Investigation Towards the Total Synthesis of Portentol *via* an Inverse Electron Demanding Diels Alder Reaction

and

Studies Towards the Total Synthesis of Brevistin

Dissertation

zur

Erlangung des Doktorgrades (Dr. rer. nat.)

der

Mathematisch-Naturwissenschaftlichen Fakultät

der

Rheinischen Friedrich-Wilhelms-Universität Bonn

vorgelegt von

Tan Hoang Luu

aus Hannover

Bonn, 2023

Angefertigt mit Genehmigung der Mathematisch-Naturwissenschaftlichen Fakultät der
Rheinischen Friedrich-Wilhelms-Universität Bonn

Erstgutachter Prof. Dr. Dirk Menche
Zweitgutachter Prof. Dr. Andreas Gansäuer

Tag der Promotion: 01.03.2024
Erscheinungsjahr: 2024

Die vorliegende Arbeit wurde in der Zeit von Oktober 2018 bis September 2023 am Kekulé-Institut für Organische Chemie und Biochemie der Mathematisch-Naturwissenschaftlichen Fakultät der Rheinischen Friedrich-Wilhelms-Universität Bonn unter der Leitung von Prof. Dr. Dirk Menche angefertigt

Danksagung

An erster Stelle gilt mein Dank Herrn Prof. Dr. *Dirk Menche* für die Aufnahme in seinen Arbeitskreis und die Vergabe der hoch interessanten Themen. Die angenehme Arbeitsatmosphäre mit dem entgegengebrachten Vertrauen und die hervorragende Ausstattung der Labore haben wesentlich zum Gelingen dieser Arbeit beigetragen. Herrn Prof. Dr. *Andreas Gansäuer* danke ich für sein Interesse an meiner Arbeit, sowie für die Übernahme des Zweitgutachtens.

Weiterhin möchte ich allen aktuellen und ehemaligen Kollegen im Arbeitskreis Menche für die positive Zeit danken. Insbesondere für die geistreichen Gespräche am Mittagstisch und dem wissenschaftlichen Input. Ganz besonders möchte ich meinen beiden Laborpartnern *Christina Braun* und *Alexander Babczyk* danken, da ohne sie meine Zeit im Labor nur halb so schön wäre. Außerdem möchte ich mich gerne bei den von mir betreuten Studenten, insbesondere *Laura Tomzcyk, Paula Toma, Ceire Horn* und *Helena Cyri* deren Bachelor- und Masterarbeiten betreuen durfte. *Max Schönenbroicher, Christina Braun* und *Alexander Babczyk* möchte ich nochmal für das Korrekturlesen dieser Arbeit danken. *Norbert Wagner* möchte ich für die Bereitstellung und der Anleitung an der Hochdruckpresse bedanken. Außerdem gilt meinem dank auch *Thorsten Frings,* der die Teflonampullen hergestellt hat. Des Weiteren gilt mein Dank der analytischen Abteilung der Universität Bonn. Für die zahlreichen NMR-Messungen danke ich Frau Dr. *Senada Nozinovic*, *Ulrike Weynand*, *Karin Prochnicki* und *Hanelore Spitz*. Ebenso bedanke ich mich bei Frau Dr. *Marianne Engeser*, *Karin Peters-Pflaumbaum* und *Christine Sondag* für die massenspektrometrischen Messungen. *Andreas J. Schneider* möchte ich für die HPLC-Trennungen und der Vermittlung seines damit verbundenen Know-hows danken. Einen besonderen dank gilt Herrn Dr. *Jochen Möllmann,* neben seiner stetigen Unterstützung während der täglichen Arbeit, hat er stets mit Rat und Tat mir zur Seite gestanden. Des Weiteren möchte ich mich noch bei *Daniel Unger* und *Laura zur Horst,* die mich seit meinem Studium begleitet haben und ohne diese ich nie soweit gekommen wäre, bedanken. Meinen Dank möchte ich auch an meine ehemaligen Mitbewohner *Jo Siebenaller* und *David Hofmeister* richten und auch *Sebastian Hütgens* möchte ich für die Stunden und Tage die wir in der Bib verbracht haben danken. *Aron Janusko* und *Lukas Lauterbach*, danke ich für die faszinierende Zeit in der Fachschaft. Abschließend möchte ich mich bei meinen Freunden und der Familie bedanken insbesondere bei meinen Eltern *Hoai* und *Tan*. Ihr habt mich jederzeit unterstützt und ich konnte mich blind auf euch verlassen. Außerdem bedanke ich mich bei *Anne Stasch* und *Reimund Stasch,* das sie mich so herzlich in ihren Kreis aufgenommen haben. Besonders unterstützt hat mich meine Freundin *Sophie*, die für mich in allen Belangen im Leben für mich da ist, insbesondere mit ihrer Stärke, Kreativität und Weisheit, wofür ich dir für immer und ewig Dankbar bin und sein werde.

Abreviation

Ac	Acetyl
acac	Acetylacetone
Alloc	Allyloxycarbonyl
Bn	Benzyl
Boc	*tert*-Butyloxycarbonyl
brsm	Based on recovered starting material
calcd	Calculated
CDI	1,1'-Carbonyldiimidazole
***c*Hex**	Cyclohexyl
COSY	Correlation spectroscopy
COMU	(1-Cyano-2-ethoxy-2-oxoethylidene aminooxy) dimethylaminomorpholino carbenium hexafluorophosphate
CSA	Camphorsulfonic acid
2CTC	2-Chlorotrityl chloride
Cyc	Cyclohexane
d	day
DCC	*N*,*N*'-Dicyclohexylcar-bodiimide
CH_2Cl_2	Dichloromethane
DIBAL-H	Diisobutylaluminiumhydrid
DIC	*N*,*N'*-Diisopropylcarbodiimide
DIPEA	*N*,*N*-Diisopropylethylamine
DMAP	4-Dimethylaminopyridine
DMDO	Dimethyldioxirane
DMF	Dimethylformamide
DMSO	Dimethyl sulfoxide
dr	Diastereomeric ratio
ee	Enantiomeric excess
EDC	1-Ethyl-3-(3-dimethylaminopropyl)carbodiimide
EI	Electron ionization
ESI	Electrospray ionization
eq.	Equivalent
et al.	And others
Et	Ethyl
Et_2O	Diethyl ether
EtOAc/EE	Ethyl acetate
$Eu(hfc)_3$	Tris-[3-(heptafluorpropyl-hydroxymethylen)-*d*-camphorato]-europium(III)

Fmoc	Fluorenylmethyloxycarbonyl
h	Hour
HATU	Hexafluorophosphate Azabenzotriazole Tetramethyl Uronium
HBTU	Hexafluorophosphate benzo-triazole tetramethyl uranium
HFIP	Hexafluoro-2-propanol
HMBC	Heteronuclear multiple bond correlation
HOAt	1-Hydroxy-7-azabenzotriazole
HOBt	Hydroxybenzotriazole
HPLC	High performance liquid chromatography
HRMS	High-resolution mass spec-trometry
HSQC	Heteronuclear single quan-tum correlation
Hz	Hertz
IEDDA	Inverse electron demanding Diels-Alder
Ipc	Isopinocampheyl
KHMDS	Potassium bis(trimethylsi-lyl)amide
K-oxyma	2-Cyano-2-(hydroxyimino)acetic acid ethyl ester
LDA	Lithium diisopropylamide
LLS	Longest linear sequence
$LiAlH_4$	Lithium Aluminum Hydride
***m*-CPBA**	*meta*-Chloroperoxybenzoic acid
Me	Methyl
MeCN	Acetonitrile
MeOH	Methanol
min	Minute
MS	Molecular sieve or mass spectrometry
NaDA	Sodium diisopropylamide
NBS	*N*-Bromosuccinimide
NMP	*N*-Methyl-2-pyrrolidone
NMR	Nuclear magnetic resonance
NOESY	Nuclear Overhauser en-hancement spectroscopy
Ph	Phenyl
PMB	*p*-Methoxybenzyl
ppm	Parts per million
***p*-TsOH**	*p*-Toluenesulfonic acid
py	Pyridine
PyBOP	Benzotriazol-1-yl-oxytripyr-rolidinophosphonium hexa-fluorophosphate
RCM	Ring-closing metathesis
r.t.	Room temperature

SAR	Structure-activity relation-ship
SPPS	Solid-phase peptide synthesis
TBAF	Tetra-*n*-butylammonium fluoride
TBAP	Tetrabutylammonium phosphate
TBS	*tert*-Butyldimethylsilyl
TCA	Trichloroacetonitril
TES	Triethylsilyl
TEMPO	(2,2,6,6-Tetramethylpiperidin-1-yl)oxyl
Teoc	2-(Trimethylsilyl)ethoxycar-bonyl
TFA	Trifluoroacetic acid
THF	Tetrahydrofuran
TLC	Thin layer chromatography
TMS	Trimethylsilyl
TMSE	2-(Trimethylsilyl)ethyl

Table of Contents

1 Abstract

1.1 Abstract Chapter I: Investigation Towards the Total Synthesis of Portentol *via* an Inverse Electron Demanding Diels-Alder Reaction

The first chapter of this doctoral thesis explores the potential for a total synthesis of portentol (**1**) through an inverse electron demanding Diels-Alder (IEDDA) reaction. Although, Trauner *et al.* had previously developed a total synthesis for portentol (**1**)[1] it continues to be an intriguing synthetic target. This is attributed to its potential bioactivity towards cancer cell lines[2] and *Mycobacterium tuberculosis* [3]. Furthermore, portentol (**1**) features eight stereocenters condenses into a bicyclic spiro structure, making it a perfect candidate for the Diels-Alder reaction. This reaction is renowned for its ability to introduce stereocenters, create a double bond, and form a six-membered ring in a single step. Additionally, achieving *exo* selectivity in the IEDDA reaction is essential to obtain the desired stereoselectivity, which poses an intriguing challenge due to the well known *endo* selectivity of the Diels-Alder reaction.[4]

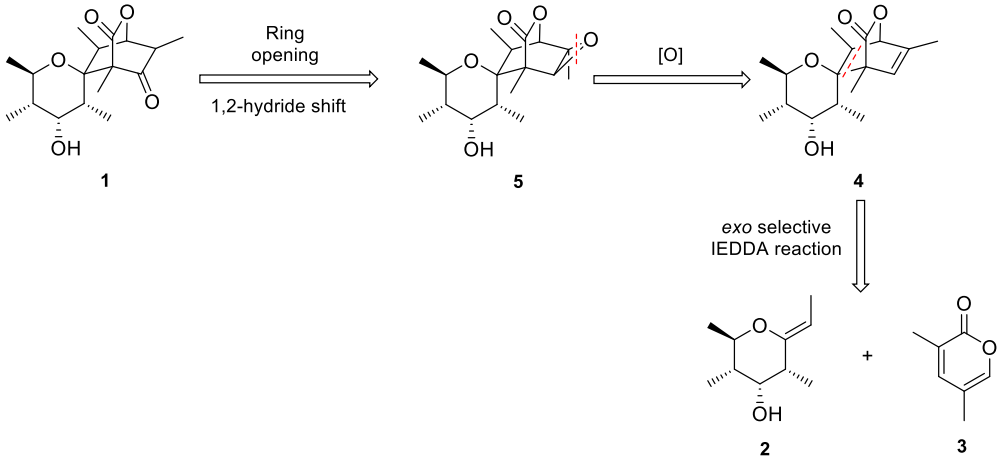

*Scheme 1-1: Retrosynthesis for portentol (**1**) showing the fragments **3** and **2** for the exo selective IEDDA reaction.*

With the goal of developing an *exo*-selective IEDDA reaction, portentol (**1**) was dissected into two primary fragments: diene (**2**) and dienophile (**3**). The synthesis of diene (**2**) had already been established, directing the focus towards devising a synthetic pathway for dienophile (**3**). Following consideration of five retrosynthetic approaches, a dependable synthesis route for dienophile (**3**) was formulated. Key steps in this approach involved the Paterson aldol reaction and the Corey-Winter elimination. Subsequently, after the successful synthesis of dienophile (**3**), investigations into the IEDDA reaction ensued. This included the utilization of various test dienophiles, screening diverse Lewis acids and conditions. In pursuit of this, a new setup for high-pressure reactions was developed, along with enhancing the electron deficiency of the

diene fragment by incorporating a 2-pyrone system with a pentafluorophenol ester moiety. While this test system provided initial insights into the mechanism of the IEDDA reaction towards portentol (**1**), applying the same setup to dienophile (**3**) proved unsuccessful due to its inherent instability. Nonetheless, it was demonstrated that by employing the *exo*-selective IEDDA reaction on analogous dienophiles, potential derivatives of portentol (**1**) could be synthesized in the future.

1.2 Abstract Chapter II: Studies Towards the Total Synthesis of Brevistin

The second chapter of this dissertation delves into brevistin (**6**), which was initially isolated in 1975 from the bacterium *Bacillus brevis* 342-14.[75] Brevistin (**6**) is a cyclic lipopeptide comprising 11 amino acids and a fatty acid chain. It exhibits antibiotic activity against Gram-positive bacteria, including bacterial strains such as *Streptococcus pyogenes, Staphylococcus aureus* and *Streptococcus pneumoniae.* [75] To further investigate its antibiotic activity it serves as an appealing target for total synthesis and presents the potential for derivatization to enhance its biological characteristics.

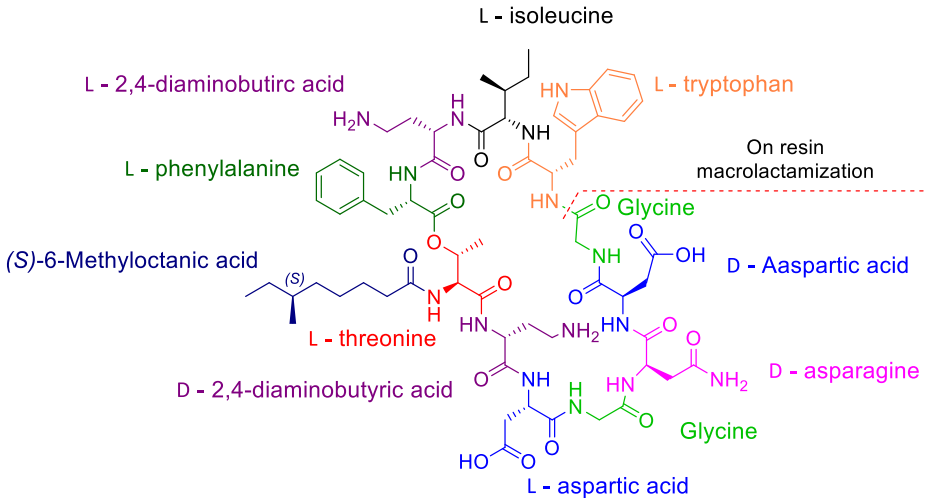

6

*Figure 1-1: Showing planned macrolactamization of brevistin (**6**).*

In the initial retrosynthetic approach, the plan was to synthesize brevistin (**6**) in a complete-on resin fashion using the solid-phase peptide synthesis (SPPS) method, followed by on-resin macrolactamization (Figure 1-1). While a portion of the peptide was successfully synthesized, unfortunately, the macrolactamization step and the completion of the linear peptide proved to be unsuccessful.

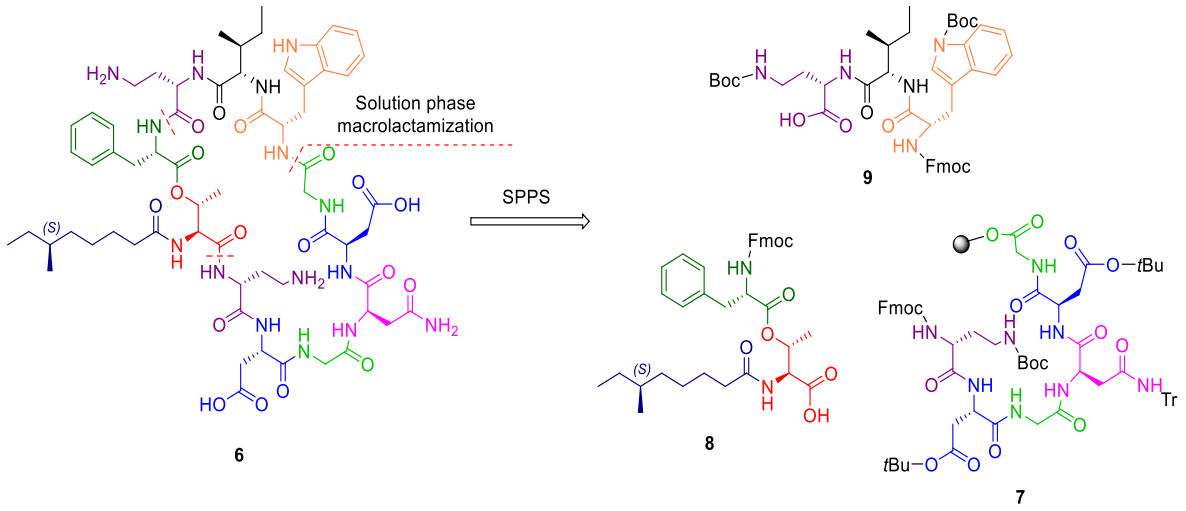

Scheme 1-2: Second retrosynthetic approach.

In a second retrosynthetic approach (Scheme 1-2), the cyclic peptide was divided into three main fragments: **7**, **8**, and **9**. Fragment **7** was synthesized using SPPS, while fragment **8** was synthesized in a solution phase. Both fragments were successfully coupled on resin, and an attempt was made to extend these coupled fragments with the last three remaining amino acids, but this endeavor proved unsuccessful. Further investigation into the coupling of the last amino acids is required, but this approach shows promising signs for the eventual successful first total synthesis of brevistin (**6**).

Chapter I: Investigation Towards the Total Synthesis of Portentol *via* an Inverse Electron Demanding Diels-Alder Reaction

2 Introduction

2.1 Overview

The history of mankind was drawn from the interaction between man and nature. Thus, man used the healing power of natural substances, especially in case of illness and injury. This resulted in the first beginnings of herbal medicine. In traditional Chinese medicine, for example, the healing properties of the leaves of the ginkgo tree have been used for almost 2000 years.[5] The medicinal effect could be attributed to the active chemical ingredients within the ginkgo extract, containing flavonoids and terpenes, which have a therapeutic effect. Studies showed that the ginkgo extract has a statistically significant effect compared to a placebo effect in improving cognition for the whole group of patients with Alzheimer's disease, vascular or mixed dementia.[6]

After extraction of herbal remedies from plants, extraction of active ingredients from prokaryotes and eukaryotes was the next step towards modern medicine. This was demonstrated by the discovery of the antibiotic penicillin in 1928 by Alexander Fleming. He found that a substance produced by the fungus *Penicillium chrysogenum* has an antibacterial effect.[7] The first chemical structure of penicillin was presented by Edward Abraham in 1942. Subsequently, the correct structure was determined by Dorothy Hodgkin in 1945 using X-ray crystallography.[8] This enabled Sheehan to develop the first total synthesis of penicillin V in 1957. He succeeded in this through a new and extremely mild method by using carbodiimide reagents to form amide bonds.[9] Hodgkin's and Sheehan's contributions now opened up the development of new β-lactam antibiotics.[7]

Today, medicinal substances are still developed through an interplay of discovery of new natural substances, subsequent structure elucidation followed by total synthesis. The synthesis of these natural products played a crucial role in derivatization for the development of more efficient drugs. The total synthesis of natural products also contributed to the development of innovative chemical reactions. These opened up new, high-yield and faster syntheses of important active ingredients.[10]

2.2 Portentol

Besides plants, fungi and bacteria, lichens, a symbiotic life form of fungi and algae or cyanobacteria, also produce biologically active substances of importance. Worldwide 17000 Lichen species are known.[11] *Roccella Portentosa* a lichen native to Chile produces the polyketide portentol (**1**), lecanoic acid **(10)**, *meso* - erythritol **(11)** and various tetrahydroxy fatty acids (Figure 2-1).[12]

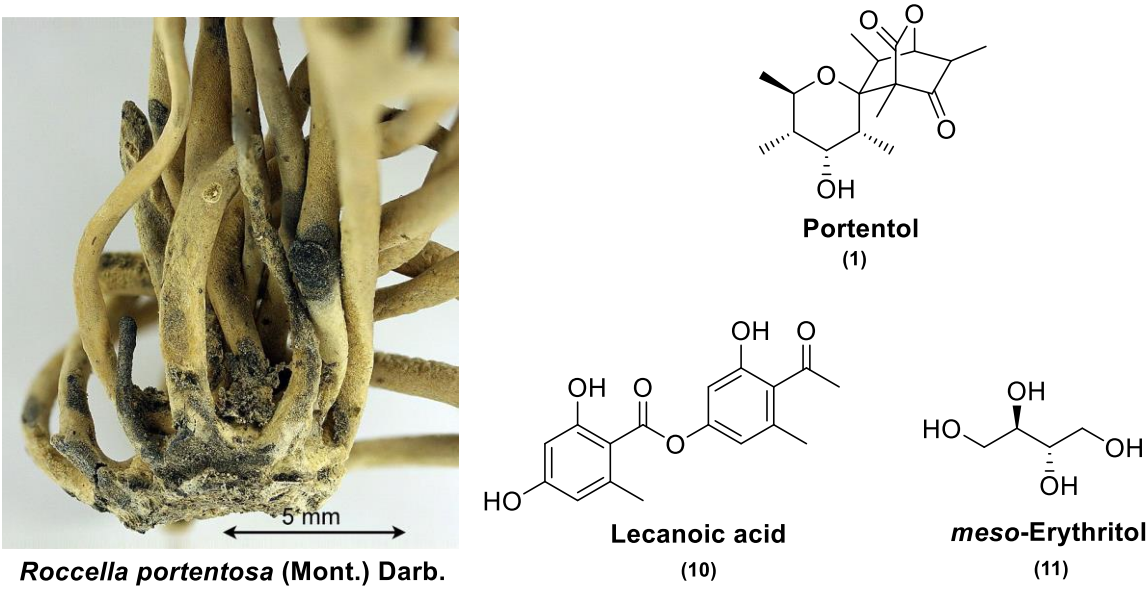

*Figure 2-1: Left: Picture of Rocella Portentosa;[13] Right: Structure of portentol **(1)**, lecanoic acid **(10)**, meso-erythritol **(11)**.*

Aberhardt and coworkers isolated portentol **1** in 1969 and could elucidate the empirical formula $C_{17}H_{26}O_5$ and right connectivity. Further investigation led to the relative stereochemistry of portentol (**1**) in 1970.[14,15] In 2004 polyketide **1** was also isolated from the brazilian nut tree *Gustavia hexapetala*. The investigators elucidated the absolute structure by 1-D and 2-D NMR analysis and confirmed the structure by single X-ray structure determination. The data was consistent with the previous findings of Aberhardt *et al*..

Furthermore, the biological activity of portentol (**1**) was tested showing growth inhibition against cancer cell lines (Table 2-1).[2]

*Table 2-1: Murine P388 Lymphocytic Leukemia Cell Line and Human Cancer Cell Line Inhibition Values (GI_{50} in µg/mL) for portentol (**1**).[2]*

Cancer Cell Line	P388	BXPC-3	MCF-7	SF-268	NCI-H460	KM20L2	DU-145
Inhibition Value	>10	7.0	>10	4.7	4.7	>10	1.3

Recently in 2020 Chandra *et al.* screened a library of 430 compounds produced by lichens to identify potent Antigen 85 complex inhibitors of *Mycobacterium tuberculosis* by using *in-silico* methods. The Antigen 85 complex was located outside the cell wall and contributed to the biosynthesis of trehalose dimycolate also known as cord factors. Those cord factors were helping *Mycobacterium tuberculosis* to survive inside the host. Portentol (**1**) showed high binding affinity to the antigen. Furthermore, computational calculations exhibited that **1** was absorbable through the human intestine, penetrates through blood-brain barriers and was a cytochrome 450 non - inhibitor. Moreover, the compound was analyzed computationally to study its toxicity characteristics where it showed non-mutagenicity, non-carcinogenicity, non-cytotoxicity, non-hepatotoxicity, and non-immunotoxicity. Making it a potential anti-tubercular drug candidate.[3]

Portentol (**1**) shows a tricyclic structure, which can be divided between a bottom fragment, the pyran ring, and the top fragment with the six-membered ring consisting a C-O bond as bridgehead. Both fragments are connected at the spiro center C-7. Furthermore, **1** contains nine stereocenters. The complex structure of portentol (**1**) makes it a challenging target for total synthesis.

2.3 Biosynthesis of Portentol

In 1970 Overton and coworkers proposed the linear precursor for **1**. The linear precursor **12** is properly formed by a polyketide synthase (PKS). However, it was not known if a type 1 or type 2 PKS is responsible for the formation of **12** and at last of portentol (**1**). Isotopic-labelling showed that acetate and malonate were incorporated into the carbon chain of **1**. The five tertiary methyl groups originated from methionine while the terminal methyl group belonged to an acetate unit.[15]

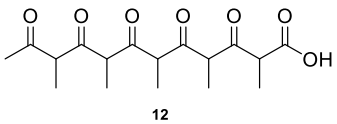

12

*Figure 2-2: Linear precursor **12** for portentol (**1**).[15]*

However, the proposed linear precursor **12** held no stereo information and contained carbons in the wrong oxidation state (Figure 2-2). Therefore, no cyclization mechanism was proposed. Later on, Trauner *et al*. proposed the following biosynthesis of portentol (**1**) (Scheme 2-1).[1,16]

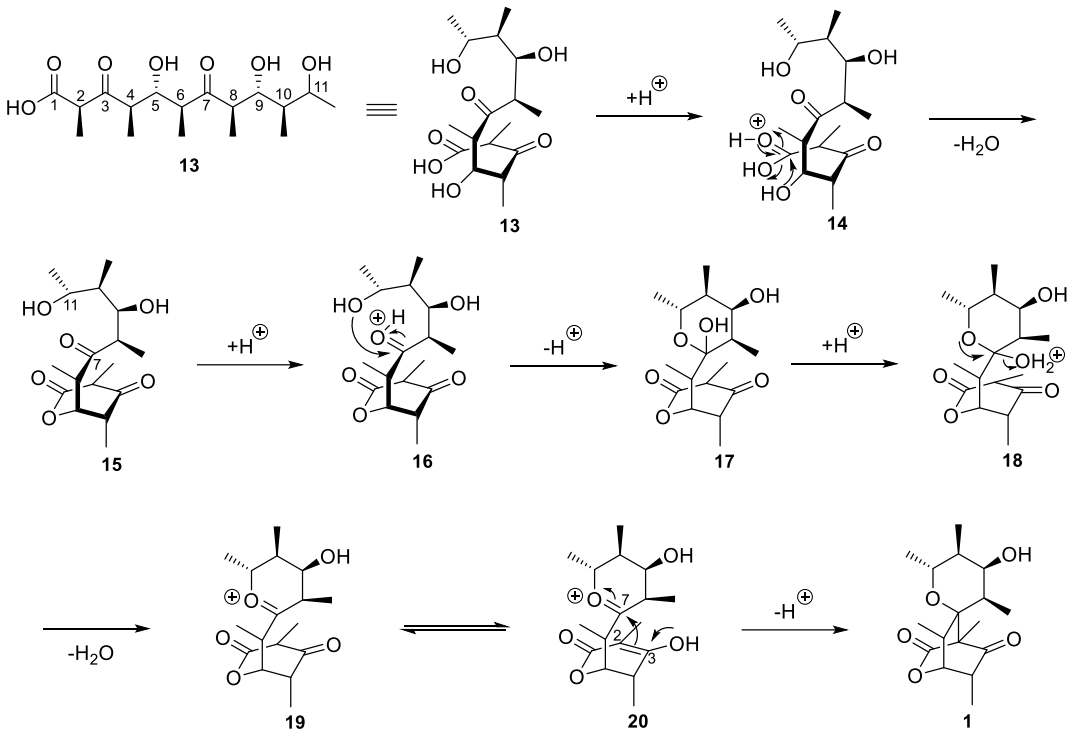

*Scheme 2-1:Proposed biosynthetic pathway towards portentol (**1**).[16]*

The mechanism began with the linear precursor **13** which held the correct stereocenters and oxidation states. The first cyclization to the pyrone ring occurred by a nucleophilic attack of the hydroxyl group at C-5 to the carboxylic acid moiety C-1, which was activated by BRØNSTED acidic conditions. Under the loss of water intermediate **15** was formed. Through protonation of **15** at the carbonyl oxygen C-7 cation **16** was formed, followed by nucleophilic attack of the hydroxy group at C-11 forming **17** under deprotonation. Hemiacetal **17** was protonated under acidic conditions and water was released giving cation **19**. The C-C bond between C-7/C-2 was formed through a cascade reaction induced by keto-enol tautomerism of the enol (C-2/C-3), establishing the spiro center. Under loss of a proton portentol (**1**) was obtained.[1,16]

2.4 Portentol as Synthetic Target

As a synthetic target, portentol (**1**) presents an interesting challenge due to the high number of stereocenters and the spiro center. A first attempt for the construction of the spirotetrahydropyran skeleton was made by van de Weghe *et al.* in 2011. Their synthetic strategy utilized polysubstituted chiral homoallylic alcohol **21** and cyclohexanone **22** in presence of a catalyst or promoter which could potentially undergo a Prins cyclization reaction to give **23** (Scheme 2-2).[17]

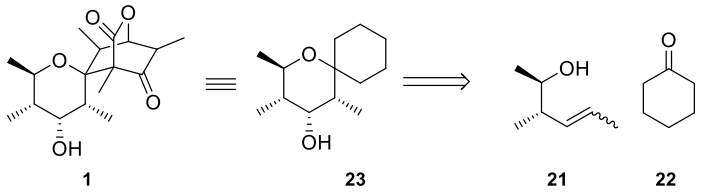

Scheme 2-2: Retrosynthetic approach by Pierre van de Weghe et al. by Prins cyclization.[17]

During their investigation of the Prins reaction, they could accomplish in the presence of TMSI, as promoter, cyclization between substituted silyl ether of homoallylic alcohol and ketones. In the case of racemic 2-methylcyclohexanone (**25**) a dynamic kinetic resolution occurred affording one stereoisomer (Scheme 2-3). The observation could be backed up by DFT calculation.[17] Nonetheless, further progress towards the total synthesis of portentol (**1**) by a Prins cyclization reaction has not been reported yet.

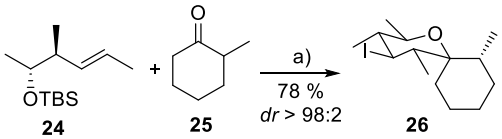

Scheme 2-3: Reagents and conditions: a) TMSI, CH_3CN or CH_2Cl_2, 0 °C.[17]

In 2015 Trauner *et al*. reported a biomimetic total synthesis of portentol (**1**). The key step of their synthetic strategy was the formation of the spirocyclic core by an intramolecular double cyclization cascade starting from the *β*-keto-*δ*-lactone **27** (Scheme 2-4). Compound **27** was formed by an *anti* aldol reaction of **28** and **29**, which were also made by aldol reaction of known compounds.[1]

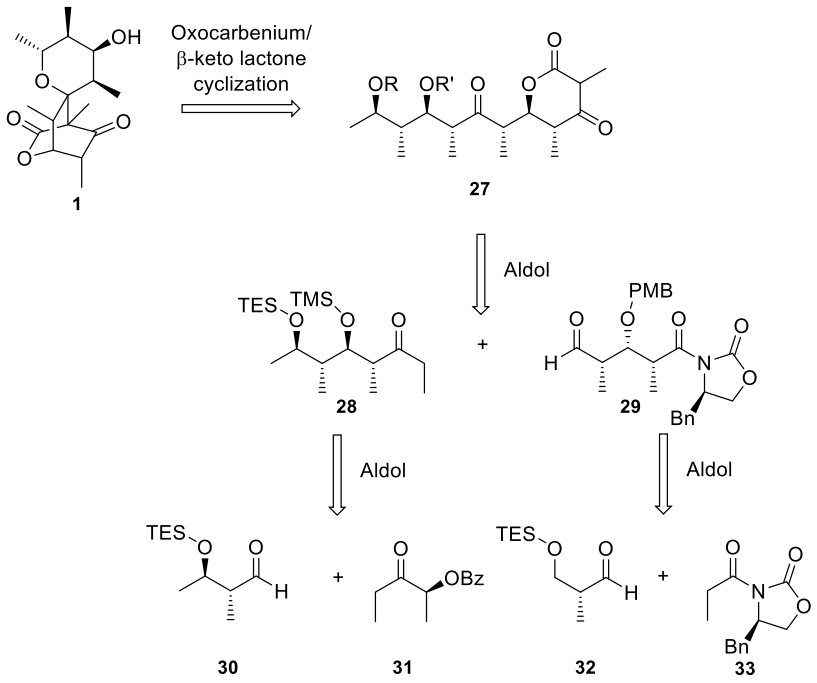

*Scheme 2-4: Retrosynthetic strategy of portentol (**1**) by Trauner et al.*[1]

The Paterson aldol reaction of the fragments **30** and **31** afforded **34** after TMS protection of the newly formed hydroxyl stereocenter followed by deprotection of the *α*-benzoate yielded ketone **28** (Scheme 2-5). The synthesis of fragment **29** started with an Evans-*syn* aldol reaction of **32** and **33**. The secondary alcohol moiety of the obtained product **36** was protected with *p*-methoxybenzyl (PMB) and yielded **37**. Desilylation of the primary alcohol and oxidation under Swern conditions yielded **29**. Both fragments were linked by a modified Evans aldol reaction, followed by deprotection of the PMB group to give compound **39**. The double cyclization cascade was induced by oxidation under Swern conditions with trifluoroacetic anhydride (TFAA) as activator, followed by deprotection of silyl groups.[1]

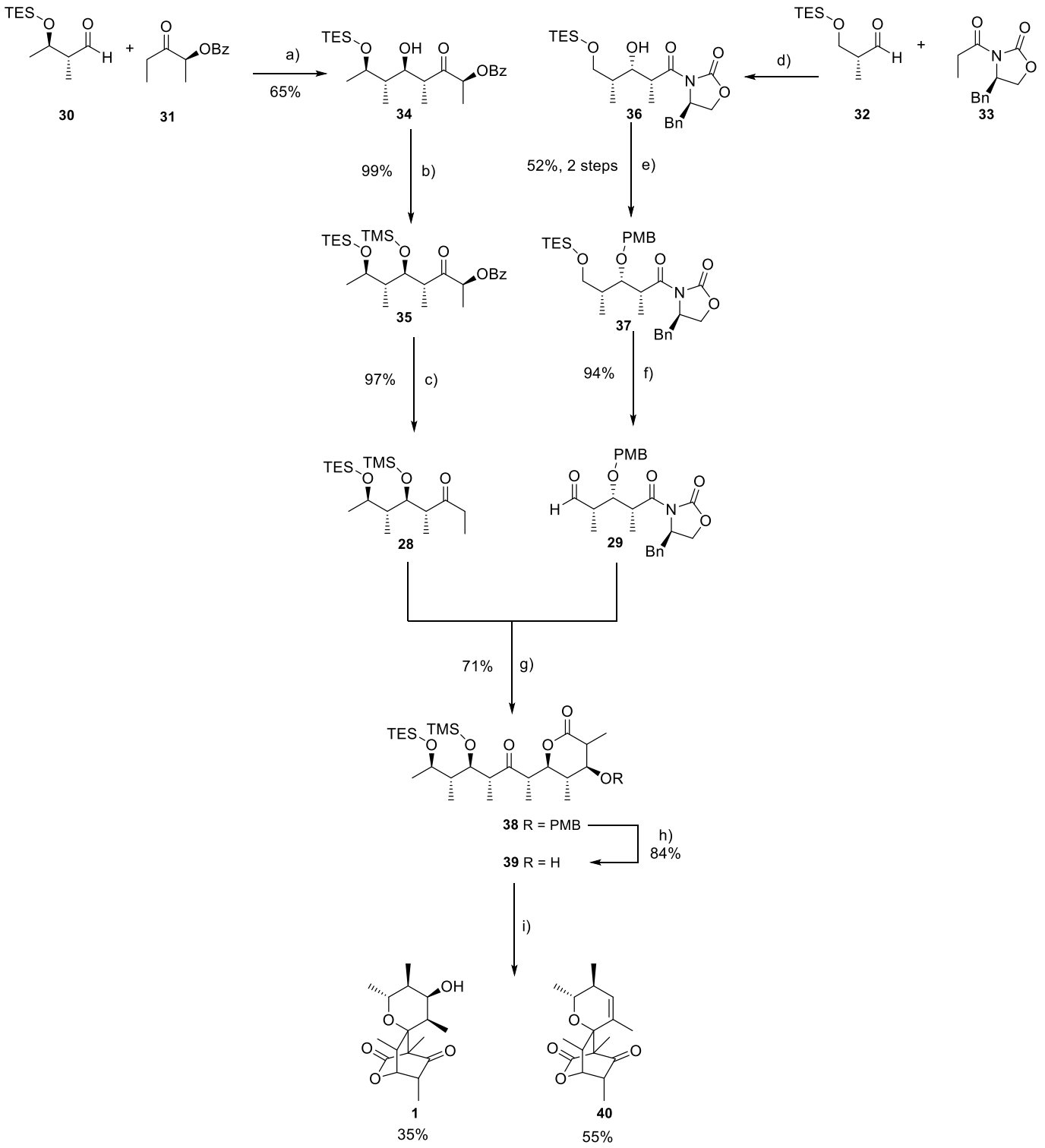

*Scheme 2-5: Reagents and conditions: a) Cy_2BCl, Et_3N, Et_2O, -78 to 0 °C, then **30**, -78 °C to -20 °C; b) TMSCl, TMS_2NH, pyridine, r.t.; c) SmI_2, THF/MeOH, 0 °C; d) Bu_2BOTf, Et_3N, CH_2Cl_2, 0 °C, then **32**, -78°C to 0 °C; e) PMB-OC(NH)CCl_3, $Sc(Otf)_3$ (1 mol%), toluene, rt; f) DMSO, $(COCl)_2$, CH_2Cl_2, -78 °C to -25 °C; Et_3N; g) Cy_2BCl, Et_3N, Et_2O, 0 °C to rt. then **29**, -78 °C to -40 °C, then pH 7 buffer, THF, H_2O_2; h) DDQ, CH_2Cl_2, rt; i) DMSO, TFAA, CH_2Cl_2, Et_3N, -78 °C, then MeOH, rt.*[1]

Trauner *et al*. proposed that after the oxidation of C-3 and desilylation **27** was generated (Scheme 2-6). Under loss of water oxocarbenium **20** was formed *in situ* during acidic workup of the desilylation. Like in the proposed biosynthesis cyclization was induced by keto-enol tautomerism to give portentol (**1**). Cation **20** was in equilibrium with its rotamer **20a** which could

not undergo cyclization fast enough due to a steric clash of the C -8 methyl group and C-9 hydroxy group with the C-2 methyl group. After elimination of water by proton transfer **41** was formed which, cyclized in the same way as **20** to yield anhydroportentol (**40**). Rotamer **41a** could not undergo cyclization due to steric hindrance between the C-2 and C-8 methyl groups and an unfavorable 1,3-axial strain between the C-6 and C-8 methyl group. Because of steric clashes of rotamers **20a** and **41a**, no stereoisomers of **1** and **40** with respect to C-7 were observed.[1]

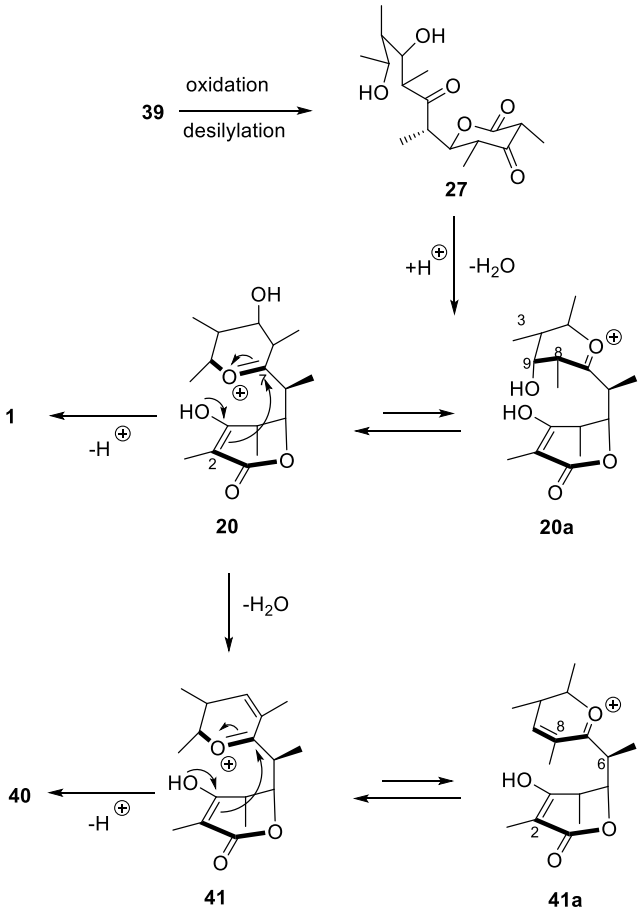

Scheme 2-6: Proposed cyclization mechanism by Trauner et al.[1]

Even after the first total synthesis of portentol (**1**), the polyketide still remained an interesting synthetic target. In 2018 Yadav *et al*. published a retrosynthetic approach using a desymmetrization strategy (Scheme 2-7).[18]

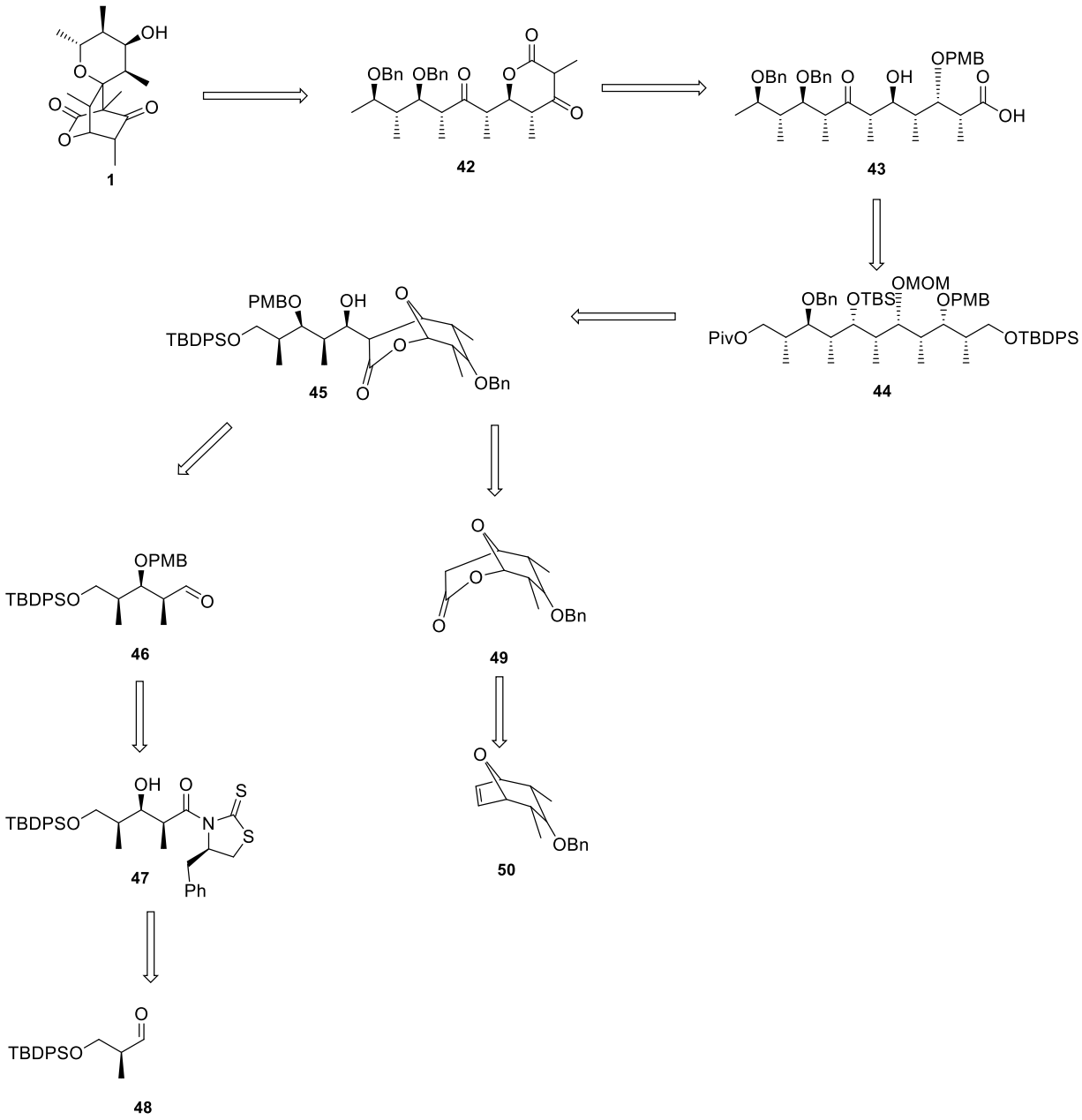

*Scheme 2-7: Retrosynthetic strategy towards portentol (**1**) by Yadav et al.[18]*

This strategy offered the formation of contiguous chiral centers by ring opening of the bicyclic precursor **45**. Compound **45** was obtained through an intermolecular aldol reaction between aldehyde **46** and the bicyclic lactone **49**, using LiHMDS as a base (Scheme 2-8).[18]

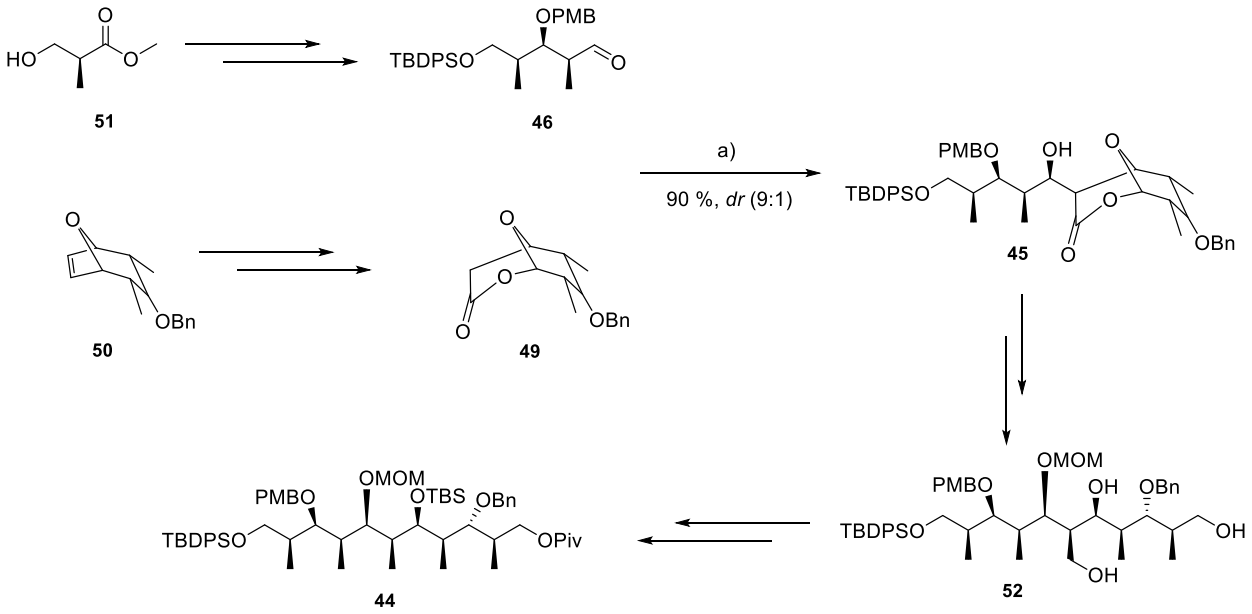

Scheme 2-8: Reagents and conditions: a) LiHMDS, THF, -78 °C.[18]

Furthermore, the free alcohol moiety of the aldol adduct **45** was protected with a MOM protecting group. Followed by a reductive cleavage of the bicyclic ring with $LiBH_4$ which gave the polyol **52**. The ring opening generated five new chiral centers within one step. After another seven steps, *Yadav et al*. succeeded in obtaining fragment **44**. Further investigations in this synthetic route are still in process and have not been reported yet.[18]

2.5 Diels-Alder Reaction

In 1928 Otto Diels and Kurt Alder reported the discovery of the cycloaddition reaction of conjugated diene and a second component with at least one π-bond, later referred as dienophile, to a cyclohexene ring.[19] The reaction later on labeled as Diels-Alder reaction was rewarded in 1950 with a Nobel Prize.[20] The formation of the six-membered framework is controlled by the interaction of the highest occupied molecular orbital (HOMO) of one component and the lowest unoccupied molecular orbital (LUMO) of the other, according to the frontier molecular orbital theory (FMO).[21]

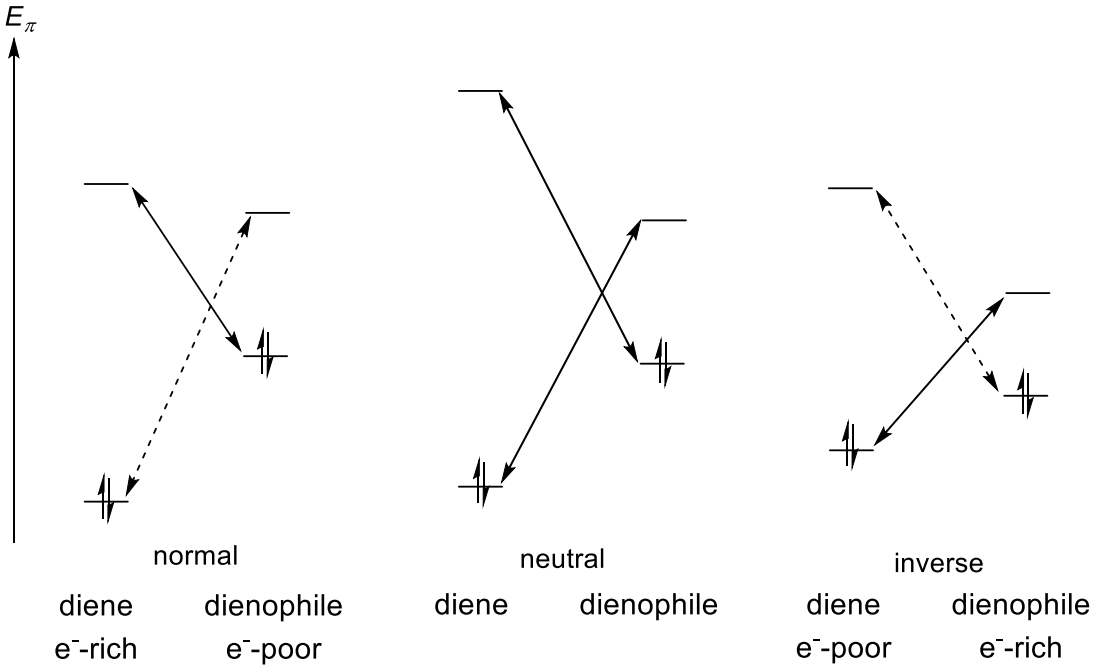

Figure 2-3: Frontier orbital interactions of Diels-Alder-reaction at different electron demand.[21]

Reactivity of the Diels-Alder reaction depends on the energy gap between HOMO and LUMO (Figure 2-3). The lower the energy difference, the lower is the transition state energy. Electron-withdrawing substituents lower the energy of both HOMO and LUMO, while electron-donating groups increase their energies. HOMO diene-controlled Diels-Alder reactions are accelerated by electron-donating substituents in the diene and by electron-withdrawing substituents in the dienophile (normal electron-demand Diels-Alder). LUMO diene-controlled Diels-Alder reactions are influenced by the electronic effect of the substituents in the opposite way (inverse electron-demand Diels-Alder). The neutral electron-demand Diels-Alder reaction is HOMO – LUMO - diene controlled and is insensitive to substituents in either the diene or the dienophile (Figure 2-3).[21]

The regiochemistry is determined by the overlap of the orbitals that have larger coefficients (Figure 2-4). The bigger the difference between the orbital coefficients of the two terminal atoms of diene and two atoms of dienophile, which form the two σ-bonds, the more regioselective the cycloaddition.[21]

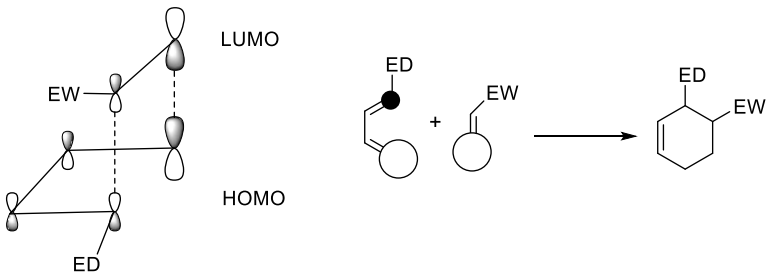

Figure 2-4: : Regioselectivity determination by FMO theory; ED: Electron donating group; EW: Electron withdrawing group.[21]

By generating two new C-C-σ-bonds up to four stereogenic centers can be established. The stereochemistry elaborated at the termini of the new σ-bonds evolves from the stereochemistry of the diene and dienophile and the topography of the cycloaddition resulting in two possible adducts named *endo* and *exo*. The spatial arrangement of reactants in which the bulkier sides of the diene and dienophile lie one above the other gives the *endo* product, while during formation of the *exo* adduct the bulkier side of one component is under the smaller side of the other. The *exo* addition mode is expected to be preferred because it suffers fewer steric repulsive interactions than the *endo* approach. However, the *endo* adduct is usually the major product because of stabilizing secondary orbital interactions in the transition state known as Alder's rule (Figure 2-5).[21]

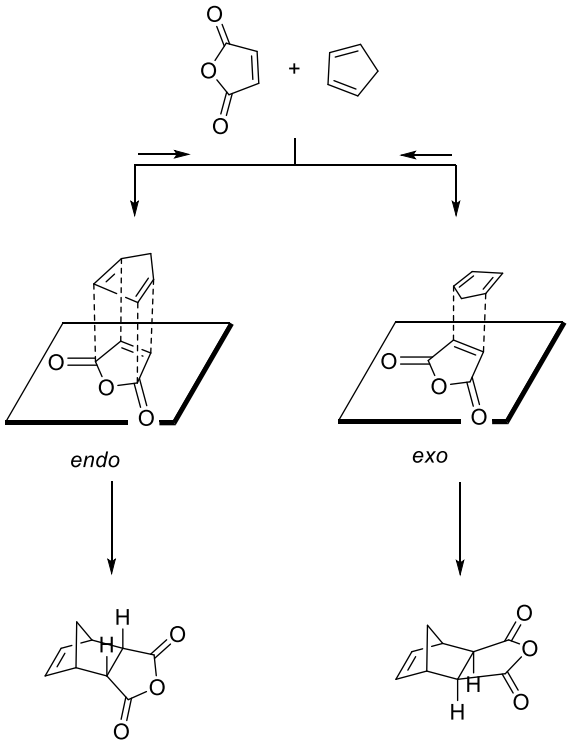

Figure 2-5: Example for endo- and exo-transition states.[21]

The possibility to create two new σ-bonds and four contiguous stereo centers shows the potential of the Diels-Alder reaction in total synthesis.

2.6 2-Pyrone the Key for the Inverse Electron Demand Diels-Alder Reaction

The behavior of 2-pyrone, which is a molecule that can act as both an electron-rich and electron-poor diene due to the presence of an electron withdrawing carboxyl group on one side and an electron donating acyloxy group on the other side. Substituted 2-pyrones are suitable for Diels-Alder reactions, with the reactivity and type of reaction determined by the electronic properties of the substituent on the pyrone ring. Electron-rich 2-pyrones participate in normal electron-demand Diels-Alder reactions (NEDDA), while electron-poor 2-pyrones participate in inverse electron-demand Diels-Alder reaction (IEDDA). Bromo- and dibromo-substituted 2-pyrones can carry out both NEDDA and IEDDA reactions flexibly (Figure 2-6).[22]

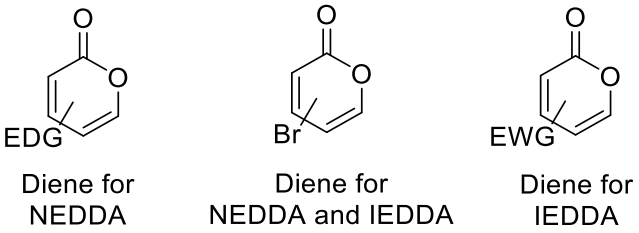

Figure 2-6: Ambiphilic capacity of 2-pyrones.[22]

3 State of Knowledge

3.1 The First Diels-Alder Reaction Approach

The first attempt to synthesize portentol (**1**) by a Diels-Alder reaction was made by Schröckeneder and Trauner. Their retrosynthetic strategy led to two main fragments (Scheme 3-1). The pyrane dienophile **3** should been derived from lactone **62**. The pyrone fragment **61** was literature known and described by Effenberger *et al.*[16,23]

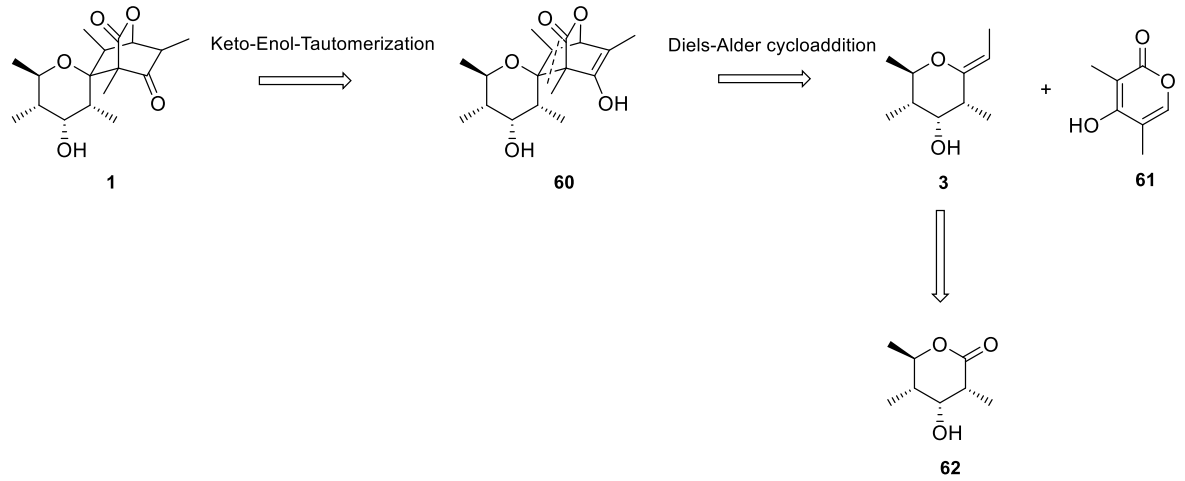

Scheme 3-1: Retrosynthetic approach by Schröckeneder and Trauner.[16]

Pyrone **61** was successfully synthesized (Scheme 3-2). However, extensive screening of the Diels-Alder reaction with pyrone **61** and its acetyl protected derivative **67** with suitable dienophiles did not yield any results. Various Lewis acids were screened under different temperature conditions and solvents.[16]

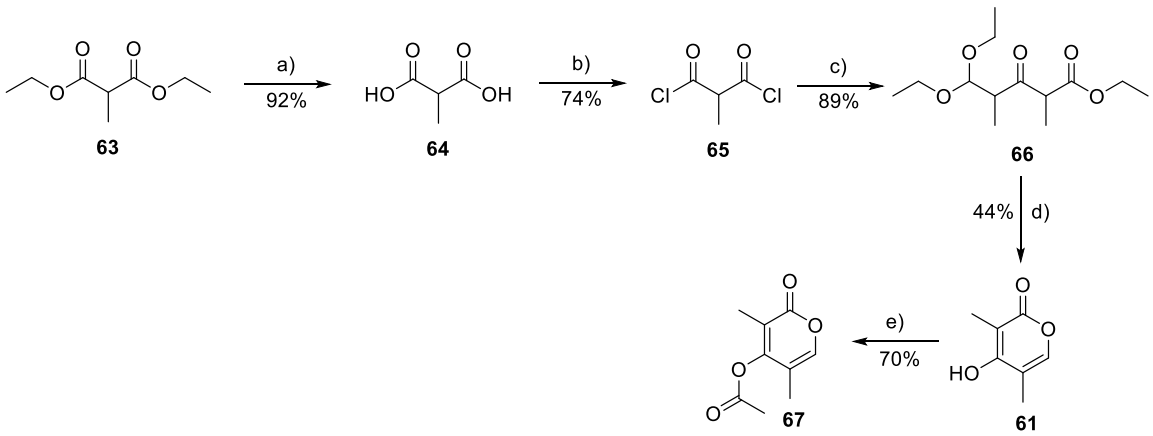

*Scheme 3-2: Synthesis of pyrone **61** and acetyl pyrone **67**; Reagents and conditions: a) KOH, THF, then HCl, from 0 °C to r.t.; b) $SOCl_2$, 50 °C; c) Ethylpropenyl ether, EtOH then NEt_3, 0°C; d) KOH, EtOH, r.t. then H_2SO_4/SO_3 from 0°C to 100 °C; e) Acetyl chloride, pyridine, DMAP, THF, from 0 °C to r.t.*[16,23]

In addition, the planned Takai-Lombardo type reaction posed a great challenge. The direct conversion of lactone **68** to enol ether **69** was unsuccessful. Conversion of lactone **68** through the hemiacetal **70** with ethylmagnesium bromide and subsequent elimination was also unsuccessful (Scheme 3-3). Thus, Schröckeneder's and Trauner's Diels-Alder reaction approach failed.[16]

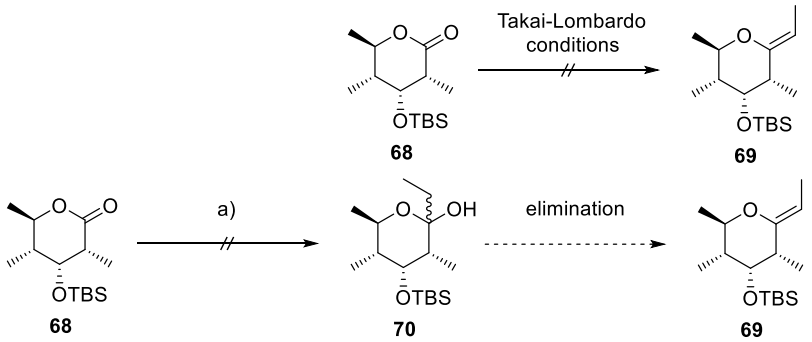

*Scheme 3-3: Top: Unsuccessful Takai-Lombardo-type reaction; Bottom: Unsuccessful two step sequence to dienophile **69**; Reagents and conditions: a) Ethylmagnesium bromide, Et_2O, from 0 °C to r.t.*[16]

3.2 A New Diels-Alder Reaction Approach

A new retrosynthetic strategy towards portentol (**1**), developed by the Menche group (Scheme 3-4), envisioned the construction of the spirocyclic core by an *exo*-selective, IEDDA reaction, too, but with pyrone **2** as diene and pyrane ring **3** as dienophile. By exchanging the hydroxypyrone **61** for the pyrone **2** in the absence of the hydroxy group the diene is expected to become electron-depleted. This is expected to favor the IEDDA.

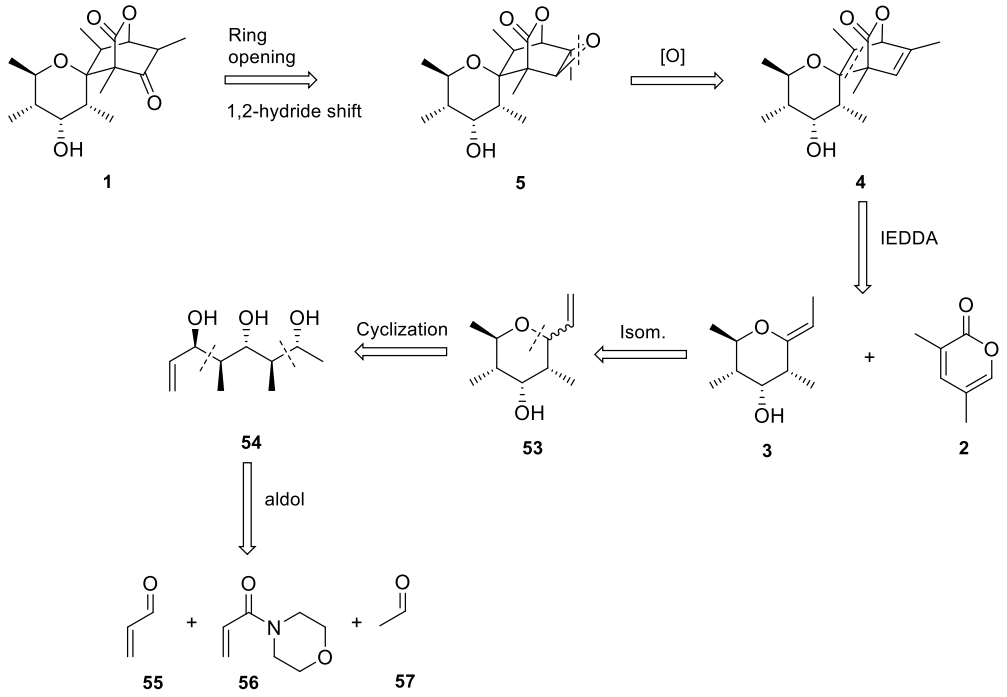

*Scheme 3-4: Retrosynthetic strategy towards portentol (**1**) via an Inverse Electron Demand Diels-Alder Reaction.*

Dienophile **3** can be present in two conformational forms: a $^{1}C_{4}$ chair conformation or a $^{4}C_{1}$ conformation. In the latter conformation all methyl groups are equatorial and the alcohol group is axial. Therefore, the methyl group at C-5 of the pyran ring does not show in axial position as in a $^{1}C_{4}$ conformation, which could prevent the diene **2** from approaching. At the same time, due its axial position in the $^{4}C_{1}$ conformation the hydroxyl group does not cause a repulsive interaction with the double bond of diene **2**. This will be the case in a $^{1}C_{4}$ conformation. Consequentially the following theoretical consideration emanates from the $^{4}C_{1}$ chair conformation.[16]

3.2.1 First Attempts for the Synthesis of Diene 2

The first approaches were pursued by Johal Ruiz and Aron Janusko. They first tried to synthesize the 3,5-dimethylpyrone (**2**). The plan involved cyclization followed by elimination of the hydroxyl group of **71**. The hydroxy moiety was envisioned to be obtained by reduction of **73**. Stereoselectivity was irrelevant, since all stereo information would be lost during cyclization and elimination. The keto group of **73** was to be released by deprotection of the dioxinone ring of **74**. Followed by the introduction of dimethoxyacetal at **75** through an orthoester condensation. **76** was to be obtained from the corresponding ethyl ester **77**. A Claisen condensation of ethyl propionate (**78**) would served as the first step (Scheme 3-5).[24]

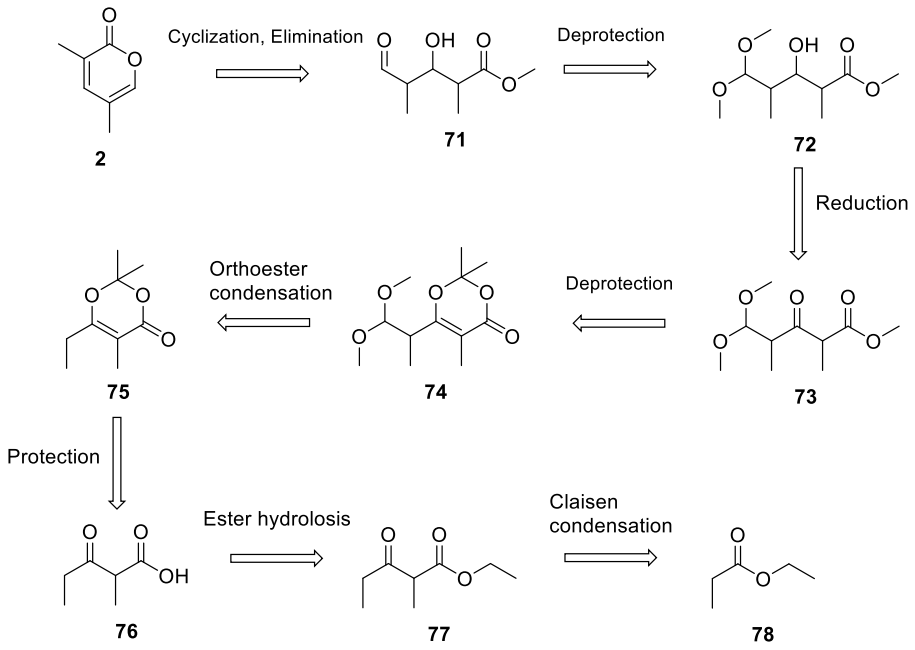

*Scheme 3-5: Retrosynthetic approach via ionic cyclization by Aron Janusko for diene **2**.[24]*

The Claisen condensation from **78** to **77** was successful, but the following ester hydrolysis to **76** could not be accomplished. An alternative route towards dioxinone **75** by Claisen condensation of *tert*-butyl propionate (**79**) and phenyl propionate followed by cleavage of the *tert*-butyl moiety under acidic conditions was successful. The synthesis proceeded up to acetal **72** until deprotection to the aldehyde under acidic conditions was unsuccessful giving multiple side products (Scheme 3-6).[24]

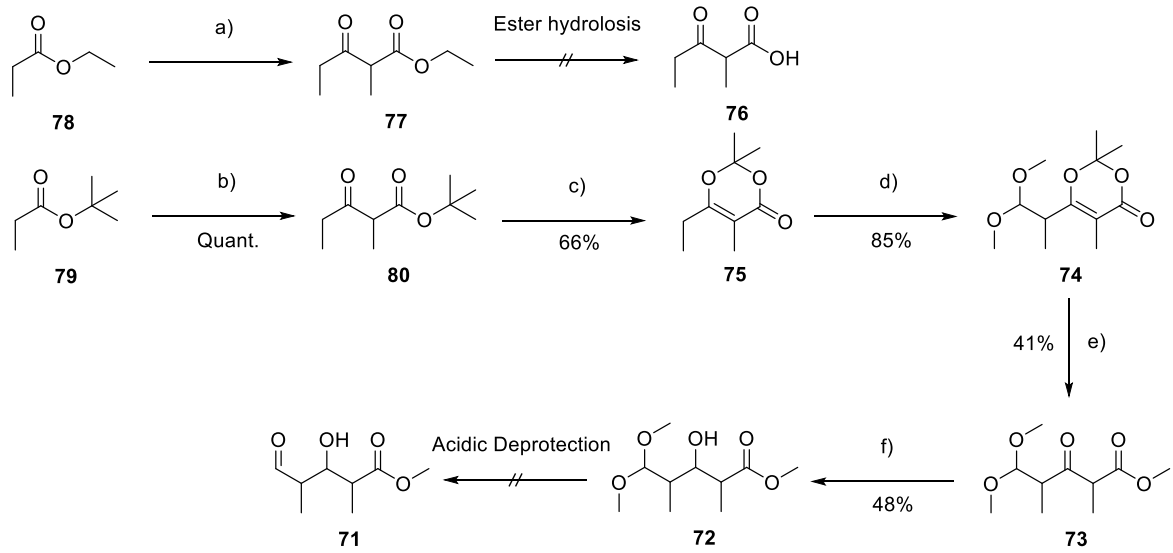

*Scheme 3-6: Synthesis of pyrone **2**; Reagents and conditions: a) KO^{t}Bu, neat, 80 °C; b) LDA, LiHMDS, THF, then phenyl propionate, -78 °C; c)H_2SO_4, Ac_2O, acetone, from 0°C to r.t.; d) TMSOTf, NEt_3, $HC(OMe)_3$, BF_3*Et_2O, CH_2Cl_2, -78°C; e) NaOMe, EtOH, r.t.; f) $NaBH_4$, MeOH, -78°C.*

In a second attempt to synthesize diene **2** the cyclization was envisioned by ring closing metathesis followed by elimination. Therefore, in the second retrosynthetic approach the

unsaturated lactone **81** was to be formed from **82** by means of an RCM. The linear precursor **83** has to been obtained by esterification of diol **84** which could been synthesize by Gringnard reaction of hydroxy acetone (**85**) using vinyl magnesium bromide (Scheme 3-7).[24]

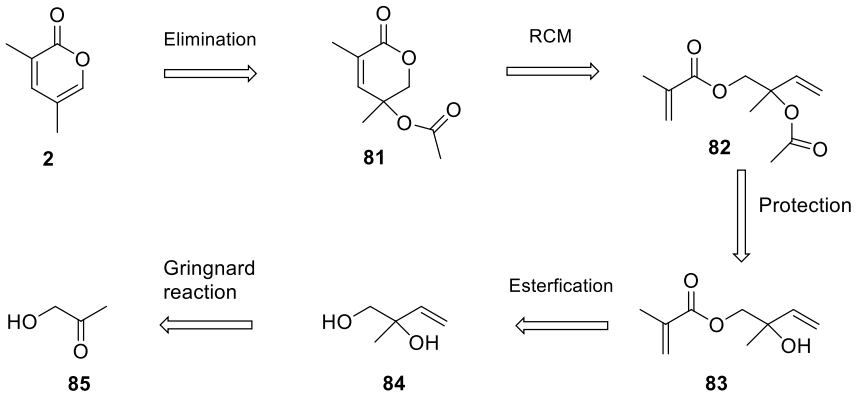

*Scheme 3-7: Retrosynthetic approach via RCM by Aron Janusko for diene **2**.[24]*

The envisaged synthetic route led successfully to the linear precursor **82** in three steps with high to moderate yields (Scheme 3-8). However, cyclization by RCM was unsuccessful. Various catalysts were tested that did not led to lactone **81**. The unprotected fragment **83** was also tested unsuccessfully under RCM conditions.[24] Thus, the synthesis of pyrone fragment **2** was unsuccessful.

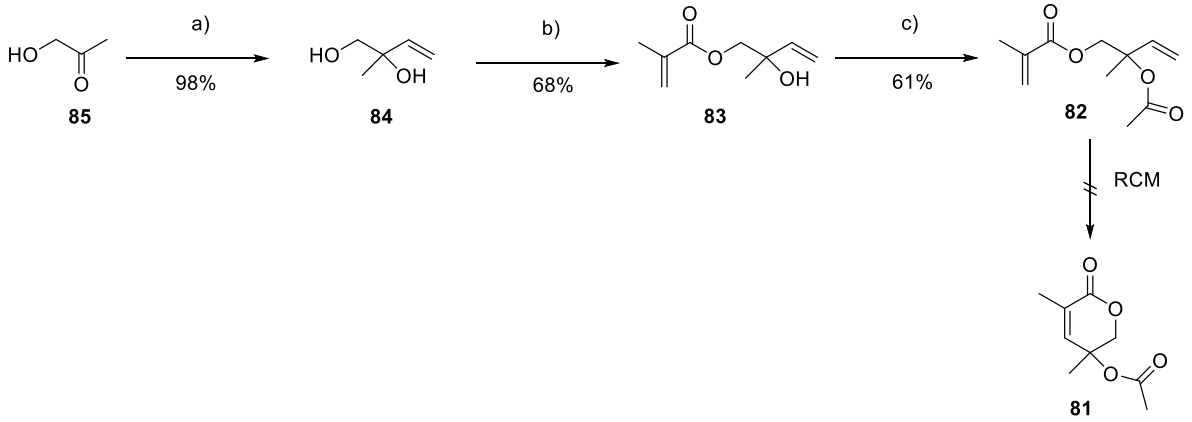

*Scheme 3-8: Synthesis of pyrone **2** via RCM; Reagents and conditions: a) Vinylmagnesium bromide, THF, from 0 °C to r.t.; b) Methacrylic acid, DCC, DMAP, 0 °C; c) Ac_2O, pyridine, DMAP (cat.), THF, r.t.[24]*

3.2.2 New Synthetic Strategy Towards Dienophile 3

As shown in section 3.2 (Scheme 3-4) a different approach towards dienophile **3** was envisioned as the approach by Schröckeneder and Trauner. Janusko and Ruiz obtained the triol **54** in five steps with moderate yields. To confirm the newly build stereo centers, triol **54** was transformed into the ortho ester **90**. Due to the rigid bicyclic structure, the configuration of

the formed stereocenters from the previous aldol addition could be confirmed by 2-D NMR analysis, such as $^{1}H,^{1}H$ - COSY and NOESY. The cyclization of compound **54** using iron trichloride hexahydrate showed small amounts of the desired product **53**. Without having performed the isomerization, the work of Janusko and Ruiz ended at this point (Scheme 3-9).[24]

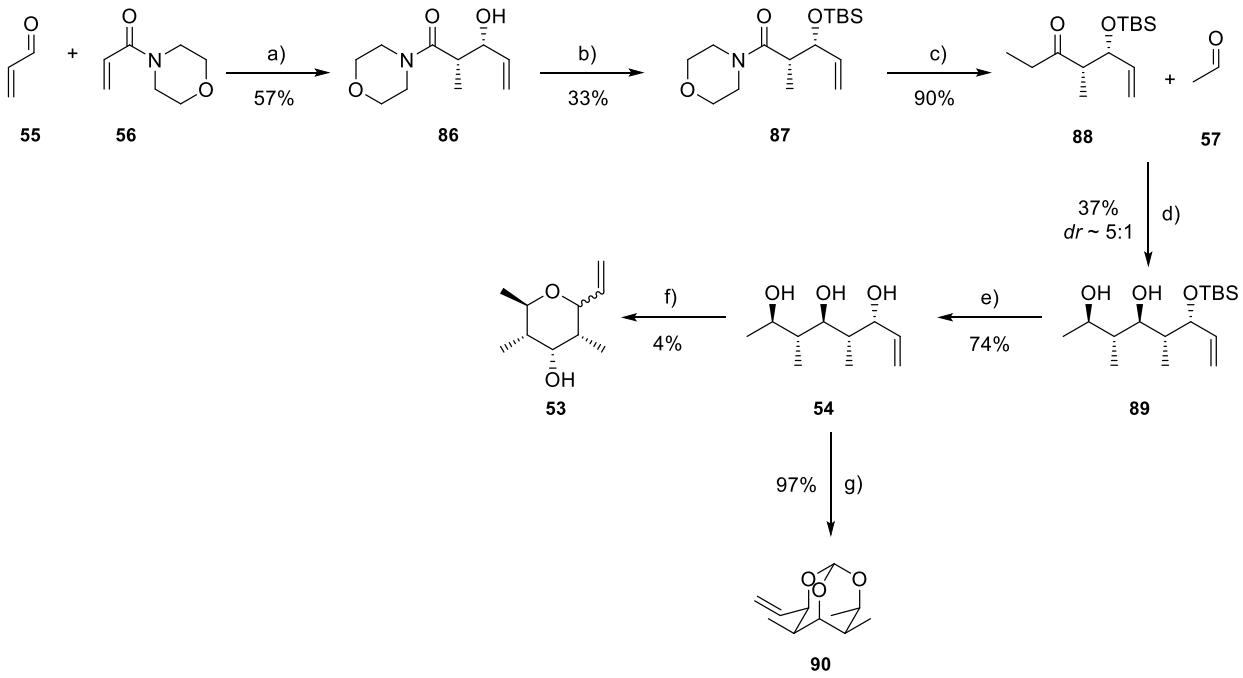

*Scheme 3-9: Reagents and conditions: a) (−)-Ipc$_2$BH, Et$_2$O, 0 °C then **56**, −78 °C then **55**, then THF/methanol/pH 7 potassium phosphate buffer; b) TBSOTf, 2,6-lutidine, CH$_2$Cl$_2$, 0 °C; c) EtLi (0.5 M in benzene/cyclohexane), THF, −78 °C; d) Cy$_2$BCl, Et$_3$N, Et$_2$O, −78 °C to 0 °C, then **57**, −78 °C to −20 °C; −20 °C to −78 °C then LiBH$_4$ (4 M in THF); e) HF·pyridine, THF, 0 °C to rt; f) FeCl$_3$·6H$_2$O, DCE, 80 °C; g) HC(OMe)$_3$, CH$_2$Cl$_2$, r.t.*[24]

3.2.3 New Synthetic Strategy Towards Diene 2 and Progress Towards Dienophile 3

The work of Janusko and Ruiz was continued by Tan Hoang Luu within the Menche group during his master thesis. First, a new synthetic strategy for diene **2** was developed. Diene **2** was envisioned by cross-alkylation of the precursor **91** which in return was planned to be obtained by an electrophilic aromatic substitution of commercially available coumalic acid (**92**) (Scheme 3-10).[25]

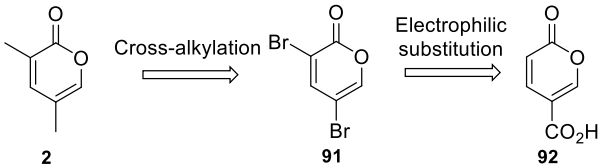

*Scheme 3-10: New retrosynthetic strategy towards **2**.*[25]

The synthesis of **2** was successfully completed. Thus, the electrophilic substitution of **92** to dibromopyrone **91** showed a yield similar to that reported in the literature.[26] The cross-alkylation was successful but the yield could not be reproduced as reported in the literature.[27] Nevertheless, this synthetic strategy proved to be the most efficient at this time, as fragment **2** could be produced quickly and cost-effectively (Scheme 3-11).

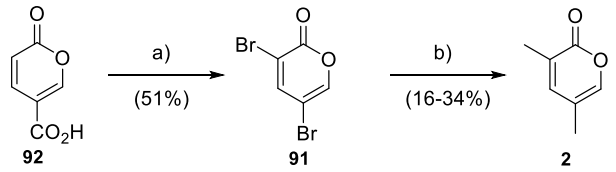

*Scheme 3-11: Synthesis towards diene **2**, Reagents and conditions: a) NBS, Bu_4NBr, $CHCl_3$, 50°C; b) $AlMe_3$, $PdCl_2(PPh_3)_2$, toluene, 100°C.[25–27]*

The synthesis of dienophile **3** was adapted by Janusko and Ruiz and an attempt was made to optimize it. Therefore, it was possible to increase the yield of triol **54**. Subsequently, the cyclization of **54** to pyrane **53** was intensively screened. However, the highest yield determined was only 14 %. In addition, the reaction proceeded with formation of several by-products which made purification of the desired product difficult. However, enough of pyrane **53** was collected to attempt isomerization under nickel catalysis to dienophile **3** (Scheme 3-12). However, this, showed only traces of the supposedly desired product, which could not be confirmed by NMR.[25]

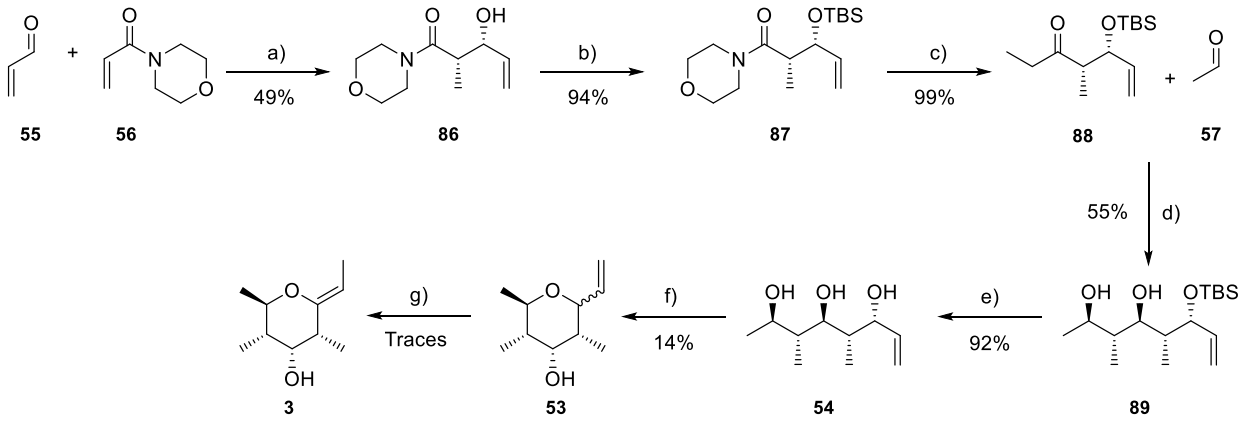

*Scheme 3-12: Reagents and conditions: a) (−)-Ipc_2BH, Et_2O, 0 °C then **56**, −78 °C then **55**, then THF/methanol/pH 7 potassium phosphate buffer; b) TBSOTf, 2,6-lutidine, CH_2Cl_2, 0 °C; c) EtLi (0.5 M in benzene/cyclohexane), THF, −78 °C; d) Cy_2BCl, Et_3N, Et_2O, −78 to 0 °C, then **57**, −78 °C to −20 °C; −20 °C to −78 °C then $LiBH_4$ (4 M in THF); e) TBAF, THF, 0 °C to rt; f) $FeCl_3 \cdot 6H_2O$, MeCN, 60 °C; g) $NiCl_2$dppb, $LiBEt_3H$, THF, rt.[25]*

3.3 First Attempts for the IEDDA Reaction

To test various conditions for the IEDDA reaction to portentol (**1**) several attempts were made to establish a test system. Schröckeneder and Trauner undertook intensive screening with

their synthesized hydroxy pyrone **61** and acetyl protected pyrone **67** respectively. Dihydroypyrane (**93**) and an *E/Z*-mixture of ethylpropenyl ether (**95**) were used as test dienophiles (Scheme 3-13). These are electronically very similar to fragment **3**. Different conditions were tested, such as temperature, solvent, time and different Lewis acids as catalysts. The desired Diels-Alder products **94** and **96** were never obtained. The screened conditions either gave no reaction at all or led to decomposition of the reactants. Thus, Schröckeneder's and Trauner's IEDDA experiments were unsuccessful.[16]

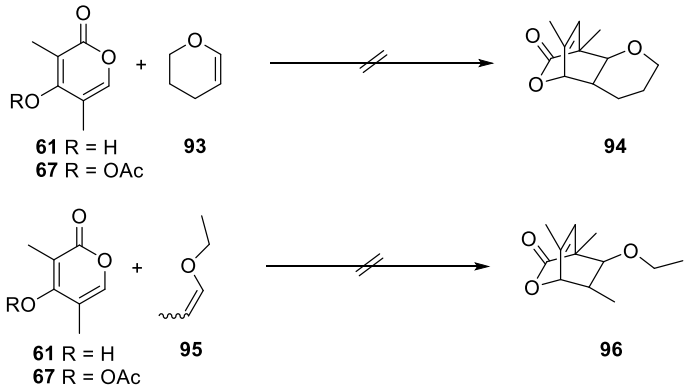

Scheme 3-13: Schröckeneder's and Trauner's test system for IEDDA reactions.[16]

3,5-Dimethylpyrone (**2**) is a more electron deficient diene, caused by the absence of the hydroxy group or the acetyl group. The regio- and stereochemical outcome of the IEDDA towards portentol (**1**) can be determined by the two transition states, which are highly favorable according to the FMO theory (Scheme 3-14). Therefore, **TS1** yields the *endo* product and **TS2** is transformed to the desired *exo* product.[4]

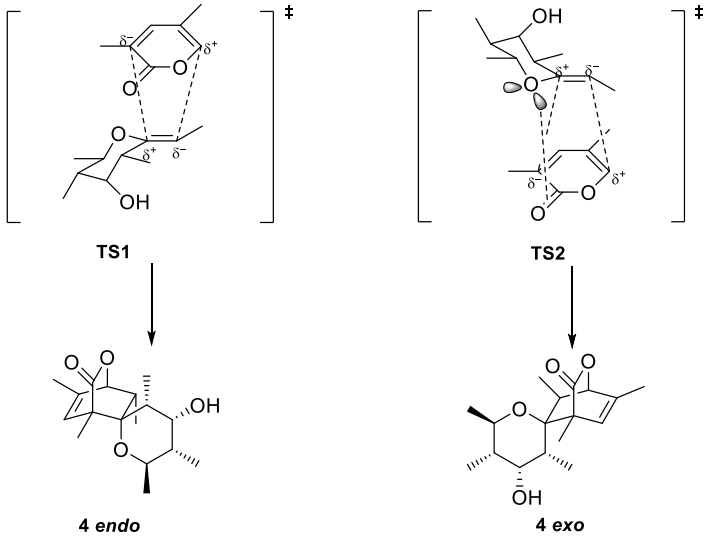

Scheme 3-14: Two favorable transition states for the IEDDA.[4]

Constructive secondary orbital interaction of the lone pair ether-oxygen with the carbonyl function can lead to a more stable transition state affording the *exo* adduct.[16] Moreover, a bulky catalyst coordinating to pyrone **2** will drive the reaction towards the desired *exo* product **4 *exo*** (Scheme 3-15).

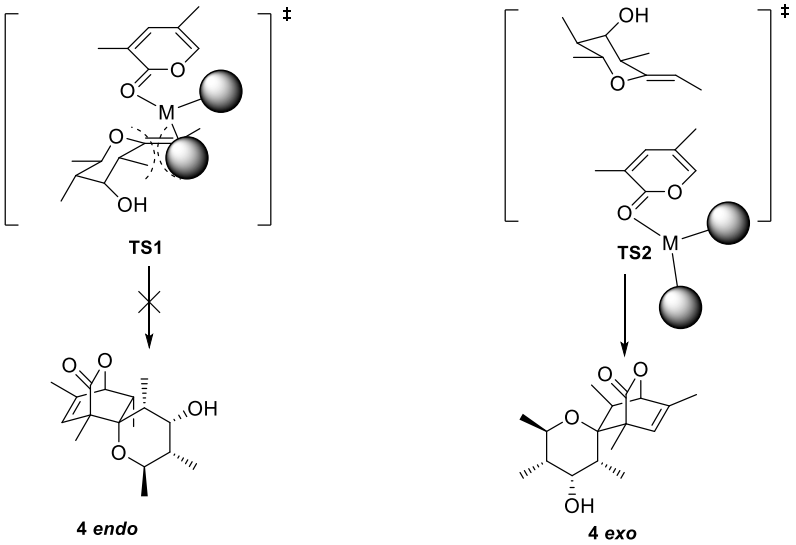

Scheme 3-15: Stereochemical effect of bulky Lewis-acid catalyst.

The presence of Lewis acid catalysts such as $AlCl_3$, $TiCl_4$, $ZnCl_2$ etc. will lead to a decrease of the LUMO energy of the diene **2**.[24] The coordination of a Lewis-acid may lead to a formation of pyryllium species **58**. This will induce a step wise reaction resulting in the Diels-Alder adduct. (Scheme 3-16).[16] In particular lanthanide base shift reagents such as $Eu(hfc)_3$, is reported by Marko *et al*. to catalyze IEDDA cycloadditions of pyrones without promoting the subsequent decarboxylation reaction under mild conditions and excellent yield.[28] Moreover, the catalyst gives the possibility to control the stereochemical outcome with chiral ligands.[28]

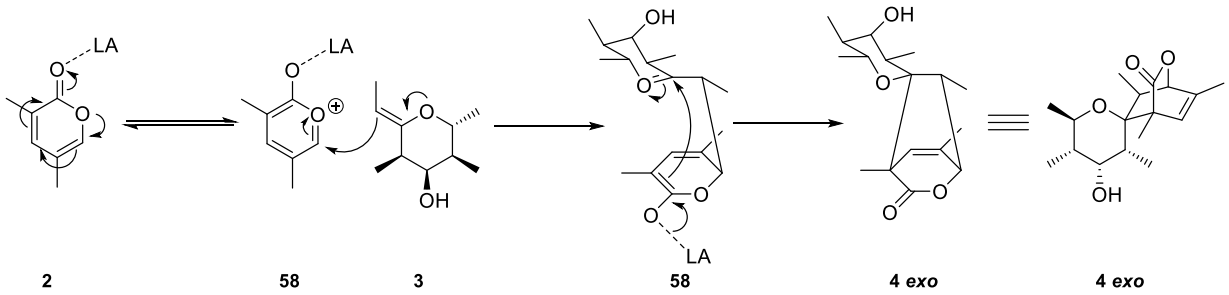

Scheme 3-16: Proposed stepwise mechanism.[16]

Posner *et al*. reported the successful [4+2] cycloaddition of unsubstituted 2-pyrone with electron-rich benzyl vinyl ether under the combined influence of high pressure (11-12 kbar)

and a catalytic amount of a Lewis acid.[29] High pressure is applied to avoid thermal reaction conditions, which would cause spontaneous extrusion of CO_2 from the initial bicyclic lactone. In addition, Diels-Alder reactions are known to have a large negative activation volume $\Delta V^{\ddagger}$ and molar reaction volume ΔV. High pressure can influence reactions characterized by negative molar and activation volumes in the aspects of acceleration, stereochemistry and changes in chemical equilibria. The effect of the pressure is given in the transition state theory (Eq. 1) stated by Evans and Polanyi. If $\Delta V^{\ddagger}$ is negative, the rate constant will increase with increasing pressure. Similarly, the effect of pressure on the reaction equilibria is given by equation two. If ΔV is negative, the application of pressure shifts the equilibrium towards the products.[21]

$$\frac{\delta \ln k}{\delta P} = -\frac{\Delta V^{\ddagger}}{RT} \qquad \text{(Equation 1)}$$

$$\frac{\delta \ln K}{\delta P} = -\frac{\Delta V}{RT} \qquad \text{(Equation 2)}$$

During Luu's master thesis, test reactions to IEDDA were undertaken. For this purpose, a high pressure reaction should be established first. Therefore, the synthesis of IEEDA product **99** was planned based a procedure published by Posner *et al.*.[29] Afterwards it was envisioned to replace diene **97** with **2** (Scheme 3-17).[25]

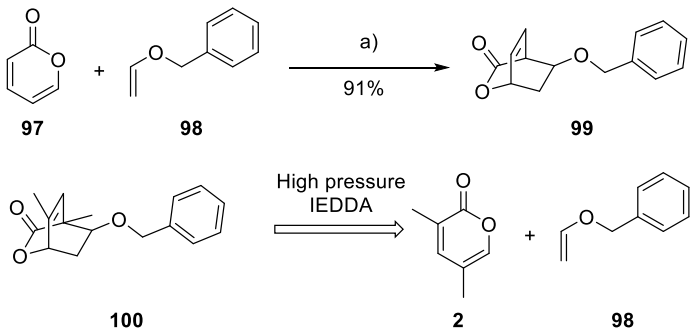

*Scheme 3-17: Top: Synthesis of **99** by Posner et al. Reagents and conditions: a) $Yb(tfc)_3$ (cat.), 11 - 12 kbar, r.t., 3 d [29]; Bottom: Retrosynthesis towards **100**.[25]*

Initially, a way had to be found to apply high pressure to the reaction. For this purpose, a piston - cylinder apparatus was used (Figure 3-1). Moreover, a suitable chemically inert reaction vessel had to be developed which would withstand the high pressure and would allow easy access to the reaction mixture. Therefore, a Teflon ampoule was developed consisting of the vessel and a double screwed cap to seal the ampoule (Figure 3-1).[25]

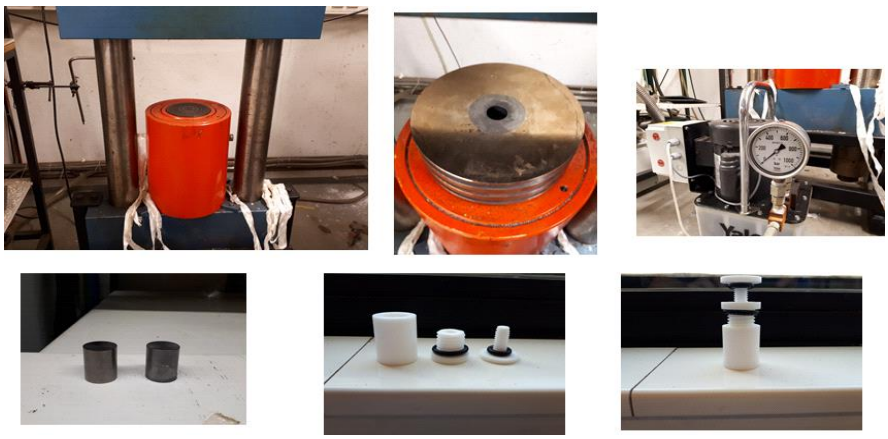

Figure 3-1: Top: From left to right: The piston-cylinder apparatus; metal mantle where the Teflon ampoule and the pistons are inserted; pressure gauge; Bottom: From left to right: The pistons; Teflon ampoule with the two screw caps.[25]

It was possible to reproduce the Diels-Alder reaction with the equipment shown, but with a lower yield (Scheme 3-18).[25] Thus, a general reaction method was successfully found and established in the Menche group for IEDDA reactions with pyrones as dienes, but has to be improved.

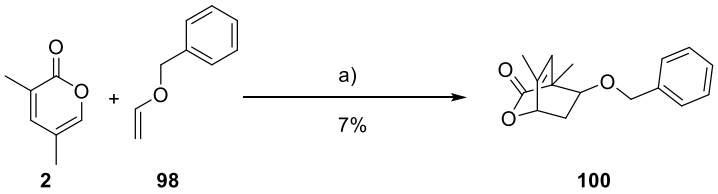

Scheme 3-18: Reagents and conditions: a) $Yb(fod)_3$ (cat.), CH_2Cl_2, 11-12 kbar, r.t., 3d. [25]

4 Project Aims

4.1 Completion of the Dienophile Fragment 3

The synthesis of portentol (**1**) by an inverse electron demanding Diels-Alder reaction proves to be a scientific challenge as shown in the previous section. In particular, the synthesis of the dienophile fragment **3** poses a special challenge. Since the target structure of dienophile **3** cannot be changed for the realization of the IEDDA reaction, the planning of an efficient synthetic route of the pyrane ring with four stereocenters and a *Z* double bond is a major challenge. The aim of this work is to develop a reliable synthesis of the southern fragment **3**. Following this, the chair conformation of the six-membered ring will be investigated. In this way it should be determined whether a $^{1}C_{4}$ or a $^{4}C_{1}$ chair conformation is present (Figure 4-1), which has a possible effect on the stereochemical course of the IEDDA reaction (see section 3.2).

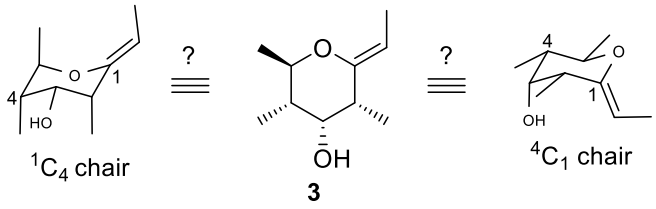

*Figure 4-1: Chair conformation of **3**; Left: $^{1}C_{4}$ chair conformation of **3**; Right: $^{4}C_{1}$ chair conformation of **3**.*

4.2 Synthesis of Portentol *via* IEDDA Reaction

Further reaction conditions for the IEDDA reaction will be investigated. For this purpose, the first successes of the high pressure Diels-Alder reaction (see section 3.3) are to be further developed and subsequently used to implement the IEDDA reaction for the synthesis of portentol (**1**). The final goal is to complete the total synthesis of **1**.

5 Results and Discussion

5.1 Synthesis of the Dienophile Fragment 3

5.1.1 Retrosynthetic Analysis

As described in section 3.2.3, iron catalyzed cyclization towards the synthesis of dienophile **3** was intensively screened. However, no condition was found to optimize this reaction. For this reason, cyclization must be achieved by a different synthetic strategy.

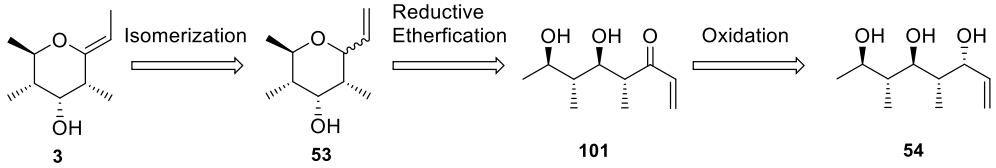

*Scheme 5-1: New retrosynthetic strategy towards dienophile **3**.*

The nickel catalyzed double bond isomerization should be further targeted as in the first retrosynthetic analysis of the Menche group. Thus, **53** was planned to be cyclized from **101** by reductive etherification. The *α-β*-unsaturated ketone **101** was obtained through oxidation of the allylic triol **54**. which was successfully synthesized previously (Scheme 5-1).

5.1.2 Synthetic Progress

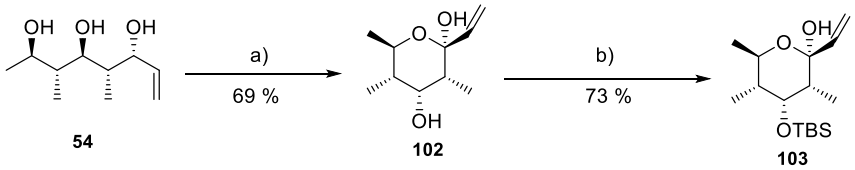

Scheme 5-2: Reagents and conditions: a) MnO_2, CH_2Cl_2, r.t., 20 h; b) TBSOTf, 2,6 lutidine, −78°C, 40 min.

Oxidation of the allylic alcohol **54** was achieved using manganese dioxide in excess. The resulting *α-β*-unsaturated ketone was cyclized to hemiacetal **102** (Scheme 5-2). The cyclization occurred through a nucleophilic attack of the free hydroxy group on the carbonyl carbon of the ketone. This step was stereoselective and could be confirmed by NMR. NOESY data showed a coupling of the hydrogen atom of the hemiacetal with the atoms H-11, and H-7 and H-5. Otherwise, no further NOESY correlations were found (Figure 5-1).

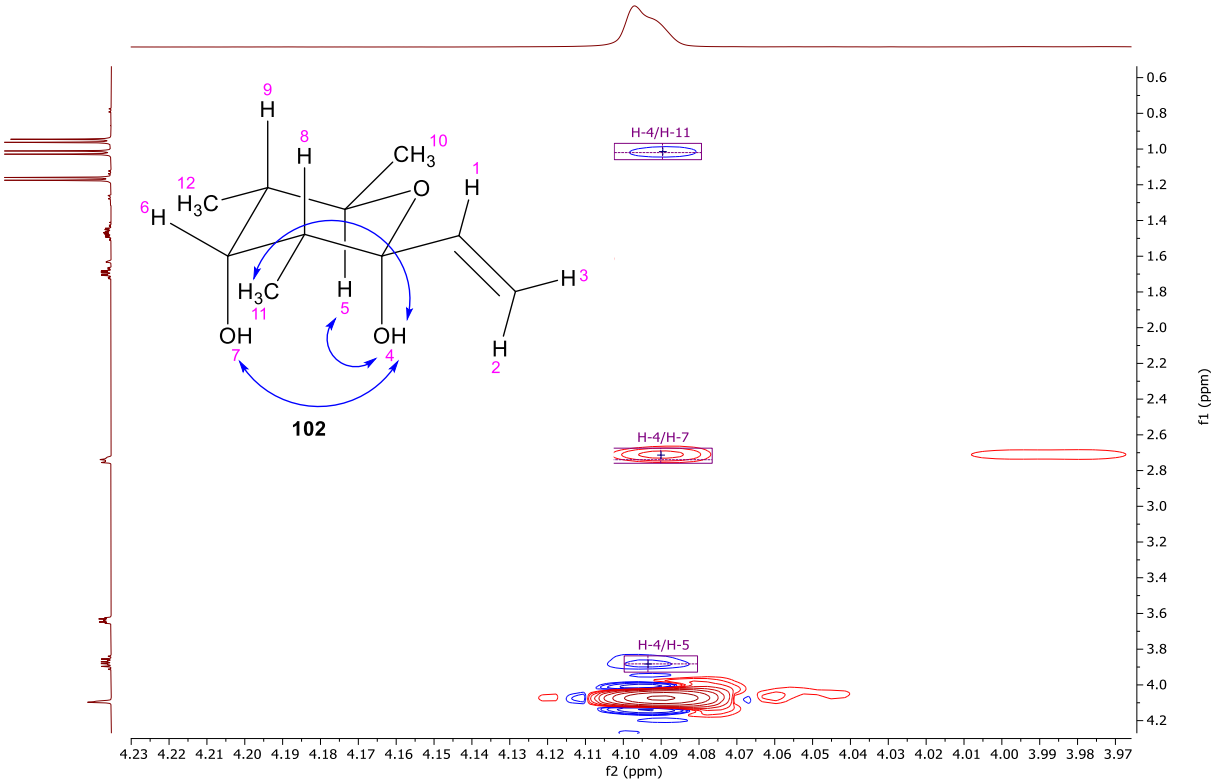

Figure 5-1: NOESY correlation of H-4.

To specifically reduce the tertiary alcohol moiety, it was decided to protect the secondary hydroxyl group. Selective protection of the secondary hydroxyl group with TBSOTf was successfully performed at −78 °C (Scheme 5-2). The two steps were completed in moderate yields.

In order to reduce the tertiary alcohol group Et_3SiH was used as reducing agent and TMSOTf as catalyst. The hydroxy group was split off under Lewis acid catalysis. The resulting allylic cation could be nucleophilically attacked by the silane (Scheme 5-3).[30,31]

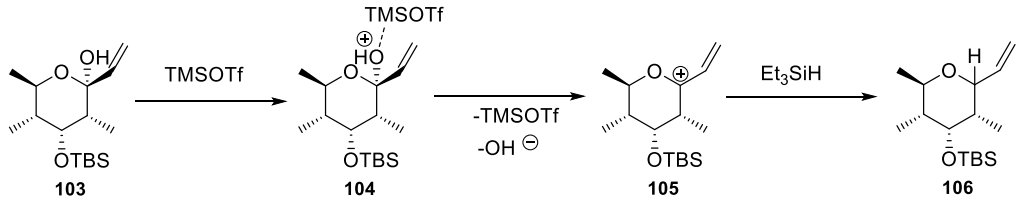

*Scheme 5-3: Theoretical mechanism of TMSOTf mediated reduction to **106**.*

However, using catalytic as well as and equimolar amounts of TMSOTf, no reaction occurred and **106** was not obtained (Table 5-1 entry 1 and entry 2). However, the exchange of Lewis acid to $BF_3{*}OEt_2$ only led to decomposition (Table 5-1 entry 3).[30,32] Next, a direct reduction of tertiary alcohols using chlorodiphenylsilane as a hydride source was tried in the presence of

catalytic amounts of indium trichloride. Here, the reaction conditions led only to decomposition, too.[33]

*Table 5-1: Conditions and reagents for reducing **103** to **106**.*

Entry	Reagents	Solvent	Temp.	Reaction Time	Yield
1	Et_3SiH 3 eq. TMSOTf 20mol%	MeCN:CH_2Cl_2 1:1	−78°C	30 min	-
2	Et_3SiH 3 eq. TMSOTf 1 eq.	MeCN: CH_2Cl_2 1:1	−78°C	60 min	-
3	Et_3SiH 2 eq. $BF_3{*}OEt_2$ 1 eq.	CH_2Cl_2	−78°C	60 min	-
4	$InCl_3$ 5 mol% Ph_2ClSiH 2 eq.	CH_2Cl_2	r.t.	3 h	-

It could be assumed that the TBS protecting group on the secondary alcohol led to steric hindrance during the reaction under the conditions shown, since both the TBS-protected secondary alcohol and the tertiary alcohol were in the axial position, preventing either the coordination of the Lewis acid or attack of the hydrid. Hence, another protecting group should been used and a benzyl protecting group should been installed to the secondary alcohol moiety of **102** using sodium hydride and benzyl bromide. However, this condition only led to decomposition of starting material. Thus, silver(I) oxide was used for the selective benzyl protection of the secondary alcohol leading to **107** with a yield of 69 % (Scheme 5-4).[34]

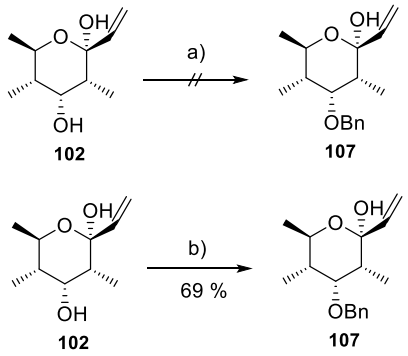

Scheme 5-4: Reagents and conditions: a) NaH, BnBr, THF, r.t., o.n.; b) Ag_2O, BnBr, CH_2Cl_2, r.t., o.n.

After the protection was completed with good yields, a next attempt was made to reduce the tertiary alcohol. Initially Et_3SiH was used as hydride source and TMSOTf as Lewis acid and first traces of the desired product **108** could be found (Table 5-2 entry 1). After the Lewis acid was exchanged to $BF_3{*}OEt_2$, a yield of 11 % was obtained (Table 5-2 entry 2). Further attempts to increase the yield remained unsuccessful (Table 5-2 entry 3 and 4).

*Table 5-2: Conditions and Reagents for reducing **107** to **108**.*

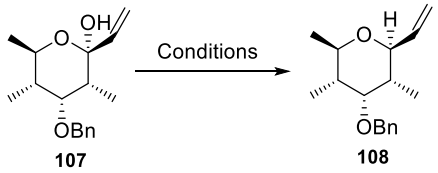

107 **108**

Entry	Reagents	Solvent	Temp.	Reaction Time	Yield
1	Et_3SiH 10 eq. TMSOTf 1 eq.	MeCN	−40°C→−20°C	3.5 h	Traces
2	Et_3SiH 2.5 eq. $BF_3 \cdot OEt_2$ 1.2 eq.	CH_2Cl_2	−78°C	10 min	11 %
3	Et_3SiH 2.5 eq. TFA 6 eq.	CH_2Cl_2	−78°C	24 h	-
4	$InCl_3$ 0.2 eq. Ph_2ClSiH 2 eq.	CH_2Cl_2	r.t.	3 h	-

Although the exchange of the protective groups led to the successful reduction of the tertiary alcohol, the yield was low revealing that the benzyl protecting group has a negative steric influence on the reduction, too. Therefore, the unprotected hemiacetal **102** was used for the reduction. Using Et_3SiH as hydride source and $BF_3 \cdot OEt_2$ as Lewis acid, **102** was successfully reduced to **109** with a good yield (Scheme 5-5). The secondary alcohol moiety was silyl protected to prevent any coordination of the free hydroxy group with the $NiCl_2$dppb catalyst of the next reaction. However, TBS protection of alcohol **109** to **106** provided only a low yield of 22 %. Yet, further attempts to optimize the yield were not made at this time.

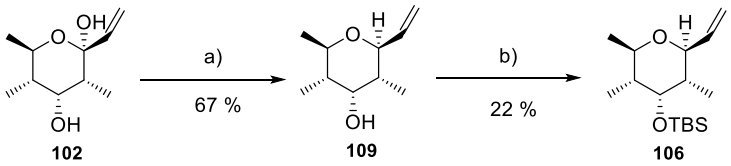

102 **109** **106**

Scheme 5-5: Reagents and conditions: a) Et_3SiH, $BF_3 \cdot OEt_2$, CH_2Cl_2, −78°C, 30 min; b) TBSOTf, 2,6 lutidine, CH_2Cl_2, 0°C to r.t., 18 h.

Now, that a reliable synthetic route to **106** was established, the *Z*-selective double bond isomerization could be tested. First, the quality of the self-synthesized catalyst dichloro[1,4-bis(diphenylphosphino)butane]nickel(II) ($NiCl_2$dppb) was checked (Figure 5-2).

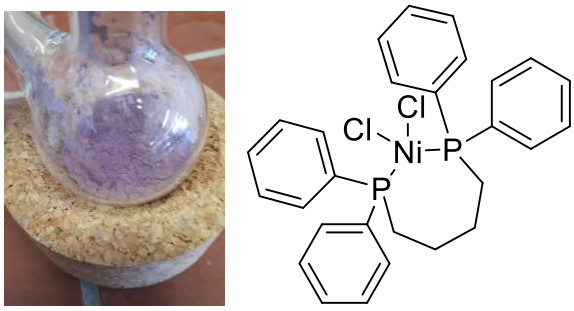

Figure 5-2: Left: $NiCl_2$dppb in a schlenk flask; Right: structure of $NiCl_2$dppb.

Therefore, the literature known synthesis of allyl ether **110** to enol ether **111** was reproduced. The reaction proceeded as described in the literature with a yield of 91 % and an *E/Z* isomeric ratio of 5:95 which was consistent with the literature (Scheme 5-6).[35]

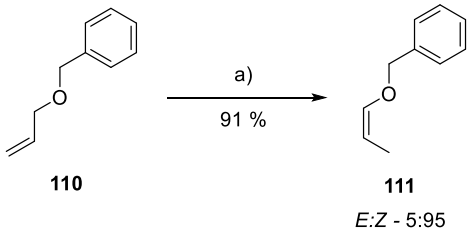

Scheme 5-6: Reagents and conditions: a) $NiCl_2$dppb, $LiBEt_3H$, THF, r.t., o.n.

The exact mechanism of the reaction is not known. Presumably, the precatalyst was first activated with the aid of the superhydride $LiBEt_3H$ and itself reduced to nickel(I). Subsequently, the nickel catalyst coordinates molecule **110** to the oxygen atom and the *α*-H atom to form **112**. At the same time, the hydride on the nickel coordinates to the double bond. The hydride was then transferred to the terminal C atom of the double bond and migrates to the vinylic site and the *α*-H atom was transferred to the nickel. This process had to be concerted and the activated nickel(I) catalyst and product **111** was released (Scheme 5-7).

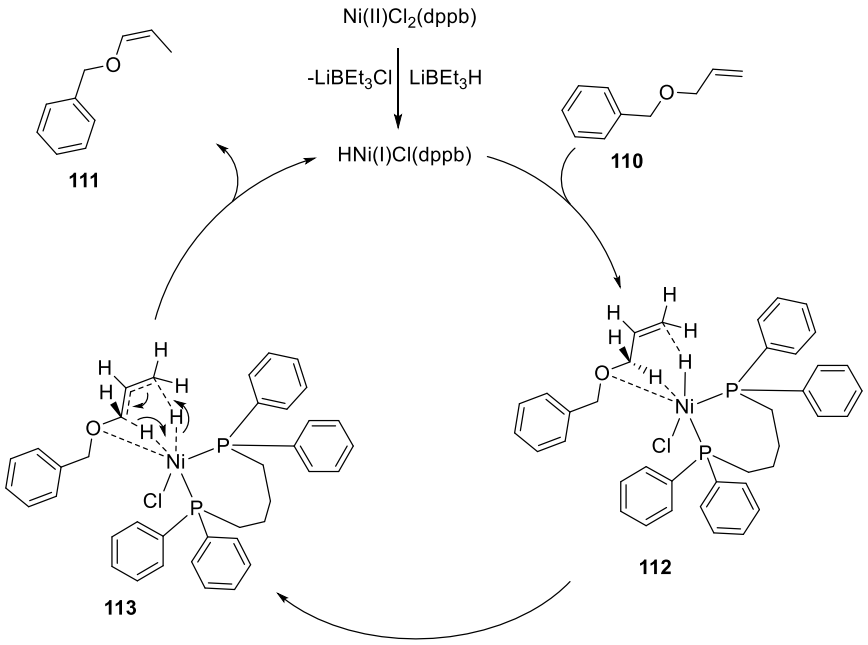

Scheme 5-7: Proposed mechanism for the Z-selective double bond isomerization with $NiCl_2$dppb.

The *Z*-selectivity of the reaction may explained by the coordination of the α-H-atom, the oxygen atom and the hydride of the nickel catalyst. The transition state that produces the *E* product was less compact than the transition state of the *Z* product. Thus, three dimensional representations of the transition states for the *E* product suggested coordination bond lengths of 2.0 Å between the nickel and the oxygen, 1.2 Å between the *α*-H atom shown in olive in Figure 5-3, and 1.8 Å between the hydride shown in brown and the carbon atom of the double bond shown in black.

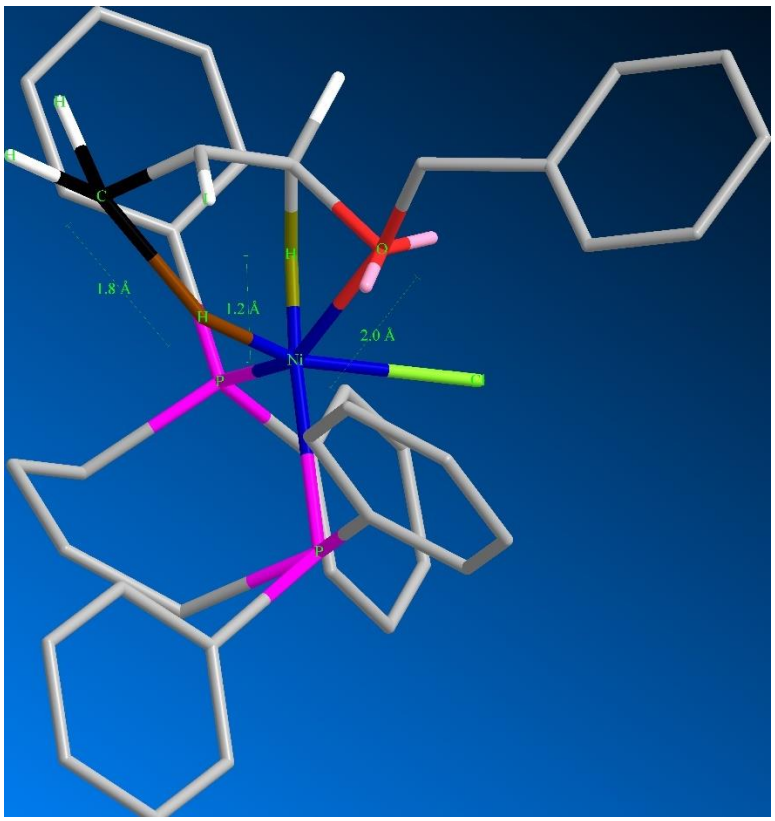

*Figure 5-3: 3-D visualization to the transition state to the E-conformer of **111**.*

In contrast, the transition state that yielded the *Z* product likely had smaller coordination bond lengths shown in Figure 5-4. This more compact transition state was probably favored over the other and would explained the higher *Z*-selectivity.

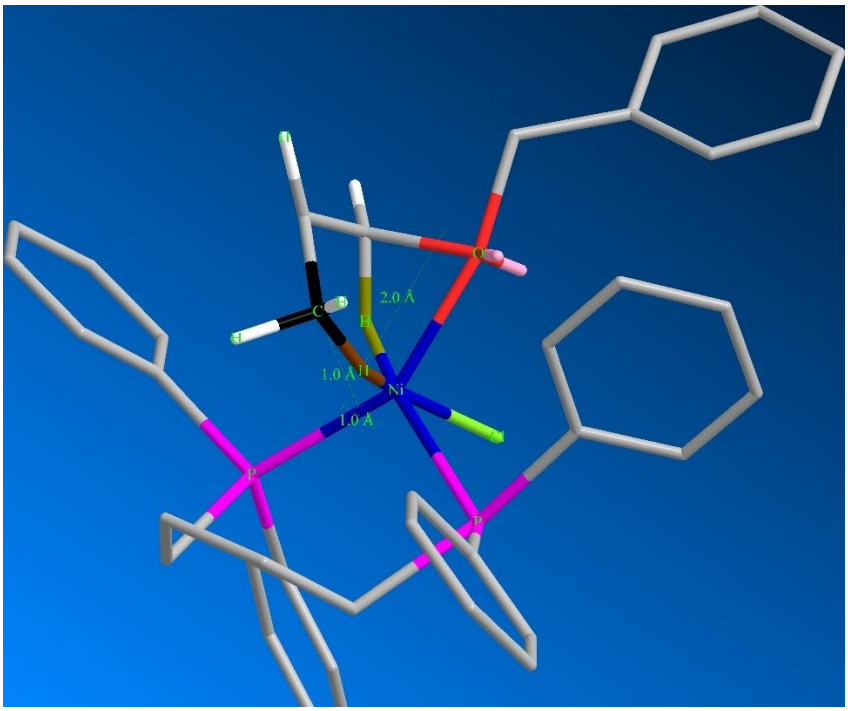

*Figure 5-4: 3-D visualization to the transition state to the Z-conformer of **111**.*

After proving that the catalyst worked, it was applied to **106**. However, no reaction was observed (Table 5-3, entry 1). Even after the temperature was increased to 70°C, there was no change in the reaction (Table 5-3, entry 2). Thereupon, other literature known conditions for double bond migration were tested. For example, the Wilkinson`s catalysis with *n*-BuLi should also led to isomerization.[35,36] However, the reaction with **106** did not result in any reaction (Table 5-3, entry 3). According to the literature, LDA also leads to *Z*-selective isomerization.[37] But these conditions also did not led to the desired product (Table 5-3, entry 4 and 5). The more reactive sodium diisopropylamide reported in the literature also showed no reaction (Table 5-3, entry 6 and 7).[38]

*Table 5-3: Conditions and Reagents for isomerization of **106** to **69**.*

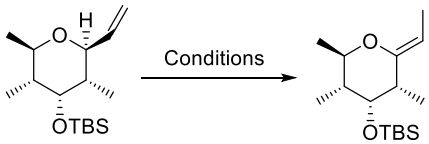

106 **69**

Entry	Reagents	Solvent	Temp.	Reaction Time	Yield
1	$NiCl_2$(dppb) 4 mol% $LiBEt_3H$ 4 mol%	THF	0°C → r.t.	24 h	-
2	$NiCl_2$(dppb) 4 mol% $LiBEt_3H$ 4 mol%	THF	70°C	24 h	-
3	Wilkinsons‘s cat. 10 mol% *n*-BuLi 0.14 eq.	THF	70°C	24 h	-
4	LDA 2 eq.	THF	−78°C → r.t.	24 h	-
5	LDA 6 eq.	THF	−78°C → r.t.	24 h	-
6	NaDA 2 eq.	THF	−78°C	24 h	-
7	NaDA 6 eq.	THF	−78°C	24 h	-

The absence of any reaction could probably be attributed to steric hindrance. For instance, Figure 5-5 showed that the activated nickel(I) catalyst could only approach the substrate from the lower side of the chair to achieve coordination of the oxygen in red, the *α*-H atom in olive and the carbon atom in black. This may led to steric repulsion of the ligands of the catalyst with **106** and the axial positioned silyl protecting group also may caused steric repulsions. Since the reactive species of the methods used with LDA and NaDA form sterically demanding complexes with THF, the unreactivity could be explained by steric hindrance, too.[37,38]

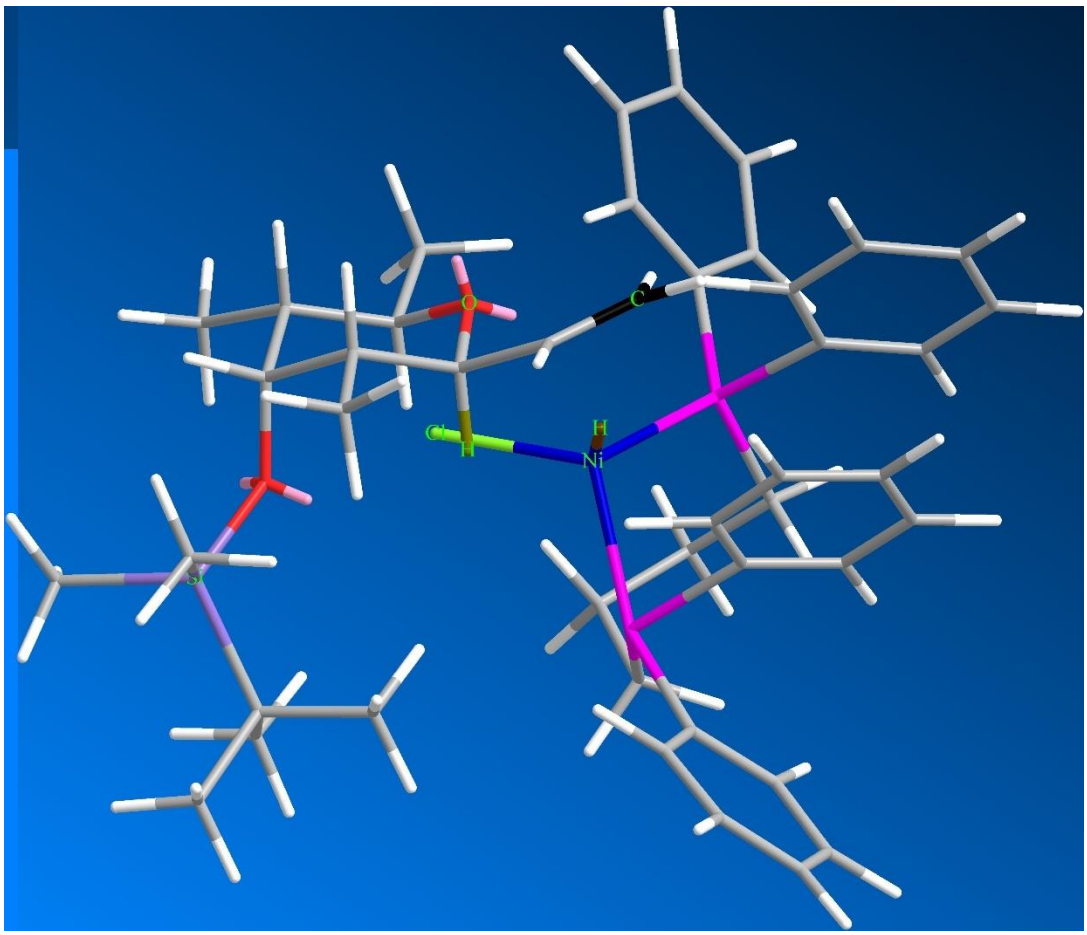

*Figure 5-5: 3-D visualization of the active Ni(I) catalyst (right) approaching **106** (left), showing steric repulsion.*

5.1.3 Conclusion and Strategic Considerations

A consistent alternative route for cyclization starting from the triol **54** was found. In addition, a synthetic route to the pyran **106** was established. However, intensive screenings of different conditions for *Z*-selective double bond isomerization were not successful, since the allyl ether **106** probably was sterically hindered for the complex coordination of the catalysts.
Therefore, the *Z*-selective double bond isomerization approach was not pursued further. Instead, a new synthesis route, based on previously synthesized compound, was developed.

5.1.4 Second Retrosynthetic Analysis

One condition for the development of the second retrosynthetic strategy for the synthesis of the dienophile **106** was that the previous established synthetic route could be used. Under this premise, the retrosynthesis shown in Scheme 5-8 was developed.

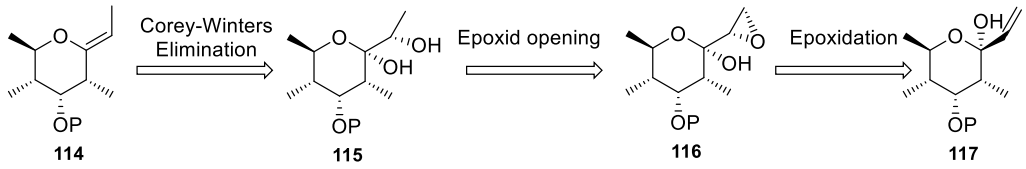

*Scheme 5-8: Second retrosynthetic strategy towards **106**.*

The *Z*-selective double bond should be achieved by Corey-Winter elimination starting from the diol **115**. The selectivity of the double bond was determined by the stereochemistry of the vicinal diol. Hence, 1,2-*syn* diols eliminate to *Z* double bonds and 1,2-*anti* diols eliminate to *E* double bonds.[39] The secondary hydroxy group was installed through a regioselective opening of the epoxide **116** and this compound had to be synthesized by stereoselective epoxidation of the terminal alkene of **117** which was already present from the previous synthesis in the unprotected form **102**.

5.1.5 Synthetic Progress of Corey-Winter Approach

In order to get the correct stereoselectivity during the epoxidation of **117**, $VO(acac)_2$ and THBP was chosen as reagents, due to hypothetical coordination of vanadium to the axial positioned tertiary alcohol leading to an epoxide on the same side as the tertiary alcohol group (Figure 5-6).[40]

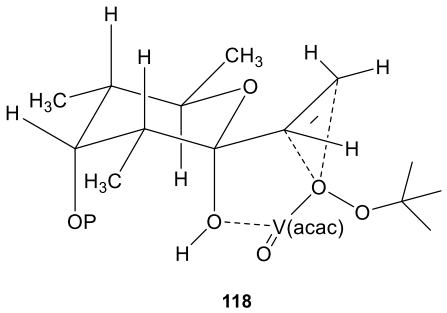

118

Figure 5-6: Theoretical coordination of the activated VO(acac)2 catalyst.

However, no change was observed during the reaction (Table 5-4, entry 1 and 2).Therefore, *m*-CPBA was used as an epoxidizing agent, too, since a directing interaction through hydrogen

bonding to the tertiary alcohol is postulated (Figure 5-7), but this method did not led to any reaction, too (Table 5-4, entry 3 and 4). [41]

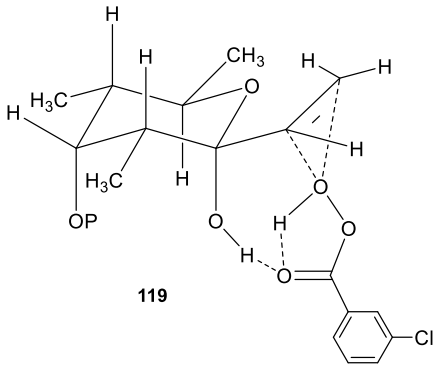

Figure 5-7: Theoretical coordination of m-CPBA.

Next, modified Sharpless epoxidation conditions were selected. According to the literature these should led to epoxidation especially for tertiary allylic alcohols.[42] But even under these conditions the reaction did not occurred (Table 5-4, entry 5 and 6). Finally, epoxidation with DMDO resulted in the desired product. However, the reaction cleaved the benzyl protecting group followed by oxidation of the secondary alcohol to ketone **121** (Table 5-4, entry 7). The silyl protecting group, on the other hand, remained stable and led to product **122** (Table 5-4, entry 8). NMR data, however, showed a diastereomeric mixture of 3:1. At this point, it was not possible to determine whether the desired *erythro* or *threo* product was present in excess (Figure 5-8). In addition, the preparation of the DMDO was extremely time consuming and only possible in small quantities.

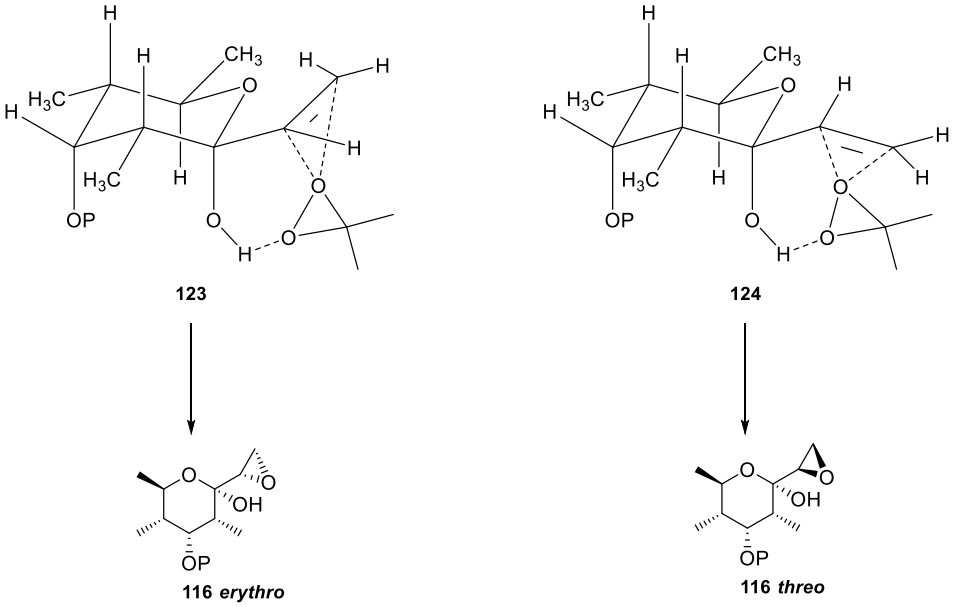

*Figure 5-8: Proposed coordination of DMDO towards **116 erythro** and **116 threo**.*

Table 5-4: Conditions and Reagents for the epoxidation.

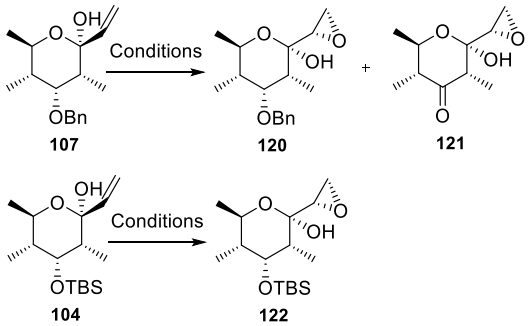

Entry	Reagents	Reactant	Solvent	Temp.	Reaction Time	Yield
1	$VO(acac)_2$ 15 mol% TBHP 2.0 eq.	**107**	Toluene	r.t.	24 h	-
2	$VO(acac)_2$ 15 mol% TBHP 2.0 eq.	**104**	THF	r.t.	24 h	-
3	*m*-CPBA 1.1 eq.	**107**	CH_2Cl_2	0°C → r.t.	24 h	-
4	*m*-CPBA 1.1 eq.	**104**	CH_2Cl_2	0°C → r.t.	24 h	-
5	$Ti(O^iPr)$ 2.1 eq. CaH_2 cat. Silica gel cat. (+)-DIPT 2.8 eq. TBHP 2.8 eq.	**107**	CH_2Cl_2	−40°C → −20°C	24 h	-
6	$Ti(O^iPr)$ 2.1 eq. CaH_2 cat. Silica gel cat. (+)-DIPT 2.8 eq. TBHP 2.8 eq.	**104**	CH_2Cl_2	−40°C → −20°C	24 h	-
7	DMDO 3.0 eq.	**107**	Acetone	r.t.	18 h	20 % of **121**
8	DMDO 3.0 eq.	**104**	Acetone	r.t.	18 h	26 % of **122** *d.r.* 3:1

Subsequently, **122** was to be converted to the vicinal diol **125** by a regioselective epoxide opening using $LiAlH_4$. The reaction yielded 37 % of the desired product **125**, but at the same time, 60 % of the silyl-deprotected epoxide **126** was obtained (Scheme 5-9). The silyl protecting group was probably cleaved, since it was diaxial to the free tertiary hydroxy group and thus a coordination of $LiAlH_4$ took place. This led to a spatial approximation to the TBS group which resulted in its removal.

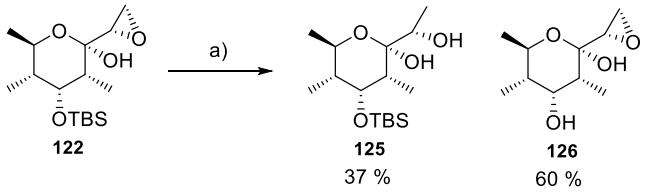

Scheme 5-9: Reagents and conditions: a) $LiAlH_4$, THF, r.t., 1 h.

Nevertheless, the isolated vicinal diol **125** was used for the Corey-Winter elimination. Thus, the thiocarbonate **127** was first formed in a reaction with the use of thiophosgene subsequent addition of 1,3-dimethyl-2-phenyl-1,3,2-diazaphospholidine to molecule **127** should led to the elimination product. Initial reaction control by TLC of the first step showed consumption of the reactant **125** with formation of a new spot. However, after completion of the second reaction and work-up, no product could be isolated (Scheme 5-10). A possible reason may be the small scale of the reaction leading in the unsuccessful synthesis of dienophile **69**.

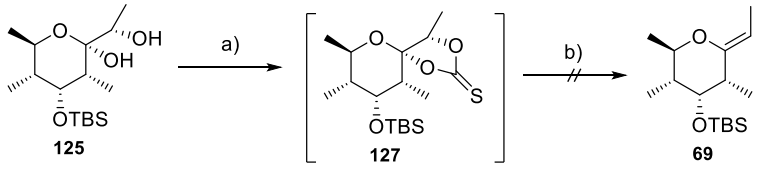

Scheme 5-10: Reagents and conditions: a) $CSCl_2$, DMAP, CH_2Cl_2, r.t., 1.5 h; b) 1,3-dimethyl-2-phenyl-1,3,2-diazaphospholidine, THF, 40°C, 20 h.

5.1.6 Conclusion and Strategic Considerations of the Corey-Winter Elimination Approach

It was possible to perform an epoxidation starting from **104** and a subsequent regioselective opening of the epoxide **122** to the vicinal diol **125**. However, the stereoselectivity of the epoxidation and the yield were very poor. The epoxide opening also gave unsatisfactory selectivity and yield. Finally, the reaction sequence for Corey-Winters elimination also showed no success.

5.1.7 Third Retrosynthetic Analysis

Since the previous retrosynthetic approaches were based on implementing the double bond at the end of the synthesis and were not very successful, this time a retrosynthesis had to be developed that would allowed the double bond to be formed at the beginning of the synthesis.

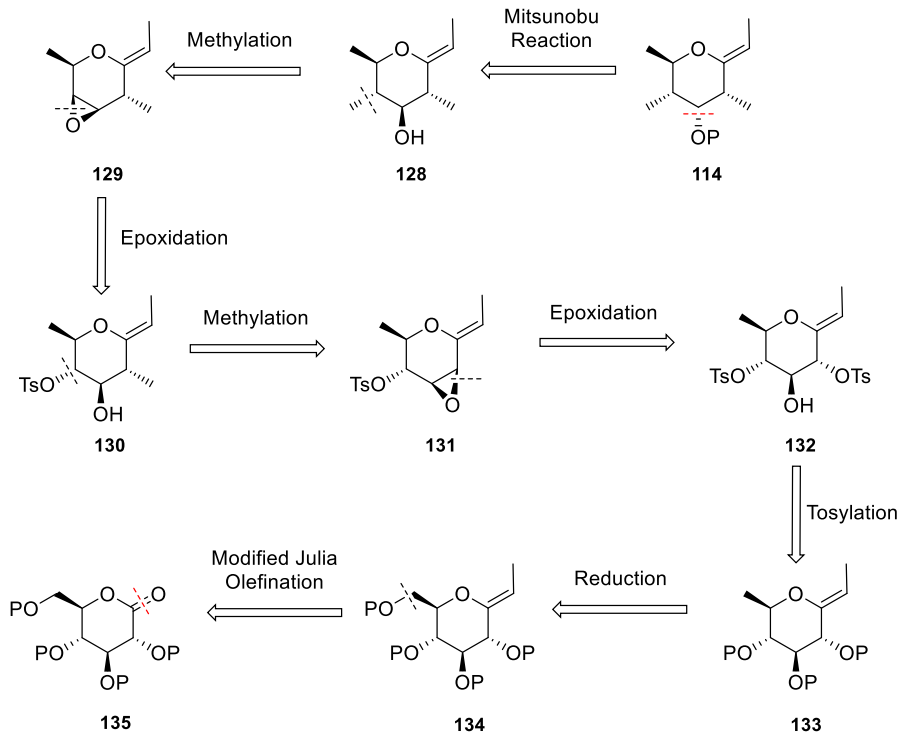

*Scheme 5-11: Third retrosynthetic strategy towards **106**.*

Based on this premise, the double bond would be constructed by a modified Julia olefination (Scheme 5-11). Gueyrard *et al*. developed this method for the synthesis of *exo* - glycals from silyl protected D-gluconolactones **136**. The previously prepared benzothiazolyl sulfone **139** was used as alkylating agent (Scheme 5-12).[43]

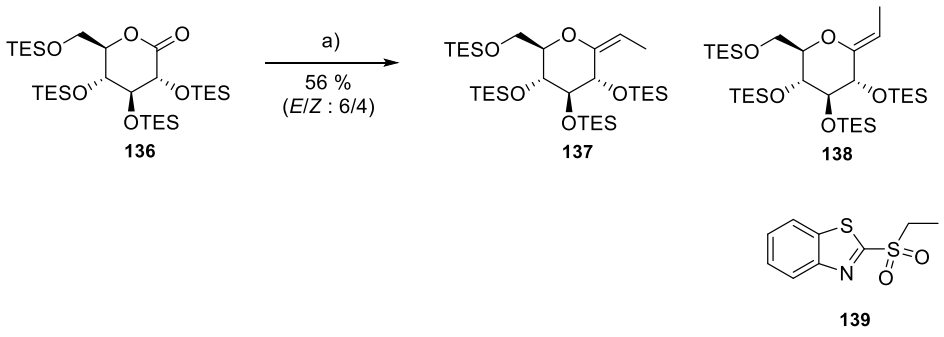

*Scheme 5-12: Work of Gueyrard et al. Reagents and conditions: a) 1. **139**, LiHMDS, THF, −78°C, 45 min; 2. DBU, THF, r.t., 30 min. [43]*

Although this reaction showed only a moderate yield and the *Z*-selectivity was low, the reaction could be carried out on a larger scale and the starting material was both cheap and readily available. In the following, the primary hydroxy group could be reduced to obtain compound **133** (Scheme 5-11). The regioselective and stereoselective substitution of the hydroxy groups by methyl groups was planned to be achieved by regioselective tosylation of the hydroxy groups followed by epoxidation and subsequent regioselective epoxid opening. This reaction sequence needed to be carried out according to the method developed by Krohn *et al*.[44,45] In

this method, levoglucosan (**140**) was regioselectively tosylated and the so called Černý epoxide **142** was subsequently formed (Scheme 5-13).[46] The epoxide was then opened by a cyano-Gilman cuprate and methylated.[44,45] This reaction sequence was envisaged to be repeated for the other side leading to molecule **128**. The last step was planned to be a Mitsunobu reaction to reverse the stereocenter of the alcohol and insert a protecting group to give dienophile **114** (Scheme 5-11).

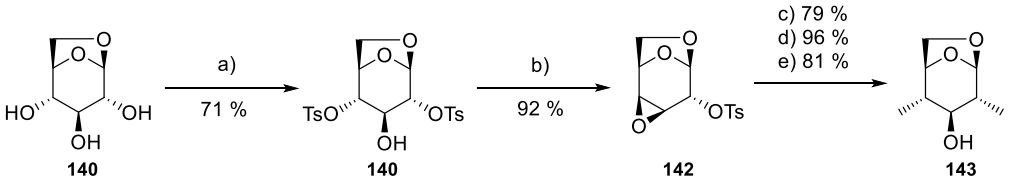

Scheme 5-13: Work of Krohn et al. Reagents and conditions: a) TsCl, Acetone/Pyrdine, 0°C, 2 h; b) NaOMe, CH_2Cl_2, r.t., 2 h; c) CuI (cat.), MeMgCl, THF, 40°C, 12 h; d) NaOMe, CH_2Cl_2, r.t., 2 h; e) CuCN, MeLi, Et_2O/THF, −78°C to −20°C, 2 h. [44]

5.1.8 Synthetic Progress of the Modified Julia Olefination Approach

The reactant used for the modified julia olefination was not triethylsilyl-protected D - gluconolactone **136**, but trimethylsilyl-protected lactone **144**, since this was available at that time at low cost and in high amounts. Besides, it was assumed that a change of the silyl protecting groups should not have a great influence on the reaction. However, this assumption turned out to be wrong. The TMS protecting groups had a positive effect on the *Z*-selectivity of the reaction while the yield remained constant (Scheme 5-14). Thus, the reaction gave an *E/Z* ratio of 1/4.4. with the TES protecting groups, the reaction showed an *E/Z* ratio of 6/4 according to Gueyrard *et al*.

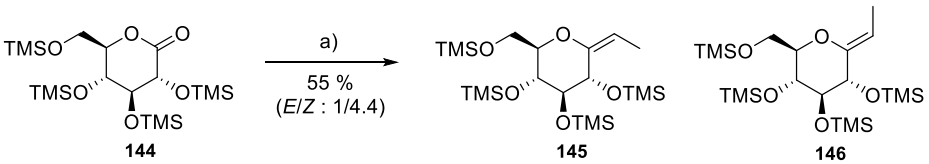

*Scheme 5-14: Reagents and conditions: a) 1. **139**, LiHMDS, THF, −78°C, 45 min; 2. DBU, THF, r.t., 1 h.*

This finding could be confirmed by NMR data. Indeed, NOE correlations were visible for the *Z*-isomer **146**, which formed the main product, between H-1 the proton of the double bond with H-2 the proton axial to the ring. In contrast, the other isomer showed no NOE correlation between these hydrogen atoms, indicating an *E* configuration of the double bond (Figure 5-9).

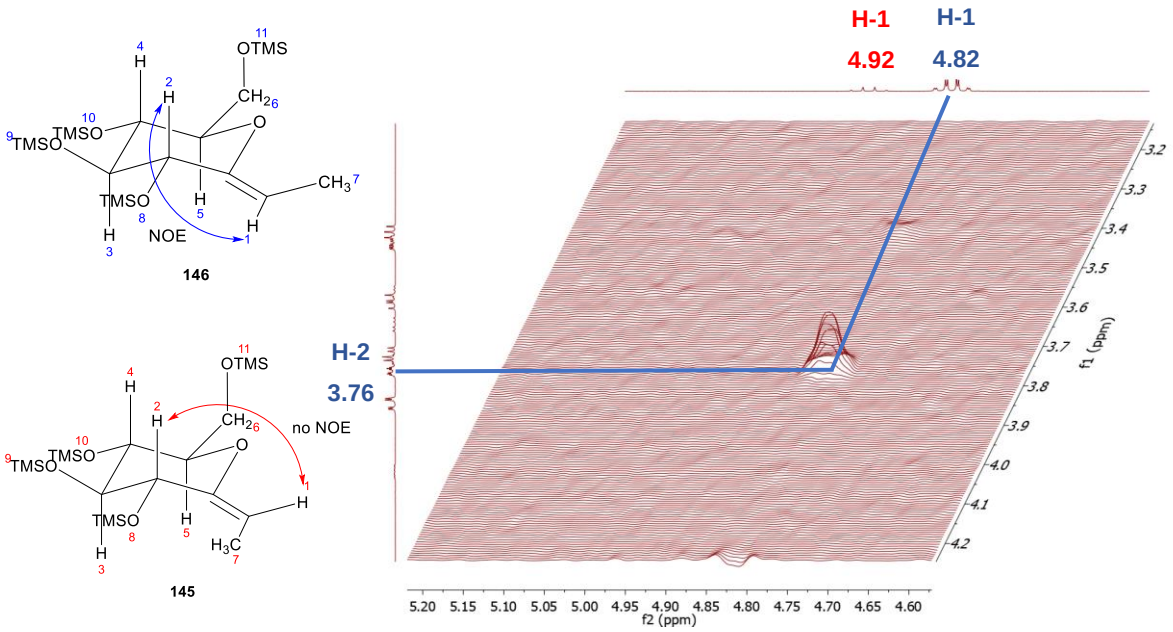

*Figure 5-9: NOE correlations of H-1 and H-2 of **146** in blue and no NOE correlation of **145** in red.*

To explain this result, a closer look at the reaction mechanism of the modified Julia olefination was needed. Julia *et al.* developed the reactions of metallated benzothiazole-2-ylsulfones, hereafter denotes as BT-sulfones, with carbonyl compounds.[47] In this case, the metallated BT-sulfone **153** was generated by the base LiHMDS. Subsequently, the sulfone **153** could perform either a *Si* side attack, shown by the red arrow in Scheme 5-15, or a *Re* side attack, shown by the green arrow. As a result of the *Si* attack, the sulfone bound axially to the ring and the carbonyl oxygen, colored brown, was equatorial to the ring. Therefore, two diastereomeric *β*-alkoxysulfones **147** were formed. One was the *syn β*-alkoxysulfone and the other was the *anti* diastereomer. *Syn* isomers eliminate to *Z* olefins and *anti* isomers to *E* olefins. Lithium coordinated the oxygen atom of the sulfone and the nitrogen atom of the heteroaromatic ring. This was followed by a Smiles rearrangement to the spirocyclic intermediate **148** which results in a transfer of the heterocycle from sulfur to oxygen. This led to the formation of the sulfinate salt **149**. DBU initiated the elimination of sulfur dioxide and lithium benzothiazolone to form *Z* alkene **146** in case for the *syn* isomer and *E* alkene **145** for the *anti* isomer.[47]

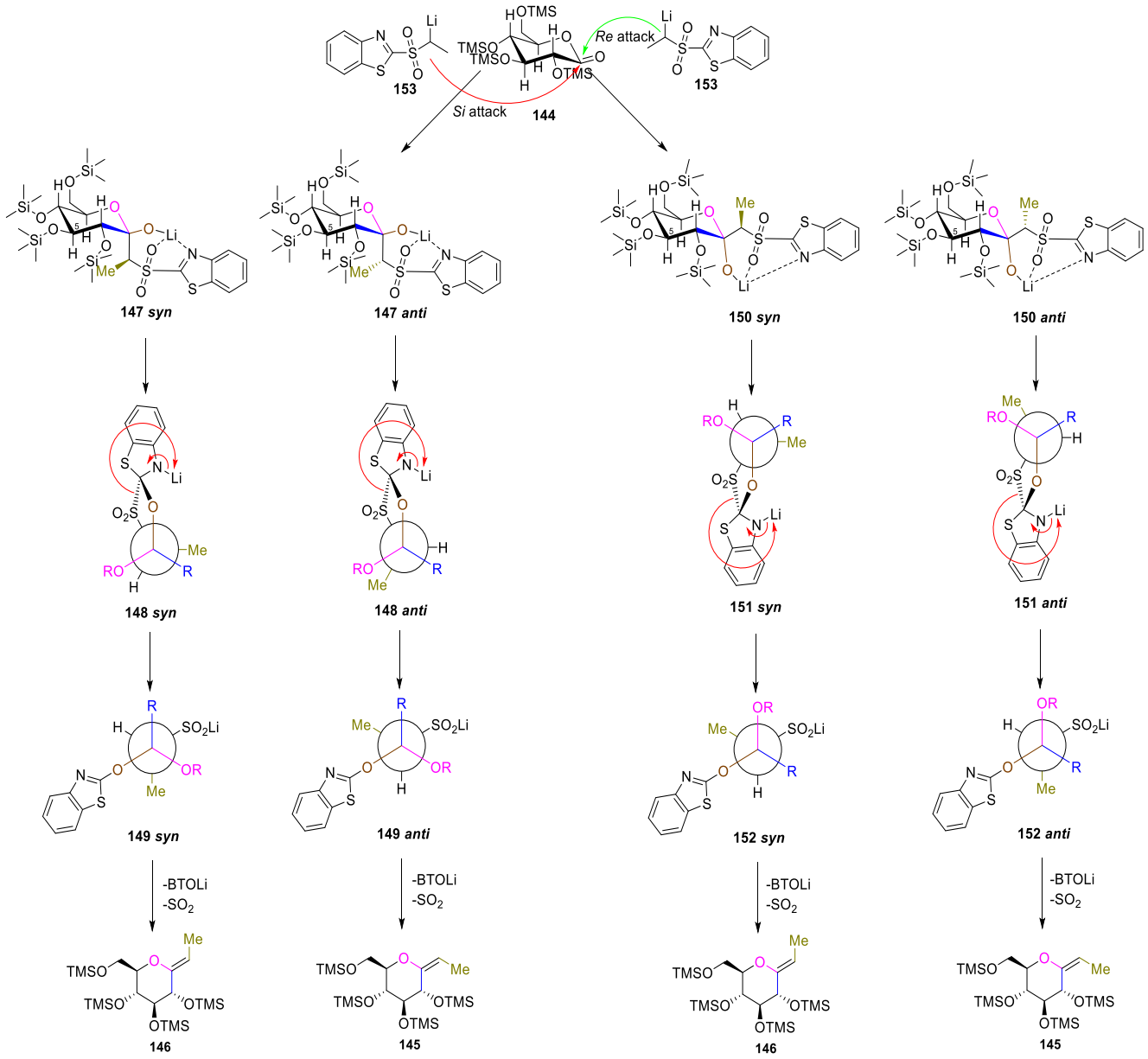

Scheme 5-15: Postulated mechanism for the modified Julia olefination.

In case of the *Re* side attack, the previously postulated mechanism was also assumed. However, the *Re* attack caused the carbonyl oxygen to be in axial position and the BT-sulfone residue in equatorial position. Since in this case the 1,3 diaxial interactions of the carbonyl oxygen and the rest of the ring were probably smaller than the 1,3 diaxial interactions of the BT-sulfone in axial position in the *Si* attack, the *Re* side attack was probably favored. An important aspect of the stereochemical course of the reaction is that there was an equilibrium between the *syn* and *anti* diastereomers of the *β*-alkoxysulfone intermediate **147** respectively intermediate **150**. This was achieved by a retroaddition/addition process.[47] Furthermore, the energy barrier of the Smiles rearrangement was larger for the *anti* isomers than for the *syn* isomers, due to interactions of the substituents during the eclipsed/gauche form of the spirocyclic transition state.[47] Thus, intermediate **148** showed spatial interactions between the methyl group, colored in olive, and the oxygen atom and the rest of the ring, colored in pink.

For **148** ***syn***, on the other hand, spatial interactions could occurred between the methyl group, colored in olive, and the rest of the ring, colored in blue. The TMS-protected hydroxyl group was located next to this residue, colored in blue. This does not seem to create such a large spatial obstacle, which meant that the *syn* isomers were preferred and thus the *Z* alkene was formed in excess. In comparison, the TES protecting groups used by Gueyrard *et al.* showed a higher *E* alkene selectivity. This was generated by the higher spatial hindrance in the *syn* isomer where the methyl group would interact with the TES protecting group. The *anti* isomer, on the other hand, showed that the hydrogen atom would been ecliptic to the residue and thus to the TES groups, and their spatial interference was lower. Thus, in the case of Gueyrard, the *anti* isomer was preferred.

The next synthetic step was the reduction of the primary hydroxy group. Since the latter had still been protected by TMS, it needed to be converted into a suitable leaving group by a silyl - tosylate exchange. For this purpose, the silyl ether **146** was treated with tosylate fluoride and DBU. At the same time, the use of polymer-bound DBU was tested in addition to the conventional base, since the use of the polymer-bound base had the advantage of processing the reaction more quickly and cleanly.

Table 5-5: Reagents and conditions for silyl-tosylate exchange.

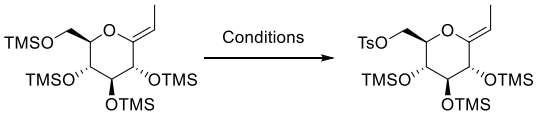

146 **154**

Entry	Reagents	Solvent	Temp.	Reaction Time	Yield
1	TsF 1.0 eq. DBU Polymer-bound 20 mol%	MeCN	r.t.	24 h	48 %
2	TsF 1.0 eq. DBU Polymer-bound 20 mol%	MeCN	78°C	24 h	10 %
3	TsF 1.0 eq. DBU 20 mol%	MeCN	r.t.	24 h	36 %
4	TsF 1.0 eq. DBU 20 mol%	MeCN	78°C	24 h	9 %

A screening showed that the optimal conditions for the selective silyl - tosylate exchange led to a yield of 48 % (Table 5-5 entry 1). At the same time, the polymer-bound DBU had proven to be a better alternative than the conventional base. The role of the base in the reaction was to react with the tosylate fluoride to form arylsulfonyl ammonium fluoride salt **155** (Scheme 5-16). This intermediate underwent an exchange between the tosylate and the silyl group. A

fluoride-silyl bond and an oxygen-arylsulfonyl bond were formed. The increased bond strength could be the driving force for the reaction. The free base was then available again for the catalytic cycle.[48]

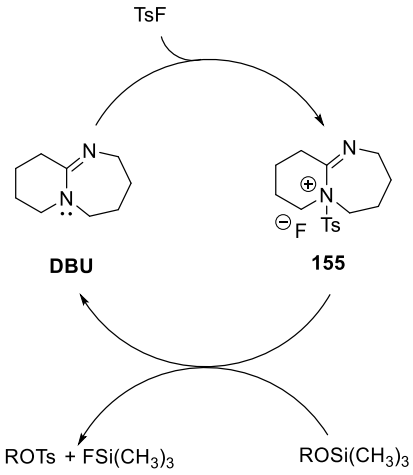

Scheme 5-16: Proposed mechanism for silyl-tosylate exchange.[48]

By selectively converting the primary TMS protected hydroxy group into a primary -OTs group, this could subsequently be reduced to a methyl group. $LiAlH_4$ and $LiBEt_3H$ were tested as reducing agents and with a yield of 66 %, $LiAlH_4$ proved to be the better reagent. In addition, only 2.0 equivalents were needed (Scheme 5-17). However, reaction control with TLC showed that a part of the starting material **154** decomposes during the reaction probably due to the TMS protecting groups which were rather unstable.

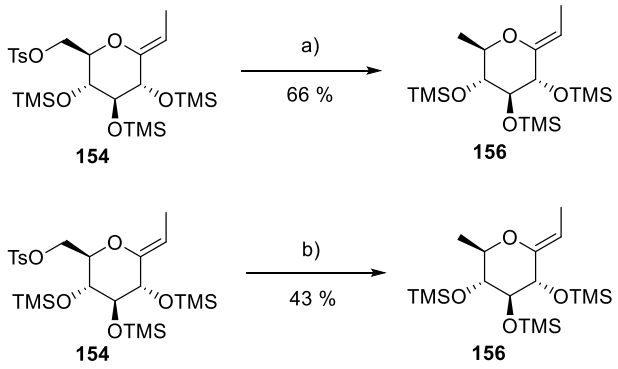

Scheme 5-17: Reagents and conditions: a) $LiAlH_4$, Et_2O, 0°C to r.t., 1d; b) $LiBEt_3H$, THF, 0°C to r.t., 1d.

In the next step, the epoxide was constructed either between C-2 and C-3 or between C-3 and C-4 by tosylating the oxygen at C-2 and C-4, followed by nucleophilic attack of the hydroxy group at C-3. For this purpose, the silyl - tosylate exchange method was used first. However, reaction control with TLC showed no reaction. Increasing the temperature only led to decomposition (Scheme 5-18). The TMS protected hydroxy groups were likely sterically

hindered, preventing any reaction from occurring. An increase in temperature then probably led to decomposition, since the TMS groups as well as the enol ether group were unstable.

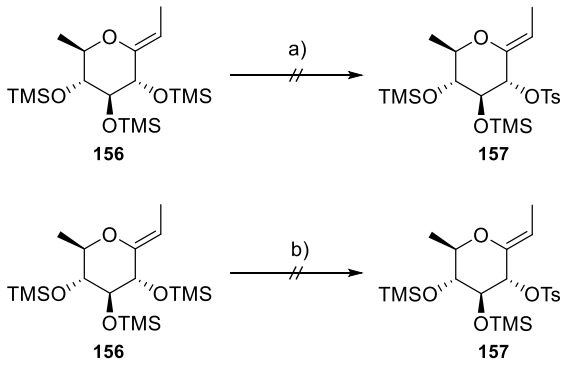

Scheme 5-18: Reagents and conditions: a) TsF, DBU Polymer-bound 20 mol%, MeCN, r.t., 24 h; b) TsF, DBU Polymer-bound 20 mol%, MeCN, 60°C, 2 h

Since no direct transformation of the silyl-protected hydroxy groups to tosylate groups was possible, the TMS protective groups were removed alternatively and a free hydroxy group was attempted to be transformed into a tosylate group. The deprotection was carried out under acidic conditions and 90 % of the triol **158** was obtained (Scheme 5-19).

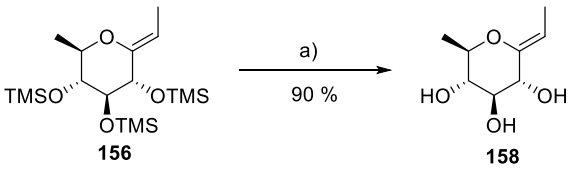

Scheme 5-19: Reagents and canditions: a) HCl, THF, H_2O, r.t., 1 h.

Attempts to tosylate compound **158** showed either no reaction or formation of multiple spots during reaction control by TLC. Isolation of the spots showed only a complex mixture of by-products that did not represented any of the desired major products. Entry four of Table 5-6 showed the attempt to monotosylate the hydroxy groups using dibutyltin oxide which was inspired by the regioselective monotosylation of secondary alcohols into glycosides.[49] However, these reaction conditions did not showed any chemical reaction. Consequently, this synthetic route was no longer feasible.

*Table 5-6: Reagents and conditions for tosylation of **158**.*

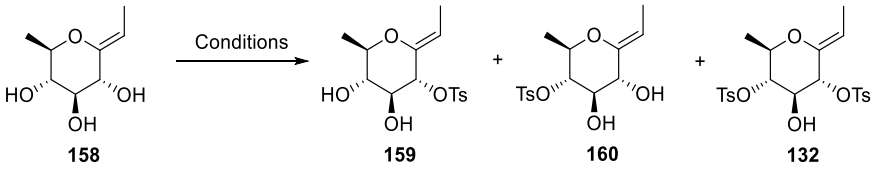

Entry	Reagents	Solvent	Temp.	Reaction Time	Yield
1	TsCl 1.10 eq.	Pyridine/CH_3Cl	0°C to r.t.	24 h	-
2	TsCl 1.00 eq.	Pyridine	−20°C	24 h	-
3	TsCl 1.00 eq. NBu_4HSO_4 0.02 eq.	NaOH 5 %/CH_2Cl_2	r.t.	24 h	-
4	Bu_2SnO 1.00 eq. TsCl 1.10 eq. DMAP 0.10 eq.	MeOH/Dioxan	reflux	10 h	-

5.1.9 Conclusion and Strategic Considerations of the Modified Julia Olefination Approach

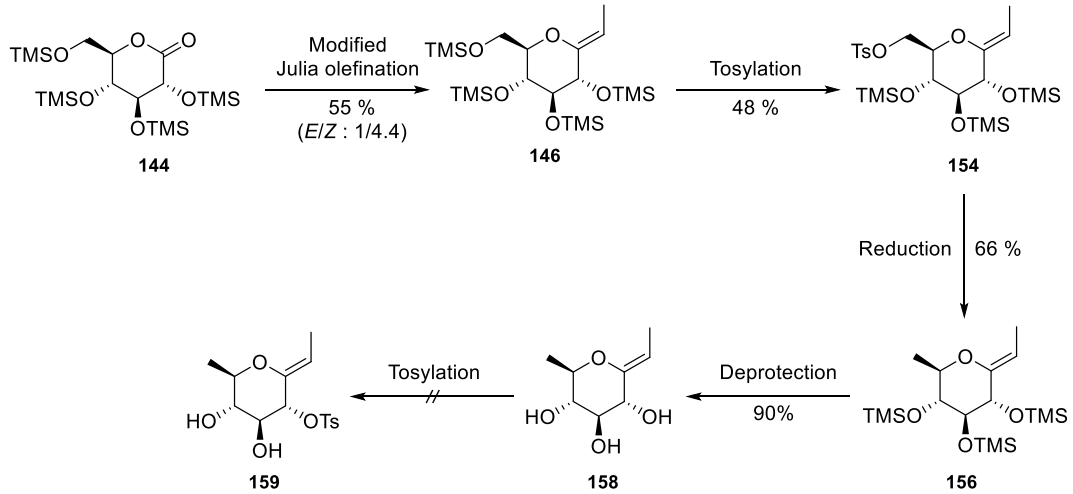

Scheme 5-20: Summary of the synthesis pathway of the modified Julia olefination approach.

In this synthetic approach, the TMS-protected lactone **144** was successfully transformed to the alkene by modified Julia olefination with a yield of 55 %. With a diastereomeric ratio of 1/4.4 (*E*/*Z*), was *Z*-isomer **146** the major product due to the selected TMS protecting group. Subsequently, the silyl tosylate exchange was carried out with a yield of 48 % using the polymer-bound amine base DBU. The following reduction at the primary site was also successful with a yield of 66 %. Deprotection of the TMS groups gave triol **158** in a yield of 90 %. However, the synthesis could not be continued because the tosylation at C-2 or at C- 4 was not successful. Nevertheless, with the help of the modified Julia olefination, the double bond

was constructed and thus the main motif of dienophile **3**. In addition, compound **158** was structurally very similar to the desired dienophile **3**, which could be utilized for testing the Diels-Alder reaction.

5.1.10 Fourth Retrosynthetic Analysis

The successful modified Julia olefination was incorporated in the next retrosynthesis. In addition, a cheap carbohydrate derivative could be utilized as a starting material, which was also available in large quantities. These aspects will be taken into account in the new retrosynthetic analysis.

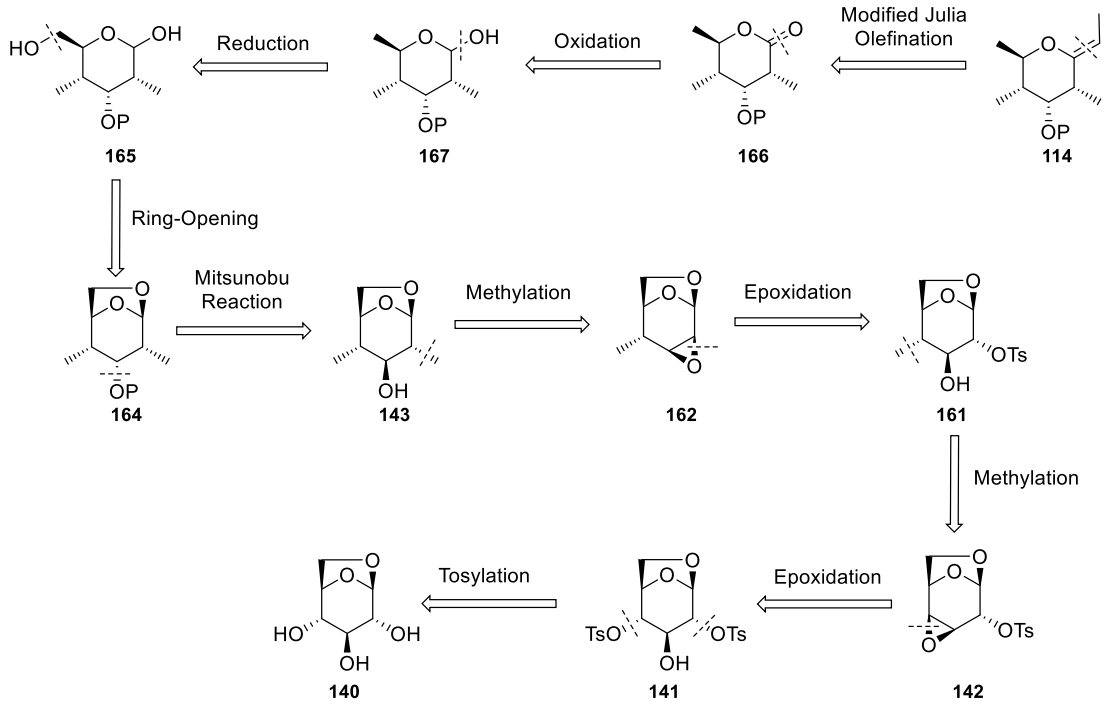

*Scheme 5-21: Fourth retrosynthetic strategy towards **106**.*

For this reason, the fourth retrosynthesis was based on levoglucosan (**140**), since it was successfully tosylated by Krohn *et al*. and subsequently methylated (Scheme 5-13). Thus, the synthesis to fragment **143** was literature known.[44,45] Next, the stereocenter of the free hydroxy group at C-3 of fragment **143** needed to be inverted and protected by a Mitsunobu reaction (Scheme 5-21). Subsequently, the anhydride **164** had to be hydrolytically opened to compound **165**, followed by reductive cleavage of the primary alcohol into compound **167**, which was envisaged to be oxidated to lactone **166**. Leading to the last step planned the modified Julia olefination to give dienophile **114**.

5.1.11 Synthetic Progress of the Levoglucosan Approach

In this synthetic route, the *Z* alkene was obtained from lactone **167** using the modified Julia olefination. Since the stereocenter at C-3 was inverted in contrast to the previously used trimethylsilyl-protected D-gluconolactone **144**, the effect of the stereocenter at C-3 for the modified Julia olefination had to be determined. For this reason, the modified Julia olefination needed to be tested on the trimethylsilyl protected D-allose lactone **168**. To synthesize **168**, it was first oxidized from commercially available D-allose (**169**) to the lactone using Shvo's catalyst **171** (Scheme 5-22).

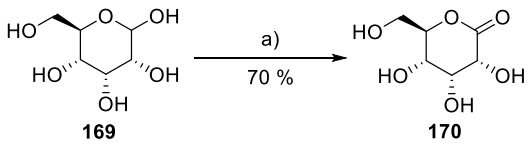

169 **170**

Scheme 5-22: Reagents and conditions: a) Shvo's cat., Cyclohexanone, DMF, r.t., 72 h.

Shvo's catalyst **171** shown in Figure 5-10 was an organoruthenium compound known to convert alcohols to esters, and other compounds. Other applications included the disproportionation of aldehydes to esters and the oxidation of secondary alcohols to ketones. In the case of D-allose, the hemiacetal of the anomeric center was oxidized to the lactone.[50]

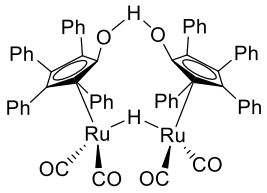

171

*Figure 5-10: Shvo's catalyst **171**.*

The dimer shown was the precatalytic form **174**, with the monomer **177** representing the reactive species. The active species was formed during the reaction of the inactive dimeric species **174** with a carbonyl compund such as cyclohexanone to **171**, which dissociates to the monomers **176** and **177** (Scheme 5-23).[50]

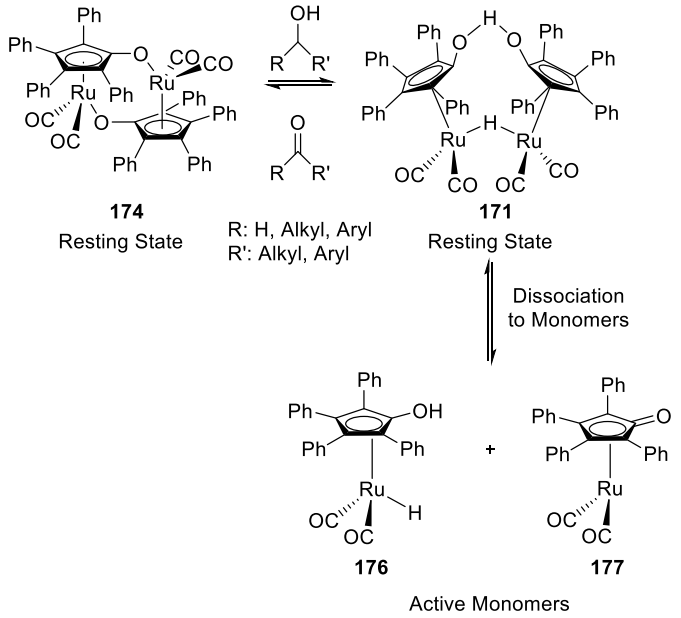

Scheme 5-23: Activation of Shvo's catalyst.[50]

The initial step of the oxidation mechanism involved the coordination of the reactive species **177** to the D-allose (**169**) through hydrogen bonds, resulting in the formation of transition state **178**. In a concerted step, the hydrogen at the alcohol of the hemiacetal was transferred to the ketone of the catalyst and the hydrogen at the carbon center was transferred to the ruthenium (Scheme 5-24). This resulted in the formation of lactone **170** and the monomer **176**. Subsequently, compound **176** was regenerated with cyclohexanone through oxidation to produce the reactive monomer species **177**.[50]

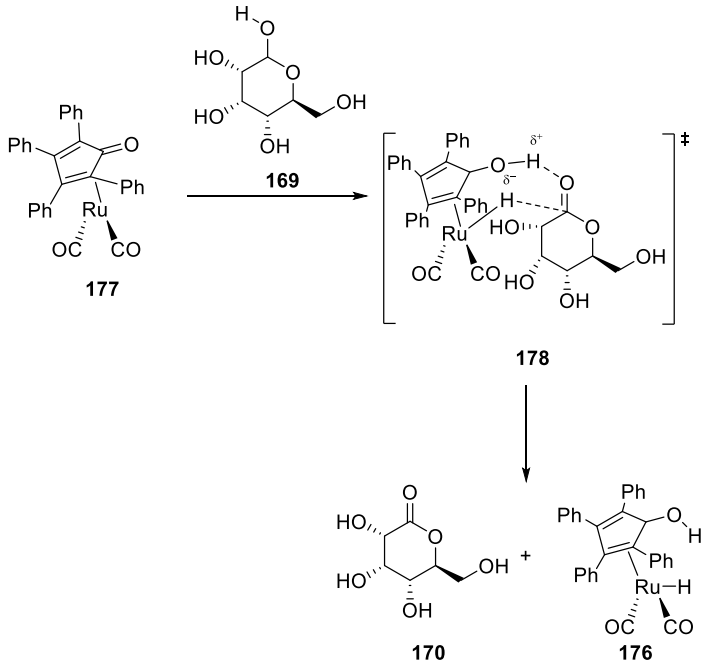

*Scheme 5-24: Proposed mechanism for oxidating **169** to **170** with Shvo's catalyst.*

To evaluate the results, it was important to consider that the reactant in solution formed an equilibrium between the anomeric pyranose **169** and furanose **172**. In aqueous solution, the sugar was primarirly present in its *β*-pyranose form. However, due to the influence of the solvent, the furanose form of sugar **172** could also be present. Therefore, during the oxidation of the sugar, both the 1,5-lactone **170** form and the 1,4-lactone **173** forms were formed. In addition, the lactones were in an equilibrium, too (Scheme 5-25).[50]

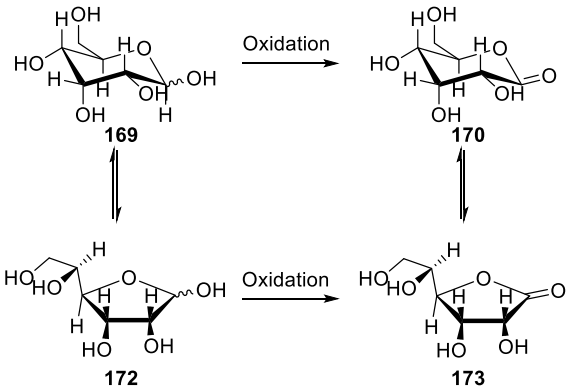

Scheme 5-25: Equilibrium of the pyranose form and the furanose form.

By ^{1}H NMR analyses, the product was found to have formed in a *δ:γ* ratio of 1:1.

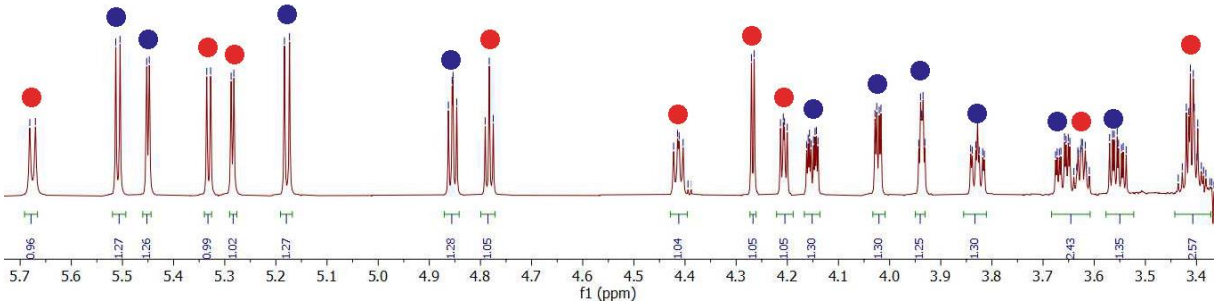

*Figure 5-11: NMR spectra of 1,5-lactone/δ-lactone **170** and 1,4-lactone/γ-lactone **173**. Marked are the signals of the pyranose form **170** (blue) and those of the furanose form **173** (red).*

*Table 5-7: ^{1}H and ^{13}C signals from **170** and **173** in D_2O (700 MHz).*

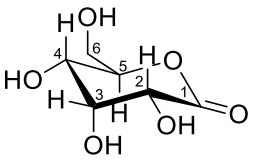

170
1,5-lactone

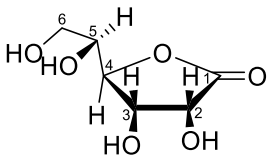

173
1,4-lactone

^{1}H	H-2	H-3	H-4	H-5	H-6	H-6‘	OH-2	OH-3	OH-4	OH-6
170.	4.02 dd	3.94 dd	3.83 ddd	4.15 ddd	3.66d dd	3.55 ddd	5.51 d	5.45 d	5.1 8d	4.85 dd
173.	4.27 d	4.21 dd	3.62 m	4.41 dd	3.40 m	3.40 m	5.68 d	5.28 d	5.33 d	4.78 pt
^{13}C	C-1	C-2	C-3	C-4	C-5	C-6				
170.	173.3	69.2	67.9	71.2	80.8	62.7				
173.	172.2	69.7	72.2	65.1	85.5	60.2				

Following protection of the four free alcohol functionalities with TMSCl, protected lactone **168** was obtained in a yield of 77 % (Scheme 5-26).[51] The reason for the low yield was likely due to the column chromatographic purification performed on silica gel and its acidic nature, which initiated partial deprotection of the silyl ethers, as TMS is known to be very acid labile. With the TMS protected allose lactone **168** obtained, the modified Julia olefination was then carried out. The reaction yielded only 21 % (Scheme 5-26).

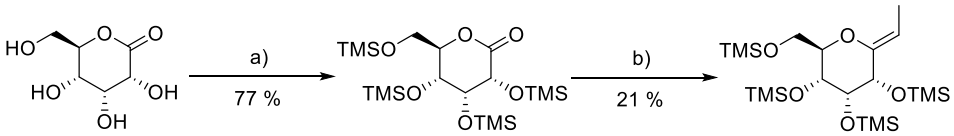

*Scheme 5-26: Reagents and condtions: a) N-Methylmorphin, TMSCl, THF, 0°C, to r.t., 60 h; b) 1. **139**, LiHMDS, THF, −78°C, 2 h; 2. DBU, THF, r.t., 1 h.*

However, the NMR data indicate that only the *Z* alkene was formed as the sole isomer. Thus, the NOESY showed a clear correlation of H-1 and H-2, which was a direct evidence of the *Z* double bond (Figure 5-12).

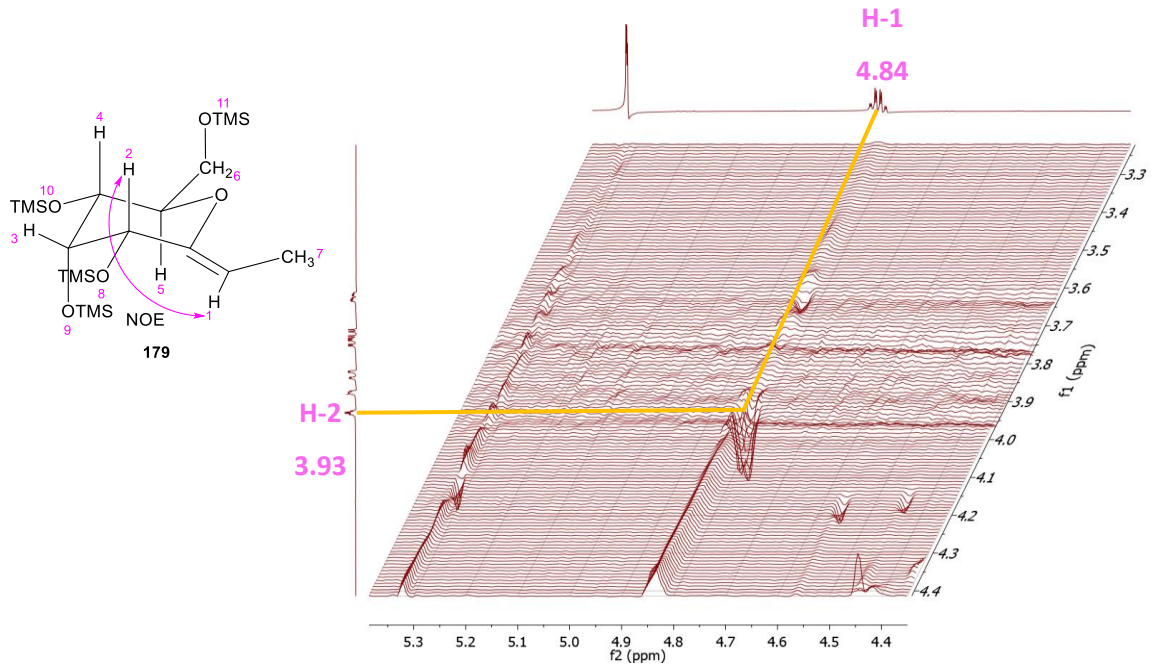

*Figure 5-12: NOE correlation showing the configuration of the Z double bond of **179**.*

*Table 5-8: NMR data for **179** in CD_2Cl_2 (700 MHz).*

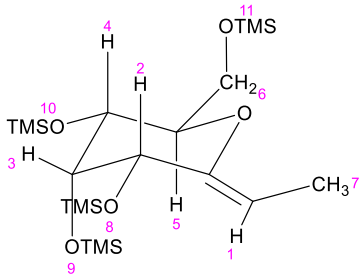

Nr.	δH [ppm] (m, J in Hz, Int.)	δC [ppm]
1	4.84 (qd, *J* = 6.9, 1.9 Hz, 1H)	102.7
2	3.93 (ddd, *J* = 2.1, 2.0, 2.0 Hz, 1H)	70.1
3	3.88 (ddd, *J* = 2.4, 2.4 Hz, 1H)	75.7
4	3.74 (dd, *J* = 9.5, 2.3 Hz, 1H)	68.5
5	3.62 (ddd, *J* = 9.5, 3.7, 1.9 Hz, 1H)	76.8
6	3.83 (dd, *J* = 11.4, 1.9Hz, 1H)	62.2
7	3.72 (dd, *J* = 11.4, 3.8 Hz, 1H)	62.2
8	1.58 (dd, *J* = 6.8, 2.0 Hz, 3H)	9.1
9	0.14 (s, 9H)	−0.2
10	0.10 (s, 9H)	0.9
11	0.15 (s, 9H)	0.4
11	0.12 (s, 9H)	−0.3
12	-	151.1

Moreover, the coupling constant between H-4 and H-5 shown in Table 5-8 was high with 9.5 Hz, indicating an *anti*-axial alignment of the hydrogen atoms. This in turn confirmed that the pyran ring must had been in a $^4C_1$ chair configuration. These results supported the underlying hypothesis that dienophile **114** to be synthesized was also present in this configuration.

The *Z*-selectivity can be explained by the mechanism of modified Julia olefination discussed in section 5.1.9. As previously described, both *Si* and *Re* side attacks were possible. However, the *Si* side attack in compound **168** was likely blocked by the axially positioned TMS protected hydroxy group. Therefore, the reaction course through the *Si* side attack intermediate was highly unlikely and did not occur. Consequently, only the reaction course through the *Re* side attack remained. In this case, the reaction proceeded only through the *syn* adduct and ultimately yielded only the *Z* alkene as product (Scheme 5-27).

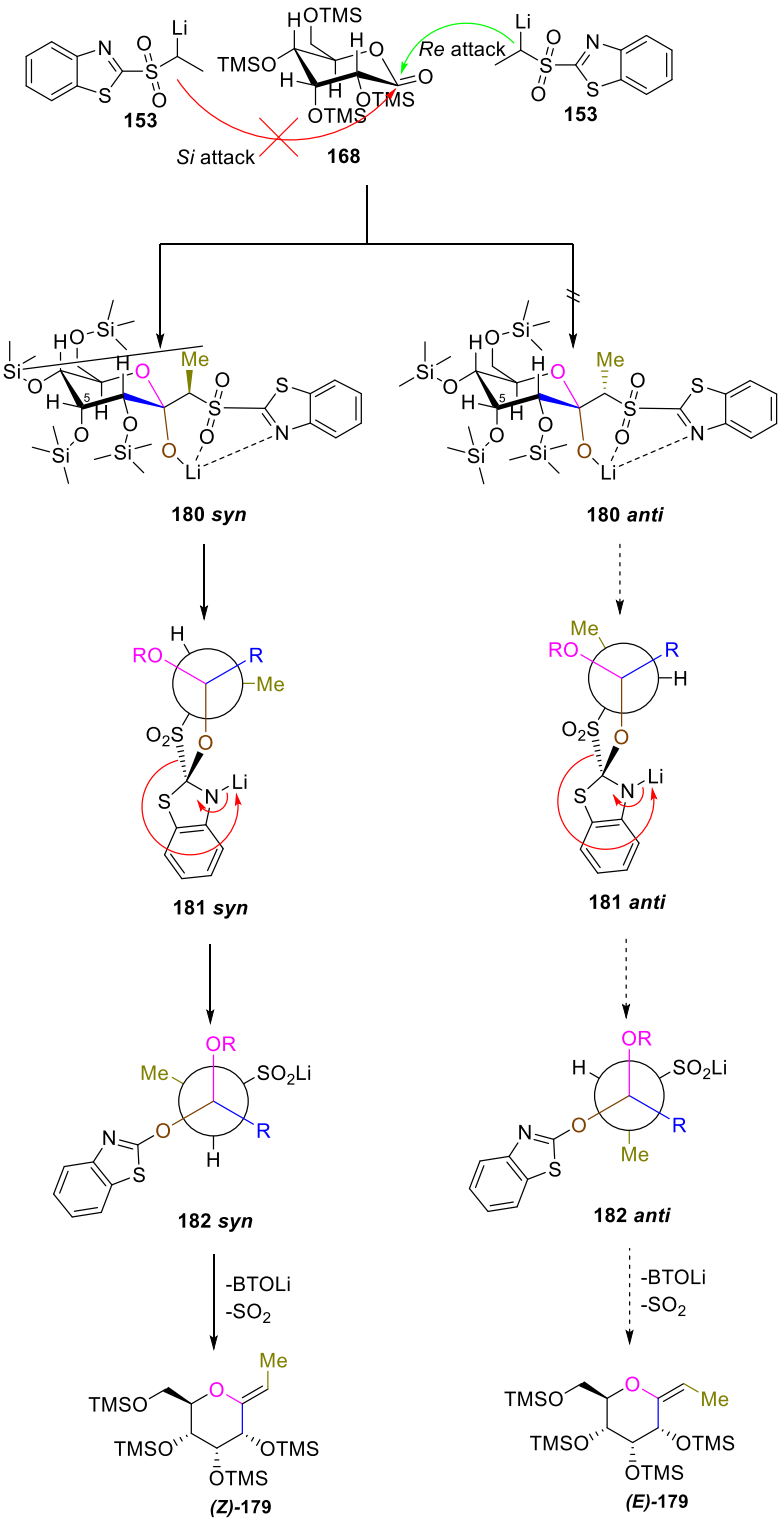

*Scheme 5-27: Postulated mechanism for the modified Julia olefination for **179**.*

Based on the information gathered from the synthesis of **179**, it was concluded that the reversed stereocenter at C-3 likely had a detrimental effect on the yield. However, it was also conceivable that with the C-3 alcohol in an axial position, the *Z*-isomer was generated. Consequently, these findings suggested that a synthesis utilizing the modified Julia olefination of lactone **167** could have potentially yielded the desired product.

The actual synthesis with Levoglucosan (**140**) could then commence. To begin, **140** was tosylated and subsequently epoxidated. This was initiated with NaOMe, which induced a nucleophilic attack of the alcohol group on C-3 onto the tosylate bound C-4. The two step synthesis gave **142** in quantitative yield. Following that, the epoxide was opened and methylated using the Grignard reagent methylmagnesium chloride. The reaction was conducted following the procedure outlined by Krohn *et al*., utilizing copper iodide as a catalyst. However, in this instance, only a yield of 28 % was achieved. The 79 % yield reported by Krohn *et al*. proved unattainable under these conditions. Substituting copper iodide with copper chloride as the catalyst resulted in a slightly improved yield of 51 %. The second epoxidation between C-3 and C-2 proceeded with quantitative yield, consistent with the literature (Scheme 5-28).[44,45]

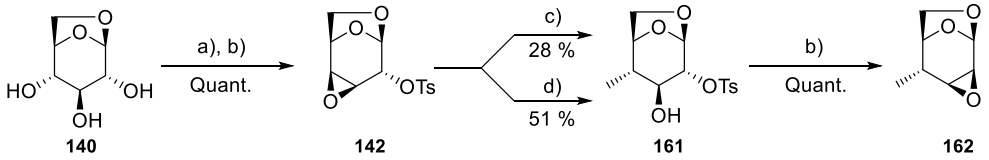

Scheme 5-28: Reagents and conditions: a) TsCl, $CHCl_3$/Pyrdine, r.t., 16 h; b) NaOMe, CH_2Cl_2/MeOH, r.t., 1 h; c) CuI 10 mol%, MeMgCl, THF,40°C, 12 h; d) CuCl 10 mol%, MeMgCl, THF,10°C 10 h. [44,45]

The second methylation through epoxide opening using the Gilman cuprate under the same reaction conditions as described by Krohn *et al.* did not exhibit any reaction (Table 5-9, entry 1).[44] Even when the reaction time was extended overnight, no change was observed in the reaction mixture (Table 5-9, entry 2). In a third approach, boron trifluoride etherate was added as an additive (Table 5-9, entry 3) and compound **143** was obtained with a low yield of 19 %. Changing the copper salt catalyst from CuCN to CuI also failed to improve the yield, resulting in a yield of only 13 % (Table 5-9, entry 4).[52] Using the conditions from the initial methylation, only a yield of 7 % could be achieved (Table 5-9, entry 5).[44,45] Lastly, the conditions of a mixed 2-thienyl higher order cyanocuprate were tested, but this reaction proceeded without formation of the product **143** (Table 5-9, entry 6).[52] Despite successfully synthesizing molecule **143**, it was not possible to attain the reported yield of 81 % as indicated by Krohn *et al*.[45] It can be ruled out that the quality of the reagents cause the deviation in yield since they were not only newly acquired, but also tested for purity and reactivity upon receipt. Consequently, the exact cause of such a significant deviation in yields remained inconclusive. Nevertheless, enough of fragment **143** was obtained to continue the synthesis for the time at being.

*Table 5-9: Reagents and conditions for the methylation of **162** to **143**.*

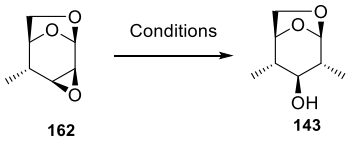

Entry	Reagents	Solvent	Temp.	Reaction Time	Yield
1	CuCN 4.00 eq. MeLi 8.00 eq.	Et_2O/THF	−78°C → −20°C	2 h	-
2	CuCN 4.00 eq. MeLi 8.00 eq.	Et_2O/THF	−78°C → −20°C	24 h	-
3	CuCN 4.00 eq. MeLi 8.00 eq. $BF_3{*}OEt_2$ 2.50 eq.	Et_2O/THF	−78°C → −20°C	16 h	19 %
4	CuI 4.00 eq. MeLi 8.00 eq.	Et_2O/THF	−10°C → −20°C	16 h	13 %
5	CuI 0.13 eq. MeMgCl 6.40 eq.	THF	−44°C → r.t.	5 h	7 %
6	Me(2-Th)Cu(CN)Li_2 1.43 eq $BF_3{*}OEt_2$ 1.43 eq.	Et_2O/THF	−78°C	16 h	-

Inversion of the free alcohol group at C-3 was achieved through a Mitsunobu reaction. Simutaneously, the hydroxy group was protected with a benzyl protecting group.[53] The reaction yielded **183** with a moderate yield of 50 % (Scheme 5-29).

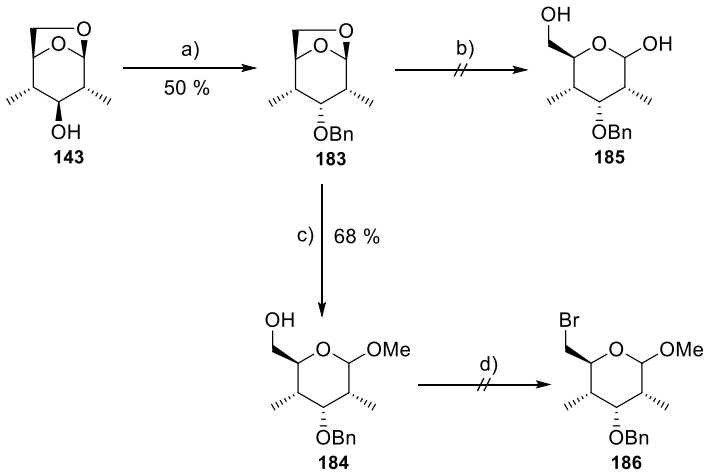

Scheme 5-29: Reagents and conditions: a) BnOH, TPP, TMAD, Benzene, 50°C, 16 h; b) BCl_3, CH_2Cl_2, 0°C to r.t., 2 h; c) p-TsOH (cat.), MeOH, 50°C, 16 h; d) Ph_3P, CBr_4, THF, 0°C, 2 h.

The subsequent step involved breaking the 1.6 anhydro bridge, which initially proved unsuccessful when attempted through hydrolytic cleavage using BCl_3, resulting in the

decomposition of the starting material. Consequently, a different approach was chosen, and the cleavage was carried out *p*-TsOH in methanol and led to the formation of the acetal **184** with a yield of 68 % (Scheme 5-29).[54]

At this stage, the primary alcohol group was to be cleaved. The plan was to first convert the primary alcohol group into a bromide using the Appel reaction and then obtain the methyl group through the Barton-McCombie reaction. However, the attempt to transform the hydroxy group into a bromide failed (Scheme 5-29). Given the lack of available material at this point and the consistently low yields obtained in previous reactions, contrary to the literature, such as the synthesis of coompound **143**, it was decided not to pursue this synthetic route any further.

5.1.12 Conclusion and Strategic Considerations of the Levoglucosan Approach

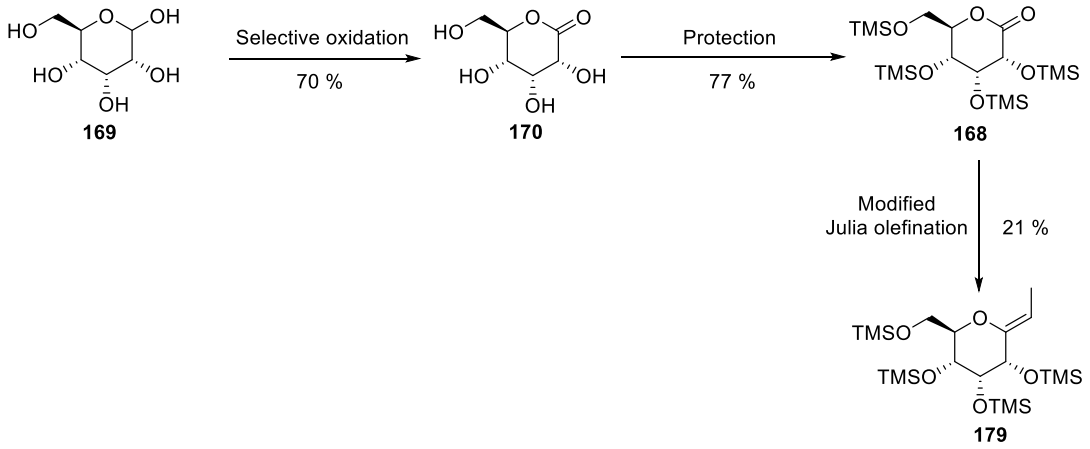

*Scheme 5-30: Summary of the synthesis towards molecule **179**.*

In this synthesis approach, the preparation of **179** based on the modified Julia olefination revealed that the stereocenter had a significant impact on diastereoselectivity (Scheme 5-30). Thus, only the *Z*-alkene was produced as the product. At the same time, compound **179** offered valuable structural insights into the final dienophile **3**.

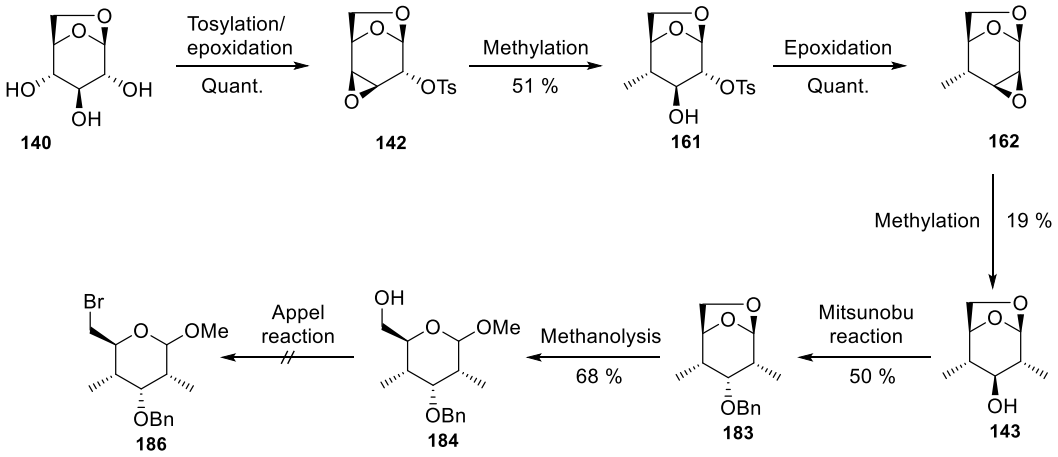

Scheme 5-31: Summary of the Levoglucosan approach.

Synthesis of dienophile **3** from levoglucosan (**140**) initially progressed smoothly. However, the second epoxide opening from molecule **162** to compound **161** could not be achieved with the expected yield of 81 % as described in the literature. Instead, only a yield of 19 % was obtained in the best case scenario. This created a significant bottleneck early in the entire synthetic pathway. Subsequent syntheses also yielded unsatisfactory results, and ultimately, the Appel reaction from **184** to **186** was unsuccessful. It was concluded that this was not the appropriate synthetic pathway for producing dienophile **3** (Scheme 5-31).

5.1.13 Fifth Retrosynthetic Analysis

In this retrosynthesis, the plan was to synthesize dienophile **3** through two different routes, building upon the previous retrosyntheses and their corresponding syntheses.

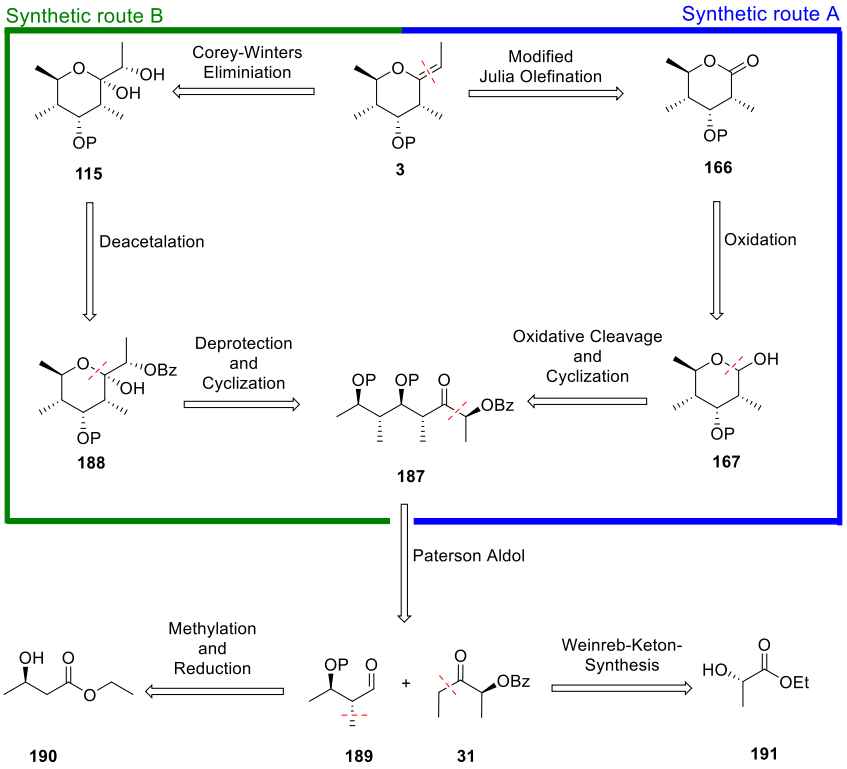

*Scheme 5-32: Fifth retrosynthetic analysis towards dienophile **3**.*

On one hand, a modified Julia olefination with lactone **166** was planned. The formation of lactone **166** would follow selective oxidation of the corresponding lactol **167**. Cyclization of fragment **187** to compound **167** could occur through cleavage and deprotection of the corresponding functional groups. This synthetic route would have been referred to as synthetic route A (Scheme 5-32, blue marking).

Additionally, the synthesis of **3** was targeted by a Corey-Winter elimination of the *syn*-diol **115**. Deacetylation of fragment **188** was planned to synthesize *syn*-diol **115**. Deprotection of the left hydroxyl group of compound **187** would led to cyclization and the formation of fragment **188**. This synthetic route would have been referred to as synthetic route B (Scheme 5-32, green marking).

Both routes would have originated from the linear fragment **187**. This component was envisaged to be synthesized by a Paterson aldol reaction of the *α, β*-chiral aldehyde **189** and the *α*-chiral ketone **31**. Aldehyde **189** would have resulted from asymmetric methylation followed by reduction. In parallel, ketone **31** was planned to be synthesized through the Weinreb ketone synthesis method. A major advantage of this synthetic route was that the

synthesis of fragment **187** was already known in the literature and had been discussed in section 2.4 (Scheme 2-5). As such, **187** corresponded to the mono-protected fragment **34**, which had been employed in the initial synthesis of portentol (**1**) by Trauner *et al*.[1]

5.1.14 Synthetic Progress of the Double Pathway Approach

The retrosyntheses to **3** proposed in Scheme 5-32 both proceed from molecule **187**, so the initial goal was to successfully synthesize this fragment.

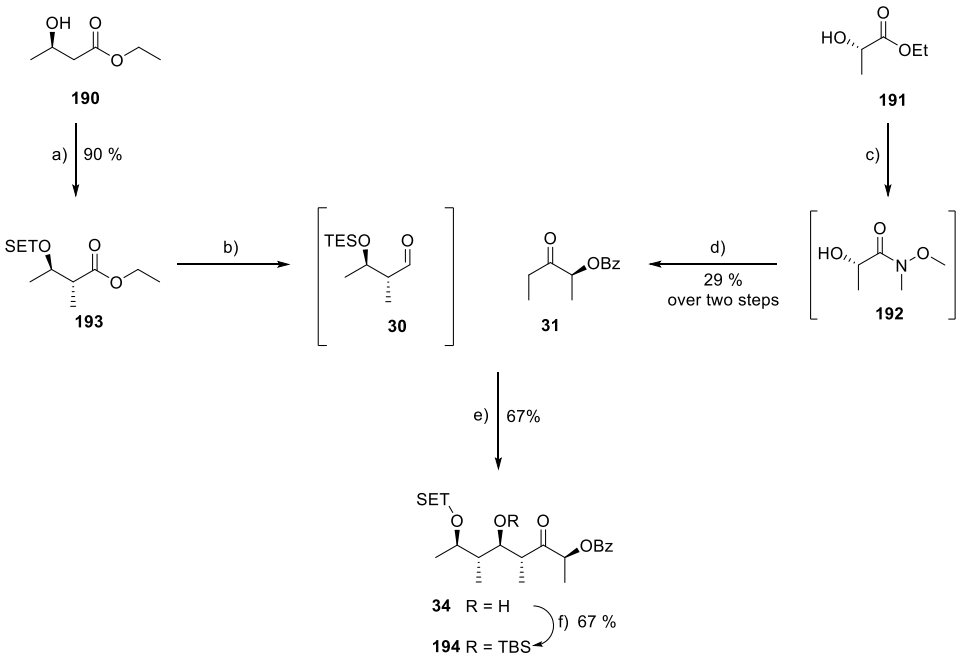

*Scheme 5-33: Reagents and conditions: a) LDA, DMI, MeI, TESCl, THF, −78 °C to 0 °C; b) DIBAL-H, CH_2Cl_2, −78°C; c) C_2H_7NO, i-PrMgCl, Et_2O/THF, −20 °C; d) EtMgBr then Bz_2O, NEt_3, DMAP, Et_2O/THF, 0 °C to rt; e) **31**, Cy_2BCl, NEt_3, Et_2O, −78 °C to 0 °C, then −78 °C, **30**, −78 °C to −20 °C;*

The synthesis started with the formation of the *α*-chiral ketone **191**, which was required for the reaction with fragment **30** (Scheme 5-33). It was synthesized according to the method developed by Paterson *et al*.[55] First, starting from the purchasable (*S*)-lactate **191**, the Weinreb amide **192** was synthesized. One of the advantages of Weinreb amides was their high selectivity in reactions with organyl metals as in the subsequent Grignard reaction. Nucleophilic addition of the organyl metal compound to the carbonyl group gave a tetrahedral intermediate, which was stabilized by chelation. Hydrolysis achieved the formation of benzyl ester **31**.[56]

After chromatographic purification, a yield of 29 % was determined, this low yield compared to the literature value of 40 %[57] could be attributed to slightly elevated temperatures during the reaction. In addition, it was likely that the Weinreb amide was not completely dry and the residual moisture led to inactivation of the Grignard compound.

The synthesis was continued with the asymmetric *α*-alkylation of *β*-hydroxy ester **190**, known as Frater-Seebach alkylation.[58]

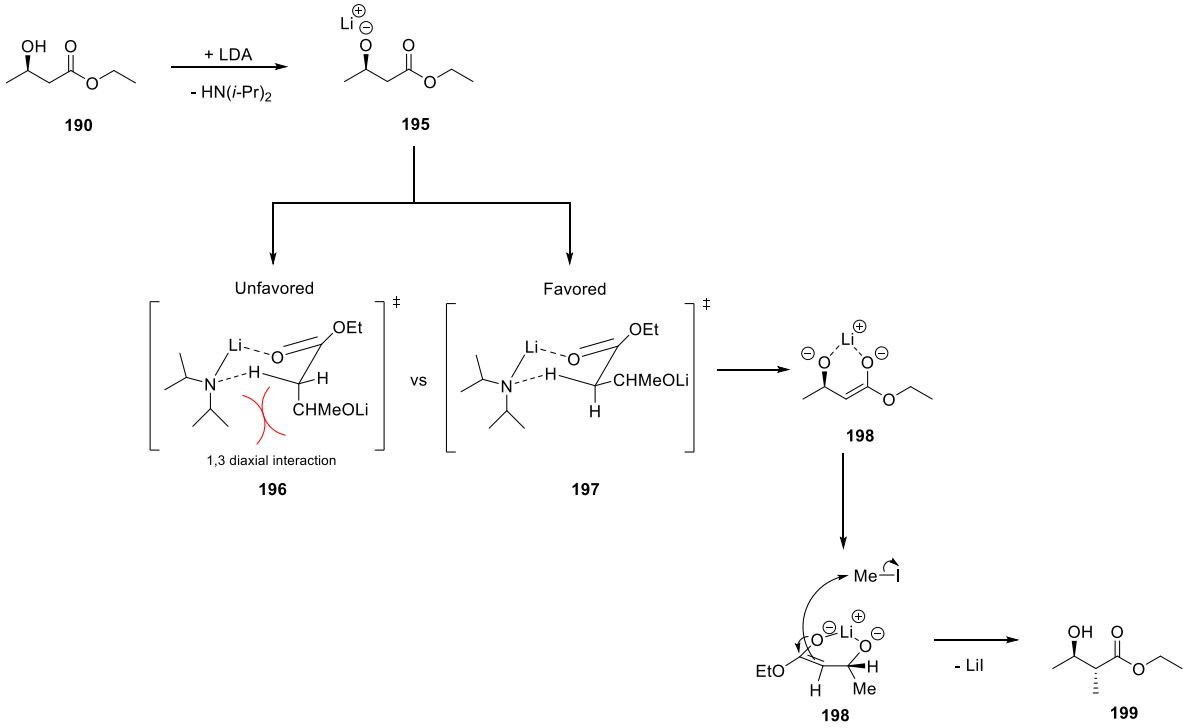

*Scheme 5-34: Mechanismen of the Frater-Seebach alkylation towards fragment **193**.*

The *in situ* prepared lithium diisopropylamide was utilized in 2.3 equivalents. The first equivalent was necessary for deprotonation of the hydroxyl group of **190**, resulting in the formation of the salt **195**. The second equivalent LDA was responsible for the abstraction of the *α*-hydrogen. Transition state **196** was destabilized to such an extent by the 1,3-diaxial interaction that deprotonation preferentially proceeded through transition state **197**, yielding in the *E*-ester enolate **198**. The formation of **198** as an intermediate was further favored by the formation of a chair like configuration, as the lithium cation formed a chelated complex, followed by the nucleophilic attack of the ester enolate **198** on methyl iodide with regeneration of the carbonyl group. The nucleophilic attack occurred stereoselectively *anti* to the hydroxyl group, as this orientation was sterically favored and no steric interaction was established by the ester group and the methyl moiety.[58] Consequently, the new stereocenter of **193** was in *R*-configuration (Scheme 5-34). The hydroxy group was subsequently protected as the triethyl silyl ether **193**.

After chromatographic purification, a yield of 61 % was obtained and NMR data revealed a diastereomeric ratio of 5:1. During the reaction, maintaining low temperatures proved challenging, and in some cases, slightly higher temperatures were reached, resulting in reduced selectivity.[58] Fragment **193** underwent partial reduction with DIBAL-H, yielding

aldehyde **30**. However, fragment **30** was not purified or isolated due to its instability. Instead, it was directly reacted with compound **31** in the Paterson aldol reaction (Scheme 5-33).

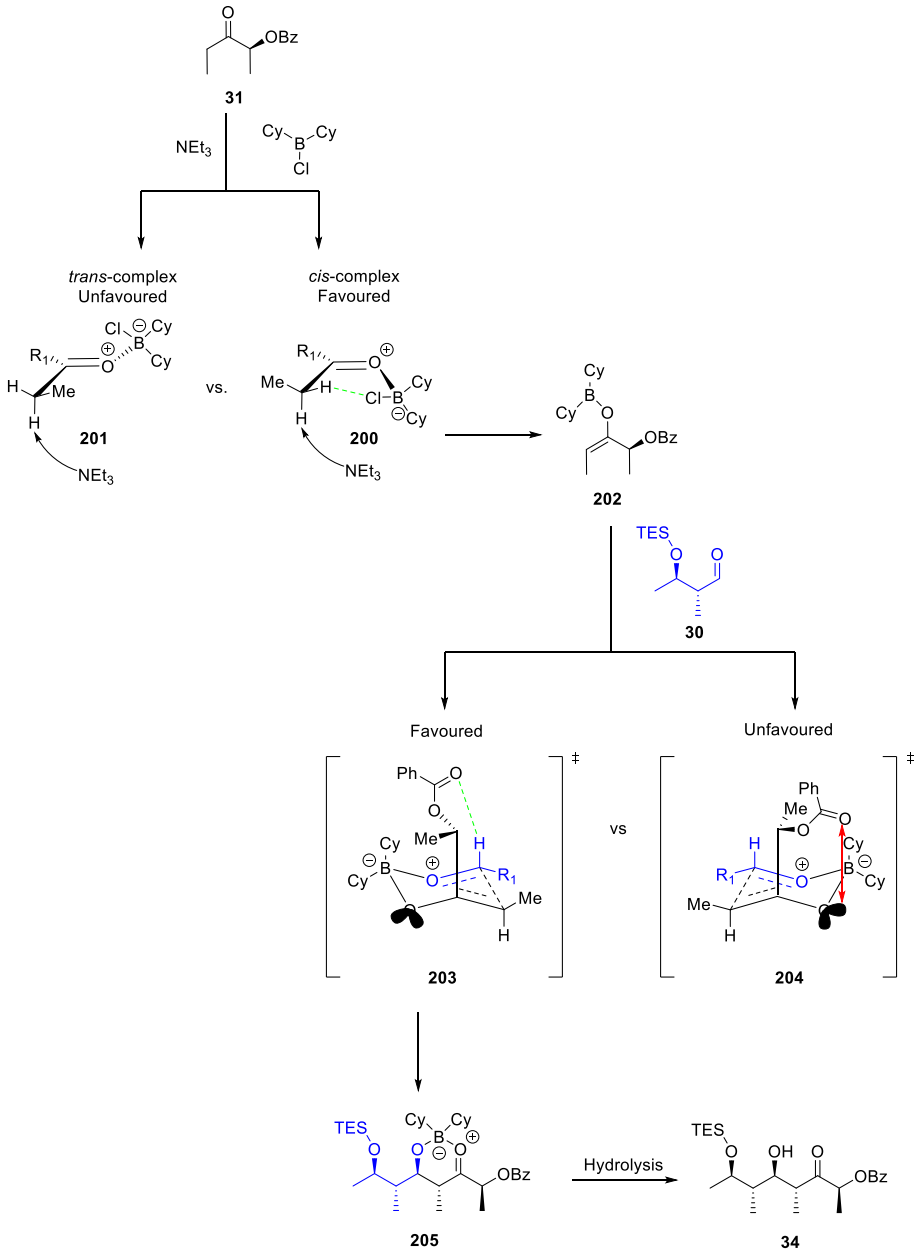

Scheme 5-35: Mechanism for Paterson anti aldol reaction.[59,60]

The reaction mechanism likely started with the enolization of the previously prepared ketone **31** using triethylamine as the base and chlorodicyclohexylborane as the Lewis acid. Chlorodicyclohexylborane coordinated with the carbonyl group in a manner aligning the B-O bond *cis* to the acidic proton. The formation of this *cis* complex **200** was favored due to the use of chlorodicyclohexylborane. The chlorine ligand, serving as the leaving group, formed a hydrogen bond with the hydrogen on the *α*-carbon. This interaction created a closed, six-membered transition state and further activated the axial proton for deprotonation. The two cyclohexyl ligands presented steric hindrance that additionally promoted the formation of the

closed transition state. Triethylamine served as a sterically less demanding base, facilitating the deprotonation of the activated axial proton. The ligands and leaving group of the Lewis acid, as well as the choice of base, played significant roles in favoring the formation of (*E*)-enolate **202**. In general, these factors contributed to achieving high stereocontrol. The use of a sterically demanding leaving group, such as triflates, small ligands like *n*-butane, and an equally sterically demanding base like diisopropylamine, would favored the formation of the *trans* complex **201** and, consequently, the (*Z*)-enolate.[60] Afterwards, (*E*)-enolate **202** attacked aldehyde **30** through the Zimmerman-Traxler transition state. To identify the favored aldol product the corresponding Zimmerman-Traxler transition states had to be examined, considering the ketone's stereochemistry at the *α*-position and the direction of the nucleophilic attack on aldehyde **30**—whether from the *Re* or *Si* side—were critical factors in this analysis.[59] It was assumed that the preference lay in the attack from the *Si* side at transition state **203**. This preference could be explained by the lower 1,3-allylic strain, as the methyl group of the ketone did not extend towards the six-membered transition state but pointed outward in the opposite direction. This orientation allowed for the formation of a hydrogen bond between the benzoate and the axially aligned hydrogen of the aldehyde (Scheme 5-35, highlighted in green). These factors significantly contributed to the stability of transition state **203** and favored the *Si* side attack. Consequently, the *anti*-product **34** was formed with high selectivity. On the other hand, the attack from the *Re* side was unfavoured. The alternative transition state **204** was not preferred and was destabilized due to repulsive forces between the free electron pairs of oxygen within the enolate and the benzoate (Scheme 5-35, highlighted in red).[59]
The Paterson reaction gave a yield of 67 % after chromatographic purification. NMR analysis showed that the *anti*- and *syn*-aldol product were present in a ratio of 5:1. The yield and the diastereomeric ratio are thus within the range of the literature values and the reaction could be successfully reproduced.[1] Subsequent protection of the hydroxy group of **34** was carried out with TBSOTf to **194** with a yield of 67 %. NMR analysis of **194** showed that it was possible to separate the diastereomers after chromatographic purification (Scheme 5-33)

After the successful synthesis of **194**, it was possible to pursue synthetic route A further.

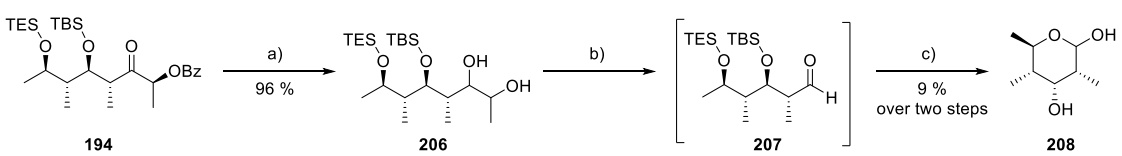

Scheme 5-36: Reagents and conditions: a) $LiBH_4$, THF, −78°C to r.t., 3 d; b) $NaIO_4$, dioxane/water, 0°C to r.t., o.n.; c) TBAF, THF, r.t. to 0 °C, 3 h.

Reduction of the keto group and the carboxylic acid ester of **194** with lithium borohydride as a strong reducing agent led to the formation of the 1,2-diol **206**, which was obtained in 96 % yield (Scheme 5-36).

The vicinal diol **206** underwent oxidative cleavage by utilizing sodium iodine periodate, which was capable of reacting with both *cis*- and *trans*-diols, making stereochemical requirements unnecessary for compound **206** [61] and yielding aldehyde **207**, which was not subjected to chromatographic purification but was directly used in further reactions.

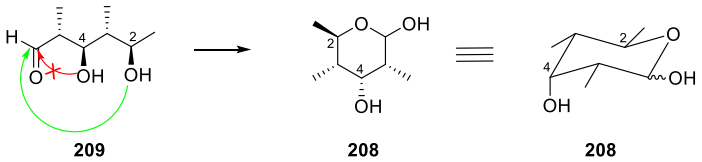

*Scheme 5-37: Cylization of **209** to **208**.*

The cyclization of the linear component **209** was initiated by deprotecting the silyl protecting groups using *tert*-butylammonium fluoride. This enabled a nucleophilic attack of the hydroxyl group in position 2 at the carbonyl group, leading to intramolecular nucleophilic addition and the formation of hemiacetal **208** (Scheme 5-37). Only the attack of the C-2 hydroxyl group was feasible, as it provided an energetically stable chair conformer. Neither the *Re* nor the *Si* side was preferentially attacked, resulting in a diastereomeric mixture of compound **208**. Deprotection and subsequent cyclization yielded a low yield of 9 % of lactol **208**.

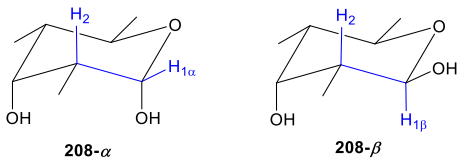

Figure 5-13: ^{1}H correlation of $H_{1\alpha}$ and $H_{1\beta}$.

Based on the ^{1}H NMR data, the anomers **208-*α*** and **208-*β*** were identified (Figure 5-13). The signal of H-1*β* in the ^{1}H NMR spectrum was identified at 4.71 ppm and exhibits a ^{3}J coupling of 8.8 Hz to H-2. The high coupling constant demonstrated the trans-axial orientation of the hydrogens and served as evidence for the formation of anomer **208-*β***. The H-1*α* signal in the ^{1}H NMR spectrum was shifted to a higher frequency of 4.94 ppm due to shielding and exhibits a lower coupling constant of 3.1 Hz.[62]

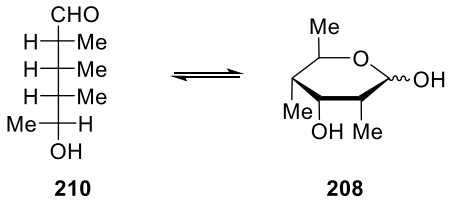

*Scheme 5-38: Open-chain Fischer projection **210** (left) and closed-chain Haworth projection **208** (right).*

Furthermore, the ^{1}H NMR data proved that the hemiacetal **208** was in equilibrium with the open-chair form (Scheme 5-38), since the characteristic singlet at 9.41 ppm could be assigned to the hydrogen of the aldehyde (Figure 5-14). This could be attributed to water in the deuterated solvent of the NMR sample or contained in the sample itself. Overall, **210**, **208-*α*** and **208-*β*** are present in a ratio of 1.5:1:0.25. It proved challenging to assign the signals from the NMR data due to the presence of anomers **208-*α***, **208-*β***, and aldehyde **210**.

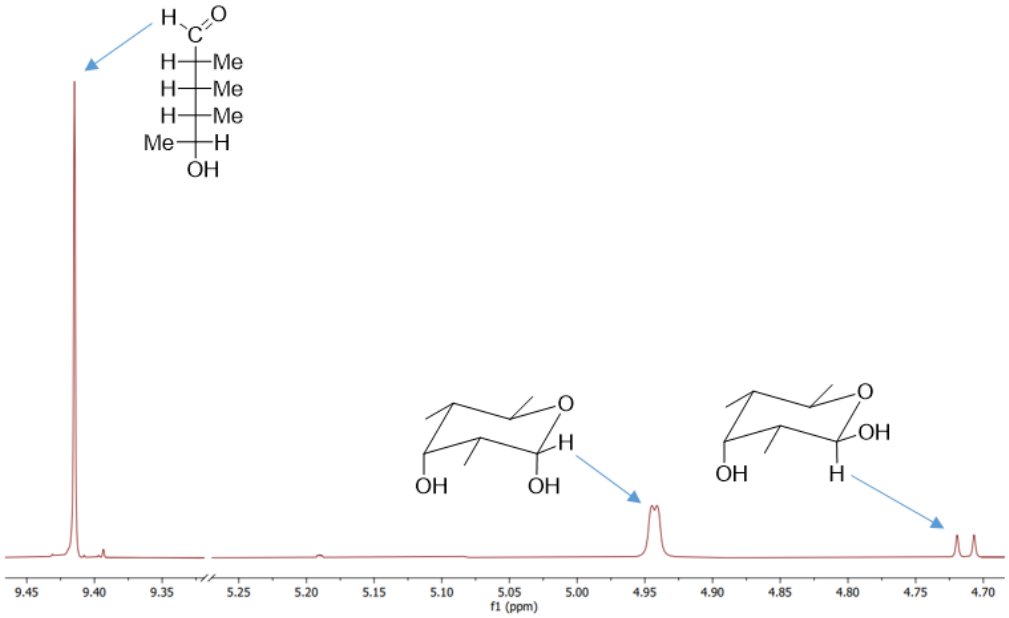

*Figure 5-14: Enlarged section of ^{1}H NMR showing characteristic signals for **208-*α***, **208-*β***, and **210**.*

It was observed that isomer **208-*α*** was formed in a larger proportion compared to isomer **208-*β***. The reason for the preferential formation of isomer **208-*α*** was the anomeric effect.

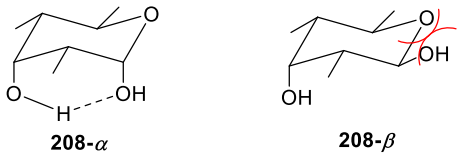

*Figure 5-15: Hydrogen bonding of **208-*α*** vs repulsion effects of **208-*β***.[63]*

The repulsive forces of the oxygen in the ring and the hydroxyl group were lowest when the latter was axially positioned. In this case, it can be assumed that a hydrogen bond was formed between the two axial hydroxyl groups resulting in a stabilized, six-membered state (Figure 5-15). In addition, the preferred axial position can be justified on the basis of electronic aspects.[63]

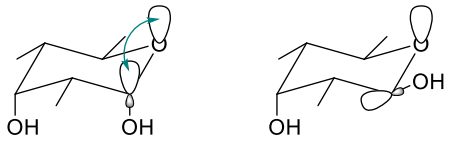

*Figure 5-16: Orbital interaction of anomer **208-α** and anomer **208-β**.[63]*

The non-bonding 2p orbital of the oxygen in the ring was likely to transfer electron density to the antibonding σ* orbital of the C-OH bond (Figure 5-16). This hyperconjugative interaction occured only when the position was antiperiplanar. In an equatorial orientation, this stereoelectronic effect could not have occurred because there would have been no optimal orbital overlap.[63]

The subsequent oxidation of lactol **208** to lactone **211** was carried out with manganese dioxide, which chemoselectively oxidized only the hydroxyl group of the anomeric center (Scheme 5-39).

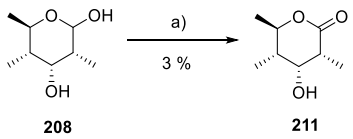

Scheme 5-39: Reagents and conditions: a) MnO_2, EtOAc, r.t., 72 h.

In the ^{13}C NMR, the characteristic signal at 173.5 ppm could be attributed to the quaternary carbon of the lactone, thus confirming that the reaction was successful, but only partially, as a low yield of 3 % was determined. The low yield of the reaction could be explained by the mechanism (Scheme 5-40).

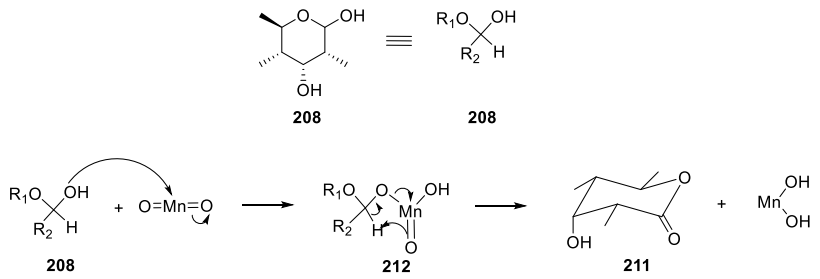

*Scheme 5-40: Mechanism of oxidation of **211**.[61]*

The nucleophilic attack of the hydroxyl group of the hemiacetal **208** on MnO_2 gave rise to a manganese ester **212** as intermediate. In a concerted reaction step, $Mn(OH)_2$ was cleaved in the +II oxidation state to give the lactone **211**. It was reasonable to assume that molecule **208-α** was the weaker nucleophile because of the hydrogen bonding involving the axially aligned hydroxy groups (Figure 5-15). Consequently, the nucleophilic attack of **208-*β*** occurred more rapidly. Hence, the nucleophilic attack on MnO_2, as described in the mechanism, was expected to primarily involve **208-*β***. However, this particular anomer was found to be in lower abundance due to the previously mentioned stabilizing effects. Furthermore, MnO_2 oxidation exhibited chemoselectivity at the anomeric center, preventing any reaction with isomer **210**. Simultaneously, the presence of aldehyde **210** increased the polarity of the reaction mixture and partially deactivated the manganese dioxide.

This partial deactivation of MnO_2 was also the reason for the preference for strongly apolar solvents. Nonetheless, the reaction had to be conducted in ethyl acetate due to solubility challenges. In contrast, synthetic route B yielded more favorable results.

In synthetic pathway B, the process commenced with the targeted removal of the TES protecting group from the linear fragment **194** (Scheme 5-41). Subsequently, this compound was cleaved using trifluoroacetic acid, thereby instigating cyclization through an intramolecular nucleophilic addition.

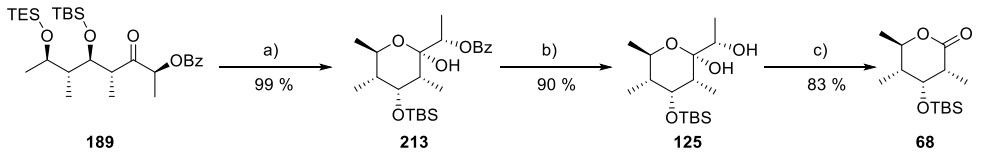

Scheme 5-41: Reagents and conditions: a) TFA, THF, H_2O, 0 °C, 4 h; b) NaOMe, CH_2Cl_2, MeOH, r.t., 16 h; c) $NaIO_4$, H_2O, r.t., 19 h.

The nucleophilic attack predominantly took place from the *Si* side of the carbonyl group. Both the TBS protecting group and the benzoyl group imposed significant steric hindrance, making an attack from the *Re* side unfavorable. Consequently, the resulting stereocenter had an *R* - configuration. Therefore, it was crucial to selectively remove only the triethylsilyl protecting group, capitalizing on the varying stability of the silyl protecting groups. The TBS protecting group, which was more sterically demanding, remained intact when treated with the trifluoroacetic acid reagent.

Subsequent basic hydrolysis of the benzoyl group gave *syn* 1,2-diol **125** in an excellent yield of 90 % (Scheme 5-41).

Following the successful synthesis of diol **125**, it was proceeded with another attempt to synthesize lactone **68** through synthesis pathway A, employing oxidative cleavage. Remarkably, this reaction yielded a high yield of 83 % (Scheme 5-41).

The lactone **68** obtained, while still bearing its TBS protecting group, was found to be identical to the lactone prepared by Trauner and Schröckeneder for the subsequent but unsuccessful Takai-Lombardo reaction (section 3.1)[16]. However, the distinctive advantage of this synthetic route lies in the fact that lactone **68** was obtained as a single isomer. In contrast, Schröckeneder obtained lactone **68** as a minor isomer within a diastereomeric mixture, with a ratio of 1:15, which proved challenging to completely separate.

Based on the NMR data, it was determined that **68** adopted a chair conformation. This determination was made based on the observed coupling constants that are commonly associated with chair conformations. For instance, the coupling constant between the hydrogens at C-5 and C-4 measured 10.7 Hz, a value typically found for trans - axial positions. Similarly, the coupling constant between the hydrogens at C-4 and C-3 was 1.4 Hz, indicating the presence of an axial and an equatorial hydrogen pair. The coupling constant between C-3 and C-2, slightly elevated at 2.6 Hz due to the nearby carbonyl group, still corresponded to the coupling constant expected between an axial and an equatorial hydrogen.

However, it's important to note that due to the planarity of the lactone group, this chair conformation was not ideal (Figure 5-17).

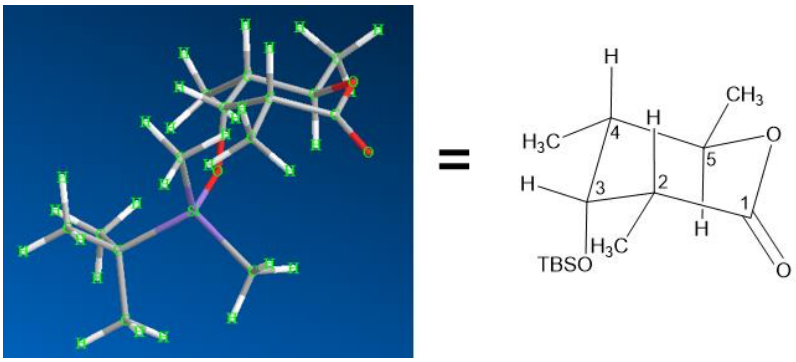

*Figure 5-17: 3D view from **68**.*

Upon obtaining lactone **68**, attempts were made to conclude synthetic pathway A by applying the modified Julia olefination method (Scheme 5-42). However, despite repeated efforts, the only observed outcome was the decomposition of the starting material. As a result, work on pathway A was halted at this juncture.

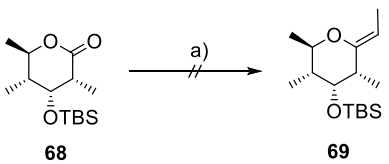

*Scheme 5-42: Reagents and conditions: a) 1. **139**, LiHMDS, THF, −78°C, 2 h; 2. DBU, THF, r.t., 1 h.*

Meanwhile, work continued on synthetic pathway B. Here, the goal was to synthesize the thiocarbonate **127**. In the initial attempt, thiophosgene was employed, akin to the procedure described in section 5.1.6. However, the objective this time was to isolate the thiocarbonate **127**. Regrettably, under these reaction conditions, only decompositions occurred, yielding unknown by-products.

Subsequently, by substituting thiophosgene with thiocarbonyldiimidazole (TCDI), it was successfully obtained product **127** with a yield of 87 % after chromatographic purification (Scheme 5-43).

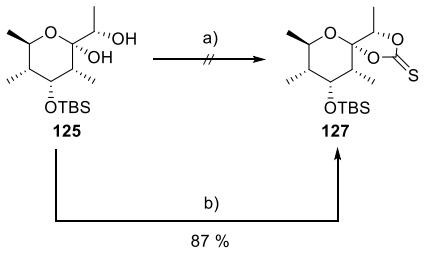

Scheme 5-43: Reagents and conditions: a) $CSCl_2$, DMAP, CH_2Cl_2, r.t., 4 h; b) TCDI, DMAP, CH_2Cl_2, r.t., 50 h.

Given the formation of a spiro center in **127**, preventing any rotation of the stereocenter, the stereochemistry established by the Frater-Seebach, Paterson-Aldol, and cyclization reactions could be validated through NMR experiments. To confirm the correct configuration of the labeled stereocenters, primarily ^{1}H, ^{1}H - COSY, and NOESY correlations were employed.

The stereocenters at C-2 and C-7 provided a reliable reference point, as these stereocenters could be traced back to commercially available reactants whose absolute configurations were known.

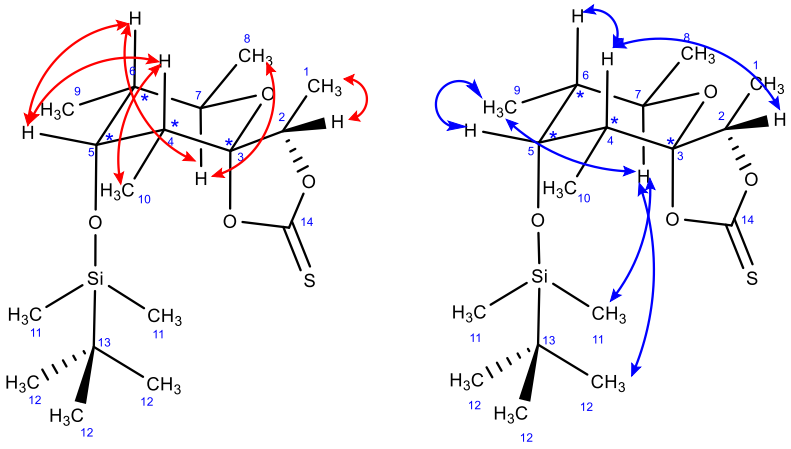

*Figure 5-18: The major ^{1}H,^{1}H-COSY correlations (left, red) and NOESY correlations (right, blue) of fragment **127**.*

The stereo center at C-6 was formed during the Frater-Seebach methylation, and the ^{1}H signals for C-7 and C-6 displayed a substantial coupling constant of 10.2 Hz, suggesting a

trans-axial orientation for the hydrogens. This observation provided strong evidence for the stereochemistry at these positions.

In the Paterson aldol reaction, both stereocenters C-4 and C-5 were established, and their respective hydrogens exhibited a low ^{3}J coupling constant of 2.2 Hz, indicating a torsion angle of 60° between them. Additionally, the correlation between C-4 and C-6 was only possible when the hydrogens at C-4 and C-6 were aligned axially upward. Furthermore, a correlation was found between the methyl group at C-9 and the hydrogen at C-5. These observations collectively confirmed the stereochemistry of stereocenters C-4, C-5, and C-6.

Regarding the C-3 stereocenter, which was a quaternary carbon, identification and final confirmation primarily relied on the ^{13}C-DEPT and HMBC data sets. As a result, the stereochemistry of C-3, C-4, C-5, and C-6, all formed during the synthesis, was considered confirmed and accurate. Consequently, fragment **127** could be used for the subsequent elimination.

The initial attempt at reductive syn-elimination involved 1,3-dimethyl-2-phenyl-1,3,2-diazaphospholidine (Table 5-10, entry 1), but no reaction was observed. Subsequently, trimethyl phosphite was employed, also serving as the solvent (Table 5-10, entry 2). Unfortunately, this led only to the formation of by-products and decomposition. Finally, triethyl phosphite was used (Table 5-10, entry 3), resulting in the successful formation of the desired dienophile **69** with a moderate yield of 63 %.

*Table 5-10: Reagents and conditions for the Corey-Winters elimination from **127** to **69**.*

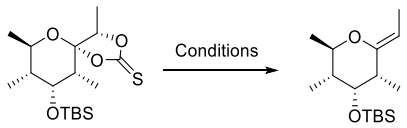

127 **69**

Entry	Reagents	Solvent	Temp.	Reaction Time	Yield
1	1,3-Dimethyl-2-phenyl-1,3,2-diazaphospholidine 6 eq.	THF	57 °C	16 h	-
2	$P(OMe)_3$	-	120 °C	16 h	-
3	$P(OEt)_3$	-	160 °C	16 h	63 %

The final structure of dienophile **69** was confirmed through NMR data analysis. The precise locations of hydrogen atoms were determined using ^{1}H,^{1}H - COSY correlations, and the quaternary carbon C-3 was identified through HMBC correlations (Figure 5-19).

The formation of the double bond was evident from the chemical shifts of the carbon atoms. For example, C-2 exhibited a chemical shift of 101.8 ppm, while C-3 displayed a chemical shift of 154.8 ppm, both of which were indicative of a typical double bond.[64]

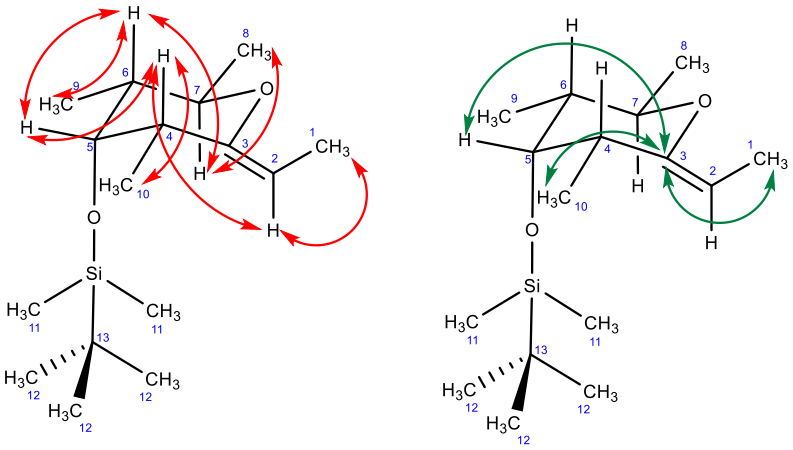

*Figure 5-19: The major $^{1}H,^{1}H$-COSY correlations (left, red) and HMBC correlations (right, green) of **69**.*

Additionally, NOESY data revealed a correlation between H-2 and H-10, indicating the formation of *Z* - alkenes (Figure 5-20, bottom). In contrast, a correlation between the methyl group H-1 and either H-10 or H-4 would suggest an *E* - alkene configuration. Since no such NOESY correlations were observed, the possibility of an *E* - alkene could be ruled out.
However, it's worth noting that there was no NOESY correlation between H-4 and H-2, which would have been expected. This could likely be explained by the fact that, aside from the double bond at C-3 and its planarity, it was not possible to achieve an ideal chair conformation due to the axial position of the TBS protecting group, pushing the equatorially located methyl groups further upward. Consequently, the axial H-4 was not in close proximity to H-2, preventing the occurrence of a NOESY correlation (Figure 5-20, top).

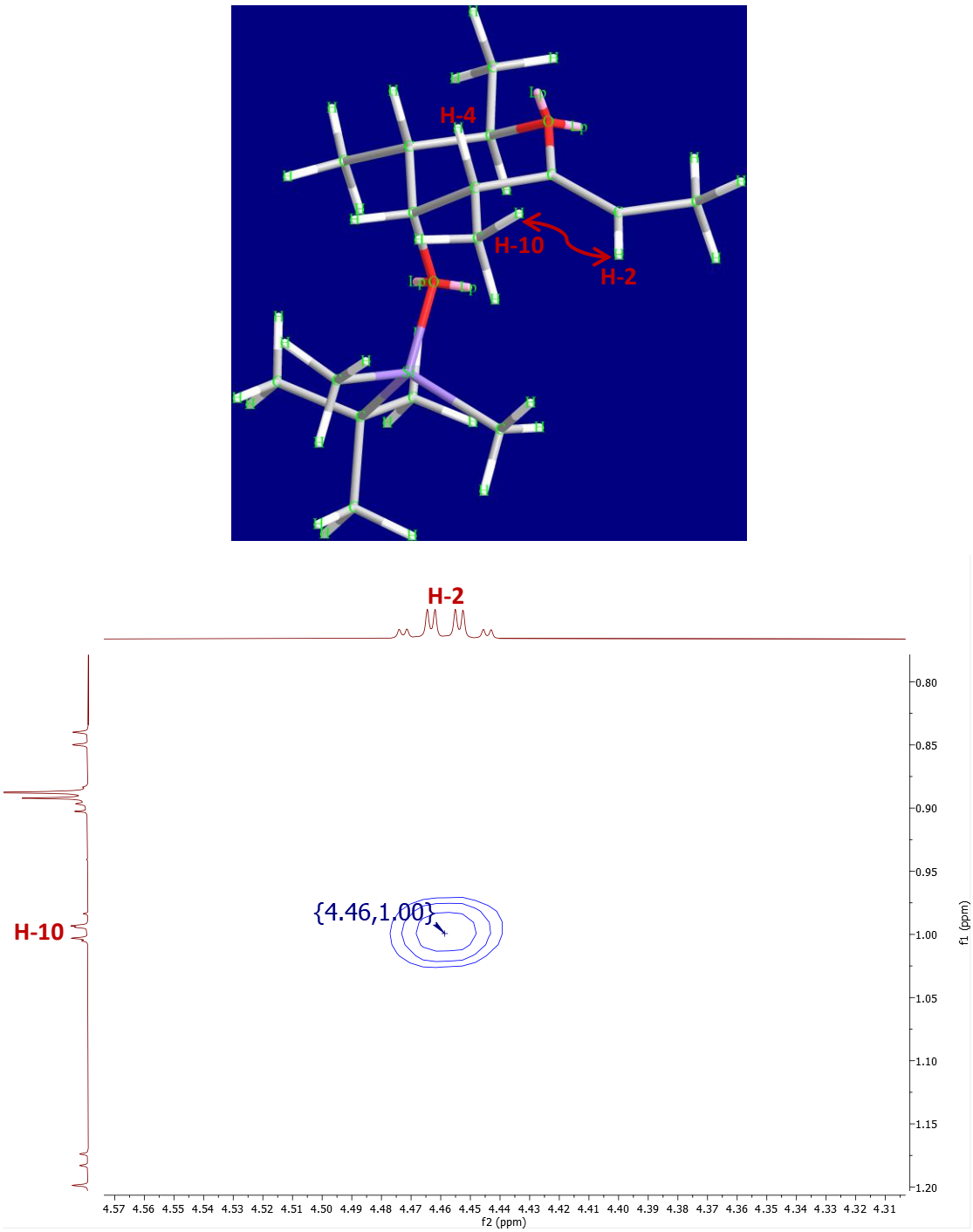

*Figure 5-20: Top: 3D visualization of **69** an the NOESY correlation between H-2 and H-10. Bottom: Section from the NOESY NMR of **69** showing the NOESY correlation between H-2 and H-10.*

Furthermore, it was possible to address whether a $^{1}C_{4}$ chair conformation or a $^{4}C_{1}$ chair conformation was present (Figure 5-21). To determine this, the coupling constant was analyzed between H-6 and H-7. A coupling constant within the higher range, typically between 8 - 11 Hz, would suggest the presence of a trans axial interaction. Conversely, if a trans equatorial position existed, a lower coupling constant in the range of 2 - 4 Hz would be expected.

With the coupling constant between H-6 and H-7 measured at 10.1 Hz, falling within the range of *trans* - axial coupling constants, it was concluded that a $^{4}C_{1}$ chair conformation was present.

This conclusion arised from the fact that in the $^4C_1$ conformation, both hydrogen atoms were positioned as *trans* - axial to each other.[62,64]

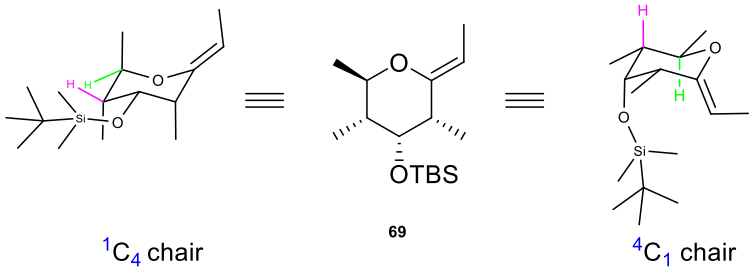

*Figure 5-21: Chair conformation of **69**; Left: $^1C_4$ chair conformation of **69**; Right: $^4C_1$ chair conformation of **69**.*

5.1.15 Conclusion of the Double Pathway Approach

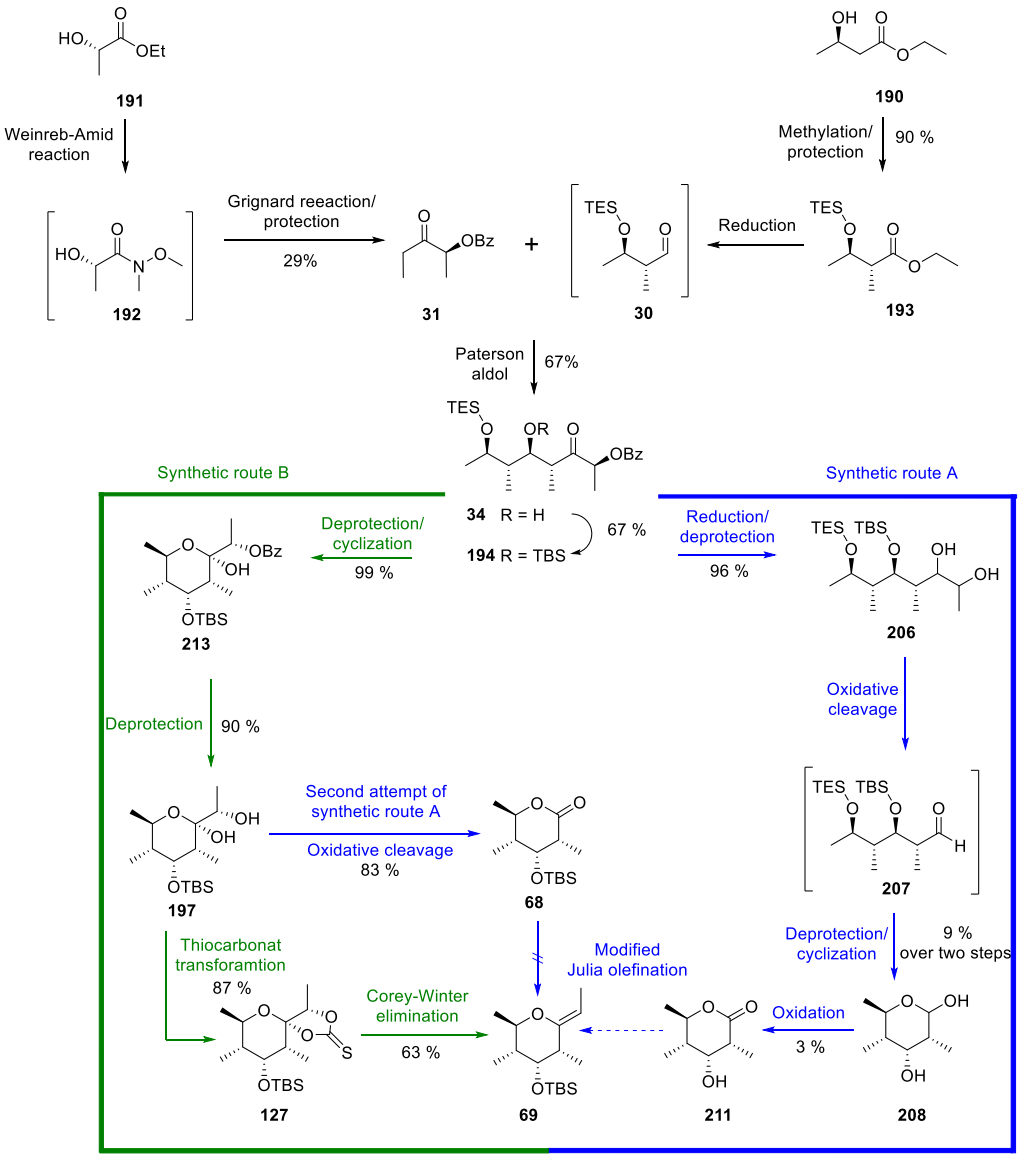

Scheme 5-44: Summary of the double synthetic pathway approach.

In summary, synthetic route B led to the desired dienophile **69**. With a total of 9 steps and a longest linear sequence of 7 steps with an overall yield of 20 %, a reliable and effective synthetic route to dienophile **69** was developed. In addition, the complete structure and conformation of dienophile **69** could be elucidated by NMR experiments.

5.2 Synthesis of Portentol *via* IEDDA Reaction

5.2.1 Synthetic Progress of the IEDDA Reaction

In Section 3.3, it was demonstrated that diene **2** underwent an IEEDA reaction, but benzyl vinyl ether (**98**) was used as the dienophile. Firstly, its double bond was only terminal, and secondly, it was a linear molecule. Since the planned dienophile **69** had both a *Z* double bond with a methyl group and was cyclic, an investigation was undertaken to determine whether these factors affected the IEDDA reaction.

Initially, the influence of the methyl group was examined using enol ether **111**, as discussed in Section 5.1.3. This molecule closely resembled benzyl vinyl ether (**98**), making it easier to compare the differences between a terminal enol ether and an allylic enol ether as dienophiles, and to elucidate the impact of the methyl group and the *Z* configuration.

The reaction conditions were chosen as previously described in section 3.3, with Yb(fod)3 as the catalyst. However, despite previously resulting in a Diels-Alder product with **98** as the dienophile, the reaction conditions used for **111** did not yield any observable reaction. This indicated that the *Z* configuration of the double bond and the presence of the methyl group had a negative influence on the reaction.

Following further research, particularly an examination of the work conducted by Posner *et al*. on IEDDA reactions under high pressure conditions, it was determined to replicate the reaction using the same conditions. However, for this attempt, zinc chloride was employed as the catalyst instead of the lanthanide-based catalyst $Yb(fod)_3$.[29] As a consequence of this modification, the Diels-Alder product **223 *exo*** was formed in a yield of 45 %, and product **223 *endo*** was obtained in a yield of 5 % (Scheme 5-45).

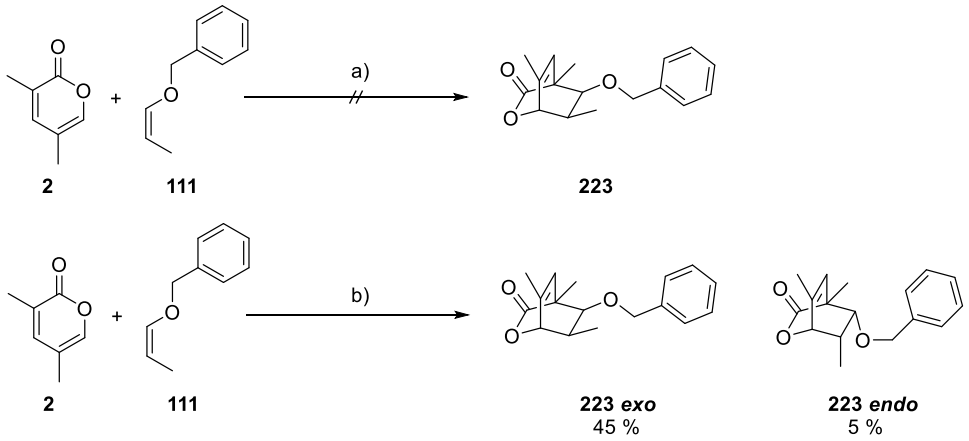

Scheme 5-45: Reagents and conditions: a) Yb(fod)$_3$ (cat.), CH_2Cl_2,11-12 kbar, r.t., 3 d; b) $ZnCl_2$ (cat.), CH_2Cl_2,11 - 12 kbar, r.t., 3 d.

The positive outcome of the reaction could be clearly attributed to the change in the catalyst from Yb(fod)$_3$ to zinc chloride. This was likely because zinc chloride was less sterically demanding in comparison. Interestingly, the main product formed was the *exo* product, with a significant excess in a 9:1 ratio.

Isomer **223 *exo*** and isomer **223 *endo*** were distinguishable through NOESY correlations. For example, the NOESY NMR data for the *exo* product revealed correlations between H-3 and H-4, indicating that they were oriented on the same side. Furthermore, H-4 exhibited correlations with H-5, supporting the conclusion that H-3, H-4, and H-5 all faced downward. Additionally, H-8 and H-10 of the methyl groups showed correlations, implying that the methyl group H-10 was equatorially positioned and pointing upwards.

In contrast, the *endo* product exhibited no NOESY correlation between H-8 and H-10, confirming that the methyl group H-10 in the *endo* product occupied an axial position (Figure 5-22).

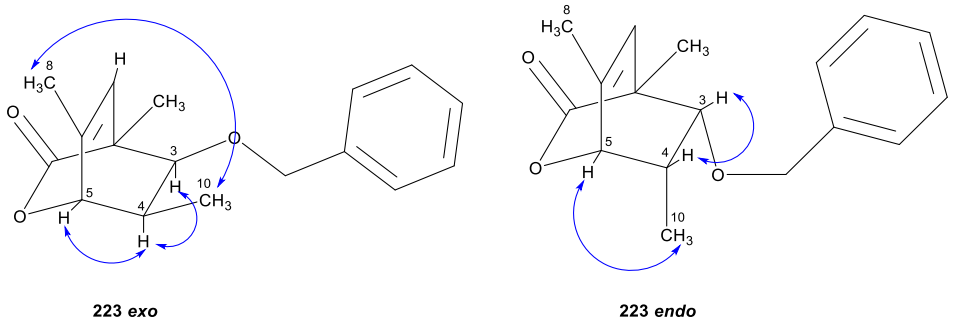

*Figure 5-22: Left: NOESY correlation of **223 exo**. Right: NOESY correlation of **223 endo**.*

In the transition state **TS 223 *exo***, dienophile **111** approached diene **2** in a manner where the methyl group of **111** was positioned beneath the oxygen of the lactone. Consequently, there were no repulsive interactions between the oxygen and the methyl group. Furthermore, in this transition state, it was unlikely that any unfavorable steric interactions occurred between $ZnCl_2$

and dienophile **111**, and there were no steric clashes between the benzyl group of **111** and diene **2** (Figure 5-23).

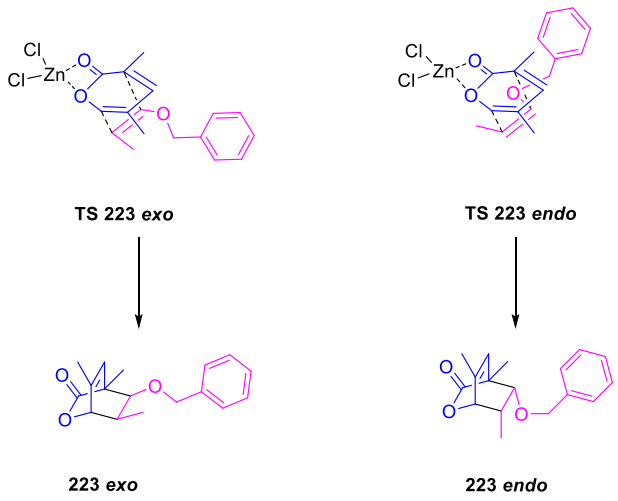

*Figure 5-23: Left: Transition state to **223** exo. Right: Transition state to **223** endo.*

In the transition state **TS 223 *endo***, however, the possibility of repulsive steric interactions between the methyl group and the benzyl group of fragment **111** with diene **2** existed. Furthermore, negative interactions with the Lewis acid and the methyl moiety were conceivable (Figure 5-23). This led to the conclusion that the diastereomeric outcome of the reaction was substrate-controlled.

Next, dienophile **179**, previously synthesized in Section 5.1.12, was employed to gain further insights into the IEDDA reaction. Compound **179** shared a highly similar structure with the final dienophile **69**, and both molecules possessed identical stereocenters. The reaction was once again conducted under high pressure conditions with $ZnCl_2$ as the catalyst. To ensure complete conversion of the substrate, the reaction was maintained under 11 - 12 kbar pressure for 7 days instead of 3 days, due to the presence of unreacted diene **2** in the previous IEDDA reaction.

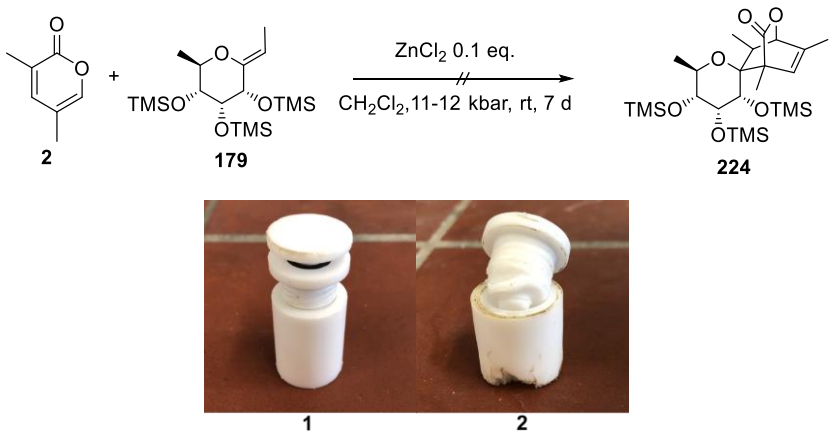

*Figure 5-24: Top: Failed high pressure reaction towards **224**. Bottom: Left: Teflon ampoule before the reaction. Right: Teflon ampoule after the reaction.*

Unfortunately, the reaction didn't succeed due to the Teflon ampoule bursting during the process, resulting in the loss of the entire reaction solution (Figure 5-24). Consequently, a new design for the Teflon ampoule was necessary to reduce the risk of bursting during high-pressure conditions and to prevent leakage issues.

With this goal in mind, the screw cap of the Teflon ampoule underwent a revision. The new design features a screw cap with an opening that tapers conically toward the bottom. This opening can be sealed using a bolt. Unlike the previous double screw cap, this new design ensured that the screw cap no longer deformed when closed, requiring only one rubber ring between the screw cap and the ampoule. The smaller rubber ring used between the two screw caps in the initial design was particularly vulnerable to organic solvents and became brittle under pressure, creating a weak point.

Furthermore, the underside of the screw cap was now slightly conical, as illustrated in Figure 5-25 on the right. This alteration aims to distribute the pressure across the entire ampoule lid more evenly. The lid was finally secured with a bolt. This design allowed for the ampoule to be initially screwed shut and then completely filled with the reaction solution before sealing it with the bolt. This approach serves two important purposes: firstly, it prevented leakage when sealing a filled ampoule, and secondly, it ensured that the ampoule was entirely filled, as the presence of air pockets could led to ampoule bursting under pressure.

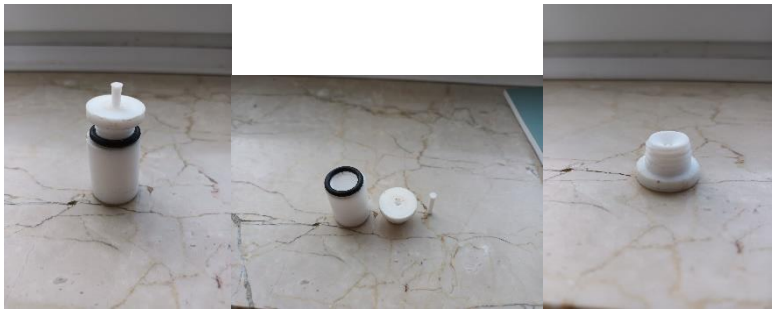

Figure 5-25: New Teflon ampoule design.

With the newly designed Teflon ampoule, the IEDDA reaction was carried out under high pressure. This time, dienophile **145**, which had been synthesized in section 5.1.9, was employed. Compound **145** was chosen due to its cost effectiveness, quicker production, and greater availability. Although it had been confirmed that the new Teflon vial withstood the conditions and met expectations, the reaction itself resulted in an unidentifiable mixture of substances and partial decomposition (Scheme 5-46).

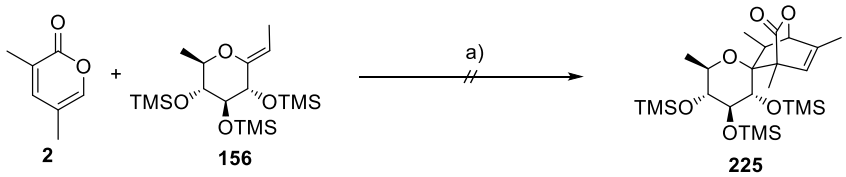

Scheme 5-46: Reagents and conditions: a) $ZnCl_2$ (cat.), CH_2Cl_2,11-12 kbar, r.t., 7 d.

The TMS protecting group of dienophile **156** was identified as the reason behind the reaction's failure. This group proved to be highly susceptible to the chosen reaction conditions. Despite the setback in the IEDDA reaction, the decision was made to proceed with the authentic dienophile **69**, as small quantities of **69** had been successfully synthesized at the time. Moreover, fragment **69** was devoid of any TMS groups.

Regrettably, the IEDDA reaction between diene **2** and dienophile **69** did not yield the desired outcome. Instead, the reaction solution exhibited a complex mixture of various substances. Notably, none of these substances proved to be the target product **226**; instead, the isolation of hemiacetal **227** was achieved (Scheme 5-47).

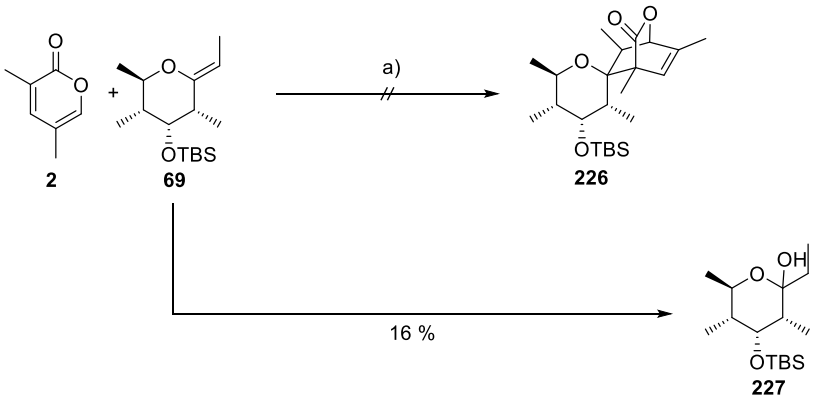

Scheme 5-47: Reagents and conditions: a) $ZnCl_2$ (cat.), CH_2Cl_2,11-12 kbar, r.t., 3 d

Subsequent experiments consistently demonstrated the production of hemiacetal **227**. Despite the substantial efforts dedicated to conducting the reaction under anhydrous conditions, the persistence of hemiacetal **227** formation indicated the presence of residual water traces.

An experiment involving the combination of dienophile **69** solely with the catalyst $ZnCl_2$ revealed that enol ether **69** exhibited instability in the presence of this Lewis acid, resulting in the formation of hemiacetal **227**. This observation indicated that $ZnCl_2$ was ill-suited as a Lewis acid catalyst for this reaction.

In pursuit of an appropriate Lewis acid catalyst, diene **2** and dienophile **69** were subjected to reactions with various Lewis acids. High pressure conditions were not chosen for several reasons: firstly, the high-pressure setup proved to be extremely time-consuming, and secondly, the available Teflon ampoules exhibited structural weaknesses after a maximum of three uses under high pressure, rendering them unsuitable for high-throughput screening. Additionally, under standard pressure conditions, the reaction progress could be monitored using TLC, a capability unavailable in high pressure processes

Table 5-11: Reagents and conditions for test screening for the IEDDA reaction.

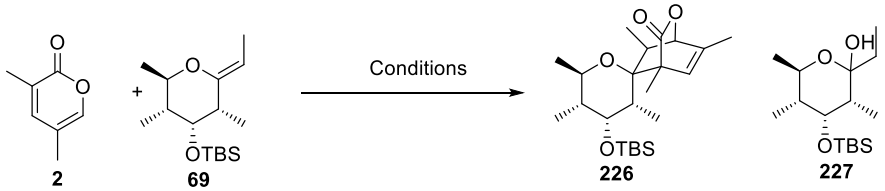

2 **69** **226** **227**

Entry	Reagents	Solvent	Temp.	Reaction Time	**226**	**227**
1	$ZnBr_2$ 10 mol%	CH_2Cl_2	r.t.	20 h	-	✓
2	$BF_3{*}OEt_2$ 10 mol%	CH_2Cl_2	r.t.	20 h	-	✓
3	$Eu(hfc)_3$ 10 mol%	CH_2Cl_2	r.t.	20 h	-	-
4	$Eu(hfc)_3$ 10 mol%	CH_2Cl_2	40 °C	20 h	-	-
5	$Eu(hfc)_3$ 10 mol%	CH_2Cl_2	45 °C	20 h	-	-

Literature described $ZnBr_2$ and $BF_3{*}OEt_2$ as reliable Lewis acid catalysts especially in the case of 2-pyrones,[22] but applying both of them as catalysts, the reactions resulted in the formation of hemiacetal **227** (Table 5-11 entry 1 and 2). $Eu(hfc)_3$, a lanthanide-based Lewis acid, had been reported to be effective in IEDDA reactions with 2-pyrones and enol ethers.[65] Noticeable $Eu(hfc)_3$, showed no formation of the hemiacetal **227**. However, also no formation of the Diels-Alder product **226** was observed (Table 5-11 entry 3). Also elevated temperatures did not lead to any reaction (Table 5-11 entry 4 and 5). This was taken as an opportunity to test the reaction with $Eu(hfc)_3$ under high pressure conditions.

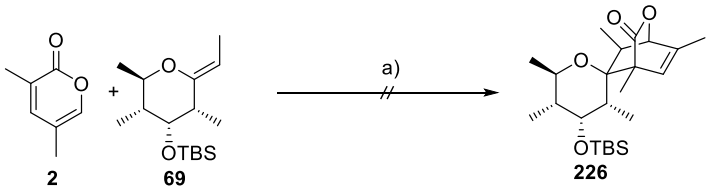

Scheme 5-48: Reagents and conditions: a) Eu(hfc)$_3$ (cat.), CH_2Cl_2,11-12 kbar, r.t., 3 d.

However, this reaction also failed to yield the desired product **226**, and no hemiacetal **227** was formed (Scheme 5-48). Instead, only decomposition product of dienophile **69** was found, although their exact structures could not be definitively determined.

To enhance the reactivity of the IEDDA reaction, it was necessary to convert the *α*-methyl group of 3,5-dimethylpyrone (**2**) into an ester group. Replacing the methyl group with a carbonyl group on the 2-pyrone ring increased the electron deficiency of the diene, thereby augmenting its reactivity in the IEDDA reaction. Additionally, the presence of a second carbonyl group at C-3 induced a chelating effect with metal-based Lewis acids, promoting the complexation of the diene and further activating it.[22] Following the IEDDA reaction, the carbonyl group could subsequently be converted back into a methyl group through reduction (Scheme 5-49).

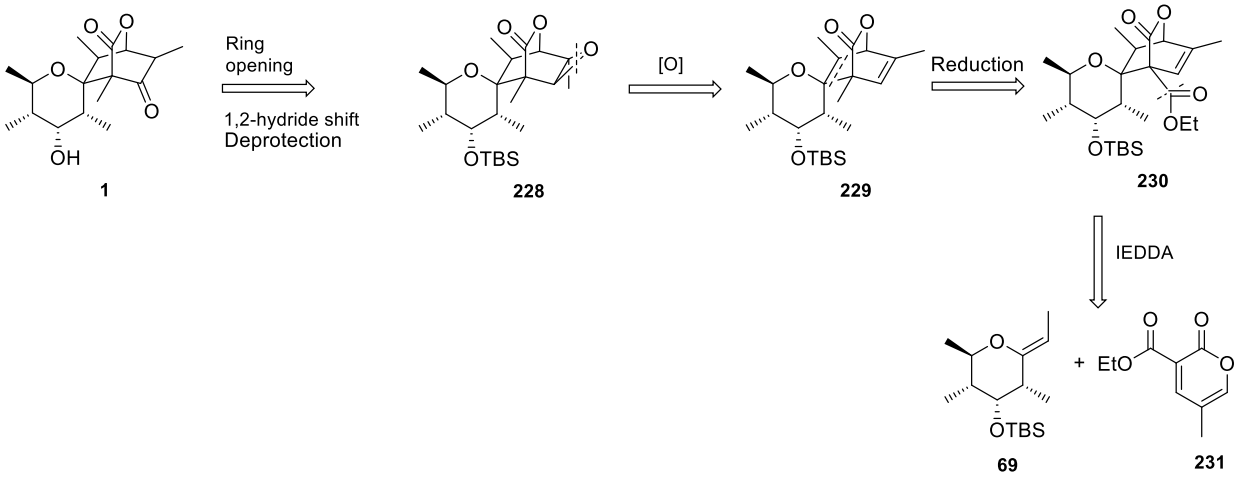

*Scheme 5-49: New retrosynthesis towards Portentol (**1**) via IEDDA reaction.*

For this reason, the known substituted 2-pyrone, **231**, as described in the literature, was synthesized. Compound **231** was obtained through a Knoevenagel condensation reaction involving 3-ethoxy-methacrolein (**232**) and diethyl malonate. The reaction yielded 50 %, which was comparable to the 54 % yield reported in the literature.[66–68]

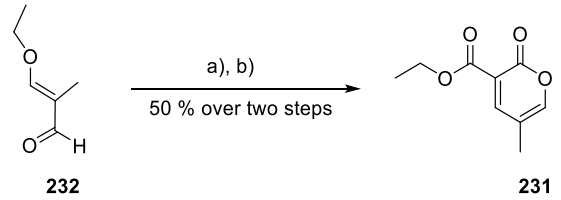

Figure 5-26: Reagents and conditions: a) 1. Diethyl malonate, $ZnCl_2$, Ac_2O, reflux, 4 h, b) HCO_2H, reflux, 1 h.[66–68]

With the new diene **231** available, a screening under normal pressure conditions was conducted to assess whether the reactivity of diene **231** was adequate for an IEDDA reaction with dienophile **69**.

Table 5-12: Reagents and conditions for test screenings for the IEDDA reaction.

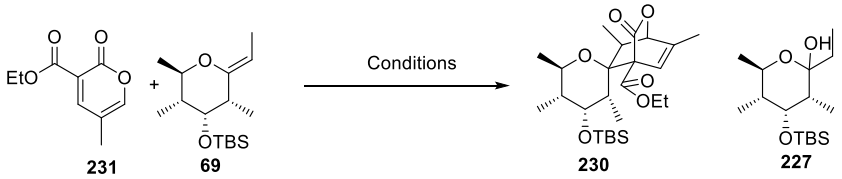

Entry	Reagents	Solvent	Temp.	Reaction Time	**230**	**227**
1	$ZnCl_2$ 10 mol%	CH_2Cl_2	r.t.	20 h	-	✓
2	$ZnBr_2$ 10 mol%	CH_2Cl_2	r.t.	20 h	-	✓
3	$Yb(OTf)_3$ 10 mol%	CH_2Cl_2	r.t.	20 h	-	✓
4	$Eu(hfc)_3$ 10 mol%	CH_2Cl_2	r.t.	20 h	-	-
5	$Eu(hfc)_3$ 100 mol%	CH_2Cl_2	r.t.	20 h	-	-
6	$Eu(hfc)_3$ 100 mol%	CH_2Cl_2	40 °C	20 h	-	-
7	$Eu(hfc)_3$ 100 mol%	CH_2Cl_2	80 °C	20 h	-	-

The Lewis acids $ZnCl_2$ and $ZnBr_2$, once again, resulted in the formation of hemiacetal **227** (Table 5-12, entries 1 and 2). Even Yb(OTf)3, which, as indicated in the literature, had shown promise in Diels-Alder reactions with diene **231**[22,66] only led to the formation of molecule **227** (Table 5-12, entry 3). Surprisingly, the catalyst Eu(hfc)3 did not yield either hemiacetal **227** or the Diels-Alder product **230** (Table 5-12, entry 4).

Attempts to increase the catalyst loading to equivalent amounts and elevate the temperature also failed to produce the desired product (Table 5-12, entries 5-7). Notably, throughout the entire screening, it was observed that dienophile **69** underwent decomposition over time. Nevertheless, the reaction with Eu(hfc)3 as a Lewis acid catalyst was tested under high pressure conditions. Unfortunately, this reaction did not result in the formation of the Diels-Alder product **230**. Instead, only the decomposition of dienophile **69** was observed (Scheme 5-50).

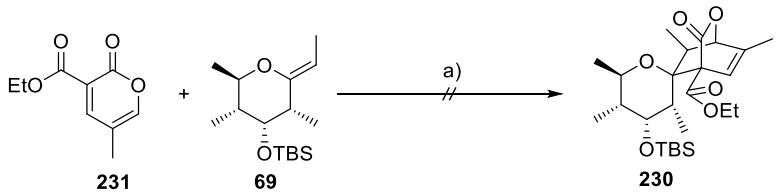

Scheme 5-50: Reagents and conditions: a) Eu(hfc)$_3$ (cat.), CH_2Cl_2,11-12 kbar, r.t., 3 d.

These results demonstrated that the Lewis acid catalysts induced the transformation of dienophile **69** into hemiacetal **227**. Additionally, dienophile **69** proved to be unstable and underwent self-decomposition, a process that may have been exacerbated by the presence of Lewis acids. Furthermore, it was possible that diene **2** remained too electron-rich for an effective IEDDA reaction. Steric hindrance and a potentially high energy barrier might have also impeded the reaction. Therefore, it was concluded that the reaction was best conducted without a Lewis acid catalyst. To optimize the IEDDA reaction, two approaches were considered.

The first option was to increase the electron density at the double bond of the dienophile. However, in this case, this was not possible since the fragment at the enol ether could not be further modified. The second option was to enhance the electron deficiency of the diene. This had already been achieved by replacing the methyl group with an ester group, a modification that allowed for the reversible transformation of the ester group back into a methyl moiety after the IEDDA reaction (Scheme 5-49).

By substituting the ethyl ester with a pentafluorophenol ester, it was feasible to make the pyrone even more electron-poor. Posner *et al.* successfully conducted an IEDDA reaction using the highly reactive pyrone **233**. The fluorinated pyrone **233**, under Lewis acid catalysis, initially did not react with the enol ether **234**. Instead, it led to the decomposition of diene **233**. However, when the reaction was conducted at a temperature of 80°C, it resulted in the successful formation of the Diels-Alder product **235** without the use of a Lewis acid (Scheme 5-51).[69]

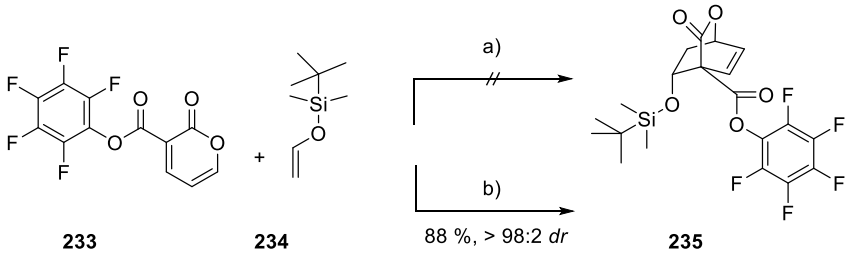

Scheme 5-51: IEDDA reaction by Posner et al. Reagents and conditions: a) Lewis acid, CH_2Cl_2, −78°C; b) CH_2Cl_2, 80°C, 4 h,[69]

A suitable diene with a pentafluorophenol group for the IEDDA reaction to portentol (**1**) could be obtained by esterification of the carboxylic acid **237** with pentafluorophenol. The carboxylic acid **237** could in turn be obtained from saponification of the already synthesized ethyl ester **231** (Scheme 5-52).

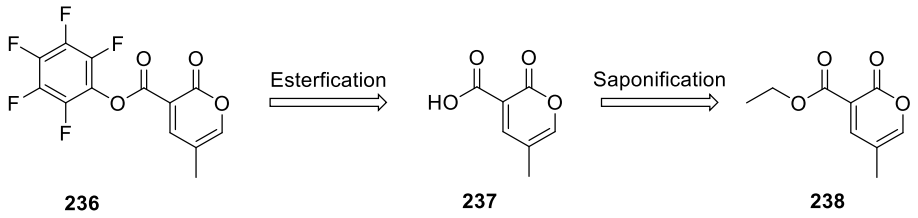

*Scheme 5-52: Retrosynthesis of diene **236**.*

However, before starting the synthesis of diene **236**, the IEDDA reaction was first tested with the known pyrone **233** to assess the applicability of this method in the context of this study. The synthesis of pentafluorophenol ester **233** was literature known.[69,70] The synthesis began with the saponification of methylester pyrone **239**. In the literature, this process yielded 78 %.[70] Initially, this yield could not be reproduced. However, no further efforts were made to optimize the reaction since a sufficient quantity of carboxylic acid **240** was obtained. The subsequent esterification to form pentafluorophenol ester **233** also resulted in a lower yield, achieving only 32 % compared to the literature yield of 71 % (Scheme 5-53).[69]

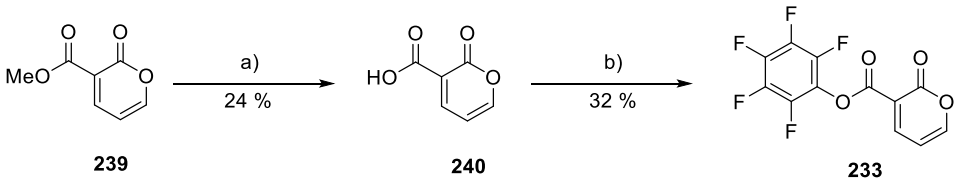

Scheme 5-53:Reagents and conditions: a) TMS_2, I_2. CH3Cl, reflux, 16 h; b) Pentafluorophenol, EDC, CH_2Cl_2, −78°C, 16 h. [69]

To confirm the reactivity of pyrone **233**, dienophile **241** was employed for the IEDDA reaction instead of dienophile **69**. The latter was only available in limited quantities, and larger quantities could not be prepared due to its instability, which was discovered later on. It was found that compound **69** could not be stored for an extended period as it tends to decompose over time. The benzyl group was chosen as an alternative because it was more stable compared to the TMS protecting groups used in the previously employed test dienophile **156**. Molecule **241** was synthesized from alkene **158**, which was prepared in section 5.1.9, through benzylation with a moderate yield of 67 %. (Scheme 5-54).

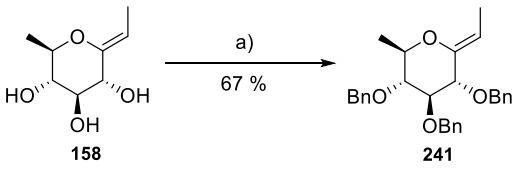

Scheme 5-54: Reagents and conditions: a) BnBr, NaH, DMF, 0°C to r.t., 16 h.

Dienophile **241** was utilized to investigate the IEEDA reaction with diene **233**. For this purpose, the reaction was conducted under three different conditions. Initially, it was carried out under normal pressure at room temperature, but TLC analysis revealed no conversion. Subsequently, the reaction was heated to 55°C, but this also did not result in any observable effect. Finally, the reaction was performed at room temperature under high pressure, leading to the formation of the Diels-Alder product **242** and hemiacetal **243** (Scheme 5-55).

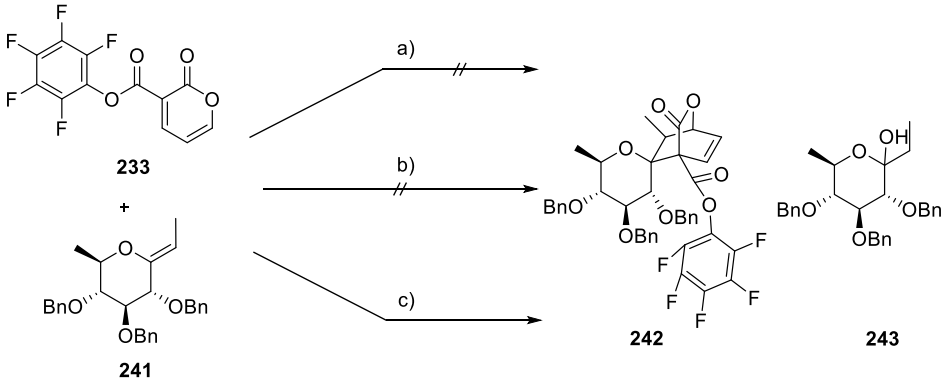

Scheme 5-55: Reagents and conditions: a) CH_2Cl_2, r.t., 24 h; b) CH_2Cl_2, 50°C, 24 h; c) CH_2Cl_2, r.t. 96 h 11-12 kbar.

Following column chromatographic separation, molecule **242** was initially detected through mass spectroscopy. However, upon conducting NMR structure elucidation of compound **242**, it was found that only trace amounts of this molecule had formed. The primary product of the IEDDA reaction turned out to be the elimination product **244**. As a result, further NMR analysis of molecule **242** was not feasible. However, despite the mixture of compounds, the structure of the other Diels-Alder product **244** could be determined by NMR analysis.

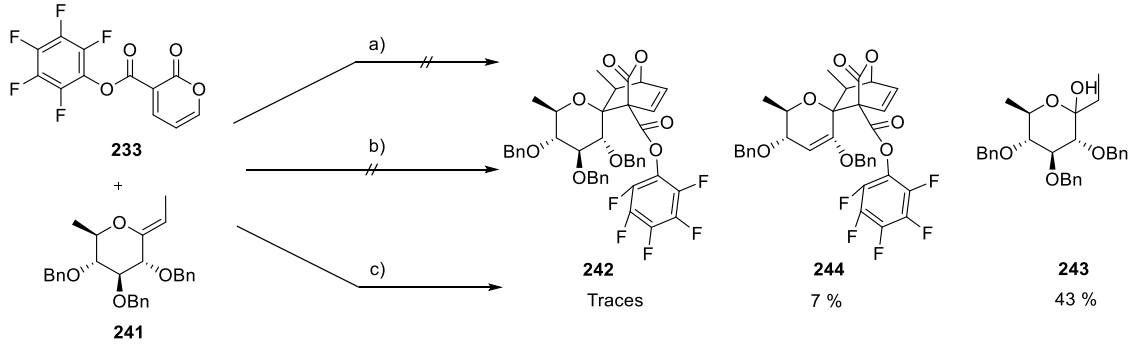

Scheme 5-56: Reagents and conditions: a) CH_2Cl_2, r.t., 24 h; b) CH_2Cl_2, 50°C, 24 h; c) CH_2Cl_2, r.t. 96 h 11-12 kbar.

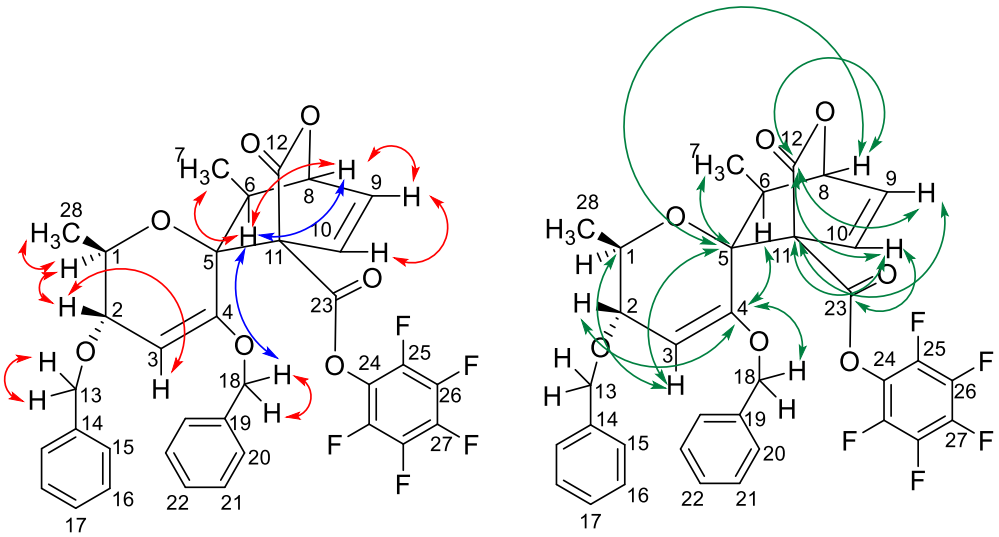

*Figure 5-27: The major $^{1}H,^{1}H$-COSY correlations (left, red), $^{1}H,^{1}H$-NOESY correlations (left, blue) and HMBC correlations (right, green) of **244**.*

The general structure of compound **244** was confirmed through $^{1}H,^{1}H$-COSY and $^{1}H,^{13}C$-HSQC NMR,. The $^{1}H,^{1}H$-COSY spectra revealed correlations between H-6 and H-8, which are characteristic of the products formed after the Diels-Alder reaction. Additionally, the $^{1}H,^{13}C$-HMBC spectra clearly demonstrated correlations between H-8 and the quaternary C-5. The elimination of benzyl alcohol at C-3 was indicated by H-3 at 5.25 ppm, exhibiting a typical low-field shift for an alkene proton. Furthermore, NOESY analysis showed a spatial correlation between H-6 and the benzylic hydrogens H-18a, H-18b, and the neighboring H-8, indicating that molecule **244** was the *exo* product. H-6 exhibited a spatial correlation to H-18 and H-8, as observed in NOESY, suggesting that H-6 was in the downward axial position. Moreover, the common coupling constant between H-6 and H-8 was measured to be 3.0 Hz.[71] According to the literature, this falls within the typical range of typical ^{3}J *exo* coupling constant for the bicyclo [2.2.2]-octane skeleton. A typical ^{3}J *endo* coupling constant for this position would be in the range of 1-2 Hz[71]

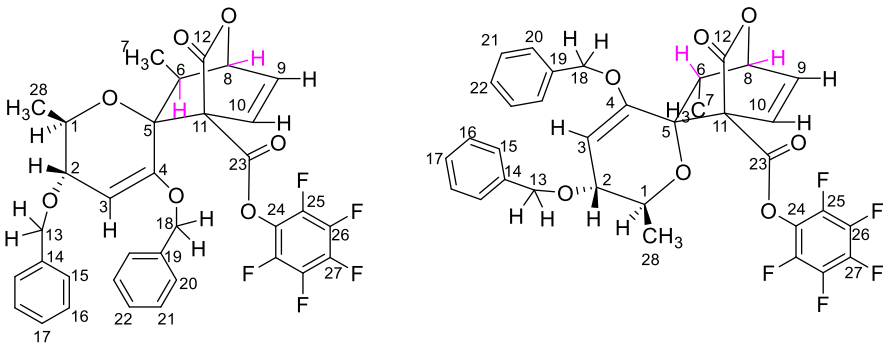

244 *exo* **244 *endo***

*Figure 5-28: Left: **244**-exo. Right: **244**-endo.*

Furthermore, the selective formation of the *exo* product could be elucidated by the proposed reaction mechanism shown in Scheme 5-57.

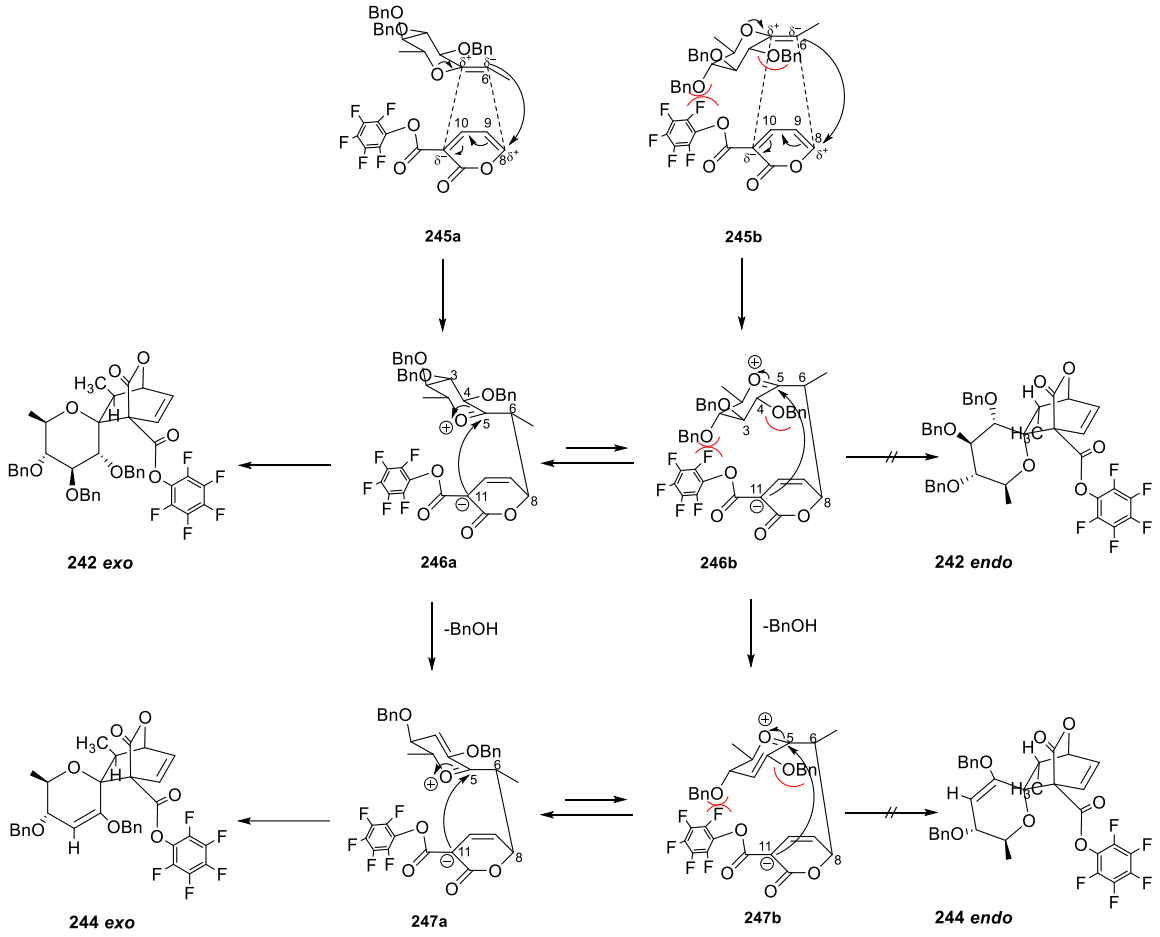

Scheme 5-57: Proposed mechanism for the IEDDA reaction.

The reaction likely initiated with a nucleophilic attack of dienophile **241** from C-6 to C-8 of pyrone **233**, facilitated by the formation of an oxocarbenium intermediate. The electron-deficient nature of diene **233** made the C-8 position susceptible to nucleophilic attack, causing a shift in the double bond from C-8/C-9 to C-9/C-10, with the electron density of the double bond at C-10/C-11 transferring to C-11. In transition state **245a** for the *exo* product, no steric interactions existed between dienophile **241** and diene **233**. In contrast, transition state **245b** for the *endo* product might have shown steric hindrance between the substituents of dienophile **241** and diene **233**, making it less favorable compared to the *exo* product transition state **245a**. Even after the initial nucleophilic attack by dienophile **241**, steric hindrance persisted in **246b**. This could be resolved by the rotation along the C-5/C-6 axis to convert **246b** into **246a**. In this equilibrium, intermediate **246a** predominated due to the absence of steric hindrance. It could then trigger ring closure through a nucleophilic attack of C-11 on C-5, yielding compound **242 *exo***.

The intermediates **246a** and **246b** closely resembled those in the final step of the first total synthesis of portentol (**1**) and the biosynthesis of it (as discussed in sections 2.3-2.4). Trauner *et al*. proposed a mechanism for the formation of anhydroportentol (**40**) under similar conditions.

In the case of the synthesis of portentol (**1**), a hydroxy group of the pyran ring was eliminated as water, resulting in the double bond. In this case, the elimination of the benzyl ether at C-3, with the proton at C-4, likely led to **247a** and **247b**, respectively. However, due to steric hindrance, the equilibrium likely favored **247a**, which could then cyclize to form molecule **244 *exo***.

The elimination of benzyl alcohol and its origin from intermediates **246a** or **246b** suggested that the mechanism had to proceeded stepwise. In a concerted mechanism, these intermediates would not have been present, and elimination would not have occurred.

The selective formation of the *exo* product supported the hypothesis that the stereochemical outcome of the IEDDA reaction to portentol (**1**) was substrate-controlled. It also confirmed the reactivity of pyrone **233**, which had been successfully activated by the pentafluorophenol group.

Encouraged by these results, another IEDDA reaction was attempted using pyrone **233** and the authentic dienophile **69** under the same conditions as before. However, the desired product **248** did not form. Instead, a complex mixture of products was generated, which could not be separated (Scheme 5-58).

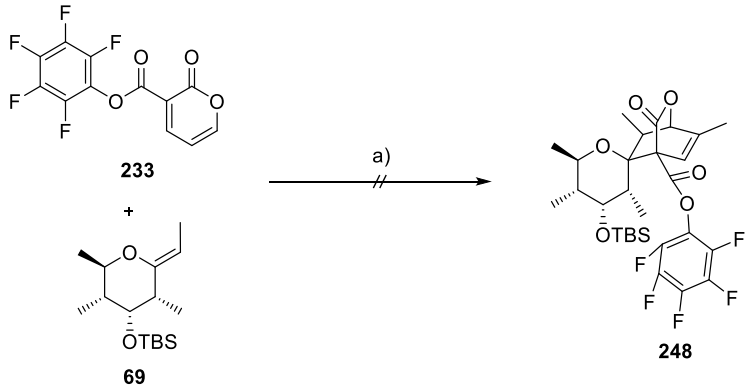

Scheme 5-58: Reagents and conditions: a) CH_2Cl_2, r.t. 96 h 11-12 kbar.

The failure of this IEDDA reaction could be attributed to the instability of dienophile **69**. It had previously been observed that **69** was extremely unstable. Even when **69** was used immediately after its synthesis for the IEDDA reaction, it resulted in the formation of an inseparable mixture. Furthermore, it was noted that shortly after isolating dienophile **69**, NMR analysis revealed its transformation into another molecule.

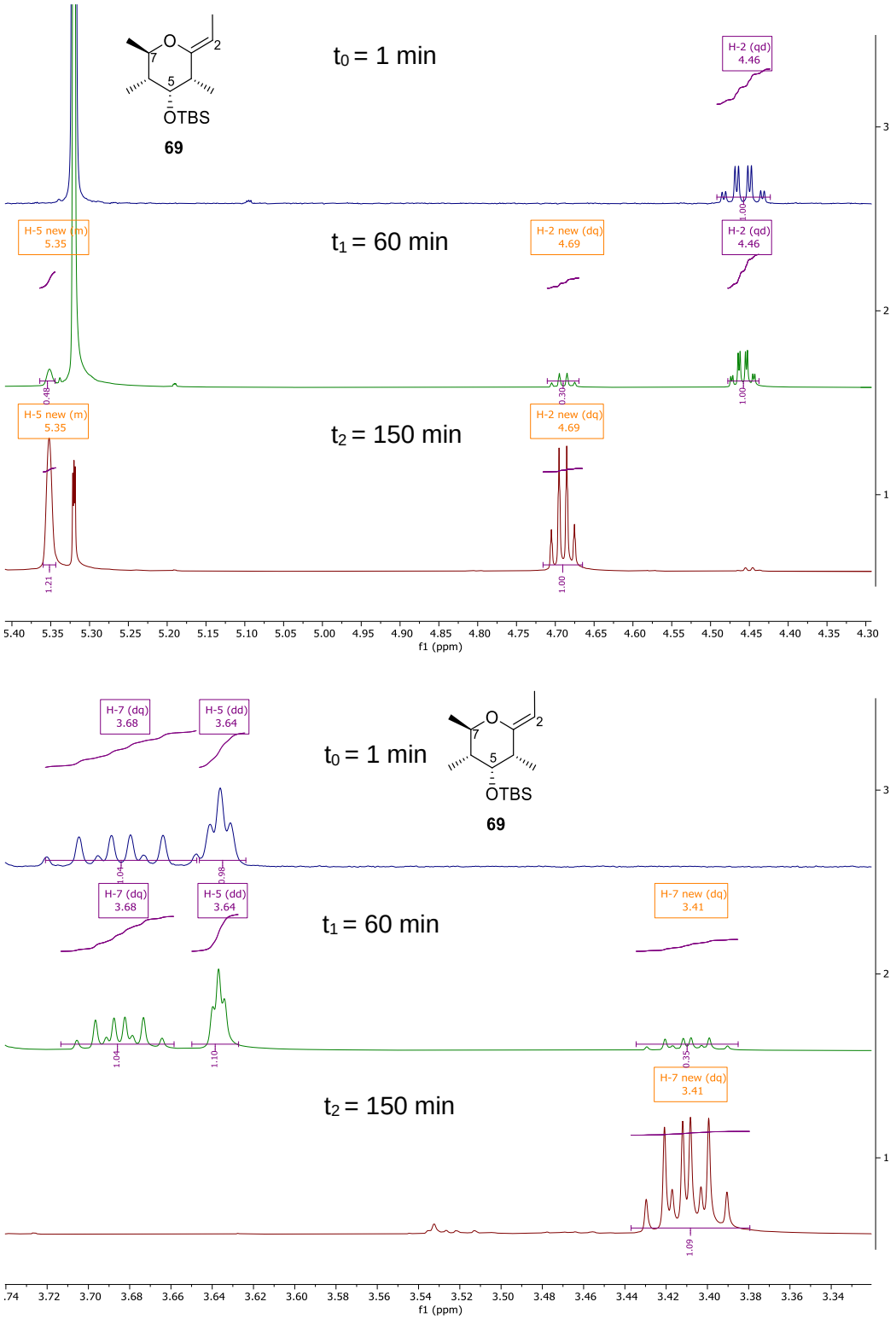

*Figure 5-29: ^{1}H-NMR of **69** during a time span of 150 min.*

To investigate the decomposition, a sample of **69** was measured over several intervals at room temperature in deuterated dry dichloromethane. After 60 minutes, new signals became apparent in the ^{1}H-NMR spectrum, while the original signals of dienophile **69** slowly decreased. This included the signals of H-2, H-5, and H-7 (Figure 5-29). After 150 minutes, the original

signals of compound **69** were no longer detectable. This led to the conclusion that dienophile **69** had completely transformed into another molecule. The structure of this newly formed molecule was revealed after an intensive structural elucidation by NMR.

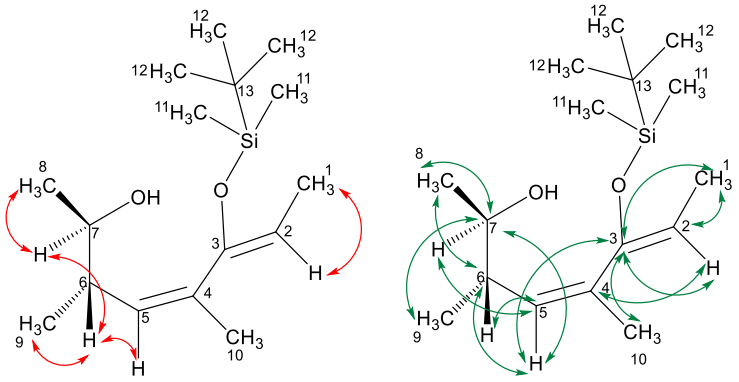

249

*Figure 5-30: The major $^{1}H,^{1}H$-COSY correlations (left, red) and HMBC correlations (right, green) of **249**.*

*Table 5-13: NMR data of **249** in CD_2Cl_2 (700 MHz).*

Nr.	δH [ppm] (m, J in Hz, Int.)	δC [ppm]
1	1.65 (dd, *J* = 6.9, 0.9 Hz, 3H)	9.8
2	4.69 (dq, *J* = 6.9, 0.8 Hz, 1H)	100.4
3	-	151.3
4	-	128.4
5	5.36 – 5.34 (m, 1H)	129.0
6	2.15 – 2.09 (m, 1H)	36.8
7	3.41 (dq, *J* = 8.9, 6.2 Hz, 1H)	77.3
8	1.28 (d, *J* = 6.2 Hz, 3H)	19.4
9	0.95 (d, *J* = 7.1 Hz, 3H)	17.6
10	1.76 (dd, *J* = 2.1, 1.4 Hz, 3H)	18.4
11	0.08 (s, 3H)	-3.5
11	0.08 (s, 3H)	-3.5
12	0.90 (s, 9H)	25.8
13	-	18.3

The transformation of dienophile **69** into diene **249** resulted in the breaking of the bond between the ring oxygen and C-3. This led to the formation of a secondary alcohol at C-7. This transformation was evident in the chemical shift of the proton at C-7, which exhibited a typical low field shift of 3.41 ppm. Furthermore, H-7 displayed correlations with H-8 and H-6 in the $^{1}H,^{1}H$ - COSY NMR. The chemical shift of H-6 was in the range of 2.15 - 2.09 ppm, and this slight low field shift was attributed to the presence of a neighboring double bond. Proton H-5, which exhibited only one correlation with H-6 in $^{1}H,^{1}H$ – COSY spectra, showed a strong low

field shift with values of 5.36 - 5.34 ppm, typical of an alkene hydrogen atom. Additionally, C-5, with a shift of 129.0 ppm in the ^{13}C - NMR, fell within the range of alkene carbon atoms. The bonding between H-5 and C-5 was confirmed by HSQC NMR. Since H-5 did not show any further correlations in COSY NMR, it was concluded that C-4 was a quaternary carbon. Moreover, C-4 did not exhibit correlations in HSQC and was absent in DEPT NMR, supporting the conclusion that C-4 must be quaternary. A similar analysis revealed that C-3 was also quaternary, with a shift of 151.3 ppm, indicating that C-3 was an alkene carbon atom still bound to an oxygen atom. HMBC data provided ^{3}J correlations of quaternary carbons with protons, confirming the positions of these carbons and protons.

However, NMR alone could not determine with certainty whether the silyl ether was attached to C-7 or C-3. Nevertheless, it was likely that the silyl protecting group was located at the oxygen on the quaternary carbon because of keto-enol tautomerism. The free enol **250** would be in equilibrium with the keto tautomer **251**, which would be the major tautomer. This would have been evident in the ^{13}C - NMR spectrum by a signal in the range of 175 - 160 ppm, typically associated with carbonyl groups. However, no such signals were found in the ^{13}C - NMR. Furthermore, there was no presence of a CH_2 group, which would be present in the keto form (Scheme 5-59). Therefore, it was reasonable to assume that the silyl protecting group was located at the quaternary carbon, and the alcohol group must be free in the secondary position

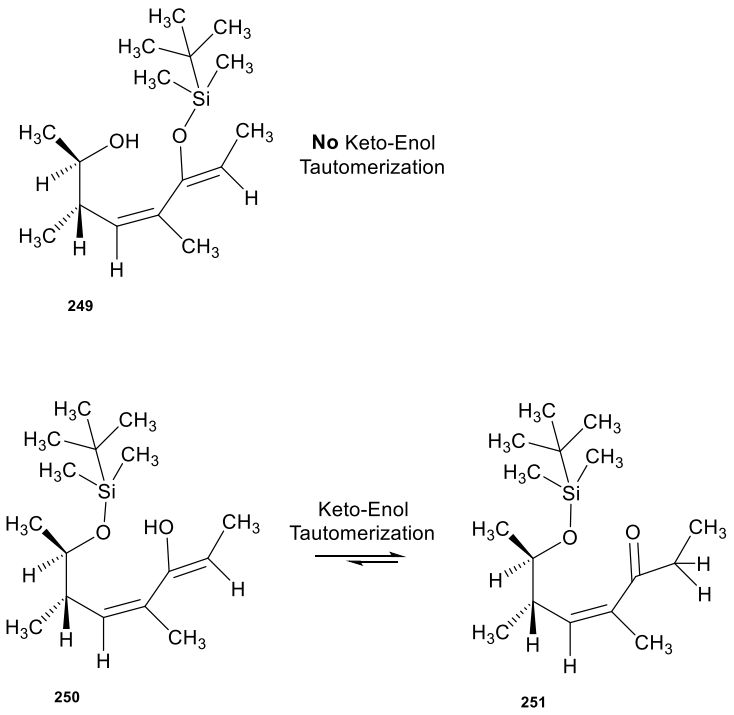

Scheme 5-59: Top: No keto-enol tautomerization. Bottom: Keto-enol tautomerization enabled.

The transformation of dienophile **69** to *α,β*-unsaturated enol **249** could be explained by a rearrangement of the OTBS group and a proton. Thus, several reaction mechanisms were possible. A first suggestion would be that the oxygen in the ring initiated by the double bond deprotonates the proton at C-4 leading to a cleavage between oxygen and C-3, followed by the formation of the double bond of the C-4/C-5 axis by elimination of the OTBS anion. This resulted in the stabilized allyl cation **252** which was likely attacked at C-3 by the OTBS anion leading to rearrangement product **249**. This sequence could have occurred either sequential, as shown in Scheme 5-60 as pathway A, or through a concerted mechanism as shown in pathway B.

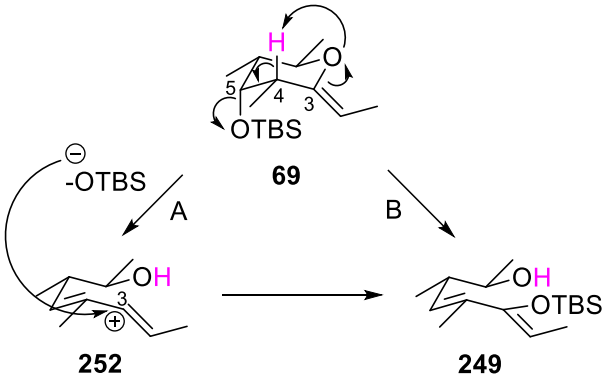

*Scheme 5-60: First proposed mechanism for the rearrangement from **69** to **249**.*

Another possible mechanism for the rearrangement involved the shift of the double bond from C-2/C-3 to the C-3/C-4 axis through resonance structure **253** through a proton transfer from C-4 to C-2. The newly formed enol **254** then underwent deprotonation at H-2, leading to the formation of a double bond between C-2/C-3. Subsequently, the double bond shifted from C-3/C-4 to C-4/C-5. This initiated the elimination of the OTBS anion, which could then attack the activated oxocarbenium **255** at C-3, resulting in the cleavage of the oxygen C-3 bond. This, in turn, led to the formation of compound **249** (Scheme 5-61).

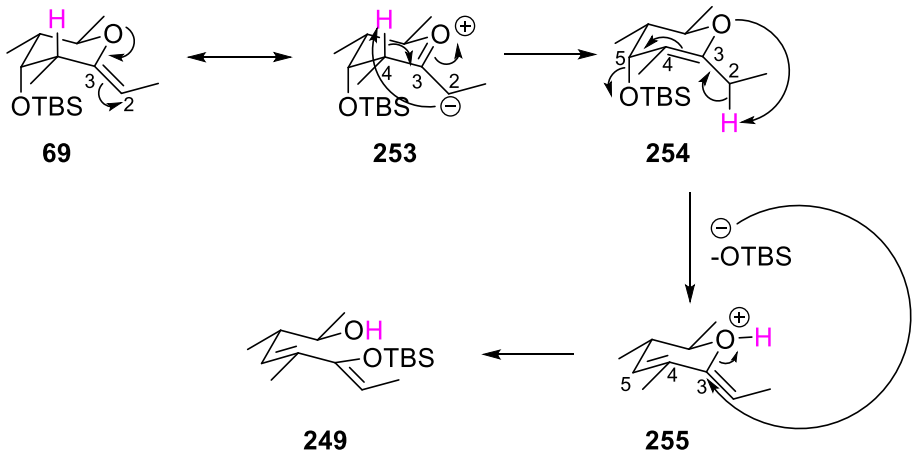

*Scheme 5-61: An alternative mechanism for the rearrangement to **249**.*

However, regardless of which of these proposed reaction mechanisms was more likely, they all highlighted a general problem with dienophile **69**. This problem stemmed from the labile nature of H-4, which was highly susceptible to elimination by the neighboring enol group. This effect was amplified by the *anti* - axial position of H-4 relative to the OTBS group. Additionally, the axial position of the oxygen atom at C-5 posed another challenge, as it was in close spatial proximity to C-3, further favoring rearrangement.

Interestingly was this lability not be observed in the previously used test dienophile **241**. On the one hand, this appeared to be more stable due to the protected alcohol groups instead of the methyl groups of the authentic dienophile **69**. Moreover, protected alcohol group at C-5 of the D-glucose based dienophile **241** was in equatorial position which did not favor the rearrangement that occurred in fragment **69**.

This destabilizing effect of the axial hydroxy group at C-5 was also observed on the previously synthesized D-allose - based dienophile **179** (see section 5.1.12). Thus, the position of the TMS protected hydroxy group had a strong negative effect on the yield of the alkene synthesis. Attempts to deprotect the D-allose enol ether **179** also led only to a complex inseparable reaction mixture (Scheme 5-62). This confirmed the relationship between the stability of the dienophile and the position of the hydroxyl group. The additional protected hydroxy groups of **179** stabilized it. However, the negative effect of the axially located liberated hydroxyl group outweighed the positive effects of the other hydroxy moiety, dramatically reducing the stability of the potential molecule **256**.

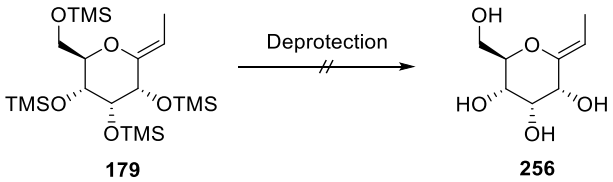

179 **256**

Scheme 5-62: Different reagents and conditions were tested for the deprotection, but only leading to an inseparable mixture.

5.2.2 Conclusion of the IEDDA Reaction

In summary, the IEDDA was optimized to the extent that it was possible to switch from a Lewis acid catalyzed system with pyrone **2** to an uncatalyzed system using the activated pentafluorophenol pyrone **233**. Therefore, side reactions initiated by catalysts could be prevented. Furthermore, the setup was optimized for high pressure reactions and it was possible to successfully perform an IEDDA reaction with fluorinated pyrone **233** under high pressure conditions. In addition, it was possible to gain more insight into the reaction mechanism of the IEDDA reaction especially for very complex dienophiles like the D-glucose based enol ether **241** and its role in the selectivity of the inverse Diels-Alder reaction. However, it was not possible to transfer these findings to the authentic dienophile **69** because of its extremely unstable nature.

6 Summary and Outlook

The inverse electron demanding Diels-Alder reaction is an effective method to build up four new stereocenters in one step. In addition, two C-C bonds are formed and a new double bond is formed. This is enabled by an electron-rich dienophile and an electron-deficient diene. The bicyclic structure of portentol (**1**) can be divided into an electron-rich dienophile, the enol ether **3**, and the electron-poor diene **2**. Previous attempts to synthesize portentol (**1**) by an IEDDA reaction failed already in the synthesis of the dienophile.[16] In this work, however, the synthesis of the dienophile fragment was successfully completed after five synthetic approaches with a total of 9 steps and an overall yield of 20 % in a longest linear sequence of 7 steps (Scheme 6-1).

*Scheme 6-1: Summary towards the synthesis of dienophile **69**.*

In addition, different cyclic enol ethers with complex stereocenters based on carbohydrates were synthesized during the synthesis approaches of the dienophile (Figure 6-1).

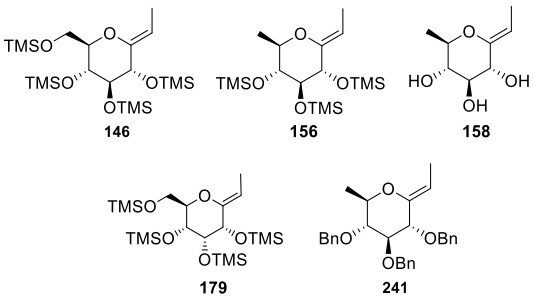

Figure 6-1: Summary of different dienophiles synthesized in this work.

Moreover, the first successes with the IEDDA reaction have been achieved under Lewis acid catalysis. As a result, a high pressure process was developed and special Teflon ampoules were designed and produced. Finally, an IEDDA reaction was successfully carried out with diene **233** and dienophile **241** without the use of a catalyst giving first insights into the reaction mechanism, the stereochemical course and the reactivity and showed that the IEDDA reaction was generally feasible, but also that dienophile **69** was extremely unstable. This property was due to the structure of the dienophile which was invariable for the total synthesis of portentol (**1**) *via* inverse electron demanding Diels-Alder reaction. The highly reactive enol ether group

was essential for the IEDDA reaction and the stereocenters of the substituents of the ring were also indispensable for the IEDDA reaction, since they control the stereochemical course of the reaction. Unable to modify the structure of the dienophile to make it more stable, the inverse electron demanding Diels-Alder towards portentol (**1**) remains unresolved.

Chapter II: Studies Towards the Total Synthesis of Brevistin

7 Introduction

7.1 Brevistin

One of the greatest threats to global health is the spread of infectious diseases. Diseases such as tuberculosis and cholera claimed millions of lives.[72] For a long time, no medical treatments were known. It was not until the discovery of the antibiotic penicillin in 1928 by the physician and bacteriologist Alexander Fleming and the subsequent work of Howard Florey, Ernst Chain, Norman Heatley and Edward Abraham at the University of Oxford who successfully took penicillin from the laboratory to the clinic as a medical treatment in 1941.[73] As of today, antibiotics are a central component of modern medicine, with a variety of different antimicrobial active substances now being used. However, the success story of antibiotics is increasingly clouded by a worrying development due to careless, often hasty and inappropriate use, as well as the massive use in livestock production. Since the use of antibacterial substances, pathogens have developed resistances that render established antibiotics ineffective.[74] To avert this antibiotic resistance crisis, it is essential to discover and develop new antibiotics.
One of these candidates is the cyclic lipopeptide brevistin (**6**), which shows antibiotic activity against Gram-positive bacteria, including the bacterial strains *Streptococcus pyogenes, Staphylococcus aureus* and *Streptococcus pneumoniae*.[75] The latter in particular are among the most common multidrug-resistant pathogens.[76]

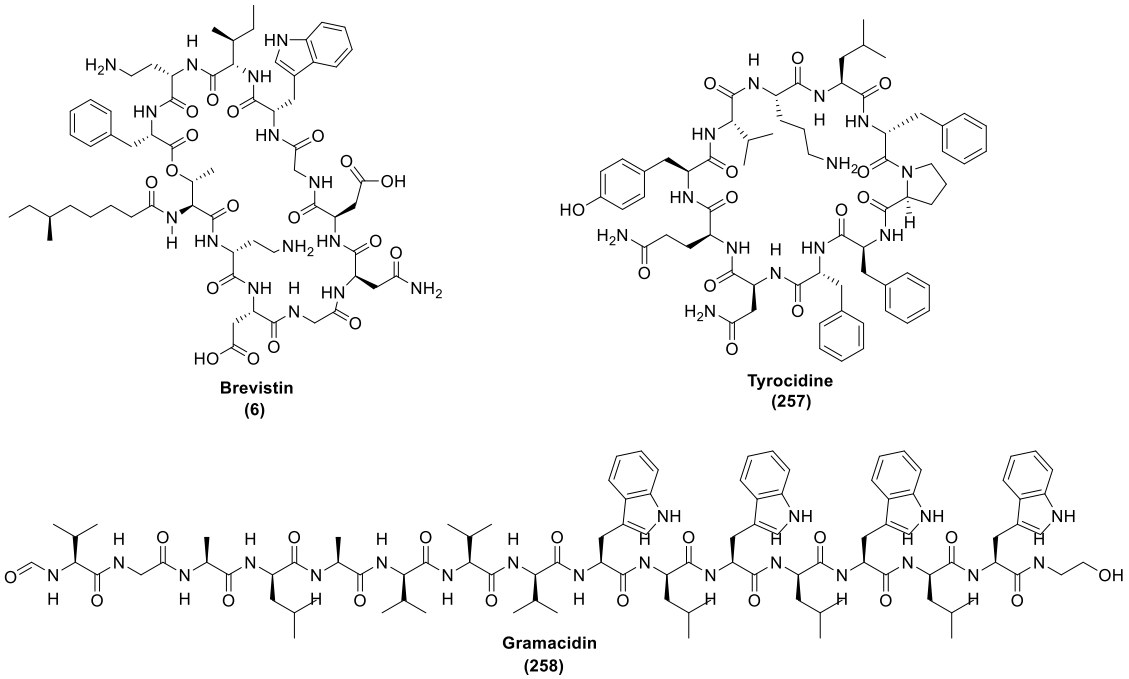

Figure 7-1: Isolated peptides from Bacillus brevis 342-14.[77]

In addition, brevistin (**6**) exhibited only low toxicity to mice. Peptide **6** was discovered in 1975 and, alongside the already established antibiotics tyrocidine (**257**) and gramicidin (**258**), it was isolated from the bacterium *Bacillus brevis* 342-14 (Figure 7-1).[77] Brevistin (**6**) is a cyclic peptide consisting of the 11 amino acids L-and D-aspartic acid, D-asparagine, L-threonine, glycine, L-isoleucine, L-phenylalanine, L-tryptophan, and L- and D-2,4 - diaminobutyric acid. Phenylalanine and threonine are linked by an intramolecular depsi bond between phenylalanine and the hydroxy group of the threonine. Also, the lipophilic fatty acid *(S)*-6-methyloctanoic acid is attached to the amino group of threonine as a side chain (Figure 7-2).[75,78]

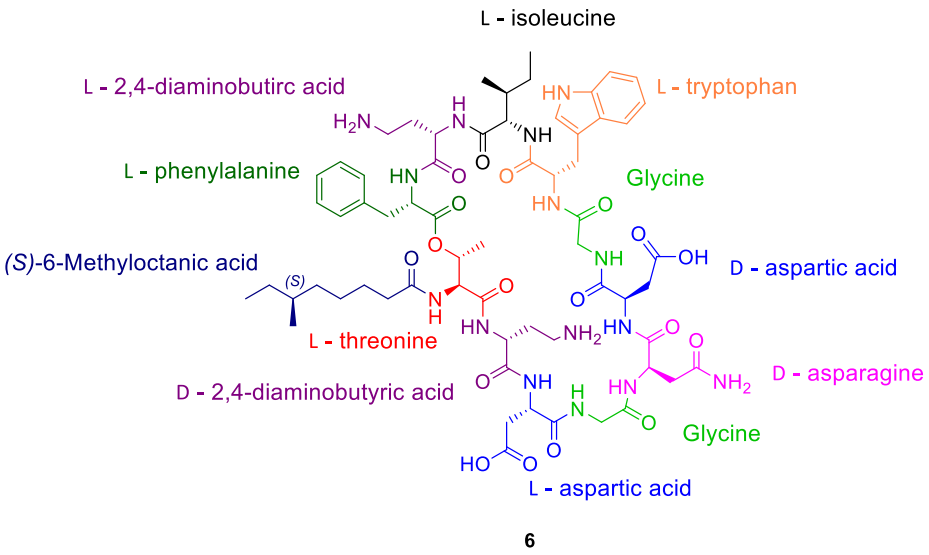

*Figure 7-2: Brevistin (**6**) and their amino acids and fatty acid.*

The non-ribosomal cyclic lipopeptide brevistin (**6**) is an interesting and challenging target for total synthesis due to its bioactivity as well as its complex structure.

7.2 Synthesis of Peptides

In order to obtain therapeutically active peptides, three different methods are generally used in addition to the isolation of the peptide from its natural source: *in vivo* expression, cell-free protein synthesis and chemical synthesis. Chemical synthesis can be further divided into liquid phase chemistry and solid phase chemistry, with solid phase synthesis being the focus of this work.[79,80]

7.2.1 Solid Phase Peptide Synthesis

In solid-phase synthesis, peptides are synthesized on an insoluble polymeric support, called resin, to which the first amino acid is covalently bound. In contrast to the usual procedure in protein biosynthesis, the synthesis does not take place from the *N*- to the *C*-terminus, but in the opposite direction from the *C*- to the *N*-terminus, to avoid side reactions and to correctly form the peptide chain, it is essential to protect the *N*-terminus of the amino acids in addition to the side chains. The elongation of the chain proceeds successively through a repetitive cycle consisting of deprotection of the amino group and coupling of the subsequent *N*-protected amino acid. Once the desired chain length has been achieved, the peptide can be obtained after global deprotection and cleavage of the solid phase (Scheme 7-1).[79,80]

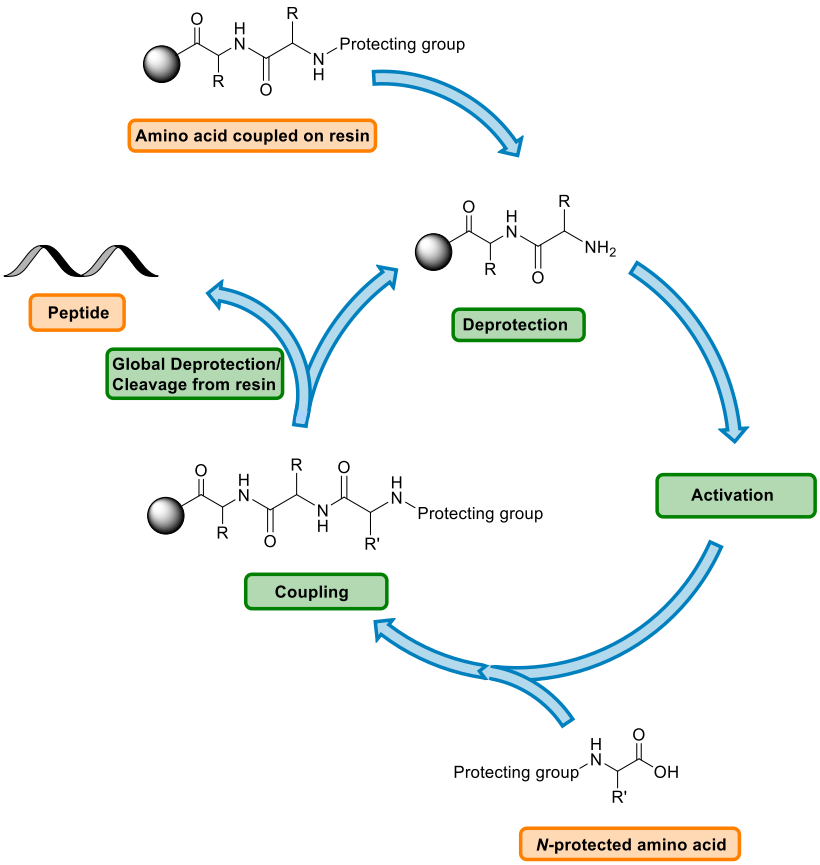

Scheme 7-1: Schematic representation of solid-phase peptide synthesis (SPPS).[81]

The most commonly used solid phase is a polystyrene-based resin. Depending on the requirements, a variety of commercially available polymeric resins with different functionalization can be purchased. For example, for peptides containing *C*-terminal acid, the Wang-resin, the HMPB-resin, the trityl chloride-resin and the 2-chlorotrityl chloride-resin are mainly used as support material (Figure 7-3).[79] The most important aspect of the resins is that the amino acid or peptide chain is temporarily immobilized on the resin as an ester, thioester,

amide or other group, but this temporary bond has to be cleavable only under specific conditions to prevent spontaneous cleavage from the resin.

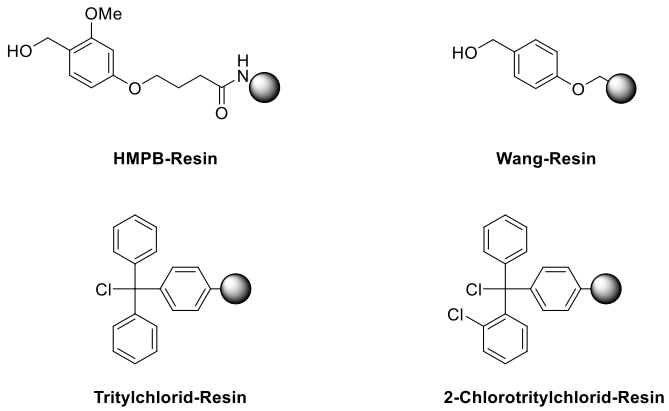

Figure 7-3: Different types of SPPS resins.[79]

These conditions must be in accordance with the selected protective groups of the amino acids at the *N*-terminus, since undesired cleavage of the protective groups may also occur. This led to the development of two protective group strategies for solid phase peptide synthesis (SPPS).

The first protective group strategy is the Boc/Bn strategy. In this strategy, the N_α group of amino acids is protected by a *tert*-butoxycarbonyl (Boc) group and the side chains of trifunctional amino acids are protected by benzyl (Bn) groups. While the temporary Boc group is cleaved off under acidic conditions, the Bn group remains intact throughout the entire synthesis and is only removed after the completion of the peptide, along with the solid phase. This is based on the stability of the peptide-resin bond and the Bn protecting group to weak acids, but the lability to strong acids, usually using hydrogen fluoride (HF).[79,80]

The second protective group strategy is based on Fmoc/*t*-Bu protection where the amino group is protected by 9-fluorenylmethoxycarbonyl protecting group (Fmoc), which can be cleaved by an E1cb mechanism under mildly basic conditions, usually by adding a dilute piperidine solution in DMF. However, the group is stable against acids. The side chains of the amino acids are protected by *tert*-butyl type protecting groups. In analogy to the Boc/Bn strategy, they are cleaved off only after the complete synthesis of the peptide, typically using concentrated TFA, along with the resin. Due to its milder reaction conditions, this strategy is the most widespread and established method for the synthesis of peptides in solid phase.[79,80]

Directly forming amide bonds from amines and carboxylic acids is not feasible because it typically results in an acid-base reaction forming an ammonium salt rather than a nucleophilic substitution. To overcome this limitation and prevent obstructive proton transfer, an additional coupling reagent is employed to activate the carboxylic acid. This activation involves converting the hydroxy group into a better leaving group, facilitating the nucleophilic attack of

the amino group. Meanwhile, a wide range of coupling reagents exists, whereby a suitable selection is essential to avoid side reactions, such as racemization or epimerization, while maintaining high reactivity.[80]

Among the most widely used coupling reagents in synthesis are carbodiimides. Probably the best known carbodiimide is the *N,N'*-dicyclohexylcarbodiimide (DCC) already used by Merrifield and introduced by Sheehan and Hess in 1955.[80]

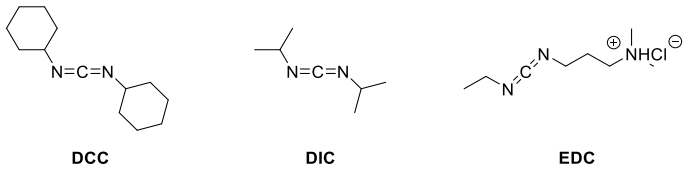

Figure 7-4: Different carbodiimide coupling reagents.

The carboxylic acid is activated *in situ*, forming an activated O-acylurea **262**. From this intermediate, two distinct reaction pathways are possible. The O-acylurea can directly react through a nucleophilic attack by the amine, yielding the desired amide **266** and generating *N,N'*-dicyclohexylurea **265** as an insoluble by-product. Alternatively, it can initially react with another *N*-protected amino acid **259** to create a symmetrical anhydride, which can then further react with an amine **263** (Scheme 7-2).

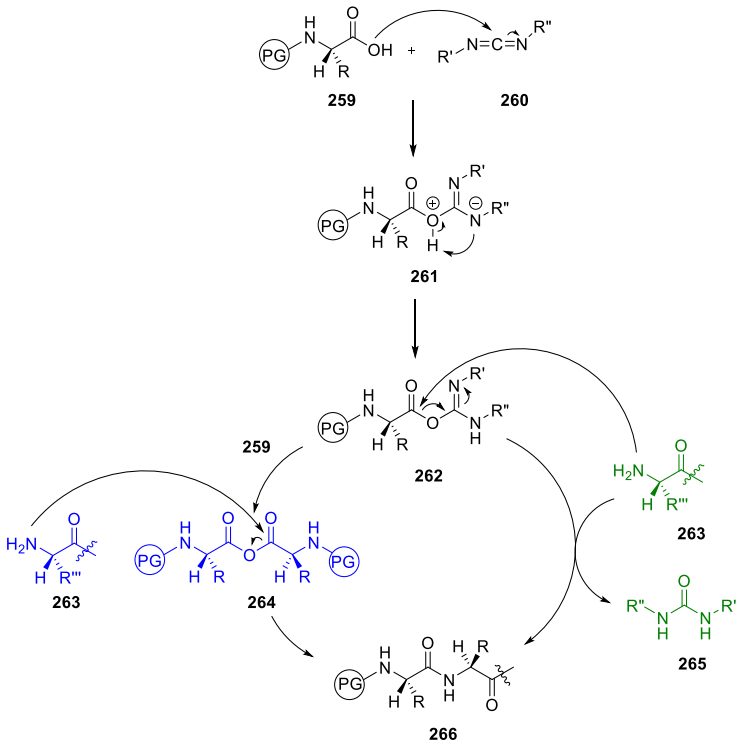

Scheme 7-2: Mechanism of coupling of two amino acids with the addition of carbodiimide coupling reagents. (PG = Protective group).

Active esters represent another category of coupling reagents. These derivatives of *N*-protected amino acids offer both sufficient shelf stability and high reactivity toward nucleophiles such as amines. Active esters are formed by reacting the free carboxyl group of amino acid **259** with a substituted hydroxyamine or substituted phenol in the presence of a carbodiimide. This reaction generates a highly reactive species **268**, which subsequently reacts with the free amino group of peptide **263** to yield compound **266**. The electrophilicity of the carbonyl carbon in peptide **268** increases due to the presence of an electron-withdrawing group **Y** on the ester. By-products of the active ester formation, such as pentafluorophenol (HOPfp), 1-hydroxybenzotriazole (HOBt), or *N*-hydroxysuccinimide (HOSu), can be effectively removed using an aqueous solution (Figure 7-5).[80]

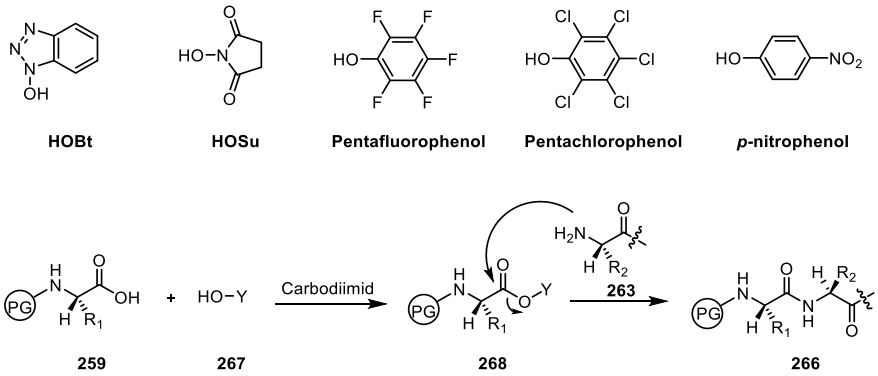

Figure 7-5: Top: Different reagents for the formation of active esters. Bottom: Mechanism of amino acid coupling with active esters.[80]

Phosphonium salts are another important class of coupling reagents. These are based on phosphonium salts of HOBt and HOAt and promote the coupling of amino acids by forming acyl phosphonium salts.[80]

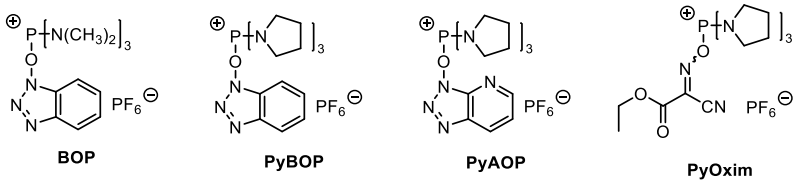

Figure 7-6: Different phosphonium salt coupling reagents.[80]

Phosphonium salts are utilized to generate reactive esters *in situ*, simplifying handling and promoting rapid coupling in peptide synthesis. Although the exact reaction mechanism remains partially understood, it is generally accepted that the reactive intermediate is an active ester, denoted as **271**, when the ligand (**L**) is bonded to a phosphorus atom by an oxygen atom. Conversely, when **L** is a chlorine or bromine atom, the active species forms a symmetrical anhydride and oxazolones. Additionally, an excess of tertiary amines, such as DIPEA, is required to convert the amino acid into a carboxylate ion **269**. The carboxylate then initiates a

nucleophilic attack on the phosphonium salt, producing an acyloxyphosphonium salt **270**, which can be directly attacked by the free amino group or initially by an oxyanion **L** to form an active ester **271**. This active ester eventually undergoes aminolysis in the presence of peptide **263**. Both pathways lead to the formation of amide bonds in compound **266**, along with the side product **273** and hexaalkylphosphorotriamide **272** (Scheme 7-3).[80]

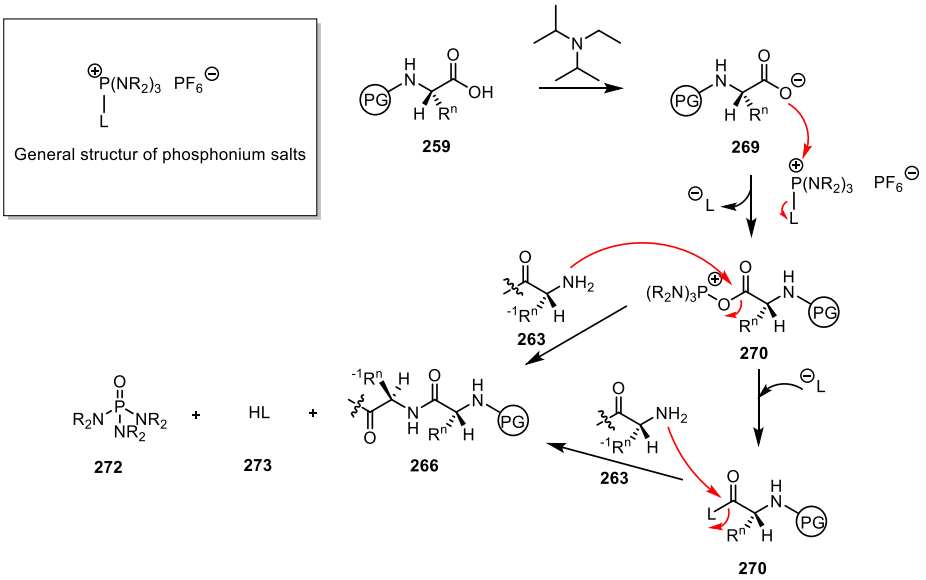

Scheme 7-3: Mechanism of amino acid coupling with phosphonium salts.[80]

The last class of coupling reagents to be presented are those of uronium and aminium salts.

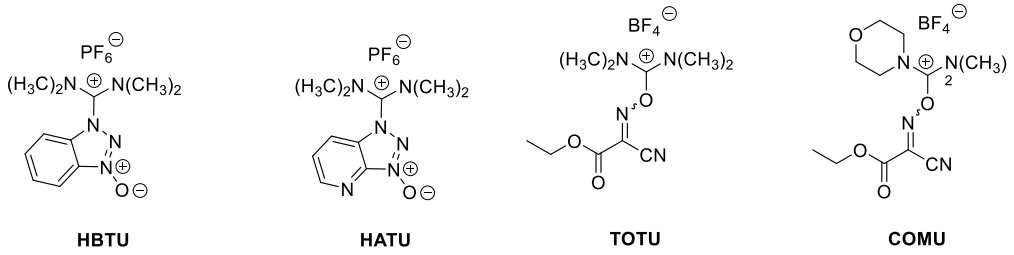

Figure 7-7: Different uronium and aminium salt coupling reagents.[80]

These reactions involve carbocations, such as **276**, which can be attacked by deprotonated carboxylic acids **275**. This results in the formation of an O - acyluronium cation (**277**) and a benzotriazoyl anion **278**. Two possible pathways can occur from this point. In one, the amine **280** directly attacks the acyl carbon, leading to the desired amide bond in peptide **282**. Alternatively, the benzotriazoyl anion **278** can attack the acyl carbon, forming a benzotriazoyl ester **281**, which undergoes further reaction with the amine **280** to yield the amide **282** (Scheme 7-4).[80]

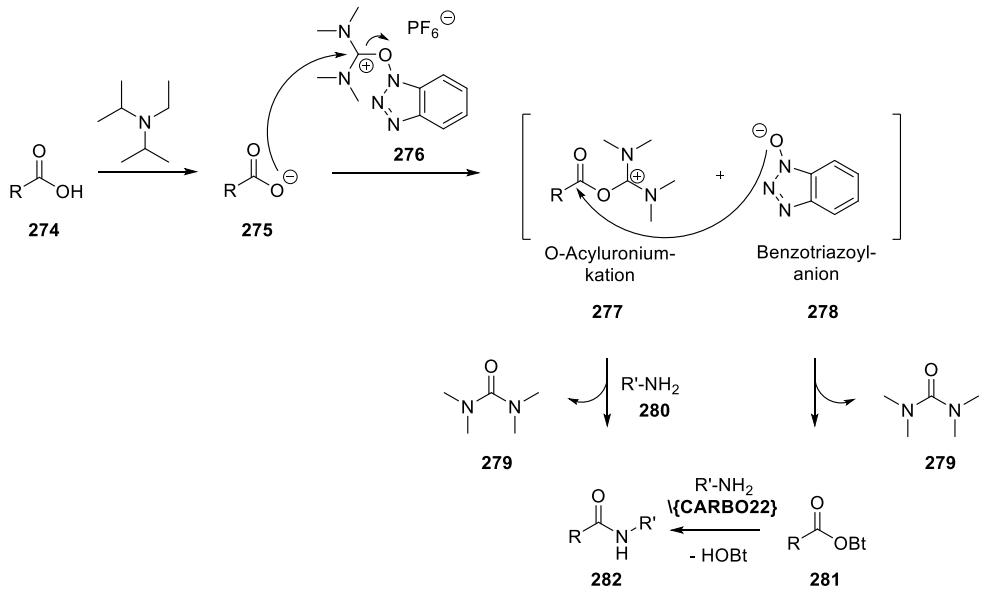

Scheme 7-4: Mechanism of amino acid coupling with uranium and aminium salts.[80]

The various coupling methods mentioned before illustrate the significant diversity of strategies available in solid-phase peptide synthesis (SPPS). These methods are crucial because they can be tailored to the specific molecule, depending on the complexity and structure of the peptide

The completeness of coupling reactions can be assessed using the Kaiser test, a qualitative method for detecting the presence or absence of free primary amino groups. This test relies on the reaction of ninhydrin with amines. A positive test results in a dark blue coloration of both the solution and the resin. Conversely, a negative test, indicating successful coupling, yields a slightly yellowish to colorless solution and resin (Figure 7-8).[82,83]

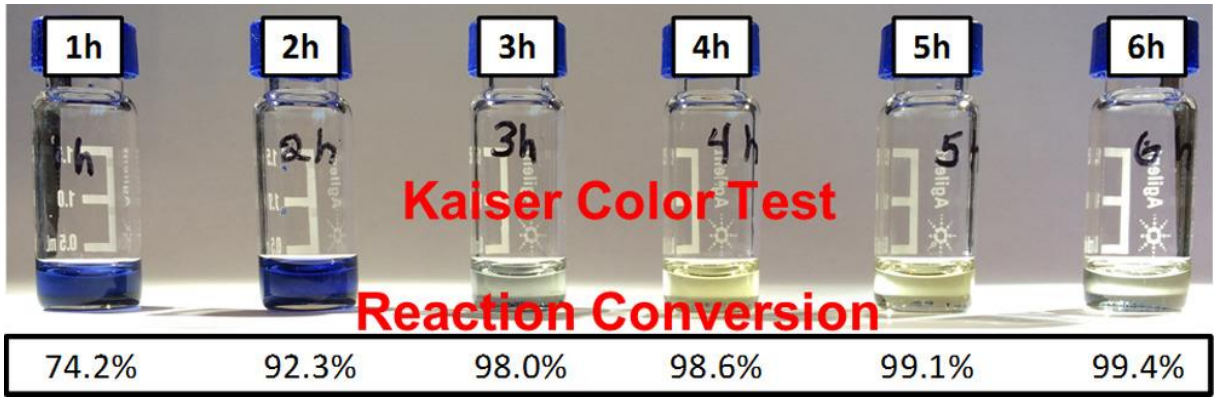

Figure 7-8: Kaiser Test by Sheng Cui et al.[82]

8 Project Aims

Brevistin (**6**) exhibits promising antibiotic properties, particularly against potential multi-resistant bacteria, making it a promising drug candidate.[75,78] Furthermore, conducting a more in-depth structural analysis would provide insights into additional properties related to biological activity. Specifically, investigating the influence of the fatty acid residue on its biological activity is of interest. For example, studies have demonstrated that altering the length and position of the fatty acid chain can enhance the bioactivity of cyclic lipopeptide antibiotics like colistin.[84]

Hence, a total synthesis becomes valuable for generating additional insight for advanced biological studies and producing derivatives to elucidate the structure-activity relationship. Ideally, this endeavor could lead to the creation of an even more potent compound. The primary objectives of this work include developing a retrosynthesis and subsequently establishing a suitable synthesis method. The ultimate aim of this project is to establish a reliable total synthesis route for brevistin (**6**).

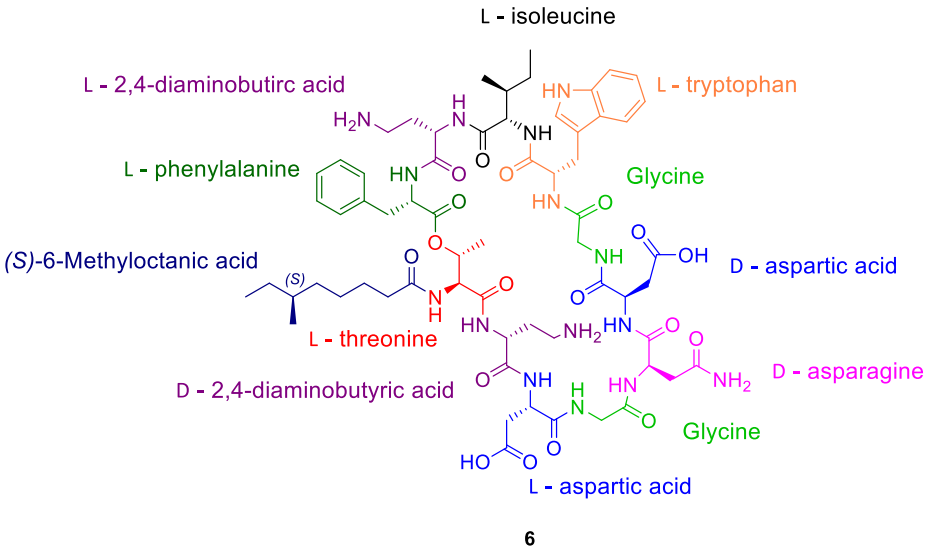

Figure 8-1: Brevistin (6).

9 Results and Discussion

9.1 Retrosynthetic Analysis of Brevistin

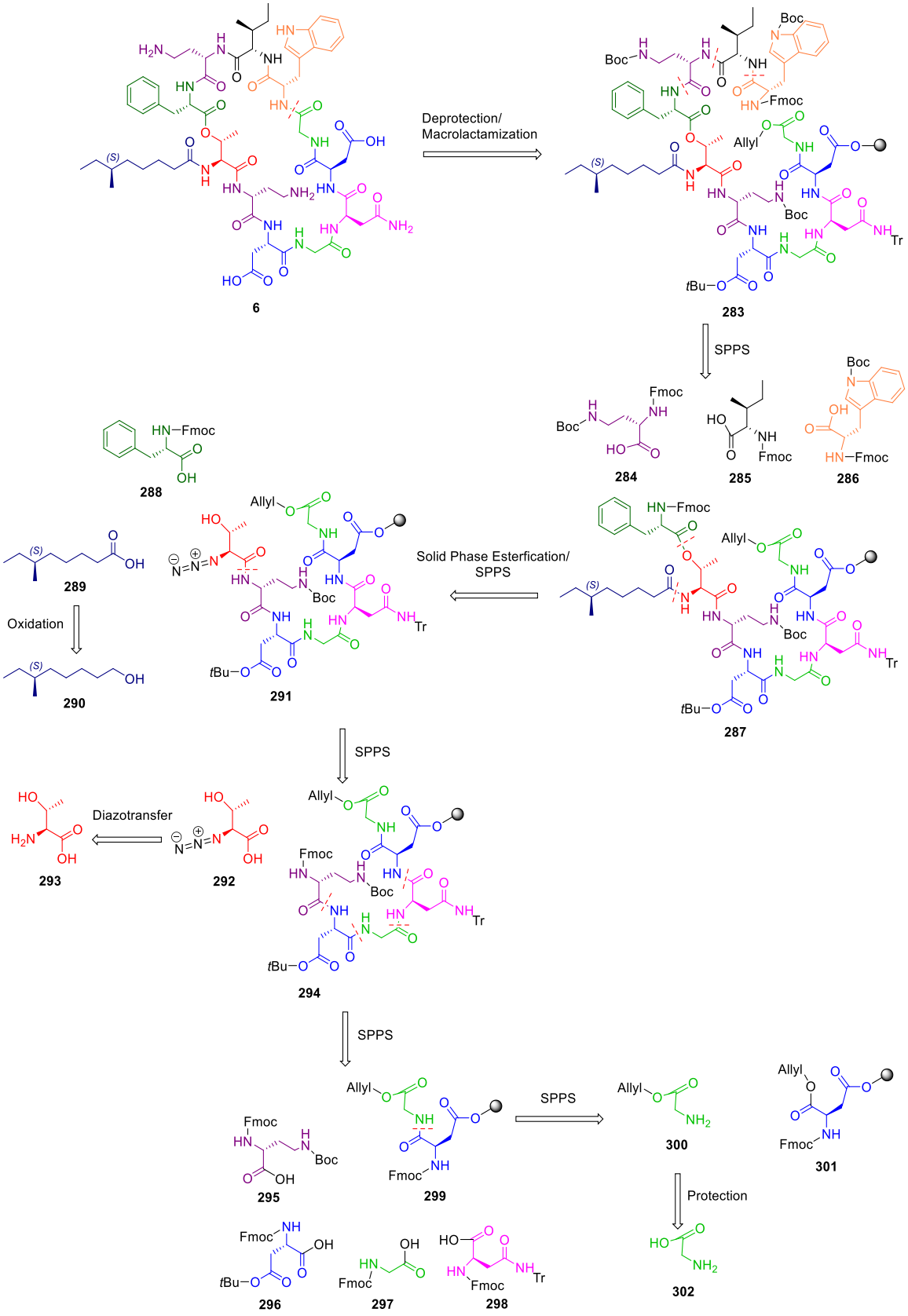

*Scheme 9-1: Retrosynthetic analysis of Brevistin (**6**) based on a SPPS Fmoc strategy.*

The retrosynthetic analysis of brevistin (**6**) drew strong inspiration from the solid-phase peptide synthesis (SPPS) of daptomycin (**303**). Taylor *et al.* developed a solid-phase total synthesis method for daptomycin (**303**), which shares a high degree of structural similarity with brevistin (**6**). Their distinctive approach was a complete on-resin synthesis of daptomycin (**303**) (Figure 9-1).[85]

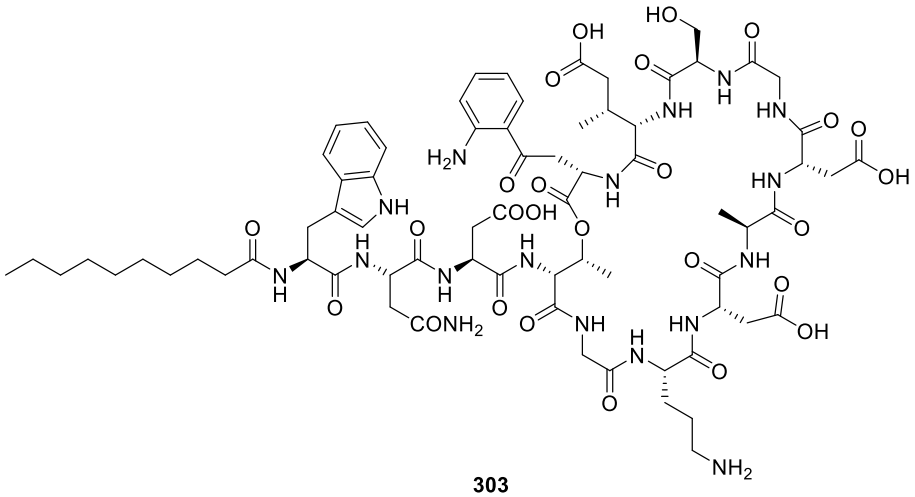

303

*Figure 9-1: Daptomycin **303**.[85]*

Accordingly, the Fmoc protective group strategy as well as the protective groups of the side chains were adapted to brevistin (**6**).[85] Similarly, the final ring closure on solid phase was envisaged for the synthesis of brevistin (**6**). Thus, macrolactamization was planned after deprotection of the tryptophan and glycine of the linear peptide **283**. Cyclization needed to be performed at this position, since epimerization was likely at the *C*-terminus due to activation by coupling reagents and this could be excluded by choosing glycine as the *C*-terminus. In addition, glycine was not sterically hindered for activation by a coupling reagent or subsequent macrolactamization.[85]

The linear precursor **283** was planned to be synthesized by the commercially available Fmoc protected amino acids **284**, **285** and **286** by SPPS method on the peptide chain **287**.

The depsi bond of **287** was envisaged to be established by solid phase esterfication with the Fmoc protected phenylalanine **288** and the alcohol group of **291**. After reduction of the azide group, the fatty acid **289** was planned to be coupled by SPPS. The optically active fatty acid **289** needed to be obtained by oxidation of the commercially available alcohol **290**.[85]

The azide group served as a special protecting group and was intended to afford the L-threonine azide **292** through diazotransfer to L-threonine (**293**). The azide **292** was envisaged to be bound to peptide chain **294** by SPPS.

The hexapeptide **294** was intended to be realized by coupling of the commercially available amino acids **295**, **296**, **297** and **298** to dipeptide **299**.[85] This suggested that the synthesis of brevistin (**6**) commenced with D-aspartic acid protected at the *N* - terminus with a Fmoc group

and an allyl group at the *C* - terminus. The free carboxy group of the side chain of D-aspartic acid needed to be bound to the resin. This would allowed the final macrolactamization on solid phase, since the resin was not bound to the *C* - terminus of the final linear peptide precursor as usual in SPPS, but to the side chain. The *C* - terminus of the D-aspartic acid **301** bound to the resin was to be extended by the previously allyl protected glycine **300**.[86] This step was planned as the second coupling step, as this should prevent steric hindrance by the growing peptide chain, which was likely at this site in a later coupling (Scheme 9-1).[85]

9.2 Synthetic Progress of the Complete on Resin Synthesis Approach

At the beginning of the synthesis of brevistin (**6**), the two non-commercially available peptide building blocks allyl protected glycine **302** and L-threonine azide **292** were synthesized first.
As ring closure was planned to occur at the carboxyl group of glycine **302** towards the end of the synthesis, it needed to be protected throughout the peptide chain formation. In this context, for the repetitive deprotection of the Fmoc group under basic conditions, the use of a metal-catalytically cleavable and base-stable allyl protection group appeared to be particularly suitable. Furthermore, literature detailing the synthesis of allyl protection was available. [86] Starting from glycine **302**, esterification was carried out under acid catalysis using allyl alcohol. The reaction proceeded as described, resulting in the quantitative yield of allyl-protected glycine in the form of ammonium tosylate salt **304** (Scheme 9-2).[86]

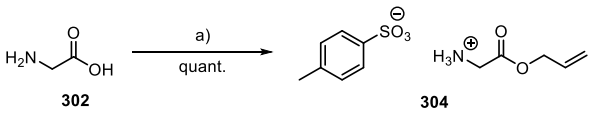

302 **304**

Scheme 9-2: Reagents and conditions: a) TsOH · H_2O, allyl alcohol, toluene, 115°C, 20.5 h.[86]

The diazotransfer reaction starting from *tert*-butyl ether protected L-threonine **305** to azide **292** was literature known, too. The triflate azide was prepared beforehand from sodium azide and triflate anhydride. Under copper sulfate catalysis, the azo group of the triflate azide was transferred to the amine of the amino acid **305**, thus building up the azide. The *tert*-butyl protecting group was cleaved by acidic aqueous work-up, thus liberating the alcohol group. The reaction proceeded as described in the literature and **292** was obtained quantitatively (Scheme 9-3).[87]

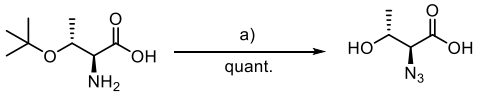

305 292

Scheme 9-3: Reagents and conditions: a) TfN_3, K_2CO3, $CuSO_4 \cdot 5\ H_2O$, CH_2Cl_2/ MeOH/ H_2O (2:2:1), r.t., 12 h.[87]

The synthesis of fatty acid **289** was also carried out, following a known literature procedure for oxidation starting from alcohol **290**. Utilizing NaClO and $NaClO_2$ in the presence of 2,2,6,6-tetramethyl-1-piperidinyloxy (TEMPO), it was able to achieve a 95 % yield of acid **289**, which closely aligned with the reported literature yield of 98 %." (Scheme 9-4).[88]

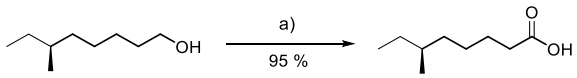

290 289

Scheme 9-4: Reagents and conditions: a) NaClO, $NaClO_2$, TEMPO, Na_2HPO_4, MeCN/ H_2O, (1:1), r.t., 16 h.[88]

After successful synthesis of all non-commercial fragments, SPPS of brevistin (**6**) could be started. The resin used for the solid phase was 2-chlorotrityl chloride-resin (Figure 7-3). This resin was chosen for the synthesis since it showed good stability during peptide synthesis and its increased steric hindrance by the trityl group prevents side chain racemization during the first amino acid coupling.[89,90] In addition, this resin was base stable and could be separated from the peptide chain by acidic conditions. This property was necessary for the planned Fmoc protection group strategy (section 7.2.1).[90]

At the beginning of the SPPS, D-aspartic acid **306** was coupled to the resin using DIPEA. Unreacted resin was then deactivated by a mixture of dichloromethane, DIPEA, and methanol, so that it could not enter into any side reactions in the further course of the synthesis. After the successful immobilization of the first amino acid by its side chain, the allyl - protected carboxylic acid group of fragment **301** was deprotected under palladium catalysis, followed by the coupling of the previously synthesized glycine **304** to the free carboxylic acid of **307** using the coupling reagent PyBOP. Subsequently, the repetitive cycle of Fmoc deprotection, coupling of the amino acid, and washing followed. In the further course of the synthesis, DIC was used as the coupling reagent. After the coupling of the amino acids **298** and **297**, the tetrapeptide **310** was obtained on solid phase.

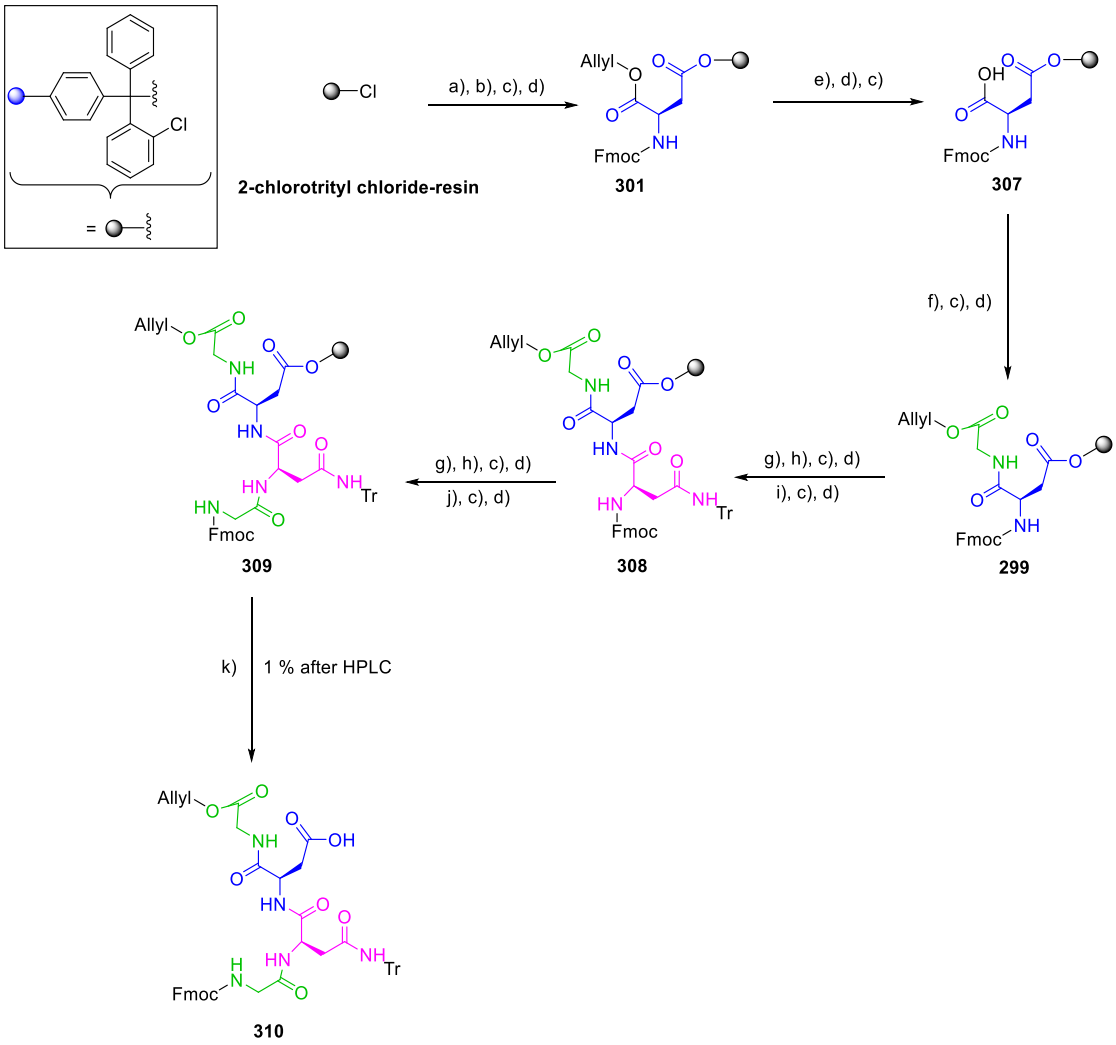

*Scheme 9-5: Reagents and conditions: a) **306**, DIPEA, CH_2Cl_2, r.t., 20 h; b) CH_2Cl_2/MeOH/DIPEA (17:2:1), 3 × 15 min; c) DMF, 3 × 3 min; d) CH_2Cl_2, 3 × 3 min; e) DMBA, $Pd(PPh_3)_4$ (cat.), CH_2Cl_2/DMF (3:1), r.t., 1 h; f) **304**, DIPEA, PyBOP, HOBt, DMF, r.t., 3 h: g) Piperidin/DMF (1:4), 5 min; h) Piperidin/DMF (1:4), 15 min; i) **298**, DIC, HOBt, DMF, r.t., 3 h; j) **297**, DIC, HOBt, DMF, r.t., 3 h; k) Acetic acid/TFE/CH_2Cl_2 (1:1:8), r.t., 1 h.*

The success of the coupling steps was confirmed by the Kaiser assay. To further investigate the progress of the SPPS so far, a part of the tetrapeptide **310** was separated from the resin while preserving the protecting groups. On the one hand, these increased the solubility of the peptide in organic solvents, and, on the other hand, the UV-active Fmoc and trityl groups helped to simplify HPLC separation. Accordingly, 1 % of the tetrapeptide **310** was obtained after HPLC separation. The structure was confirmed by NMR structure elucidation, and the exact mass was confirmed by positive ESI-MS.

Although the previous structure of the peptide chain was confirmed, the yield was extremely low at 1 % after semi-preparative HPLC. A typical yield for such a short peptide chain would be between 60 % - 70 %.[89,91] The very low yield can be explained by the fact that the 2 - chlorotrityl chloride-resin was from an older batch and was therefore largely hydrolyzed and thus deactivated. Nevertheless, it was decided to proceed with the SPPS.

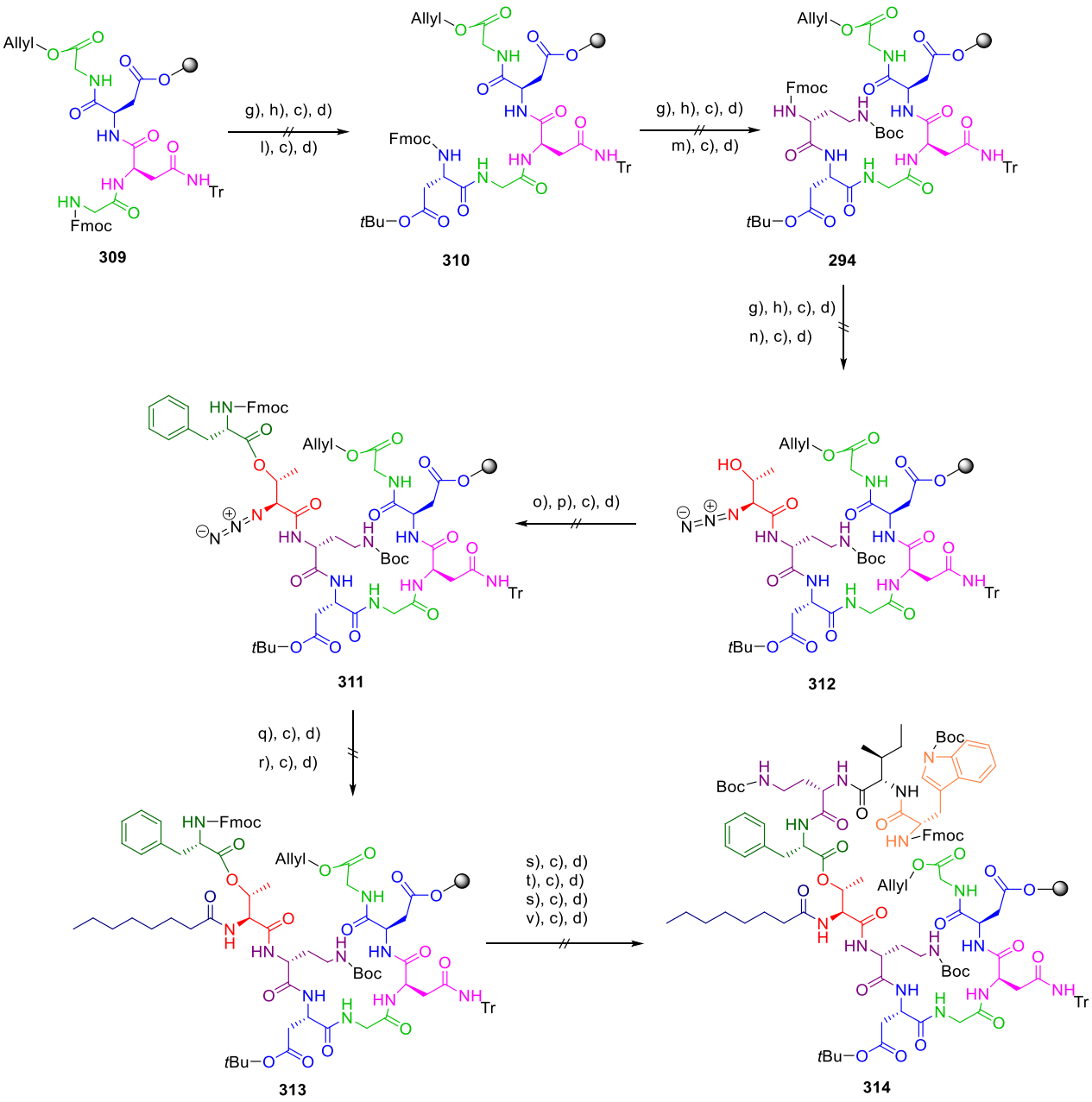

*Scheme 9-6: Reagents and conditions: c) DMF, 3 × 3 min; d) CH_2Cl_2, 3 × 3 min; l) **296**, DIC, HOBt, DMF, r.t., 3 h; m) **295**, DIC, HOBt, DMF, r.t., 3 h; n) **292**, DIC, HOBt, DMF, r.t., 3 h; o) **288**, DIC, CH_2Cl_2, r.t., 1 h; p) DMAP (cat.), CH_2Cl_2, 20 h; q) $P(Me)_3$, Dioxan/H_2O (2:1), r.t., 1 h; r) **291**, DIC, HOBt, DMF, r.t., 3 h; s) 2 – methylpiperidine/DMF (1:4), 3 x 10 min; t) **285**, DIC, HOBt, DMF, r.t., 3 h; v) **286**, DIC, HOBt, DMF, r.t., 3 h.*

The commercially available amino acids **296** and **295** and the previously synthesized threonine azide **292** were coupled to the solid phase. Subsequently, phenylalanine **288** was coupled to the peptide chain **291** by esterification. Phenylalanine **288** was first converted to its anhydride with DIC and then esterified with DMAP by nucleophilic attack of the free alcohol group of molecule **291**. The azide group was then reduced on solid phase with the aid of $P(Me)_3$, followed by coupling of fatty acid **312**. In this synthesis step, it was decided not to use the optically active fatty acid **289**, since the precursor alcohol **290** was very expensive and only available in small quantities. Instead, the commercially available octanoic acid **312** was used.

This fatty acid was structurally very similar to the authentic fatty acid **289**. In addition, octanoic acid **312** was available in large quantities at low cost. The peptide chain **313** was extended through SPPS with L-2,4-diaminobutyric acid **284**, L-isoleucine **285** and L-tryptophan. Fmoc deprotection at this step was performed with a 20 % 2-methylpiperidine solution instead of a 20 % piperidine solution as before, to prevent basic cleavage of the ester bond, as 2-methylpiperidine was a weaker base than piperidine, but was still basic enough to cleave Fmoc (Scheme 9-6).[85]

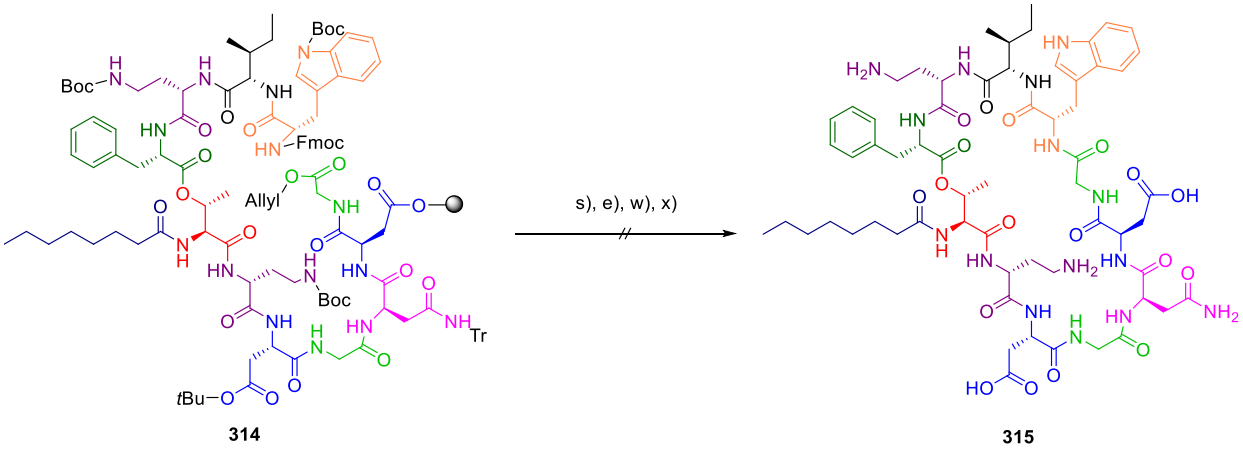

Scheme 9-7: Reagents and conditions: s) 2 – methylpiperidine/DMF (1:4), 3 x 10 min; e) DMBA, Pd(PPh$_3$)$_4$ (cat.), CH$_2$Cl$_2$/DMF (3:1), r.t., 1 h; w) DIPEA, PyBOP, HOAt, Triton X-100 1 % v/v, CH$_2$Cl$_2$DMF/NMP, (3:2:2), r.t., 13 h; x) TFA/Thioanisol/TIS/H$_2$O, (88:2:5:5), r.t., 2 h.

At the end of the SPPS, the Fmoc group and the allyl protecting group were removed from **314**. The ring was then closed using PyBOP and HOAt, followed by cleavage of the peptide from the resin. These conditions were successfully applied to the synthesis of daptomycin (**303**). In this case, it did not lead to the desired peptide **315**. Instead, an unidentifiable peptide was found by semi preparative HPLC and the structure could not be elucidated by NMR analysis.

9.3 Conclusion and Strategic Considerations of the Complete-on Resin Synthesis Approach

This synthetic approach proved promising at the beginning. However, the elongation of the peptide turned out to be a black box due to a pure solid phase synthesis. After each coupling, it was assumed that the coupling had been successful based on the Kaiser test, but no structural information about the peptide during synthesis or the efficiency of the individual couplings could be obtained. In addition, due to the hydrolysis of the resin, the loading of the resin was initially very low, which had a significant negative effect on the yield. At the same time, no further screening of the cyclization could be carried out.

9.4 Second Retrosynthetic Analysis of Brevistin

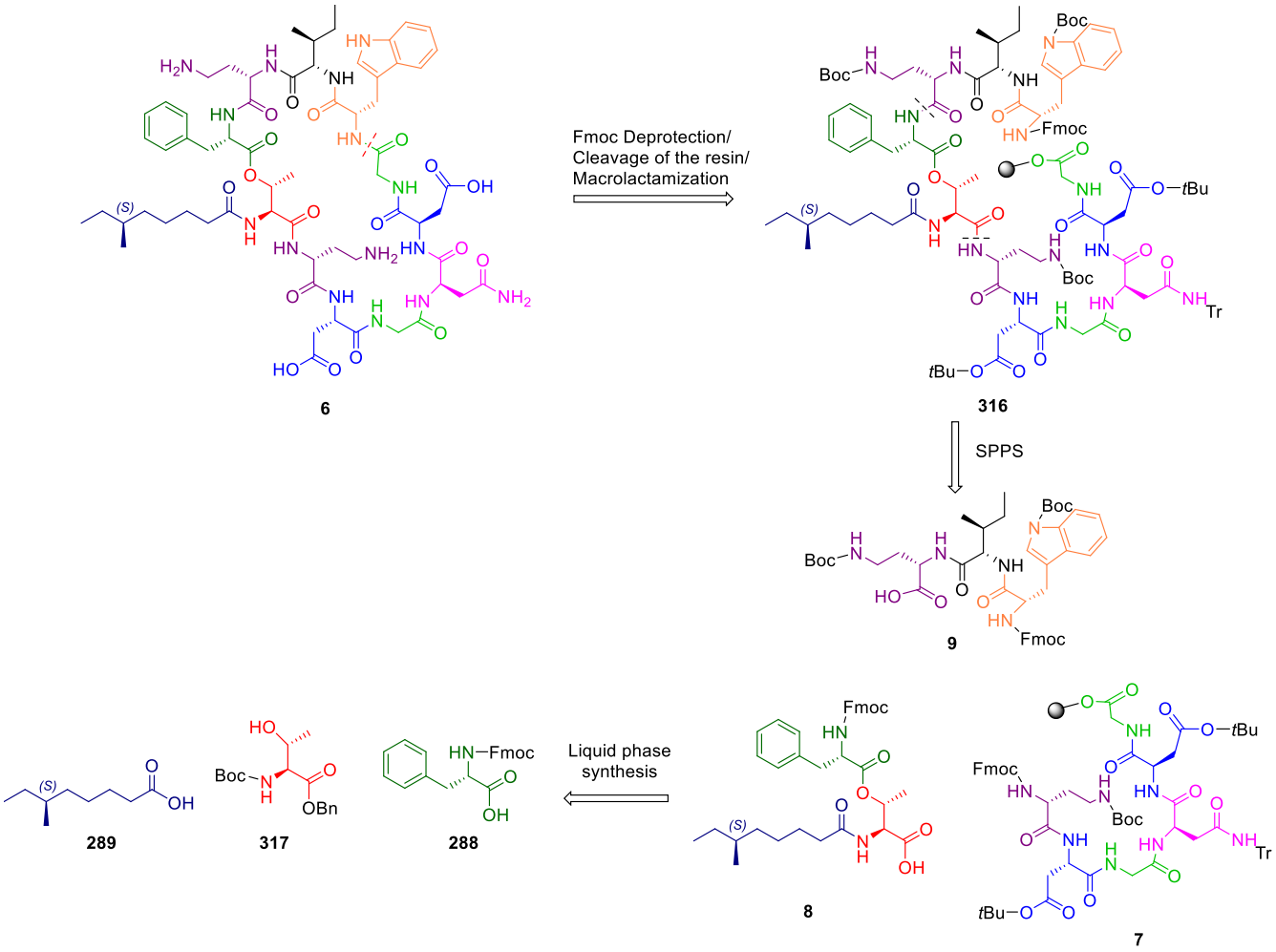

*Scheme 9-8: Second retrosynthetic analysis of brevistin **6**.*

It was envisioned that brevistin (**6**) would continue to be synthesized by SPPS. However, the final macrolactamization would no longer be carried out in solid-phase but in the liquid phase. This had the advantage that the course of the reaction could be controlled at any time. As a result, the first amino acid to be immobilized on solid phase was glycine. This would form the *C* - terminus of peptide chain **316**, and as planned in the last retrosynthesis, the ring would be closed between glycine and tryptophan. The linear precursor **316** could be divided into three fragments. The first fragment was the hexapeptide **7**. This was proposed to be assembled by SPPS and to remain on the resin. The dipeptide **8** was to be synthesized in the liquid phase. For this purpose, the protected L-threonine **317** needed to be esterified with phenylalanine, and then the fatty acid had to be coupled with the amine group of the threonine. It was envisaged that dipeptide **8** would be coupled to the hexapeptide **7** through SPPS method, and subsequently, the last three amino acids needed to be coupled to the peptide chain on resin. (Scheme 9-8).

9.5 Synthetic Progress of the Dual Phase Approach

The synthesis began with the synthesis of fragment **8**. Initially, L-threonine **317** and phenylalanine **288** were esterified using EDC and DMAP. The literature known reaction proceeded as reported with a yield of 67 %.[92] The obtained dipeptide **318** was deprotected from Boc with a yield of 93 %. The free amine group of threonine was coupled to a fatty acid using the coupling reagent HATU. First, octanoic acid **312** was coupled to dipeptide **319** as a test reaction. After deprotection of the benzyl group by hydrogenation, fragment **320** was obtained with a yield of 70 % in two steps. The authentic fragment **8** with the optically active fatty acid **289** was obtained in the same way with a yield of 70 %, too (Scheme 9-9).

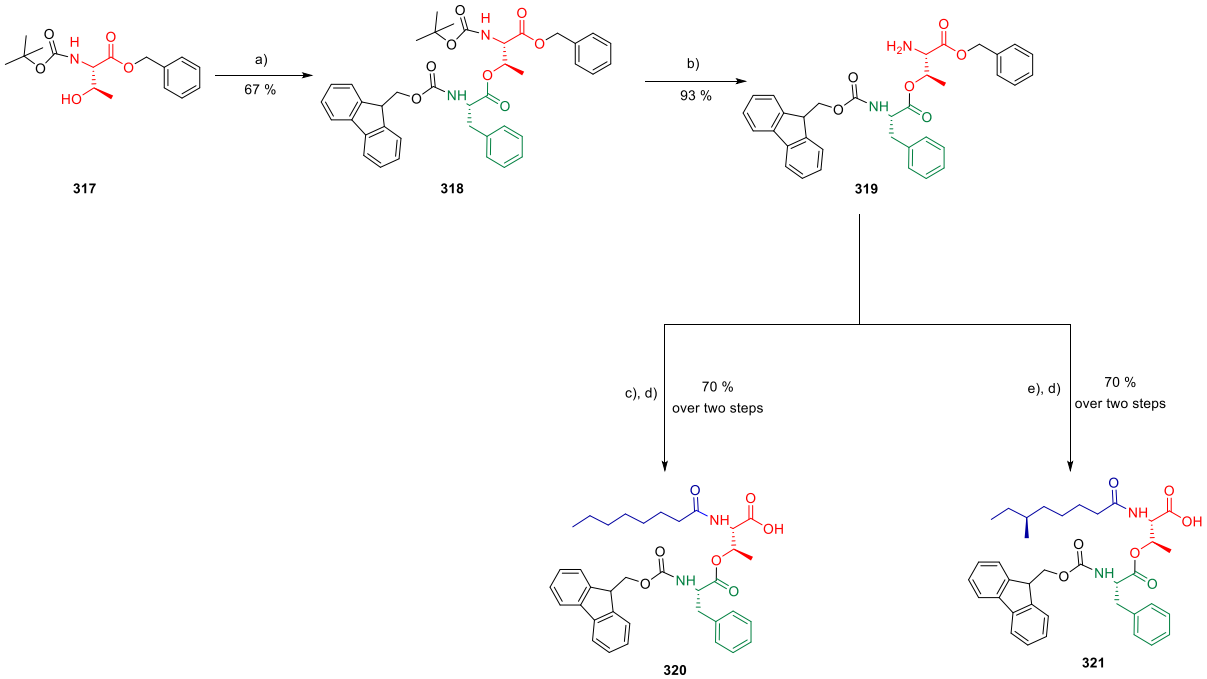

*Scheme 9-9: Reagents and conditions: a) HO-L-Phe-Fmoc, EDC*HCl, DMAP (cat.), CH_3Cl, r.t., 20 h; b) CH_2Cl_2/TFA (1:1), r.t. 2 h; c) Octanoic acid, HATU, DIPEA, DMF, r.t. o.n.; d) Pd/C, H_2 atmospeher, AcOEt, r.t., 20 h; e)* ***289****, HATU, DIPEA, DMF, r.t. o.n..*

Fragment **7** was synthesized by SPPS. In contrast to the first solid-phase synthesis shown in section 8.2, the *C* - terminus of glycine **297** was immobilized on the 2-chlorotrityl chloride resin to obtain **321** and instead of DIC, HBTU was used as coupling agent (section 7.2.1), which showed more efficient and faster couplings than the carbodiimide-based coupling reagents, especially for short peptide chains. Accordingly, D-aspartic acid **322** was coupled using HBTU. Furthermore, the amino acids D-aspargine **298**, glycine **297**, L-aspartic acid **296** and D-2,4-diaminobutyric acid **295** were coupled using the same method. Subsequently, a small part of the solid phase peptide **7** was cleaved from the resin to verify the successful couplings.

After semi-preparative HPLC, 64 % of the hexapeptide **325** was obtained and the structure was confirmed by NMR analysis and ESI-MS.

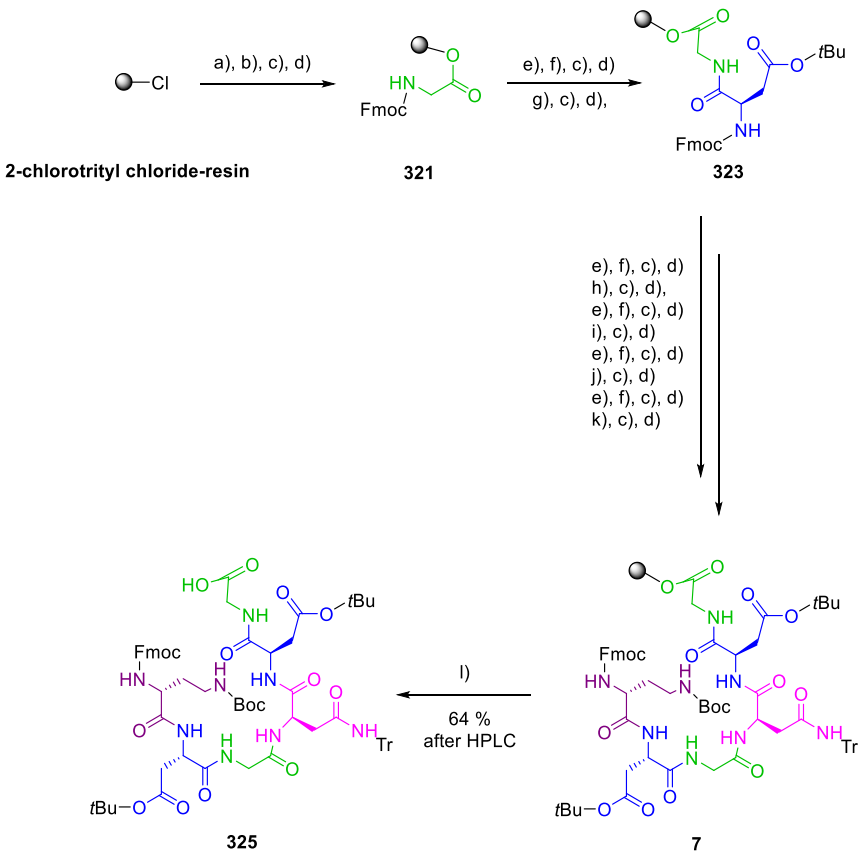

*Scheme 9-10: Reagents and conditions: a) **297**, DIPEA, CH_2Cl_2, r.t., 20 h; b) CH_2Cl_2/MeOH/DIPEA (17:2:1), 3 × 15 min; c) DMF, 3 × 3 min; d) CH_2Cl_2, 3 × 3 min; e) Piperidin/DMF (1:4), 5 min; f) Piperidin/DMF (1:4), 15 min; g) **322,** HBTU, HOBt, DIPEA, DMF, r.t., 1 h; h) **298** HBTU, HOBt, DIPEA, DMF, r.t., 1 h;i) **297** HBTU, HOBt, DIPEA, DMF, r.t., 1 h; j) **296** HBTU, HOBt, DIPEA, DMF, r.t., 1 h; k) **295** HBTU, HOBt, DIPEA, DMF, r.t., 1 h; l) HFIP/CH_2Cl_2 (1:4), r.t., 3 h*

Detailed amino acid and protecting group identification was achieved by $^{1}H,^{13}C$ - HSQC and $^{1}H,^{1}H$ - COSY NMR. TOCSY NMR data also supported to identify the spin systems of the amino acids and by HMBC NMR the connectivity of the amino acids and thus the peptide chain of fragment **325** was confirmed (Figure 9-2).

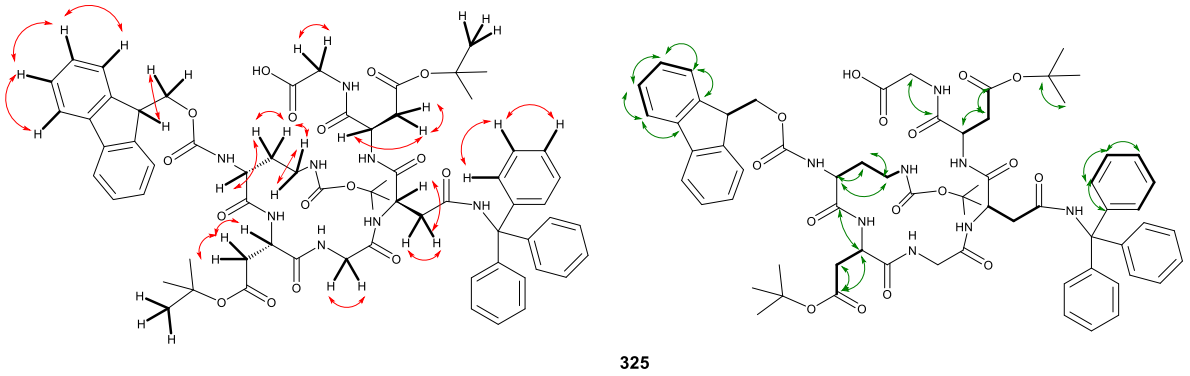

Figure 9-2: Left: Bold line shows $^{1}H,^{13}C$-HSQC correlations and red double-headed arrows show $^{1}H,^{1}H$-COSY correlations. Right: Green double-headed arrows show $^{1}H,^{13}C$-HMBC correlations and bold line shows $^{1}H,^{1}H$-TOCSY correlations.

After the structure of hexapeptide **7** was confirmed, the synthesis was continued. The previously synthesized lipodipeptide **8** was coupled to the peptide chain **7** bound to the resin using the coupling reagents K-oxyma and DIC, which was reported to be used for coupling of larger peptides.[93] Subsequently, a portion of the peptide was separated from the resin for structural analysis of the coupling product. Following semi-preparative HPLC, the desired product was obtained with a yield of 11 % (Scheme 9-11).

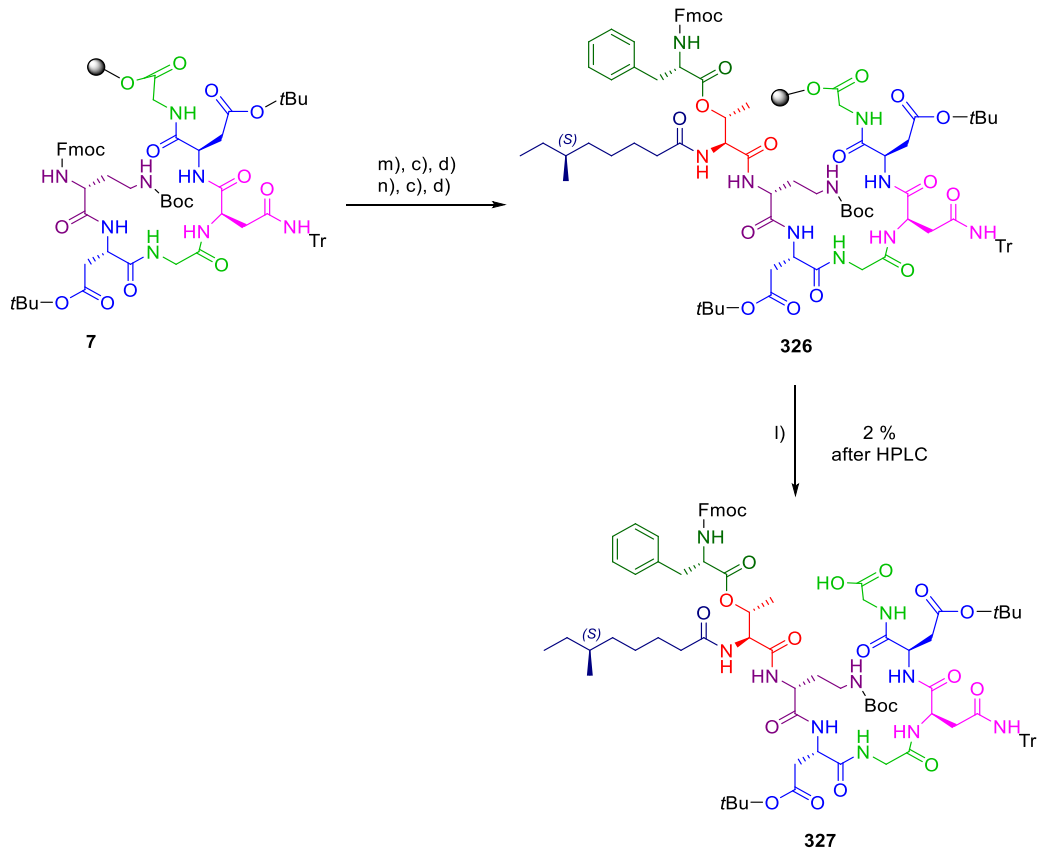

*Scheme 9-11: Reagents and conditions: m) Methylpiperidin/DMF (1:4), 3 × 10 min; n) **8**, K - Oxyma, DIC, DMF, r.t., 24 h.*

^{1}H,^{1}H - COSY NMR and TOCSY NMR confirmed the presence of all amino acids and the fatty acid. HSQC and HMBC NMR confirmed the connectivity of the amino acids of peptide **327**. Additionally, the exact mass was confirmed by ESI-MS. The low yield of 2 % could have been explained by the fact that the fragment **8** was probably sterically hindered during coupling due to its size. For optimization, the reaction could have either been performed twice, or a different coupling reagent could have been used. However, it was decided to proceed with the synthesis first, since fragment **8** had been completely used.

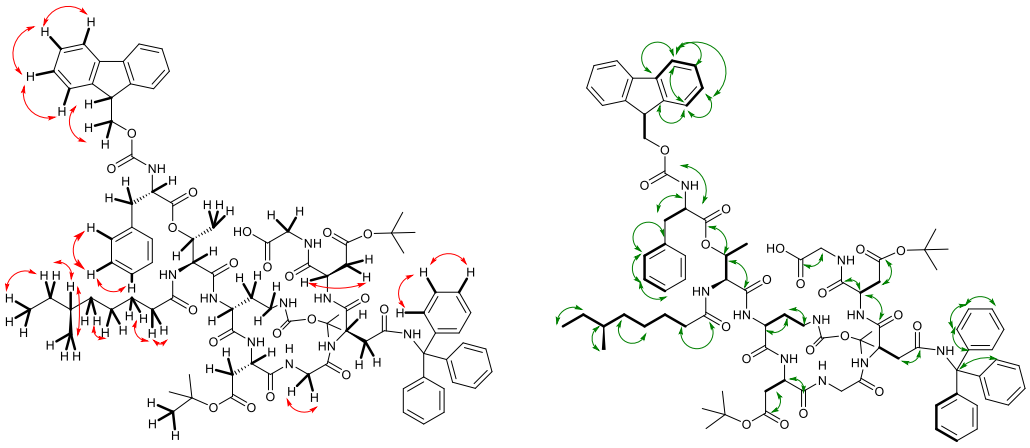

327

Figure 9-3: Left: Bold line shows ^{1}H,^{13}C-HSQC correlations and red double-headed arrows show ^{1}H,^{1}H-COSY correlations. Right: Green double-headed arrows show ^{1}H,^{13}C-HMBC correlations and bold line shows ^{1}H,^{1}H-TOCSY correlations.

The solid-phase synthesis was completed. Accordingly, the amino acids **284**, **285**, and **286** were coupled to the resin-bound peptide by SPPS as before. Subsequently, the last Fmoc

group was cleaved off, and the peptide was released from the resin (Scheme 9-12). However, NMR structural analysis showed that it was not the desired peptide **328**.

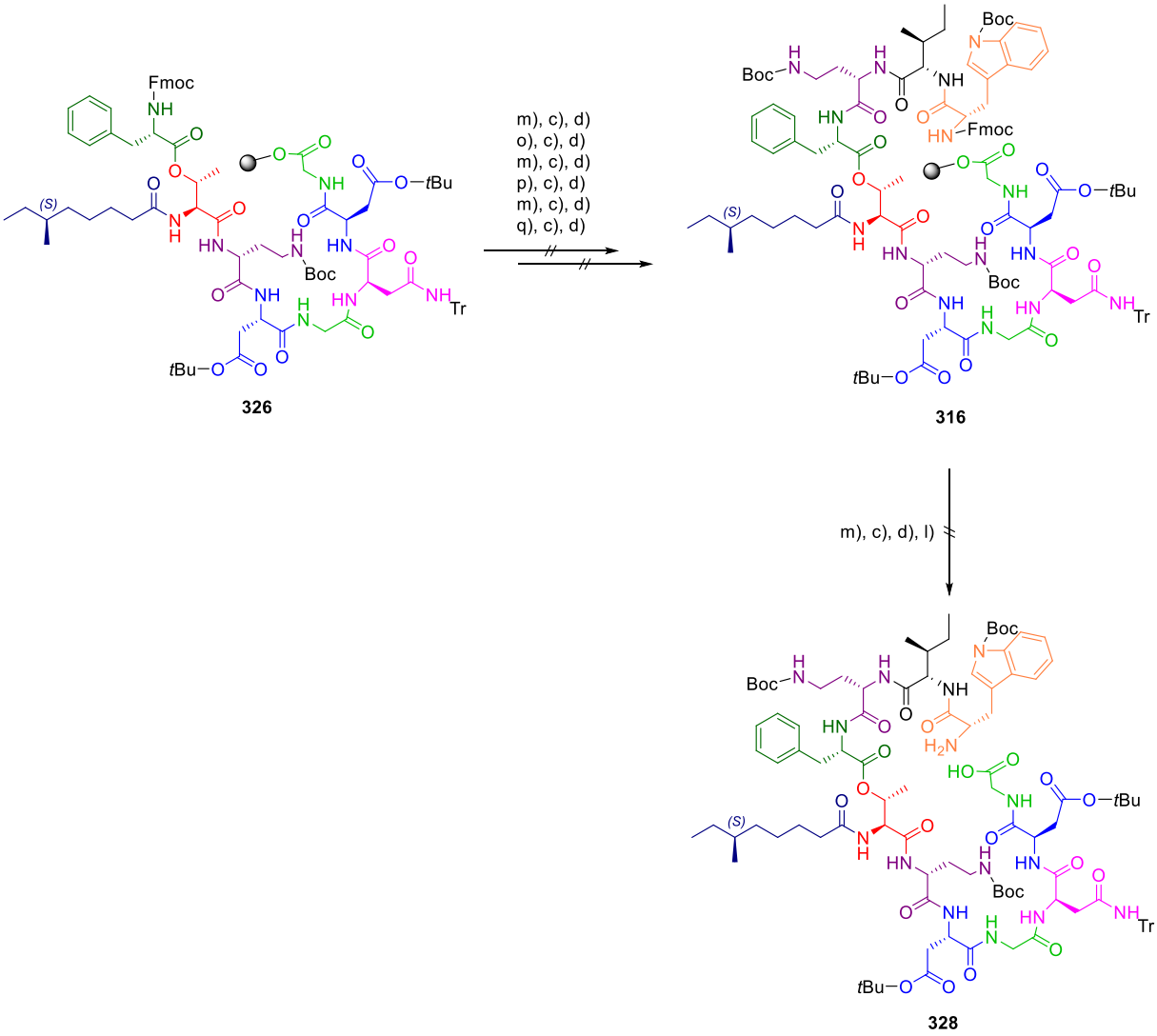

Scheme 9-12: Reagents and conditions: o) ***284*** *HBTU, HOBt, DIPEA, DMF, r.t., 1 h; p)* ***285*** *HBTU, HOBt, DIPEA, DMF, r.t., 1 h; q)* ***286*** *HBTU, HOBt, DIPEA, DMF, r.t., 1 h.*

Instead, peptide **329** was identified by NMR analysis. The NMR data showed no signals for the threonine, phenylalanine and fatty acid groups. However, all signals of the hexapeptide fragment **325** were present. Also the signals of the amino acids L-2,4-diaminobutyric acid **284**, L-isoleucine **285** and L-tryptophan **286** were identified. Given that the peptide underwent separation through both analytical HPLC and semi-preparative HPLC, it provided assurance that it constituted a single molecule rather than two distinct substances.

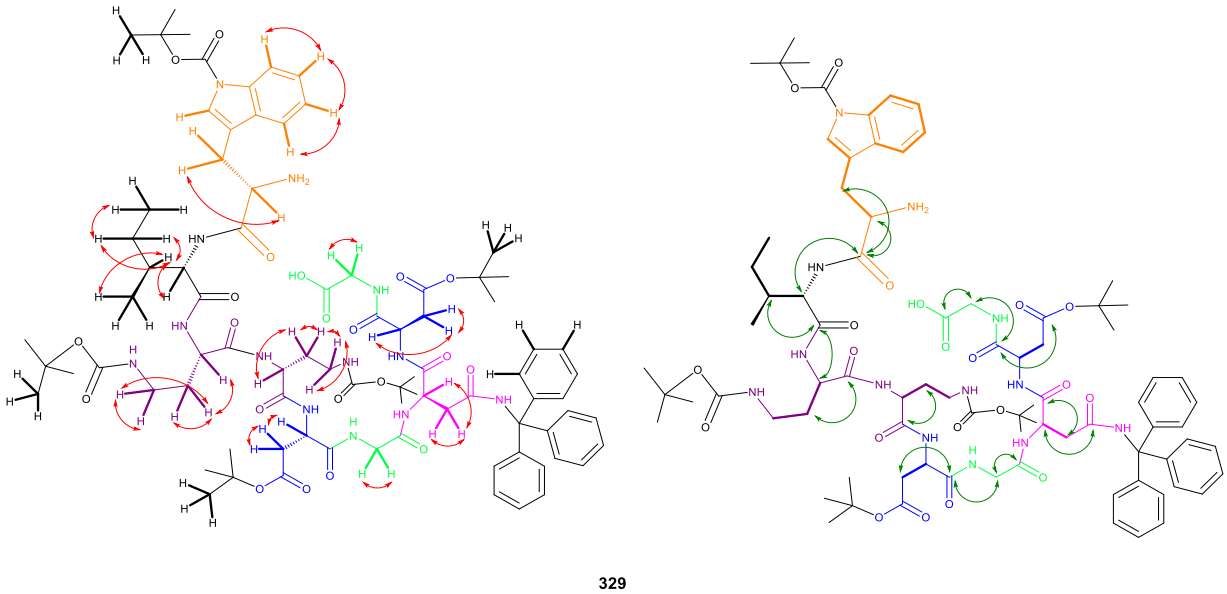

329

Figure 9-4: Left: Bold line shows $^{1}H,^{13}C$-HSQC correlations and red double-headed arrows show $^{1}H,^{1}H$-COSY correlations. Right: Green double-headed arrows show $^{1}H,^{13}C$-HMBC correlations and bold line shows $^{1}H,^{1}H$-TOCSY correlations (Full NMR table see appendix).

Therefore, the last three amino acids were coupled to the hexapeptide fragment **325** and not to the fragment **326** as planned. Two effects probably caused the failure of the synthesis. First, hexapeptide **7** was still bound in excess to the resin, so that this was also extended by the solid-phase synthesis. The second effect was probably that the peptide to be coupled, **327**, was sterically shielded, especially by the fatty acid chain, and thus did not undergo a coupling reaction.

9.6 Conclusion of the Dual Phase Approach

In summary, in this synthesis approach, the lipopeptide fragment **8** was achieved in four steps with an overall yield of 44 %. In addition, the hexapeptide fragment **325** was obtained by SPPS in 64 % yield. Subsequently, it was possible to couple both fragments using solid phase synthesis. However, the subsequent coupling of the last three amino acids through SPPS was unsuccessful. The last three amino acids coupled to the incorrect peptide chain which was bound to the resin. To prevent this, coupling reagents needed to be screened. In addition, it would be possible to deactivate the reactive *N* - termini of the non-expandable peptide chains on the resin. In this manner, the unbound *N* - termini of undesired peptide chains are chemically linked to a reagent, a process commonly referred to as capping. Another viable option would be to introduce the fatty acid chain at a later stage.

10 Summary and Outlook

This work laid the first foundation for the synthesis of brevistin (**6**). The first synthetic successes were achieved, such as a modular fragment synthesis. For instance, the dual phase approach described in section 9.5 allowed the fragment synthesized in liquid phase to be modified in such a way that instead of the fatty acid, a protective group was first installed on the α amine of the threonine. Thus, either the silyl-based 2-(trimethylsilyl)ethoxycarbonyl (Teoc) protecting group or, as in section 9.2, the azide threonine could be used (Figure 10-1).

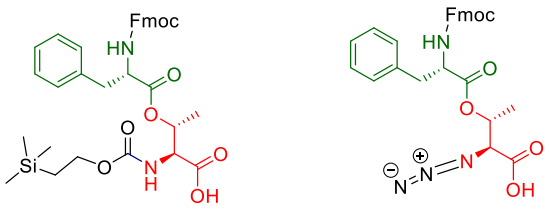

330 **331**

*Figure 10-1: Left: Possible Teoc protected dipeptide fragment **330**. Right: Possible azide protected dipeptide fragment **331**.*

This would allowed the fatty acid to be introduced into the peptide at a later time and would eliminate the possible negative steric effects of the non-polar fatty acid chain. In addition, the fatty acid could be changed flexibly, which would lead to a simplified synthesis of derivatives and investigation of the effect of the fatty acid on the bioactivity.

If further coupling of the fragments or continuation of the synthesis on solid phase is not possible, it would be possible to protect the coupling product **327** at the *C* - terminus and to couple this to the possible tripeptide fragment **333** in liquid phase (Scheme 10-1). In addition, suitable conditions for the cyclization of the linear precursor still have to be found. Thus, brevistin (**6**) remains an exciting synthetic target.

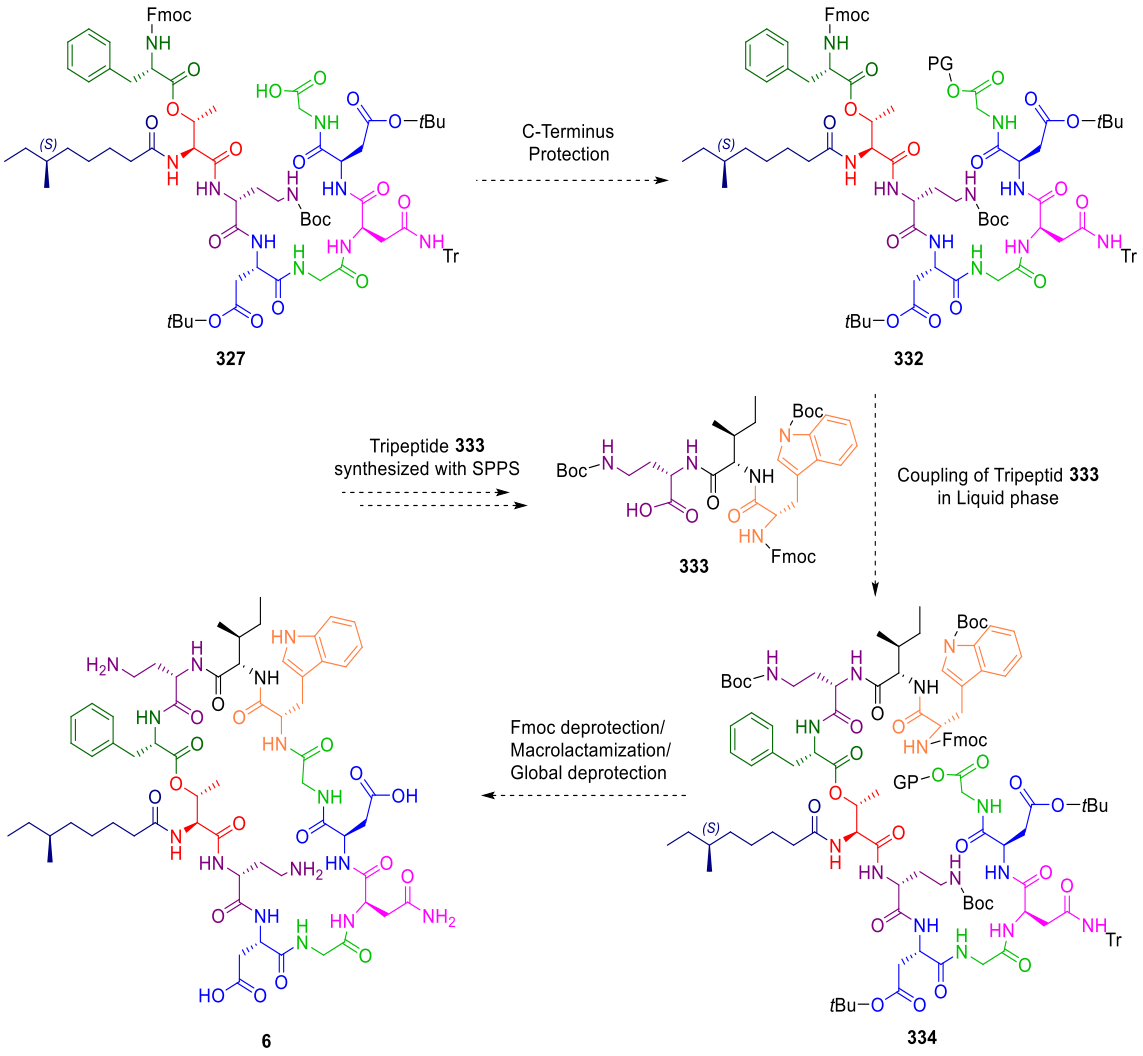

Scheme 10-1: Alternative synthetic route for coupling in liquid phase.

11 Experimental Part

11.1 Gerneral Methods

Reaction conditions: All reagents were purchased from commercial suppliers (*Sigma-Aldrich*, *TCI*, *Acros*, *AlfaAesar*, *Iris Biotech*) in the highest purity grade available and used without further purification. Anhydrous solvents (THF, CH_2Cl_2, MeCN, Et_2O, toluene) were obtained from a solvent drying system MB SPS-800 (*MBraun*) and stored over molecular sieves (3 or 4 Å). Unless stated otherwise, all non-aqueous reactions were performed under an argon atmosphere in flame-dried glassware. The reactants were handled using standard *Schlenk* techniques. Temperatures above r.t. (23 °C) refer to oil bath or heat-on temperatures, which were controlled by a temperature modulator. For cooling, the following baths were used: water/ice (0 °C), MeCN/dry ice (−40 °C) and acetone/dry ice (−78 °C) as well as a *Huber* TC100E-F-NR cryostat.

TLC monitoring was performed with silica gel 60_{F254} pre-coated polyester sheets (0.2 mm silica gel, *Macherey-Nagel*) and visualized using UV light and staining with a solution of CAM (1.0 g $Ce(SO_4)_2$), 2.5 g $(NH_4)_6Mo_7O_{24}$, 8 mL conc. H_2SO_4 in 100 mL H_2O) and subsequent heating.

Purification methods: For column chromatography, silica gel (pore size 60 Å, 40-63 µm) was used from *Merck* or *Aldrich*. Compounds were eluated using the stated mixtures under pressure of nitrogen or air. Solvents for column chromatography were distilled prior to use. For ion exchange chromatography, Dowex® 50WX8, 100–200 mesh by *Acros* was used. Gel permeation chromatography was performed using SephadexTM LH–20 purchased from *GE Healthcare*.

Preparative thin-layer chromatography was performed on alumina backed silica gel sheets (20x20 cm, pore size 60 Å) coated with a fluorescent indicator purchased from *Merck*. The crude product was applied as a solution in CH_2Cl_2 (20 µL) and using a *Hamilton* syringe. Detection was carried out under UV light and the desired areas were scrapped off and stirred 1 h with EtOAc or CH_2Cl_2. After filtration, the silica gel was washed (EtOAc or CH_2Cl_2) and the solvent was removed under reduced pressure.

Semi-preparative and analytical HPLC analyses were performed on *Knauer Wissenschaftliche Geräte GmbH* systems with support from *Andreas J. Schneider*. The solvents for HPLC were purchased in HPLC grade. The chromatograms were recorded by UV-detection at 240, 215, 210 and 205 nm.

Table 11-1: HPLC configuration for preparative HPLC

	System A	System B	System C
series	PLATINblue	Azura	PLATINblue
pumps	binary, HPG P1 system, 10 mL	binary, HPG P 6.1L, 10 mL	binary, HPG P1 system, 5 mL
pressure	750 bar	700 bar	1000 bar
autosampler	AS1 with 10 µL injection loop	3950 with 100 µL injection loop	AS1 with 10 µL injection loop
mixing chamber	static, SmartMix 350 µL	integrated static mixing chamber, 100 µL	static, SmartMix 100 µL
column heater	T1	CT 2.1	T1
detection type	PDA UV/VIS detection PDA1, D2/Hg halogen lamps, 190-1000 nm	PDA UV/VIS detection DAD 6.1L, D2/Hg halogen lamps, 190-1020 nm	PDA UV/VIS detection PDA1, D2/Hg halogen lamps, 190-1000 nm
degasser	analytical 2-channel-online-degasser	analytical 2-channel-online-degasser	analytical 2-channel-online-degasser

Analytical methods: All NMR spectra were recorded on *Bruker* spectrometers at the University of Bonn under supervision of Dr. *Senada Nozinovic* with operating frequencies of 125 (^{13}C), 150 (^{13}C), 175 (^{13}C), 400 (^{1}H), 500 (^{1}H), 600 (^{1}H) and 700 MHz (^{1}H) in deuterated solvents obtained from *Deutero* and *Carl Roth*. Spectra were measured at room temperature unless stated otherwise and chemical shifts are reported in ppm relative to (Me)4Si (δ = 0.00 ppm) and were calibrated to the residual signal of undeuterated solvents.[229] Data for 1H-NMR spectra are reported as follows: chemical shift (multiplicity, coupling constants (*J*) reported in hertz, number of hydrogens, assignment). Abbreviations used are: s (singlet), d (doublet), t (triplet), q (quartet), quint (quintet), m (multiplet), br (broad). Overlapped and not resolved signals are reported as multiplets. Atom numbering was chosen randomly and is shown for the isolated products in the respective schemes.

Mass spectra (MS) and high resolution mass spectra (HRMS) were recorded on the documented systems in Table 11-2 at the University of Bonn under supervision of Dr. *Marianne Engeser*

Table 11-2: Used MS systems for MS and HRMS.

	manufacturer	**measurements**
MAT 95 XL	*Thermo Finnigan* (Bremen)	EI
MAT 90	*Thermo Finnigan* (Bremen)	EI, LIFDI, CI, FAB
MALDI autoflex II TOF/TOF	*Bruker Daltonik* (Bremen)	MALDI
micrOTOF-Q	*Bruker Daltonik* (Bremen)	ESI, APCI, nano-ESI, MS/MS, LC-MS, DC-MS
Orbitrap XL	*Thermo Fisher Scientific* (Bremen)	ESI, APCI, APPI, nano-ESI
Apex IV FT-ICR	*Bruker Daltonik* (Bremen)	ESI, nano-ESI, MALDI, EI, CI

Optical rotation data were measured using an *Anton Paar* modular compact polarimeter MCP 150, with either a 10 mm cuvette (0.2 ml) or a 100 mm cuvette (0.7 ml), using a LED (589 nm) as a light source. The optical rotation was measured autonomously five times and the specific rotation was calculated.

$$[\boldsymbol{\alpha}]_{\boldsymbol{D}}^{\boldsymbol{T}} = \frac{\boldsymbol{\alpha}_{\boldsymbol{D}}^{\boldsymbol{T}}}{\boldsymbol{l} * \boldsymbol{c}}$$

[α]: specific rotation, D: light source (589 nm), T: temperature, α: optical rotation, l: path length of the cuvette, c: concentration [g/100 mL]

11.2 Experimental Data

11.2.1 Syntheses Portentol Project

(2S,3R,4R,5S,6R)-3,5,6-trimethyl-2-vinyltetrahydro-2H-pyran-2,4-diol (102)

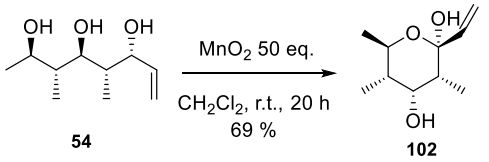

54 102

Chemical Formula: $C_{10}H_{18}O_3$
Exact Mass: 186,1256
Molecular Weight: 186,2510

To a stirred solution of **54** (30.0 mg, 0.16 mmol, 1.00 eq.) in CH_2Cl_2 (5.00 mL) was added MnO_2 (691 mg, 7.95 mmol, 50.0 eq.) and stirred at room temperature for 20 h. The solution was filtered over a pad of Celite and concentrated under reduced pressure. The crude product was purified by flash column chromatography (*n*-pentan:diethylether = 2:1) to yield **102** as a white solid (17.4 mg, 0.09 mmol, 69 %).

***R*f** = 0.5 (cyclohexane: ethyl acetate 1:1).

$[\alpha]_D^{20}$= −0.8° (*c* = 1.02 in CH_2Cl_2).

^{1}H-NMR (400 MHz, CD_2Cl_2): *δ* [ppm] = 5.77 (ddd, *J* = 17.3, 10.7, 0.5 Hz, 1H), 5.39 (dd, *J* = 17.3, 1.7 Hz, 1H), 5.18 (dd, *J* = 10.7, 1.7 Hz, 1H), 4.11 – 4.08 (m, 1H), 3.88 (dq, *J* = 10.3, 6.2 Hz, 1H), 3.64 (dt, *J* = 6.7, 2.5 Hz, 1H), 2.77 – 2.72 (m, 1H), 1.69 (qdd, *J* = 7.1, 2.6, 0.7 Hz, 1H), 1.47 (dqd, *J* = 10.4, 6.9, 2.5 Hz, 1H), 1.17 (d, *J* = 6.2 Hz, 3H), 1.02 (d, *J* = 7.2 Hz, 3H), 0.95 (d, *J* = 6.9 Hz, 3H).

^{13}C-NMR (101 MHz, CD_2Cl_2): *δ* [ppm] = 139.9 (CH) , 115.2 (CH_2) , 98.9 (C_q) , 74.6 (CH) , 65.6 (CH), 42.3 (CH), 41.0 (CH), 19.0 (CH_3), 13.9 (CH_3), 12.6 (CH_3).

HRMS (ESI-TOF) m/z: $[M+Na]^+$Calculated for $C_{10}H_{18}O_3Na^+$ 209.1148, found: 209.1154

(*2S*,*3R*,*4R*,*5R*,*6R*)-4-((*tert*-butyldimethylsilyl)oxy)-3,5,6-trimethyl-2-vinyltetrahydro-2*H*-pyran-2-ol (103)

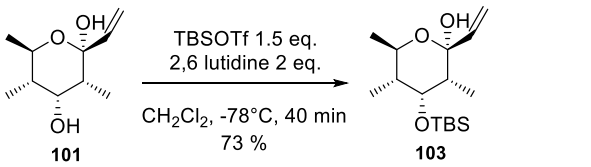

Chemical Formula: $C_{16}H_{32}O_3Si$
Exact Mass: 300,2121
Molecular Weight: 300,5140

A stirred solution of **102** (10.4 mg, 0.06 mmol, 1.00 eq.) in dry CH_2Cl_2 (2.00 mL) was cooled to –78 °C. 2,6-lutidine (13.0 µL, 0.11 mmol, 2.00 eq.) and *tert*-butylmethylsilyl triflat (TBSOTf) (15.0 µL, 0.07 mmol, 1.20 eq.) were added consecutively dropwise. The reaction stirred at –78 °C for 45 min. The solution was quenched with a saturated aqueous ammonium chloride solution (1.50 mL). The phases were separated and the aqueous layer was extracted with CH_2Cl_2 (3 x 3.0 mL). The combined organic layers were dried over $MgSO_4$, filtered and concentrated under reduced pressure. The crude product was purified by flash column chromatography (*n*-pentan:diethylether = 10:1) to yield **103** as a white solid (12.3 mg, 0.04 mmol, 73 %).

***R*f** = 0.6 (cyclohexane: ethyl acetate 1:1).

$[\alpha]_D^{20}$= −1.2° (*c* = 0.86 in CH_2Cl_2).

^{1}H-NMR (500 MHz, CD_2Cl_2): *δ* [ppm] = 5.69 (ddd, *J* = 17.2, 10.6, 1.2 Hz, 1H), 5.43 – 5.38 (m, 2H), 5.14 (dd, *J* = 10.6, 2.1 Hz, 1H), 3.92 – 3.85 (m, 2H), 1.70 (qd, *J* = 7.2, 2.1 Hz, 1H), 1.53 – 1.45 (m, 1H), 1.15 (d, *J* = 6.2 Hz, 3H), 0.96 (d, *J* = 3.2 Hz, 13H), 0.91 (d, *J* = 7.0 Hz, 3H), 0.15 (s, 3H), 0.13 (s, 3H).

^{13}C-NMR (125 MHz, CD_2Cl_2): *δ* [ppm] =140.1 (CH), 115.7 (CH_2), 99.1 (C_q), 77.8 (CH), 65.8 (CH), 43.7(CH), 42.3 (CH), 26.4 (CH_3), 19.5 (CH_3), 18.7 (C_q), 15.6 (CH_3), 14.6 (CH_3), -3.3 (CH_3), -3.4 (CH_3).

HRMS (ESI-TOF) m/z: $[M+Na]^+$Calculated for $C_{16}H_{32}O_3SiNa^+$ 323.2013, found: 323.2013.

(2S,3R,4R,5R,6R)-4-(benzyloxy)-3,5,6-trimethyl-2-vinyltetrahydro-2H-pyran-2-ol (107)

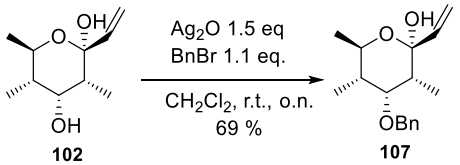

Chemical Formula: $C_{17}H_{24}O_3$
Exact Mass: 276,1725
Molecular Weight: 276,3760

To a stirred solution of **102** (17.2 mg, 0.09 mmol, 1.00 eq.) in CH_2Cl_2 (1.00 mL) was added Ag_2O (32.10 mg, 0.14 mmol, 1.50 eq.) and Benzyl bromide (12.03 µL, 0.10 mmol, 1.10 eq.) at room temperature over night. The solution was filtered over a pad of silica gel and concentrated under reduced pressure. The crude product was purified by flash column chromatography (cyclohexan:ethyl acetat = 8:1) to yield **107** as a white solid (17.50 mg, 0.06 mmol, 69 %)

R_f = 0.3 (cyclohexane: ethyl acetate 5:1).

^{1}H NMR (500 MHz, CD_2Cl_2) δ [ppm] = 7.41 – 7.30 (m, 5H), 5.69 (ddd, *J* = 17.2, 10.6, 1.2 Hz, 1H), 5.40 (dd, *J* = 17.2, 2.0 Hz, 1H), 5.26 (dd, *J* = 1.2, 0.6 Hz, 1H), 5.15 (dd, *J* = 10.6, 2.0 Hz, 1H), 4.67 (d, *J* = 10.7 Hz, 1H), 4.63 (d, *J* = 10.8 Hz, 1H), 3.86 (dq, *J* = 10.2, 6.2 Hz, 1H), 3.63 (t, *J* = 2.5 Hz, 1H), 1.79 (qd, *J* = 7.1, 2.4 Hz, 1H), 1.58 – 1.54 (m, 1H), 1.15 (d, *J* = 6.2 Hz, 3H), 1.04 (d, *J* = 7.1 Hz, 3H), 1.00 (d, *J* = 6.9 Hz, 3H).

^{13}C NMR (126 MHz, CD_2Cl_2) δ [ppm] = 140.1, 138.5, 129.1, 128.6, 128.4, 115.9, 98.9, 84.8, 77.3, 66.5, 43.1, 42.4, 19.6, 14.8, 13.8.

HRMS (ESI-TOF) m/z: $[M+H]^+$Calculated for $C_{17}H_{24}O_3Na^+$ 299.1618, found: 299.1618.

(2R,3R,4R,5R,6S)-4-(benzyloxy)-2,3,5-trimethyl-6-vinyltetrahydro-2H-pyran (108)

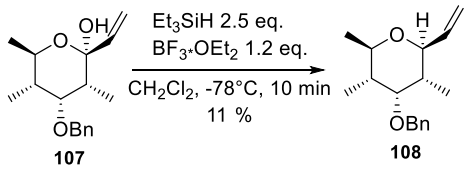

Chemical Formula: $C_{17}H_{24}O_2$
Exact Mass: 260,1776
Molecular Weight: 260,3770

A stirred solution of **107** (8.80 mg, 0.03 mmol, 1.00 eq.) in dry CH_2Cl_2 (1.00 mL) was cooled to –78 °C. Et_3SiH (12.70 µL, 0.08 mmol, 2.50 eq.) and $BF_3{\cdot}OEt_2$ (4.70 µL, 0.04 mmol, 1.20 eq.) were added consecutively dropwise. The reaction stirred at –78 °C for 10 min. The solution was quenched with a saturated sodium bicarbonat (1.50 mL). The phases were separated and the aqueous layer was extracted with CH_2Cl_2 (3 x 3.00 mL). The combined organic layers were dried over Na_2SO_4, filtered and concentrated under reduced pressure. The crude product was purified by flash column chromatography (cyclohexan:ethyl acetate = 15:1) to yield **108** as a brownish oil (0.90 mg, 3.46 µmol, 11 %).

***R*f** = 0.3 (cyclohexane: ethyl acetate 15:1).

^{1}H NMR (500 MHz, CD_2Cl_2) δ [ppm] = 7.40 – 7.32 (m, 4H), 7.31 – 7.25 (m, 1H), 5.72 (ddd, *J* = 17.2, 10.4, 7.6 Hz, 1H), 5.21 (ddd, *J* = 17.2, 2.0, 1.0 Hz, 1H), 5.12 (ddd, *J* = 10.4, 2.1, 0.7 Hz, 1H), 4.62 (d, *J* = 1.3 Hz, 2H), 3.86 (dd, *J* = 10.3, 7.6 Hz, 1H), 3.59 (dq, *J* = 10.0, 6.3 Hz, 1H), 3.47 (t, *J* = 2.5 Hz, 1H), 1.61 – 1.54 (m, 1H), 1.52 – 1.47 (m, 3H), 1.12 (d, *J* = 6.2 Hz, 3H), 0.96 (d, *J* = 6.9 Hz, 3H), 0.92 (d, *J* = 6.9 Hz, 3H).

^{13}C NMR (126 MHz, CD_2Cl_2) δ [ppm] = 139.9, 139.0, 128.8, 128.0, 127.9, 117.1, 83.0, 79.6, 76.4, 73.3, 44.2, 42.1, 19.9, 14.8, 14.5.

HRMS (ESI-TOF) m/z: $[M+Na]^+$Calculated for $C_{17}H_{24}O_2Na^+$ 283.1669, found: 283.1669.

(2R,3S,4R,5R,6S)-2,3,5-trimethyl-6-vinyltetrahydro-2H-pyran-4-ol (109)

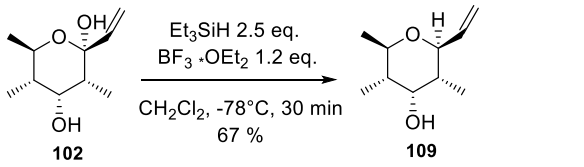

Chemical Formula: $C_{10}H_{18}O_2$
Exact Mass: 170,1307
Molecular Weight: 170,2520

A stirred solution of **102** (60.0 mg, 0.30 mmol, 1.00 eq.) in dry CH_2Cl_2 (2.00 mL) was cooled to –78 °C. Et_3SiH (128.2 µL, 0.80 mmol, 2.50 eq.) and BF_3*OEt_2 (47.7 µL, 0.40 mmol, 1.20 eq.) were added consecutively dropwise. The reaction stirred at –78 °C for 30 min. The solution was quenched with a saturated sodium bicarbonat (1.50 mL). The phases were separated and the aqueous layer was extracted with CH_2Cl_2 (3 x 3.00 mL). The combined organic layers were dried over Na_2SO_4, filtered and concentrated under reduced pressure. The crude product was purified by flash column chromatography (*n*-pentan:diethylether = 5:1) to yield **109** as a colorless oil (37.2 mg, 0.2 mmol, 67 %).

***R*$_f$** = 0.6 (cyclohexane: ethyl acetate 5:1).

^{1}H NMR (500 MHz, CD_2Cl_2) δ [ppm] = 5.72 (ddd, *J* = 17.2, 10.4, 7.6 Hz, 1H), 5.19 (ddd, *J* = 17.2, 2.1, 1.0 Hz, 1H), 5.11 (ddd, *J* = 10.4, 2.1, 0.8 Hz, 1H), 3.87 (dd, *J* = 9.5, 7.3 Hz, 1H), 3.74 (t, *J* = 2.1 Hz, 1H), 3.60 (dq, *J* = 9.8, 6.3 Hz, 1H), 1.48 (dqd, *J* = 10.1, 7.0, 2.1 Hz, 1H), 1.45 – 1.35 (m, 1H), 1.09 (d, *J* = 6.3 Hz, 3H), 0.86 (d, *J* = 6.9 Hz, 3H), 0.81 (d, *J* = 7.0 Hz, 3H).

^{13}C NMR (125 MHz, CD_2Cl_2) δ [ppm] = 139.2, 116.8, 78.8, 76.2, 72.4, 44.3, 42.3, 19.9, 15.3, 15.1.

HRMS (ESI-TOF) m/z: $[M+Na]^+$Calculated for $C_{10}H_{18}O_2Na^+$ 193.1199, found: 193.1199.

tert-butyldimethyl(((2R,3R,4R,5S,6S)-2,3,5-trimethyl-6-vinyltetrahydro-2H-pyran-4 yl)oxy)silane (106)

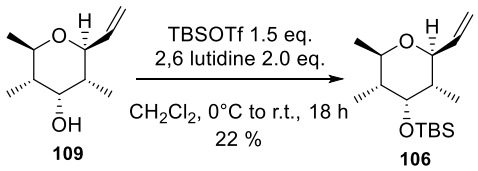

Chemical Formula: $C_{16}H_{32}O_2Si$
Exact Mass: 284,2172
Molecular Weight: 284,5150

A stirred solution of **109** (9.20 mg, 0.05 mmol, 1.00 eq.) in dry CH_2Cl_2 (1.0 mL) was cooled to 0 °C. 2,6-lutidine (12.5 µL, 0.11 mmol, 2.00 eq.) and *tert*-butylmethylsilyl triflat (TBSOTf) (18.6 µL, 0.08 mmol, 1.20 eq.) were added consecutively dropwise. The reaction was allowed to warm up to room temperature and stirred at this temperature for 18 h. The solution was quenched with a saturated aqueous ammonium chloride solution (1.50 mL). The phases were separated and the aqueous layer was extracted with CH_2Cl_2 (3 x 3.00 mL). The combined organic layers were dried over Na_2SO_4, filtered and concentrated under reduced pressure. The crude product was purified by flash column chromatography (*n*-pentan:diethylether = 10:1) to yield **106** as a colorless oil (3.40 mg, 0.01 mmol, 22 %).

R_f = 0.6 (cyclohexane: ethyl acetate 10:1).

^{1}H-NMR (500 MHz, CD_2Cl_2): δ [ppm] = 5.69 (ddd, *J* = 17.2, 10.6, 1.2 Hz, 1H), 5.43 – 5.38 (m, 2H), 5.14 (dd, *J* = 10.6, 2.1 Hz, 1H), 3.92 – 3.85 (m, 2H), 1.70 (qd, *J* = 7.2, 2.1 Hz, 1H), 1.53 – 1.45 (m, 1H), 1.15 (d, *J* = 6.2 Hz, 3H), 0.96 (d, *J* = 3.2 Hz, 13H), 0.91 (d, *J* = 7.0 Hz, 3H), 0.15 (s, 3H), 0.13 (s, 3H).

^{13}C-NMR (125 MHz, CD_2Cl_2): δ [ppm] = 140.1 (CH), 115.7 (CH_2), 99.1 (C_q), 77.8 (CH), 65.8 (CH), 43.7(CH), 42.3 (CH), 26.4 (CH_3), 19.5 (CH_3), 18.7 (C_q), 15.6 (CH_3), 14.6 (CH_3), -3.3 (CH_3), -3.4 (CH_3).

HRMS (ESI-TOF) m/z: $[M+Na]^+$Calculated for $C_{16}H_{32}O_2SiNa^+$ 307.2064, found: 307.2064.

(Z)-((prop-1-en-1-yloxy)methyl)benzene (111)

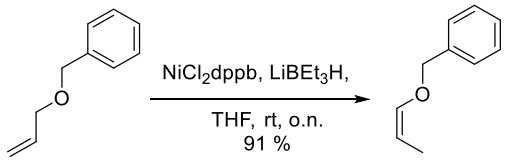

110 **111**

E:Z - 5:95
Chemical Formula: $C_{10}H_{12}O$
Exact Mass: 148,0888
Molecular Weight: 148,2050

A stirred solution of **110** (2.40 g, 16.0 mmol, 1.00 eq.) in dry THF (8.0 mL) was cooled to 0 °C. $NiCl_2$dppb (0.26 g, 0.64 mmol, 0.04 eq.) was added to the solution and $LiBEt_3H$ (1 M in THF, 0.64 mL, 0.64 mmol, 0.04 eq.) was added dropwise. The reaction was allowed to warm up to room temperature and stirred at this temperature over night. The solution was quenched with a saturated sodium bicarbonate solution (5.00 mL). The phases were separated and the aqueous layer was extracted with Et_2O (3 x 7.00 mL). The combined organic layers were dried over Na_2SO_4, filtered and concentrated under reduced pressure. The crude product was purified by flash column chromatography (*n*-pentan:diethylether = 5:1) to yield **111** as a colorless oil (2.17 g, 14.6 mmol, 91 %).[35]

R_f = 0.6 (cyclohexane: ethyl acetate 5:1/ 5 %w $AgNO_3$).
^{1}H NMR (500 MHz, $CDCl_3$) δ [ppm] = 7.36 (dtd, *J* = 7.1, 6.3, 1.4 Hz, 5H), 6.04 (dq, *J* = 6.2, 1.7 Hz, 1H), 4.80 (s, 2H), 4.45 (qd, *J* = 6.8, 6.2 Hz, 1H), 1.63 (dd, *J* = 6.8, 1.7 Hz, 3H).
^{13}C NMR (125 MHz, $CDCl_3$) δ [ppm] = 145.3, 138.0, 128.6, 127.9, 127.4, 102.0, 73.7, 9.5.
HRMS (ESI-TOF) m/z: $[M+H]^+$Calculated for $C_{10}H_{13}O^+$ 149.0961, found: 149.0961.

(2R,3R,5R,6R)-2-hydroxy-3,5,6-trimethyl-2-((S)-oxiran-2-yl)tetrahydro-4H-pyran-4-one (121)

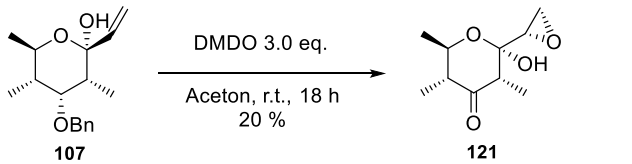

Chemical Formula: $C_{10}H_{16}O_4$
Exact Mass: 200,1049
Molecular Weight: 200,2340

To a stirred solution of DMDO (0.07 M in Acetone, 3.70 mL, 0.26 mmol, 3.00 eq.) was added **107** (22.5 mg, 0.09 mmol, 1.00 eq.). The reaction was stirred at room temperature for 18 h. The solution was concentrated under reduced pressure. The crude product was purified by flash column chromatography (cyclohexane:ethyl acetate = 8:1) to yield **121** as a white solid (3.4 mg, 0.02 mmol, 20 %)

R_f = 0.3 (cyclohexane: ethyl acetate 8:1).
$[\alpha]_D^{20}$= −44.4° (*c* = 0.36 in CH_2Cl_2).
^{1}H NMR (500 MHz, CD_2Cl_2) δ [ppm] = 3.89 (dq, *J* = 10.0, 6.1 Hz, 1H), 3.21 (dd, *J* = 4.0, 2.8 Hz, 1H), 2.82 (dd, *J* = 5.0, 4.0 Hz, 1H), 2.78 (qd, *J* = 6.8, 1.2 Hz, 1H), 2.70 (dd, *J* = 5.0, 2.8 Hz, 1H), 2.33 (dqd, *J* = 10.1, 6.6, 1.2 Hz, 1H), 1.34 (d, *J* = 6.2 Hz, 3H), 0.99 (d, *J* = 0.5 Hz, 3H), 0.97 (d, *J* = 0.7 Hz, 3H).
^{13}C NMR (126 MHz, CD_2Cl_2) δ [ppm] = 207.5, 99.4, 73.2, 51.6, 45.0, 45.1, 20.6, 9.9, 9.0.
HRMS (ESI-TOF) m/z: $[M+H]^+$Calculated for $C_{10}H_{17}O_4^+$ 201.1120, found: 201.1121.

(2R,3R,4R,5R,6R)-4-((tert-butyldimethylsilyl)oxy)-3,5,6-trimethyl-2-(oxiran-2-yl)tetrahydro-2H-pyran-2-ol (122)

Chemical Formula: $C_{16}H_{32}O_4Si$
Exact Mass: 316,2070
Molecular Weight: 316,5130

To a stirred solution of DMDO (0.05 M in Acetone, 5.24 mL, 0.25 mmol, 3.00 eq.) was added **107** (24.5 mg, 0.08 mmol, 1.00 eq.). The reaction was stirred at room temperature for 18 h. The solution was concentrated under reduced pressure. The crude product was purified by flash column chromatography (*n*-pentan:diethylether = 15:1) to yield **122** as a white solid (3.40 mg, 0.02 mmol, 26 % *d.r.* 3:1)

R_f = 0.3 (cyclohexane: ethyl acetate 5:1).

NMR data for major isomer:

^{1}H NMR (700 MHz, CD_2Cl_2) δ [ppm] = 3.89 – 3.84 (m, 2H), 2.93 (dd, *J* = 4.0, 2.6 Hz, 1H), 2.88 (dd, *J* = 6.1, 2.5 Hz, 1H), 2.64 (dd, *J* = 6.1, 4.0 Hz, 1H), 1.85 (qd, *J* = 7.2, 2.1 Hz, 1H), 1.50 – 1.45 (m, 1H), 1.16 (d, *J* = 6.3 Hz, 3H), 1.10 (d, *J* = 7.2 Hz, 3H), 0.94 (s, 8H), 0.89 (d, *J* = 7.0 Hz, 3H), 0.15 (s, 3H), 0.13 (s, 4H).

^{13}C NMR (175 MHz, CD_2Cl_2) δ [ppm] = 97.1, 78.3, 66.1, 54.8, 44.2, 43.4, 40.8, 26.3, 19.3, 18.6, 15.4, 14.5, -3.3, -3.4.

HRMS (ESI-TOF) m/z: $[M+H]^+$Calculated for $C_{16}H_{33}O_4Si^+$ 317.2143, found: 317.2144.

(2R,3R,4R,5R,6R)-4-((tert-butyldimethylsilyl)oxy)-2-((S)-1-hydroxyethyl)-3,5,6-trimethyltetrahydro-2H-pyran-2-ol (125)

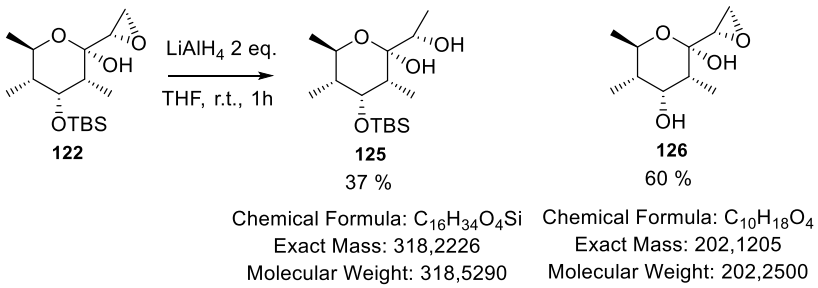

To a stirred solution of **122** (6.20 mg, 0.01 mmol, 1.00 eq.) in dry THF (3.00 mL) was added dropwise $LiAlH_4$ (1 M in THF, 24.2 µL, 0.02 mmol, 2.00 eq.). The reaction stirred at room temperature for 1 h. The solution was cooled to 0°C and was diluted with ethyl acetate (2.00 mL) and water (2.00 mL). The mixture was quenched with a saturated Rochell salt solution (3.00 mL) and was allowed to warm up to room temperature and stirred for 30 min at this temperature. The phases were separated and the aqueous layer was extracted with ethyl acetate (3 x 3.00 mL). The combined organic layers were dried over Na_2SO_4, filtered and concentrated under reduced pressure. The crude product was purified by flash column chromatography (cyclohexan:ethyl acetate = 5:1) to yield **125** as a white solid (1.40 mg, 4.00 µmol, 37%) and **126** as a white solid (1.46 mg, 7.20 µmol, 60 %).

Data for **125**:

***R*f** = 0.5 (cyclohexane: ethyl acetate 1:1).

^{1}H NMR (700 MHz, CD_2Cl_2) δ [ppm] = 3.89 – 3.83 (m, 2H), 3.62 (q, *J* = 6.4 Hz, 1H), 2.52 (dd, *J* = 5.9, 4.1 Hz, 1H), 2.06 (qd, *J* = 7.2, 2.1 Hz, 1H), 1.47 – 1.42 (m, 1H), 1.15 (d, *J* = 6.2 Hz, 3H), 1.13 (d, *J* = 6.4 Hz, 3H), 1.06 (d, *J* = 7.2 Hz, 3H), 0.94 (s, 9H), 0.89 (d, *J* = 7.1 Hz, 3H), 0.15 (s, 3H), 0.13 (s, 3H).

^{13}C NMR (175 MHz, CD_2Cl_2) δ [ppm] = 100.7, 79.3, 70.2, 66.2, 43.8, 38.5, 26.5, 19.6, 18.8, 16.1, 15.6, 14.8, -3.1, -3.3.

HRMS (ESI-TOF) m/z: $[M+H]^+$Calculated for $C_{16}H_{35}O_4Si^+$ 319.2299, found: 319.2299.

Data for **126**:

***R*f** = 0.3 (cyclohexane: ethyl acetate 1:1).

^{1}H NMR (700 MHz, CD_2Cl_2) δ [ppm] = 3.84 (dq, *J* = 10.3, 6.2 Hz, 1H), 3.54 (s, 1H), 3.22 (d, *J* = 1.5 Hz, 1H), 2.95 (dd, *J* = 4.0, 2.8 Hz, 1H), 2.74 (dd, *J* = 5.3, 4.0 Hz, 1H), 2.72 (dd, *J* = 5.3, 2.8 Hz, 1H), 1.90 (qdd, *J* = 7.2, 2.9, 1.3 Hz, 1H), 1.45 (dtd, *J* = 13.7, 6.9, 2.6 Hz, 1H), 1.18 (d, *J* = 6.2 Hz, 3H), 1.07 (d, *J* = 7.2 Hz, 3H), 0.95 (d, *J* = 6.9 Hz, 3H).

^{13}C NMR (175 MHz, CD_2Cl_2) δ [ppm] = 97.4, 74.9, 66.7, 54.8, 44.9, 43.0, 40.0, 19.4, 14.4, 14.4, 13.4.

HRMS (ESI-TOF) m/z: $[M+H]^+$Calculated for $C_{10}H_{19}O_4^+$ 203.1278, found: 203.1278.

(((3R,4S,5R,6R,Z)-2-ethylidene-6-(((trimethylsilyl)oxy)methyl)tetrahydro-2H-pyran-3,4,5-triyl)tris(oxy))tris(trimethylsilane) (146)

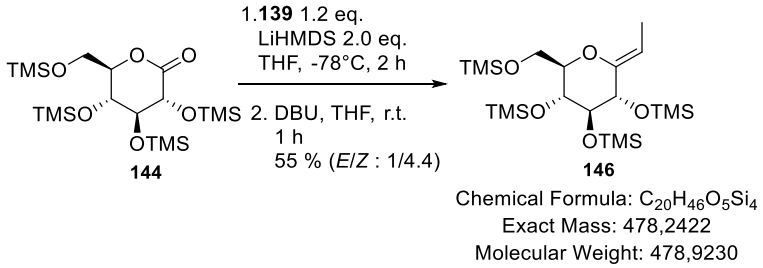

Protected lactone **144** (6.20 g, 13.28 mmol, 1.00 eq.) was dissolved in dry THF (57.0 mL) and the solution was cooled down to –78°C. BT-Sulphone **139** (3.62 g, 15.94 mmol, 1.20 eq.) was added to the solution. Afterwards LiHMDS (26.5 mL, 26.56 mmol, 2.00 eq.) was added slowly over a periode of 15 minutes. The resulting light yellow mixture was allowed to warm up to r.t. and stirred for one hour. The reaction mixture was quenched with CH_2Cl_2 (50.0 mL) and dest. water (10.0 mL). The aqueous phase was extracted with dichlormethane (3 x 10.0 mL) and the combined organic phases were washed with dest. water (5.00 mL), brine (5.00 mL) and dried over Na_2SO_4. The solvent was removed under reduced pressure yielding the crude product as a bright yellow oil. The crude product was dissolved with dry THF (150 mL) and DBU (4.70 g, 26.6 mmol, 2.00 eq.) was added. The reaction was stirred at r.t. for one hour before the solvent was removed *in vacuo*. The resulting oil was purified by flash column chromatography (*n*-pentane:diethylether = 50:1) to give the alkene **146** (3.50 g, 7.30 mmol, 46 %) as an colorless oil.

R_f: = 0.6 (cyclohexane: ethyl acetate 10:1).

$[\alpha]_D^{20}$= +46.2° (*c* = 0.86 in CH_2Cl_2).

^{1}H-NMR (500 MHz, CD_2Cl_2) δ [ppm] = 4.82 (qd, *J* = 6.8, 1.3 Hz, 1H), 3.85 (dd, *J* = 11.5, 2.0 Hz, 1H), 3.78 – 3.75 (m, 1H), 3.72 (dd, *J* = 11.5, 4.3 Hz, 1H), 3.59 (dd, *J* = 9.6, 7.2 Hz, 1H), 3.46 – 3.39 (m, 2H), 1.58 (dd, *J* = 6.8, 1.4 Hz, 3H), 0.20 – 0.10 (m, 43H).

^{13}C-NMR (125 MHz, CD_2Cl_2) δ [ppm] = 151.9, 103.8, 79.1, 76.4, 73.1, 72.5, 69.6, 9.1.

HRMS (ESI-TOF) m/z: Calculated for $[M+H]^+$ $C_{20}H_{47}O_5Si_4^+$ 479.2495, found: 479.2493.

((2R,3R,4S,5R,Z)-6-ethylidene-3,4,5-tris((trimethylsilyl)oxy)tetrahydro-2H-pyran-2-yl)methyl 4-methylbenzenesulfonate (154)

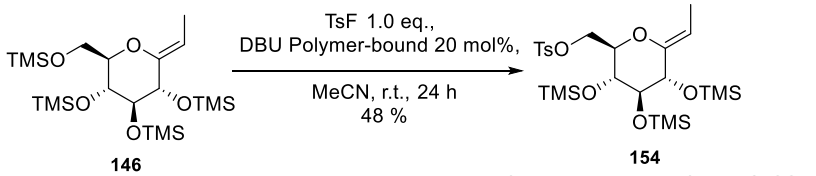

146 **154**

Chemical Formula: $C_{24}H_{44}O_7SSi_3$
Exact Mass: 560,2116
Molecular Weight: 560,9240

To a solution of TMS ether **146** (2.11 g, 4.40 mmol, 1.00 eq.) and TsF (766.70 mg, 4.40 mmol, 1.00 eq.) in MeCN (8.30 mL) DBU polymer bound (1,5 mmol/g, 1.70 g, 0.88 mmol, 0.20 eq.) was added. The mixture was stirred for 24 h at r.t. covered in aluminiumfoil. The solution was filtered over a pad of celite and concentrated under reduced pressure. The crude product was purified by flash column chromatography (cyclohexane:diethylether = 30:1) to yield **154** as a colourless oil (1.18 g, 2.11 mmol, 48 %)

R_f: = 0.4 (cyclohexane: ethyl acetate 10:1).

^{1}H-NMR (700 MHz, CD_2Cl_2) δ [ppm] = 7.81 – 7.76 (m, 2H), 7.38 – 7.33 (m, 2H), 4.80 (dtd, *J* = 6.9, 6.1, 1.3 Hz, 1H), 4.27 (dd, *J* = 10.6, 2.1 Hz, 1H), 4.08 (ddd, *J* = 10.7, 5.6, 1.3 Hz, 1H), 3.72 (dt, *J* = 6.5, 1.4 Hz, 1H), 3.68 (ddd, *J* = 9.7, 5.6, 2.2 Hz, 1H), 3.48 – 3.43 (m, 1H), 3.40 (t, *J* = 6.6 Hz, 1H), 1.49 (dd, *J* = 6.8, 1.3 Hz, 3H), 0.25 – -0.01 (m, 31H).

^{13}C-NMR (175 MHz, CD_2Cl_2) δ [ppm] = 150.7, 145.5, 133.4, 130.2, 128.4, 104.3, 79.5, 76.9, 73.4, 73.0, 70.0, 21.8, 9.5.

HRMS (ESI-TOF) m/z: Calculated for $[M+Na]^+$ $C_{24}H_{44}O_7Si_3SNa^+$ 583.2008, found: 583.2001.

(((3R,4S,5R,6R,Z)-2-ethylidene-6-methyltetrahydro-2H-pyran-3,4,5-triyl)tris(oxy))tris(trimethylsilane) (156)

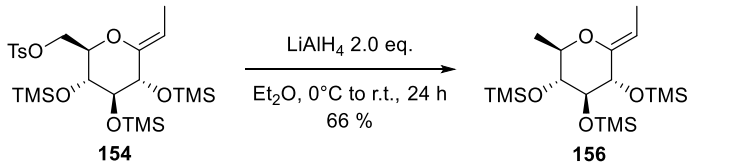

Chemical Formula: $C_{17}H_{38}O_4Si_3$
Exact Mass: 390,2078
Molecular Weight: 390,7420

Methode A:

Tosylated species **154** (409 mg, 729.2 µmol, 1.00 eq.) was dissolved in dry diethylether (0.80 mL). The mixture was cooled to 0°C before Lithiumaluminiumhydrid (1 M in THF, 1.50 mL, 1.46 mmol, 2.00 eq.) were slowly added. The solution was stirred for 1 hour at 0°C. After that the cooling bath was removed and the mixture stirred at r.t., covered with aluminiumfoil, for another 24 h. After 24 h the mixture was again cooled to 0°C and ethyl acetate (1.50 mL), dest. water (1.50 mL) and sat.-Rochelle-salt-solution (1.50 mL) were slowly added successively. The solution was stirred for further 30 minutes at 0°C. The solution was allowed to warm up to r.t., extracted with ethyl acetate (3 x 1.00 mL) and dried over Na_2SO_4. After evaporation of the solvent under reduced pressure the crude product was purified by flash column chromatography (cyclohexane:ethylactate = 20:1) to yield **156** (187 mg, 477.8 µmol, 66 %) as a colorless oil.

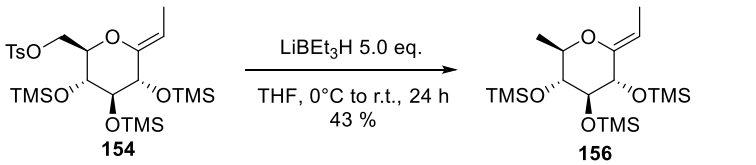

Chemical Formula: $C_{17}H_{38}O_4Si_3$
Exact Mass: 390,2078
Molecular Weight: 390,7420

Methode B:

Tosylated species **154** (68.6 mg, 122.3 µmol, 1.00 eq.) was dissolved in dry THF (0.90 mL). The mixture was cooled to 0°C before $LiBEt_3H$ (1 M in THF, 0.98 mL, 980 µmol, 5.00 eq.) were slowly added. The solution was stirred for 1 hour at 0°C. After that the cooling bath was removed and the mixture stirred at r.t., covered with aluminiumfoil, for another 24 h.

After 24 h the mixture was again cooled to 0°C and pentane (2.00 mL) and a saturated aqueous ammonium chloride solution (0.60 mL) were slowly added successively. The solution was stirred for further 30 minutes at 0°C. The solution was allowed to warm up to r.t., extracted with pentane (3 x 1.00 mL). The combined organic layers were washed with dest. water (5.00 mL),

brine (5.00 mL) and dried over Na_2SO_4. After evaporation of the solvent under reduced pressure the crude product was purified by flash column chromatography (cyclohexane:ethylactate = 20:1) to yield **156** (20.3 mg, 52.0 µmol, 43 %) as a colorless oil.

R_f: = 0.5 (cyclohexane: ethyl acetate 10:1).

^{1}H-NMR (500 MHz, CD_2Cl_2) δ [ppm] = 4.86 (qd, *J* = 6.8, 1.5 Hz, 1H), 3.77 (dp, *J* = 7.4, 1.5 Hz, 1H), 3.74 – 3.67 (m, 1H), 3.44 (dq, *J* = 9.2, 6.3 Hz, 1H), 3.36 – 3.30 (m, 1H), 3.25 (dd, *J* = 9.2, 7.6 Hz, 1H), 1.72 (dd, *J* = 7.3, 0.4 Hz, 1H), 1.57 (dd, *J* = 6.8, 1.6 Hz, 3H), 1.43 (d, *J* = 6.9 Hz, 2H), 1.28 (d, *J* = 6.3 Hz, 3H), 1.14 (d, *J* = 6.4 Hz, 1H), 0.90 (t, *J* = 7.4 Hz, 2H), 0.21 – 0.06 (m, 61H).

^{13}C-NMR (125 MHz, CD_2Cl_2) δ [ppm] = 152.4, 150.7, 126.5, 112.6, 103.3, 98.5, 79.5, 78.1, 77.4, 76.7, 76.6, 75.2, 73.7, 71.3, 69.7, 32.3, 21.2, 19.2, 19.0, 10.3, 9.6, 6.9, 1.4, 1.3, 1.2.

HRMS (ESI-TOF) m/z: Calculated for $[M+Na]^+$ $C_{17}H_{38}O_4Si_3Na^+$ 413.1970, found: 413.1971.

(3R,4S,5S,6R,Z)-2-ethylidene-6-methyltetrahydro-2H-pyran-3,4,5-triol (158)

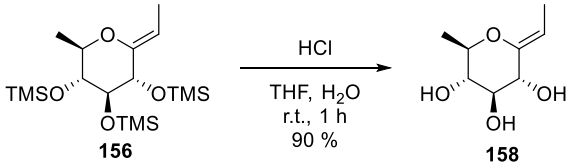

Chemical Formula: $C_8H_{14}O_4$
Exact Mass: 174,0892
Molecular Weight: 174,1960

Protected enol ether **156** (54.8 mg, 0.14 mmol, 1.00 eq.) was dissolved in THF (1.45 mL). Dest. water (0.30 mL) and HCl (0.06 mL, 0.14 mmol, 1.00 eq., 1 M) were added and the solution was stirred for 1 hour at r.t. The mixture was quenched with a saturated sodium bicarbonate solution (3.00 mL) and the aqueous phase was extracted with ethyl acetate (5 x 2.00 mL). The solvent was removed *in vacuo* and the residue was purified by flash column chromatography (ethyl acetate 100%) to yield **158** as a white solid (22.0 mg, 0.13 mmol, 90 %).

R_f: = 0.2 (ethyl acetate 100%).

$[\alpha]_D^{20}$= +75.0° (*c* = 0.21 in MeOH).

^{1}H-NMR (500 MHz, CD_2Cl_2) δ [ppm] =5.06 (qd, *J* = 6.8 Hz, *J* = 2.0 Hz,1H), 3.80 – 3.73 (m, 1 H, H-4), 3.27 (dd, *J*= 9.1 Hz, *J* = 6.1 Hz, 1H), 3.22 – 3.11 (m, 2 H), 1.56 (dd, *J* = 6.8 Hz, *J* = 2.1 Hz, 3H), 1.32 (d, *J* = 6.1 Hz, 3H).

^{13}C-NMR (125 MHz, CD_2Cl_2) δ [ppm] = 206.2, 102.5, 79.4, 77.8, 76.5, 72.5, 18.6, 9.5.

HRMS (ESI-TOF) m/z: Calculated for $[M–H]^-$ $C_8H_{13}O_4^-$ 173.0819, found: 173.0819.

(3*R*,4*R*,5*S*,6*R*)-3,4,5-trihydroxy-6(hydroxymethyl)-tetrahydro-2*H*-pyran-2-one (170)

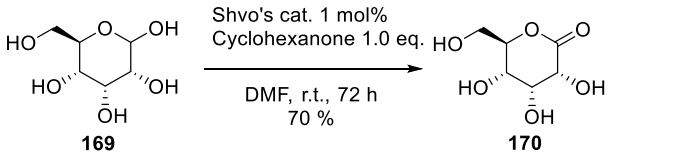

Chemical Formula: $C_6H_{10}O_6$
Exact Mass: 178,0477
Molecular Weight: 178,1400

D-Allose (**169**) (500 mg, 2.78 mmol, 1.00 eq.) was dissolved in dry DMF (10.0 mL) and dry cyclohexanone (20.0 mL, 2.78 mmol, 1.00 eq.) was added to the stirring solution. The combined mixture was stirred at r.t. until *D*-Allose (**169**) was completely dissolved. Then Shvo's catalyst (37.6 mg, 34.7 µmol, 0.01 eq.) was added and the mixture stirred at r.t. under exclusion of light. The color changed from light yellow to orange. The reaction was quenched with anhydrous acetone (10.0 mL) and the solvent was removed *in vacuo*. The remaining precipitate was taken up with anhydrous acetone (10.0 mL) and centrifuged (2500 rpm, 5 min) until the residual solid was white and the supernatant solution without color. The residual white solid was dried *in vacuo* to constant weight yielding **170** (1.39 g, 7.79 mmol, 70 %).

R_f: = 0.1 (ethyl acetate 100%).

$[\alpha]_D^{20}$= +45.5° (*c* = 0.51 in MeOH).

NMR data for 1,5 Lactone **170**

^{1}H-NMR (700 MHz, DMSO-d_6): δ [ppm] = 5.51 (d, *J* = 5.8 Hz, 1H), 5.45 (d, *J* = 3.6 Hz, 1H), 5.18 (d, *J* = 7.0 Hz, 1H), 4.85 (dd, *J* = 6.3, 5.1 Hz, 1H), 4.15 (ddd, *J* = 9.5, 4.0, 2.2 Hz, 1H), 4.02 (dd, *J* = 5.8, 2.4 Hz, 1H), 3.94 (dd, *J* = 3.9, 2.1 Hz, 1H), 3.83 (ddd, *J* = 9.3, 6.9, 2.2 Hz, 1H), 3.66 (ddd, *J* = 12.2, 5.1, 2.2 Hz, 1H), 3.55 (ddd, *J* = 12.3, 6.3, 4.1 Hz, 1H).

^{13}C-NMR (176 MHz, DMSO-d_6): δ [ppm] = 173.3, 80.8, 71.2, 69.2, 67.3, 62.7.

NMR data for 1,4 Lactone **173**

^{1}H-NMR (700 MHz, DMSO-d_6): δ [ppm] = 5.68 (d, *J* = 7.7 Hz, 1H), 5.33 (d, *J* = 5.3 Hz, 1H), 5.28 (d, *J* = 3.8 Hz, 1H), 4.78 (t, *J* = 5.5 Hz, 1H), 4.41 (dd, *J* = 7.6, 5.4 Hz, 1H), 4.27 (d, *J* = 3.8 Hz, 1H), 4.21 (dd, *J* = 5.5, 3.7 Hz, 1H), 3.64 – 3.60 (m, 1H), 3.44 – 3.38 (m, 2H).

^{13}C-NMR (176 MHz, DMSO-d_6): δ [ppm] = 172.2, 85.5, 72.2, 69.7, 65.1, 60.2.

HRMS (ESI-TOF) m/z: Calculated for $[M+H]^+$ $C_6H_{11}O_6^+$ 179.0550, found: 179.0550.

Synthesis of (3*R*,4*R*,5*R*,6*R*)-3,4,5-tris((trimethylsilyl)oxy)-6 (((trimethylsilyl)oxy)methyl)tetrahydro-2*H*-pyran-2-one (168)

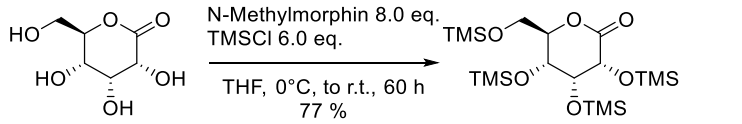

170 **168**

Chemical Formula: $C_{18}H_{42}O_6Si_4$
Exact Mass: 466,2058
Molecular Weight: 466,8680

Lactone **170** (1.30 g, 7.30 mmol, 1.00 eq.) was dissolved in dry THF (20.0 mL) and cooled down to 0°C. NMM (6.50 mL, 58.4 mmol, 8.00 eq.) and TMSCl (5.50 mL, 43.8 mmol, 6.00 eq.) were slowly added subsequently. The resulting mixture was stirred at 0°C for one hour before the reaction was allowed to warm up to r.t. and stirred for further 60 h. The reaction was quenched by diluting the solution with dry pentane (30.0 mL) and dest. water (2.00 mL). The organic layer was extracted with dry pentane (2 x 15.0 mL) and washed with sat. Na_2HPO_4-solution (2 x 10.0 mL). The combined organic layers were dried over Na_2SO_4 and the solvent was removed under reduced pressure. The crude product was purified by flash column chromatography (cyclohexane:ethylacetate = 20:1) yielding as colorless oil protected lactone **168** (2.63 g, 5.62 mmol, 77 %).

R_f: = 0.5 (cyclohexane: ethyl acetate 10:1).

$[\alpha]_D^{20}$= +52.6° (*c* = 1.05 in CH_2Cl_2).

^{1}H-NMR (500 MHz, CD_2Cl_2) δ [ppm] = 4.30 (dt, *J* = 9.0, 2.2 Hz, 1H), 4.08 – 4.00 (m, 3H), 3.82 (dd, *J* = 11.8, 2.0 Hz, 1H), 3.73 (dd, *J* = 11.8, 2.4 Hz, 1H), 0.28 – 0.02 (m, 39H).

^{13}C-NMR (125 MHz, CD_2Cl_2) δ [ppm] = 171.5, 80.8, 75.5, 71.4, 66.5, 61.1.

HRMS (ESI-TOF) m/z: Calculated for $[M+H]^+$ $C_{18}H_{43}O_6Si_4^+$ 467.2131, found: 467.2122.

(((3*R*,4*R*,5*R*,6*R*,*Z*)-2-ethylidene-6(((trimethylsilyl)oxy)methyl)tetrahydro-2*H*-pyran-3,4,5 triyl)tris(oxy))tris(trimethylsilane) (179)

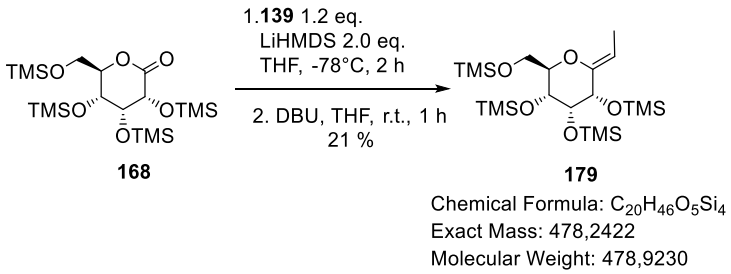

Chemical Formula: $C_{20}H_{46}O_5Si_4$
Exact Mass: 478,2422
Molecular Weight: 478,9230

Protected lactone **168** (2.45 g, 5.25 mmol, 1.00 eq.) was dissolved in dry THF (57.0 mL) and the solution was cooled down to –78°C. BT-Sulphone **139** (1.43 g, 6.30 mmol, 1.20 eq.) was added to the solution. Afterwards LiHMDS (10.5 mL, 10.50 mmol, 2.00 eq.) was added slowly over a period of 15 minutes. The resulting light yellow mixture was allowed to warm up to r.t. and stirred for one hour. The reaction mixture was quenched with CH_2Cl_2 (50.0 mL) and dest. water (10.0 mL). The aqueous phase was extracted with dichlormethane (3 x 10.0 mL) and the combined organic phases were washed with dest. water (5.00 mL), brine (5.00 mL) and dried over Na_2SO_4. The solvent was removed under reduced pressure yielding the crude product as an bright yellow oil. The crude product was dissolved with dry THF (150 mL) and DBU (3.00 g, 5.25 mmol, 1.00 eq.) was added. The reaction was stirred at r.t. for one hour before the solvent was removed *in vacuo*. The resulting oil was purified by flash column chromatography (pentane:diethylether = 50:1) to give the alkene **179** (0.53 g, 1.10 mmol, 21 %) as an colorless oil.

R_f: = 0.5 (cyclohexane: ethyl acetate 10:1).

$[\alpha]_D^{20}$= +42.2° (*c* = 1.05 in CH_2Cl_2).

^{1}H-NMR (700 MHz, CD_2Cl_2) δ [ppm] = 4.84 (qd, *J* = 6.9, 1.9 Hz, 1H), 3.93 (h, *J* = 2.0 Hz, 1H), 3.88 (t, *J* = 2.4 Hz, 1H), 3.83 (dd, *J* = 11.4, 1.9 Hz, 1H), 3.76 – 3.71 (m, 2H), 3.62 (ddd, *J* = 9.5, 3.7, 1.9 Hz, 1H), 1.58 (dd, *J* = 6.8, 2.0 Hz, 3H), 0.17 – 0.08 (m, 39H).

^{13}C-NMR (175 MHz, CD_2Cl_2) δ [ppm] = 151.1, 102.7, 76.8, 75.7, 70.1, 68.1,61.7, 9.1.

HRMS (ESI-TOF) m/z: Calculated for $[M+H]^+$ $C_{20}H_{47}O_5Si_4^+$ 479.2495, found: 479.2490.

(1R,2S,4S,5R,6R)-3,7,9-trioxatricyclo[4.2.1.02,4]nonan-5-yl4-methylbenzenesulfonate (142)

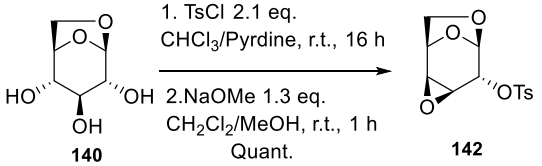

Chemical Formula: $C_{13}H_{14}O_6S$
Exact Mass: 298,0511
Molecular Weight: 298,3090

To a stirred solution of **140** (10.0 g, 61.7 mmol, 1.00 eq.) in dry pyridine (50.0 mL) was added dropwise a solution of tosyl chloride (24.7 g, 130 mmol, 2.10 eq.) in dry chloroform (65.0 mL) and pyridine (50.0 mL). The reaction stirred at room temperature for 24 h. The solution was diluted with water (40.0 mL). The phases were separated and the aqueous layer was extracted with dichloromethane (2 x 150 mL). The combined organic layers were washed with 10 % sulfuric acid (4 x 150 mL). The phases were separated and the collected organic layers were dried over $MgSO_4$, filtered and concentrated under reduced pressure. The crude product was dried over high vacuum for 24 h. Without further purification was the resulting white solid dissolved in dry methanol (25.0 mL) and dry dichloromethane (50.0 mL). The stirred solution was cooled to 0°C and NaOMe (4.33 g, 80.2 mmol, 1.30 eq.) was added. The reaction was allowed to warm up to r.t. and stirred for one hour at this temperature. The solution was diluted with water (50.0 mL). The phases were separated and the aqueous layer was extracted with dichloromethane (2 x 40.0 mL). The combined organic layers were washed with water (2 x 50.0 mL). The phases were separated and the collected organic layers were dried over $MgSO_4$, filtered and concentrated under reduced pressure. The residual white solid was dried *in vacuo* to constant weight yielding **142** (18.4 g, 61.8 mmol, Quant.).

R_f: = 0.4 (cyclohexane: ethyl acetate 1:1).

$[\alpha]_D^{20}$= −42.2° (*c* = 1.10 in CH_2Cl_2).

^{1}H-NMR (500 MHz, $CDCl_3$) δ [ppm] = 7.84 (dd, *J* = 8.2 Hz, *J* = 1.5 Hz, 2H), 7.37 (d, *J* = 8.2 Hz, 2H), 5.17 (d, J = 1.1 Hz, 1H), 4.83 (td, *J* = 4.2 Hz, *J* = 3.4 Hz, *J* = 0.8 Hz, 1H), 4.40 (dd, *J* = 1.1 Hz, *J* = 0.6 Hz, 1H), 3.95 (d, *J* = 4.8 Hz, *J* = 0.9 Hz, 1H), 3.61 (dd, *J* = 3.6 Hz, *J* = 2.7 Hz, 1H), 3.50 (dd, *J* = 4.8 Hz, *J* = 3.5 Hz, 1H), 3.14 (dd, *J* = 2.7 Hz, *J* = 0.9 Hz, 1H), 2.46 (s, 3 H).

^{13}C-NMR (125 MHz, $CDCl_3$) δ [ppm] = 145.8, 133.0, 130.4 (2C), 128.2 (2C), 98.2, 71.9, 71.8, 64.9, 53.0, 47.8, 21.9.

HRMS (ESI-TOF) m/z: Calculated for $[M+H]^+$ $C_{13}H_{15}O_6S^+$ 299.0584, found: 299.0585.

(1S,2S,3S,4R,5R)-3-hydroxy-2-methyl-6,8-dioxabicyclo[3.2.1]octan-4-yl4-methylbenzenesulfonate (161)

Method A:

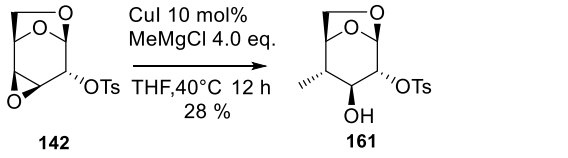

Chemical Formula: $C_{14}H_{18}O_6S$
Exact Mass: 314,0824
Molecular Weight: 314,3520

To a stirred solution of **142** (18.9 g, 63.7 mmol, 1.00 eq.) and purified CuI (1.21 g, 6.37 mmol, 0.10 eq.) in dry THF (300 mL) was added dropwise a solution of MeMgCl (3 M in THF, 85.0 mL, 255 mmol, 4.00 eq.) at – 44°C. The reaction was allowed to warm up to r.t. and heated to 40°C and stirred for 12 h at this temperature. The solution was cooled to 0°C and quenched with a saturated NH_4Cl solution (500 mL). The mixture was allowed to warm up to r.t. and the phases were separated and the aqueous layer was extracted with dichloromethane (2 x 250 mL). The combined organic layers were washed with 10 % NH_4OH (4 x 350 mL). The phases were separated and the collected organic layers were dried over $MgSO_4$, filtered and concentrated under reduced pressure. The crude product was purified by flash column chromatography (cyclohexane:ethylacetate = 1:1) yielding as light yellow solid **161** (5.61 g, 17.8 mmol, 28 %).

Methode B:

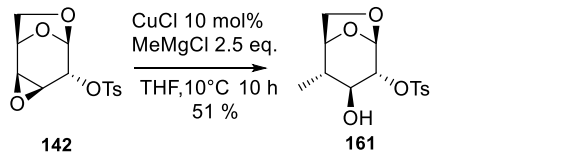

Chemical Formula: $C_{14}H_{18}O_6S$
Exact Mass: 314,0824
Molecular Weight: 314,3520

To a stirred solution of **142** (15.2 g, 51.2 mmol, 1.00 eq.) and CuCl (0.51 g, 5.12 mmol, 0.10 eq.) in dry THF (300 mL) was added dropwise a solution of MeMgCl (3 M in THF, 42.7 mL, 128 mmol, 2.50 eq.) at 10°C. The reaction stirred at this temperature for 10 h. The solution

was cooled to 0°C and quenched with a saturated NH_4Cl solution (300 mL). The mixture was allowed to warm up to r.t. and the phases were separated and the aqueous layer was extracted with dichloromethane (2 x 100 mL). The combined organic layers were washed with 10 % NH_4OH (4 x 150 mL). The phases were separated and the collected organic layers were dried over $MgSO_4$, filtered and concentrated under reduced pressure. The crude product was purified by flash column chromatography (cyclohexane:ethylacetate = 1:1) yielding as light yellow solid **161** (8.20g, 26.1 mmol, 51 %).

R_f: = 0.3 (cyclohexane: ethyl acetate 1:1).

$[\alpha]_D^{20}$= −52.3° (*c* = 1.05 in CH_2Cl_2).

^{1}H-NMR (400 MHz, CD_2Cl_2) δ [ppm] = 7.83 – 7.77 (m, 2H), 7.43 – 7.36 (m, 2H), 5.24 (d, *J* = 1.5 Hz, 1H), 4.28 – 4.24 (m, 1H), 4.12 (dq, *J* = 2.0, 1.1 Hz, 1H), 4.01 (dd, *J* = 7.0, 0.8 Hz, 1H), 3.65 (dd, *J* = 7.1, 5.1 Hz, 1H), 3.53 (tq, *J* = 3.8, 1.3 Hz, 1H), 2.46 (s, 3H), 1.18 (d, *J* = 7.4 Hz, 3H).

^{13}C-NMR (125 MHz, CD_2Cl_2) δ [ppm] = 145.2, 133.8, 130.0 (x2), 127.9 (x2), 99.1, 79.2, 76.8, 72.1, 68.4, 38.8, 21.6,17.5.

HRMS (ESI-TOF) m/z: Calculated for $[M+H]^+$ $C_{14}H_{19}O_6S^+$ 315.0897, found: 315.0897.

(1R,2S,4S,5R,6S)-5-methyl-3,8,9-trioxatricyclo[4.2.1.02,4]nonane (162)

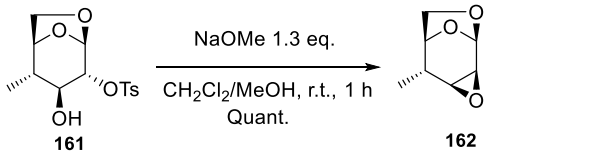

Chemical Formula: $C_7H_{10}O_3$
Exact Mass: 142,0630
Molecular Weight: 142,1540

A stirred solution of **161** (8.20 g, 26.1 mmol, 1.00 eq.) in dry methanol (45.0 mL) and dry dichloromethane (200 mL) was cooled to 0°C and NaOMe (1.84 g, 34.2 mmol, 1.30 eq.) was added. The reaction was allowed to warm up to r.t. and stirred for one hour at this temperature. The solution was diluted with water (50.0 mL). The phases were separated and the aqueous layer was extracted with dichloromethane (2 x 40.0 mL). The combined organic layers were washed with water (2 x 50.0 mL). The phases were separated and the collected organic layers were dried over $MgSO_4$, filtered and concentrated under reduced pressure. The residual white solid was dried *in vacuo* to constant weight yielding **162** (4.04 g, 28.4 mmol, Quant.).

R_f: = 0.4 (cyclohexane: ethyl acetate 1:1).

$[\alpha]_D^{20}$= −22.2° (*c* = 1.26 in CH_2Cl_2).

^{1}H-NMR (400 MHz, CD_2Cl_2) δ [ppm] = 5.62 – 5.59 (m, 1H), 4.08 (dddd, *J* = 5.9, 2.1, 1.3, 0.8 Hz, 1H), 3.69 – 3.63 (m, 2H), 3.31 (ddd, *J* = 3.9, 3.2, 0.7 Hz, 1H), 2.84 (ddd, *J* = 3.9, 1.3, 0.5 Hz, 1H), 2.08 (qt, *J* = 7.3, 0.8 Hz, 1H), 1.53 (s, 2H), 1.20 (d, *J* = 7.4 Hz, 3H).

^{13}C-NMR (125 MHz, $CDCl_3$) δ [ppm] = 98.3, 73.7, 68.7, 53.9, 51.6, 34.6, 16.7.

HRMS (ESI-TOF) m/z: Calculated for $[M+H]^+$ $C_7H_{11}O_3^+$ 143.0703, found: 143.0705.

(1S,2S,3S,4R,5R)-2,4-dimethyl-6,8-dioxabicyclo[3.2.1]octan-3-ol (143)

Method from Table 4-9 entry 3:

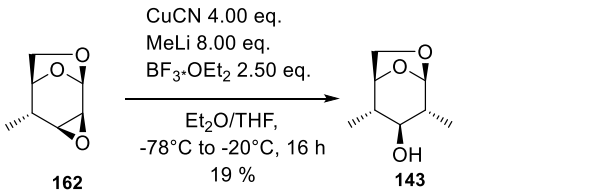

162 **143**

Chemical Formula: $C_8H_{14}O_3$
Exact Mass: 158,0943
Molecular Weight: 158,1970

A stirred solution of CuCN (126 mg, 1.41 mmol, 4.00 eq.) in freshly distilled dry Et_2O (3.34 mL) was cooled to -78°C and MeLi (1.6 M in Et_2O, 1.76 mL, 2.81 mmol, 8.00 eq.) was added over a period of 5 min. The solution was then warmed to 0°C and during this time the suspension became transparent. After stirring for 10 min at 0°C, the mixture was cooled to –78°C and a solution of epoxide **162** (50.0 mg, 0.35 mmol, 1.00 eq.) in dry THF (4.45 mL) and BF_3*Et_2O (0.11 mL, 0.88 mmol, 2.50 eq.) were added. The solution was stirred at –78°C for 1 h and was then warmed up to –20°C and stirred for 15 h. The reaction was quenched by dropwise addition of water (6 mL) and then a saturated aqueous NH_4Cl solution (6.00 mL) was added. The biphasic mixture was stirred until the aqueous phase turned blue. The aqueous phase was washed with diethyl ether (5 × 5.00 mL), and the combined organic phases were dried over Na_2SO_4, filtered and concentrated under reduced pressure. The crude product was purified by flash column chromatography (cyclohexane:ethylacetate = 1:1) yielding as light yellow solid **143** (41.8 mg, 0.27 mmol, 19 %).

Method from Table 4-9 entry 4:

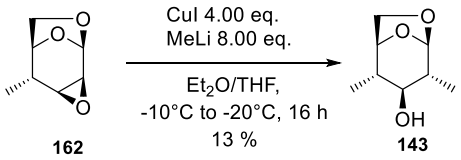

162 **143**

Chemical Formula: $C_8H_{14}O_3$
Exact Mass: 158,0943
Molecular Weight: 158,1970

A stirred solution of CuI (269 mg, 1.41 mmol, 4.00 eq.) in freshly distilled dry Et_2O (3.34 mL) was cooled to –10°C and MeLi (1.6 M in Et_2O, 1.76 mL, 2.81 mmol, 8.00 eq.) was added over a period of 5 min. The solution was then warmed to 0°C and during this time the suspension became transparent. After stirring for 10 min at 0°C, the mixture was cooled to –20°C and a solution of epoxide **162** (50.0 mg, 0.35 mmol, 1.00 eq.) in dry THF (4.45 mL) was added. The solution was stirred for 16 h at this temperature. The reaction was quenched by dropwise addition of water (6.00 mL) and then a saturated aqueous NH_4Cl solution (6.00 mL) was added. The aqueous phase was washed with diethyl ether (5×5 mL), and the combined organic phases were dried over Na_2SO_4, filtered and concentrated under reduced pressure. The crude product was purified by flash column chromatography (cyclohexane:ethylacetate = 1:1) yielding as light yellow solid **143** (41.8 mg, 0.27 mmol, 13 %).

Method from Table 4-9 entry 5:

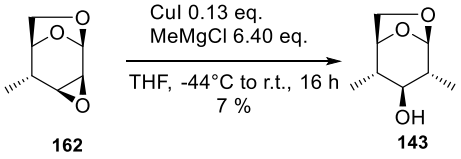

162 **143**

Chemical Formula: $C_8H_{14}O_3$
Exact Mass: 158,0943
Molecular Weight: 158,1970

To a stirred solution of **162** (50.0 mg, 0.35 mmol, 1.00 eq.) and purified CuI (8.67 mg, 0.05 mmol, 0.13 eq.) in dry THF (8.00 mL) was added dropwise a solution of MeMgCl (3 M in THF, 0.75 mL, 2.24 mmol, 6.40 eq.) at – 44°C. The reaction was allowed to warm up to r.t. and stirred for 5 h at this temperature. The solution was cooled to 0°C and quenched with a saturated NH_4Cl solution (10.0 mL). The mixture was allowed to warm up to r.t. and the phases were separated and the aqueous layer was extracted with dichloromethane (2 x 25.0mL). The

combined organic layers were washed with 10 % NH_4OH (4 x 15.0 mL). The phases were separated and the collected organic layers were dried over $MgSO_4$, filtered and concentrated under reduced pressure. The crude product was purified by flash column chromatography (cyclohexane:ethylacetate = 1:1) yielding as light yellow solid **143** (3,88 mg, 24.5 µmol, 7 %).

R_f: = 0.27 (cyclohexane: ethyl acetate 1:1).

$[\alpha]_D^{20}$= −62.7° (*c* = 1.01 in CH_2Cl_2).

^{1}H-NMR (500 MHz, CD_2Cl_2) δ [ppm] = 3.82 – 3.73 (m, 1H), 3.66 (ddd, *J* = 10.8, 5.5, 2.8 Hz, 1H), 3.50 (dt, *J* = 11.6, 5.8 Hz, 1H), 3.07 – 3.00 (m, 1H), 2.70 (p, *J* = 7.3 Hz, 1H), 2.39 (d, *J* = 1.9 Hz, 1H), 2.38 (d, *J* = 1.3 Hz, 1H), 2.13 (dq, *J* = 13.4, 6.7 Hz, 1H), 1.09 (d, *J* = 7.2 Hz, 3H), 0.91 (d, *J* = 6.7 Hz, 3H).

^{13}C-NMR (125 MHz, CD_2Cl_2) δ [ppm] = 74.3, 64.9, 51.8, 48.4, 24.40, 22.7, 22.6, 13.8.

HRMS (ESI-TOF) m/z: Calculated for $[M+Na]^+$ $C_8H_{14}O_3Na^+$ 158.0943, found: 158.0945.

(1S,2S,3R,4R,5R)-3-(benzyloxy)-2,4-dimethyl-6,8-dioxabicyclo[3.2.1]octane (183)

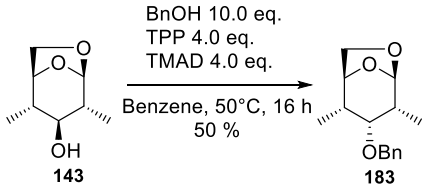

Chemical Formula: $C_{15}H_{20}O_3$
Exact Mass: 248,1412
Molecular Weight: 248,3220

To a stirred solution of **143** (50.0 mg, 0.32 mmol, 1.00 eq.) and benzyl alcohol (0.33 mL, 3.16 mmol, 10.0 eq.) in benzene (8.00 mL) were added triphenylphosphine (330 mg, 1.26 mmol, 4.00 eq.) and TMAD (217 mg, 1.26 mmol, 4.00 eq.). The mixture was stirred for 16 h at 50°C. The solution was filtered over a pad of celite and concentrated under reduced pressure. The crude product was purified by flash column chromatography (chloroform:ethyl acetate = 24:1) to yield **183** as a colorless oil (39.7 mg, 0.16 mmol, 50 %).

R_f: = 0.57 (cyclohexane: ethyl acetate 1:1).

$[\alpha]_D^{20}$= −2.0° (*c* = 1.08 in CH_2Cl_2).

^{1}H-NMR (500 MHz, CD_2Cl_2) δ [ppm] = 7.38 – 7.32 (m, 4H), 7.27 (ddt, *J* = 7.1, 5.6, 2.3 Hz, 1H), 4.34 (ddt, *J* = 6.0, 1.6, 0.8 Hz, 1H), 3.89 (t, *J* = 6.5 Hz, 1H), 3.77 (dd, *J* = 7.2, 1.0 Hz, 1H), 3.69 (dd, *J* = 7.2, 5.4 Hz, 1H), 2.26 – 2.17 (m, 1H), 2.12 – 2.05 (m, 1H), 1.17 (d, *J* = 7.2 Hz, 3H), 1.03 (d, *J* = 7.4 Hz, 3H)

^{13}C-NMR (125 MHz, $CDCl_3$) δ [ppm] = 139.4, 128.7, 127.8, 127.7, 105.5, 78.3, 72.3, 70.0, 68.1, 39.5, 37.7, 13.5, 11.6.

HRMS (ESI-TOF) m/z: Calculated for $[M+H]^+$ $C_{15}H_{21}O_3^+$ 249.1485, found: 249.1484.

((2S,3S,4R,5R)-4-(benzyloxy)-6-methoxy-3,5-dimethyltetrahydro-2H-pyran-2-yl)methanol (184)

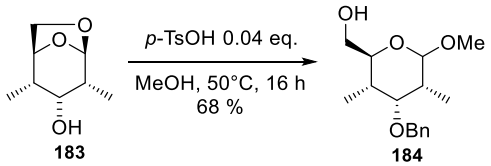

Chemical Formula: $C_{16}H_{24}O_4$
Exact Mass: 280,1675
Molecular Weight: 280,3640

To a stirred solution of **183** (20.0 mg, 0.08 mmol, 1.00 eq.) in dry methanol (8.00 mL) was added *p*-TsOH (0.55 mg, 3.22 µmol, 0.04 eq.). The mixture was stirred for 16 h at 50°C. The reaction was neutralized with Amberlite IRA-400 and filtered. The solution was concentrated under reduced pressure. The crude product was purified by flash column chromatography (cyclohexane: ethyl acetate = 2:1) to yield **184** as a colourless oil (15.3 mg, 0.05 mmol, 68 %).

R_f: = 0.43 (cyclohexane: ethyl acetate 1:1).
^{1}H-NMR (400 MHz, CD_2Cl_2) δ [ppm] = 7.39 – 7.31 (m, 13H), 7.31 – 7.23 (m, 2H), 4.40 (d, *J* = 8.8 Hz, 1H), 3.80 – 3.61 (m, 4H), 3.59 – 3.51 (m, 4H), 2.00 (s, 3H), 1.04 (d, *J* = 6.9 Hz, 4H), 0.96 (d, *J* = 6.9 Hz

Ethyl (2*R*,3*R*)-2-methyl-3-((triethylsilyl)oxy)butanoate (193)

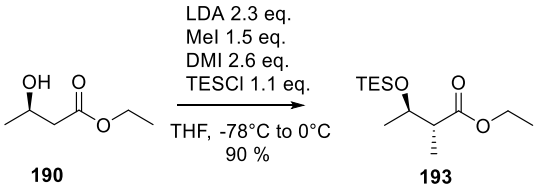

190 **193**

Chemical Formula: $C_{13}H_{28}O_3Si$
Exact Mass: 260,1808
Molecular Weight: 260,4490

To a solution of *i*-Pr_2NH (2.90 mL, 20.7 mmol, 2.38 eq.) in THF (20.0 mL) was added dropwise a solution of *n*-BuLi (10.0 mL, 2.0 M in cyclohexane, 20.0 mmol, 2.30 eq.) at -78 °C. Then the reaction was stirred für 10 minutes at 0 °C and cooled back to -78 °C. (R)-ethyl 3-hydroxybutanoate (**190**) (1.15 g, 8.70 mmol, 1.00 eq.) was dissolved in THF (2.00 mL) and added dropwise over 10 minutes. The mixture was stirred at -78 °C for 10 minutes, then for 10 minutes at 0 °C and cooled back to -78 °C. 1,3-dimethyl-2-imidazolidinone (2.50 mL, 23.2 mmol, 2.70 eq.) was added. Afterwards Methyliodid (0.80 mL, 12.9 mmol, 1.50 eq.) was added. The mixture was stirred for 1 hour at -78 °C and 1.5 hours at 0 °C. After the addition of Triethylsilylchlorid (TESCl, 1.60 mL, 9.53 mmol,1.10 eq.), the reaction was stirred at 0 °C for 30 minutes. The mixture was quenched with a saturated aqueous ammonium chlorid solution (20.0 mL) and destilled water (15.0 mL). The phases were separated and the aqueous layer was extracted with Et_2O (3 x 50.0 mL). The combined organic layers were dried over Na_2SO_4, filtered and concentrated under reduced pressure. The crude product was purified by flash column chromatography (n-pentane:diethyl ether = 10:4) to yield **193** (1.39 g, 5.34 mmol, 61 %) as colorless oil.

R_f = 0.5 (cyclohexane:ethyl acetat, 10:1).

$[\alpha]_D^{20}$= −37.6° (*c* = 1.03 in CH_2Cl_2).

^{1}H-NMR (400 MHz, $CDCl_3$): δ [ppm] = 4.12 (q, J = 7.1 Hz, 2H), 4.05 (dq, J = 7.3, 6.2 Hz, 1H), 2.49 (qd, J = 7.4, 6.2 Hz, 1H), 1.26 (t, J = 7.1, 1.4 Hz, 3H), 1.13 (d, J = 6.2 Hz, 3H), 1.08 (d, J = 7.1 Hz, 3H), 0.94 (t, J = 8.0 Hz, 9H), 0.64-0.55 (m, 6H).

^{13}C-NMR (125 MHz, $CDCl_3$): δ [ppm] = 175.3 (C_q), 70.1 (CH), 60.3 (CH_2), 48.3 (CH), 20.6 (CH_3), 14.3 (CH_3), 12.6 (CH_3), 7.0 (3 x CH_3), 5.0 (3 x CH_2).

Diastereomeric ratio 5:1

HRMS (ESI): *m/z*: calc for $[M+H]^+$: $C_{13}H_{29}O_3Si^+$ 261.1880, found: 261.1886.

(2*R*, 3*R*)-2-methyl-3-((triethylsilyl)oxy)butanal (193)

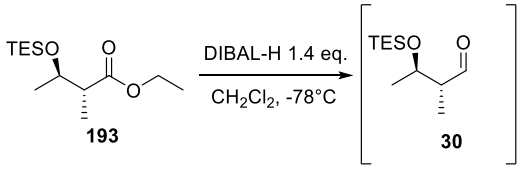

Chemical Formula: $C_{11}H_{24}O_2Si$
Exact Mass: 216,1546
Molecular Weight: 216,3960

To a solution of the ester **193** (2.17 g, 8.33 mmol, 1.00 eq.) in CH_2Cl_2 (8.30 mL) was added DIBAL-H (11.8 mL, 1.0 M in CH_2Cl_2) portionwise via syringe pumpe over 30 minutes at -78 °C. Then the reaction was stirred at -78 °C for an hour. After that, EtOAc (0.60 mL) was added slowly at - 78 °C. A saturated sodium potassium tartrate solution (15.0 mL) was added and the reaction stirred for 2h at room temperature. The phases were separated and the aqueous layer was extracted with CH_2Cl_2. The combined organic layers were dried over Na_2SO_4, filtered and concentrated under reduced pressure to yield **30**, which was not further purified but used immediately for the next reaction.

(*S*)-2-hydroxy-*N*-methoxy-*N*-methylpropanamide (SYN5DEN1)

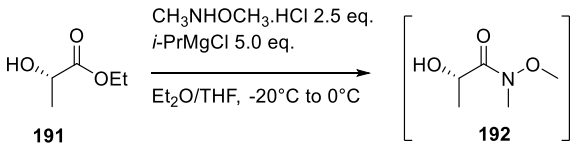

Chemical Formula: $C_5H_{11}NO_3$
Exact Mass: 133,0739
Molecular Weight: 133,1470

(*S*)-lactate (**191**) (9.65 mL, 84.7 mmol, 1.00 eq.) and N,O-dimethylhydroxylamine hydrochloride (20.7 g, 0.21 mol, 2.50 eq.) were dissolved in Et_2O/THF (1:1, 250 mL). Then *i*-PrMgCl (0.21 L, 0.42 mol, 5.00 eq.) was added at -20 °C over 30 minutes. The mixture was stirred for 30 minutes at -20 °C and 30 minutes at 0 °C. The mixture was quenched with a saturated aqueous ammonium chlorid solution (200 mL) and destilled water (200 mL). The phases were separated and the aqueous layer was extracted with Et_2O (3 x 300 mL). The combined organic layers were dried over $MgSO_4$, filtered and concentrated under reduced pressure to yield **192**. The crude product was not further purified but used immediately for the next reaction.

(*S*)-3-oxopentan-2-yl benzoate (31)

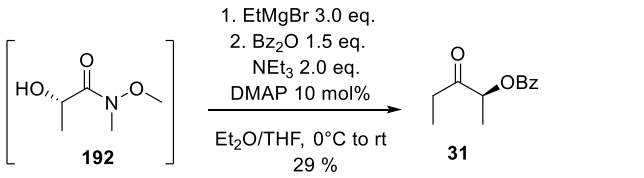

Chemical Formula: $C_{12}H_{14}O_3$
Exact Mass: 206,0943
Molecular Weight: 206,2410

EtMgBr (48.4 mL, 145 mmol, 3.00 eq.) was added to a solution of **192** at 0°C over the course of 30 minutes. Then the mixture was allowed to warm at room temperature and was stirred for 30 minutes. The mixture was quenched with saturated aqueous ammonium chlorid solution (270 mL). The phases were separated and the aqueous layer was extracted with Et_2O (150 mL) and CH_2Cl_2 (2 x 150 mL). The combined organic layers were dried over $MgSO_4$, filtered and concentrated under reduced pressure to about 125 mL.

Afterwards, Bz_2O (16.4 g, 72.6 mmol, 1.50 eq.), NEt_3 (13.4 mL, 96.8 mmol, 2.00 eq.) and DMAP (0.59 g, 4.84 mmol, 10 mol%) were added. The mixture stirred for 20 hours and was then quenched with ethylendiamine (3.59 mL, 53.7 mmol, 1.11 eq.) and destilled water (140 mL). The phases were separated and the aqueous layer was extracted with Et_2O (4 x 140 mL) The combined organic layers were dried over $MgSO_4$, filtered and concentrated under reduced pressure. The crude product was purified by flash column chromatography (n-pentane:diethyl ether = 4:1) to yield **31** (4.01 g, 19.4 mmol, 23 %) as colorless oil.

R_f = 0.5 (cyclohexane:ethyl acetate, 2:1).

$[\alpha]_D^{20}$= +26.6° (*c* = 1.02 in CH_2Cl_2).

^{1}H-NMR (500 MHz, $CDCl_3$): δ [ppm] = 8.12-8.06 (m, 2H), 7.59 (tt, J = 7.5, 1.3 Hz, 1H), 7.46 (tt, J = 8.1, 1.6 Hz, 2H), 5.36 (q, 7.0 Hz, 1H), 2.65 (dq, J = 7.3, 18.3 Hz, 1H), 2.53 (dq, J = 18.3, 7.2 Hz, 1H), 1.53 (d, J = 7.0 Hz, 3H), 1.10 (t, J = 7.2 Hz, 3H).

^{13}C-NMR (125 MHz, $CDCl_3$): δ [ppm] = 208.7 (C_q), 166.1 (C_q), 133.5 (CH), 129.9 (CH), 129.7 (CH), 129.6 (CH), 128.6 (2 x CH), 75.3 (C_q), 31.6 (CH_2), 16.7 (CH_3), 7.4 (CH_3).

HRMS (ESI): *m/z*: calc for $[M+H]^+$: $C_{12}H_{15}O_3^+$ 207.1016, found: 207.1016.

(2*S*,4*R*,5*R*,6*S*,7*R*)-5-hydroxy-4,6-dimethyl-3-oxo-7-((triethylsilyl)oxy)octan-2-yl benzoate (34)

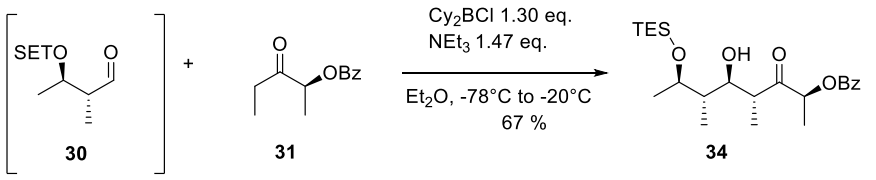

Chemical Formula: $C_{23}H_{38}O_5Si$
Exact Mass: 422,2489
Molecular Weight: 422,6370

At first, Cy_2BCl (10.8 mL, 10.8 mmol, 1.30 eq.) was added to a solution of the ketone **31** (4.01 g, 19.4 mmol, 1.50 eq.) in Et_2O (57.0 mL), followed by NEt_3 (1.73 mL, 12.5 mmol, 1.50 eq.). The reaction mixture was stirred at -78°C for 5 minutes, then at 0°C for 2 hours and then cooled back to -78°C. The aldehyd **30** (1.39 g, 5.34 mmol, 1.00 eq.) in Et_2O (2.35 mL + 2.35 mL to rinse) was added dropwise over the course of 10 minutes. The reaction was stirred for 2 hours at -78°C and then stored overnight at -20°C. The mixture was quenched with MeOH (9.5 mL), phosphate buffer with pH 7 (18.8 mL, 1M) and H_2O_2 (30%, 4.7 mL) at 0°C. The reaction was stirred for one hour at room temperature. After that Na_2SO_3 was added carefully at 0°C. The phases were separated and the aqueous layer was extracted with Et_2O (3 x 100 mL) The combined organic layers were dried over Na_2SO_4, filtered and concentrated under reduced pressure. The crude product was purified by flash column chromatography (n-pentane: ethyl acetate = 10:1) to yield **34** (2.32 g, 4.58 mmol, 80 %) as colorless oil.

R_f = 0.4 (cyclohexane:ethyl acetate, 10:1).

$[\alpha]_D^{20}$= +29.6° (*c* = 0.98 in CH_2Cl_2).

^{1}H-NMR (500 MHz, $CDCl_3$): δ [ppm] = 8.11-8.06 (m, 2H), 7.62-7.55 (m, 1H), 7.49-7.43 (m, 2H), 5.45 (q, J = 7.0 Hz, 1H), 4.17 (qd, J = 6.3, 4.6 Hz, 1H), 3.46-3.41 (m, 2H), 3.19-3.10 (m, 1H), 1.78-1.72 (m, 1H), 1.57 (d, J = 7.2 Hz, 3H), 1.39 (d, J = 7.2 Hz, 3H), 1.10 (d, J = 6.3 Hz, 3H), 1.00-0.90 (m, 9H), 0.87 (d, J = 7.0 Hz, 3H), 0.61-0.52 (m, 6H).

^{13}C-NMR (125 MHz, $CDCl_3$): δ [ppm] = 213.1 (C_q), 166.0 (C_q), 133.6 (CH), 130.0 (C_q), 129.6 (2 x CH), 128.7 (2 x CH), 77.9 (CH), 74.8 (CH), 69.5 (CH), 45.0 (CH), 43.4 (CH), 19.2 (CH_3), 16.3 (CH_3), 15.4 (CH_3), 12.4 (CH_3), 7.0 (3 x CH_3), 5.1 (3 x CH_2).

Diastereomeric ratio 5:1

HRMS (ESI): *m/z*: calc for $[M+H]^+$: $C_{23}H_{39}O_5Si^+$ 423.2561, found:. 423.2561.

(2*S*,4*R*,5*R*,6*R*,7*R*)-5-((*tert*-butyldimethylsilyl)oxy)-4,6-dimethyl-3-oxo-7-((triethylsilyl)oxy)octan-2-yl benzoate (194)

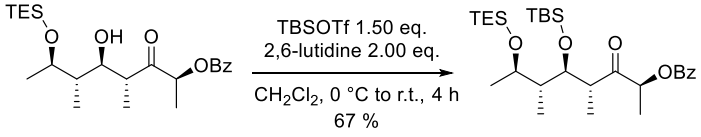

34 **194**

Chemical Formula: $C_{29}H_{52}O_5Si_2$
Exact Mass: 536,3353
Molecular Weight: 536,9000

At first, a stirred solution of **34** (2.32 g, 4.58 mmol, 1.00 eq.) in CH_2Cl_2 (21.1 mL) was cooled to 0 °C. 2,6-lutidine (1.28 mL, 10.9 mmol, 2.00 eq.) and TBSOTf (1.89 mL, 8.24 mmol, 1.50 eq.) were added dropwise over the course of 10 minutes. The reaction was allowed to warm to room temperature and was stirred for 4 hours. The mixture was then quenched with saturated aqueous ammonium chlorid solution (27.0 mL). The phases were separated and the aqueous layer was extracted with CH_2Cl_2 (3 x 15.0 mL) The combined organic layers were dried over Na_2SO_4, filtered and concentrated under reduced pressure. The crude product was purified by flash column chromatography (cyclohexane: ethyl acetate = 35:1) to yield **194** (1.65 g, 3.07 mmol, 67 %) as colorless oil.

R_f = 0.4 (cyclohexane:ethy acetate, 20:1)
$[\alpha]_D^{20}$= −14.6° (*c* = 1.03 in CH_2Cl_2).
^{1}H-NMR (500 MHz, $CDCl_3$): δ [ppm] = 8.11-8.05 (m, 2H), 7.61-7.54 (m, 1H), 7.49-7.41 (m, 2H), 5.50 (q, J = 6.9 Hz, 1H), 4.29 (dd, J = 7.8, 3.9 Hz, 1H), 3.90 (dq, J = 7.5, 6.1 Hz, 1H), 3.21-3.07 (m, 1H), 1.80-1.70 (m, 1H), 1.51 (d, J = 6.9 Hz, 3H), 1.17 (d, J = 7.0 Hz, 3H), 1.10 (d, J = 6.1 Hz, 3H), 0.94 (t, J = 7.9 Hz, 9H), 0.85 (s, 9H), 0.84 (d, J = 3.1 Hz, 3H), 0.58 (q, J = 7.9 Hz, 6H), 0.05 (s, 3H), -0.04 (s, 3H).
^{13}C-NMR (125 MHz, $CDCl_3$): δ [ppm] = 208.7 (C_q), 165.9 (C_q), 133.4 (CH), 130.0 (2 x CH), 130.0 (C_q), 128.6 (2 x CH), 74.8 (CH), 74.3 (CH), 69.4 (CH), 46.7 (CH), 46.5 (CH), 26.2 (3 x CH_3), 21.6 (CH_3), 18.3 (C_q), 15.7 (CH_3), 13.4 (CH_3), 10.8 (CH_3), 7.1 (3 x CH_3), 5.5 (3 x CH_2), - 4.1 (CH_3), - 4.7 (CH_3).
HRMS (ESI): *m/z*: calc for $[M+H]^+$: $C_{29}H_{53}O_5Si_2^+$ 537.3426 , found:. 537.327.

(4*S*,5*S*,6*R*,7*R*)-5-((*tert*-butyldimethylsilyl)oxy)-4,6-dimethyl-7-((triethylsilyl)oxy)octane-2,3-diol (206)

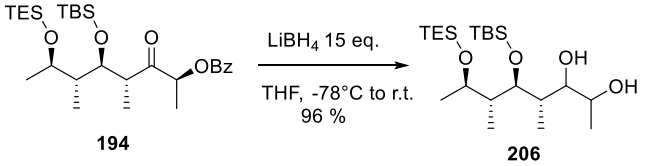

194 **206**

Chemical Formula: $C_{22}H_{50}O_4Si_2$
Exact Mass: 434,3248
Molecular Weight: 434,8080

To a stirred solution of **194** (100 mg, 0.186 mmol, 1.00 eq.) in THF (5.6 mL) was added $LiBH_4$ (1.40 mL, 2.80 mmol, 15.0 eq.) at -78 °C in one portion. The mixture was stirred for 2 hours at -78 °C and then allowed to warm to room temperature for 3 days. Distilled water (3.50 mL), saturated aqueous ammonium chloride solution (0.30 mL) and Et_2O (1.50 mL) were added at 0 °C carefully. The phases were separated and the aqueous layer was extracted with Et_2O (3 x 10.0 mL) The combined organic layers were dried over $MgSO_4$, filtered and concentrated under reduced pressure. The crude product was purified by flash column chromatography (cyclohexane: ethyl acetate = 5:1) to yield **206** (77.3 mg, 0.18 mmol, 96 %) as white solid.

R_f = 0.2 (cyclohexane:ethy acetate, 5:1).
HRMS (ESI): *m/z*: calc for $[M+H]^+$: $C_{22}H_{51}O_4Si_2^+$ 435.3320, found: 435.3317.
No clean NMR spectra has been obtained

(2*R*,3*R*,4*R*,5*R*)-3-((*tert*-butyldimethylsilyl)oxy)-2,4-dimethyl-5-((triethylsilyl)oxy)hexanal (207)

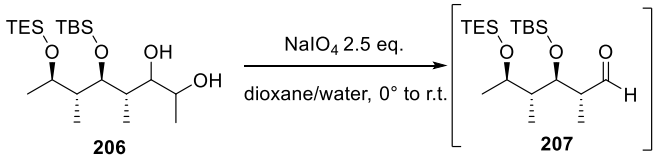

206 **207**

Chemical Formula: $C_{20}H_{44}O_3Si_2$
Exact Mass: 388,2829
Molecular Weight: 388,7390

To a stirred solution of **206** (77.3 mg, 0.18 mmol, 1.00 eq.) in dioxan and water (4.02 mL, 2:1) was added $NaIO_4$ (96.7 mg, 0.45 mmol, 2.50 eq.) at 0 °C portionwise. The mixture was stirred vigorously for one night. Then the reaction was diluted with CH_2Cl_2 (20 mL) and quenched with distilled water (2.70 mL). The phases were separated and the aqueous layer was extracted with CH_2Cl_2 (3 x 5.00 mL) The combined organic layers were dried over $MgSO_4$, filtered and concentrated under reduced pressure. The crude product was not further purified and used immediately for the next reaction.

(3*R*,4*R*,5*S*,6*R*)-3,5,6-trimethyltetrahydro-2*H*-pyran-2,4-diol (208)

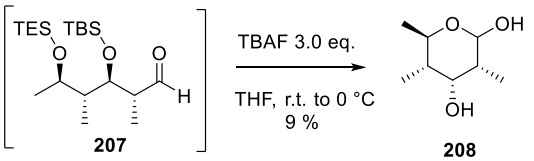

207 **208**

Chemical Formula: $C_8H_{16}O_3$
Exact Mass: 160,1099
Molecular Weight: 160,2130

A mixture of **207** (77.3 mg, 0.178 mmol, 1.00 eq.) in 1.0 M TBAF in THF (0.534 mL, 0.53 mmol, 3.00 eq.) was stirred at room temperature for 2 hours. TBAF in THF (0.178 mL, 0.18 mmol, 1.00 eq.) was added additionally. After 1 more hour the reaction was quenched with sat. $NaHCO_3$ (2.15 mL) and stirred for 5 minutes at 0 °C. The phases were separated and the aqueous layer was extracted with Et_2O (3 x 10.0 mL) The combined organic layers were dried over Na_2SO_4, filtered and concentrated under reduced pressure. The crude product was purified by flash column chromatography (cyclohexane: ethyl acetate = 1.5:1) to yield **208** (2.45 mg, 15.3 µmol, 9 %).

R_f = 0.4 (cyclohexane:ethy acetate, 1:1).
HRMS (ESI): *m/z*: calc for $[M-H]^+$: $C_8H_{15}O_3^+$ 159.1016, found: 159.1011.
*No clean NMR spectra has been obtained because the product existed as **208-α**, **208-β** and **210**.*

(3*R*,4*R*,5*S*,6*R*)-4-hydroxy-3,5,6-trimethyltetrahydro-2H-pyran-2-one (211)

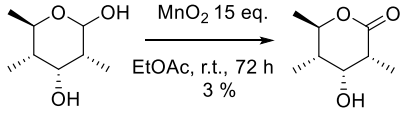

208 **211**

Chemical Formula: $C_8H_{14}O_3$
Exact Mass: 158,0943
Molecular Weight: 158,1970

To a mixture of **208** (2.45 mg, 15.3 µmol, 1.00 eq.) in EtOAc (0.87 mL) was added MnO_2 (113.5 mg, 1.30 mmol, 15.0 eq.) in portion at room temperature. The solution was stirred for 3 days. Then the reaction was filtered through a Celite-Filter and concentrated under reduced pressure to yield **211** (0.068 mg, 0.43 µmol, 3 %) as white solid.
$[\alpha]_D^{20}$= −23.2° (*c* = 0.45 in CH_2Cl_2).
^{1}H-NMR (500 MHz, CD_2Cl_2): δ [ppm] = 4.43 (dq, J = 10.6, 6.4 Hz, 1H), 3.82-3.80 (m, 1H), 2.53 (qd, J = 7.2, 3.0 Hz, 1H), 1.85-1.80 (m, 1H), 1.34 (d, J = 6.4 Hz, 3H), 1.27 (d, J = 7.2 Hz, 3H), 1.16 (d, J = 6.3 Hz, 3H).
^{13}C-NMR (125 MHz, CD_2Cl_2): δ [ppm] = 173.5 (C_q), 78.1 (CH), 73.3 (CH), 42.6 (CH), 41.1 (CH), 20.2 (CH_3), 16.3 (CH_3), 12.9 (CH_3).
HRMS (ESI): *m/z*: calc for $[M+H]^+$: $C_8H_{15}O_3Na^+$ 159.1016, found: 159.1015.

(S)-1-((2*R*,3*R*,4*R*,5*R*,6*R*)-4-((*tert*-butyldimethylsilyl)oxy)-2-hydroxy-3,5,6-trimethyltetrahydro-2*H*-pyran-2-yl)ethyl benzoate (213)

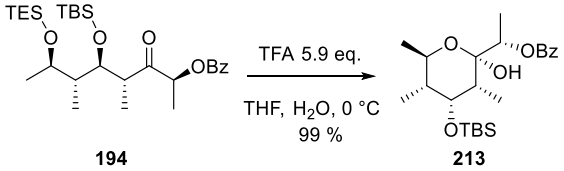

194 **213**

Chemical Formula: $C_{23}H_{38}O_5Si$
Exact Mass: 422,2489
Molecular Weight: 422,6370

A stirred solution of **194** (1.65 g, 3.07 mmol, 1.00 eq.) in H_2O (2.54 mL) in THF (42.3 mL) was cooled to 0 °C. TFA (0.85 mL, 11.0 mmol, 5.90 eq.) was added and stirred for 4 hours. The reaction was quenched with sat. $NaHCO_3$ (60.0 mL) and Et_2O (60.0 mL). The phases were separated and the aqueous layer was extracted with Et_2O (2 x 115 mL) The combined organic layers were dried over Na_2SO_4, filtered and concentrated under reduced pressure. The crude product was purified by flash column chromatography (cyclohexane: ethyl acetate = 10:1) to yield **213** (1.28 g, 3.04 mmol, 99 %) as white solid.

R_f = 0.3 (n-pentane:ethyl acetate, 10:1).

$[\alpha]_D^{20}$= −4.6° (*c* = 0.88 in CH_2Cl_2).

^{1}H-NMR (500 MHz, CD_2Cl_2): δ [ppm] = 8.06-8.02 (m, 2H), 7.58-7.53 (m, 1H), 7.47-7.42 (m, 2H), 5.50 (s, OH), 5.22 (q, J = 6.6 Hz, 1H), 3.92 (dq, J = 10.2, 6.2 Hz, 1H), 3.86 (pseudo-t, J = 2.2 Hz, 1H), 1.86 (qd, J = 7.2, 2.2 Hz, 1H), 1.53-1.45 (m, 1H), 1.29 (d, J = 6.6 Hz, 3H), 1.22 (d, J = 6.2 Hz, 3H), 1.12 (d, J = 7.2 Hz, 3H), 0.94 (s, 9H), 0.91 (d, J = 7.1 Hz, 3H), 0.16 (s, 3H), 0.13 (s, 3H).

^{13}C-NMR (125 MHz, CD_2Cl_2): δ [ppm] = 166.4 (C_q), 133.1 (C_q), 131.4 (CH), 130.0 (2 x CH), 128.7 (2 x CH), 99.8 (C_q), 79.0 (CH), 73.8 (CH), 65.8 (CH), 43.6 (CH), 40.2 (CH), 26.4 (3 x CH_3), 18.7 (CH_3), 15.4 (CH_3), 15.07 (CH_3), 14.9 (CH_3), -3.2 (CH_3), -3.55 (CH_3).

HRMS (ESI): *m/z*: calc for $[M\text{-}OH]^+$: $C_{23}H_{37}O_4^+$ 405.2456 , found: 405.2454.

(3*R*,4*R*,5*R*,6*R*)-4-((*tert*-butyldimethylsilyl)oxy)-3,5,6-trimethyltetrahydro-2*H*-pyran-2-one (125)

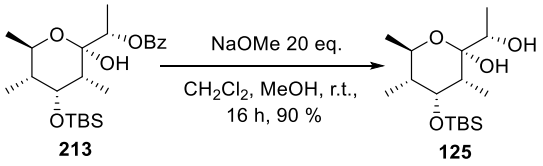

213 **125**

Chemical Formula: $C_{16}H_{34}O_4Si$
Exact Mass: 318,2226
Molecular Weight: 318,5290

To a stirred mixture of **213** (0.83 g, 1.97 mmol, 1.00 eq.) in CH_2Cl_2 (11.6 mL) were added MeOH (69.5 mL) and NaOMe (1.95 g, 35.9 mmol, 20.0 eq.) at room temperature. The reaction was stirred for 16 hours. The solution was quenched at 0 °C with saturated aqueous ammonium chlorid solution (115 mL). The phases were separated and the aqueous layer was extracted with CH_2Cl_2 (3 x 35.0 mL). The combined organic layers were dried over Na_2SO_4, filtered and concentrated under reduced pressure. The crude product was purified by flash column chromatography (cyclohexane: ethyl acetate = 5:1) to yield **125** (0.56 g, 1.77 mmol, 90 %) as white solid.

R_f = 0.5 (cyclohexane:ethy acetate, 1:1).
$[\alpha]_D^{20}$= +10.0° (*c* = 0.80 in CH_2Cl_2).
^{1}H-NMR (500 MHz, CD_2Cl_2): δ [ppm] = 5.61 (s, OH), 3.89-3.83 (m, 1H), 3.82 (pseudo-t, J = 2.2 Hz, 1H), 3.71 (p, J = 6.5 Hz, 1H), 2.31 (d, J = 6.4 Hz, 1H), 1.74 (qd, J = 7.2, 2.2 Hz, 1H), 1.49-1.39 (m, 1H), 1.16 (d, J = 6.3 Hz, 3H), 1,08 (d, J = 6.5 Hz, 3H), 1.02 (d, J = 7.2 Hz, 3H), 0.95 (s, 9H), 0.89 (d, J = 7.0 Hz, 3H), 0.15 (s, 3H), 0.13 (s, 3H).
^{13}C-NMR (125 MHz, CD_2Cl_2): δ [ppm] = 100.3 (C_q), 78.9 (CH), 71.1 (CH), 66.0 (CH), 43.7 (CH), 39.7 (CH), 26.3 (3 x CH_3), 19.3 (C_q), 18.7 (CH), 17.3 (CH_3), 15.4 (CH_3), 14.5 (CH_3), -3.3 (CH_3), -3.5 (CH_3).
HRMS (ESI): *m/z*: calc for $[M\text{-}OH]^+$: $C_{16}H_{33}O_3^+$ 301.2193 , found: 301.2193.

(4*S*,5*S*,7*R*,8*R*,9*R*,10*R*)-9-((*tert*-butyldimethylsilyl)oxy)-4,7,8,10-tetramethyl-1,3,6-trioxaspiro[4.5]decane-2-thione (127)

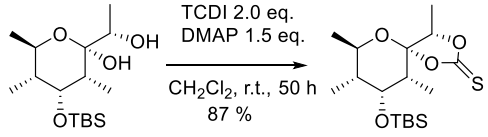

125 **127**

Chemical Formula: $C_{17}H_{32}O_4SSi$
Exact Mass: 360,1791
Molecular Weight: 360,5840

To a stirred solution of **125** (99 mg, 0.31 mmol, 1.00 eq.) in CH_2Cl_2 (5.29 mL) was added DMAP (51.4 mg, 0.42 mmol, 1.50 eq.) and Thiocarbonyldiimidazol (111.4 mg, 0.63 mmol, 2.00 eq.). The reaction was stirred for 50 hours at room temperature without any exposure to sunlight. The solution was filtered through a micro-flash chromatography and concentrated under reduced pressure to yield **127** (97.6 mg, 0.27 mmol, 87 %) as white solid.

R_f = 0.5 (cyclohexane:ethyl acetate, 3:1).

$[\alpha]_D^{20}$= +81.1° (*c* = 1.04 in CH_2Cl_2).

^{1}H-NMR (400 MHz, CD_2Cl_2): δ [ppm] = 4.69 (q, J = 6.5 Hz, 1H), 4.12 (dq, J = 10.2, 6.3 Hz, 1H), 3.75 (pseudo-t, J = 2.4 Hz, 1H), 1.80 (qd, J = 7.0, 2.7 Hz, 1H), 1.48 (dqd, J = 10.1, 7.0, 2.0 Hz, 1H), 1.36 (d, J = 6.6 Hz, 3H), 1.16 (d, J = 6.3 Hz, 3H), 1.06 (d, J = 7.1 Hz, 3H), 0.99 (s, 10H), 0.90 (d, J = 7.0 Hz, 3H), 0.10 (s, 3H), 0.08 (s, 3H).

^{13}C-NMR (125 MHz, CD_2Cl_2): δ [ppm] = 191.9 (C_q), 112.1 (C_q), 82.9 (CH), 73.5 (CH), 69.7 (CH), 42.6 (CH), 40.5 (CH), 26.3 (3 x CH_3), 18.8 (C_q), 18.8 (CH_3), 15.3 (CH_3), 13.8 (CH_3), 13.1 (CH_3), -3.1 (CH_3), -3.3 (CH_3).

HRMS (ESI): *m/z*: calc for $[M+H]^+$: $C_{17}H_{33}O_4SSi^+$ 361.1863, found: 361.1863.

(3*R*,4*R*,5*R*,6*R*)-4-((*tert*-butyldimethylsilyl)oxy)-3,5,6-trimethyltetrahydro-2*H*-pyran-2-one (68)

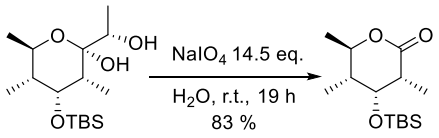

125 **68**

Chemical Formula: $C_{14}H_{28}O_3Si$
Exact Mass: 272,1808
Molecular Weight: 272,4600

Silica supported $NaIO_4$ (985 mg, 4.60 mmol, 14.5 eq.) was added to solution of **125** (100 mg, 0.31 mmol, 1.00 eq.) in CH_2Cl_2 (21.0 mL). The reaction was stirred for 19 hours at room temperature. The organic layers were dried over Na_2SO_4, filtered and concentrated under reduced pressure. No further purification was needed. The reaction yielded **68** (71.2 mg, 0.26 mmol, 83 %) as white solid.

R_f = 0.3 (cyclohexane:ethyl acetate, 6:1).
$[\alpha]_D^{20}$= +2.2° (*c* = 0.91 in CH_2Cl_2).
^{1}H-NMR (400 MHz, CD_2Cl_2): δ [ppm] = 4.45 (dq, J = 10.6, 6.4 Hz, 1H), 3.84 (dd, J = 2.6, 1.4 Hz, 1H), 2.52 (qd, J = 7.1, 2.6 Hz, 1H), 1.77 (dqd, J = 10.7, 6.8, 1.4 Hz, 1H), 1.35 (d, J = 6.4 Hz, 3H), 1.25 (d, J = 7.2 Hz, 3H), 1.00 (d, J = 6.9 Hz, 3H), 0,90 (s, 9H), 0,09 (s, 3H), 0,08 (s, 3H).
^{13}C-NMR (125 MHz, CD_2Cl_2): δ [ppm] = 173.8 (C_q), 78.1 (CH), 74.5 (CH), 43.9 (CH), 42.1 (CH), 26.2 (3 x CH_3), 20.1 (CH_3), 18.5 (C_q), 15.3 (CH_3), 14.1 (CH_3), -3.4 (CH_3), -3.4(CH_3).
HRMS (ESI): *m/z*: calc for $[M+H]^+$: $C_{14}H_{29}O_3Si^+$ 273.1880, found: 273.1877.

***tert*-butyl(((*3R,4R,5R,6R,Z*)-2-ethylidene-3,5,6-trimethyltetrahydro-2H-pyran-4-yl)oxy)dimethylsilane (69)**

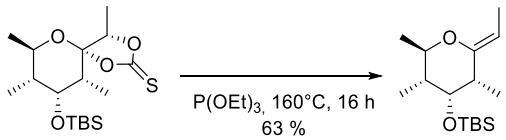

127 **69**

Chemical Formula: $C_{16}H_{32}O_2Si$
Exact Mass: 284,2172
Molecular Weight: 284,5150

A stirred solution of **127** (100 mg, 0.28 mmol, 1.00 eq.) in $P(OEt)_3$ (6.33 mL) was heated to 160 °C and stirred for 16 hours. The reaction was diluted with CH_2Cl_2 (10 mL). The solution was concentrated under reduced pressure. The crude product was purified by flash column

chromatography (*n*-pentan:diethylether = 40:1, neutral alox as solid phase) to yield **69** (50.1 mg, 0.18 mmol, 63 %) as colorless oil.

R_f = 0.5 (*n*-pentane: diethylether, 40:1).

*Table 11-3: NMR data of **69** in CD_2Cl_2 (700 MHz).*

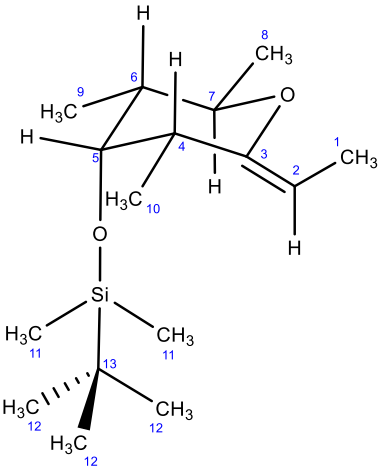

Nr.	δH [ppm] (m, J in Hz, Int.)	δC [ppm]
1	1.55 (dd, J = 6.6, 2.0 Hz, 3H)	9.9
2	4.46 (qd, J = 6.7, 1.8 Hz, 1H)	101.8
3	-	154.8
4	2.26 (dqd, J = 9.0, 6.9, 2.1 Hz, 1H)	41.1
5	3.64 (dd, J = 2.1, 2.1 Hz, 1H)	76.1
6	1.60 (dqd, J = 10.1, 7.0, 2.0 Hz, 1H)	44.3
7	3.68 (dq, J = 10.0, 6.3 Hz, 1H)	74.8
8	1.20 (d, J = 6.4 Hz, 3H)	19.7
9	0.84 (d, J = 7.0 Hz, 3H)	15.5
10	1.00 (d, J = 7.0 Hz, 3H)	15.1
11	0.04 (s, 3H)	-3.1
11	0.06 (s, 3H)	-3.5
12	0.89 (s, 9H)	26.3
13	-	18.9

HRMS (ESI): *m/z*: calc for $[M+H]^+$: $C_{16}H_{33}O_2Si^+$ 285.2244, found: 285.2242.

(1S,4S,7R)-8-(benzyloxy)-4,6,7-trimethyl-2-oxabicyclo[2.2.2]oct-5-en-3-one (223 *exo*)

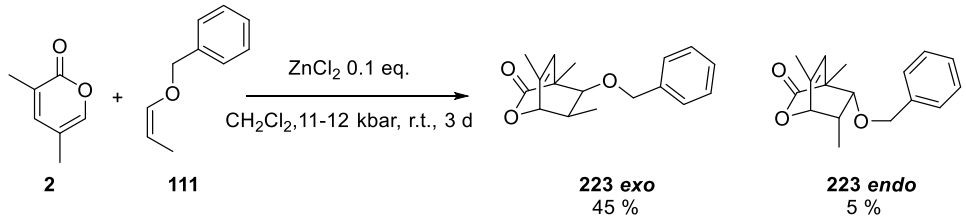

Chemical Formula: $C_{17}H_{20}O_3$
Exact Mass: 272,1412
Molecular Weight: 272,3440

A solution of **2** (45.3 mg, 0.37 mmol, 1.00 eq.) in dry CH_2Cl_2 (1.50 mL), zink chloride (5.00 mg, 0.04 mmol, 0.10 eq.) and **111** (270 mg, 1.83 mmol, 5.00 eq.) were added to a teflon vial. The vial was closed and kept at 11 – 12 kbar at room temperature for 3 days. After depressurizing the mixture was washed with destilled water (3.00 mL). The phases were separated and the aqueous layer was extracted with CH_2Cl_2 (2 x 2.00 mL). The combined organic layers were dried over $MgSO_4$, filtered and concentrated under reduced pressure. The crude product was purified by flash column chromatography (cyclohexane:ethyl acetate = 10:1) to yield **223 *exo*** as a light yellow oil (44.6 mg, 0.16 mmol, 12 %) and **223 *endo*** as light yellow oil (4.6 mg, 0.02 mmol, 5 %).

R_f for **223 *exo*** = 0.5 (cyclohexane:ethyl acetate, 1:1).
R_f for **223 *endo*** = 0.5 (cyclohexane:ethyl acetate, 1:1).
$[\alpha]_D^{20}$= −1.1° (*c* = 0.90 in CH_2Cl_2) for **223 *exo***.

*Table 11-4: NMR data of **223** exo and **223** endo in $CDCl_3$ (500 MHz).*

	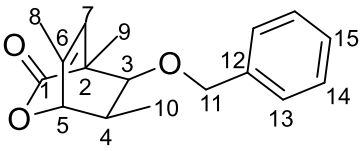 **223 *exo***		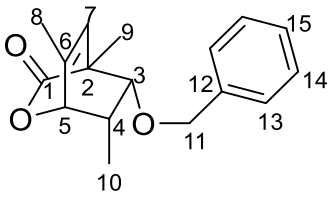 **223 *endo***	
Nr.	δH [ppm] (m, J in Hz, Int.)	δC [ppm]	δH [ppm] (m, J in Hz, Int.)	δC [ppm]
1	-	175.3	-	175.2
2	-	50.1	-	65.5
3	3.61 (d, *J* = 7.8 Hz, 1H)	77.7	3.50 (d, *J* = 9.0 Hz, 1H)	78.1
4	2.65 (ddt, *J* = 7.4, 7.4, 3.4 Hz, 1H)	38.6	2.25 (ddt, *J* = 8.8, 7.3, 1.3 Hz, 1H)	41.5
5	4.64 (dd, *J* = 3.4, 2.2 Hz, 1H)	82.0	4.52 (d, *J* = 1.9 Hz, 1H)	82.6

6	-	139.5	-	141.0
7	5.65 (td, *J* = 1.9, 1.0 Hz, 1H)	127.1	5.57 (td, *J* = 2.0, 1.9 Hz, 1H)	127.1
8	1.91 (d, *J* = 1.8 Hz, 3H)	19.6	1.84 (d, *J* = 1.8 Hz, 3H)	17.8
9	1.45 (s, 3H)	16.1	1.48 (s, 3H)	15.8
10	0.94 (d, *J* = 7.4 Hz, 3H)	12.1	1.14 (d, *J* = 7.3 Hz, 3H)	17.9
11a **11b**	4.59 (d, *J* = 11.3 Hz, 1H) 4.48 (d, *J* = 11.4 Hz, 1H)	75.3	4.58 (m, 1H) 4.50 (m, 1H)	72.3
12	-	137.6	-	137.7
13	7.32 (m, 2H)	128.3	7.32 (m, 2H)	128.3
14	7.35 (m, 2H)	128.6	7.35 (m, 2H)	128.6
15	7.30 (m, 2H)	128.2	7.30 (m, 2H)	128.0

HRMS (ESI): *m/z*: calc for $[M+H]^+$: $C_{17}H_{21}O_3^+$ 273.1485, found: 273.1482.

2-oxo-2H-pyran-3-carboxylic acid (240)

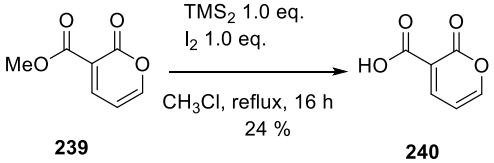

239 **240**

Chemical Formula: $C_6H_4O_4$
Exact Mass: 140,0110
Molecular Weight: 140,0940

A stirred solution of hexamethyldisilane (0.95 g, 6.50 mmol, 1.00 eq.) and iodine (1.65 g, 6.50 mmol, 1.00 eq.) was heated at 65 °C in a dry 50 mL round-bottomed flask equipped with a reservoir and a long reflux condenser. A violent exothermic reaction occurred, and a homogeneous reddish brown solution resulted, which was heated under reflux for 1.5 h to form a colorless liquid (hexamethyldisilane was quantitatively converted to iodotrimethylsilane). Pyrone **239** (1.0 g, 6.50 mmol, 1.00 eq.) in dry $CHCl_3$ (10.0 mL) of was added, and the mixture was heated at reflux for 16 h. The reaction mixture was cooled to 25 °C, and 2.00 mL of water was added. The mixture was strirred for 10 min and then dissolved with CH_2Cl_2 (20.0 mL). Saturated aqueous sodium thiosulfate (2.00 mL) was added, and the mixture was stirred until complete decoloration was evident. The organic layer was separated, and the aqueous layer was extracted with CH_2Cl_2 (3 x 30.0 mL). The combined organic solution was then washed with saturated sodium thiosulfate solution (1 x 20.0 mL), dried ($MgSO_4$), filtered, and evaporated under reduced pressure, and the residue was dried using a vacuum pump. **240** was recrystallized from toluene to yield (0.22 g, 1.56 mmol, 24 % yield) yellow crystals

^{1}H-NMR (400 MHz, $CDCl_3$): δ [ppm] = 8.56 (dd, *J* = 6.9, 2.2 Hz, 1H), 7.82 (dd, *J* = 5.1, 2.2 Hz, 1H), 6.66 (dd, *J* = 6.9, 5.0 Hz, 1H).

^{13}C-NMR (125 MHz, $CDCl_3$): δ [ppm] = 164.1, 157.8, 148.8, 117.4, 106.3.

perfluorophenyl 2-oxo-2H-pyran-3-carboxylate (233)

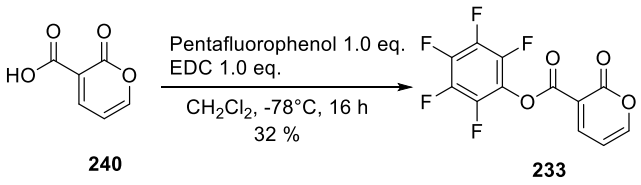

240 **233**

Chemical Formula: $C_{12}H_3F_5O_4$
Exact Mass: 305,9951
Molecular Weight: 306,1440

To a solution of pyrone **240** (150 mg, 1.07 mmol, 1.00 eq.) and pentafluorophenol (196 mg, 1.07 mmol, 1.00 eq.) in CH_2Cl_2 (7.50 mL) was added EDC (205 mg, 1.07 mmol, 1.00 eq.) at -78 ºC. The reaction was stirred for 16 hours at -78 ºC, upon which time it became an orange/red solution. Cold MeOH (2.50 mL) was added *via* syringe, and after stirring for 5 min., a brine solution (6.00 mL) was added. The reaction mixture was allowed to warm to room temperature and was extracted with CH_2Cl_2 (3 x 1.50 mL). The combined organic layers were dried over Na_2SO_4, filtered and concentrated under reduced pressure. The crude product was purified by flash column chromatography (cyclohexane: ethyl acetate = 1:1) to yield **233** (105 mg, 0.35 mmol, 32 %) as light yellow solid.

R_f = 0.3 (cyclohexane:ethyl acetate, 1:1).
^{1}H-NMR (500 MHz, $CDCl_3$): δ [ppm] = 8.46 (dd, *J* = 6.9, 2.3 Hz, 1H), 7.84 (dd, *J* = 5.0, 2.3 Hz, 1H), 6.49 (dd, *J* = 6.9, 5.0 Hz, 1H).
^{13}C-NMR (125 MHz, $CDCl_3$): δ [ppm] = 158.7, 158.5, 156.1, 151.5, 142.5, 142.5, 142.4, 142.4, 142.3, 141.0, 140.0, 139.9, 139.9, 139.9, 139.8, 139.2, 139.1, 138.5, 136.7, 136.6, 136.6, 124.7, 114.6, 106.0, 77.3, 77.2, 77.0, 76.7.
HRMS (ESI): *m/z*: calc for $[M+H]^+$: $C_{12}H_4F_5O_4^+$ 307.0030, found 307.0023.

(*3R,4S,5R,6R,Z*)-3,4,5-tris(benzyloxy)-2-ethylidene-6-methyltetrahydro-2*H*-pyran (241)

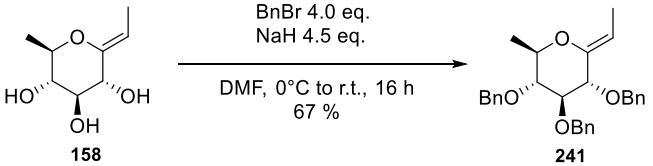

158 **241**

Chemical Formula: $C_{29}H_{32}O_4$
Exact Mass: 444,2301
Molecular Weight: 444,5710

Enol ether **158** (100 mg, 0.55 mmol, 1.00 eq.) was dissolved in dry DMF (3.00 mL) and cooled down to 0°C. NaH (100 mg, 2.47 mmol, 4.50 eq.) and BnBr (0.26 mL, 2.19 mmol, 4.00 eq.) were slowly added subsequently. The resulting mixture was stirred at 0°C for one hour before the reaction was allowed to warm up to r.t. and stirred for further 16 h. The reaction was quenched by diluting the solution with methanol (1.00 mL) and dest. Water (2.00 mL). The phases were separated and the aqueous layer was extracted with Et_2O (3 x 10.0 mL). The combined organic layers were dried over Na_2SO_4 and the solvent was removed under reduced pressure. The crude product was purified by flash column chromatography (*n*-pentan:ethylacetate = 20:1) yielding **241** (160 mg, 0.37 mmol, 77 %) as white solid.

R_f = 0.3 (*n*-pentan:ethylacetate; 20:1).

$[\alpha]_D^{20}$= +23.1° (*c* = 1.34 in CH_2Cl_2)

^{1}H-NMR (700 MHz, CD_2Cl_2): δ [ppm] = 7.36 – 7.27 (m, 15 H, H-12, H-12‘, H-13, H-13’, H-14, H-15, H-15’, H-16, H-16‘, H-17, H-18, H-18‘, H-19, H-19‘, H-20), 4.90 (qd, 1 H, H-2, $^4J_{2,4}$ = 6.8 Hz, , $^3J_{2,1}$ = 1.2 Hz), 4.80 – 4.54 (m, 6H, H-9, H- 10, H-11), 3.90 – 3.85 (m, 1 H, H-4), 3.75 (dq, 1 H, H-7, $^3J_{7,6}$ = 9.9 Hz, $^3J_{7,8}$ = 6.2 Hz), 3.63 (t, 1 H, H-5, $^3J_{5,6}$ = 6.6 Hz, $^3J_{5,4}$ = 6.6 Hz), 3.27 (dd, 1H, H-6, $^3J_{6,7}$ = 9.7 Hz, $^3J_{6,5}$ = 7.1 Hz), 1.63 (d, 3 H, H-1, $^3J_{1,2}$ = 1.3 Hz), 1.35 (d, 3 H, H-8, $^3J_{8,7}$ = 6.2 Hz).

^{13}C-NMR (175 MHz, CD_2Cl_2): δ [ppm] = 148.8 (C-3), 139.0 – 138.8 (C-21, C-22, C-23), 128.7 – 128.6 (C-13, C-13’, C-16, C-16’, C-19, C-19’), 128.3 – 128.2 (C-14, C-17, C-20), 128.0 – 127.9 (C-12, C-12’, C-15, C-15’, C-18, C-18’), 104.4 (C-2), 84.9 – 72.2 (C-9, C-10, C-11), 84.1 (C-6), 79.6 (C-4), 74.5 (C-5), 74.0 (C-7), 18.7 (C-8), 9.7 (C-1).

HRMS (ESI): *m/z*: calc for $[M+H]^+$: $C_{29}H_{33}O_4^+$ 445.2373, found: 445.2377.

perfluorophenyl(*1S,2S,3S,3'R,4S,4'S,5'R,6'R*)-3',4',5'-tris(benzyloxy)-3,6'-dimethyl-6-oxo-3',4',5',6'-tetrahydro-5-oxaspiro[bicyclo[2.2.2]octane-2,2'-pyran]-7-ene-1-carboxylate (242)

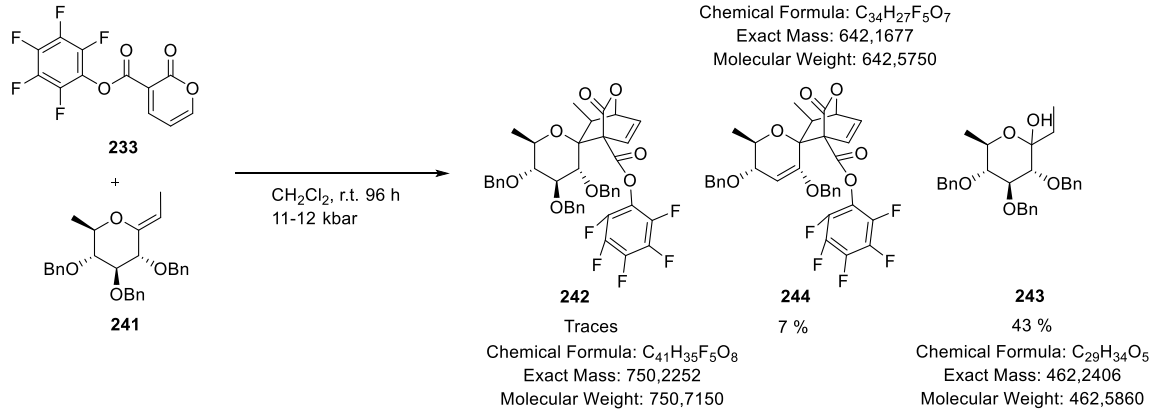

A solution of \cmpdPYRON3} (11.5 mg, 0.04 mmol, 1.00 eq.) in dry CH_2Cl_2 (1.50 mL) and **241** (50.0 mg, 0.11 mmol, 3.00 eq.) were added to a teflon vial. The vial was closed and kept at 11 – 12 kbar at room temperature for 96 hours. After depressurizing the mixture was washed with distilled water (3.00 mL). The phases were separated and the aqueous layer was extracted with CH_2Cl_2 (2 x 2.00 mL). The combined organic layers were dried over Na_2SO_4, filtered and concentrated under reduced pressure. The crude product was purified by flash column chromatography (cyclohexane:ethyl acetate = 7:1) to yield **242** in traces and **244** as light yellow solid (2.30 mg, 2.60 µmol, 7%).

R_f = 0.3 (cyclohexane:ethyl acetate, 5:1).

*Table 11-5: NMR data of **244** in CD_2Cl_2 (700 MHz).*

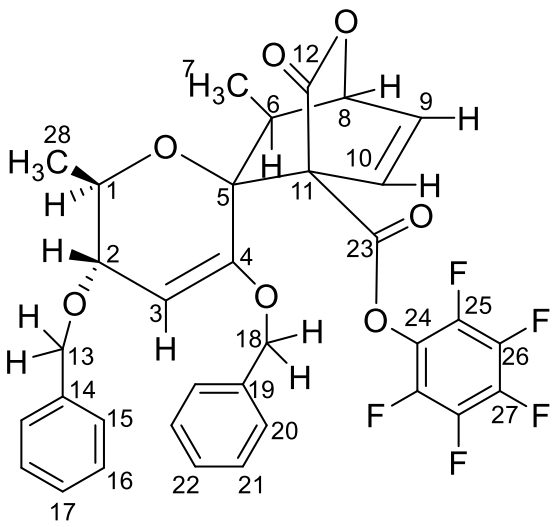

244

Nr.	δH [ppm] (m, J in Hz, Int.)	δC [ppm]
1	3.53 (dq, *J* = 8.6, 6.0 Hz, 1H)	70.8
2	3.76 (dd, *J* = 8.6, 1.5 Hz, 1H)	76.5
3	5.25 (d, *J* = 1.5 Hz, 1H)	100.1
4	-	152.8
5	-	79.8
6	2.88 (qd, *J* = 7.4, 3.0 Hz, 1H)	45.6
7	0.89 (d, *J* = 7.4 Hz, 3H))	13.0
8	4.96 (ddd, *J* = 5.0, 3.0, 2.0 Hz, 1H)	78.2
9	6.69 (dd, *J* = 7.8, 5.1 Hz, 1H)	131.0
10	6.96 (dd, *J* = 7.8, 1.9 Hz, 1H)	131.6
11	-	64.1
12	-	167.1
13a **13b**	4.64 (d, *J* = 11.7 Hz, 1H) 4.51 (d, *J* = 11.7 Hz, 1H)	71.1
14	-	138.9
15	7.36 – 7.23 (m, 2H)	128.1
16	7.36 – 7.23 (m, 2H)	128.7
17	7.36 – 7.23 (m, 1H)	128.7
18a **18b**	4.84 (d, *J* = 12.2 Hz, 1H) 4.81 (d, *J* = 11.8 Hz, 1H)	70.7
19	-	136.5
20	7.36 – 7.23 (m, 2H)	127.8
21	7.36 – 7.23 (m, 2H)	128.7
22	7.36 – 7.23 (m, 1H)	128.3
23	-	164.1
24	-	134.8
25	-	130.0
26	-	141.7
27	-	131.5
28	1.20 (d, *J* = 6.0 Hz, 3H)	18.0

For 242:

HRMS (ESI): *m/z*: calc for $[M+H]^+$: $C_{41}H_{35}O_8F_5NH_4^+$ 768.2590, found: 768.2592.

11.2.2 Syntheses Brevistin Project

2-(allyloxy)-2-oxoethan-1-aminium 4-methylbenzenesulfonate (304)

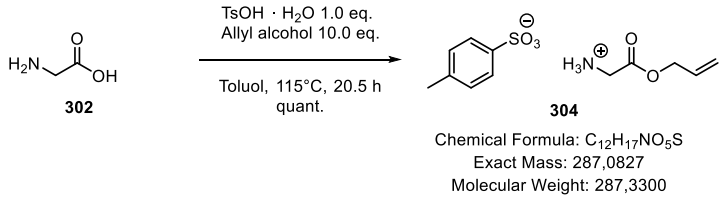

To a mixture of glycine **302** (0.98 g, 13.0 mmol, 1.00 eq.) and TsOH · H_2O (2.73 g, 14.3 mmol, 1.10 eq.) were added toluol (500 ml) in a one-necked, round bottom flask. The suspension was stirred vigorously. Then allyl alcohol (8.83 g, 130 mmol, 10.0 eq.) was added additionally and the reaction flask was fitted with a Dean-Stark trap. The mixture was stirred at 115°C overnight with concomitant azeotropic removal of water. After cooling down to room temperature the Dean-Stark trap was removed and the product was concentrated under reduced pressure to yield a yellow oil. The product was precipitated with cold diethyl ether, filtered by vacuum filtration and was again concentrated under reduced pressure to a quantitative yield of **304** (1.89 g, 6.58 mmol) as a pale yellow solid.

R_f = 0.5 (MeCN : H_2O, 4 : 1).

^{1}H-NMR (500 MHz, DMSO-d_6): δ [ppm] = 7.47 (d, J = 8.0 Hz, 2H), 7.11 (d, J = 8.0 Hz, 2H), 5.93 (ddt, J = 5.5 Hz, 10.7 Hz, 17.3 Hz, 1H), 5.38 (dd, J = 1.6 Hz, 17.2 Hz, 1H), 5.28 (dd, J = 1.44 Hz, 10.52 Hz, 1H), 4.70 (dt, J = 1.5 Hz, 5.5 Hz, 2H), 3.88 (s, 2H), 2.29 (s, 3H).

^{13}C-NMR (125 MHz, DMSO-d_6)**:** δ [ppm] = 167.4 (C_q), 145.8 (C_q), 137.6 (C_q), 131.8 (CH), 128.0 (CH), 125.5 (CH), 118.6 (CH_2), 65.7 (CH_2), 39.7 (CH_2), 20.8 (CH_3).

HRMS (ESI): m/z: calc for $[M\text{-OTs}]^+$: $C_5H_{10}O_2N^+$ 116.0706, found: 116.0706.

(*3S,4R*)-3-azido-4-hydroxypentan-2-one (292)

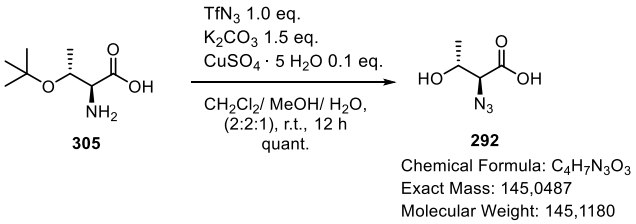

305 **292**

Chemical Formula: $C_4H_7N_3O_3$
Exact Mass: 145,0487
Molecular Weight: 145,1180

A solution of sodium azide in distilled H_2O (4.50 mL) with CH_2Cl_2 (7.50 mL) was cooled in an ice bath. While stirring Triflyl anhydride (0.93 mL, 5.55 mmol) was added dropwise over 5 min. The mixture was further stirred for 2 h. The phases were seperated and the aqueous layer was extracted with CH_2Cl (2 × 3.75 mL). The combined organic layers were washed with saturated Na_2CO_3 (1 × 3.75 mL) and used without further purification.

To a mixture of H-Thr(tBu)-OH **305** (978 mg, 5.58 mmol, 1.00 eq.), K_2CO_3 (116 mg, 8.38 mmol 1.50 eq.), $Cu^{II}SO_4$ pentahydrate (13.9 mg, 55.8 µmol, 0.10 eq.) in distilled H_2O (18.0 mL) and CH_3OH (36.0 mL) was added triflyl azide in CH_2Cl_2 (30.0 mL) and was stirred at room temperature for 12 hours. The phases were seperated with CH_2Cl_2 (50.0 mL) and the organic phase was washed with distilled H_2O (3 × 25.0 mL). The aqueous phase was acidified with HCl (10%) to pH 2 and was extracted with CH_2Cl_2 (3 × 50.0 mL). The combined organic phases were dried over Na_2SO_4 and the organic solvents were removed under reduced pressure to a quantitative yield of **292** (943 mg, 6.50 mmol, quant.) as a colorless oil.

$[\boldsymbol{\alpha}]_{\boldsymbol{D}}^{\boldsymbol{20}}$= −27.0° (*c* = 1.26 in CH_2Cl_2)
^{1}H-NMR (700 MHz, D_2O): δ [ppm] = 4.27 (dq, J = 4.9 Hz, 6.6 Hz, 1H), 3.60 (d, J = 4.9 Hz, 1H), 1.34 (d, J = 6.6 Hz, 3H).
^{13}C-NMR (125 MHz, D_2O)**:** δ [ppm] = 173.0 (C_q), 68.2 (CH), 67.4 (CH), 19.0 (CH_3).
HRMS (ESI): m/z: calc for $[M-H]^+$: $C_4H_6O_3N_3^+$ 144.0415, found: 144.0416.

(*S*)-6-methyloctanoic acid (289)

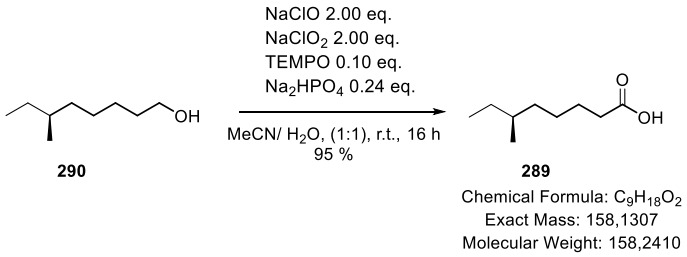

290 **289**

Chemical Formula: $C_9H_{18}O_2$
Exact Mass: 158,1307
Molecular Weight: 158,2410

A stirred solution of **290** (0.98 g, 13.0 mmol, 1.00 eq.), TEMPO (0.98 g, 13.0 mmol, 1.00 eq.), aqueous Na_2HPO_4 (0.98 g, 13.0 mmol, 1.00 eq.) in MeCN () were added NaClO (0.98 g, 13.0 mmol, 1.00 eq.) and a solution of $NaClO_2$ (0.98 g, 13.0 mmol, 1.00 eq.) in H_2O (). The mixture was stirred for 16 hours at room temperature. The reaction was quenched with a saturated $Na_2S_2O_3$ (). The phases were separated and the aqueous layer was extracted with ethyl acetate (3 x 10 mL). The combined organic extracts were washed with 1 N HCl () and dried over Na_2SO_4 and the solvent was removed under reduced pressure. The crude product was purified by flash column chromatography (*n*-pentan:ethylacetate = 20:1) yielding **289** (160 mg, 0.37 mmol, 77 %) as colorless oil.

R_f = 0.2 (*n*-pentan:ethylacetate; 10:1).

$[\alpha]_D^{20}$= −7.1° (*c* = 1.02 in CH_2Cl_2)

^{1}H-NMR (700 MHz, $CDCl_3$): δ [ppm] = 2.40 – 2.33 (m, 2H), 1.68 – 1.57 (m, 2H), 1.41 – 1.26 (m, 5H), 1.20 – 1.05 (m, 2H), 0.88 – 0.82 (m, 6H).

^{13}C-NMR (175 MHz, $CDCl_3$)**:** δ [ppm] = 179.3, 36.3, 34.4, 29.6, 26.7, 25.2, 19.3, 11.5.

HRMS (ESI): m/z: calc for $[M-H]^-$: $C_9H_{17}O_3^-$ 157.1234, found: 157.1235.

(*8R,11R*)-11-((2-(allyloxy)-2-oxoethyl)carbamoyl)-1-(9*H*-fluoren-9-yl)-3,6,9-trioxo-8-(2-oxo-2-(tritylamino)ethyl)-2-oxa-4,7,10-triazatridecan-13-oic acid (310)

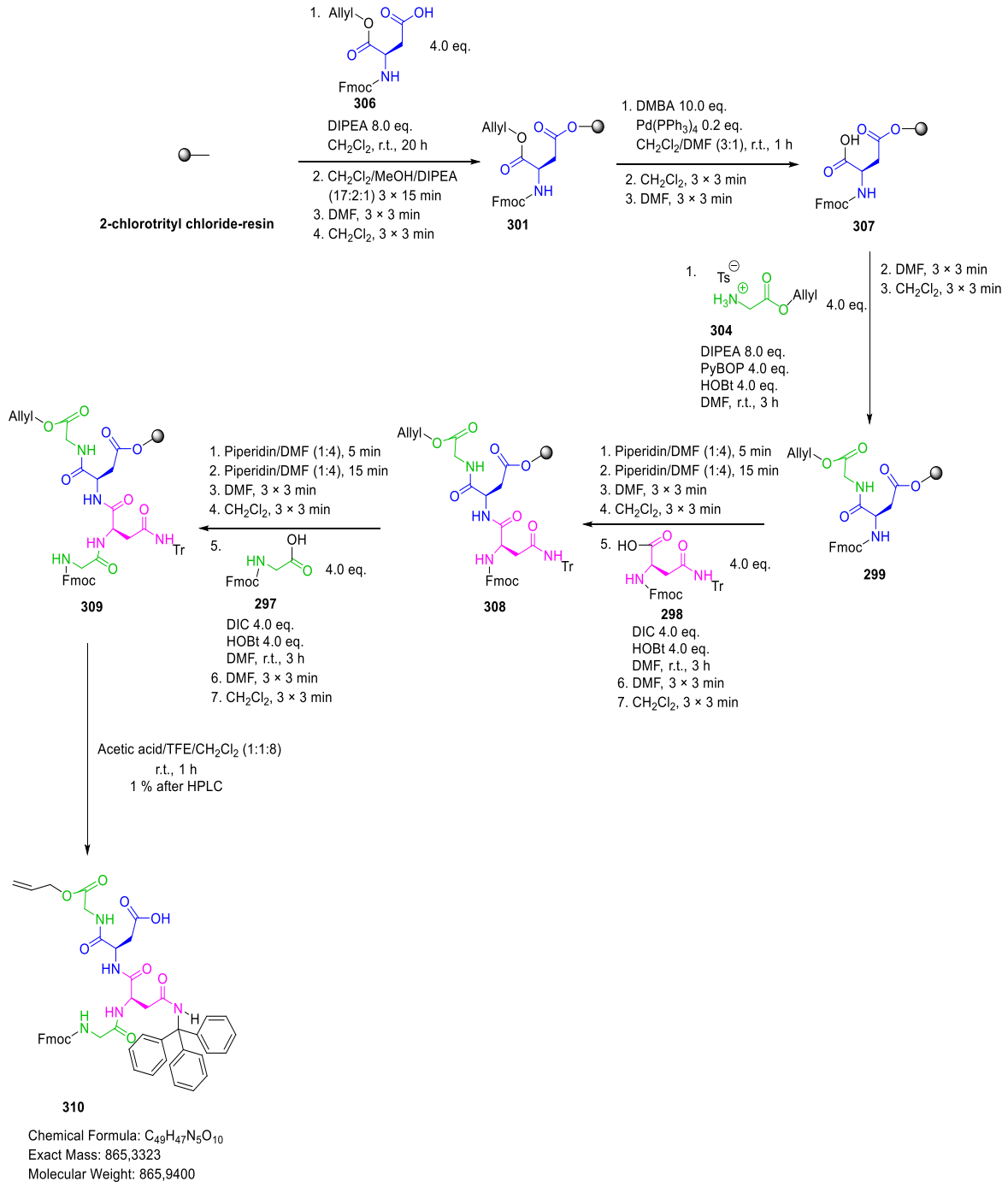

The resin (2-ClTr, 42.0 mg, 50.0 µmol, 1.00 eq.) was placed in a 10 mL polypropylene syringe fitted with a polyethylene preinserted frit and was rinsed with dry CH_2Cl_2 (6 × 3 min). The resin was preswollen in CH_2Cl_2 (1.50 mL) for 15 min. FmocAspOallyl **306** (78.1 mg, 0.20 mmol, 4.00 eq.) and DIPEA (0.07 mL, 0.40 mmol, 8.00 eq.) were stirred at room temperature for 5 min in dry CH_2Cl_2 (1.50 mL). The swollen resin was loaded with the solution and the mixture agitated overnight. The resin was capped with dry CH_2Cl_2 : MeOH : DIPEA (1.50 mL, 17:2:1,

3 × 15 min), followed by washing the resin with dry DMF (3 × 3 min) and dry CH_2Cl_2 (3 × 3 min). After removing the allyl group by adding 1,3-dimethylbarbituric acid (DMBA, 78.1 mg, 0.50 mmol, 10.00 eq.) and cat. $Pd(PPh_3)_4$ (11.6 mg, 0.01 mmol, 0.20 eq.) in dry DMF : CH_2Cl_2 (1.50 mL, 1:3) for 1 h, the resin was washed with CH_2Cl_2 (3 × 3 min) and DMF (3 × 3 min). A mixture of $TsO^{-+}H_3NGlyOallyl$ **304** (57.5 mg, 0.20 mmol, 4.00 eq.) and PyBOP/HOBt/DIPEA (4.00 : 4.00 : 8.00 eq.) in dry DMF (1.50 mL) was added to the resin for 3h to give peptide **299**. The resin was washed with DMF (3 × 3 min) and CH_2Cl_2 (3 × 3 min). The removal of the Fmoc group in peptide **299** and all subsequent peptides up to the synthesis of peptide **310** was performed with 20% piperidine in DMF (1.50 mL, 1 × 5 min, 1 × 15 min). After each deprotection the resin was washed with DMF (3 × 3 min) and CH_2Cl_2 (3 × 3 min). All Fmoc amino acids (4.00 eq.) (Fmoc-D-Asn(Trt)OH **298**, Fmoc-Gly-OH **297**) were coupled with diisopropyl carbodiimide (DIC, 4.00 eq.) and HOBt (4.00 eq.) in dry DMF (1.50 mL) for 3-4 h, followed by washing the resin with DMF (3 × 3 min) and CH_2Cl_2 (3 × 3 min). The peptide was cleaved fully protected from the resin using acetic acid: TFE : CH_2Cl_2 (1:1:8 , 2.00 mL) and agitated for 1h. The resin was filtered and was washed with the remaining mixture. The filtrates were combined and 15 times the volume of hexane was added. The organic solvents were removed under reduced pressure. The crude product was lyophilized. For analytical purpose, separation was achieved after performing semi-preparative HPLC with analytical HPLC (50% ACN/water, retention time 12.1 min for fraction 1 and 18.7 min for fraction 2, using a KNAUER Eurospher II 100-5 C18P; 5 µm 250x16mm + precolumn 5.2 mg; 265 nm for semi-preparative and a Eurospher II 100-3 C18P; 3µm; 2,0 x 100mm - 265 nm for analytical HPLC) to yield **310** (0.5 mg, 0,58 µmol, 1 %) as white, amorphous solid.

*Table 11-6: Top: Tetrapeptide **310**. Bottom: NMR data of **310** in CD_3OD (500 MHz).*

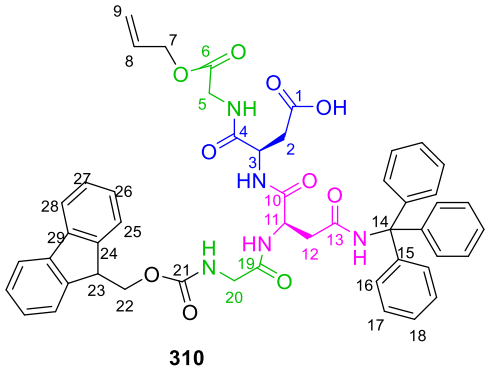

310

Nr.	δH [ppm] (m, J in Hz, Int.)	δC [ppm]
1	-	172.8
2a **2b**	2.98 (dd, J = 6.4 Hz, 15.5 Hz, 1H), 2.83 (dd, J = 6.0 Hz, 15.6 Hz, 2H)	38.9

3	4.69 (pt, J = 6.5 Hz, 1H)	51.9
4	-	171.8
5a **5b**	3.48 – 3.42 (m, 1H), 3.64 (d, J = 17.5 Hz, 1H)	42.0
6	-	170.7
7	4.55 – 4.50 (m, 2H)	66.6
8	5.88 (ddt, J = 5.7 Hz, 10.8 Hz, 16.4 Hz, 1H)	133.3
9a **9b**	5.28 (dd, J = 1.8 Hz, 17.5 Hz, 1H) 5.19 (d, J = 10.7 Hz, 1H)	118.6
10	-	170.7
11	4.69 (pt, J = 6.5 Hz, 1H)	51.9
12a **12b**	2.98 (dd, J = 6.4 Hz, 15.5 Hz, 1H) 2.83 (dd, J = 6.0 Hz, 15.6 Hz, 2H)	38.9
13	-	172.8
14	-	71.7
15	-	3 x 145.3
16	7.26 – 7.14 (m, 6H)	6 x 128.8
17	7.26 – 7.14 (m, 6H)	6 x 130.0
18	7.26 – 7.14 (m, 3H)	3 x 127.8
19	-	170.7
20	3.79 (s, 2H)	45.1
21	-	-
22a/b	4.31 (dd, J = 9.11 Hz, 10.3 Hz, 2H)	68.3
23	4.19 (pt, J = 6.9 Hz, 1H)	48.3
24	-	2 x 145.9
25	7.63 (dd, J = 4.8 Hz, 7.5 Hz, 2H)	2 x 126.3
26	7.29 (pt, J = 7.6, 2H)	2 x 128.2

27	7.38 (pt, J = 7.5 Hz, 2H)	2 x 128.7
28	7.79 (d, J = 7.6 Hz, 2H)	2 x 120.9
29	-	2 x 142.6

HRMS (ESI): m/z: calc for $[M+Na]^+$: $C_{49}H_{47}O_{10}N_5Na^+$ 888.3226, found: 888.3201.

Benzyl O-((((9H-fluoren-9-yl)methoxy)carbonyl)-L-phenylalanyl)-N-(tert-butoxycarbonyl)-L-threoninate (318)

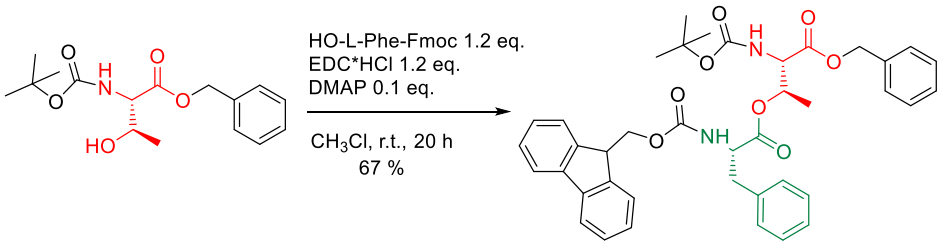

317 318

Chemical Formula: $C_{40}H_{42}N_2O_8$
Exact Mass: 678,2941
Molecular Weight: 678,7820

In a stirring solutionat 0 °C of Boc-Thr-Obz **317** (1.25 g, 4.05 mmol, 1.00 eq.), Fmoc-L-Phe-OH (1.87 g, 4.82 mmol, 1.20 eq.) and DMAP (49.5 mg, 0.41 mmol, 0.10 eq.) in dry $CHCl_3$ (50.0 mL) was added EDC·HCl (0.93 g, 4.82 mmol, 1.20 eq.). The mixture was slowly warmed to r.t. over 2 h and after it was stirred additionally 20 h under argon, the reaction was quenched with a saturated solution of NH_4Cl (25.0 mL), diluted with ethyl acetate (50.0 mL), and washed with water (1x 50.0 mL). After the collected organic phase was washed further with HCl 1 N (30.0 mL), water (30.0 mL), saturated $NaHCO_3$ (30.0 mL), and brine (30.0 mL), it was dried over $MgSO_4$, and the solvent was evaporated under reduced pressure. The resulting crude product was purified by silica gel column chromatography (ethyl acetate: cyclohexane = 1:4) to yield **318** as a white solid (1.84 g, 2.71 mmol, 67 %).

R_f = 0.33 (ethyl acetate: cyclohexane 1:4)

$[\alpha]_D^{20}$= −12.9° (*c* = 0.93 in MeOH)

^{1}H NMR (700 MHz, CD_2Cl_2): δ [ppm] = 7.81 – 7.76 (m, 2H, 2xH_{Ar}), 7.60 – 7.55 (m, 2H, 2xH_{Ar}), 7.43 – 7.36 (m, 2H, 2xH_{Ar}), 7.34 – 7.24 (m, 10H, 10xH_{Ar}), 7.14 – 7.10 (m, 2H, 2xH_{Ar}), 5.42 – 5.36 (m, 1H, H-8), 5.21 (d, *J* = 7.9 Hz, 1H, H-N_{Phe}), 5.13 (d, *J* = 11.8 Hz, 1H, H-6), 5.10 – 5.05 (m, 2H, H-6, H-N_{Thr}), 4.45 – 4.39 (m, 3H, H-4, H-11, H-15), 4.33 (dd, *J* = 10.7, 6.9 Hz, 1H, H-

15), 4.22 (t, *J* = 6.9 Hz, 1H, H-16), 3.08 – 2.93 (m, 2H, H-12), 1.44 (s, 9H, H-1), 1.20 (d, *J* = 6.5 Hz, 3H, H-9).

^{13}C NMR (175 MHz, CD_2Cl_2) δ [ppm] =170.9 (CO-10), 170.1 (CO-5), 156.1 (CO-3), 155.8 (CO-14), 144.4 (C-20), 144.3 (C-17), 141.7(C-18,C-19) 136.4 (C-13), 135.8 (C-7), 129.7-120.4 (18xCH_{Ar}), 80.4 (C-2), 72.5 (CH-8), 67.9 (CH_2-6), 67.2 (CH_2-15), 57.5 (CH-4), 55.2(CH-11), 47.6 (CH-16), 38.3 (CH_2-12), 28.4 (CH_3-1), 16.8 (CH_3-9).

HRMS (ESI-TOF) *m/z*: $[M+H]^+$Calcd for $C_{40}H_{43}N_2O_8^+$ 679.3014, found 679.3014.

benzyl *O*-((((9*H*-fluoren-9-yl)methoxy)carbonyl)-*L*-phenylalanyl)-N-octanoyl-*L*-threoninate (336)

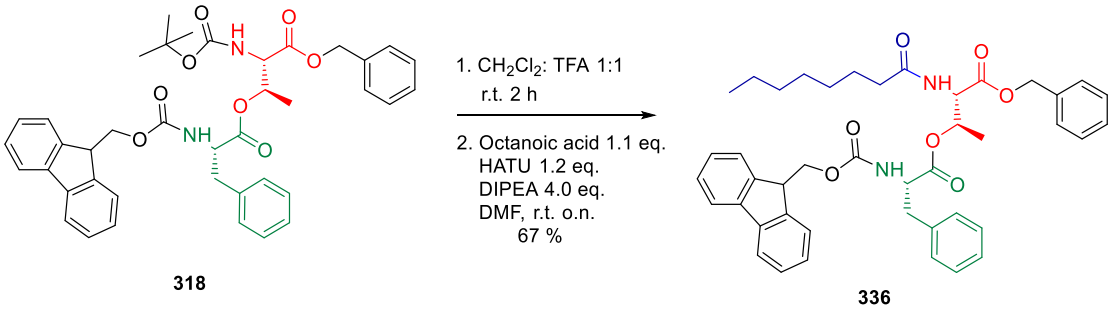

318

336

Chemical Formula: $C_{43}H_{48}N_2O_7$
Exact Mass: 704,3462
Molecular Weight: 704,8640

In a solution of **318** (2.69 g, 3.96 mmol, 1.00 eq.) in CH_2Cl_2 (32.0 mL) and TFA (32.0 mL) was added. The mixture was stirred for 2.5 h at room temperature. The solvent was removed under reduced pressure to afford a TFA ammonium salt, which was used for the next step without purification. TFA ammonium salt was dissolved with HATU (1.06 g, 2.79 mmol, 1.20 eq.), DIEA (2.05 mL, 11.6 mmol, 5.00 eq.), and octanoic acid (0.4 mL, 2.55 mmol, 1.10eq.) in DMF (50.0 mL) at 0 °C. The mixture was slowly warmed to room temperature and stirred for 16 h under argon. Then, water was added slowly and with small portions to quench the reaction. The organic phase was separated and was washed with water (2 x 30.0 mL), whereas the aqueous phase was extracted with ethyl acetate (3 x 30.0 ml). The combined organic phase was washed with brine and dried over MgSO4 and the solvent was evaporated under reduced pressure. The resulting crude product was purified by silica gel column chromatography (ethyl acetate: cyclohexane= 1:4) to yield **336** (1.10 g, 1.55 mmol, 67 %) as a light yellow oil.

R_f = 0.51 (ethyl acetate: cyclohexane 1:1)

$[\alpha]_D^{20}$= −0.9° (*c* = 1.07 in MeOH)

^{1}H NMR (500 MHz, CD_2Cl_2) δ [ppm]: 7.79 – 7.77 (m, 2H, 2xH_{Ar}), 7.59 – 7.56 (m, 2H, 2xH_{Ar}), 7.43 – 7.38 (m, 2H, 2xH_{Ar}), 7.35 – 7.23 (m, 10H, 10xH_{Ar}), 7.16 – 7.11 (m, 2H, 2xH_{Ar}), 6.01 (d, *J* = 9.1 Hz, 1H, H-N_{Thr}), 5.44 – 5.37 (m, 1H, H-13), 5.22 (d, *J* = 7.8 Hz, 1H H-N_{Phe}), 5.16 – 5.04 (m, 2H, 2xH-11), 4.78 (dd, *J* = 9.2, 2.7 Hz, 1H, H-9), 4.46 – 4.37 (m, 2H, H-16, H-20), 4.33 (dd, *J* = 10.7, 6.8 Hz, 1H, H-20), 4.22 (t, *J* = 6.8 Hz, 1H, H-21), 3.02 (t, *J* = 6.4 Hz, 2H,2xH-17), 2.24 – 2.19 (m, 2H, 2xH-7), 1.62 – 1.53 (m, 2H,2xH-5), 1.36 – 1.20 (m, 8H,2xH-2, 2xH-3, 2xH-4, 2xH-6), 1.15 (d, *J* = 6.4 Hz, 3H, 3xH-14), 0.95 – 0.83 (m, 3H, 3xH-1).

^{13}C NMR (125 MHz, CD_2Cl_2) δ [ppm]:173.7 (CO-8), 171.0 (CO-15), 169.9 (CO-10), 155.9 (C-19), 144.4 (C-22), 144.2 (C-22'), 141.7 (2xC-23), 136.4 (C-18), 135.8 (C-12), 129.7, 129.6-120.4 (18xCH_{Ar}), 72.4 (CH-13), 68.0 (CH_2-11), 67.3 (CH_2-20), 55.6 (CH-9), 55.2 (CH-16), 47.6 (CH-21), 38.2 (CH_2-17), 36.7 (CH_2-7), 32.1 (CH_2-3), 29.6 (CH_2-6), 29.4 (CH_2-5), 26.0 (CH_2-4), 23.0 (CH_2-2), 17.1 (CH_3-14), 14.2(CH_3-1).

HRMS (ESI-TOF) *m/z*: $[M+H]^+$Calcd for $C_{43}H_{49}N_2O_7^+$ 705.3567, found 705.3567.

benzyl*O*-((((9*H*-fluoren-9-yl)methoxy)carbonyl)-*L*-phenylalanyl)-*N*-((*S*)-6-methyloctanoyl)-*L*-threoninate (337)

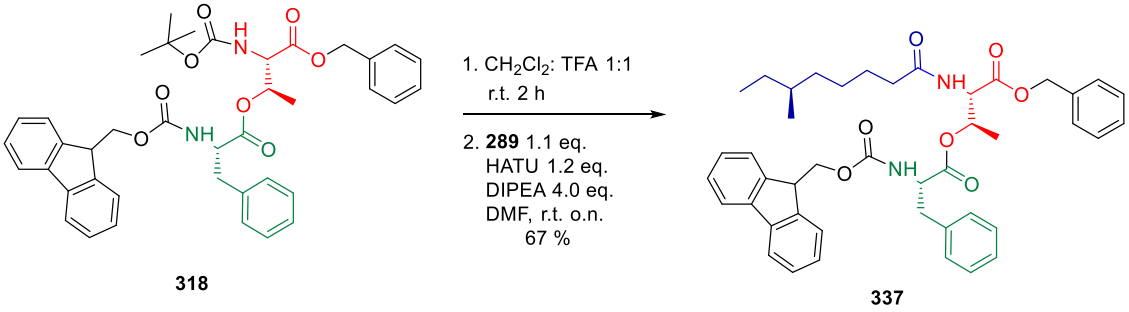

318

337

Chemical Formula: $C_{44}H_{50}N_2O_7$
Exact Mass: 718,3618
Molecular Weight: 718,8910

In a solution of **318** (1.57 g, 2.31 mmol 1.00 eq.) in CH_2Cl_2 (15.0 mL) and TFA (15.0 mL) was added. The mixture was stirred for 2.5 h at room temperature. The solvent was removed under reduced pressure to afford a TFA ammonium salt, which was used for the next step without purification. The raw material was dissolved with HATU (1.06 g, 2.77 mmol, 1.20 eq.), DIEA (2.05 mL, 11.61 mmol, 5.00 eq.), and **289** (0.4 mL, 2.55 mmol, 1.10 eq.) in DMF (50.0 mL) at 0 °C. The mixture was slowly warmed to room temperature and stirred for 16 h under argon. Then, water was added slowly and with small portions to quench the reaction. The organic phase was separated and was washed with water (2 x 30.0 mL), whereas the aqueous phase was extracted with ethyl acetate (3 x 30.0 ml). The combined organic phase was washed with brine and dried over MgSO4 and the solvent was evaporated under reduced pressure. The resulting crude product was purified by silica gel column chromatography (ethyl acetate: cyclohexane= 1:4) to yield **337** (1.10 g, 1.55 mmol, 67 %) as a light yellow oil.

R_f = 0.51 (ethyl acetate: cyclohexane 1:1)

$[\alpha]_D^{20}$= −1.1° (*c* = 0.90 in MeOH)

^{1}H NMR (700 MHz, Aceton-d_6) δ [ppm] = 7.86 (dt, *J* = 7.6, 0.9 Hz, 2H), 7.64 (dd, *J* = 17.5, 7.5 Hz, 2H), 7.41 (tt, *J* = 7.5, 0.9 Hz, 2H), 7.37 (d, *J* = 7.2 Hz, 2H), 7.34 – 7.20 (m, 10H), 6.83 (d, *J* = 8.2 Hz, 1H), 5.46 (qd, *J* = 6.5, 3.0 Hz, 1H), 5.15 (d, *J* = 12.4 Hz, 1H), 5.12 (d, *J* = 12.3 Hz, 1H), 4.84 (dd, *J* = 9.2, 3.0 Hz, 1H), 4.44 (td, *J* = 8.5, 5.9 Hz, 1H), 4.31 – 4.26 (m, 2H), 4.20 (t, *J* = 7.3 Hz, 1H), 3.13 (dd, *J* = 13.9, 5.9 Hz, 1H), 3.02 (dd, *J* = 13.9, 8.8 Hz, 1H), 2.34 – 2.20 (m, 2H), 1.58 (tt, *J* = 13.2, 7.7 Hz, 3H), 1.38 – 1.27 (m, 2H), 1.18 (s, 11H), 1.16 – 1.04 (m, 2H), 0.93 – 0.78 (m, 7H).

^{13}C NMR (125 MHz, Aceton-d_6) δ [ppm] = 173.7, 170.4, 142.1, 142.1, 137.9, 130.2, 129.3, 129.2, 129.1, 128.9, 128.6, 128.6 127.9, 127.6, 126.1, 120.8, 72.1, 68.1, 67.8, 67.3, 56.4, 56.2, 47.9, 38.0, 37.1, 36.5, 35.1, 31.6, 27.5, 27.31, 26.7, 26.0, 19.5, 19.5, 17.2, 11.7.

HRMS (ESI-TOF) *m/z*: $[M+Na]^+$Calcd for $C_{44}H_{50}N_2O_7Na^+$ 741.3510, found 741.3513.

***O*-((((9*H*-fluoren-9-yl)methoxy)carbonyl)-*L*-phenylalanyl)-*N*-octanoyl-*L*-threonine (320)**

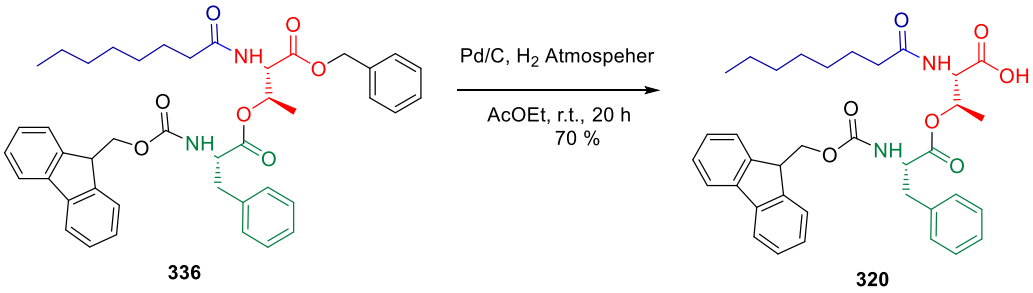

336

320

Chemical Formula: $C_{36}H_{42}N_2O_7$
Exact Mass: 614,2992
Molecular Weight: 614,7390

Into a stirring solution of compound **336** (1.217 g, 1.727 mmol, 1.00 eq.) in ethyl acetate (45.0 mL) was added Pd/C (10% Pd) (120 mg). The reaction mixture was stirred under a hydrogen atmosphere for 26 h at room temperature. The catalyst was filtered through Celite and the solvent was evaporated under reduced pressure. The crude product was purified via column chromatography (0.1% acetic acid in methanol: CH_2Cl_2 = 0.5: 9.5), to yield compound **320** (886.4 mg, 1.44 mmol, 84 %) as a yellow solid.

R_f= 0.24 (0.1% acetic acid in methanol: CH_2Cl_2 0.5: 9.5)

$[\alpha]_D^{20}$= +4.3° (*c* = 0.94 in MeOH)

^{1}H NMR (500 MHz, CD_2Cl_2) δ [ppm] = 7.79 – 7.75 (m, 2H, 2xHAr), 7.56 – 7.52 (m, 2H, 2xHAr), 7.42 – 7.37 (m, 2H, 2xHAr), 7.33 – 7.24 (m, 4H, 4xHAr), 7.19 – 7.14 (m, 2H, 2xHAr), 7.06 – 7.00 (m, 1H, , 1xHAr), 6.33 (d, *J* = 8.8 Hz, 1H, H-NThr), 5.49 – 5.39 (m, 2H, H-10, H-NPhe),

4.76 (dd, *J* = 8.9, 3.0 Hz, 1H, H-9), 4.55 (q, *J* = 7.2 Hz, 1H, H-13), 4.37 (dd, *J* = 10.6, 7.2 Hz, 1H, H-17), 4.29 (dd, *J* = 10.5, 6.7 Hz, 1H, H-17), 4.17 (t, *J* = 7.0 Hz, 1H, H-18), 3.06 (dd, *J* = 7.0, 2.3 Hz, 2H, 2xH- 14), 2.23 (t, *J* = 7.6 Hz, 2H,2xH-7), 1.63 – 1.55 (m, 2H, 2xH.5), 1.30 – 1.22 (m, 8H, 2xH-2, 2xH- 3, 2xH-4, 2xH-6), 1.19 (d, *J* = 6.4 Hz, 3H, 3xH-11), 0.90 – 0.84 (m, 3H, 3xH-1).

^{13}C NMR (125 MHz, CD_2Cl_2) δ [ppm] = 179.0 (CO-OH), 174.7 (CO-8), 171.2 (C-12), 156.4 (CO-16), 144.3 (C-19´), 144.1 (C-19), 141.7 (C-20), 136.3 (C-15), 129.7-120.4 (13xCHAr), 72.1 (CH-10), 67.6 (CH2-17), 55.8 (CH-9), 55.4 (CH-13), 47.5 (CH-18) , 38.3 (CH2-14), 36.6 (CH2-7), 32.1 (CH2-3), 29.6 (CH2-6), 26.0 (CH2-5, CH2-4), 23.0 (CH2-2), 17.2 (CH3-11), 14.2 (CH3-1).

HRMS (ESI-TOF) *m/z*: $[M+H]^+$Calcd for $C_{36}H_{43}N_2O_7^+$ 615.3069, found 615.3069.

O-((((9*H*-fluoren-9-yl)methoxy)carbonyl)-*L*-phenylalanyl)-*N*-((*S*)-6-methyloctanoyl)-*L*-threonine (321)

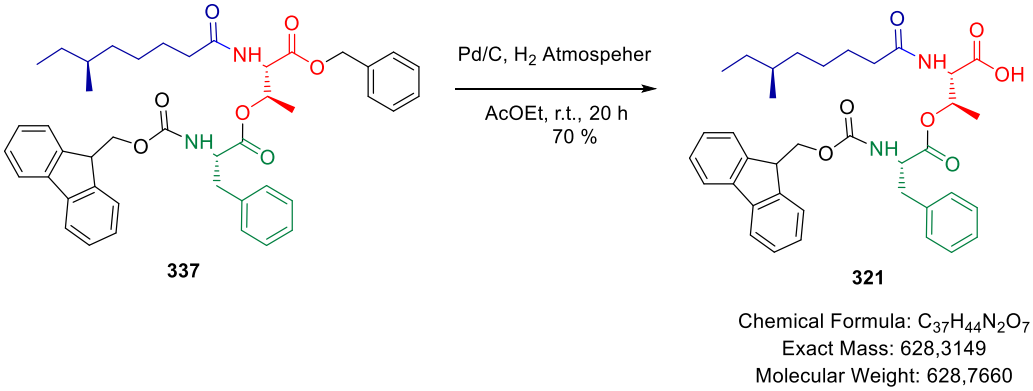

Into a stirring solution of compound **337** (1.22 g, 1.73 mmol, 1.00 eq.) in ethyl acetate (45.0 mL) was added Pd/C (10% Pd) (120 mg). The reaction mixture was stirred under a hydrogen atmosphere for 26 h at room temperature. The catalyst was filtered through Celite and the solvent was evaporated under reduced pressure. The crude product was purified via column chromatography (0.1% acetic acid in methanol: CH_2Cl_2 = 0.5: 9.5), to yield compound **321** (886 mg, 1.44 mmol, 84 %) as a yellow solid.

R_f= 0.24 (0.1% acetic acid in methanol: CH_2Cl_2 0.5: 9.5)

$[\alpha]_D^{20}$= +6.9° (*c* = 0.86 in MeOH)

^{1}H NMR (700 MHz, CD_2Cl_2) δ [ppm] = 7.81 – 7.69 (m, 3H), 7.51 (s, 2H), 7.37 (s, 2H), 7.31 – 7.10 (m, 9H), 4.55 (d, *J* = 99.4 Hz, 2H), 4.29 (d, *J* = 64.6 Hz, 3H), 4.14 (s, 2H), 3.03 (d, *J* = 22.3 Hz, 2H), 2.18 (s, 2H), 1.57 (d, *J* = 29.1 Hz, 2H), 1.23 (s, 18H), 0.81 (d, *J* = 11.5 Hz, 10H).

^{13}C NMR (175 MHz, CD_2Cl_2) δ [ppm] = 141.6, 129.7, 129.0, 128.1, 127.5, 125.4, 120.3, 69.26, 47.4, 36.7, 34.7, 31.4, 29.8, 27.2, 26.36, 19.3, 11.5.

HRMS (ESI-TOF) *m/z*: $[M+H]^+$ Calcd for $C_{37}H_{45}N_2O_7^+$ 629.3221, found 629.3226

((*R*)-2-((*R*)-2-(2-((*S*)-2-((*R*)-2-((((9*H*-fluoren-9-yl)methoxy)carbonyl)amino)-4-((*tert*-butoxycarbonyl)amino)butanamido)-4-(*tert*-butoxy)-4-oxobutanamido)acetamido)-4-oxo-4-(tritylamino)butanamido)-4-(*tert*-butoxy)-4-oxobutanoyl)glycine (325)

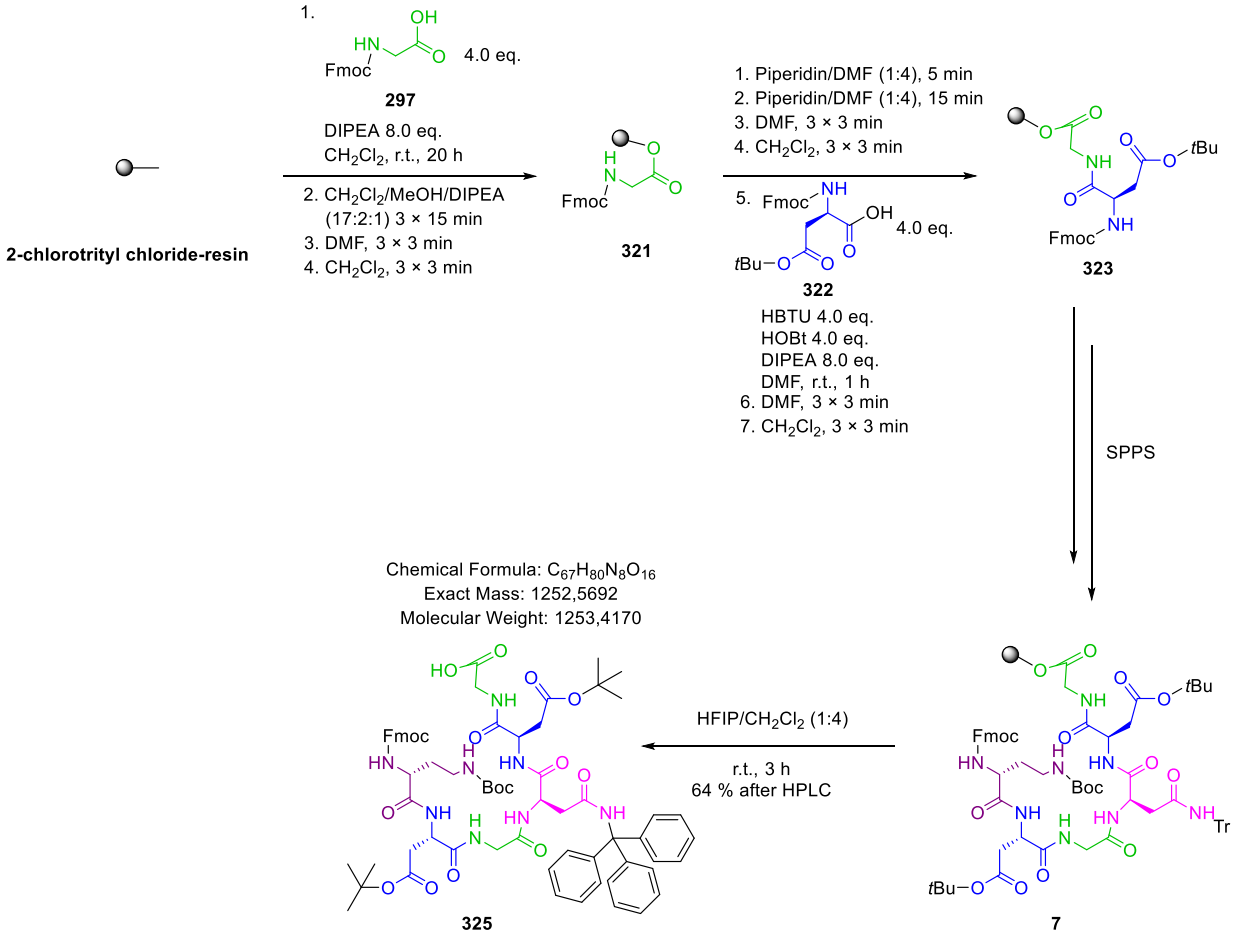

a) Functionalization of the resin

A syringe containing frit was loaded with 2-chloro-trityl chloride resin (300 mg, initial loading 1.5 mmol/g). The resin was swollen in 3 mL dry dichloromethane (CH_2Cl_2) for 40 min. The solvent was removed and a solution of Fmoc-gly-OH (268.2 mg, 0.90 mmol) and DIPEA (0.15 mL, 0.88 mmol) in 3 mL DMF) was added. The syringe was shaken 1 h at room temperature. After draining the solvent, the resin was washed with DMF (3 x 3min shaking with 3 mL) and CH_2Cl_2 (3 x 3 min shaking with 3 mL).

b) Capping of free reaction sites

3 mL of a solution of CH_2Cl_2, methanol and DIPEA (17:2:1) was added to the resin and the syringe was shaken for 15 min at room temperature. This was repeated twice. The reaction

solution was removed, and the resin was washed with DMF (3 x 5 min shaking with 3 mL) and CH_2Cl_2 (3 x 5 min shaking with 3 mL).

c) Deprotection (Removal of Fmoc)

The resin was shaken 5 min at room temperature with 20 % piperidine/DMF (3 mL). The deprotection solution was removed and the resin was loaded again with 20 % piperidine/DMF (3 mL) and was shaken for 15 min at room temperature. After removal of the deprotection solution, the resin was washed with DMF (3 x 3 min shaking with 3 mL) and CH_2Cl_2 (3 x 3 min shaking with 3 mL).

d) Coupling

The resin was loaded with a solution of amino acid (for Fmoc-D-Asp(O*t*Bu)-OH, Fmoc-D-Asn(Trt)-OH, Fmoc-gly-OH, Fmoc-L-Asp(O*t*Bu)-OH 4 eq. and Fmoc-D-Dap(Boc)-OH 2.38 eq.), HBTU (same equivalents as the used amino acid), HOBt (same equivalents as the used amino acid) and DIPEA (twice equivalents as the used amino acid) in DMF (3 mL). The resin was shaken 60 min at room temperature, washed with DMF (3 x 3 min shaking with 3 mL) and CH_2Cl_2 (3 x 3 min shaking with 3 mL).

e) Cleavage from the solid phase

For analytical purpose 0.017 mmol of resin were cleaved from the resin. A solution of 20 % 1,1,1,3,3,3-hexafluoro-2-propanol (HFIP) in CH_2Cl_2 (3 mL) was added to the dry resin and shaken for 3 h at room temperature. The solvent was collected, and the resin was washed further 2 x with 20 % HFIP/ CH_2Cl_2. The solvent was removed under reduced pressure and the residue dissolved in *tert*-butanol and water and lyophilized. For analytical purpose, separation was achieved after performing semi-preparative HPLC with analytical HPLC (60 % ACN/ 40 % 50 mM NH_4Ac pH 4,80 buffer, retention time 10.14 min, using a KNAUER Eurospher II 100-5 C18P; 5 µm 250x16mm + precolumn ; 265 nm for semi-preparative) to yield 30.5 mg (0.011 mmol, 64 %) of the hexapeptide **325** as a white solid.

R_f - value: 0.15 (6:4 MeCN:20 mmol ammonium acetate buffer).

^{1}H-NMR: **(700 MHz, MeOD, 298 K) δ [ppm]:**

7.80 (d, 2H, H-2, $^3J_{2,3}$ = 7.5 Hz), 7.68 (dd, 2H, H-5, $^3J_{5,4}$ = 7.5 Hz), 7.40 (m, 2H, H-3), 7.32 (m, 2H, H-4), 7.26 (dd, 6H, H-31, $^3J_{31,30}$ = 8.4 Hz, $^3J_{31,32}$ = 6.9 Hz), 7.24 – 7.18 (m, 9 H, H-30, H-32), 4.81 (dd, 1 H, H-25, $^3J_{25,26b}$ = 7.7 Hz, $^3J_{25,26a}$ = 5.8 Hz), 4.63 (dt, 2H, H-17, H-34, $^3J_{34,35b}$ = $^3J_{17,18a}$ = 6.2 Hz), 4.38 (d, 2H, H-8, $^3J_{8,7}$ = 7.4 Hz), 4.23 (t, 1H, H-7, $^3J_{7,8}$ = 7.1 Hz), 4.08 (dd, 1H, H-10, $^3J_{10,11b}$ = 8.4 Hz,

$^{3}J_{10,11a}$ = 5.9 Hz), 3.88 (d, 1H, H-40a, $^{2}J_{40a,40b}$ = 16.8 Hz), 3.74 (d, 1H, H-40b, $^{2}J_{40b,40a}$ = 16.8 Hz), 3.66 (d, 1H, H-23a, $^{2}J_{23a,23b}$ = 17.5 Hz), 3.37 (s, 1H, H-23b), 3.15 (dt, 1H, H-12a, $^{2}J_{12a,12b}$ = 13.7 Hz, $^{3}J_{12a,11a}$ = 6.7 Hz), 3.06 (dt, 1H, H-12b, $^{2}J_{12b,12a}$ = 13.9 Hz, $^{3}J_{12b,11b}$ = 7.0 Hz), 3.01 (dd, 1H, H-18a, $^{2}J_{18a,18b}$ = 15.6 Hz, $^{3}J_{18a,17}$ = 7.1 Hz), 2.88 - 2.77 (m, 3H, H-18b, H-26a, H-35a), 2.64 (dd, 1H, H-35b, $^{2}J_{35b,35a}$ = 16.6 Hz, $^{3}J_{35b,34}$ = 8.5 Hz), 2.56 (dd, 1H, H-26b, $^{2}J_{26b,26a}$ = 16.3 Hz, $^{3}J_{26b,25}$ 7.7 Hz), 1.92 (dt, 1H, H-11a, $^{2}J_{11a,11b}$ = 13.6 Hz, $^{3}J_{11a,10}$ = $^{3}J_{11a,12a}$ = 6.8 Hz), 1.81 (dt, 1H, H-11b, $^{2}J_{11b,11a}$ = 13.9 Hz, $^{3}J_{11b,10}$ = $^{3}J_{11b,12b}$ =7.1 Hz), 1.45 (m, 18H, H-21, H-38), 1.40 (s, 9H, H-15).

^{13}C-NMR: **(176 MHz, MeOD, 298 K) δ [ppm]:**

175.1 (C-41), 173.5 (C-27), 172.9 (C-36), 172.8 (C-19), 171.7 (C-39), 171.5 (C-22), 171.4 (C-16), 158.8 (C-33), 158.5 (C-24), 145.8 (C-13), 145.3 (C-9), 145.2 (C-29), 142.6 (C-6), 130.0 (C-1), 129.7 (C-31), 128.8 (C-30, C-3), 128.2 (C-32), 127.8 (C-2), 126.3 (C-4), 120.9 (C-5), 82.5 (C-20), 82.3 (C-37), 80.2 (C-28), 71.7 (C-14), 68.1 (C-8), 54.6 (C-10), 51.9 (C-34), 51.3 (C-25), 48.4 (C-7), 43.9 (C-40), 42.3 (C-23), 39.0 (C-18), 38.9 (C-25), 38.2 (C-26), 38.0 (C-12), 37.9 (C-18), 37.7 (C-35), 33.2 (C-11), 28.8 (C-15), 28.3 (C-21, C-38).

HRMS (ESI-TOF) *m/z*: $[M+H]^+$ Calcd for $C_{67}H_{81}N_8O_{16}^+$ 1253.5765, found 1253.5767

((*R*)-2-((*R*)-2-(2-((*S*)-2-((*R*)-2-((*2S,3R*)-3-(((((9*H*-fluoren-9-yl)methoxy)carbonyl)-*L*-phenylalanyl)oxy)-2-((*S*)-6-methyloctanamido)butanamido)-4-((*tert*-butoxycarbonyl)amino)butanamido)-4-(*tert*-butoxy)-4-oxobutanamido)acetamido)-4-oxo-4-(tritylamino)butanamido)-4-(*tert*-butoxy)-4-oxobutanoyl)glycine (327)

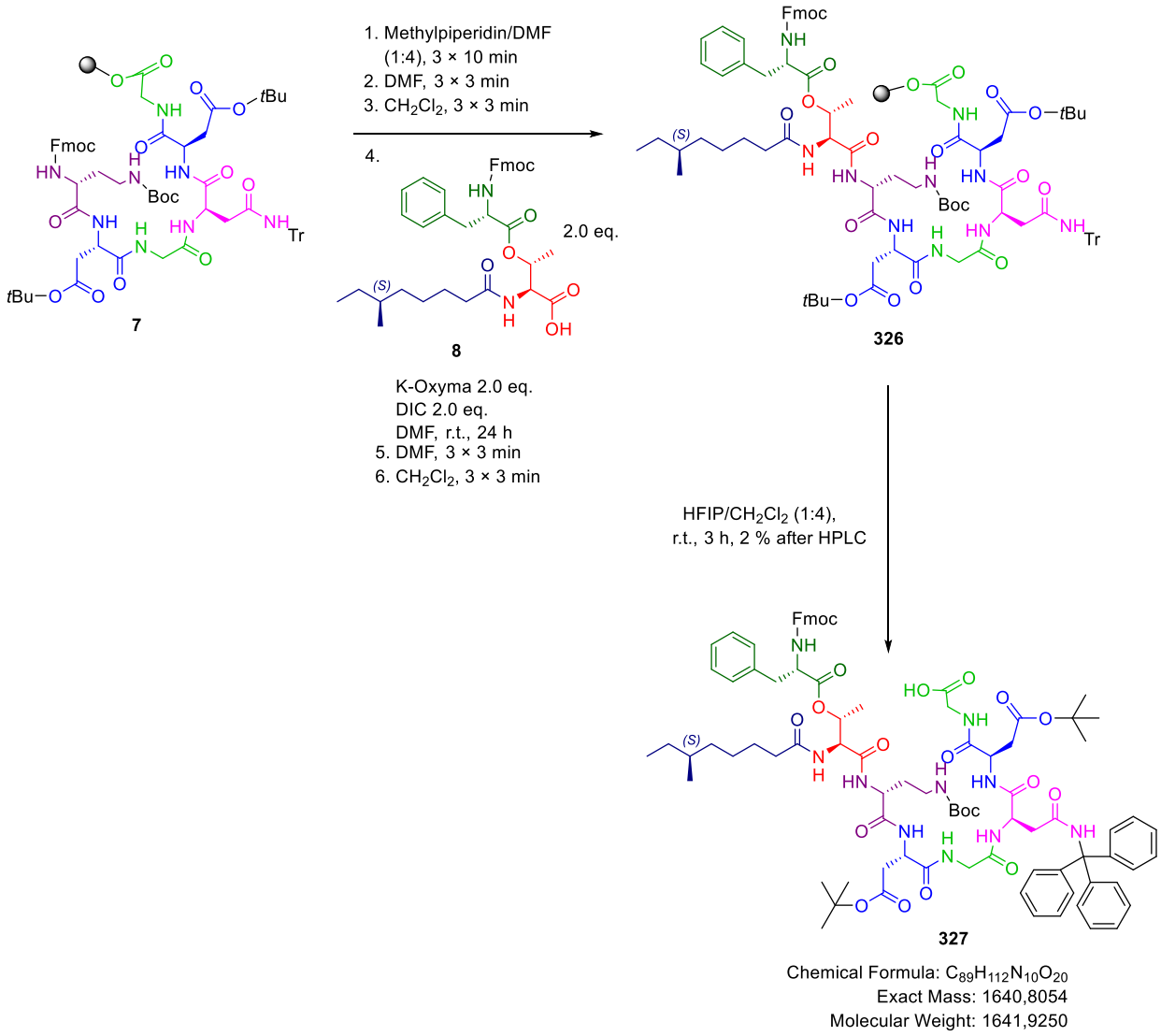

The resin (352 mg, 0.23 mmol, 1.00 eq.) was swollen in 3 mL dichloromethane (CH_2Cl_2) for 10 min. The solvent was removed, and the resin was shaken with 20 % piperidine/DMF (3.00 mL) for 5 min at room temperature. The deprotection solution was removed and the resin was loaded again with 20 % piperidine/DMF (3.00 mL) and was shaken for 15 min at room temperature. After removal of the deprotection solution, the resin was washed with DMF (3 x 3min shaking with 3 mL) and CH_2Cl_2 (3 x 3 min shaking with 3.00 mL). The solvent was removed under reduced pressure. Resin (353,8 mg, 0.56 mmol, 2.00 eq.), *N*,*N'*-di(propan-2-yl)methanediimine (DIC) (0.87 µL, 0.56 mmol, 2.00 eq.) and K-oxyma (101.3 mg, 0.56 mmol, 2.00 eq.) were dissolved in 2.30 mL DMF in a Schlenk tube under an argon atmosphere. The dried resin was then added under argon and the reaction mixture stirred for 24 hours. The reaction mixture was removed, and the resin was dried under vacuum. A solution of 20 % HFIP

in CH_2Cl_2 (1.00 mL) was added to a portion of the dry resin (70.9 mg) and shaken for 3 h at room temperature. The solvent was collected, and the resin was washed further 2 x with 20 % HFIP/ CH_2Cl_2. The solvent was removed under reduced pressure and the residue dissolved in *tert*-butanol (1.00 mL) and water (1.00 mL) and lyophilized. For analytical purpose, separation was achieved after performing semi-preparative HPLC with analytical HPLC (60 % ACN/ 40 % 50 mM NH_4Ac pH 4,80 buffer, retention time 11.92 min for fraction 1 and 18.93 min for fraction 2, using a KNAUER Eurospher II 100-5 C18P; 5 µm 250x16mm + precolumn ; 265 nm for semi-preparative) to yield 8.20 mg (2 %, 0.005 mmol) of **327** as a white solid

R_f- = 0.13 (8:2 MeCN:20 mmol ammonium acetate buffer).

$[\alpha]_D^{20}$= 46.9° (*c* = 0.32 in CH_2Cl_2)

^{1}H-NMR: **(700 MHz, MeOD, 298 K) δ [ppm]:**

7.80 (d, 2H, H-2, $^3J_{2,3}$ = 7.5 Hz), 7.65 (dd, 2H, H-5, $^3J_{5,4}$ = 7.5 Hz), 7.40 (dd, 2H, H-3, $^3J_{3,2}$ = $^3J_{3,4}$ = 7.7 Hz), 7.31 (td, 2H, H-4, $^3J_{4,3}$ = $^3J_{4,5}$ = 7.5 Hz, $^4J_{4,2}$ = 1.1 Hz), 7.30 - 7.18 (m, 20H, H-13, H-14, H-15, H-50, H-51, H-52), 4.83 (q, 1H, H-17, $^3J_{17,18}$ = 7.9 Hz), 4.66 (t, 1 H, H-54, $^3J_{54,55}$ = 7.5 Hz), 4.56 - 4.47 (m, 1H, H-19), 4.40 - 4.31 (m, 4H, H-8, H-10, H-37), 4.30 - 4.27 (m, 1H, H-45), 4.20 (t, 1H, H-7, $^3J_{7,8}$ = 7.0 Hz), 3.89 - 3.81 (m, 2H, H-60), 3.66 (d, 1H, H-43a, $^2J_{43a,43b}$ = 17.1 Hz), 3.37 (m, 1H, H-43b), 3.06 (ddd, 2H, H-31), 3.01 (dd, 2H, H-32, $^2J_{32,32}$ = 13.4 Hz, $^3J_{32a,31}$ = 7.7 Hz), 2.91 - 2.77 (m, 4H, H-55, H-38), 2.70 - 2.62 (m, 2H, H-46), 2.56 (dd, 2H, H-11, $^2J_{11,11}$ = 13.9 Hz, $^3J_{11,10}$ = 7.0 Hz), 1.90 (m, 1H, H-21a), 1.61 (m, 1H, H-21b), 1.50 - 1.33 (m, 37H, H-18, H-22, H-23, H-24, H-25, H-27, H-30, H-35, H-41, H-58), 0.94 - 0.82 (m, 9H, H-18, H-26, H-28).

^{13}C-NMR: **(176 MHz, MeOD, 298 K) δ [ppm]:**

174.6 (C-61), 174.4 (C-47, C-20), 173.4 (C-56, C-39), 172.9 (C-29), 171.6 (C-42, C-59), 171.5 (C-16, C-36), 171.2 (C-44), 158.4 (C-53), 145.8 (C-33), 145.3 (C-49), 145.2 (C-6), 142.6 (C-1), 138.2 (C-12), 130.5 (C-15, C-14), 130.0 (C-14, C-15), 129.6 (C-13), 128.8 (C-50), 128.2 (C-51), 128.2 (C-3), 127.9 (C-4), 126.4 (C-52), 126.3 (C-5), 121.0 (C-2), 82.4 (C-40, C-57), 80.2 (C-48), 71.7 (C-34), 68.2 (C-8), 58.3 (C-10), 52.5 (C-45), 52.2 (C-54), 51.9 (C-19), 51.3 (C-17), 49.5 (C-7), 43.9 (C-60), 39.1 (C-43), 38.5 (C-55), 38.2 (C-31), 37.9 (C-32), 37.5 (C-38), 36.7 (C-46), 35.5 (C-11), 32.6 (C-21), 30.6 (C-37), 28.8 (C-35), 28.3 (C-58, C-41), 27.8 (C-30), 27.1 (C-25), 19.6 (C-30), 17.5 (C-24), 17.4 (C-27), 17.3 (C-22), 17.2 (C.23), 17.1 (C-28), 11.8 (C-26).

HRMS (ESI-TOF) *m/z*: $[M+H]^+$ Calcd for $C_{89}H_{113}N_{10}O_{20}^+$ 1641.8127, found 1641.81

12 References

[1] B. Cheng, D. Trauner, *J. Am. Chem. Soc.* **2015**, *137*, 13800.

[2] G. R. Pettit, Q. Zhang, V. Pinilla, D. L. Herald, D. L. Doubek, J. A. Duke, *J. Nat. Prod.* **2004**, *67*, 983.

[3] R. Pant, A. Joshi, T. Joshi, P. Maiti, M. Nand, T. Joshi, V. Pande, S. Chandra, *J. Mol. Graph.* **2021**, *103*, 107822.

[4] X. Jiang, R. Wang, *Chem. Rev.* **2013**, *113*, 5515.

[5] *Spektrum.de https://www.spektrum.de/news/heilpflanzen-kraeuter-fuer-die-seele/1848205* (accessed 2023-01-09).

[6] S. Weinmann, S. Roll, C. Schwarzbach, C. Vauth, S. N. Willich, *BMC Geriatr* **2010**, *10*, 14.

[7] P. M. Wright, I. B. Seiple, A. G. Myers, *Angew. Chem. Int. Ed.* **2014**, *53*, 8840.

[8] a) D. S. Jones, J. H. Jones, *Biogr. Mems Fell. R. Soc.* **2014**, *60*, 5; b) D. Crowfoot, C. W. Bunn, B. W. Rogers-Low, A. Turner-Jones in *Chemistry of Penicillin* (Ed.: H. T. Clarke), Princeton University Press, **1949**, pp. 310–366.

[9] J. C. Sheehan, K. R. Henery-Logan, *J. Am. Chem. Soc.* **1959**, *81*, 3089.

[10] a) P. S. Baran, *J. Am. Chem. Soc.* **2018**, *140*, 4751; b) K. C. Nicolaou, D. Vourloumis, N. Winssinger, P. S. Baran, *Angew. Chem. Int. Ed.* **2000**, *39*, 44.

[11] *Live Science* https://www.livescience.com/55008-lichens.html (accessed 2023-01-10).

[12] S. Huneck, G. Follmann, W. A. Weber, G. Trotet, *Zeitschrift für Naturforschung B* **1967**, *22*, 671.

[13] *Roccella portentosa - Pictures of Tropical Lichens*. https://www.tropicallichens.net/3675.html (accessed 2023-01-10).

[14] J. Aberhart, K. H. Overton, *Chem. Comm.* **1969**, 162.

[15] D. J. Aberhart, A. Corbella, K. H. Overton, *J. Chem. Soc. D* **1970**, 664.

[16] A. Schröckeneder, *Dissertation*, Ludwig-Maximilians-Universität, München, **2013**.

[17] M. Jacolot, M. Jean, N. Levoin, P. van de Weghe, *Org. Lett.* **2012**, *14*, 58.

[18] G. C. Kumar, V. Satyanarayana, K. Muralikrishna, J. S. Yadav, *ChemistrySelect* **2018**, *3*, 11316.

[19] O. Diels, K. Alder, *Justus Liebigs Ann. Chem.* **1928**, *460*, 98.

[20] K. C. Nicolaou, S. A. Snyder, T. Montagnon, G. Vassilikogiannakis, *Angew. Chem. Int. Ed.* **2002**, *41*, 1668.

[21] F. Fringuelli, A. Taticchi, *The Diels-Alder reaction*. *Selected practical methods*, Wiley, Chichester, **2002**.

[22] G. Huang, C. Kouklovsky, A. de La Torre, *Chemistry (Weinheim an der Bergstrasse, Germany)* **2021**, *27*, 4760.

[23] F. Effenberger, T. Ziegler, K.H. Schönwälder, *Chem. Ber.* **1985**, *118*, 741.

[24] A. Janusko, *Master Thesis*, Rheinische Friedrich-Wilhelms-Universität Bonn, Bonn, **2017**.

[25] Tan Hoang Luu, *Master Thesis*, Rheinischen Friedrich-Wilhelms-Universität Bonn, Bonn, **2018**.

[26] H.-K. Cho, *Org. Synth.* **2015**, *92*, 148.

[27] K. Ryu, Y.-S. Cho, S.-I. Jung, C.-G. Cho, *Org. Lett.* **2006**, *8*, 3343.

[28] I. E. Markó, G. R. Evans, *Synlett* **1994**, *1994*, 431.

[29] G. H. Posner, Y. Ishihara, *Tetrahedron Lett.* **1994**, 75.

[30] K. Li, K. Vanka, W. H. Thompson, J. A. Tunge, *Org. Lett.* **2006**, *8*, 4711.

[31] T. Yamanoi, Y. Nara, S. Matsuda, Y. Oda, A. Yoshida, K. Katsuraya, M. Watanabe, *Synlett* **2007**, *2007*, 785.

[32] S. Zhanga, X.L. Yub, W.J. Wang, J.W. Wanga, Gui Long Zhao, *Indian J. Chem. Sect. B* **2014**, *53*, 1205.

[33] M. Yasuda, Y. Onishi, M. Ueba, T. Miyai, A. Baba, *J. Org. Chem.* **2001**, *66*, 7741.

[34] A. Bouzide, G. Sauvé, *Tetrahedron Lett.* **1997**, *38*, 5945.

[35] A. Wille, S. Tomm, H. Frauenrath, *Synth.* **1998**, *1998*, 305.

[36] G.-J. Boons, S. Isles, *J. Org. Chem.* **1996**, *61*, 4262.

[37] C. Su, P. G. Williard, *Org. Lett.* **2010**, *12*, 5378.

[38] R. F. Algera, Y. Ma, D. B. Collum, *J. Am. Chem. Soc.* **2017**, *139*, 11544.

[39] Block, E. Olefin Synthesis by Deoxygenation of Vicinal Diols. In *Organic reactions*; Wiley Online Library, **2004**; pp 457–566..

[40] a) D. H. R. Barton, S. Bath, D. C. Billington, S. D. Gero, B. Quiclet-Sire, M. Samadi, *J. Chem. Soc., Perkin Trans. 1* **1995**, 1551; b) S. Kazemi, Á. B. Martín, D. Sordi, M. C. Kroon, C. J. Peters, I. W. Arends, *Green Processing and Synthesis* **2012**, *1*.

[41] M. Freccero, R. Gandolfi, M. Sarzi-Amadè, A. Rastelli, *J. Org. Chem.* **2005**, *70*, 9573.

[42] *Asymmetric Epoxidation of Methyl Gibberellate by the Modified Sharpless Reagent*. https://www.tandfonline.com/doi/epdf/10.1080/00397918908053055?needAccess=true&role=button (accessed 2023-04-20).

[43] S. Habib, F. Larnaud, E. Pfund, T. Mena Barragán, T. Lequeux, C. Ortiz Mellet, P. G. Goekjian, D. Gueyrard, *Org. Biomol. Chem.* **2014**, *12*, 690.

[44] K. Krohn, D. Gehle, U. Flörke, *Justus Liebigs Ann. Chem.* **2005**, *2005*, 2841.

[45] K. Krohn, I. Ahmed, M. Al Sahli, *J. Carbohydr. Chem.* **2008**, *27*, 379.

[46] M. Černý, V. Gut, J. Pacák, *Collect. Czech. Chem. Commun.* **1961**, *26*, 2542.

[47] P. R. Blakemore, *J. Chem. Soc., Perkin Trans. 1* **2002**, 2563.

[48] V. Gembus, F. Marsais, V. Levacher, *Synlett* **2008**, *2008*, 1463.

[49] Y. Tsuda, M. Nishimura, T. Kobayashi, Y. Sato, K. Kanemitsu, *Chem. Pharm. Bull.* **1991**, *39*, 2883.

[50] M. Bierenstiel, *Dissertation*, Ludwig-Maximilians-Universität, München, **2005**.

[51] R. Lin, D. C. Hoerr, L. E. Weaner, R. Salter, *J. Labelled Compd. Rad.* **2017**, *60*, 616.

[52] Lipshutz, B. H. Synthetic Procedures Involving Organocopper Reagents. In *Organometallics in Synthesis: A Manual*; Schlosser, M. A., Ed.; Wiley, **1994**; pp 283–382.

[53] S. Kozai, T. Fuzikawa, K. Harumoto, T. Maruyama, *Nucleosides, nucleotides & nucleic acids* **2003**, *22*, 145.

[54] M. Nakata, N. Akiyama, J. Kamata, K. Kojima, H. Masuda, M. Kinoshita, K. Tatsuta, *Tetrahedron* **1990**, *46*, 4629.

[55] I. Paterson, D. J. Wallace, S. M. Velázquez, *Tetrahedron Lett.* **1994**, *35*, 9083.

[56] S. Nahm, S. M. Weinreb, *Tetrahedron Lett.* **1981**, *22*, 3815.

[57] S. Scheeff, D. Menche, *Org. Lett.* **2019**, *21*, 271.

[58] A. A. Khan, S. H. Chee, B. L. Stocker, M. S. M. Timmer, *Eur. J. Org. Chem.* **2012**, *2012*, 995.

[59] I. Paterson, D. J. Wallace, S. M. Velázquez, *Tetrahedron Lett.* **1994**, *35*, 9083.

[60] C. Bonini, R. Racioppi, G. Righi, L. Rossi, *Tetrahedron: Asymmetry* **1994**, *5*, 173.

[61] R. Brückner, *Reaktionsmechanismen*. *Organische Reaktionen, Stereochemie, moderne Synthesemethoden*, Springer Spektrum, Berlin, Heidelberg, **2015**.

[62] A. Babczyk, L. M. Wingen, D. Menche, *Eur. J. Org. Chem* **2020**, *2020*, 6645.

[63] K. B. Wiberg, W. F. Bailey, K. M. Lambert, Z. D. Stempel, *T J. Org. Chem.* **2018**, *83*, 5242.

[64] M. Hesse, H. Meier, B. Zeeh, *Spektroskopische Methoden in der organischen Chemie*. *102 Tabellen*, Thieme, Stuttgart, **2005**.

[65] I. E. Markó, G. R. Evans, *Tetrahedron Lett.* **1994**, *35*, 2767.

[66] X.-W. Liang, Y. Zhao, X.-G. Si, M.-M. Xu, J.-H. Tan, Z.-M. Zhang, C.-G. Zheng, C. Zheng, Q. Cai, *Angew. Chem. Int. Ed.* **2019**, *58*, 14562.

[67] V. Kvita, H. Sauter, *Helv. Chim. Acta* **1990**, *73*, 883.

[68] V. Nair, D. E. Vietti, C. S. Cooper, *J. Am. Chem. Soc.* **1981**, *103*, 3030.

[69] R. D. Slack, M. A. Siegler, G. H. Posner, *Tetrahedron Lett.* **2013**, *54*, 6267.

[70] G. H. Posner, C.-G. Cho, T. E. N. Anjeh, N. Johnson, R. L. Horst, T. Kobayashi, T. Okano, N. Tsugawa, *J. Org. Chem.* **1995**, *60*, 4617.

[71] G. Gurudata, J. B. Stothers, *Can. J. Chem.* **1969**, *47*, 3515.

[72] a) T. R. Navin, S. J. N. McNabb, J. T. Crawford, *Emerging Infectious Diseases* **2002**, *8*, 1187; b) P. K. M. Jensen, S. L. Grant, M. L. Perner, Z. Z. Hossain, J. Ferdous, R. Sultana, S. Almeida, M. Phelps, A. Begum, *APMIS : acta pathologica, microbiologica, et immunologica Scandinavica* **2021**, *129*, 421.

[73] American Chemical Society. *Alexander Fleming Discovery and Development of Penicillin - Landmark - American Chemical Society*.

https://www.acs.org/education/whatischemistry/landmarks/flemingpenicillin.html#top (accessed 2023-06-27).

[74] a) M. J. Martin, S. E. Thottathil, T. B. Newman, *American journal of public health* **2015**, *105*, 2409; b) C. L. Ventola, *Pharm. Ther.* **2015**, *40*, 277.

[75] J. Shoji, R. Sakazaki, Y. Wakisaka, K. Koizumi, M. Mayama, *J. Antibiot.* **1976**, *29*, 375.

[76] C. Cillóniz, C. Garcia-Vidal, A. Ceccato, A. Torres in *Antimicrobial Resistance in the 21st Century* (Eds.: I. W. Fong, D. Shlaes, K. Drlica), Springer International Publishing, Cham, **2018**, pp. 13–38.

[77] X. Yang, A. E. Yousef, *World J. Microbiol. Biotechnol.* **2018**, *34*, 57.

[78] J. Shoji, T. Kato, *J. Antibiot* **1976**, *29*, 380.

[79] W. Hou, X. Zhang, C.-F. Liu, *Trans. Tianjin Univ.* **2017**, *23*, 401.

[80] D. M. M. Jaradat, *Amino acids* **2018**, *50*, 39.

[81] A. Duro-Castano, I. Conejos-Sánchez, M. Vicent, *Polymers* **2014**, *6*, 515.

[82] T.-L. Hwang, K. Ranganathan, Y.-Q. Fang, R. D. Crockett, S. Osgood, S. Cui, *Org. Process Res. Dev.* **2018**, *22*, 1007.

[83] A. Patgiri, M. Z. Menzenski, A. B. Mahon, P. S. Arora, *Nat. Protoc.* **2010**, *5*, 1857.

[84] S. K. Jensen, T. T. Thomsen, A. Oddo, H. Franzyk, A. Løbner-Olesen, P. R. Hansen, *Int. J. Mol. Sci.* **2020**, *21*.

[85] C. R. Lohani, R. Taylor, M. Palmer, S. D. Taylor, *Org. Lett.* **2015**, *17*, 748.

[86] B. K. W. Chung, C. J. White, C. C. G. Scully, A. K. Yudin, *Chem. Sci.* **2016**, *7*, 6662.

[87] J. T. Lundquist, J. C. Pelletier, *Org. Lett.* **2001**, *3*, 781.

[88] Z. Yang, X. Jin, M. Guaciaro, B. F. Molino, *J. Org. Chem.* **2012**, *77*, 3191.

[89] P. Athanassopoulos, K. Barlos, D. Gatos, O. Hatzi, C. Tzavara, *Tetrahedron Lett.* **1995**, *36*, 5645.

[90] J. E. Cyr, D. A. Pearson, D. M. Wilson, C. A. Nelson, M. Guaraldi, M. T. Azure, J. Lister-James, L. M. Dinkelborg, R. T. Dean, *J. Med. Chem.* **2007**, *50*, 1354.

[91] P. K. Chinthakindi, A. Benediktsdottir, P. I. Arvidsson, Y. Chen, A. Sandström, *Eur. J. Org. Chem.* **2020**, *2020*, 3796.

[92] T. Yoshiya, A. Taniguchi, Y. Sohma, F. Fukao, S. Nakamura, N. Abe, N. Ito, M. Skwarczynski, T. Kimura, Y. Hayashi et al., *Org. Biomol. Chem.* **2007**, *5*, 1720.

[93] P. Cherkupally, G. A. Acosta, L. Nieto-Rodriguez, J. Spengler, H. Rodriguez, S. N. Khattab, A. El-Faham, M. Shamis, Y. Luxembourg, R. Prohens et al., *Eur. J. Org. Chem.* **2013**, *2013*, 6372.

13 Appendix

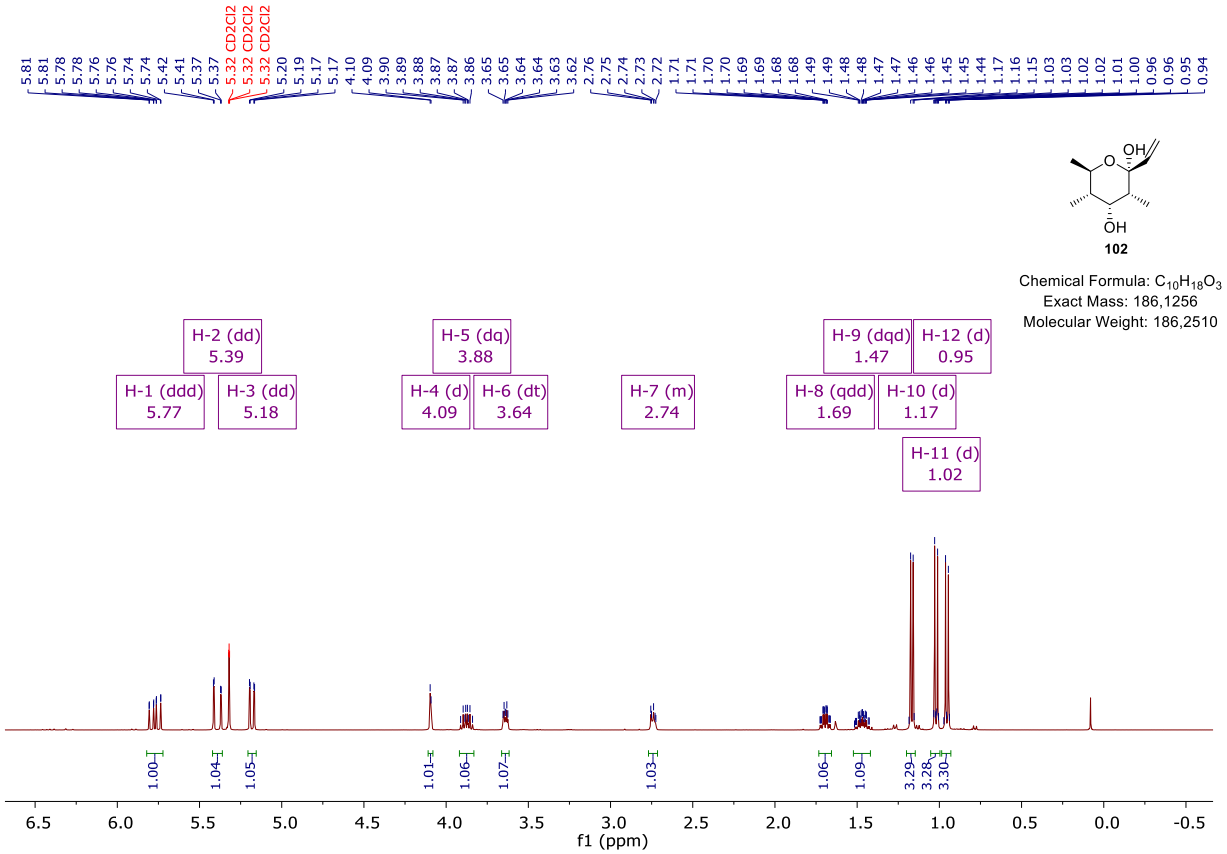

^{1}H-NMR spectrum of **102** (400 MHz, CD_2Cl_2)

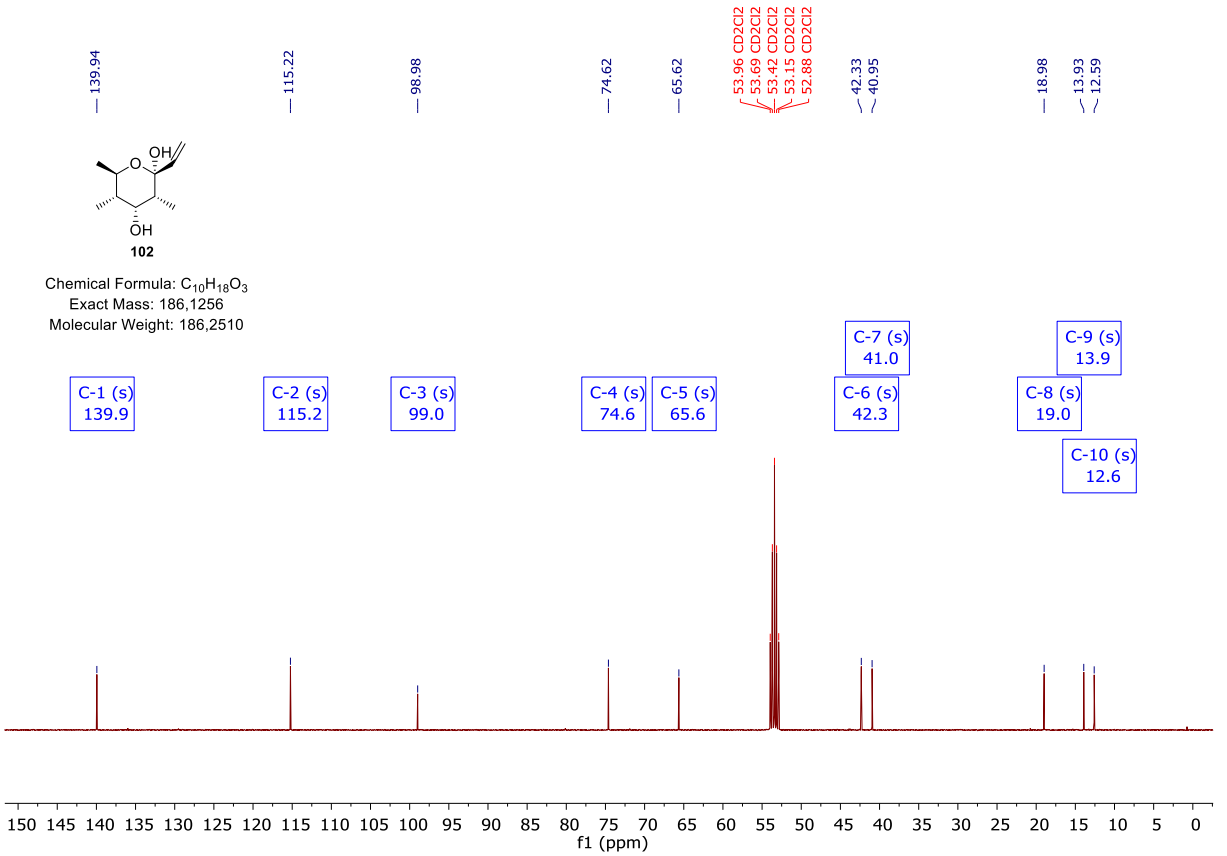

^{13}C-NMR spectrum of **102** (101 MHz, CD_2Cl_2)

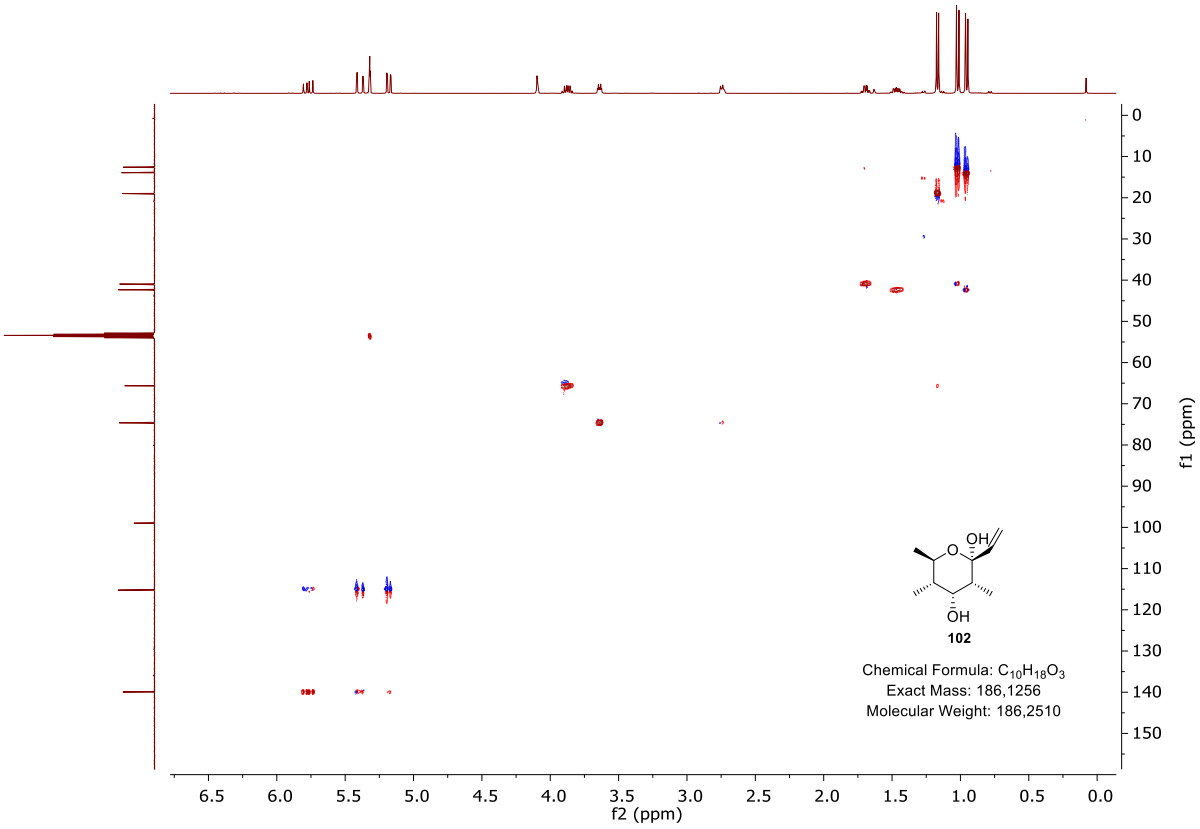

^{1}H, ^{13}C-HSQC spectrum of **102** (400 MHz, 101 MHz, CD_2Cl_2)

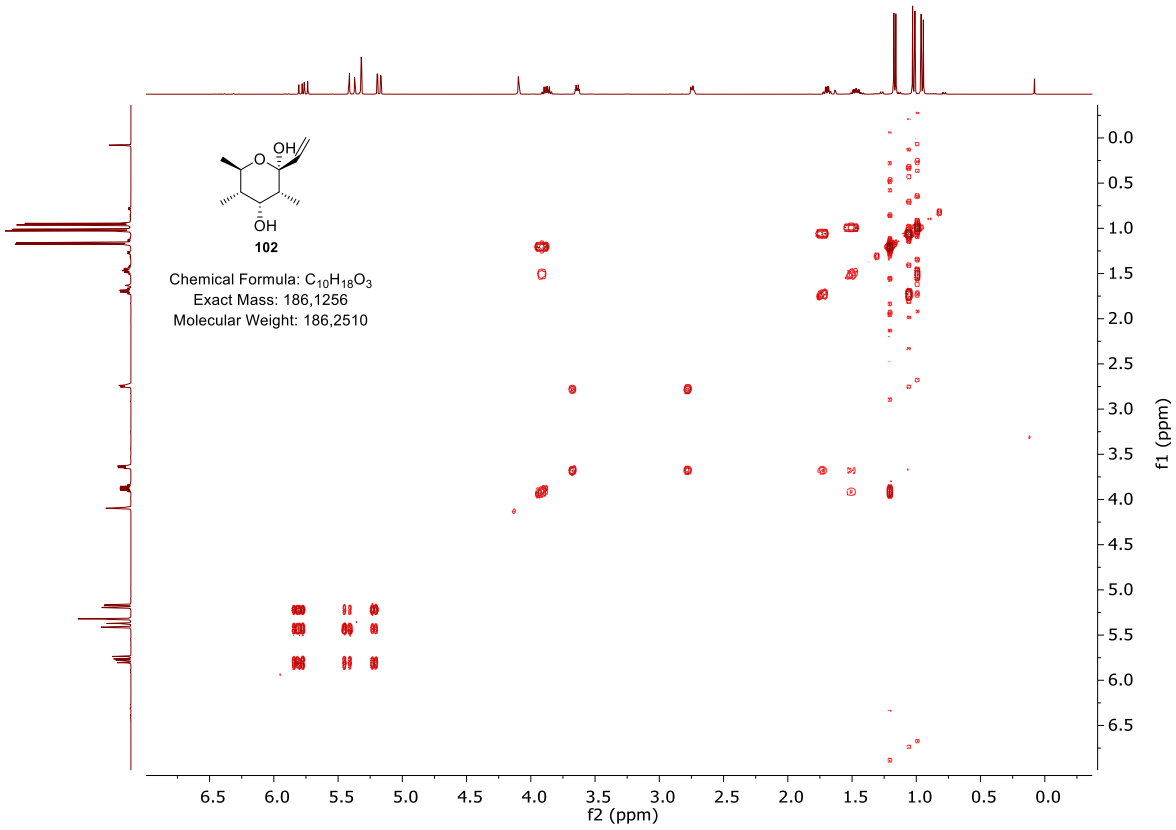

^{1}H, ^{1}H-COSY spectrum of **102** (400 MHz, CD_2Cl_2)

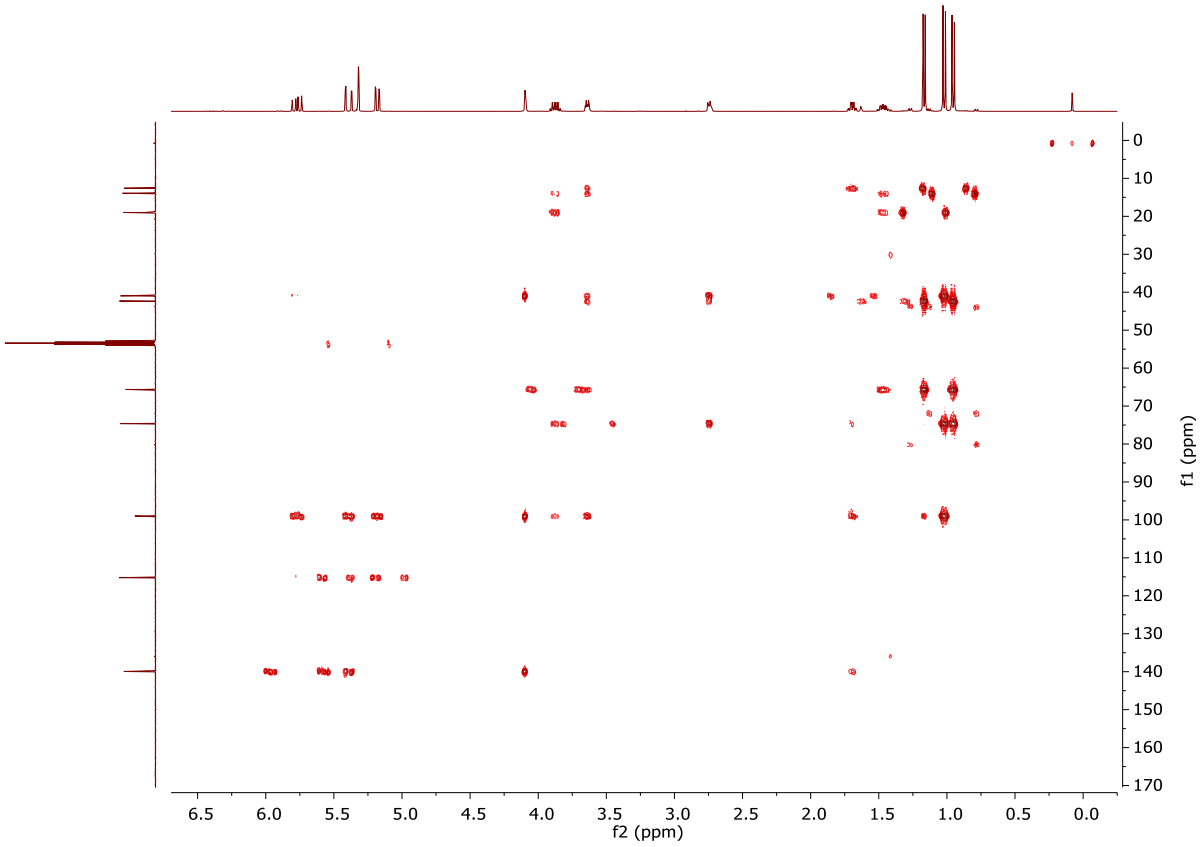

^{1}H, ^{13}C-HMBC spectrum of **102** (400 MHz, 101 MHz, CD_2Cl_2)

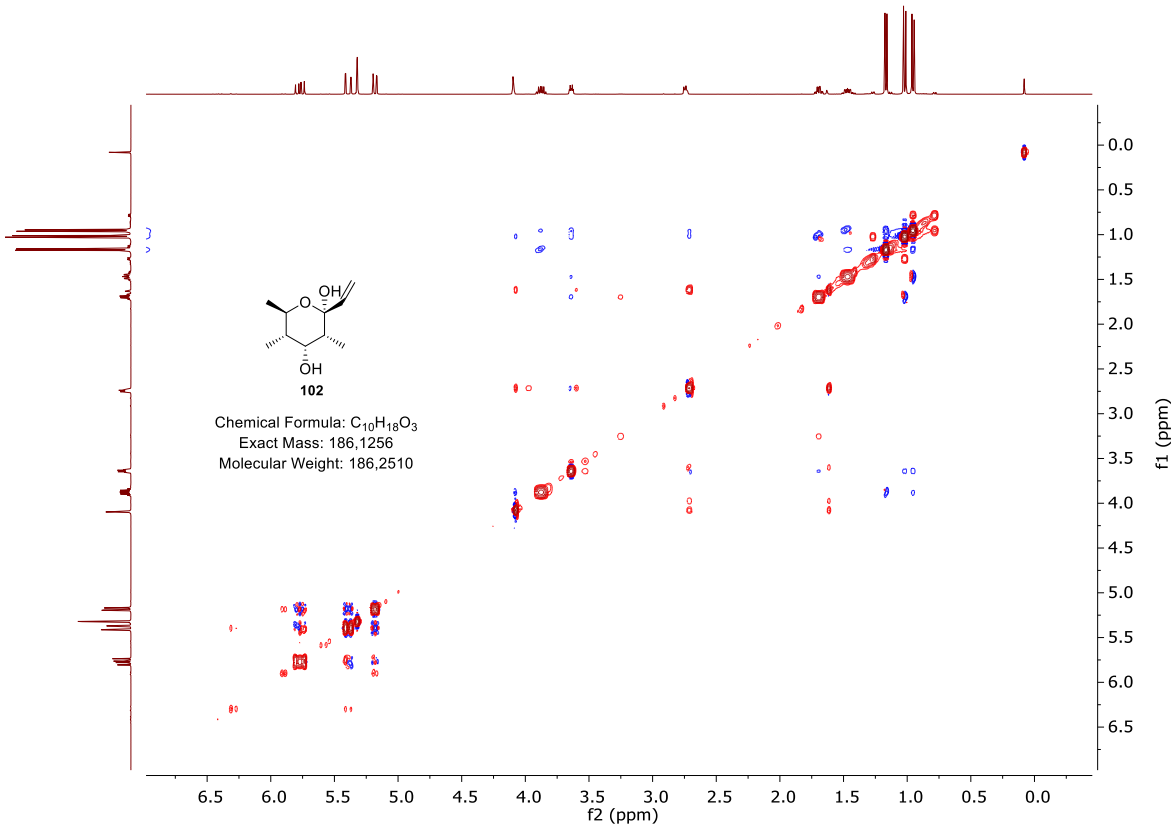

^{1}H, ^{1}H-NOESY spectrum of **102** (400 MHz, CD_2Cl_2)

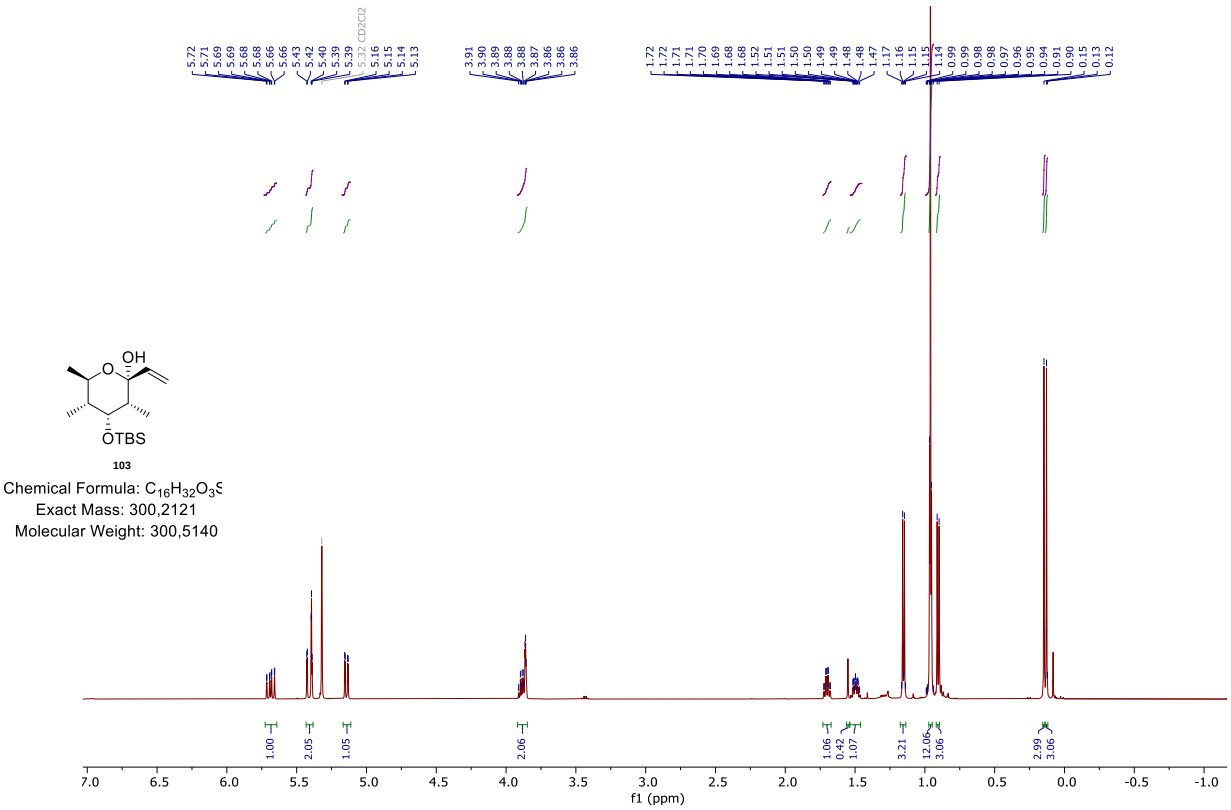

^{1}H-NMR spectrum of **103** (400 MHz, CD_2Cl_2)

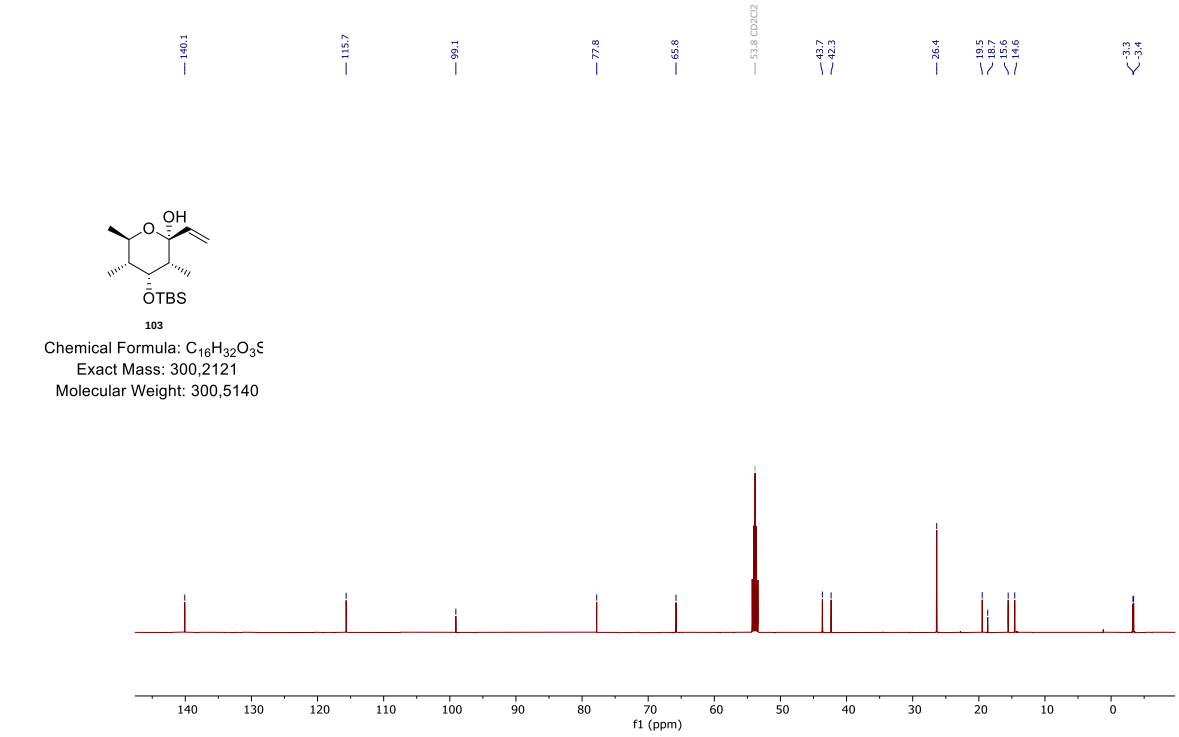

^{13}C-NMR spectrum of **103** (101 MHz, CD_2Cl_2)

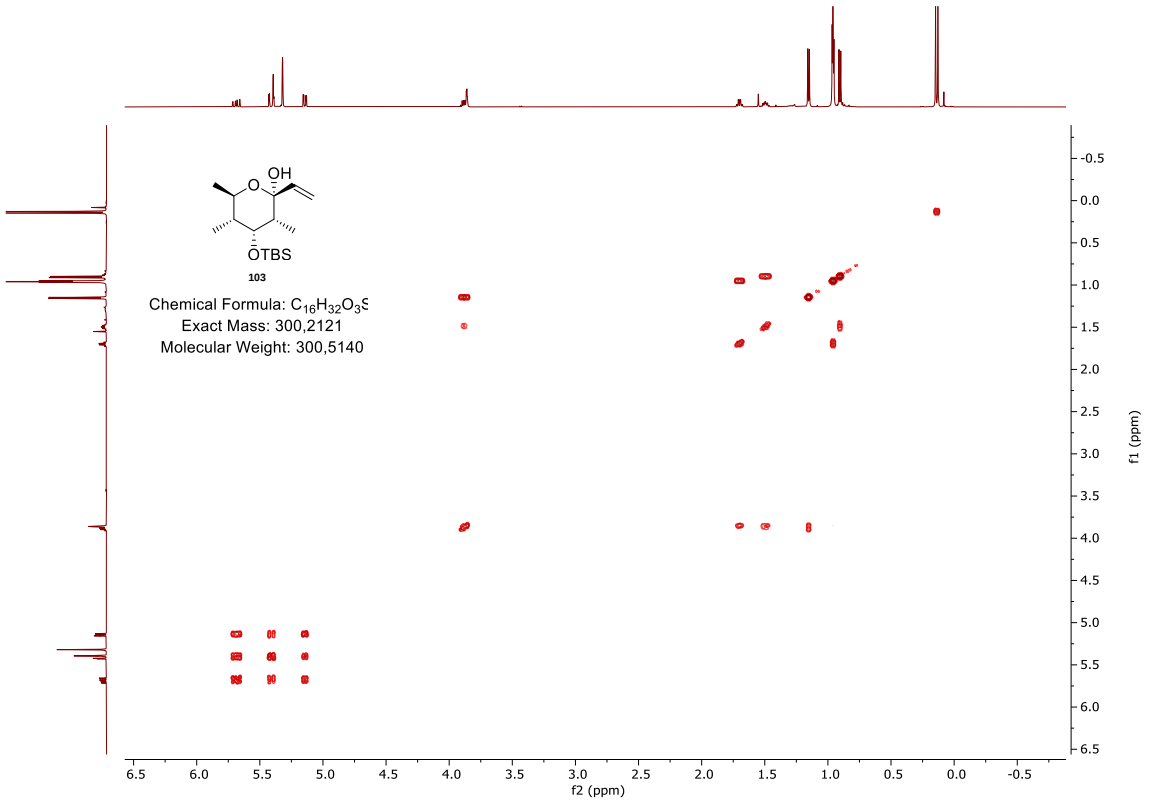

^{1}H, ^{1}H-COSY spectrum of **103** (400 MHz, CD_2Cl_2)

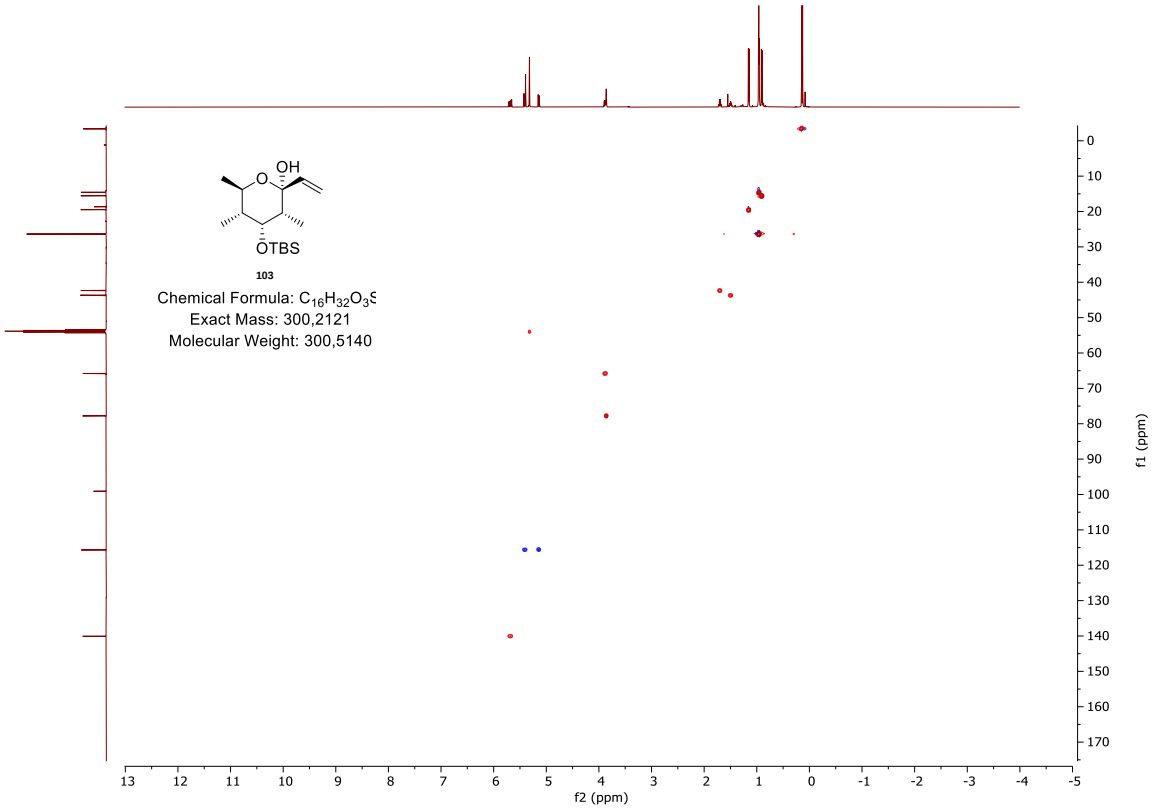

^{1}H, ^{13}C-HSQC spectrum of **103** (400 MHz, 101 MHz, CD_2Cl_2)

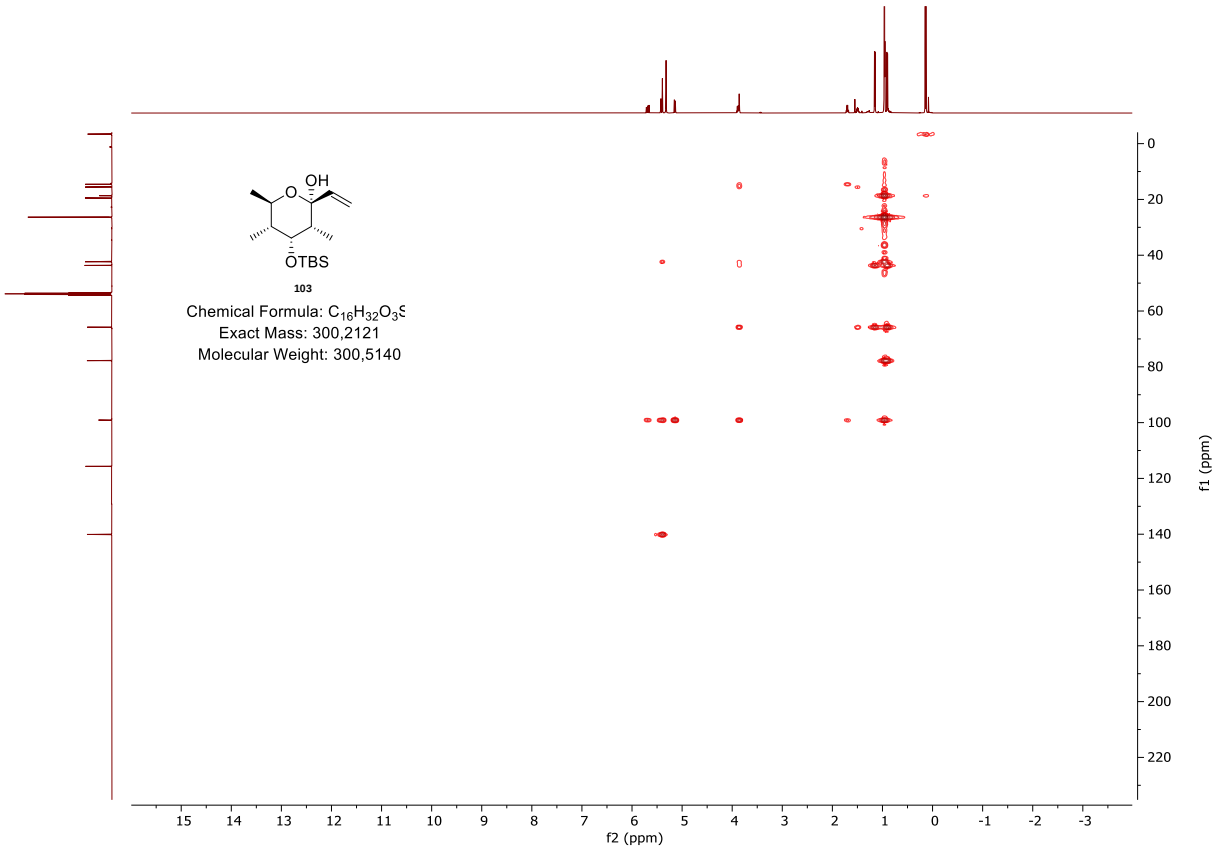

^{1}H, ^{13}C-HMBC spectrum of **103** (400 MHz, 101 MHz, CD_2Cl_2)

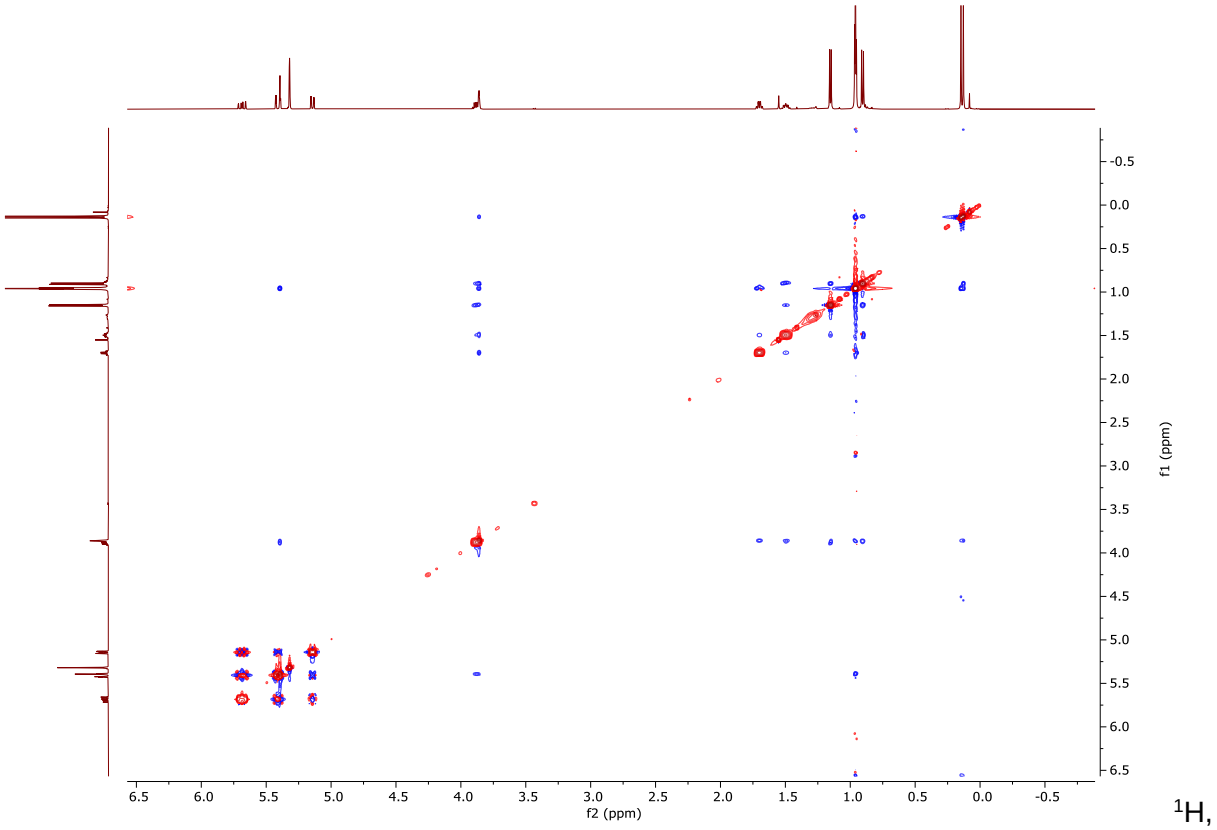

^{1}H,

^{1}H -NOESY spectrum of **103** (400 MHz, CD_2Cl_2)

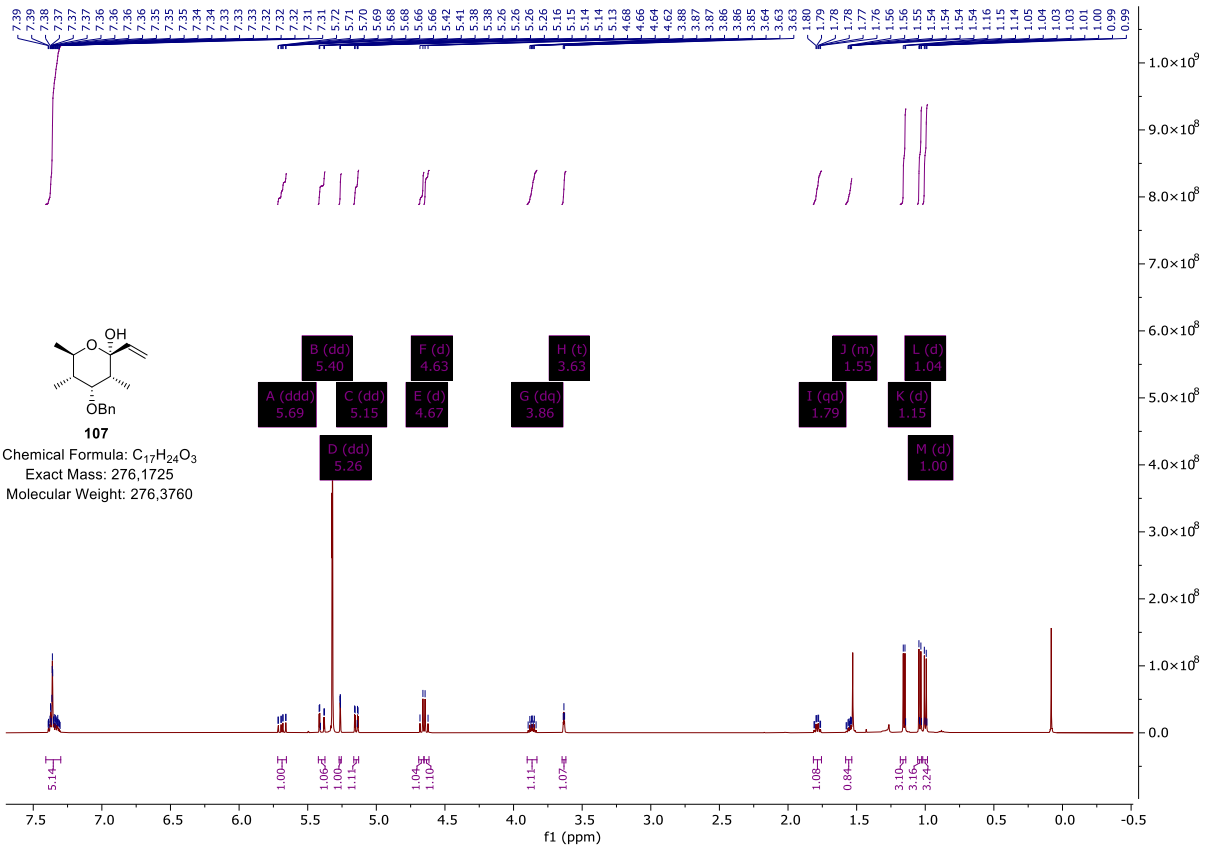

^{1}H-NMR spectrum of **107** (500 MHz, CD_2Cl_2)

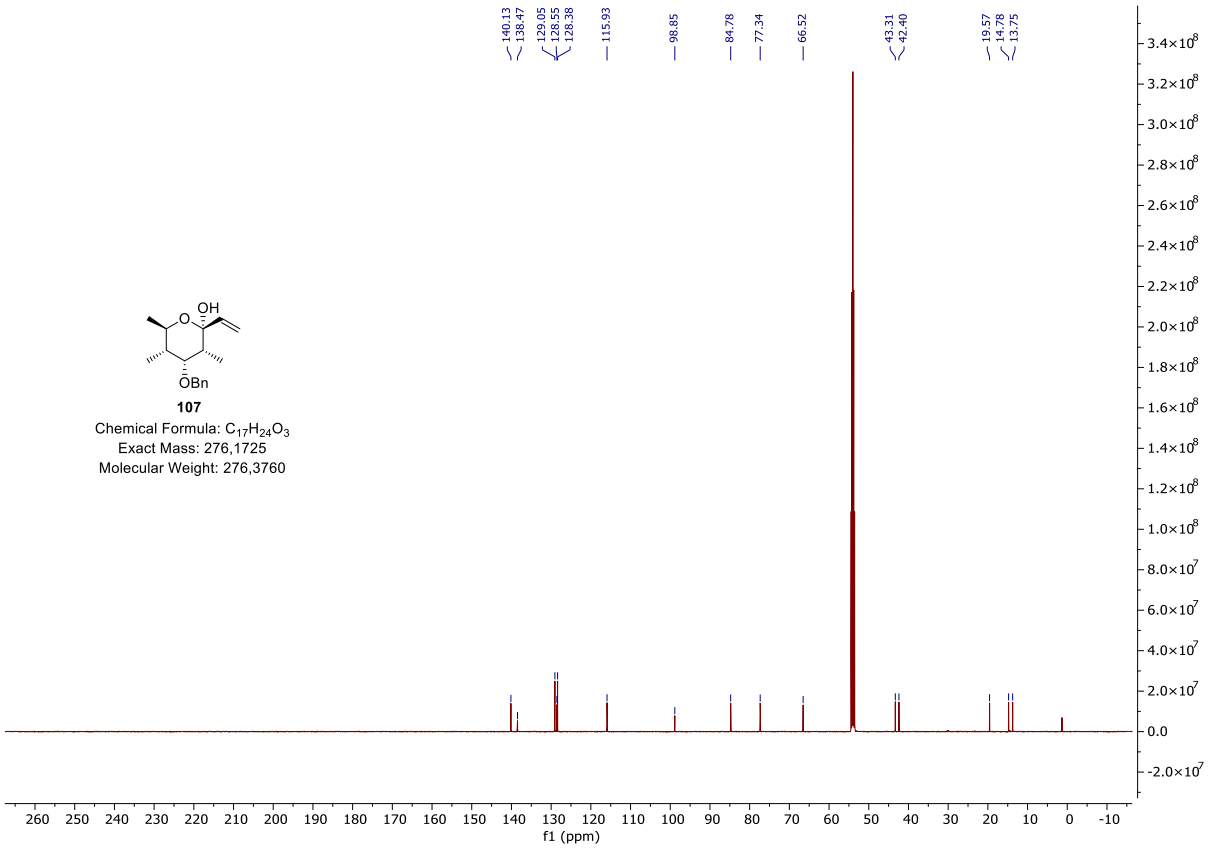

^{13}C-NMR spectrum of **107** (125 MHz, CD_2Cl_2)

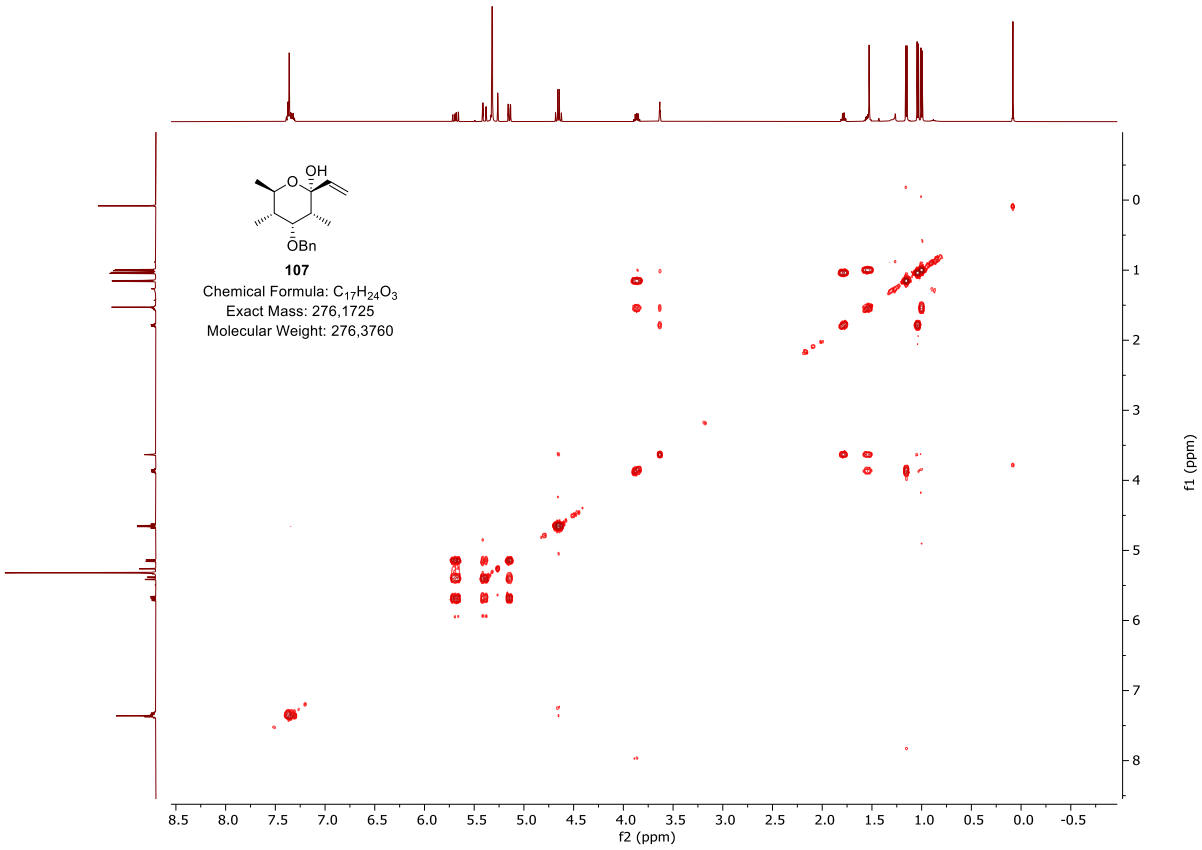

^{1}H, ^{1}H -COSY spectrum of **107** (500 MHz, CD_2Cl_2)

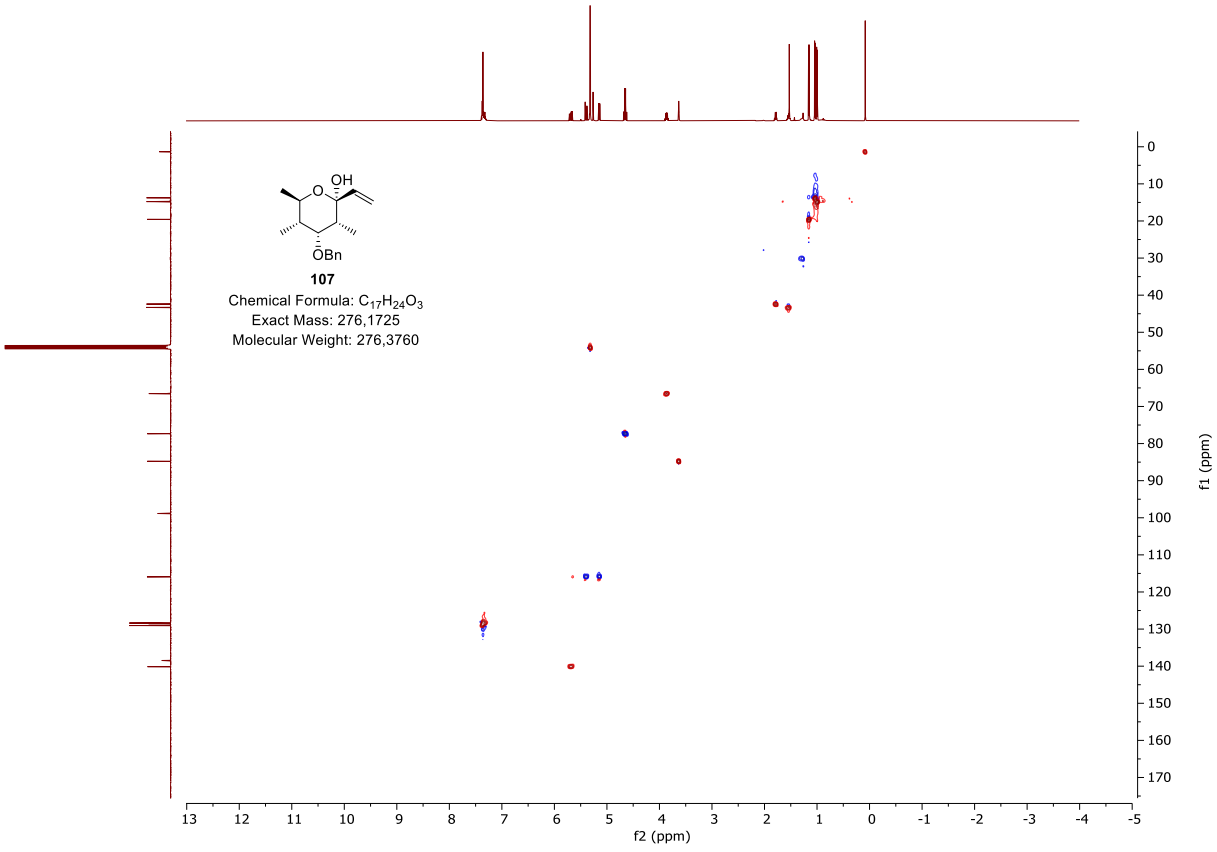

^{1}H, ^{13}C-HSQC spectrum of **107** (500 MHz, 125 MHz, CD_2Cl_2)

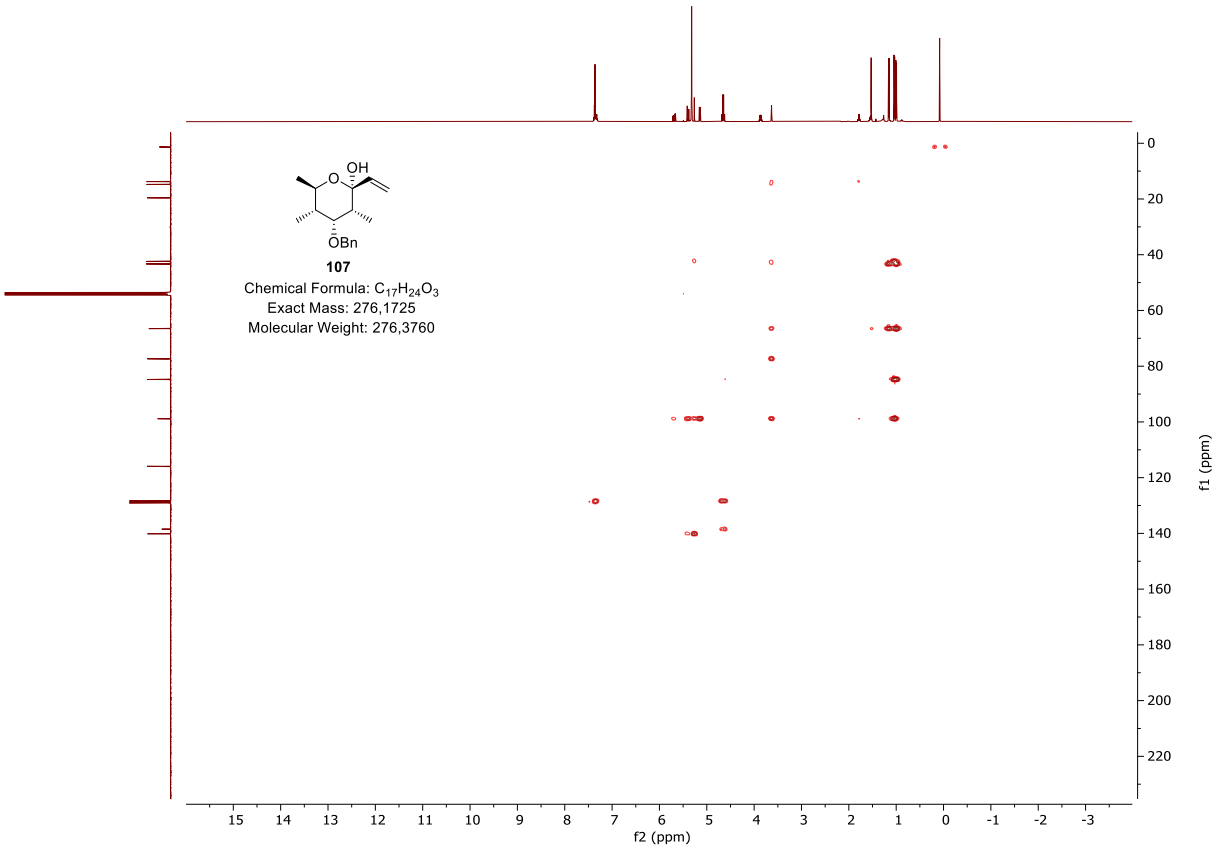

^{1}H, ^{13}C-HMBC spectrum of **107** (500 MHz, 125 MHz, CD_2Cl_2)

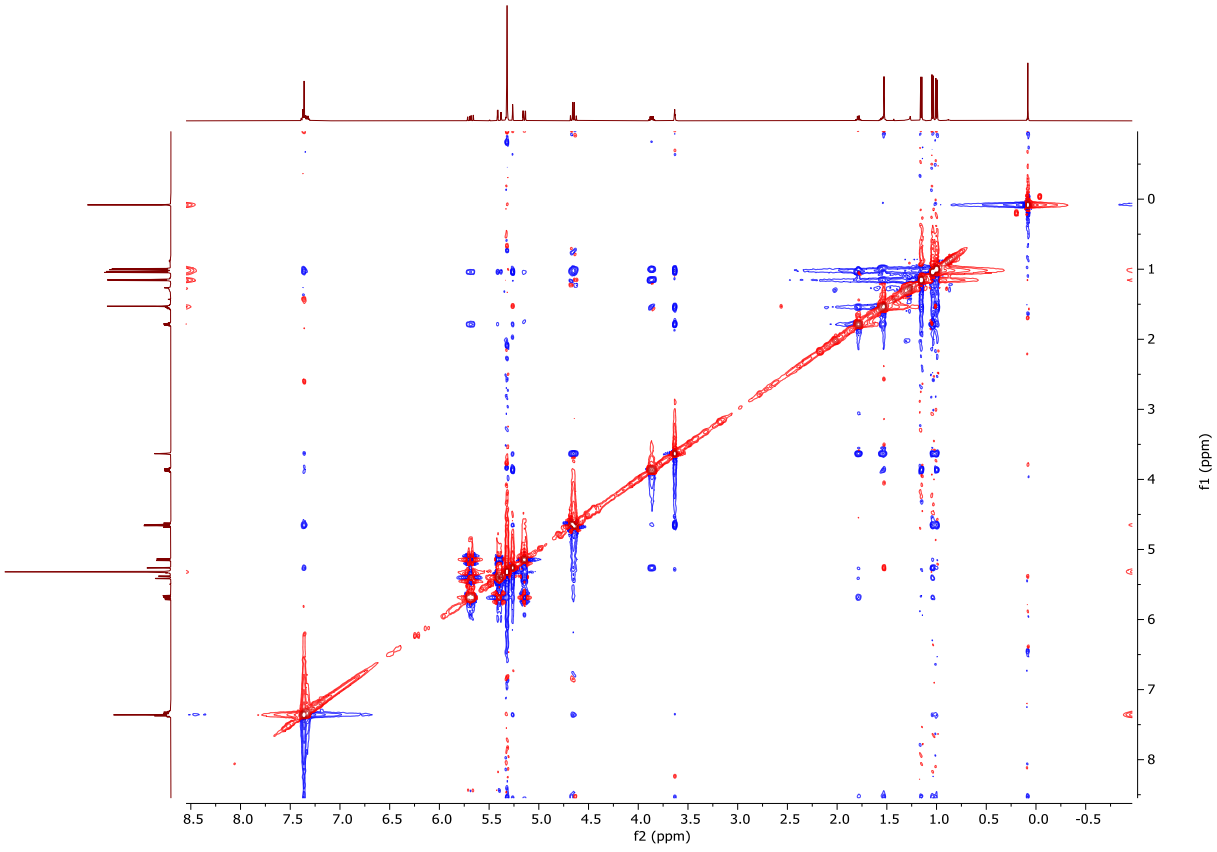

^{1}H, ^{1}H -NOESY spectrum of **107** (500 MHz, CD_2Cl_2)

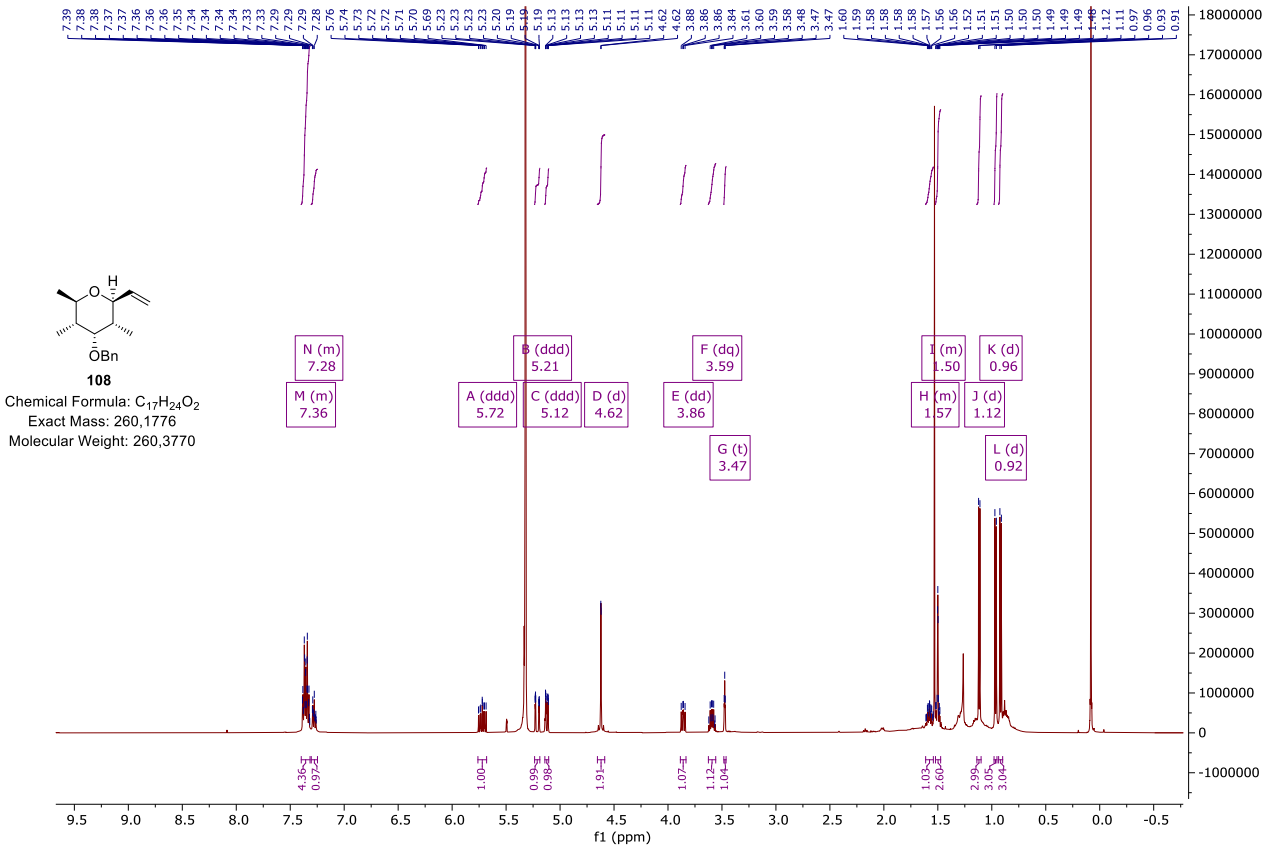

108
Chemical Formula: $C_{17}H_{24}O_2$
Exact Mass: 260,1776
Molecular Weight: 260,3770

^{1}H-NMR spectrum of **108** (500 MHz, CD_2Cl_2)

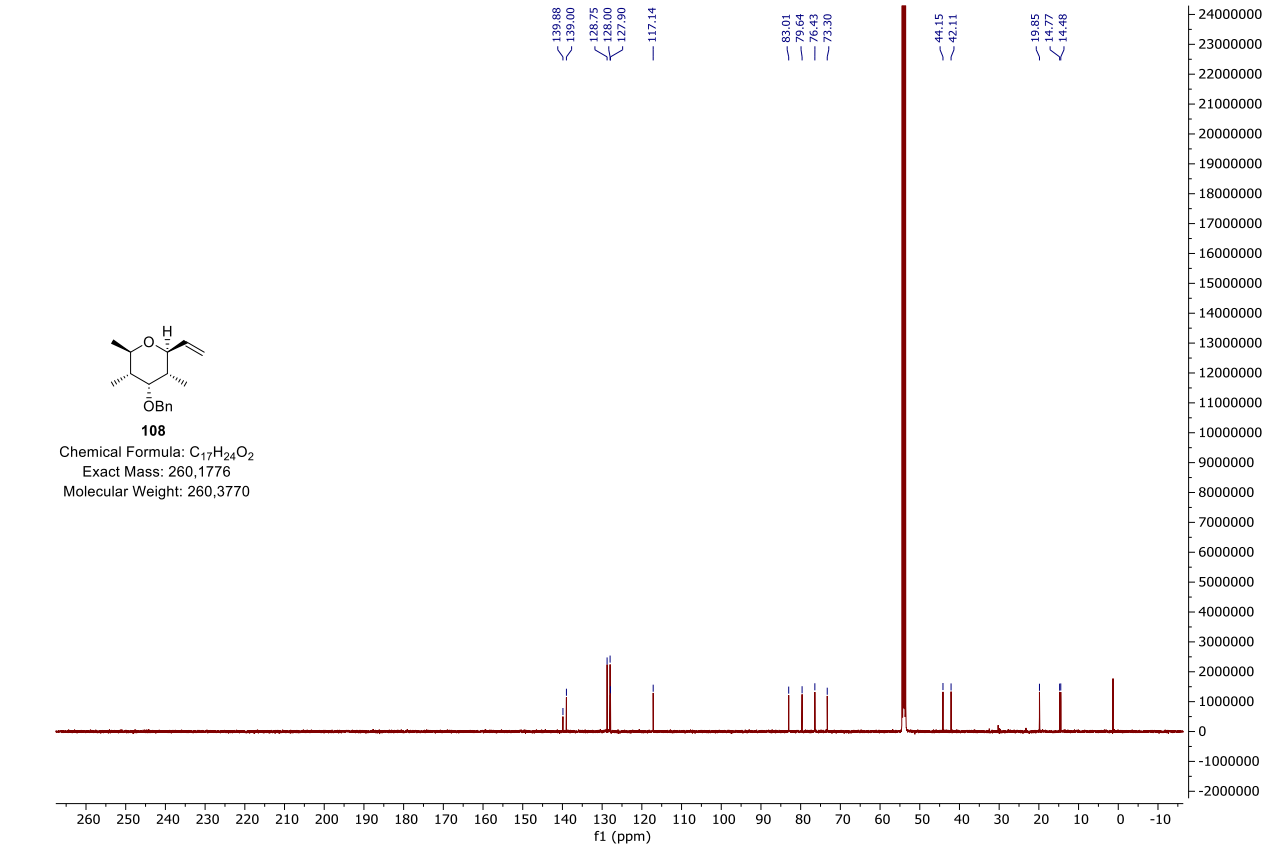

108
Chemical Formula: $C_{17}H_{24}O_2$
Exact Mass: 260,1776
Molecular Weight: 260,3770

^{13}C-NMR spectrum of **108** (125 MHz, CD_2Cl_2)

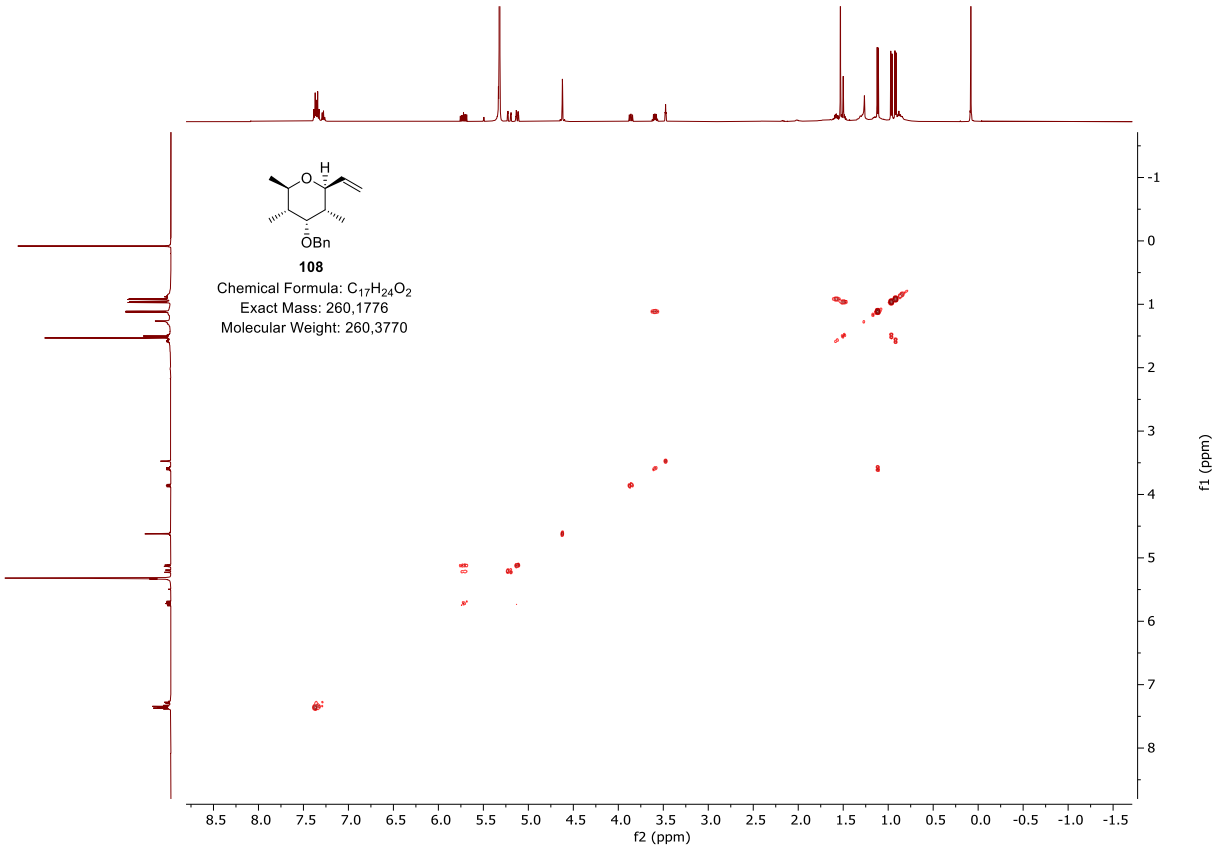

^{1}H, ^{1}H -COSY spectrum of **108** (500 MHz, CD_2Cl_2)

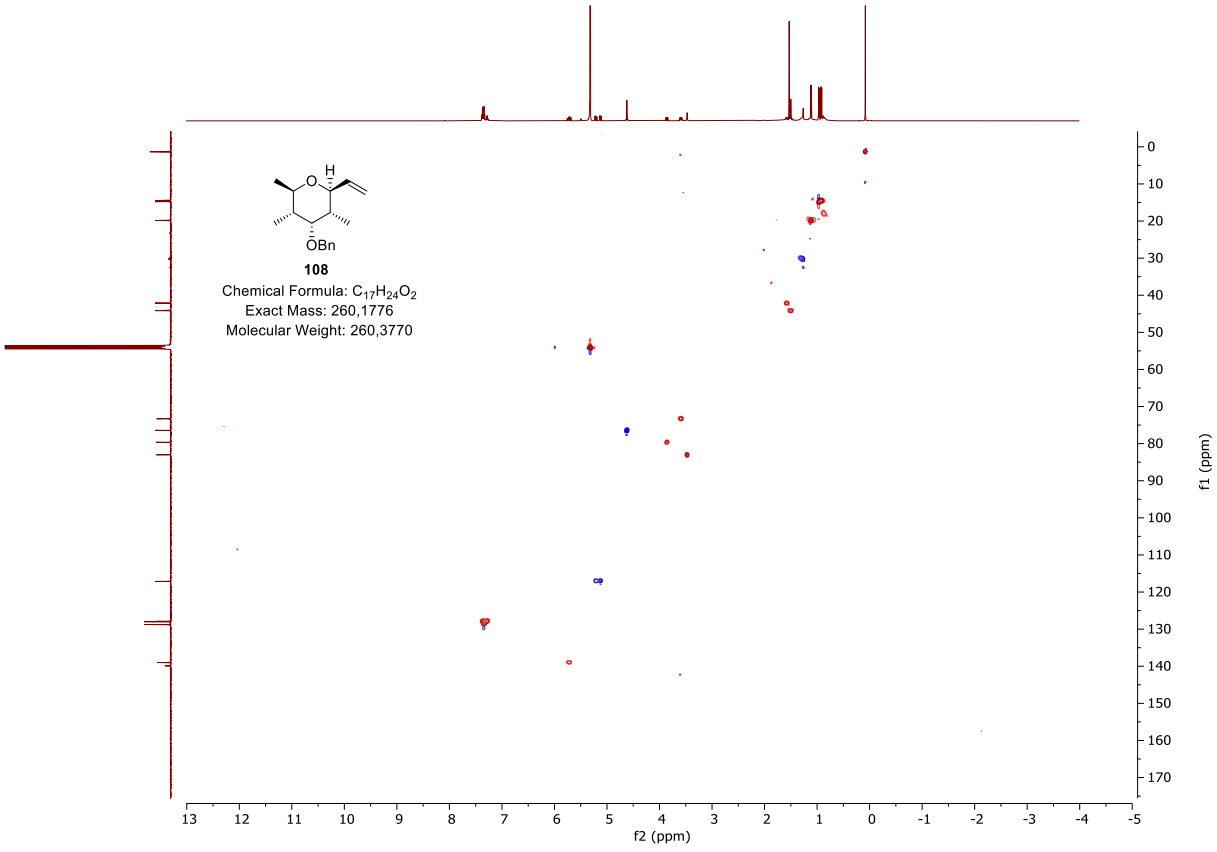

^{1}H, ^{13}C-HSQC spectrum of **108** (500 MHz, 125 MHz, CD_2Cl_2)

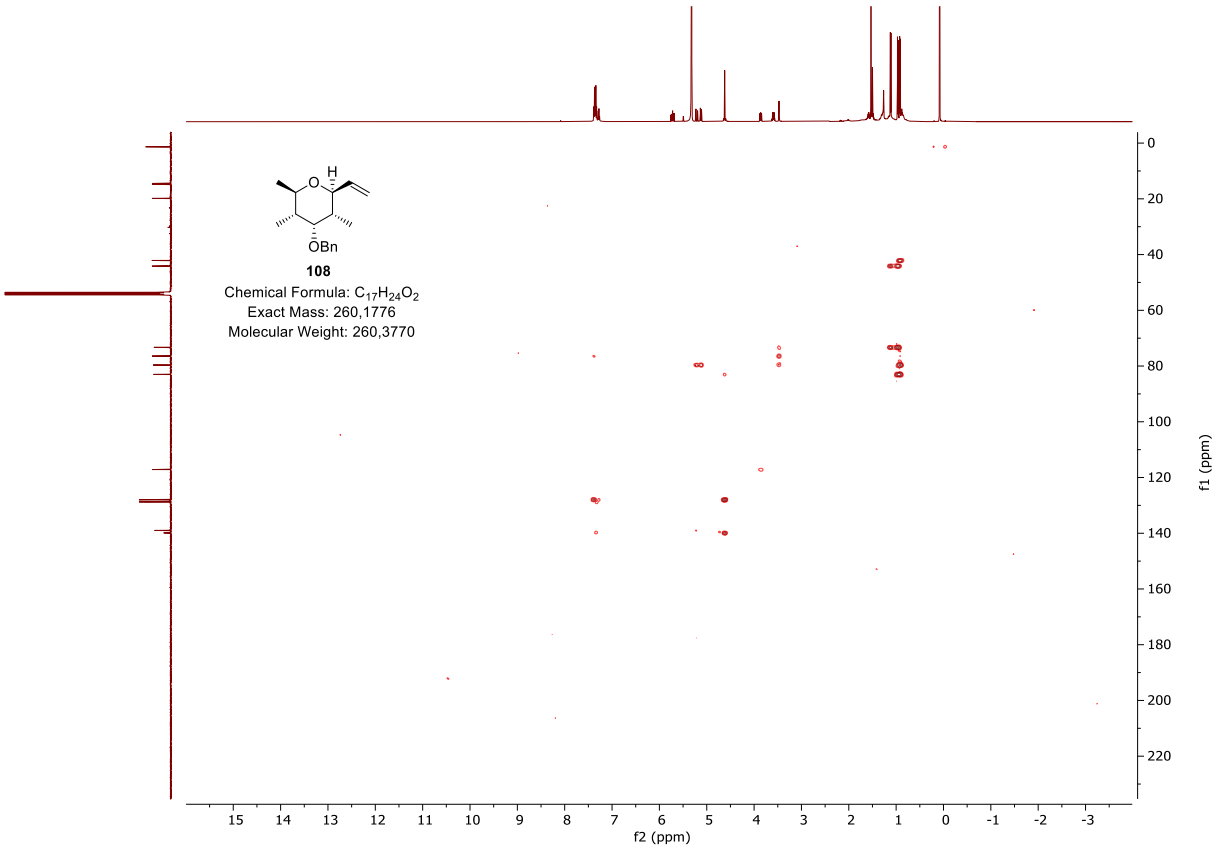

^{1}H, ^{13}C-HMBC spectrum of **108** (500 MHz, 125 MHz, CD_2Cl_2)

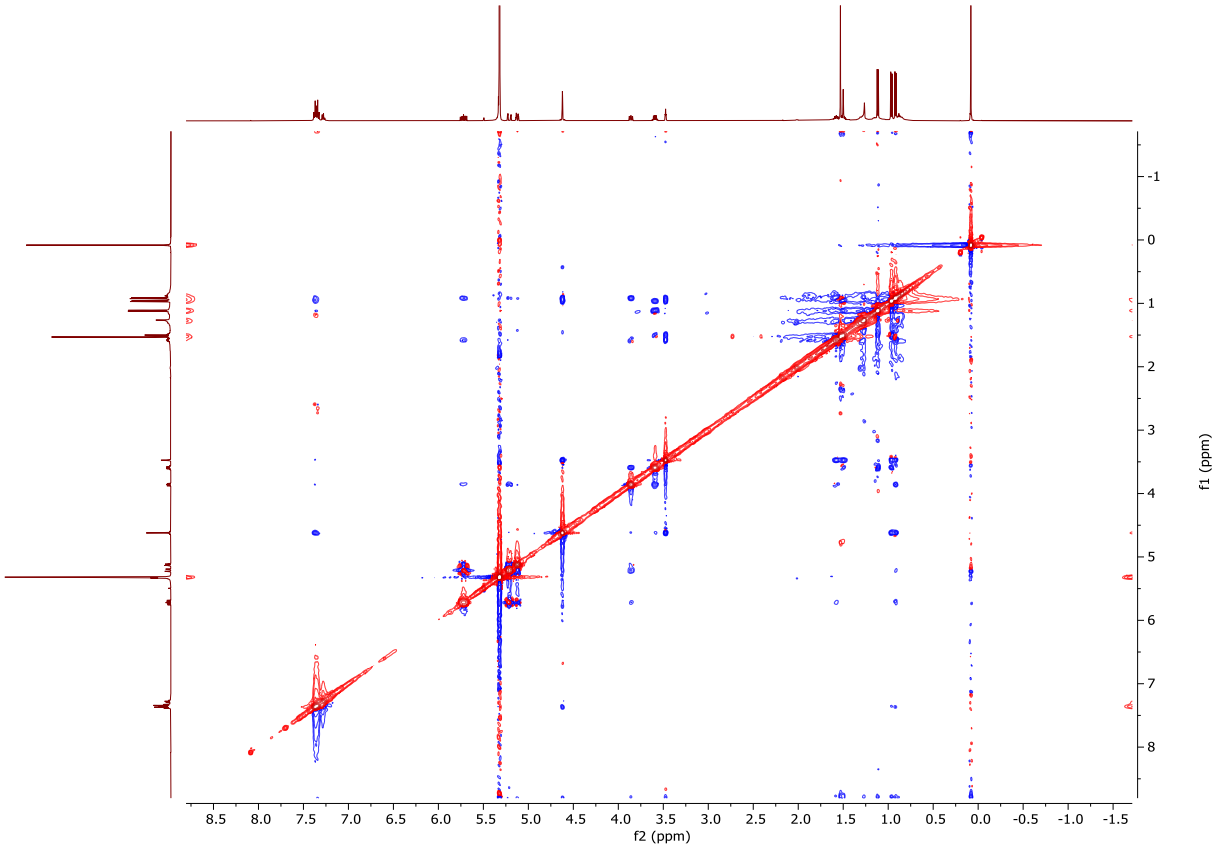

^{1}H, ^{1}H -NOESY spectrum of **108** (500 MHz, CD_2Cl_2)

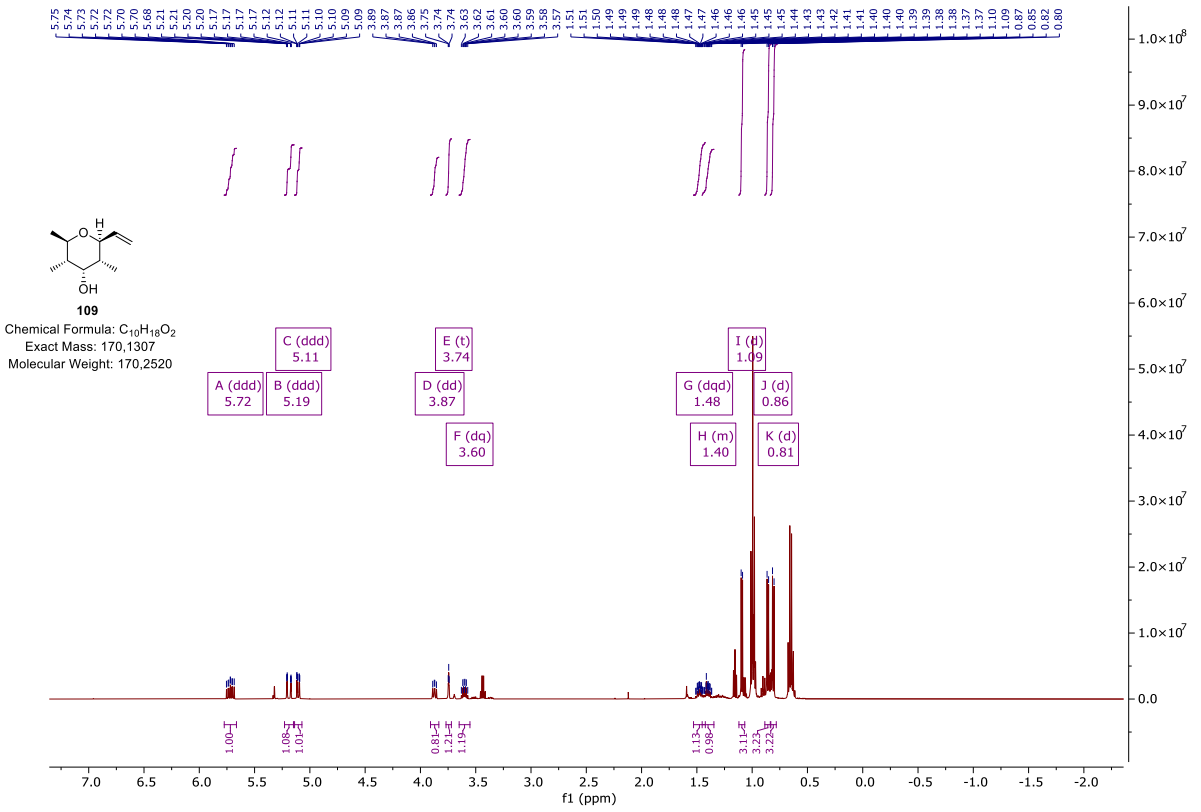

^{1}H-NMR spectrum of **109** (500 MHz, CD_2Cl_2).

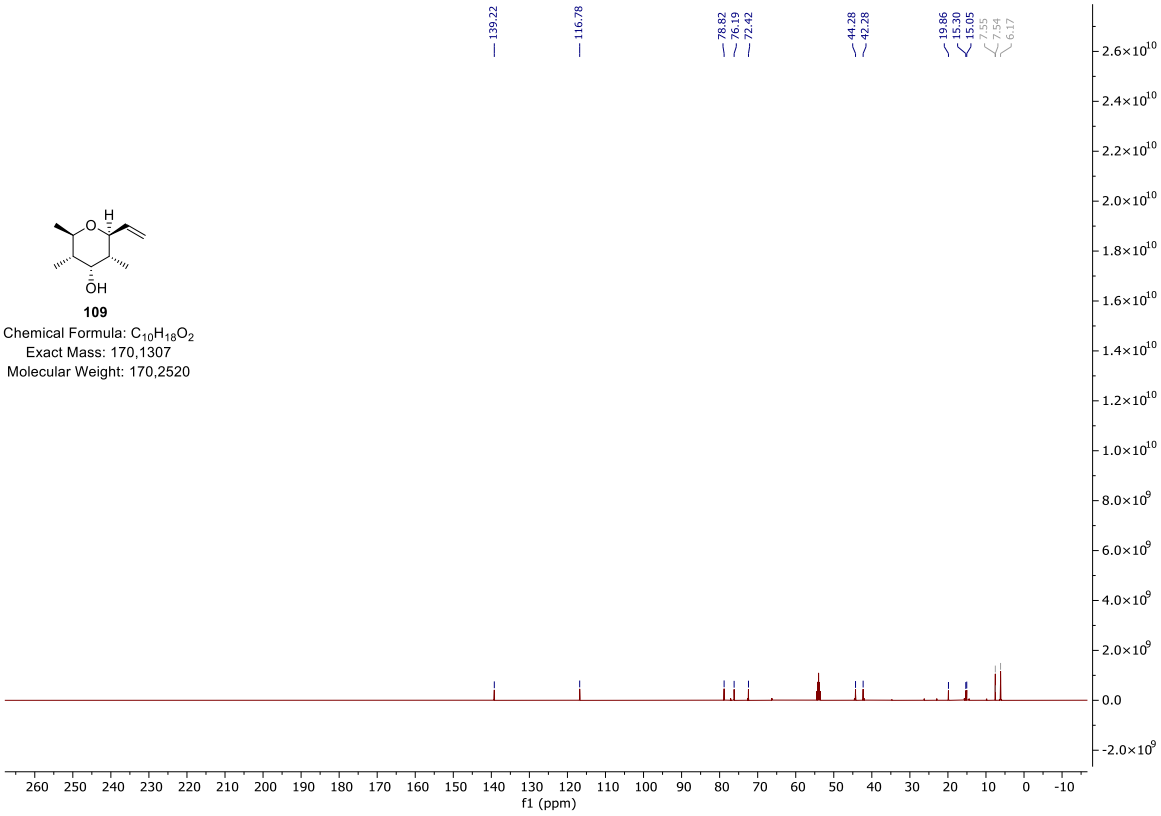

^{13}C-NMR spectrum of **109** (125 MHz, CD_2Cl_2).

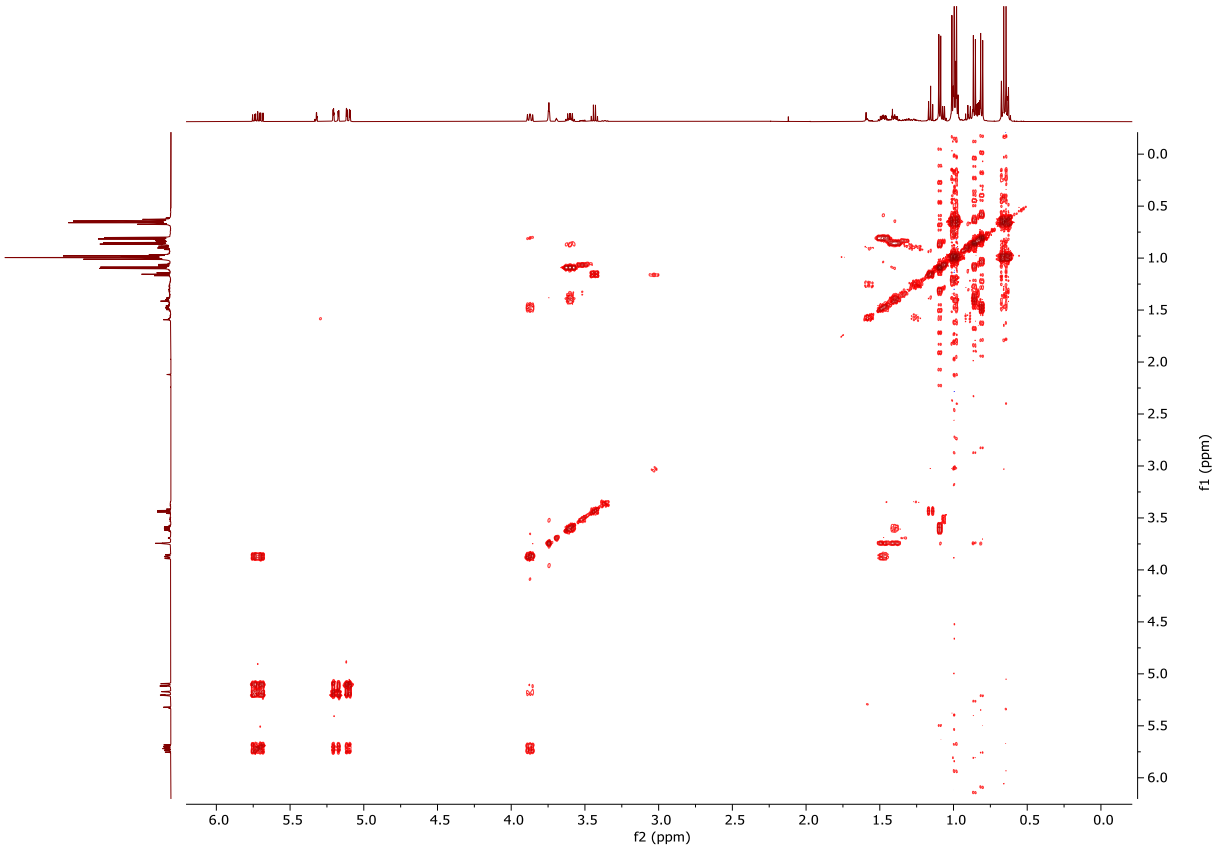

^{1}H, ^{1}H-COSY spectrum of **109** (500 MHz, CD_2Cl_2).

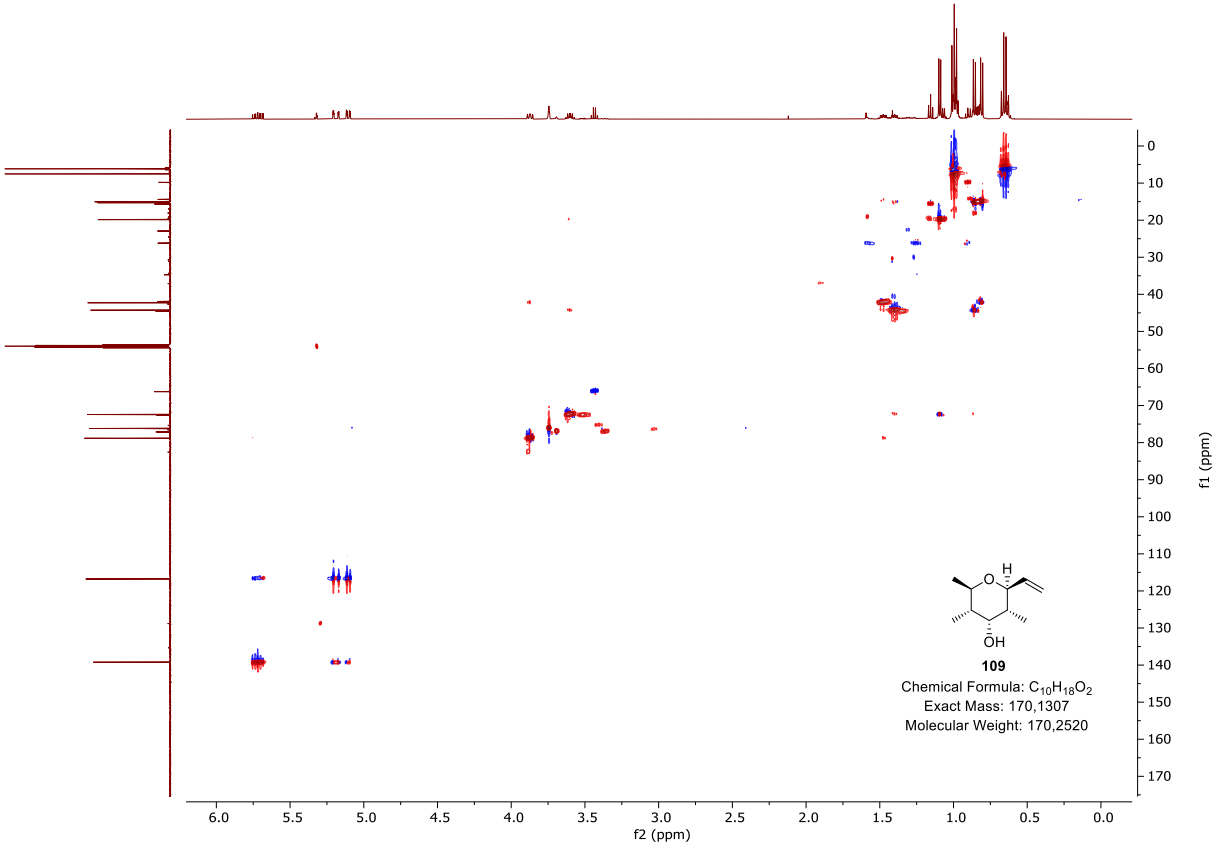

^{1}H, ^{13}C-HSQC spectrum of **109** (500 MHz, 125 MHz, CD_2Cl_2).

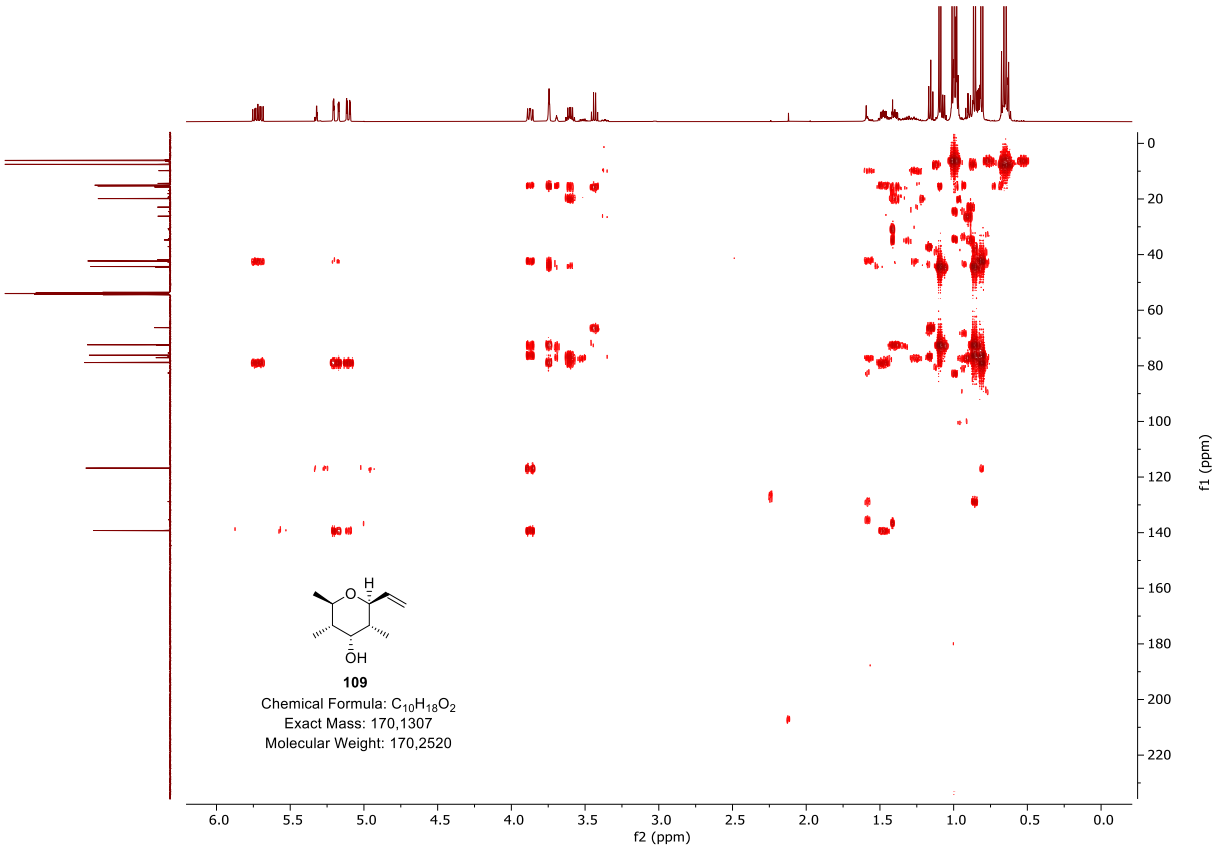

^{1}H, ^{13}C-HMBC spectrum of **109** (500 MHz, 125 MHz, CD_2Cl_2).

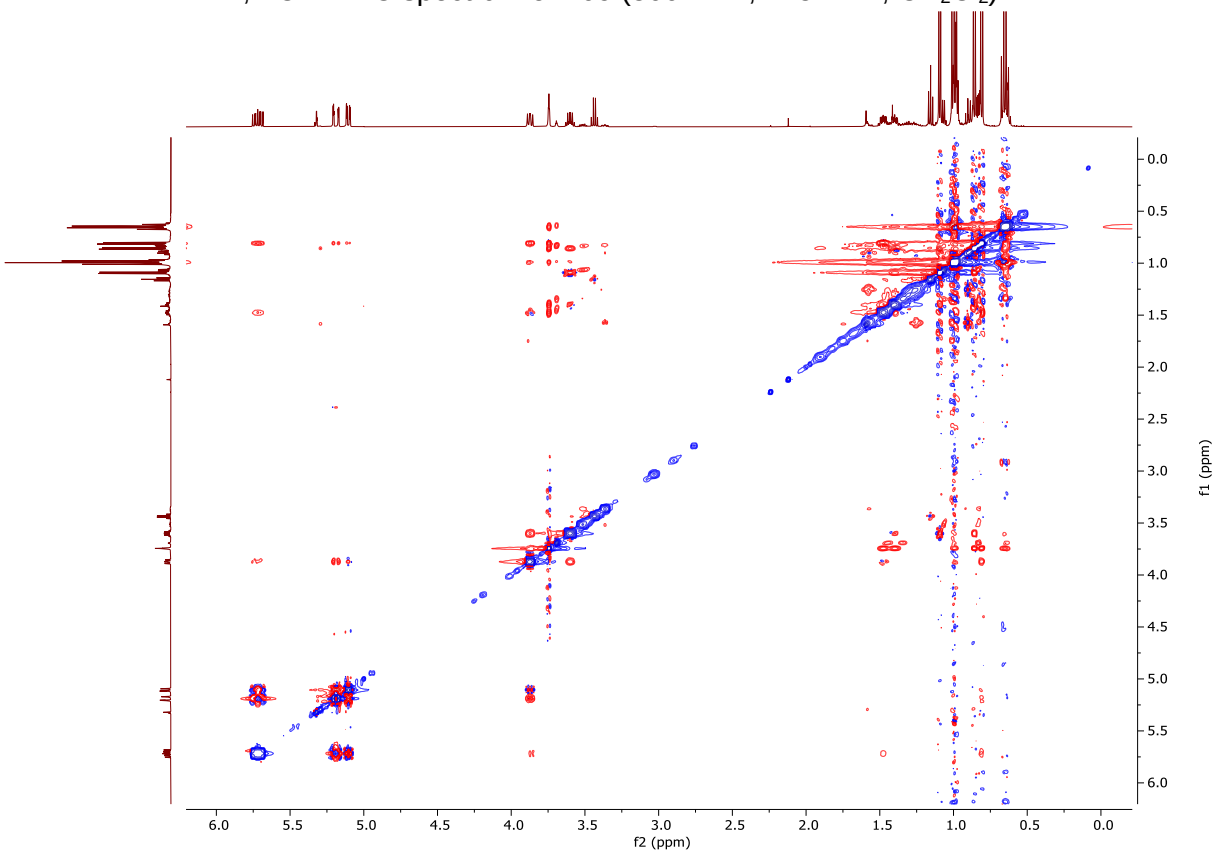

^{1}H, ^{1}H-NOESY spectrum of **109** (500 MHz, CD_2Cl_2).

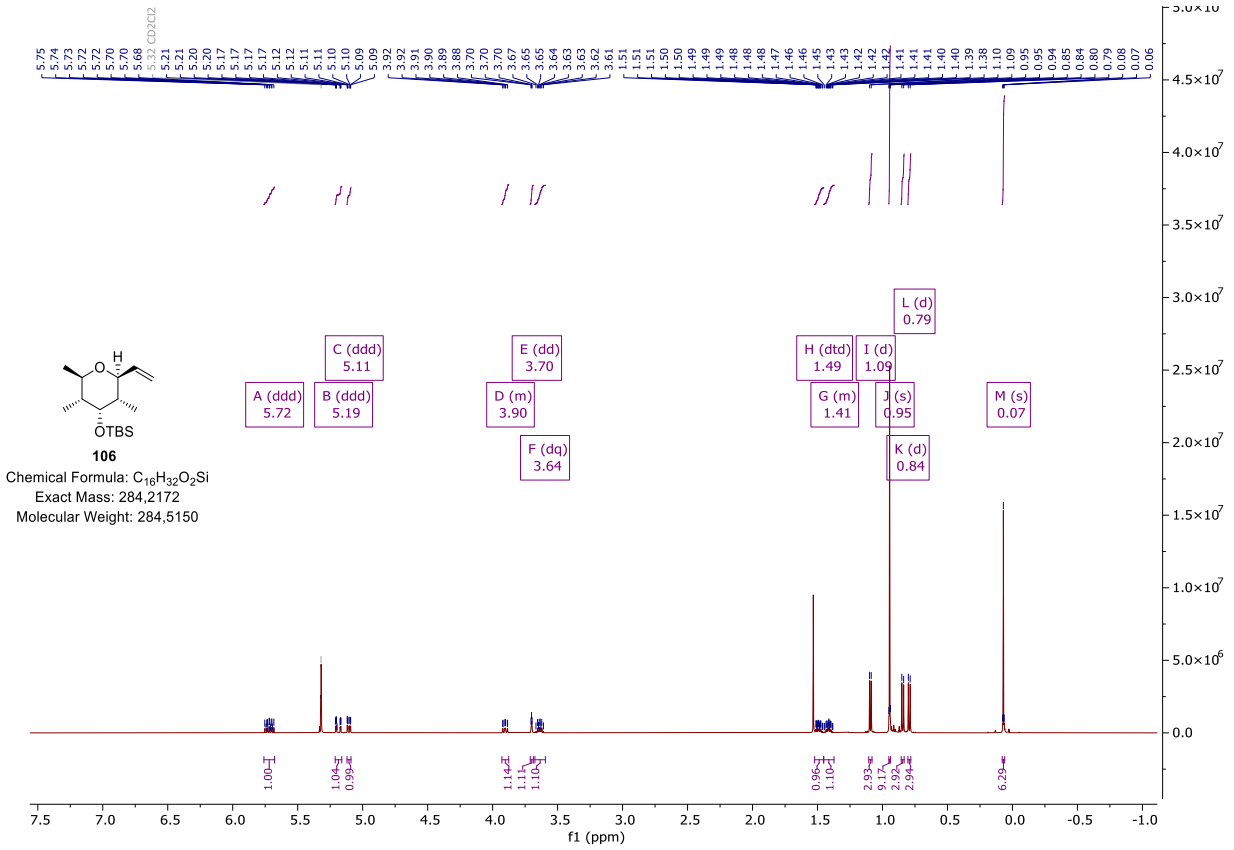

^{1}H-NMR spectrum of **106** (500 MHz, CD_2Cl_2).

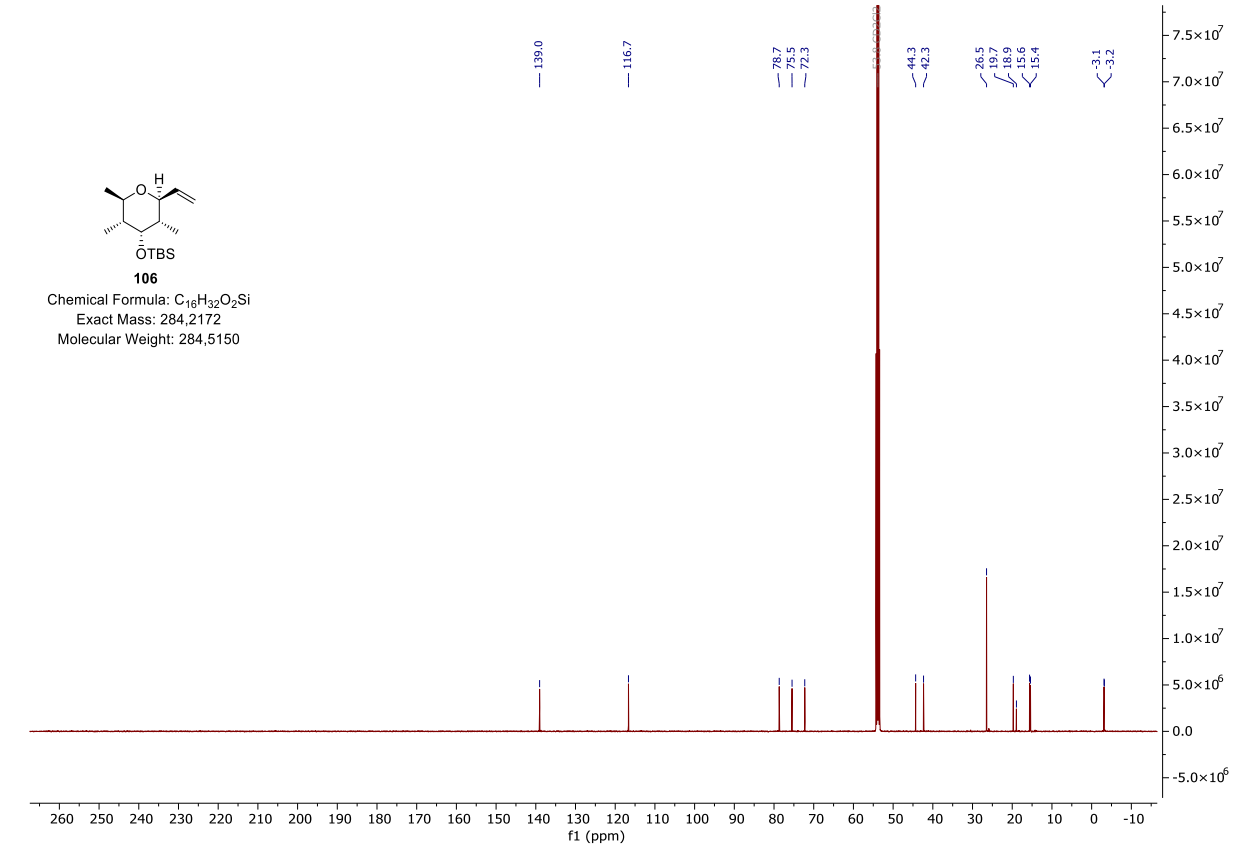

^{13}C-NMR spectrum of **106** (125 MHz, CD_2Cl_2).

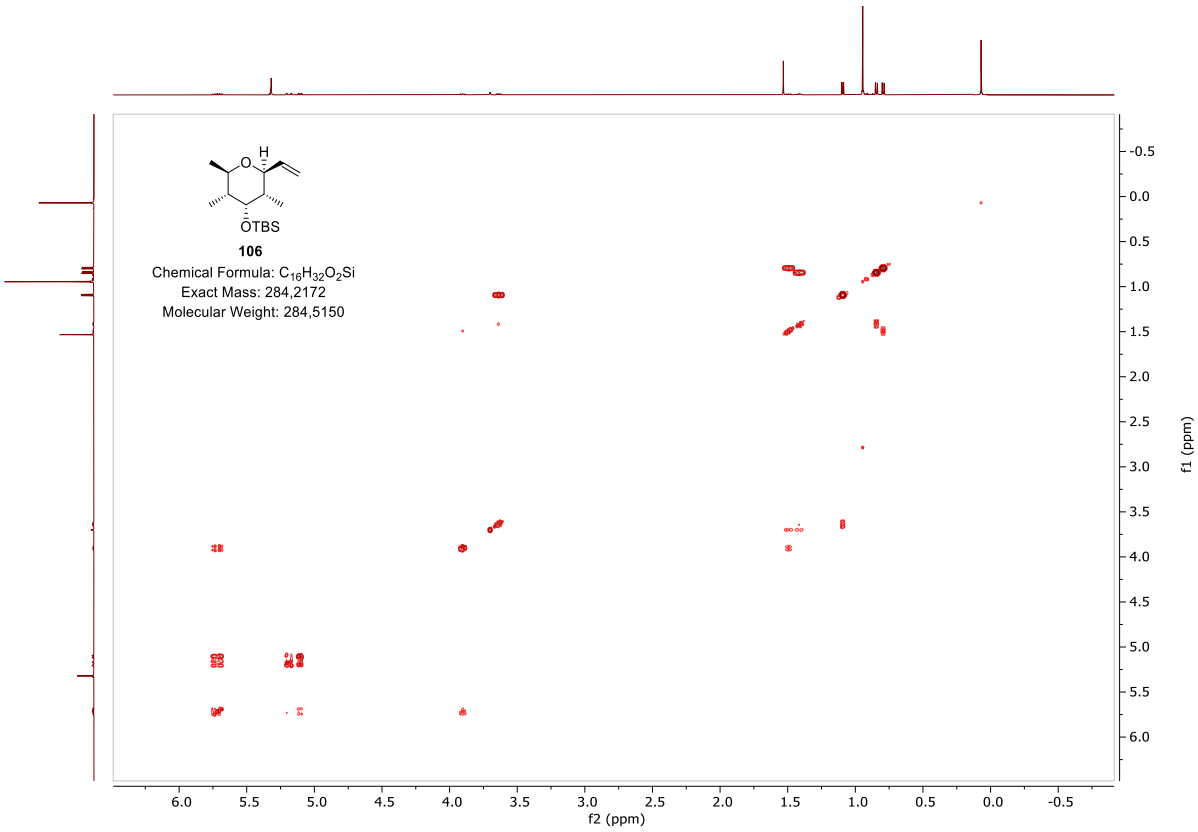

^{1}H, ^{1}H -COSY spectrum of **106** (500 MHz, CD_2Cl_2).

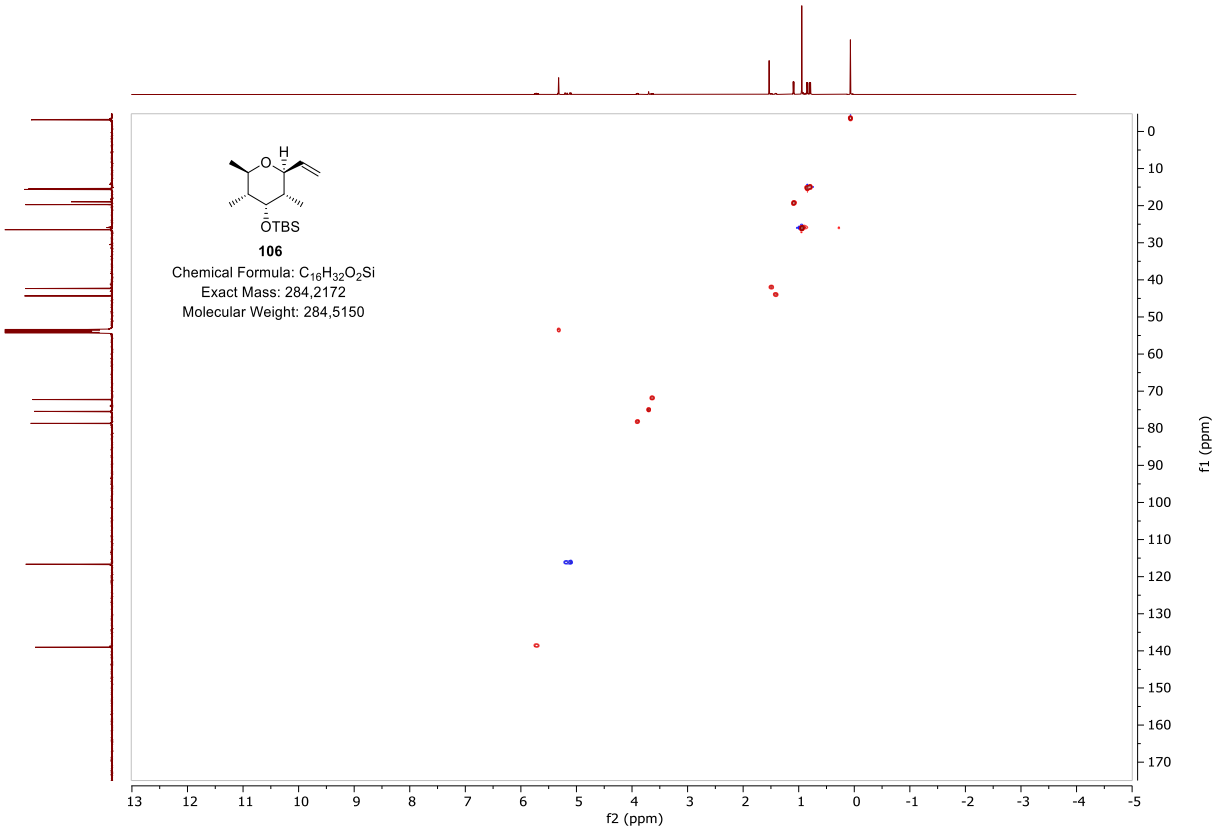

^{1}H, ^{13}C-HSQC spectrum of **109** (500 MHz, 125 MHz, CD_2Cl_2).

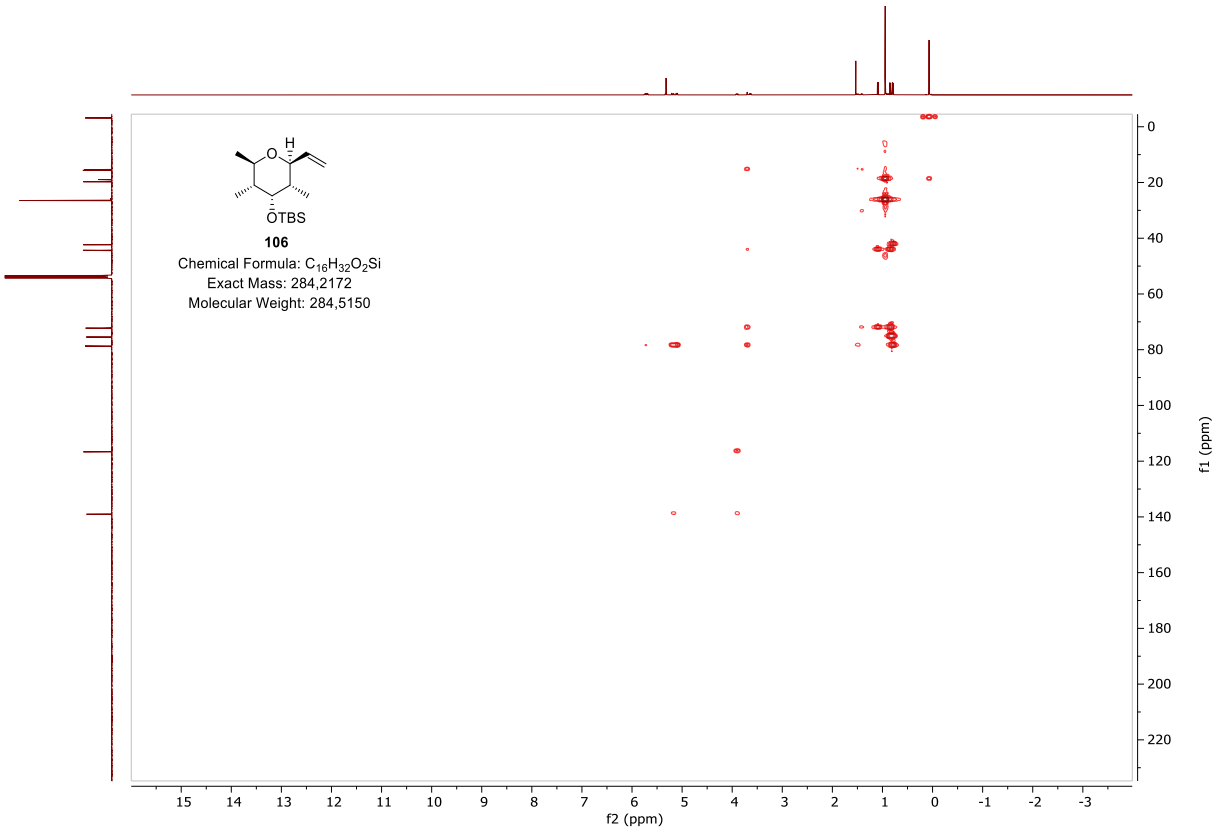

^{1}H, ^{13}C-HMBC spectrum of **106** (500 MHz, 125 MHz, CD_2Cl_2).

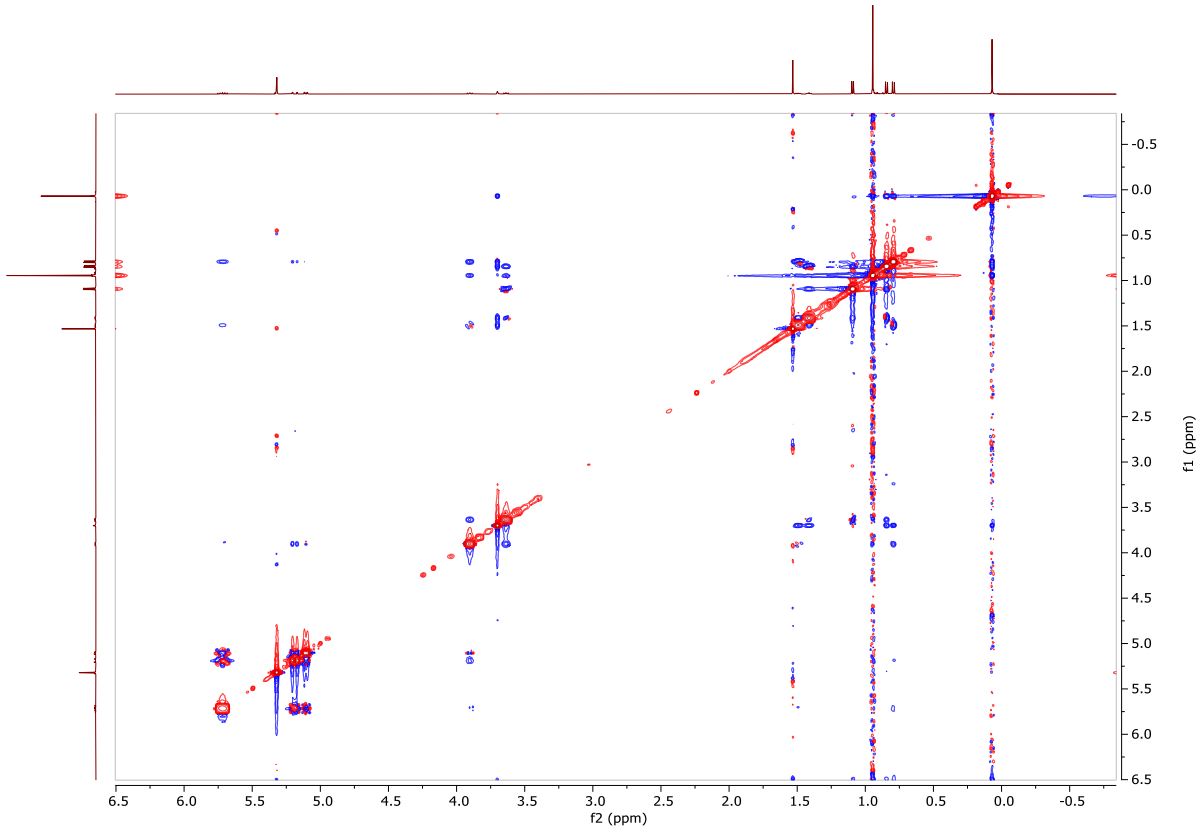

^{1}H, ^{1}H -NOESY spectrum of **106** (500 MHz, CD_2Cl_2).

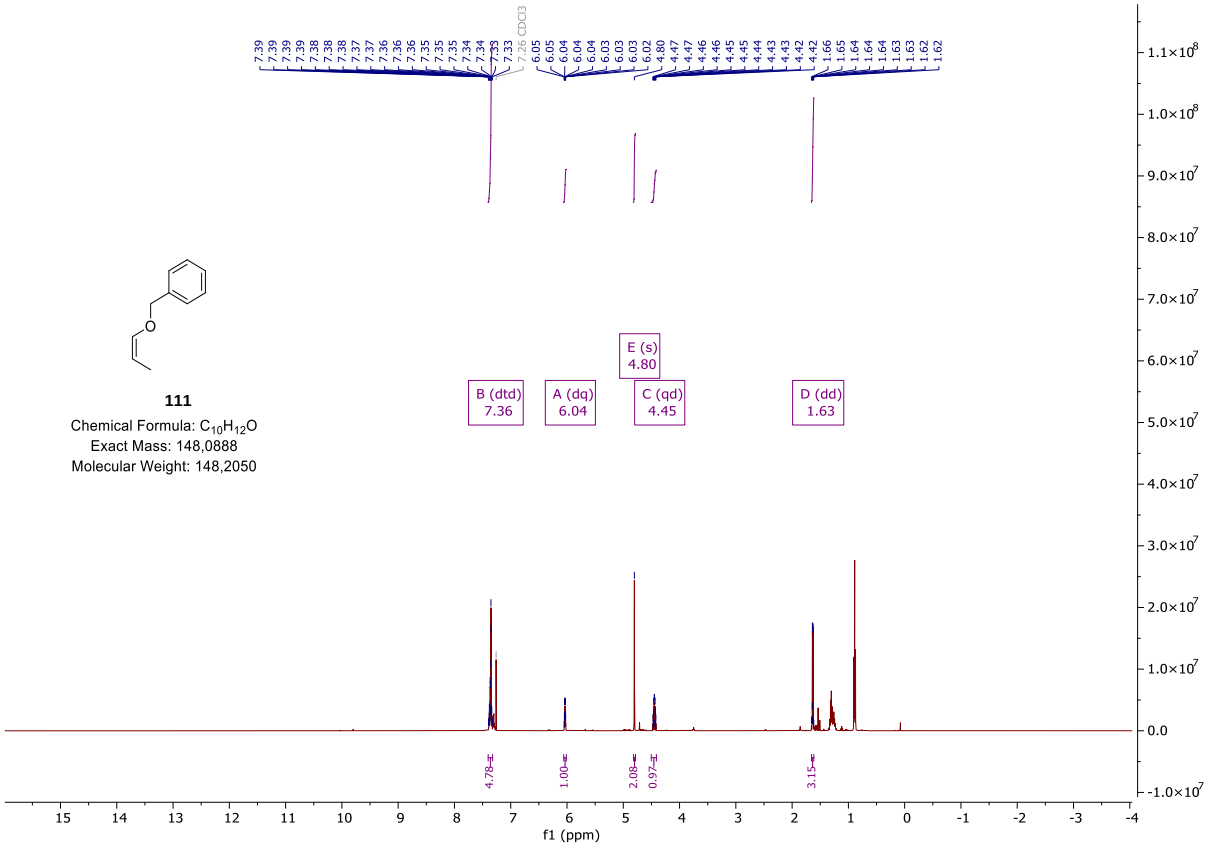

^{1}H-NMR spectrum of **111** (500 MHz, $CDCl_3$).

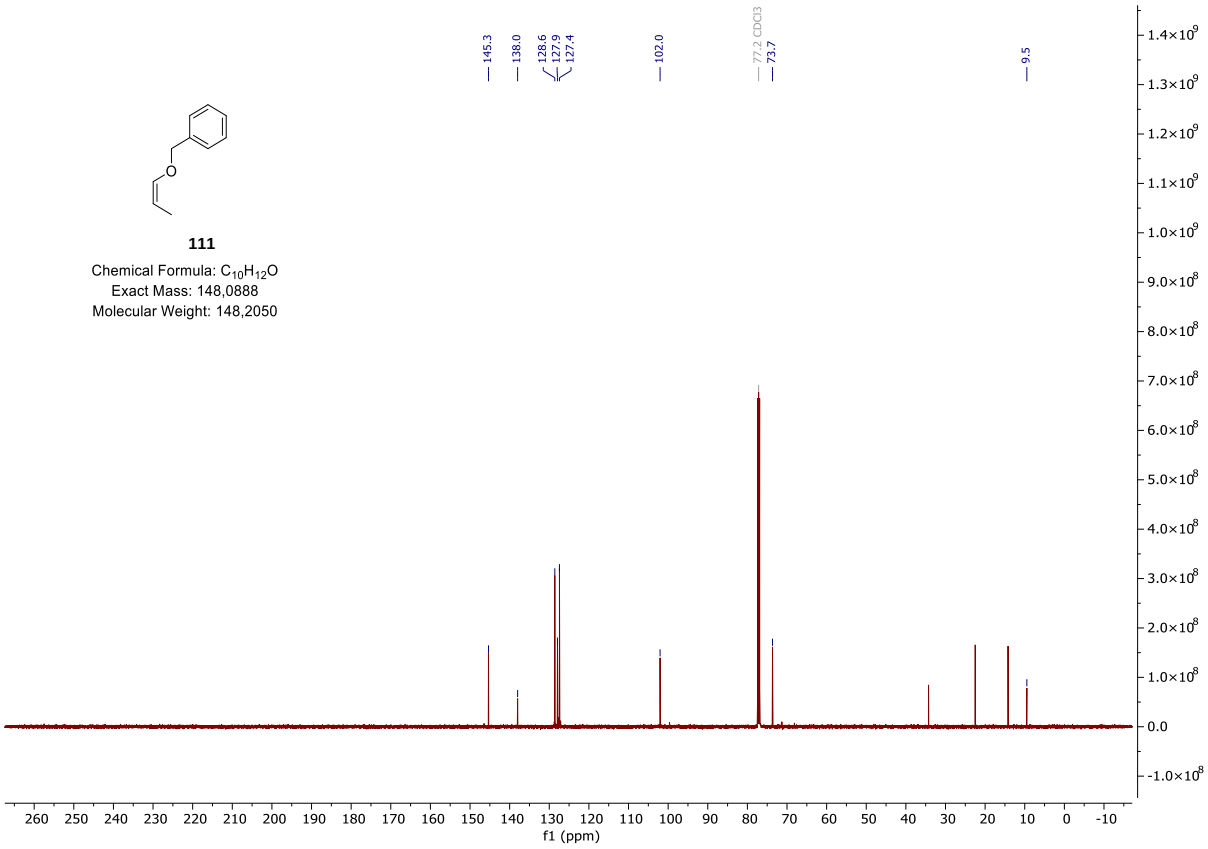

^{13}C-NMR spectrum of **111** (125 MHz, $CDCl_3$).

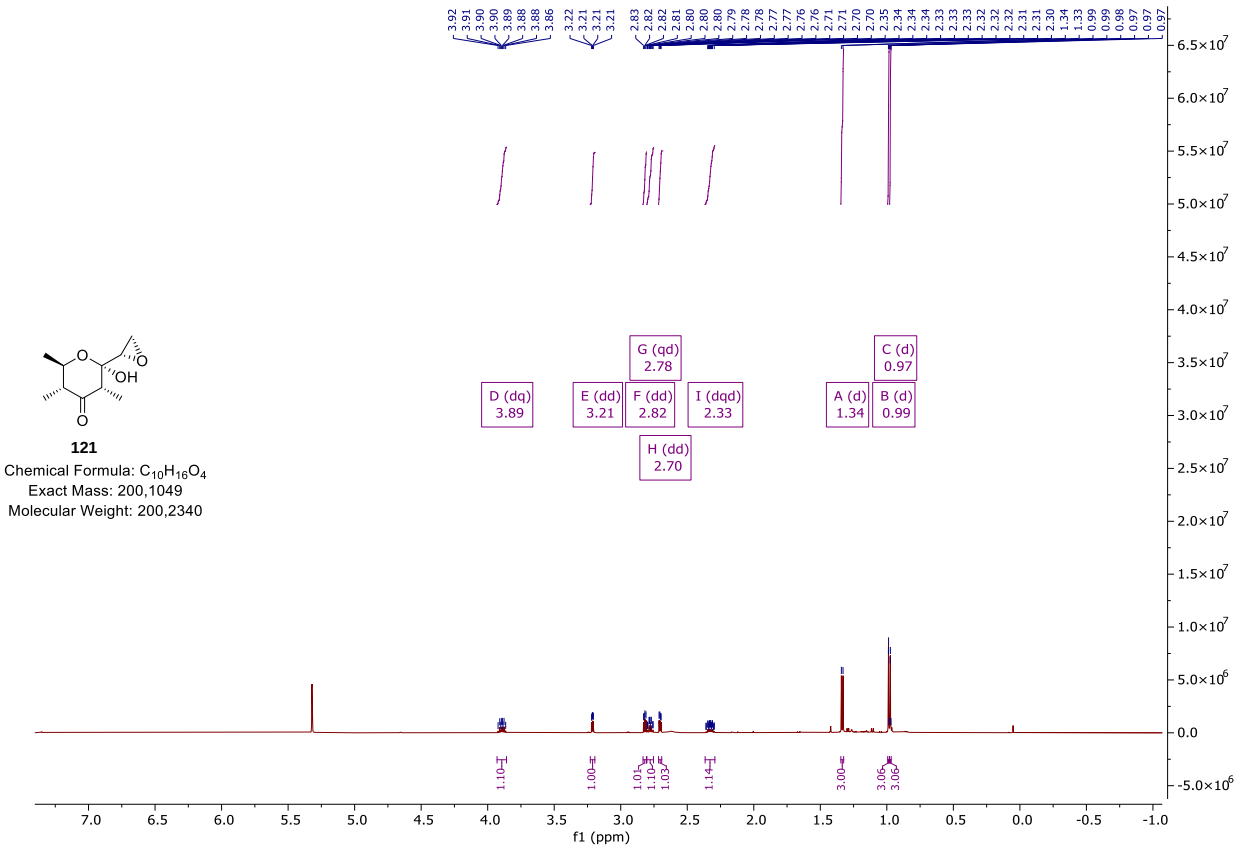

^{1}H-NMR spectrum of **121** (500 MHz, CD_2Cl_2).

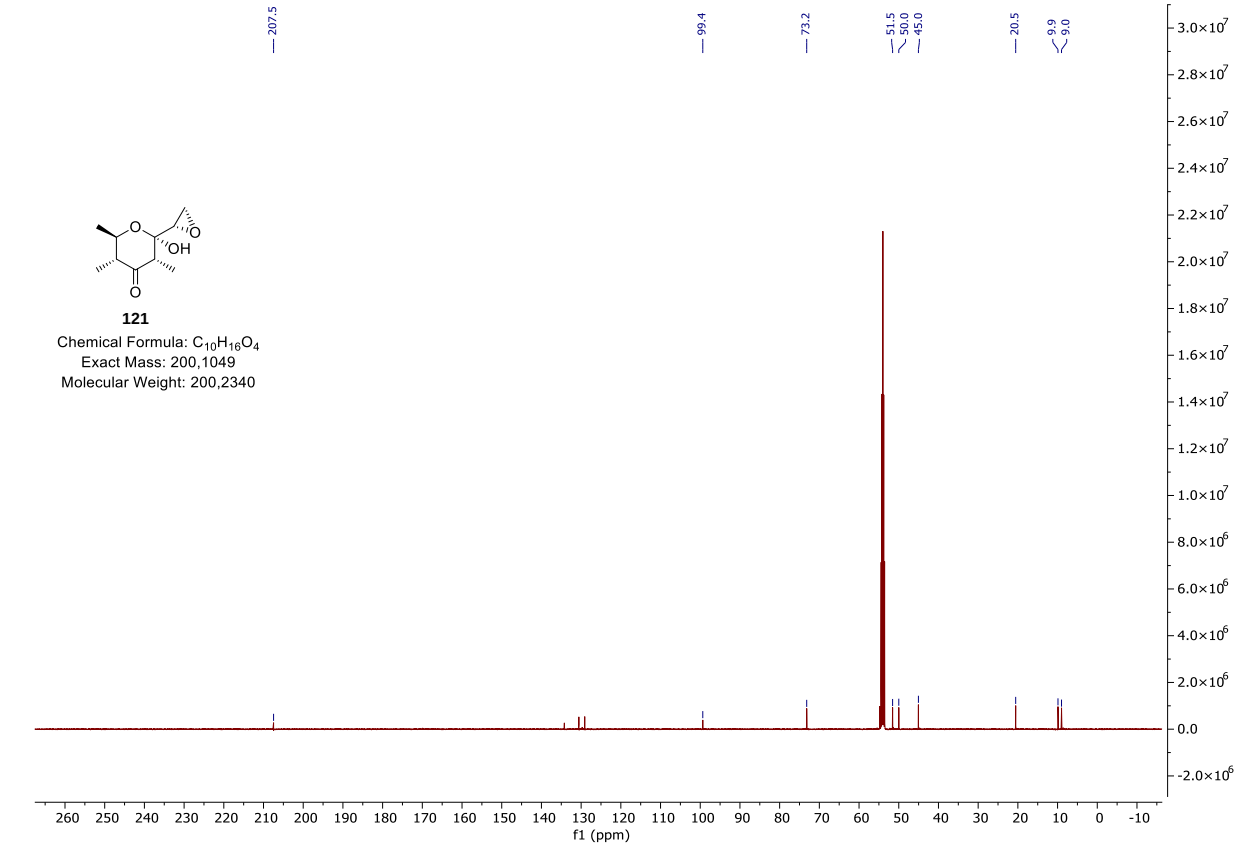

^{13}C-NMR spectrum of **121** (125 MHz, CD_2Cl_2).

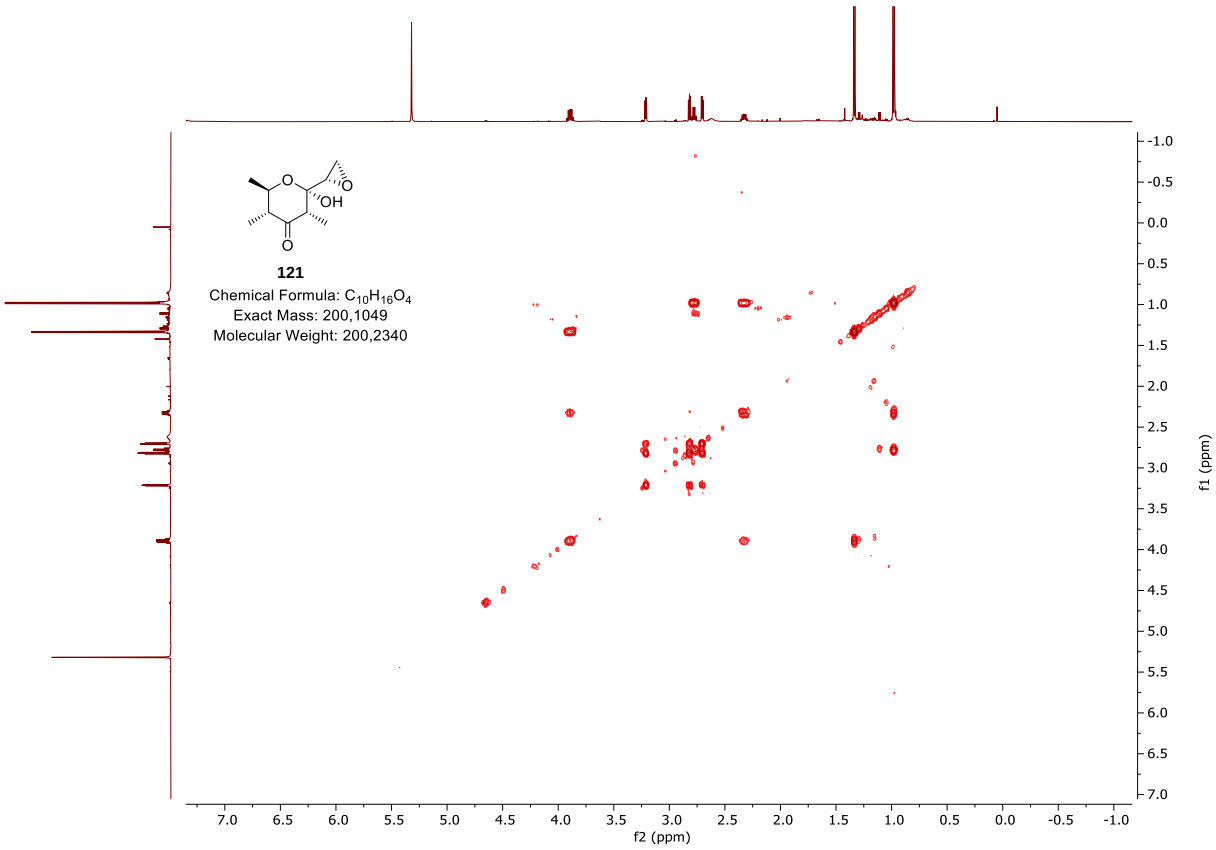

^{1}H, ^{1}H -COSY spectrum of **121** (500 MHz, CD_2Cl_2).

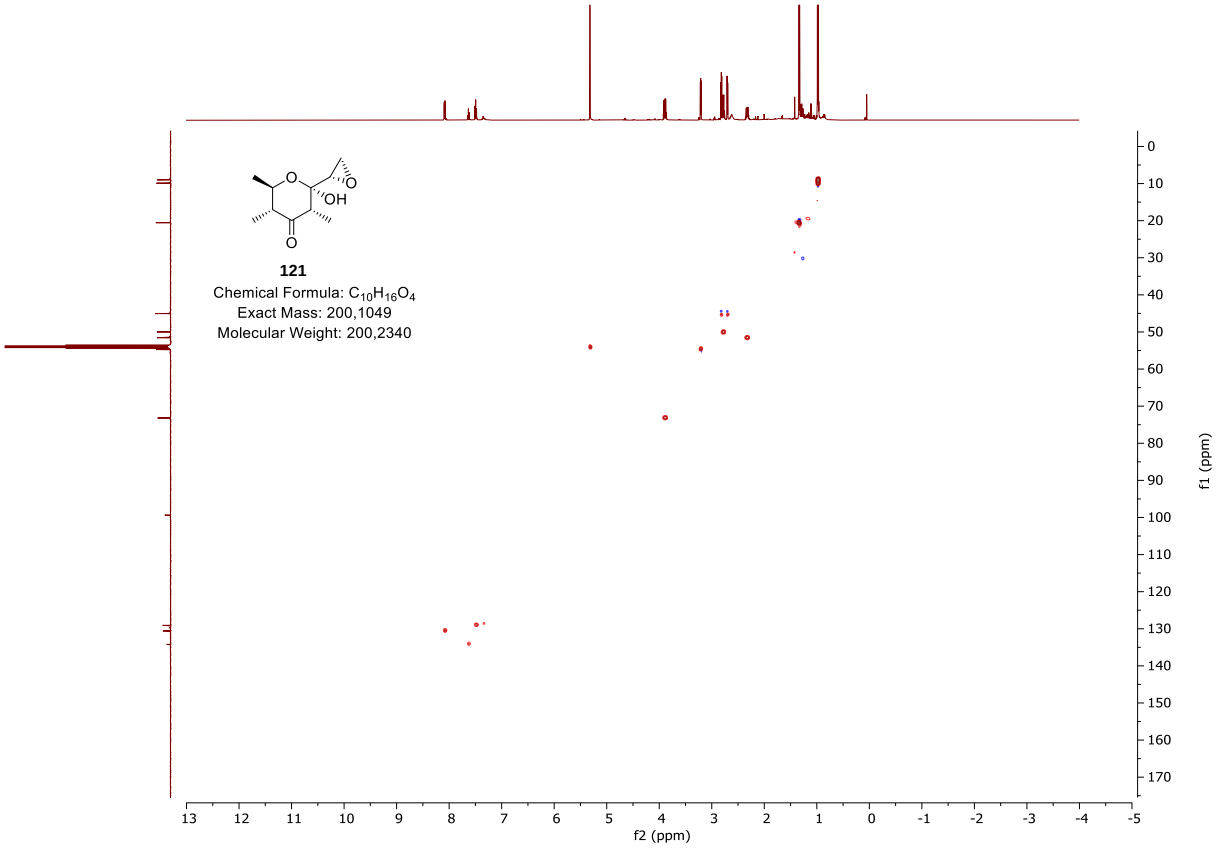

^{1}H, ^{13}C-HSQC spectrum of **121** (500 MHz, 125 MHz, CD_2Cl_2).

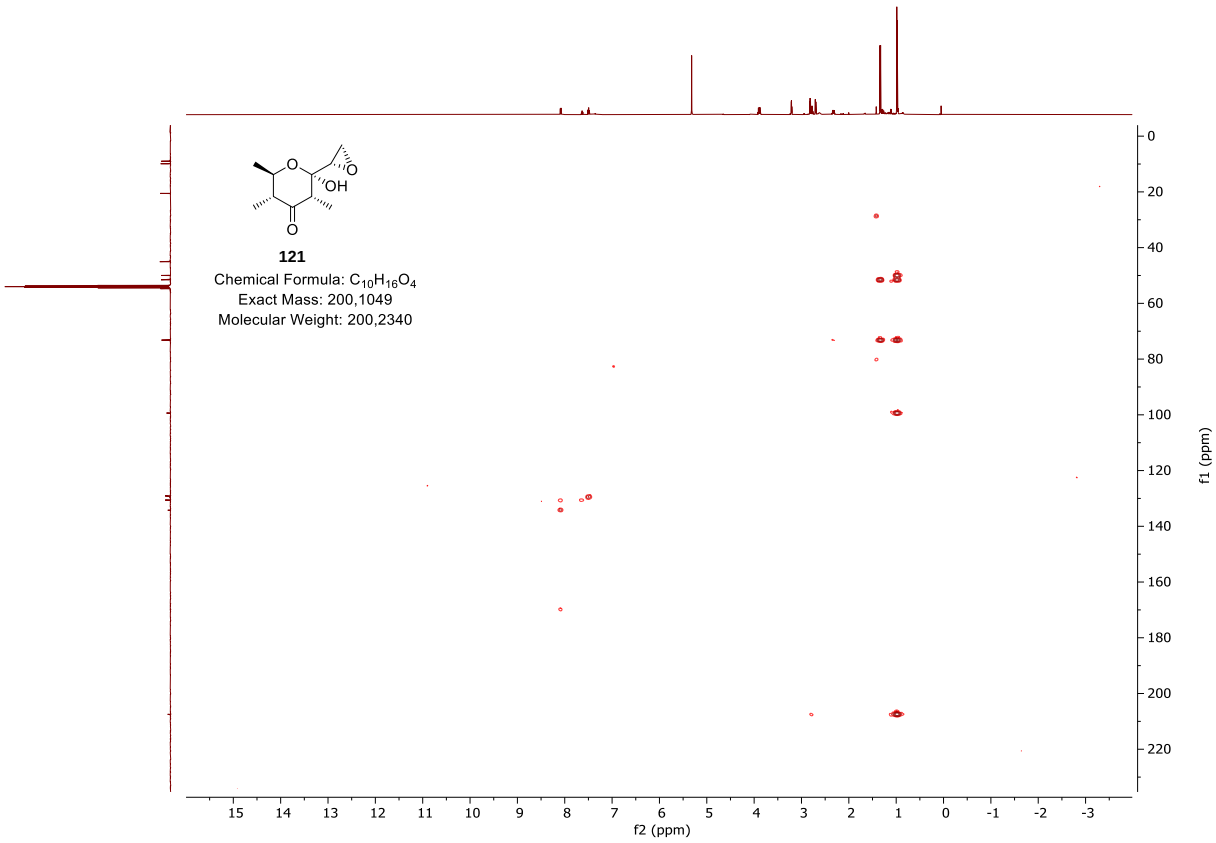

^{1}H, ^{13}C-HMBC spectrum of **121** (500 MHz, 125 MHz, CD_2Cl_2).

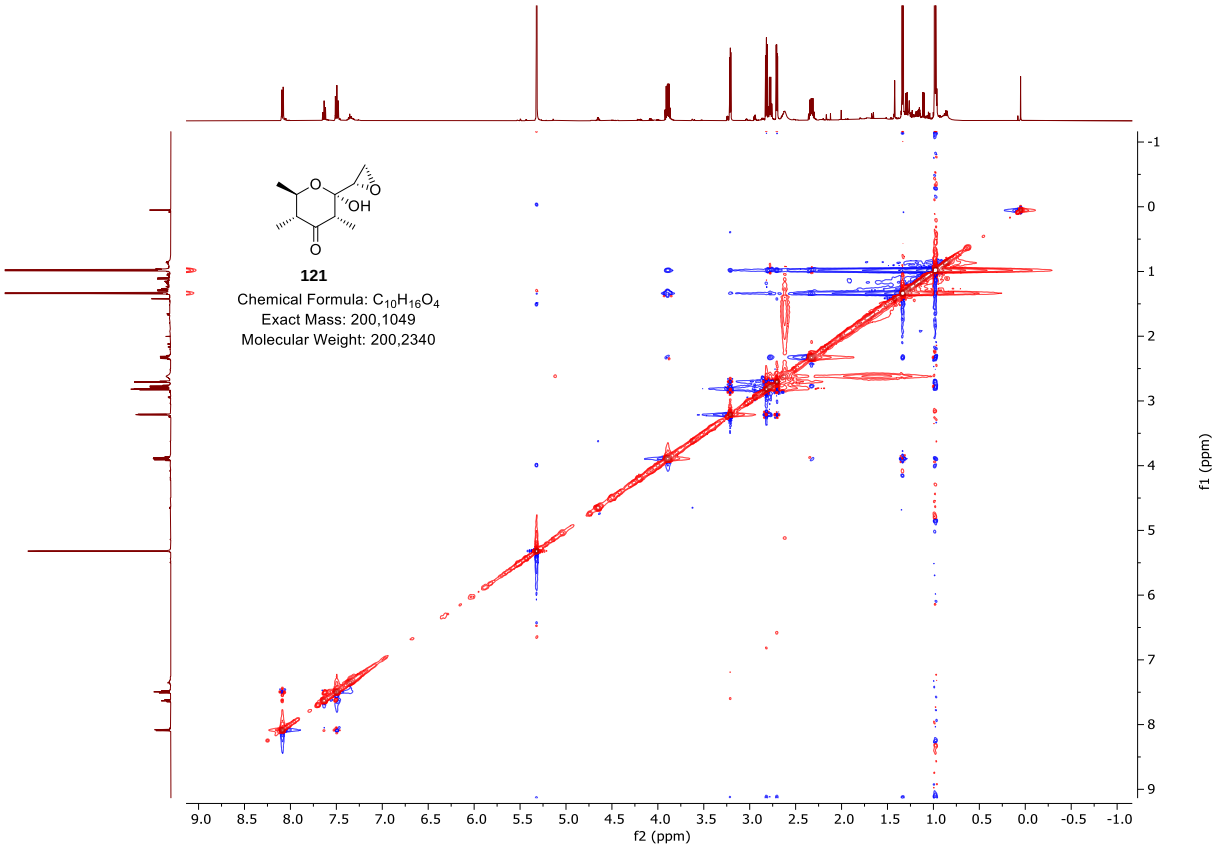

^{1}H, ^{1}H -NOESY spectrum of **121** (500 MHz, CD_2Cl_2).

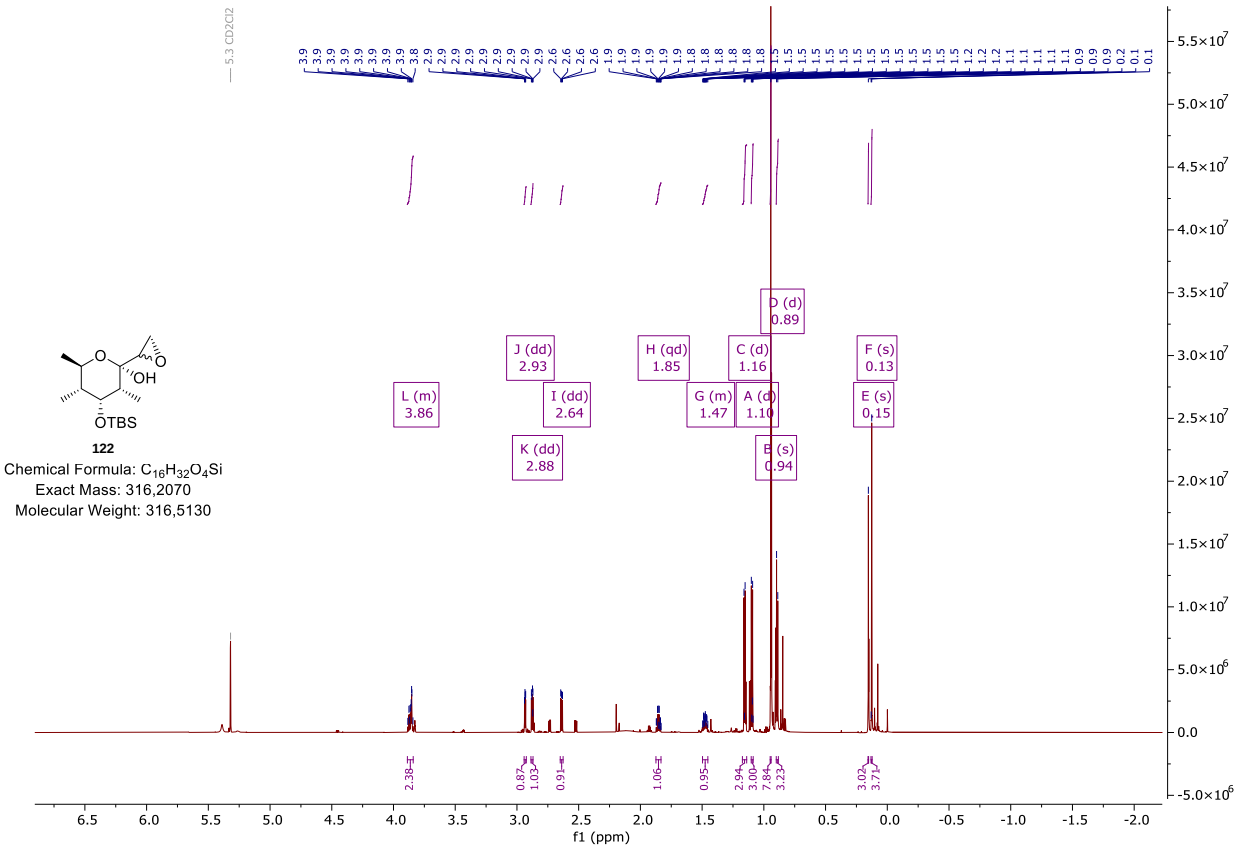

^{1}H-NMR spectrum of **122** (700 MHz, CD_2Cl_2).

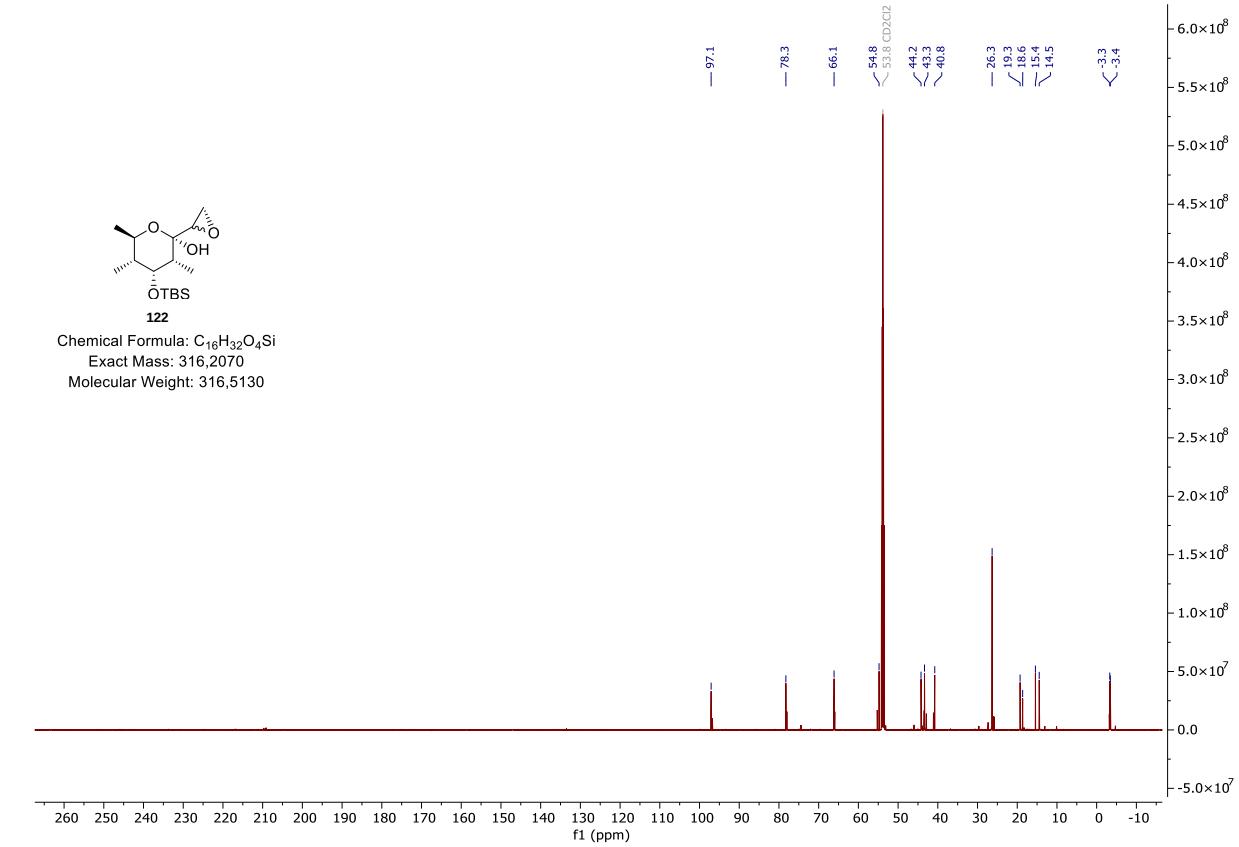

^{13}C-NMR spectrum of **122** (175 MHz, CD_2Cl_2).

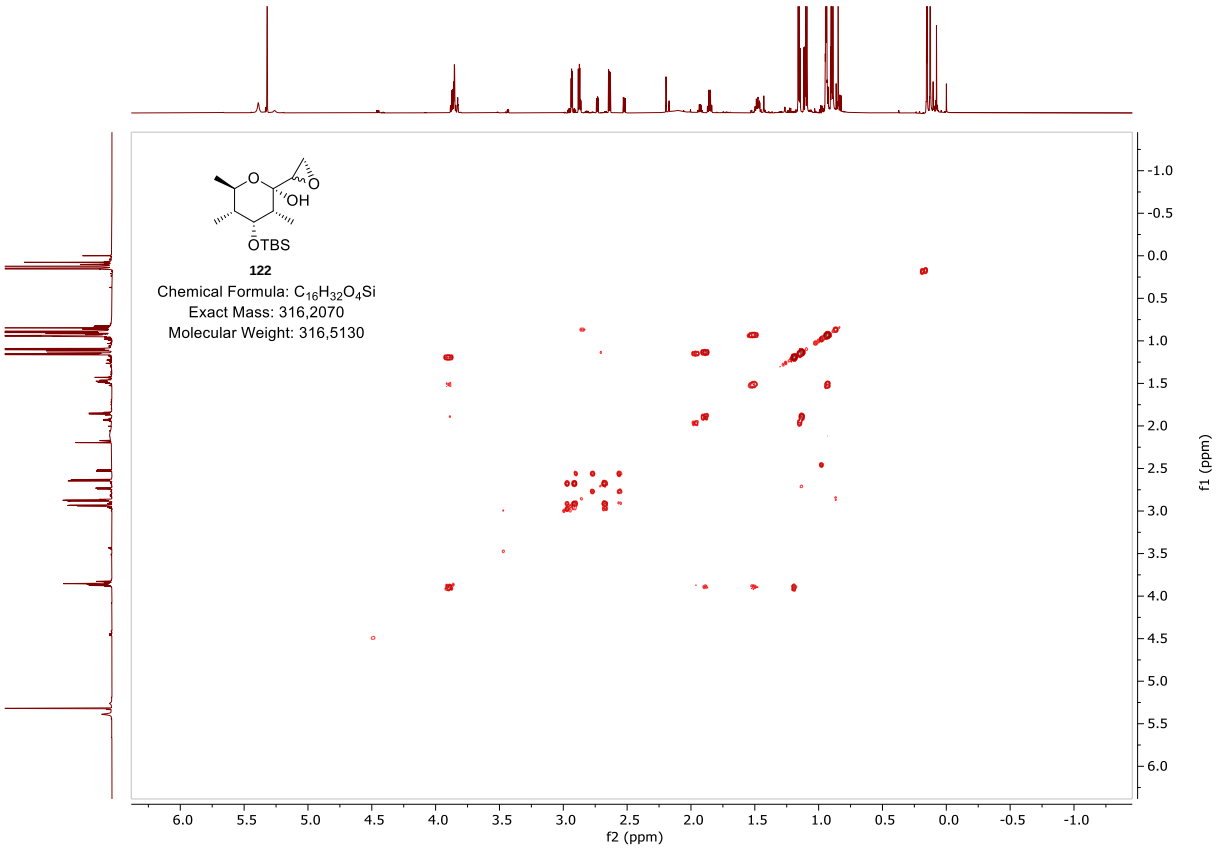

^{1}H, ^{1}H -COSY spectrum of **122** (700 MHz, CD_2Cl_2).

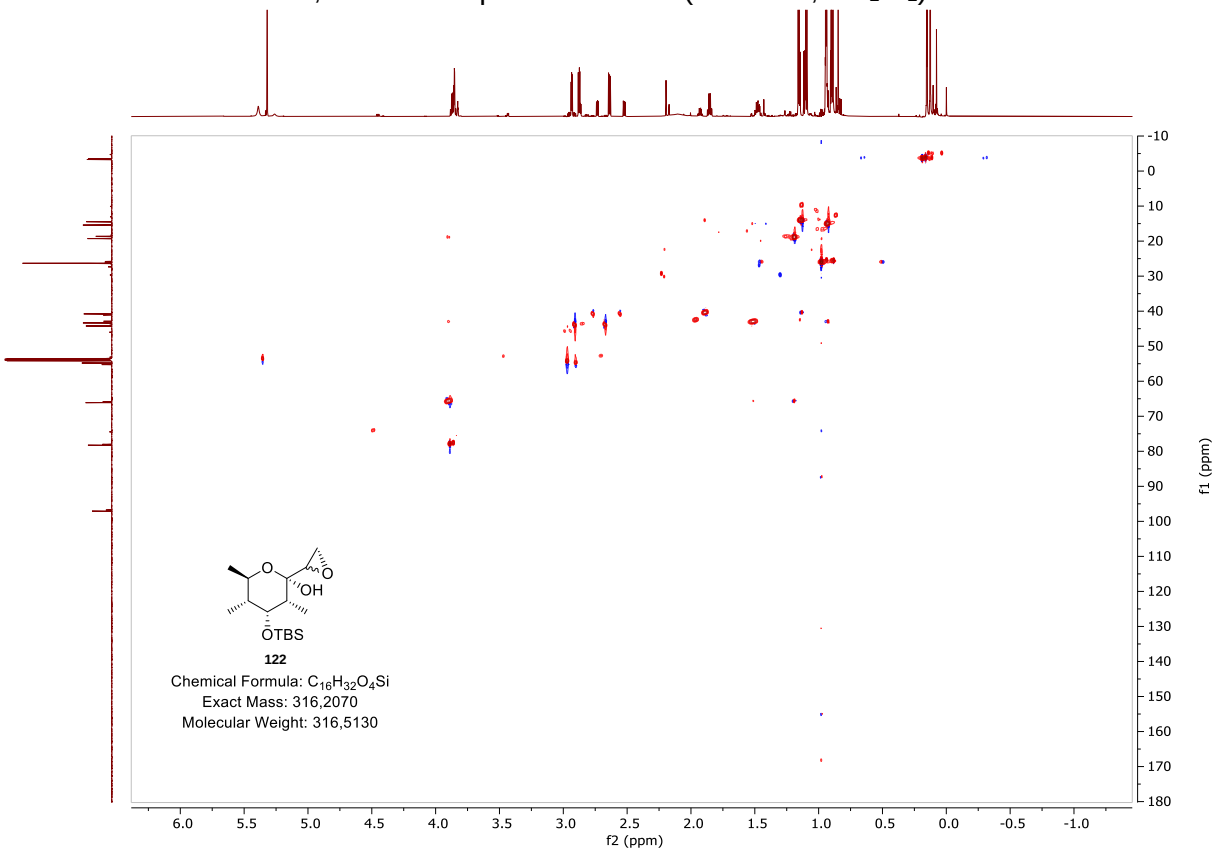

^{1}H, ^{13}C-HSQC spectrum of **122** (700 MHz, 175 MHz, CD_2Cl_2).

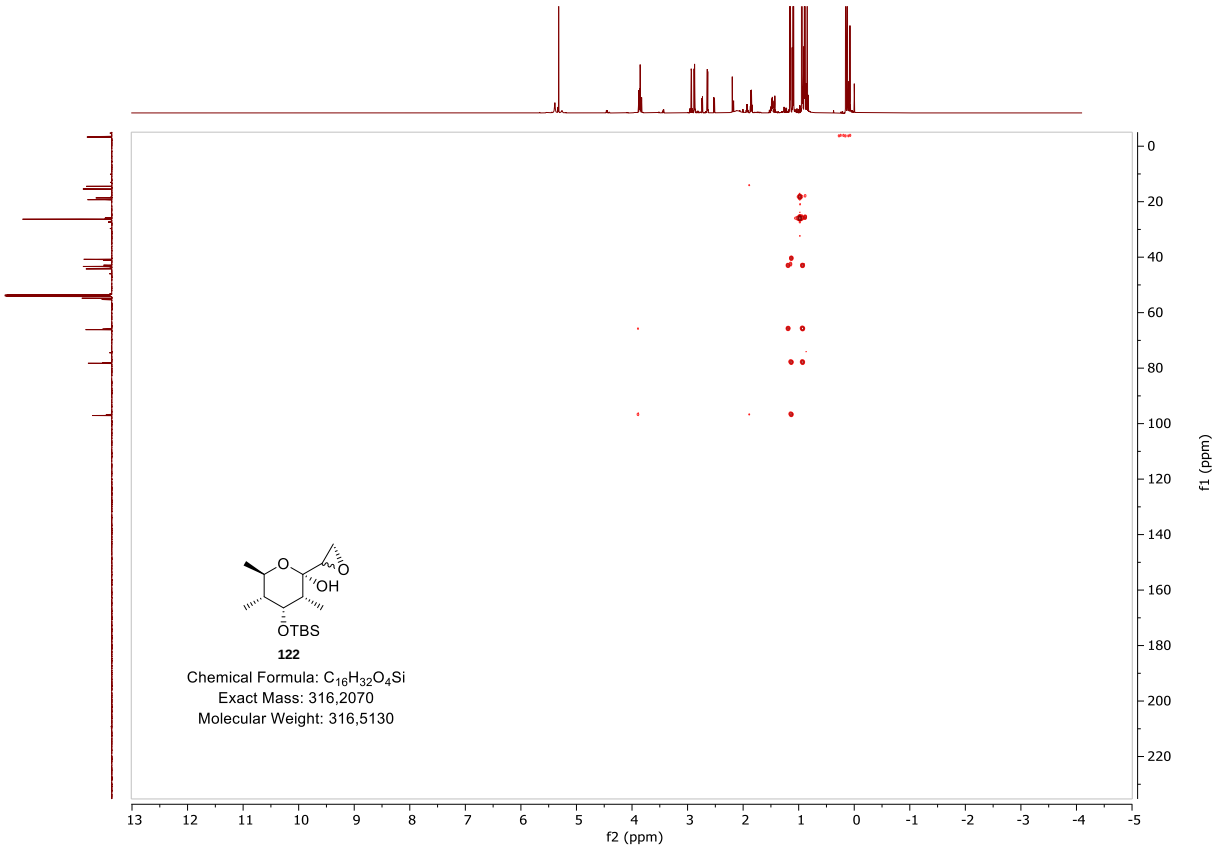

^{1}H, ^{13}C-HMBC spectrum of **122** (700 MHz, 175 MHz, CD_2Cl_2).

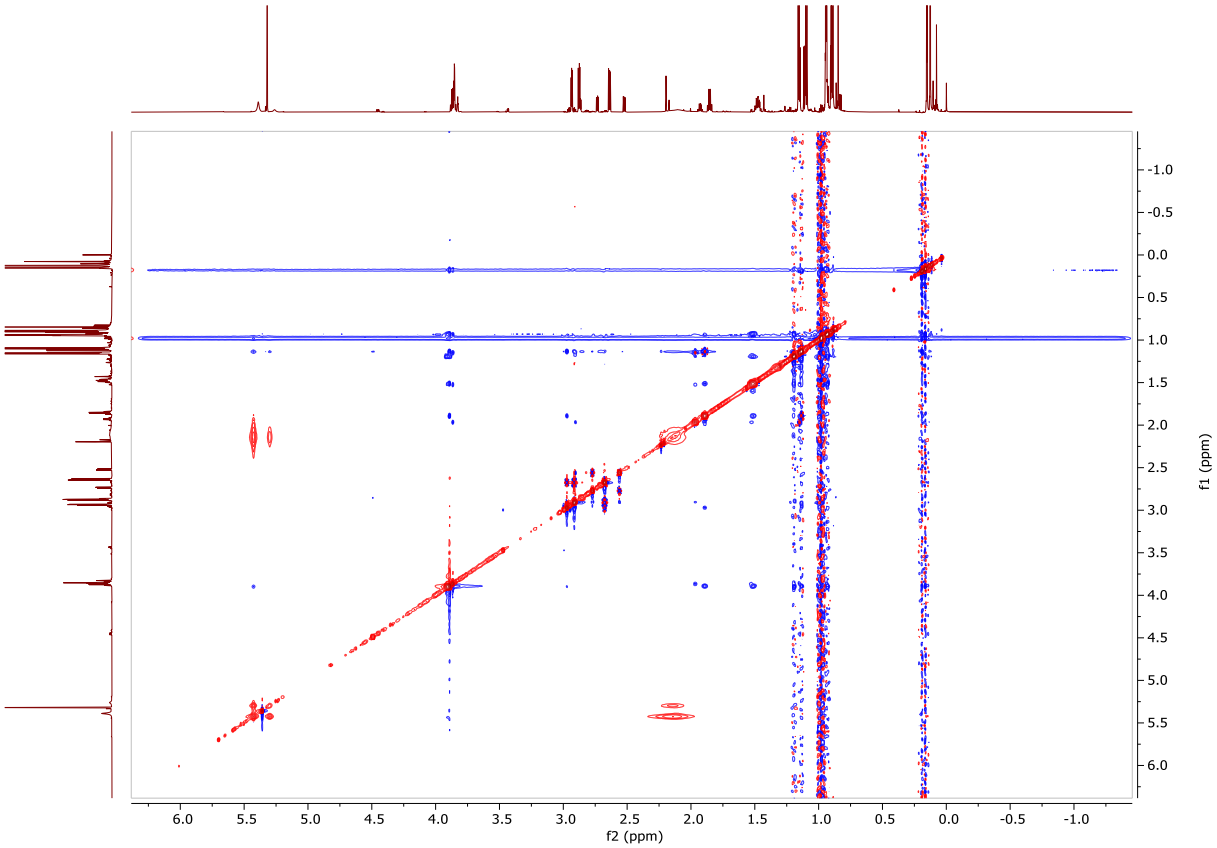

^{1}H, ^{1}H -NOESY spectrum of **122** (700 MHz, CD_2Cl_2).

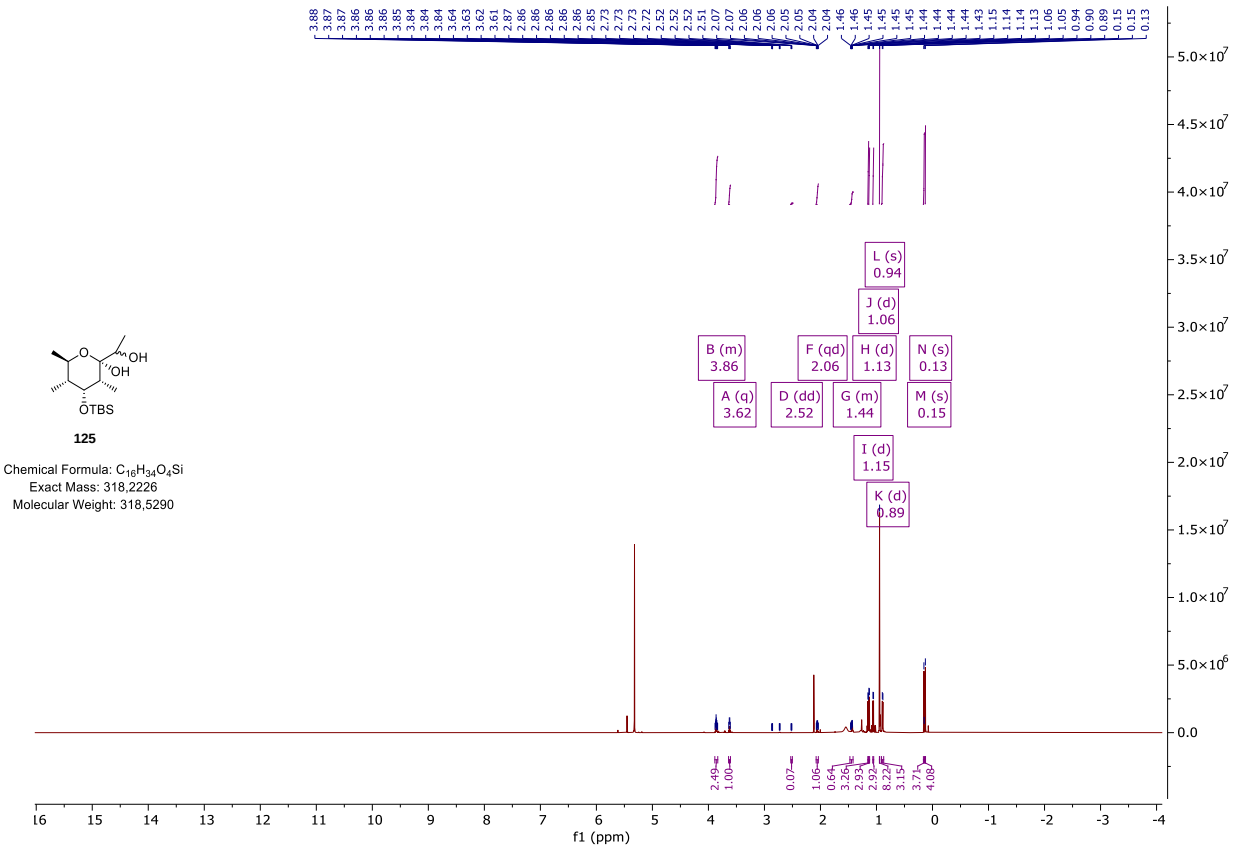

^{1}H-NMR spectrum of **125** (700 MHz, CD_2Cl_2).

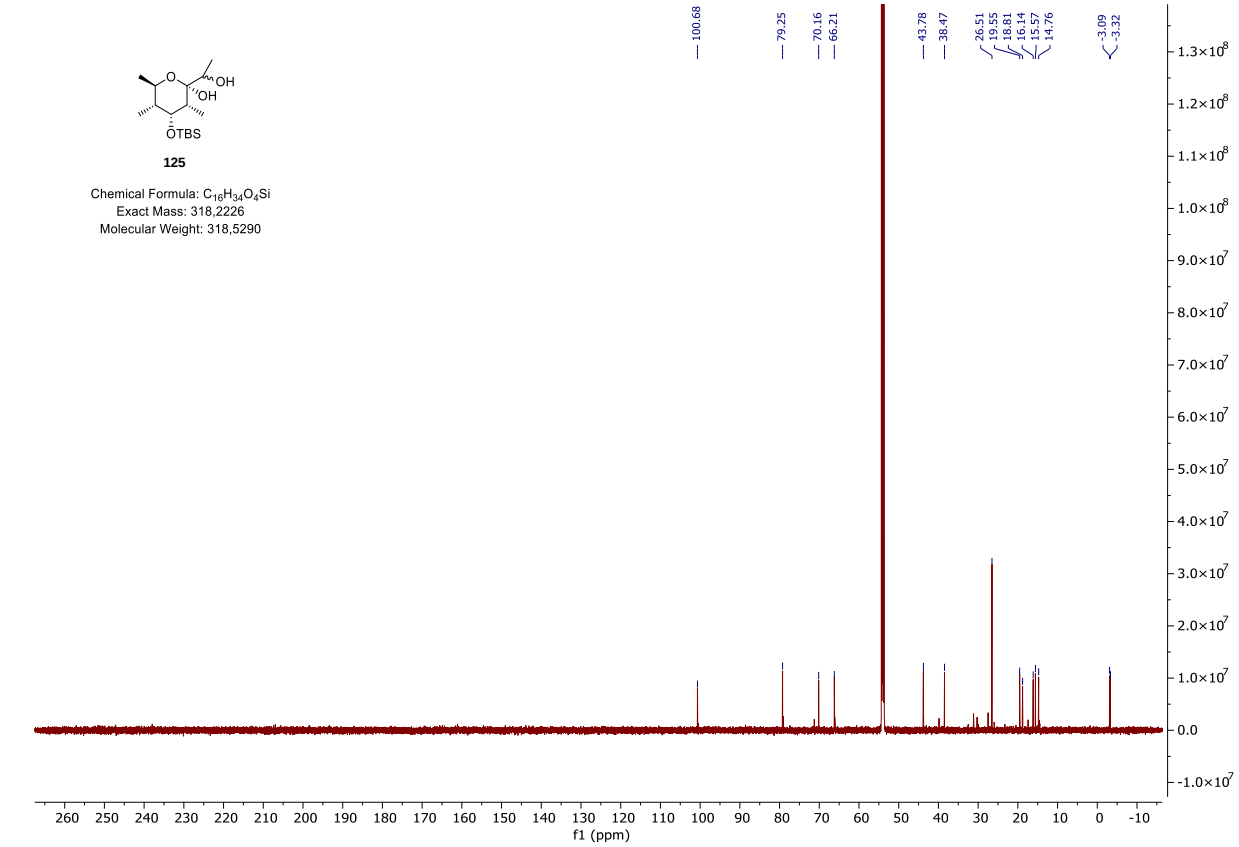

^{13}C-NMR spectrum of **125** (175 MHz, CD_2Cl_2).

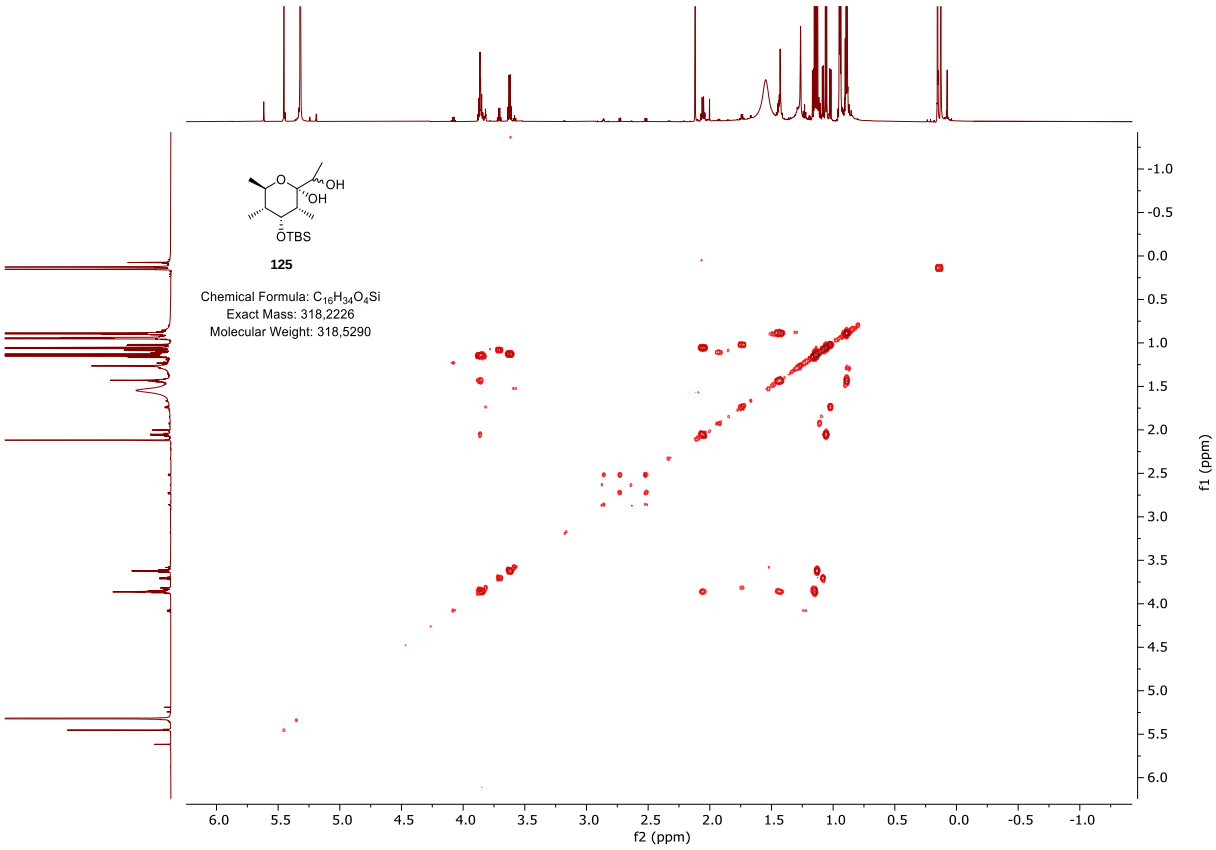

^{1}H, ^{1}H -COSY spectrum of **125** (700 MHz, CD_2Cl_2).

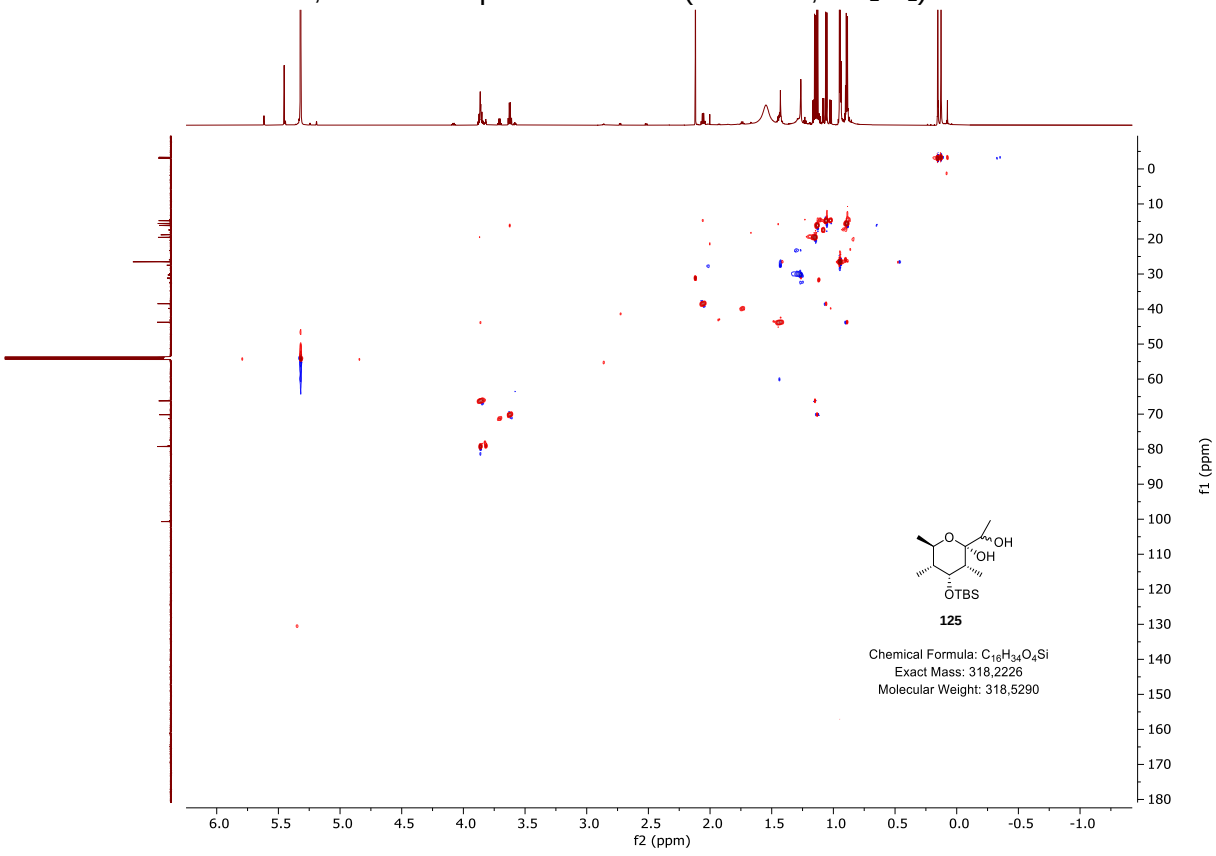

^{1}H, ^{13}C-HSQC spectrum of **125** (700 MHz, 175 MHz, CD_2Cl_2).

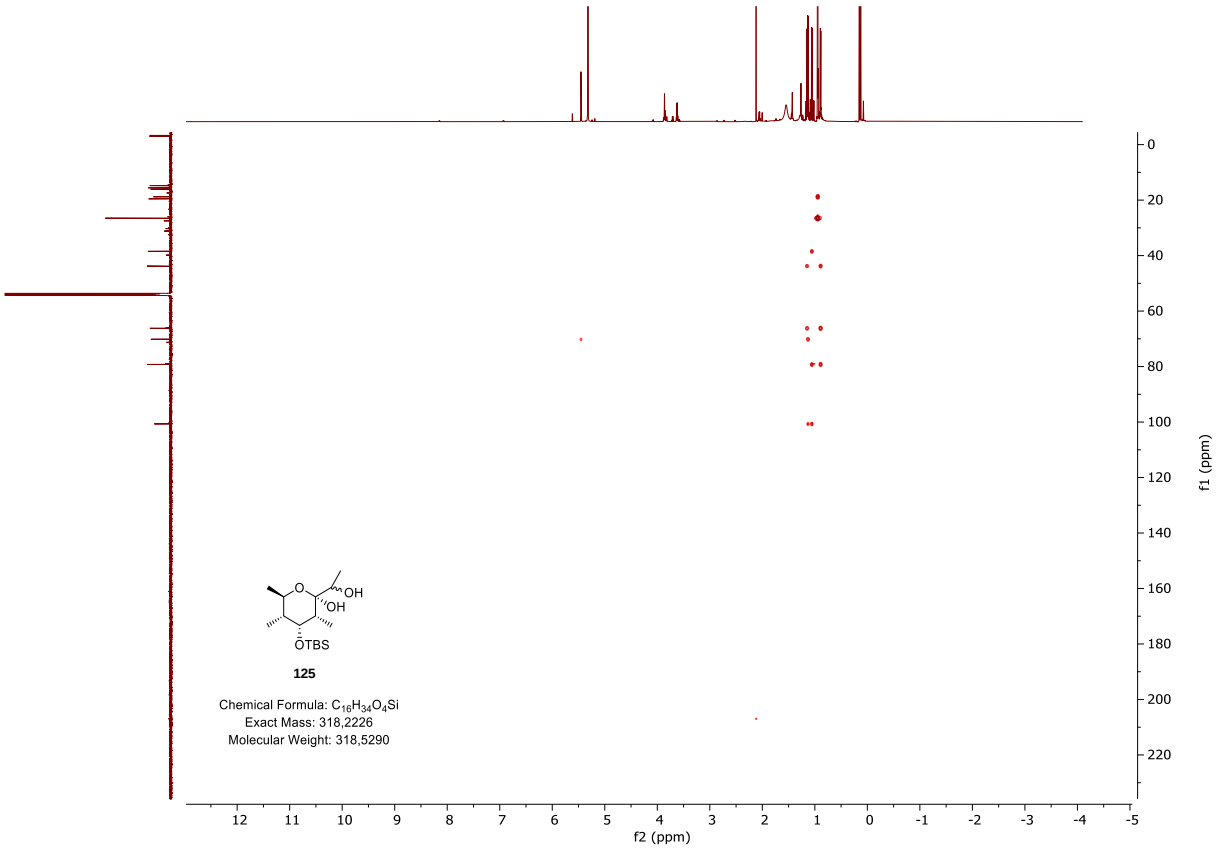

^{1}H, ^{13}C-HMBC spectrum of **125** (700 MHz, 175 MHz, CD_2Cl_2).

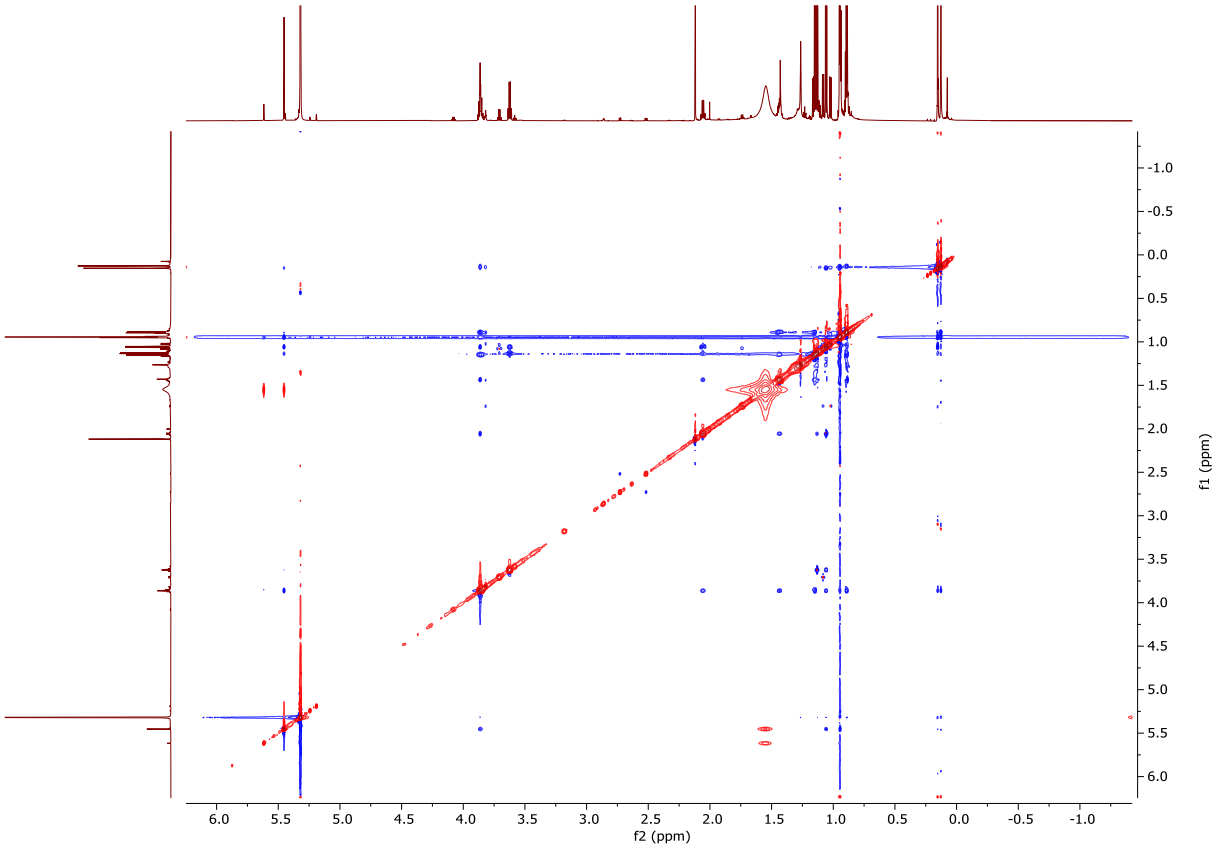

^{1}H, ^{1}H -NOESY spectrum of **125** (700 MHz, CD_2Cl_2).

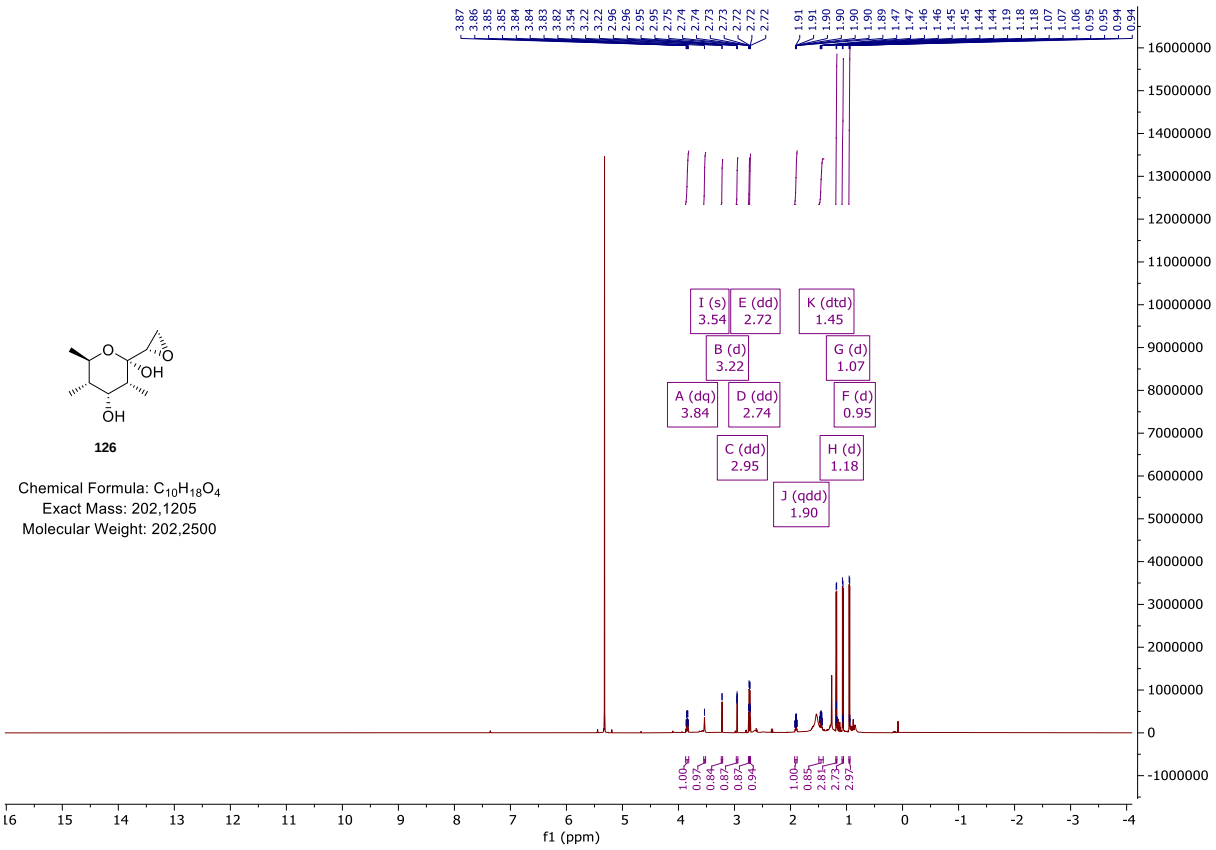

126

Chemical Formula: $C_{10}H_{18}O_4$
Exact Mass: 202,1205
Molecular Weight: 202,2500

^{1}H-NMR spectrum of **126** (700 MHz, CD_2Cl_2).

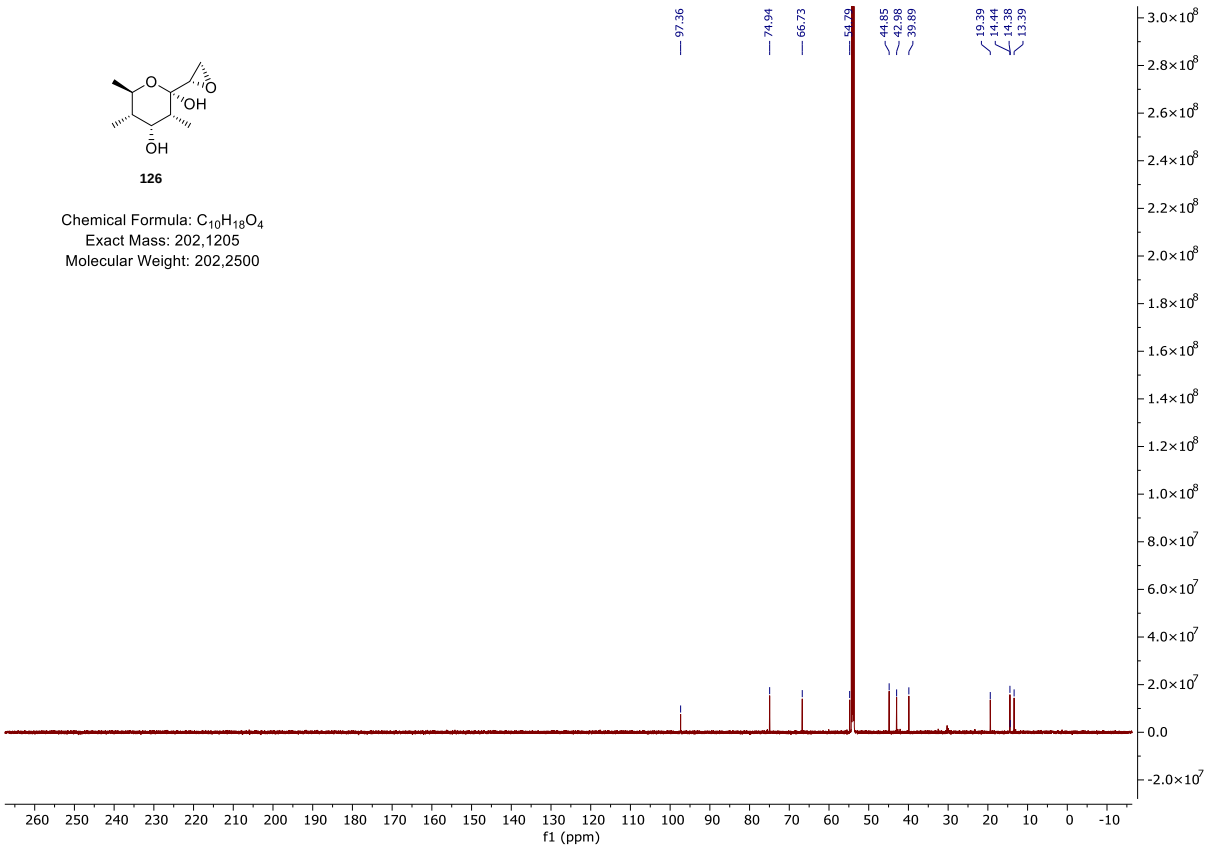

126

Chemical Formula: $C_{10}H_{18}O_4$
Exact Mass: 202,1205
Molecular Weight: 202,2500

^{13}C-NMR spectrum of **126** (175 MHz, CD_2Cl_2).

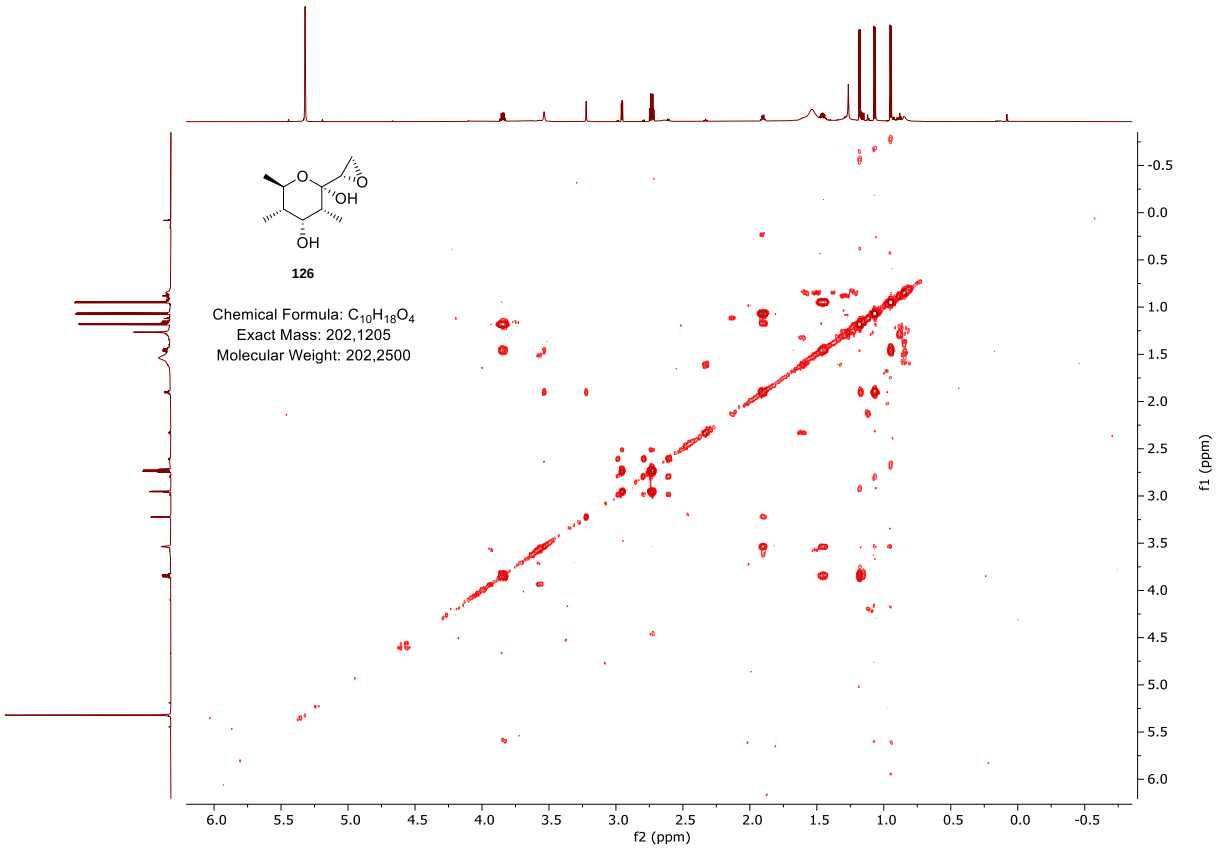

^{1}H, ^{1}H-COSY spectrum of **126** (700 MHz, CD_2Cl_2).

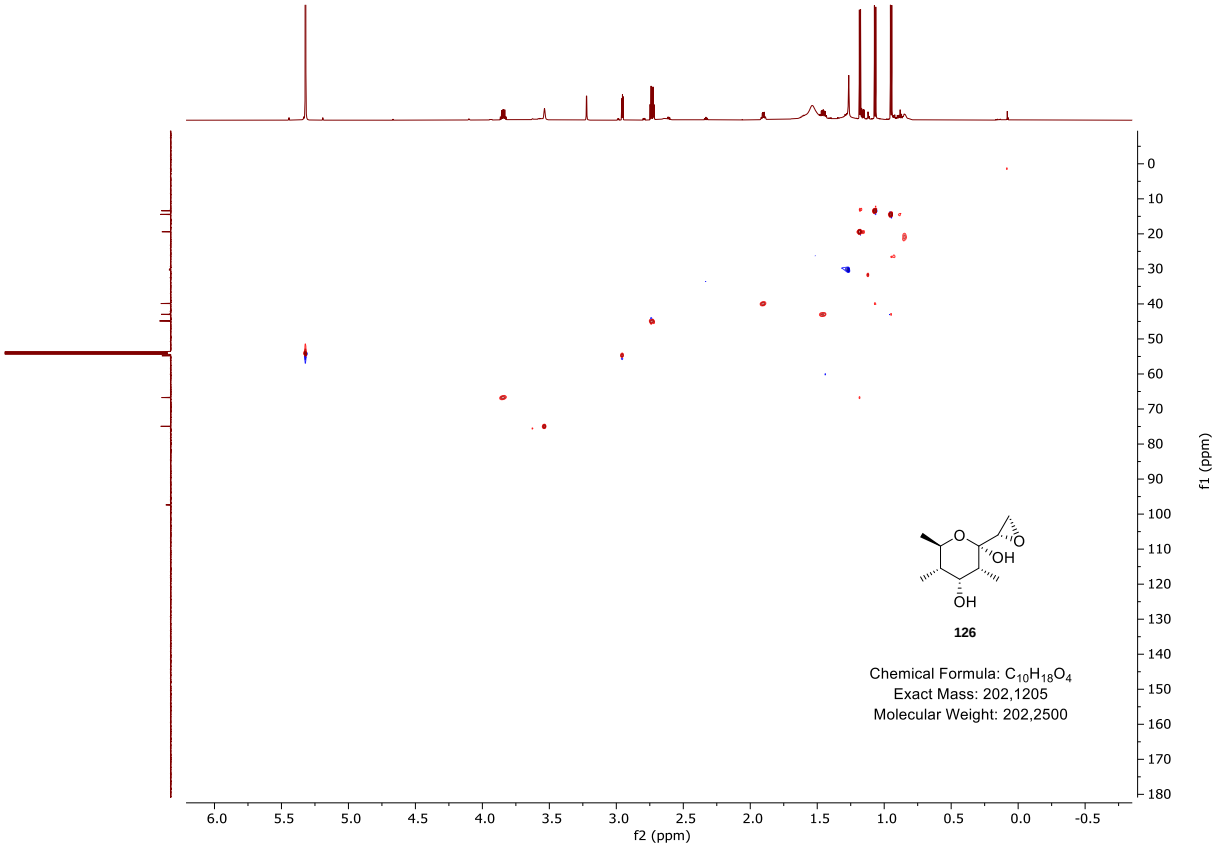

^{1}H, ^{13}C-HSQC spectrum of **126** (700 MHz, 175 MHz, CD_2Cl_2).

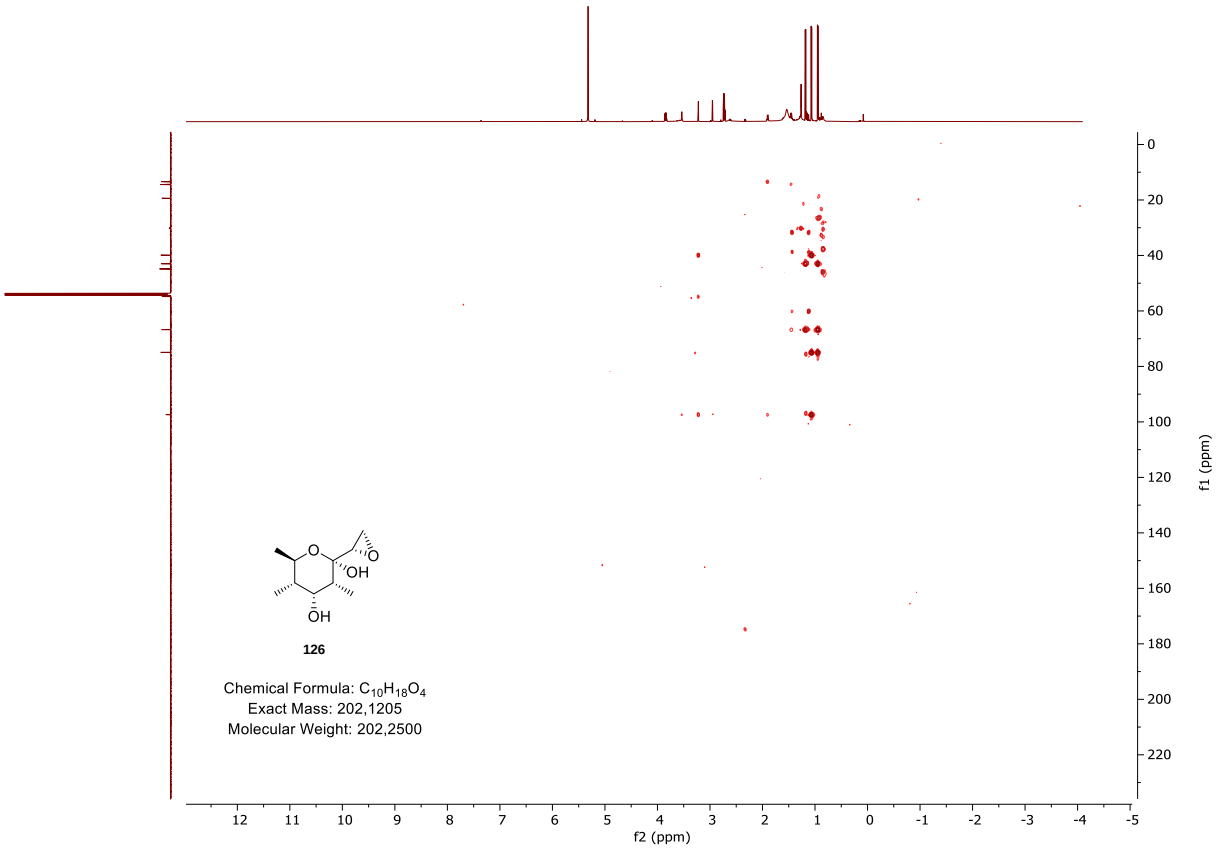

^{1}H, ^{13}C-HMBC spectrum of **126** (700 MHz, 175 MHz, CD_2Cl_2).

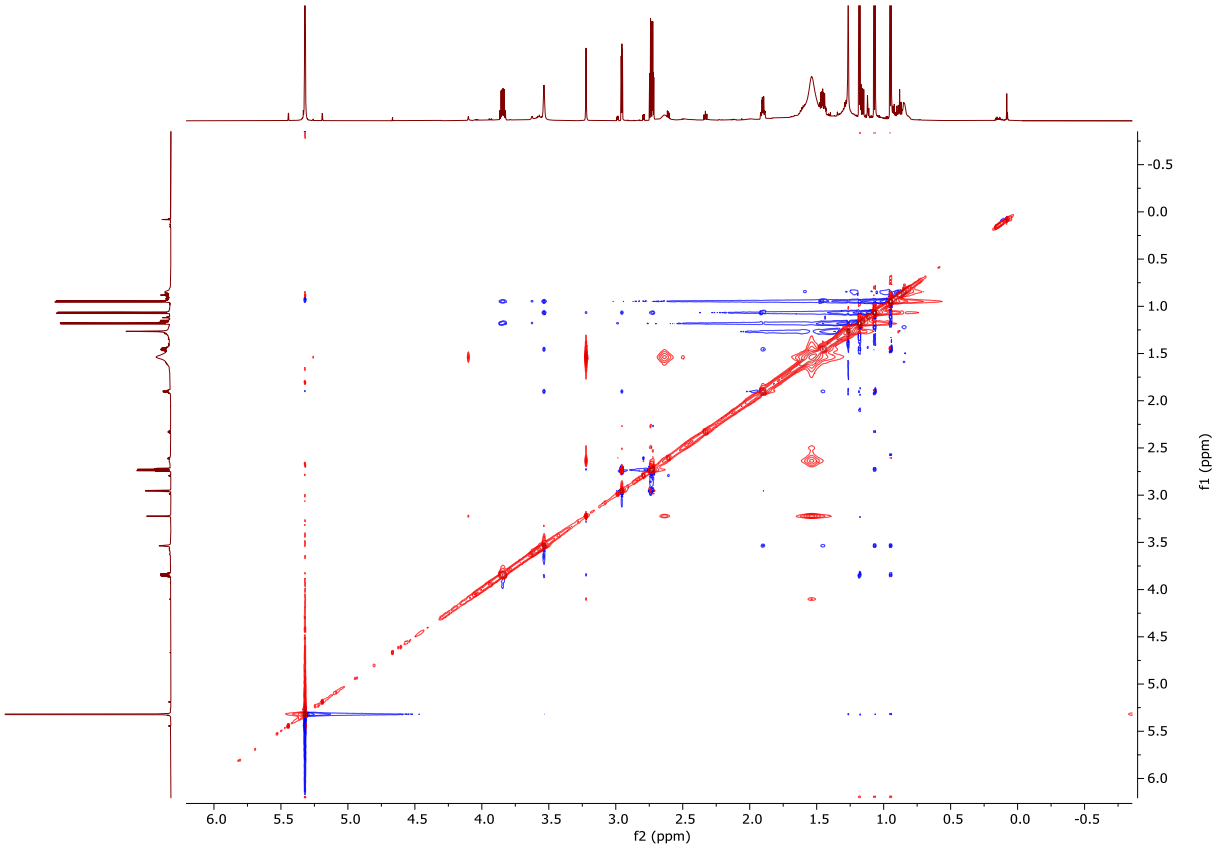

^{1}H, ^{1}H-NOESY spectrum of **126** (700 MHz, CD_2Cl_2).

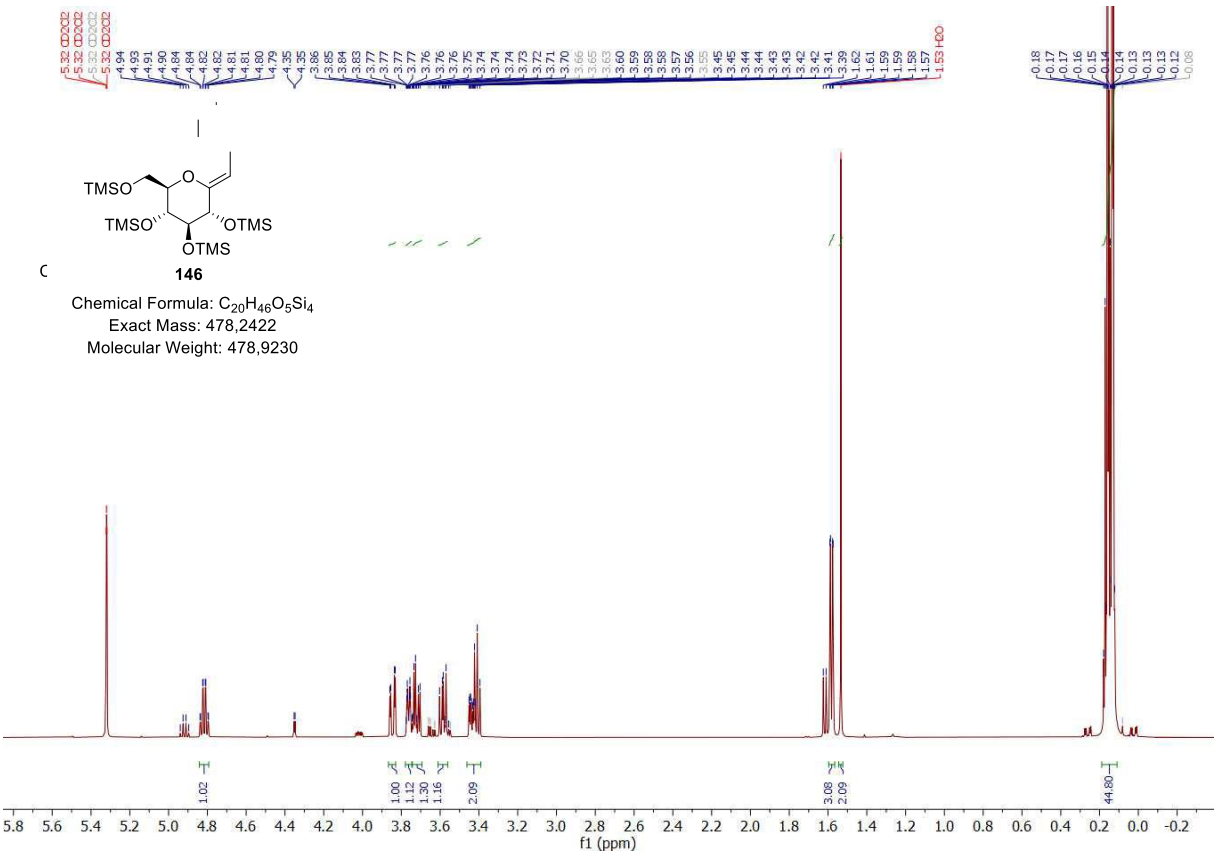

^{1}H – NMR spectrum of **146** (500 MHz, CD_2Cl_2)

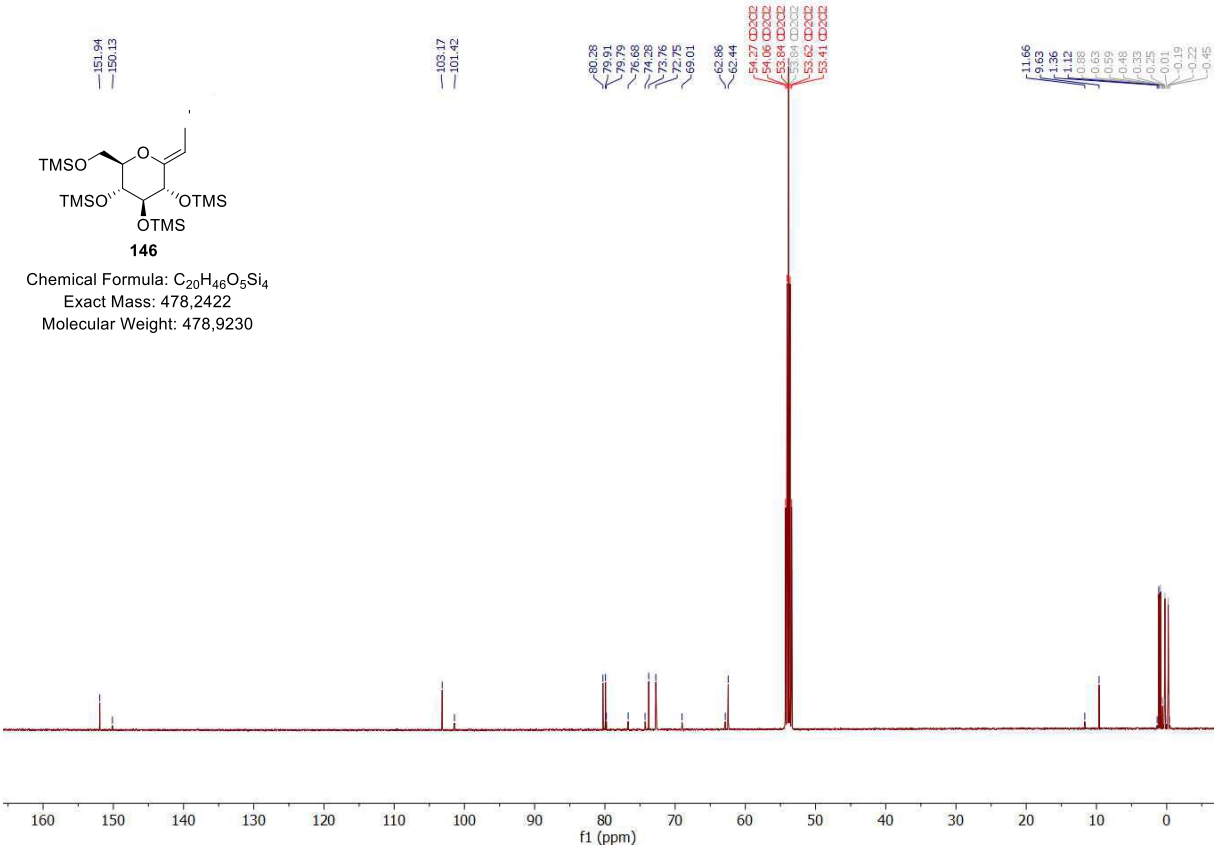

^{13}C – NMR spectrum of **146** (125 MHz, CD_2Cl_2)

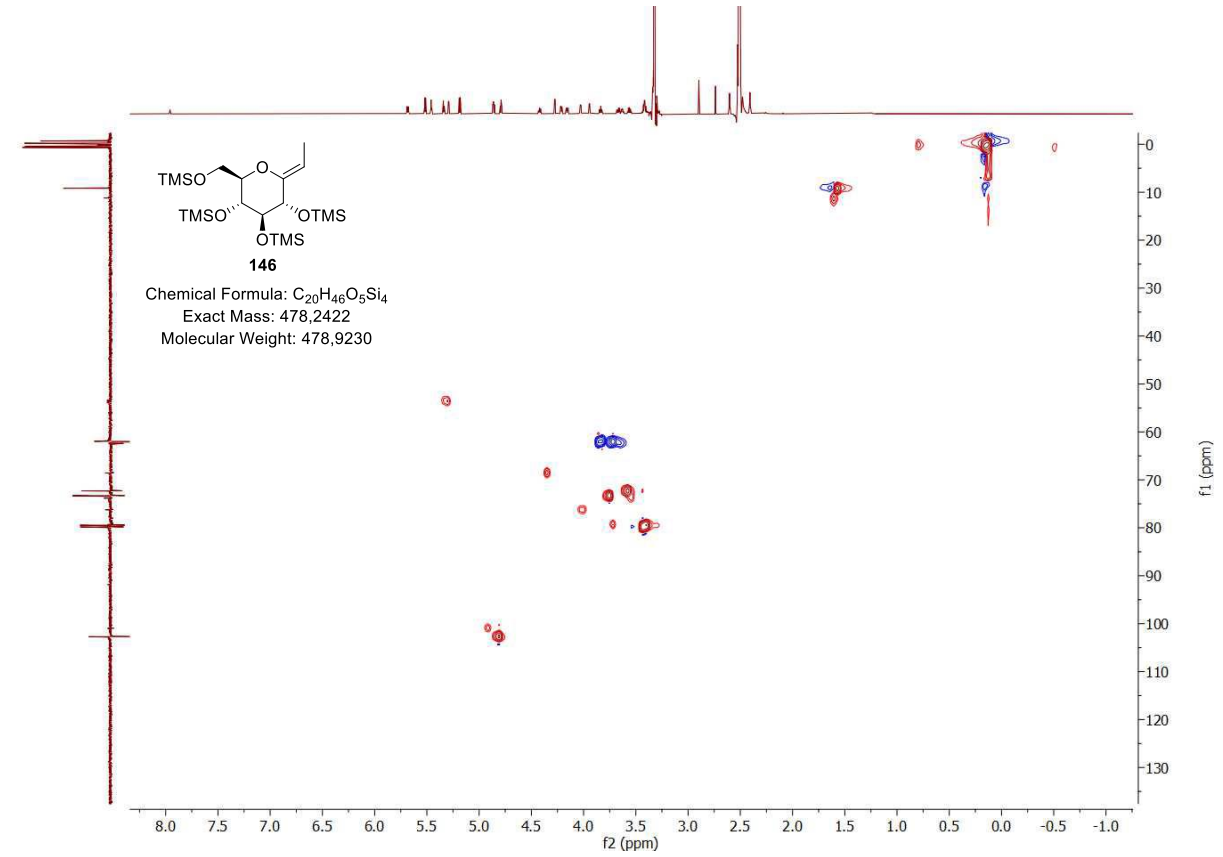

^{1}H, ^{13}C – HSQC spectrum of **146** (500 MHz, 125 MHz, CD_2Cl_2)

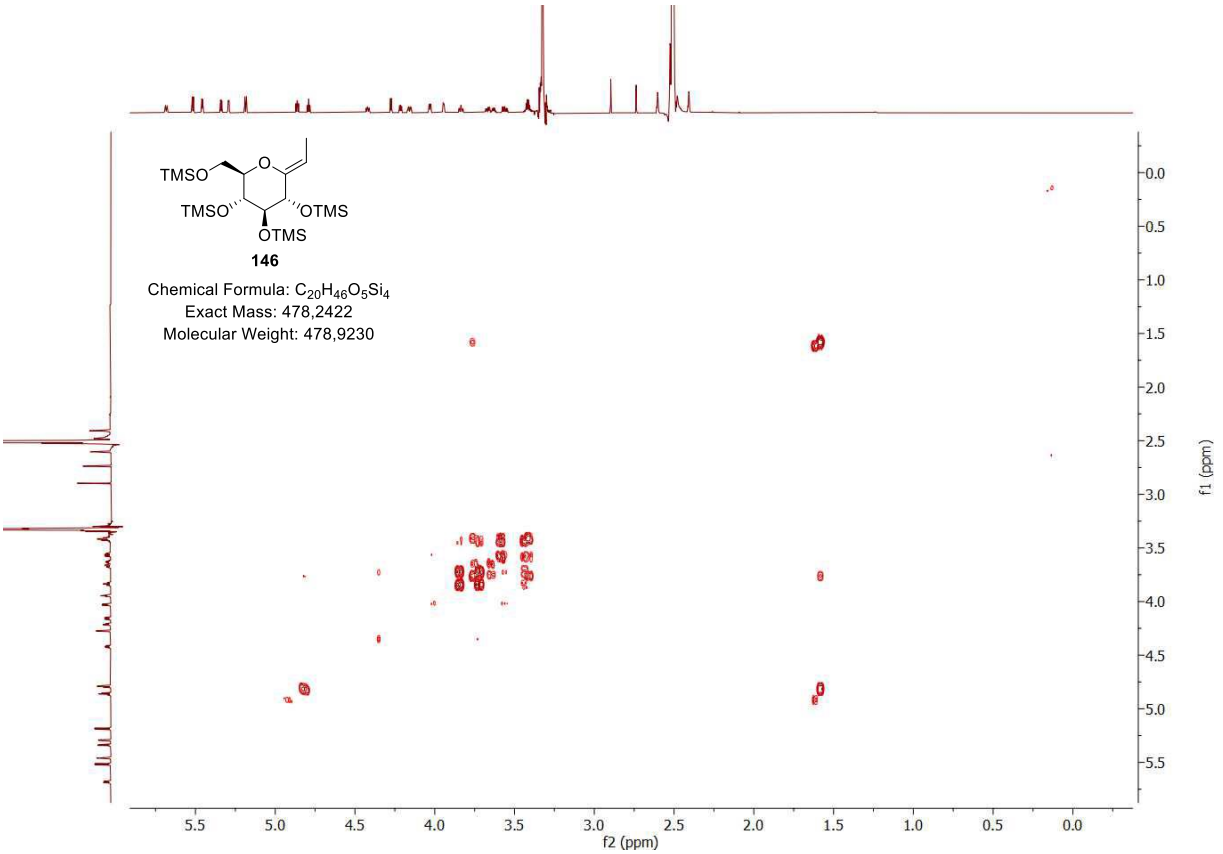

^{1}H, ^{1}H –COSY spectrum of **146** (500 MHz, CD_2Cl_2)

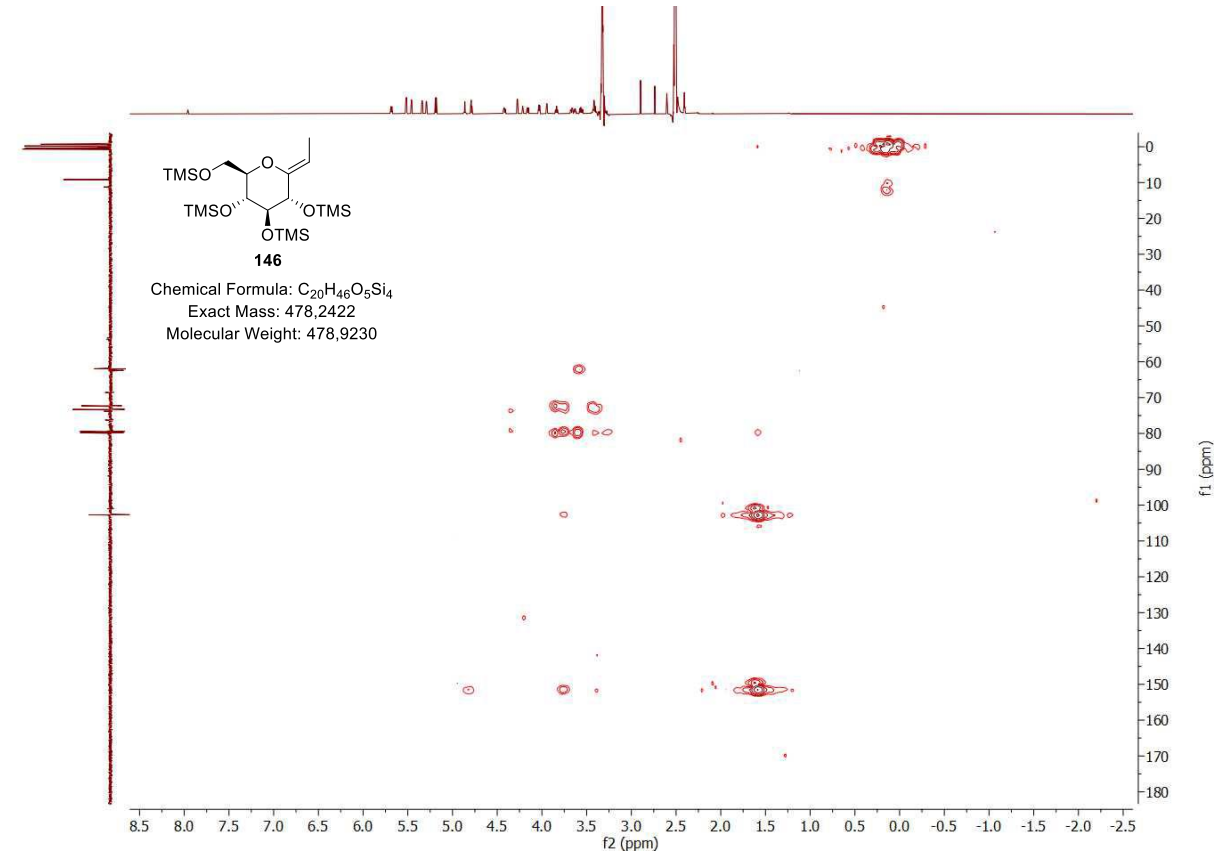

^{1}H, ^{13}C –HMBC spectrum of **146** (500 MHz, 125 MHz, CD_2Cl_2)

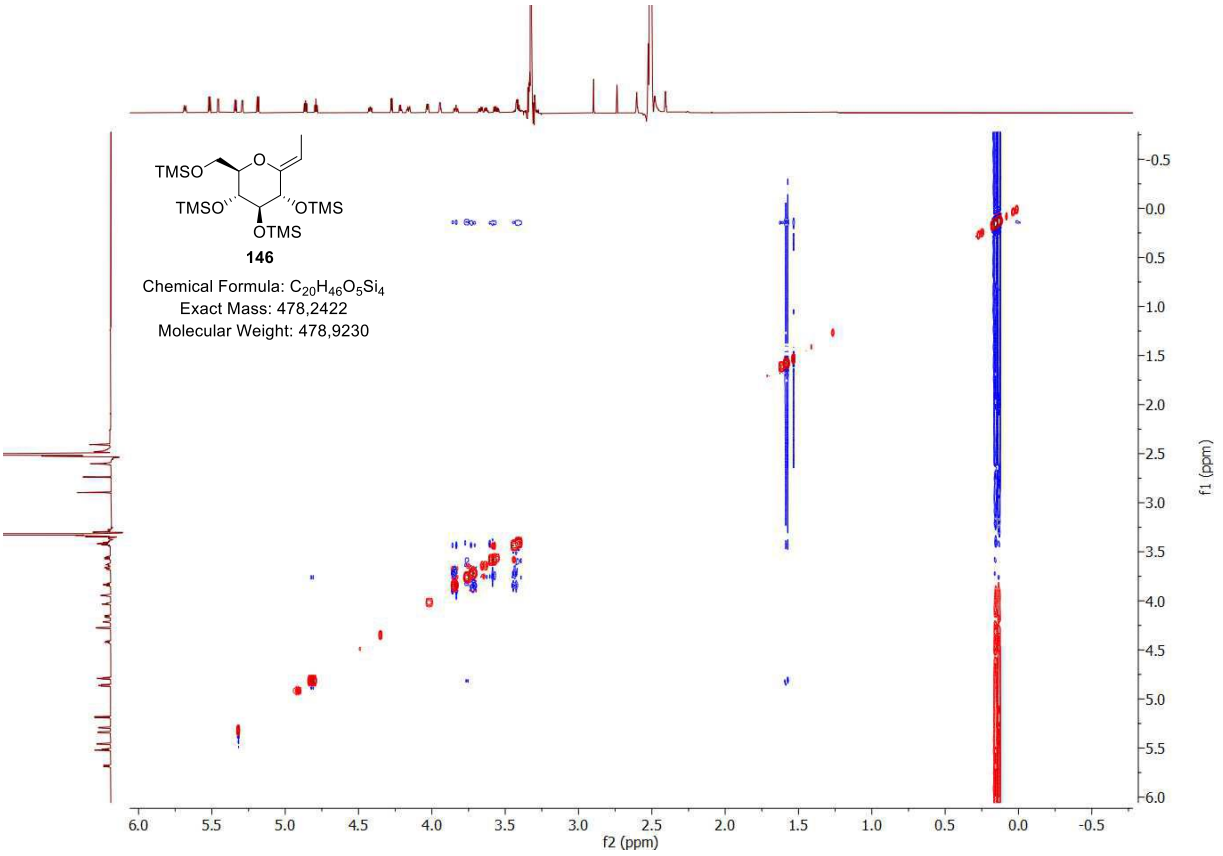

^{1}H, ^{1}H –NOESY spectrum of **146** (500 MHz, CD_2Cl_2)

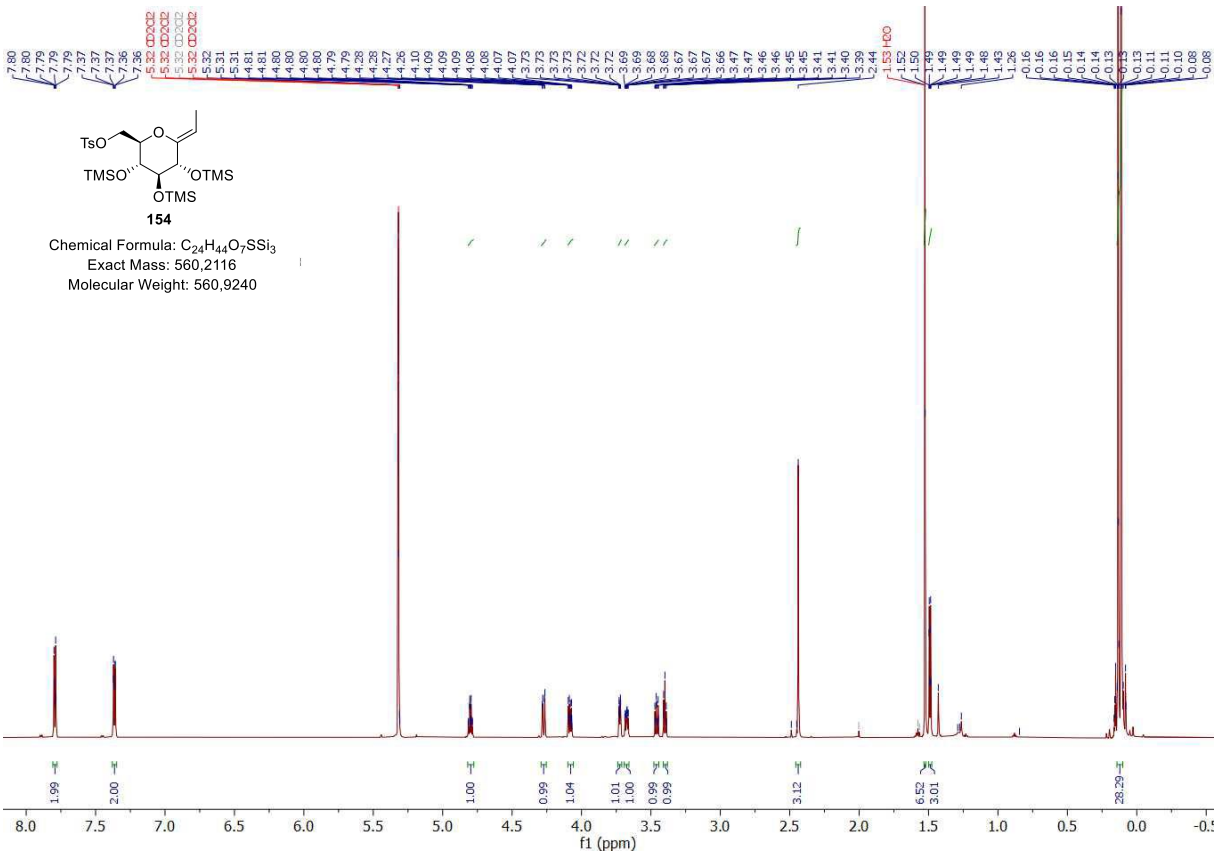

^{1}H – NMR spectrum of **154** (700 MHz, CD_2Cl_2)

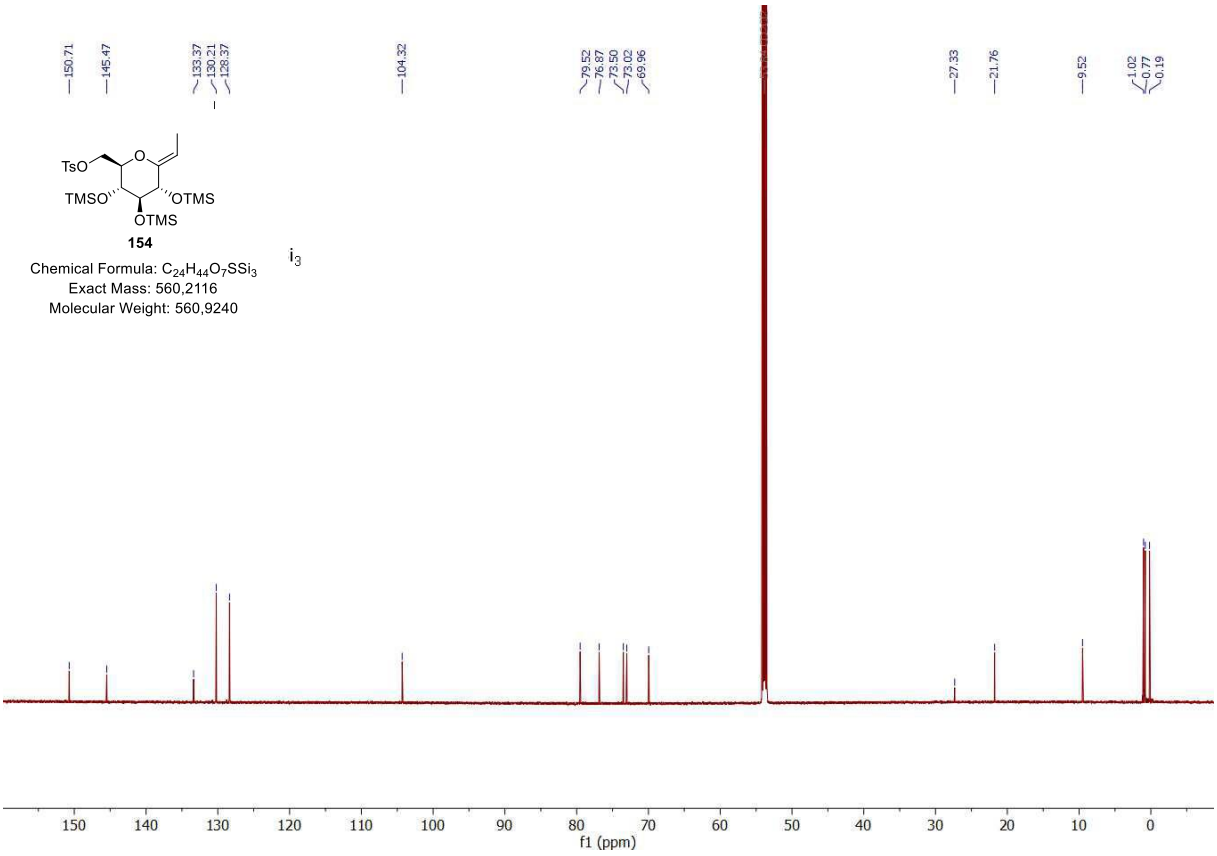

^{13}C – NMR spectrum of **154** (175 MHz, CD_2Cl_2)

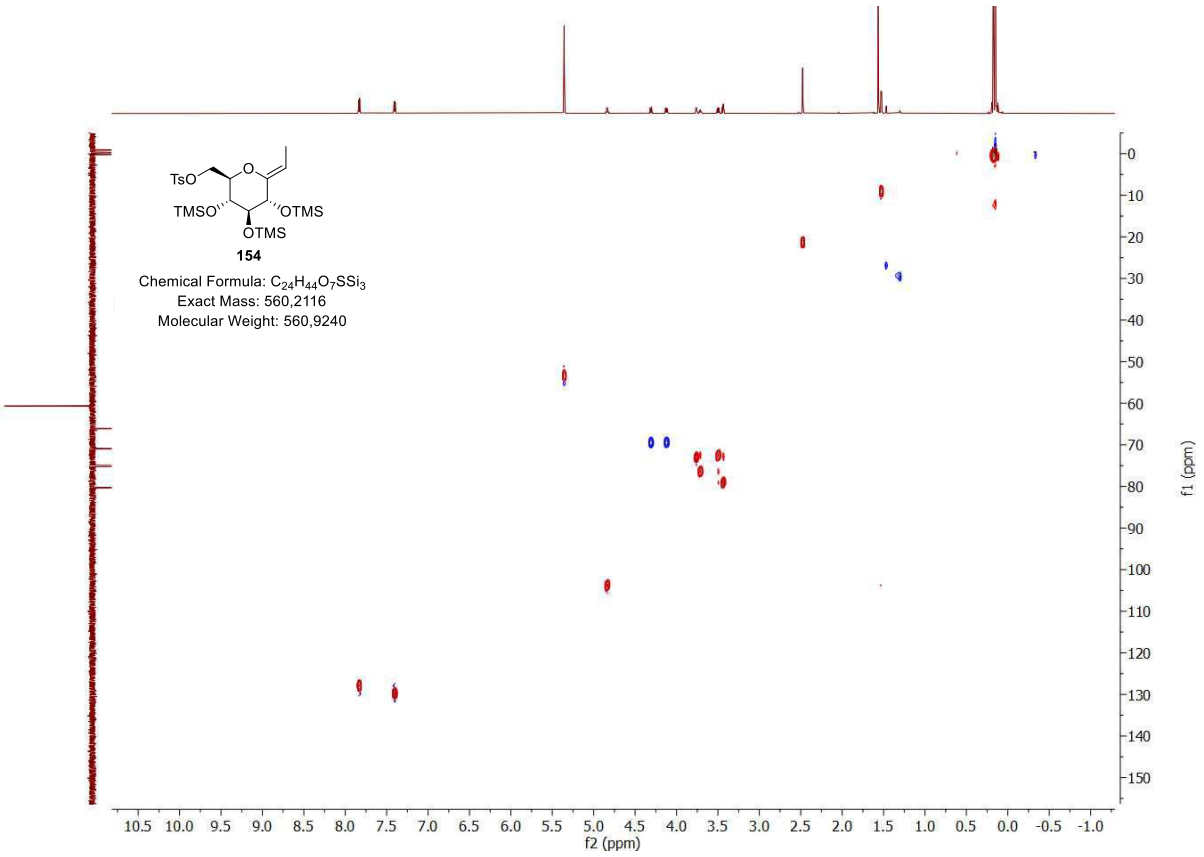

^{1}H, ^{13}C – HSQC spectrum of **154** (700 MHz, 175 MHz, CD_2Cl_2)

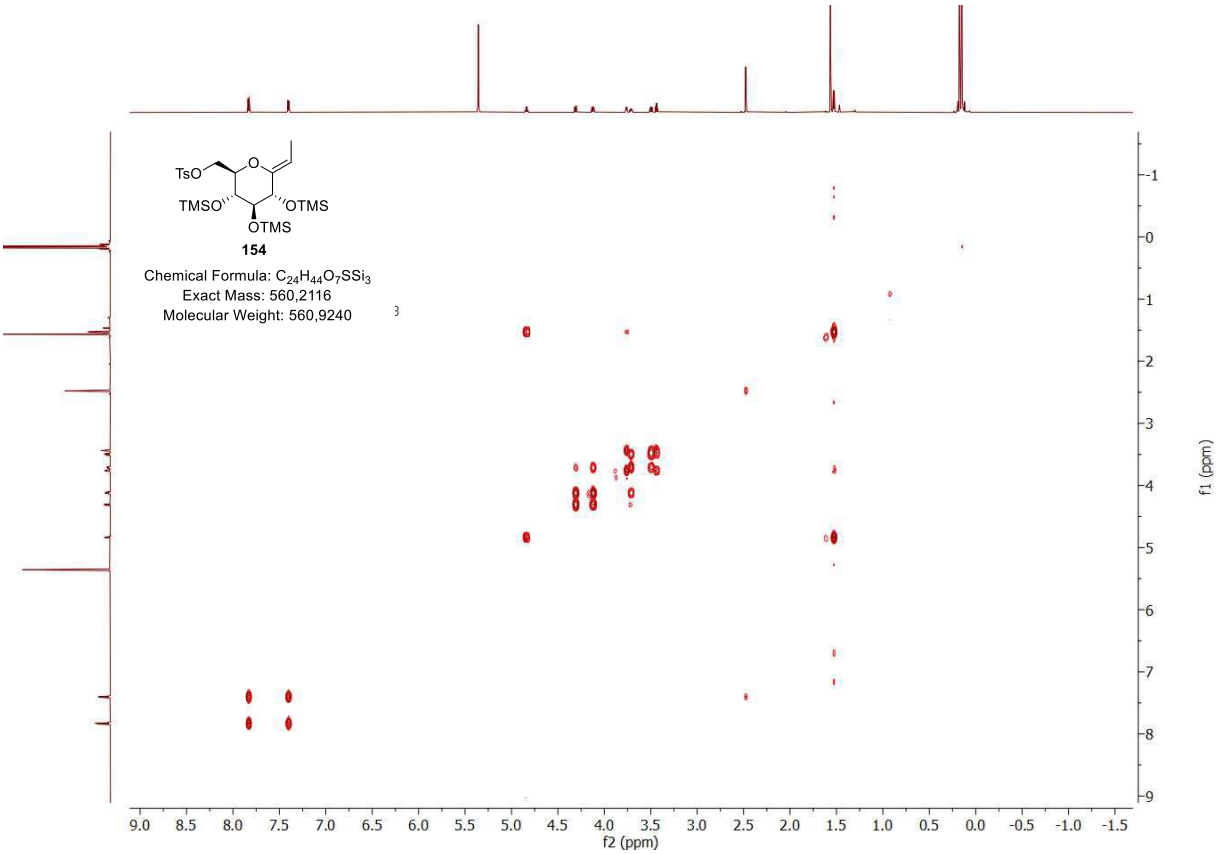

^{1}H, ^{1}H –COSY spectrum of **154** (700 MHz, CD_2Cl_2)

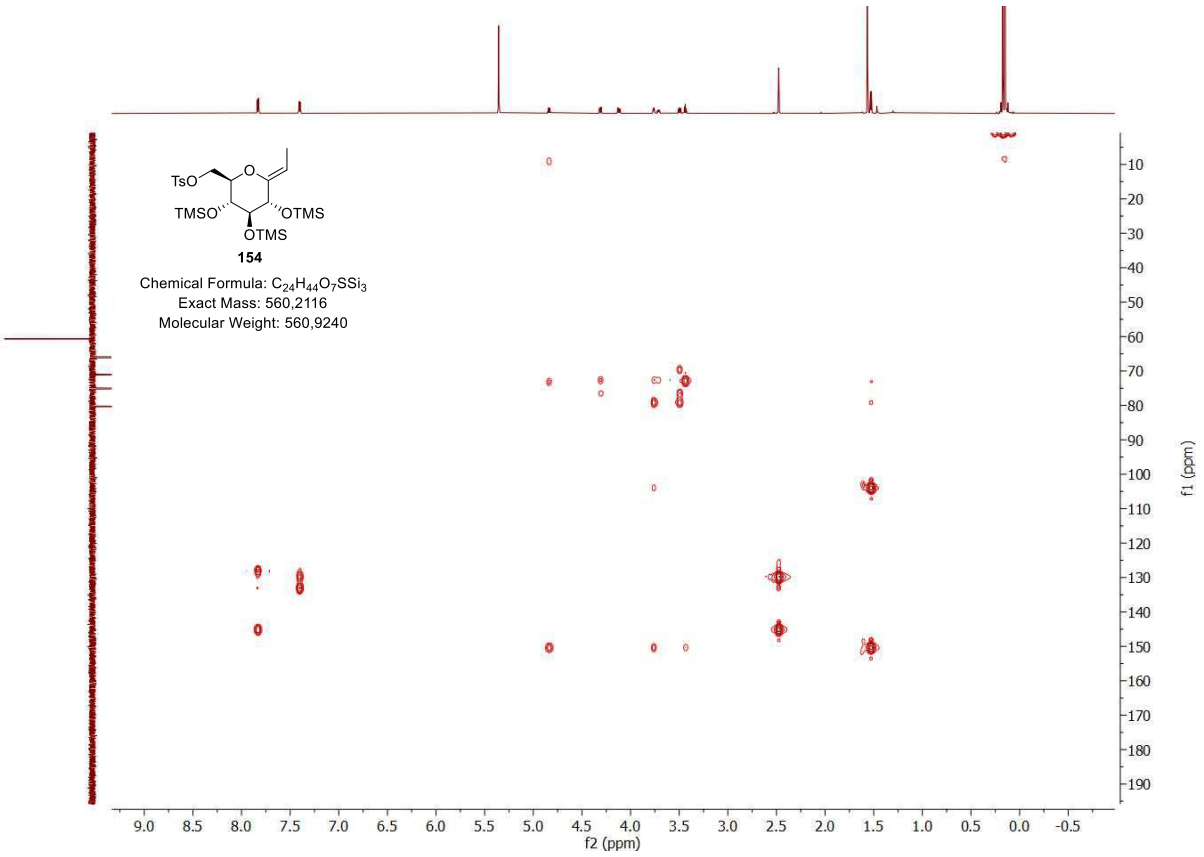

^{1}H, ^{13}C –HMBC spectrum of **154** (700 MHz, 175 MHz, CD_2Cl_2)

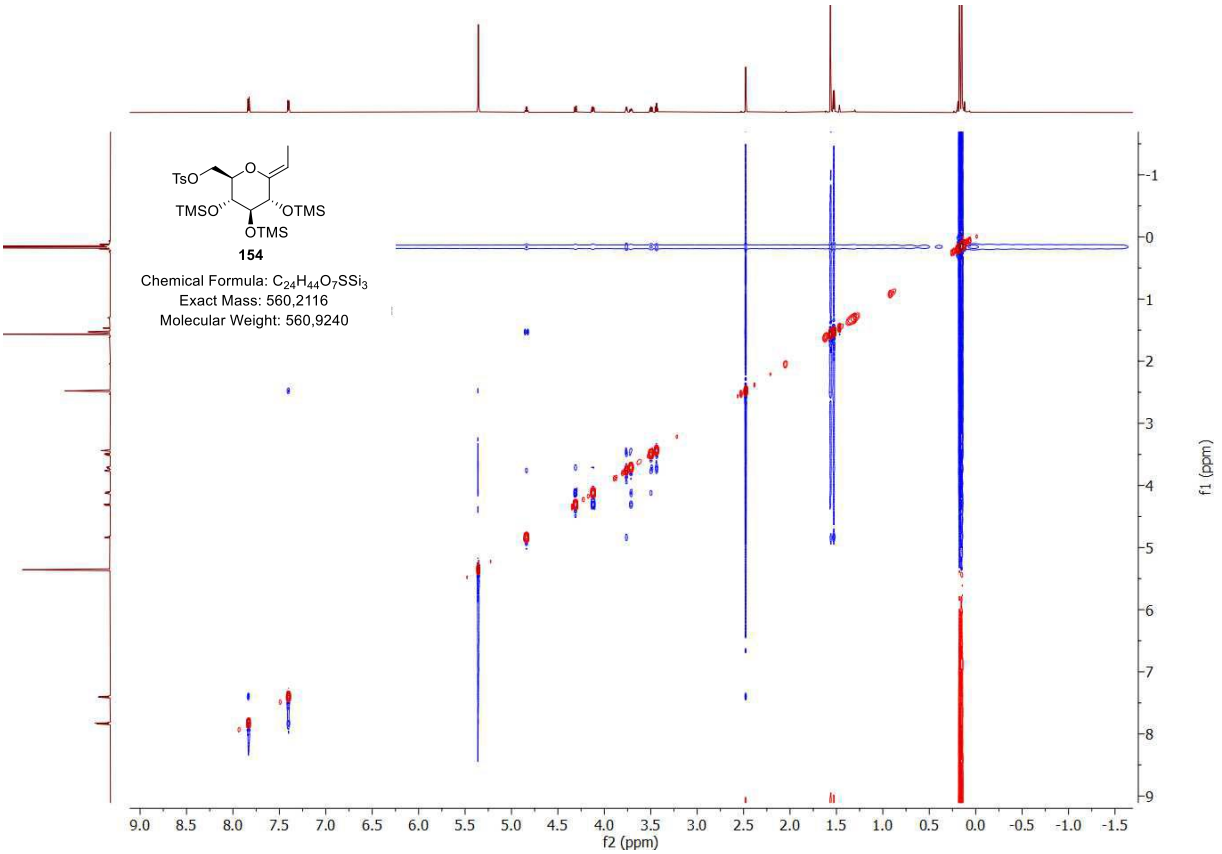

^{1}H, ^{1}H –NOESY spectrum of **154** (700 MHz, CD_2Cl_2)

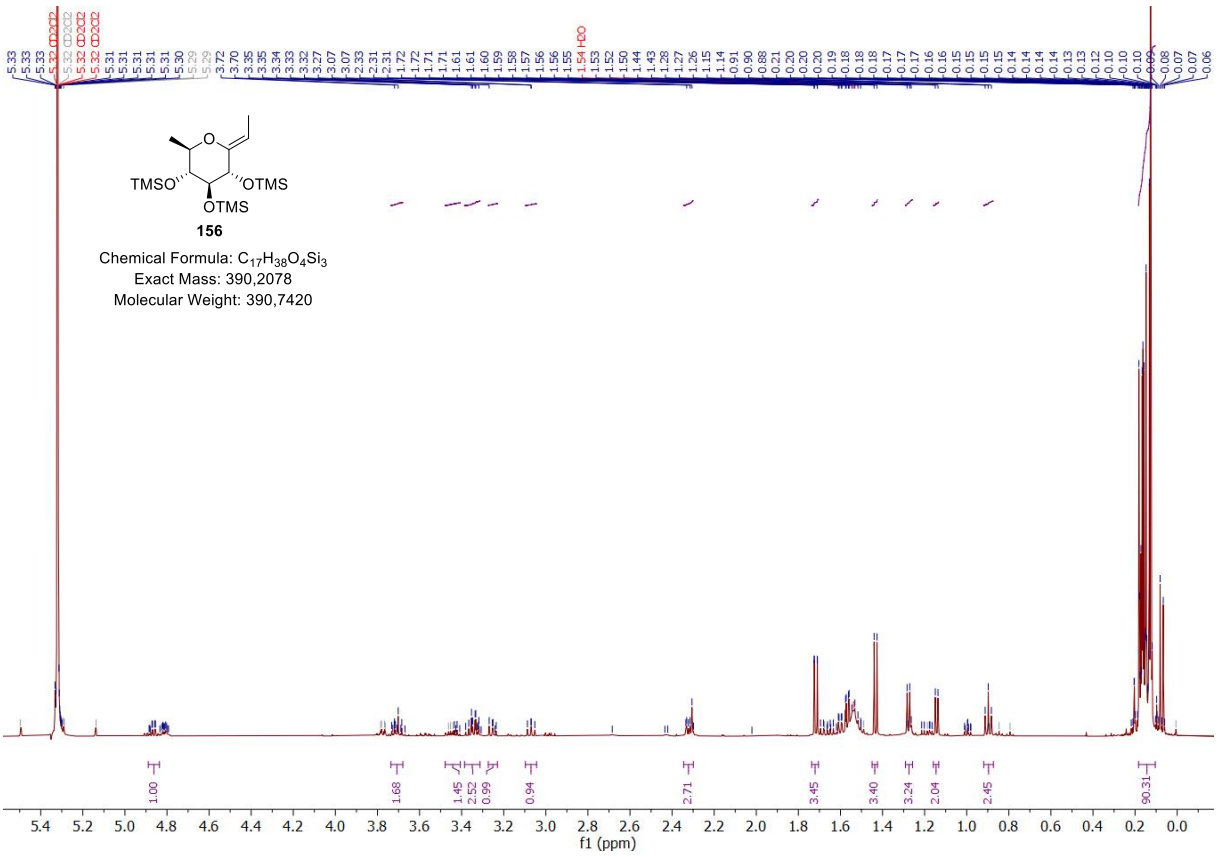

^{1}H – NMR spectrum of **156** (500 MHz, CD_2Cl_2)

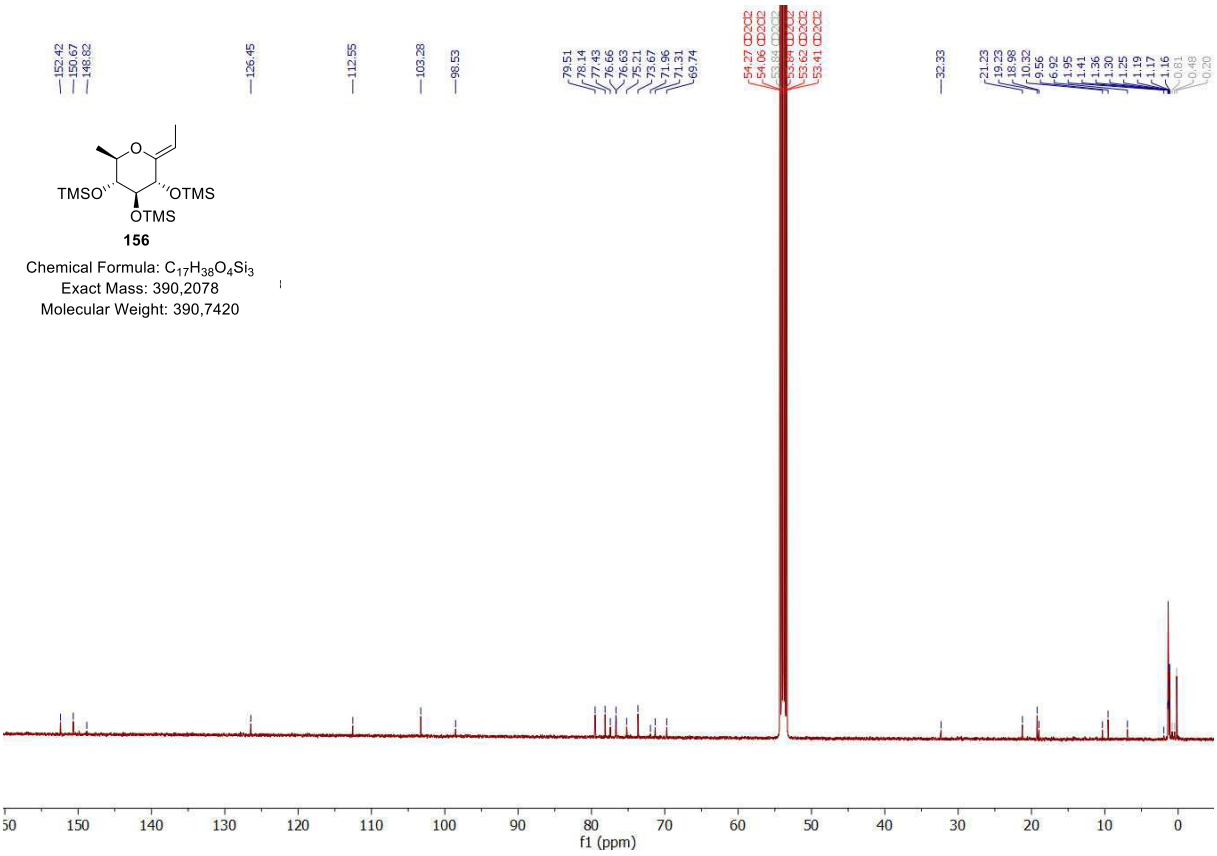

^{13}C – NMR spectrum of **156** (125 MHz, CD_2Cl_2)

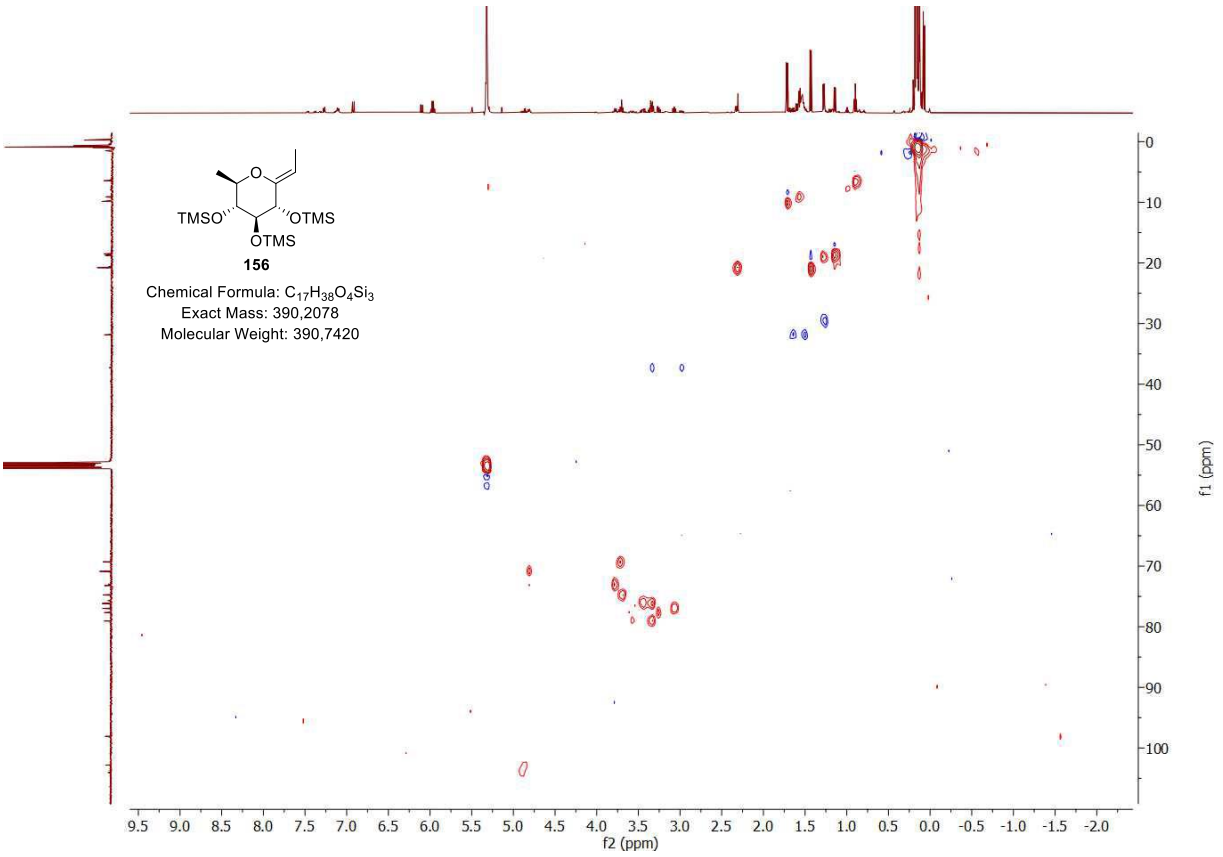

^{1}H, ^{13}C – HSQC spectrum of **156** (500 MHz, 125 MHz, CD_2Cl_2)

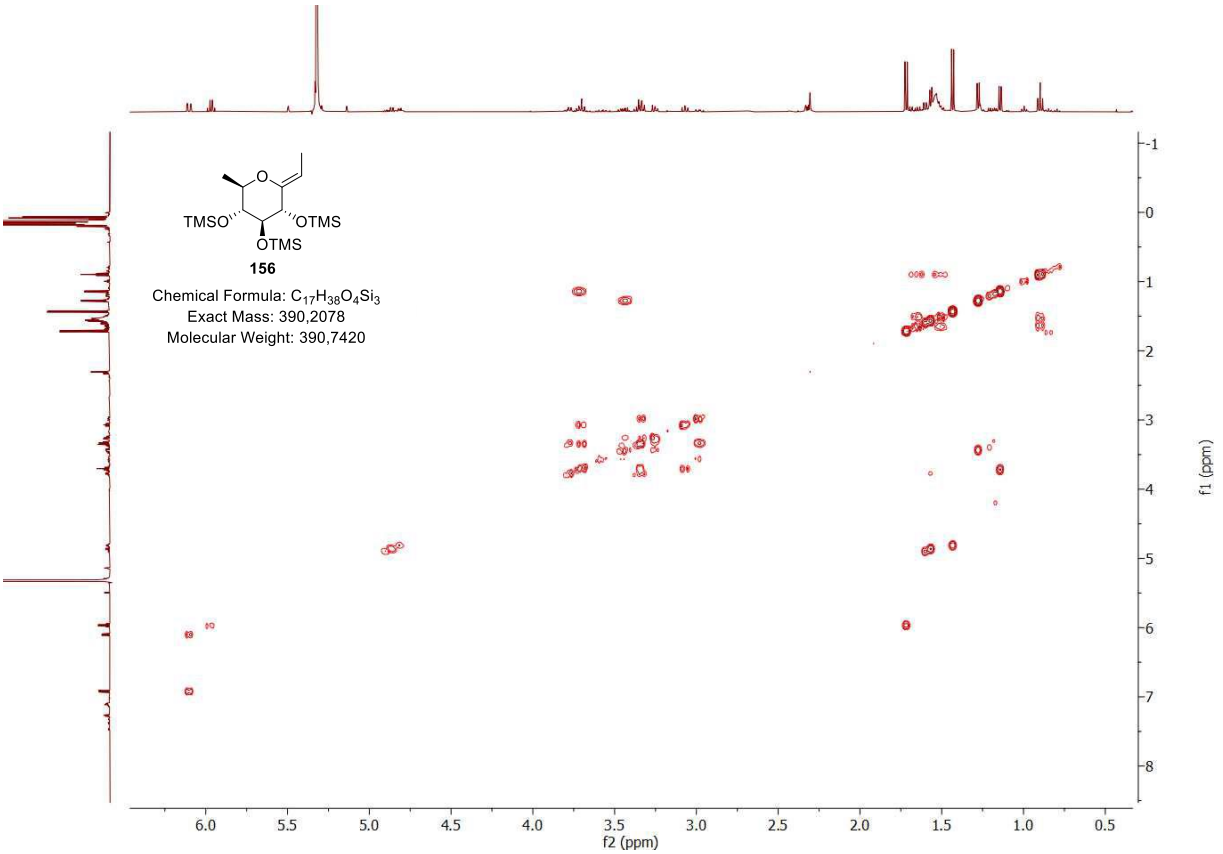

^{1}H, ^{1}H –COSY spectrum of **156** (500 MHz, CD_2Cl_2)

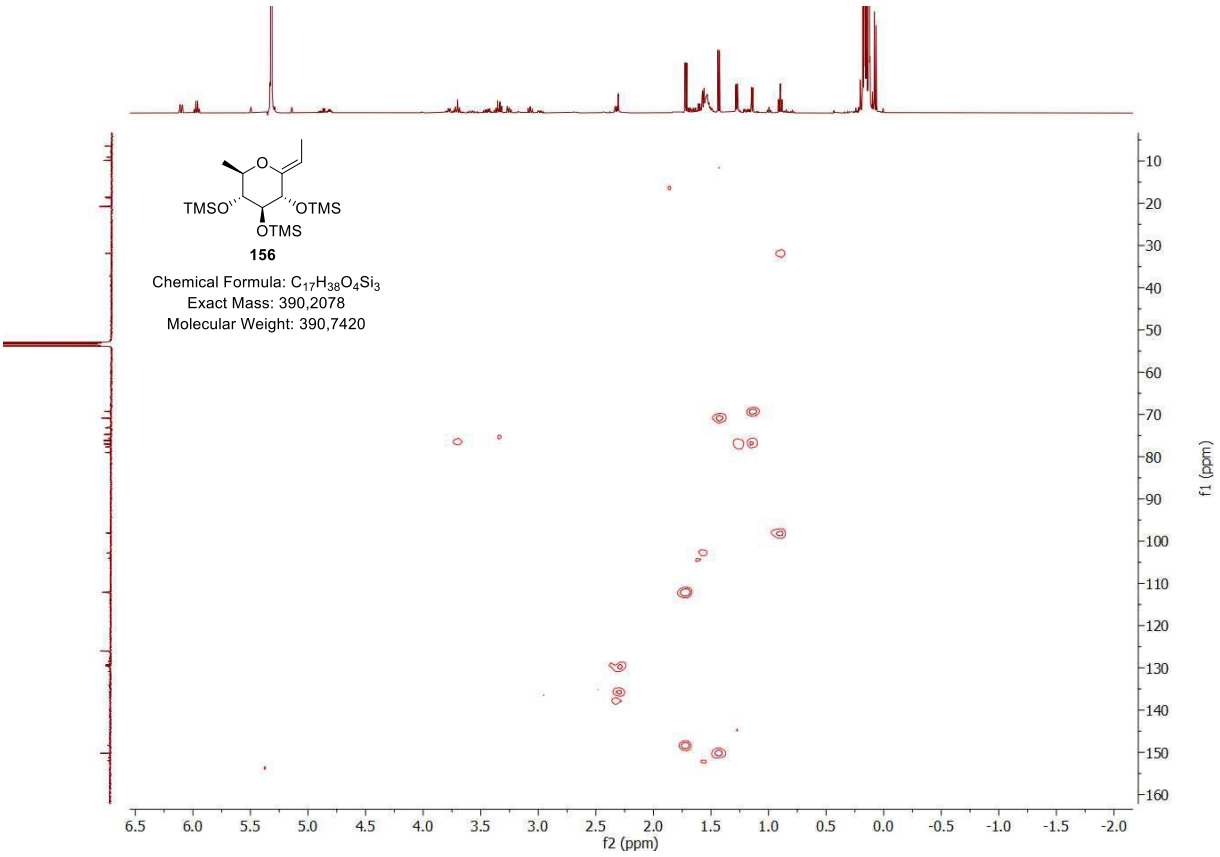

^{1}H, ^{13}C –HMBC spectrum of **156** (500 MHz, 125 MHz, CD_2Cl_2)

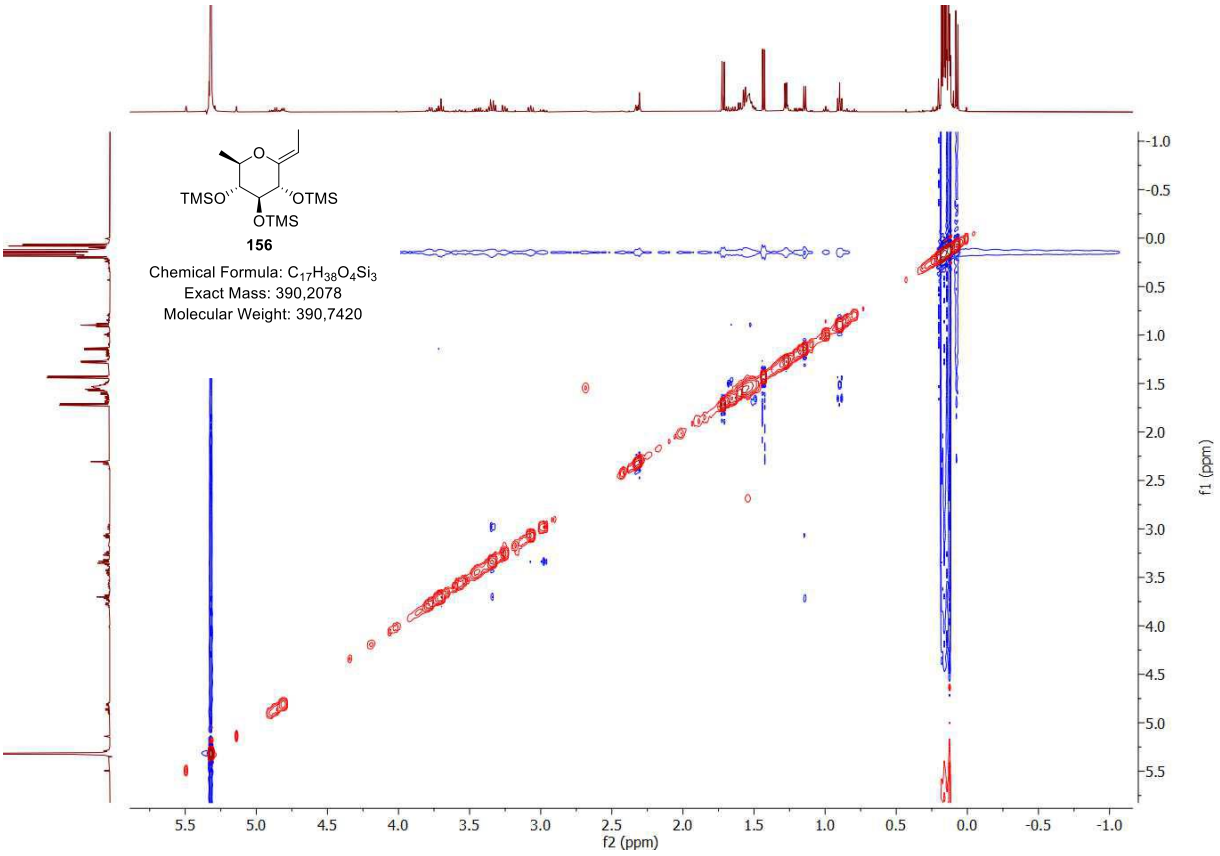

^{1}H, ^{1}H –NOESY spectrum of **156** (500 MHz, CD_2Cl_2)

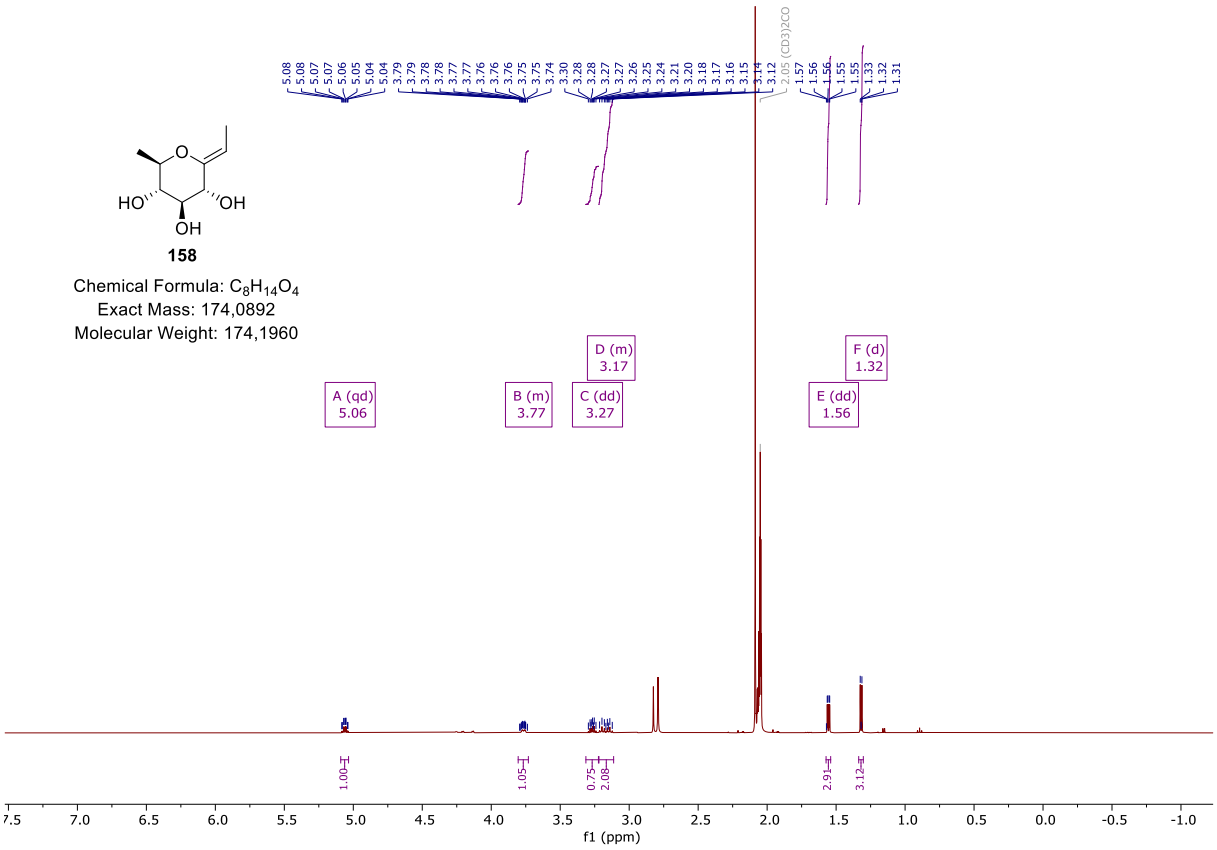

^{1}H – NMR spectrum of **158** (500 MHz, Acetone-d6)

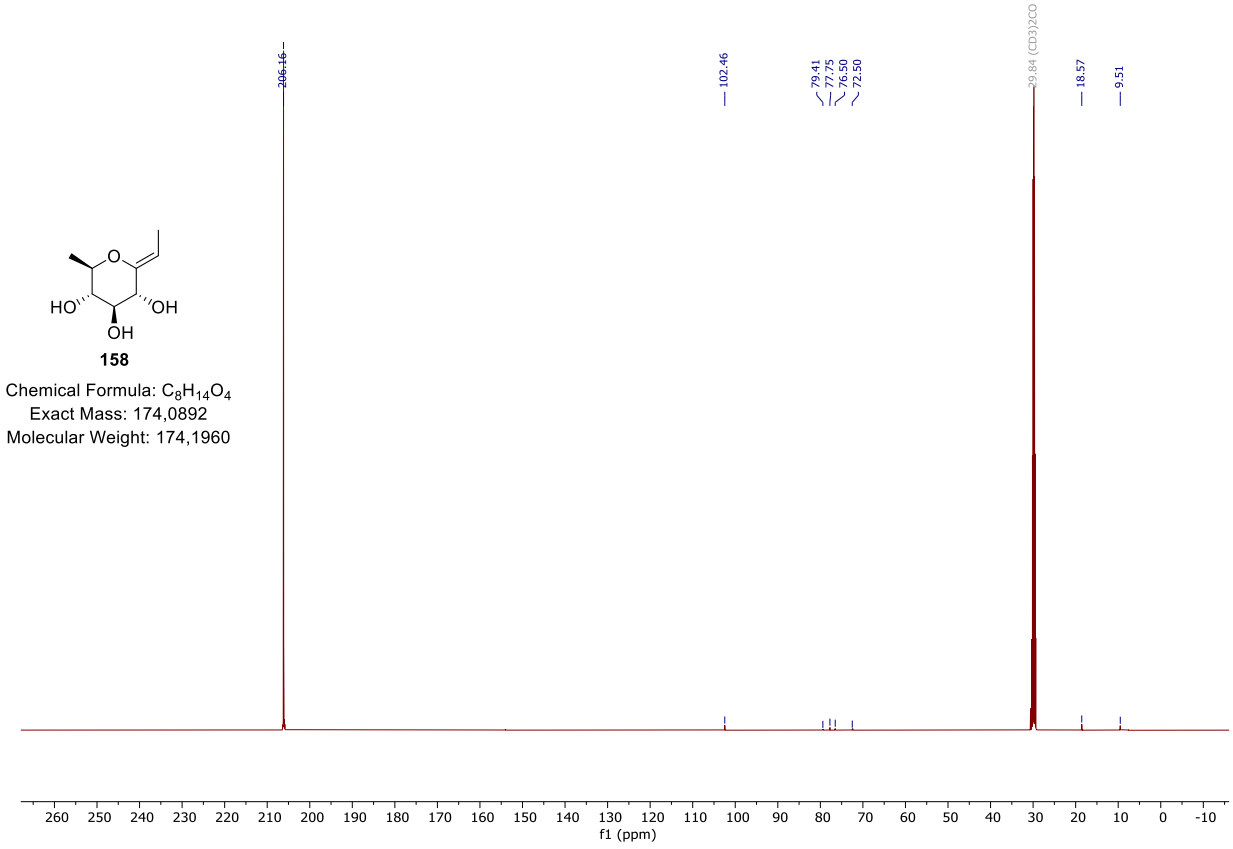

^{13}C – NMR spectrum of **158** (125 MHz, Acetone-d6)

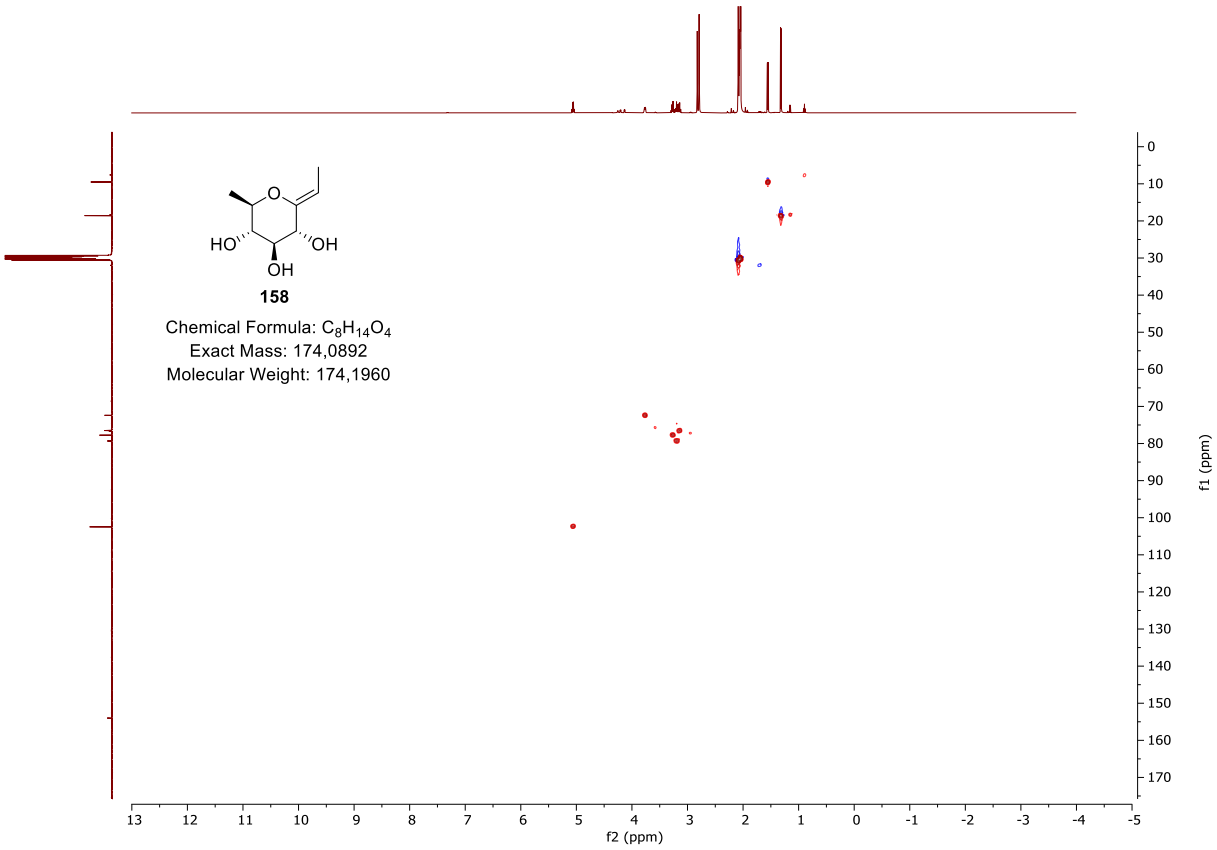

^{1}H, ^{13}C – HSQC spectrum of **158** (500 MHz, 125 MHz, Acetone-d6)

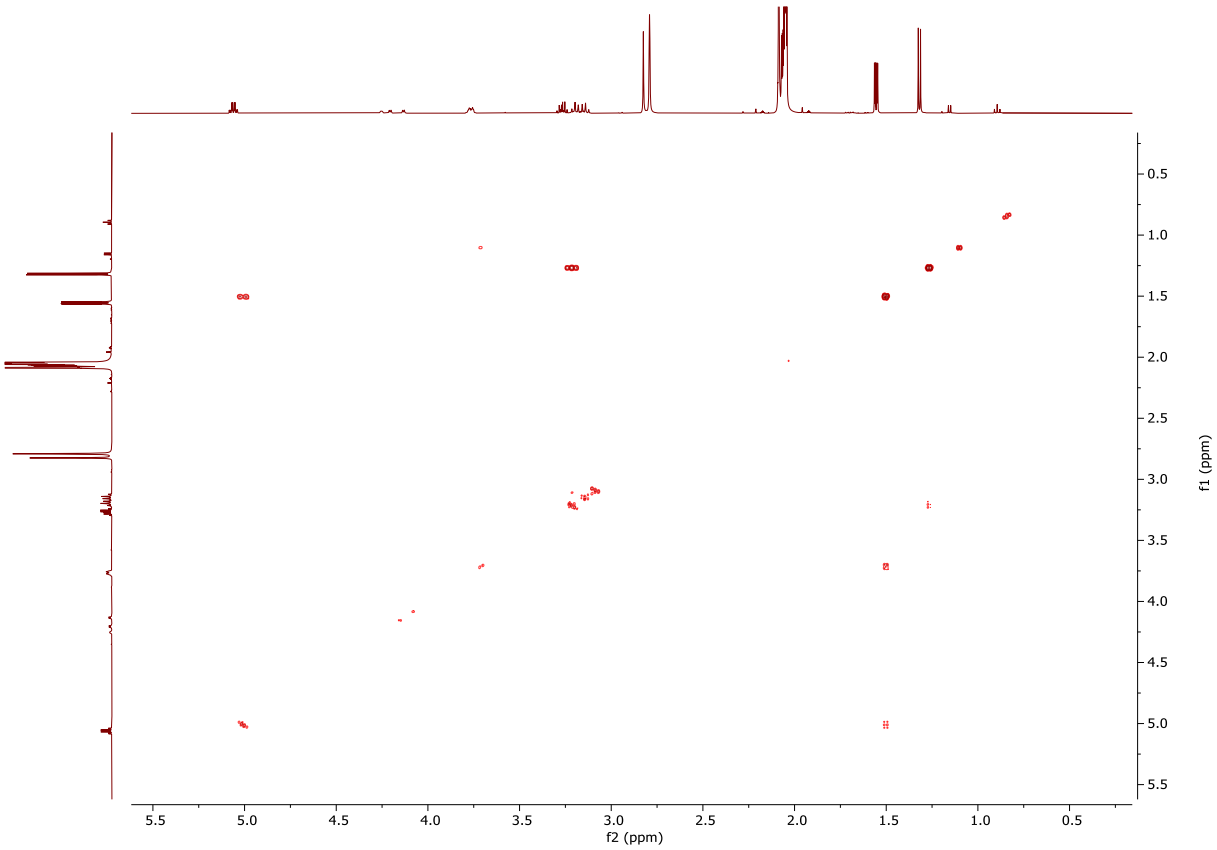

^{1}H, ^{1}H –COSY spectrum of **158** (500 MHz, Acetone-d6)

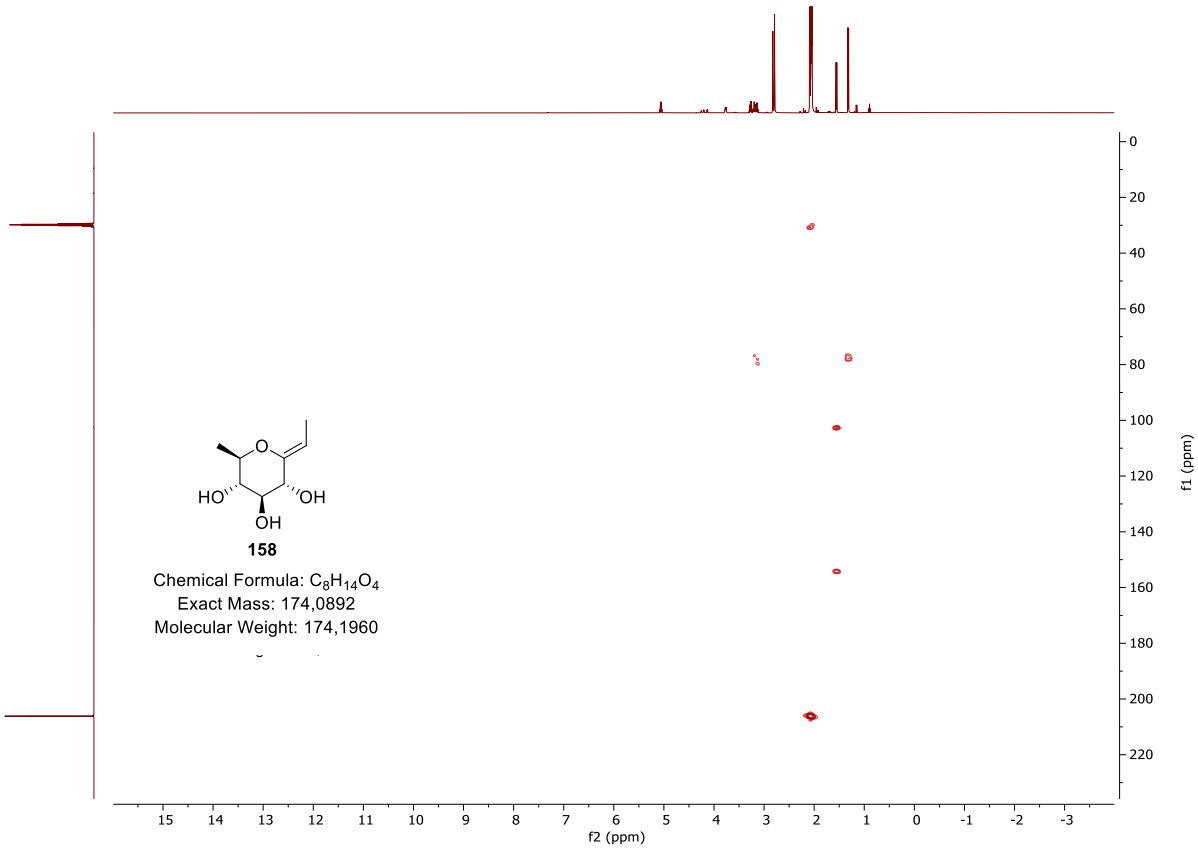

^{1}H, ^{13}C –HMBC spectrum of **158** (500 MHz, 125 MHz, Acetone-d6)

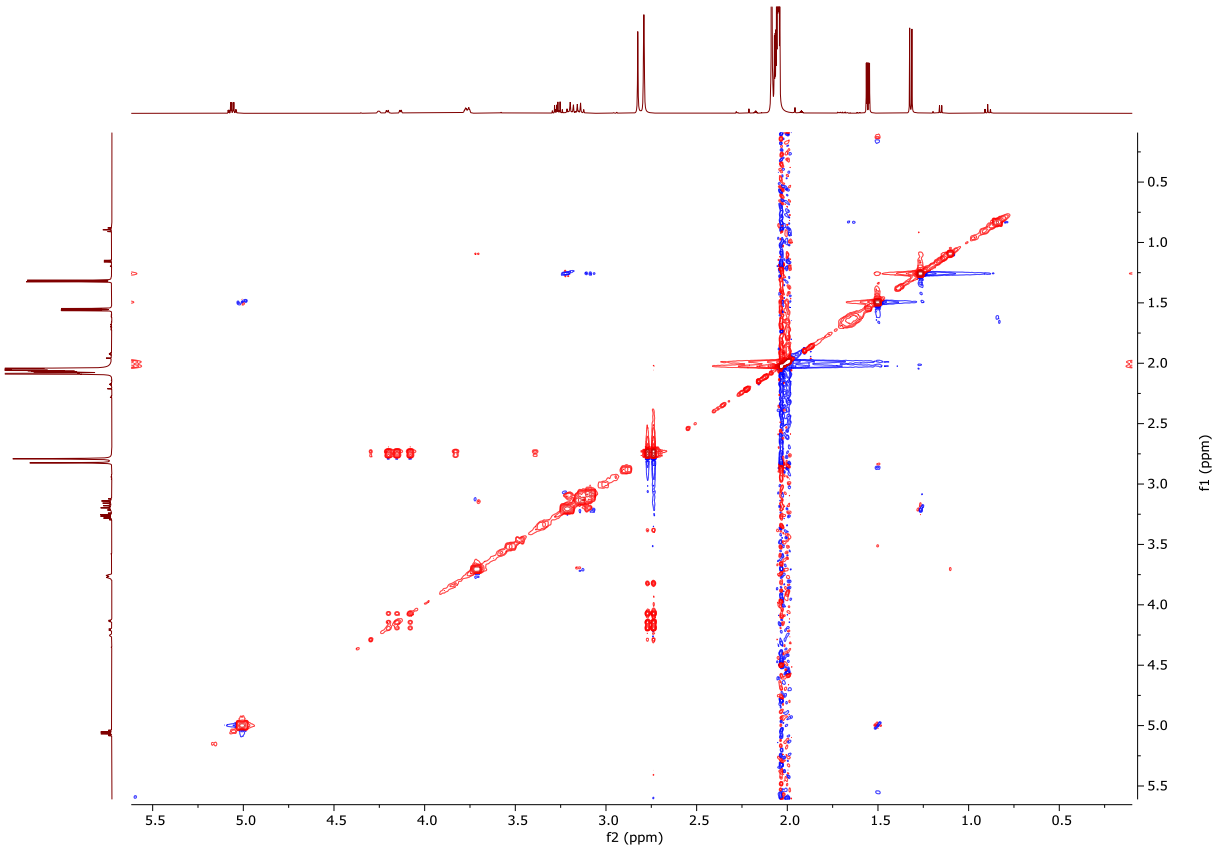

^{1}H, ^{1}H –NOESY spectrum of **158** (500 MHz, Acetone-d6)

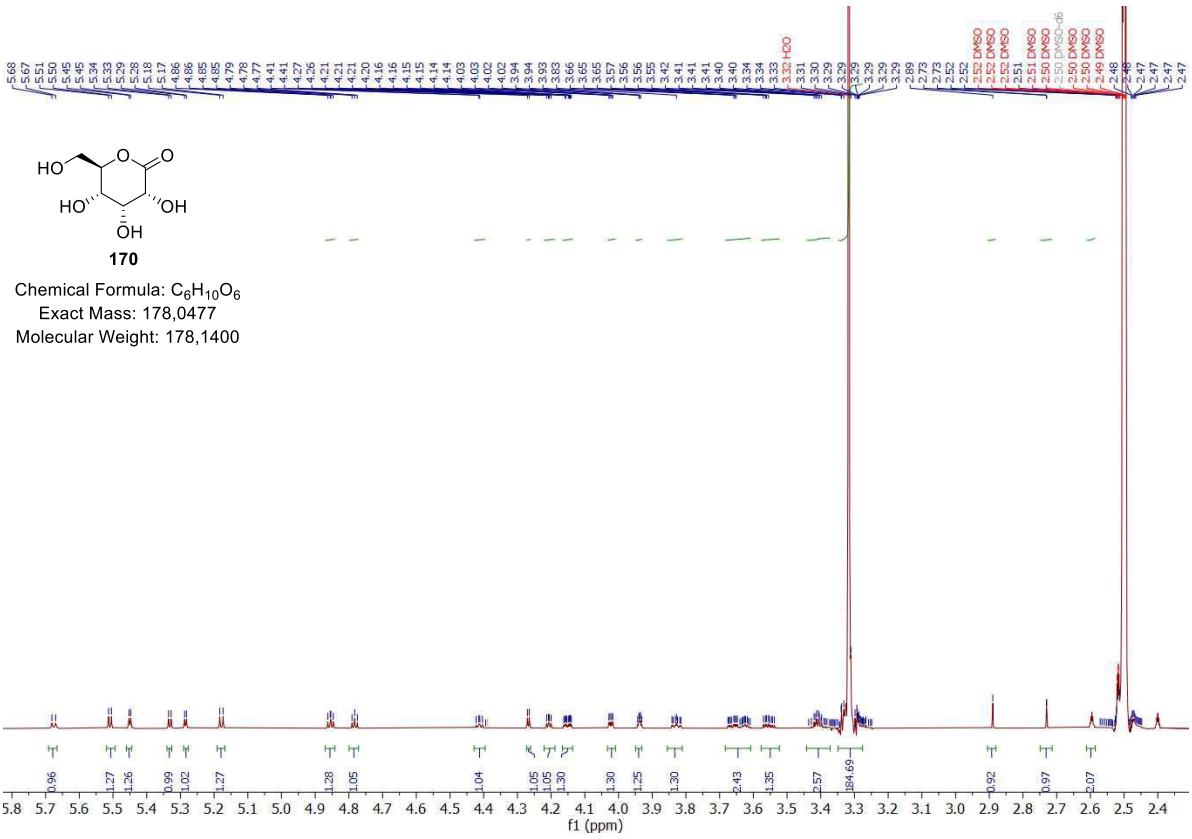

^{1}H – NMR spectrum of **170** (700 MHz, DMSO-d6)

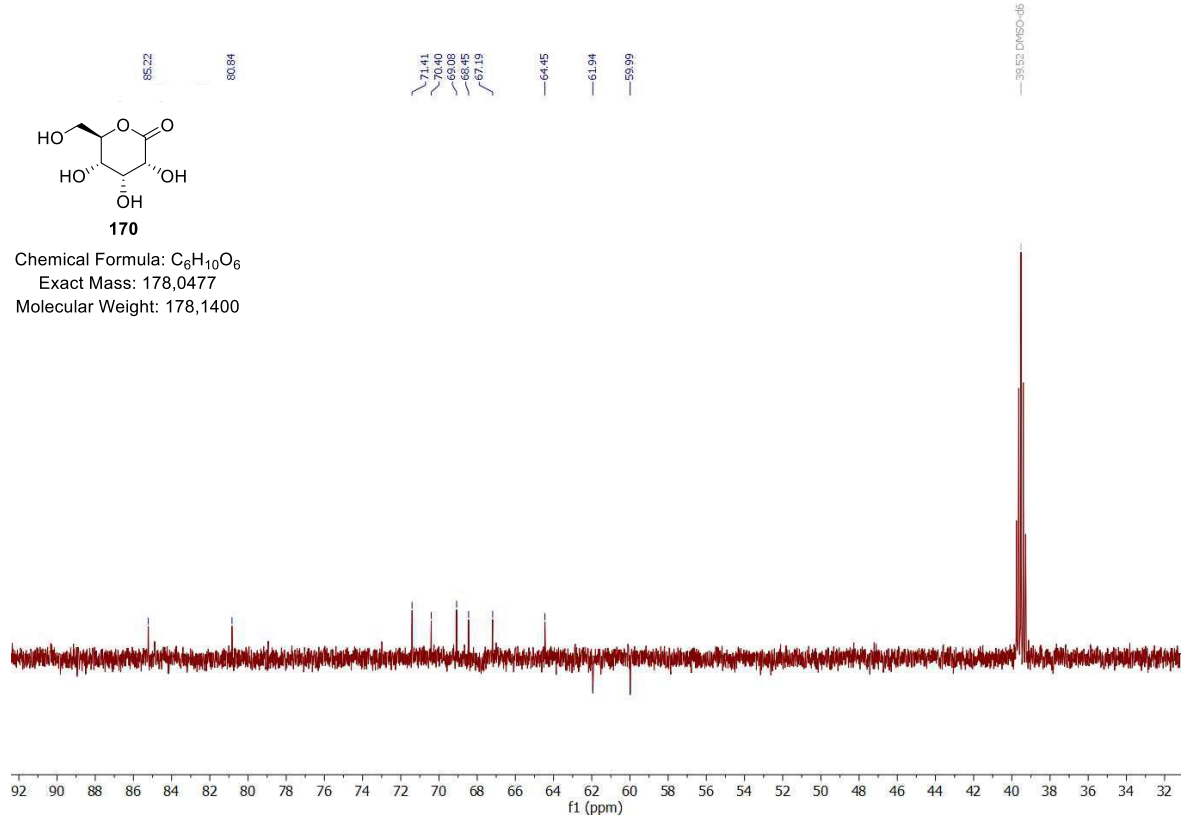

^{13}C – NMR spectrum of **170** (175 MHz, DMSO-d6)

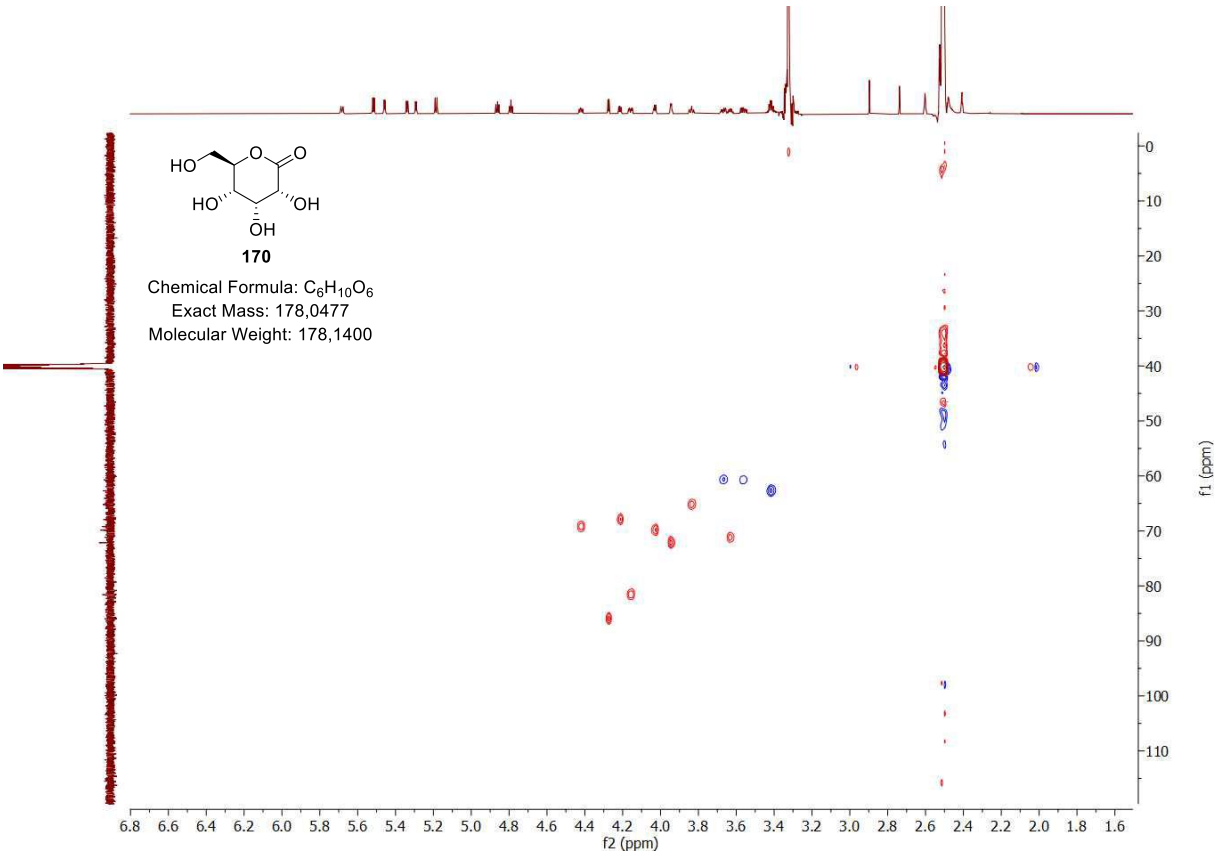

^{1}H, ^{13}C – HSQC spectrum of **170** (700 MHz, 175 MHz, DMSO-d6)

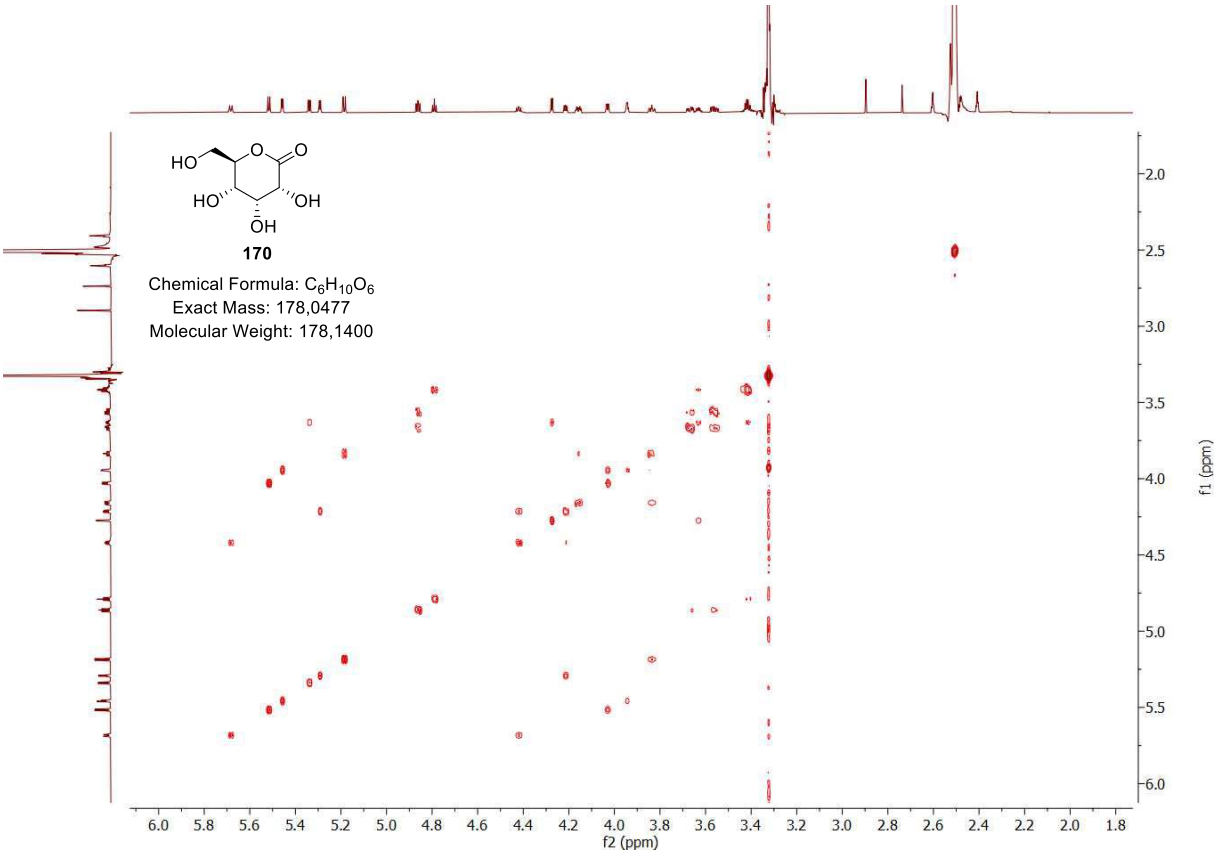

^{1}H, ^{1}H –COSY spectrum of **170** (700 MHz, DMSO-d6)

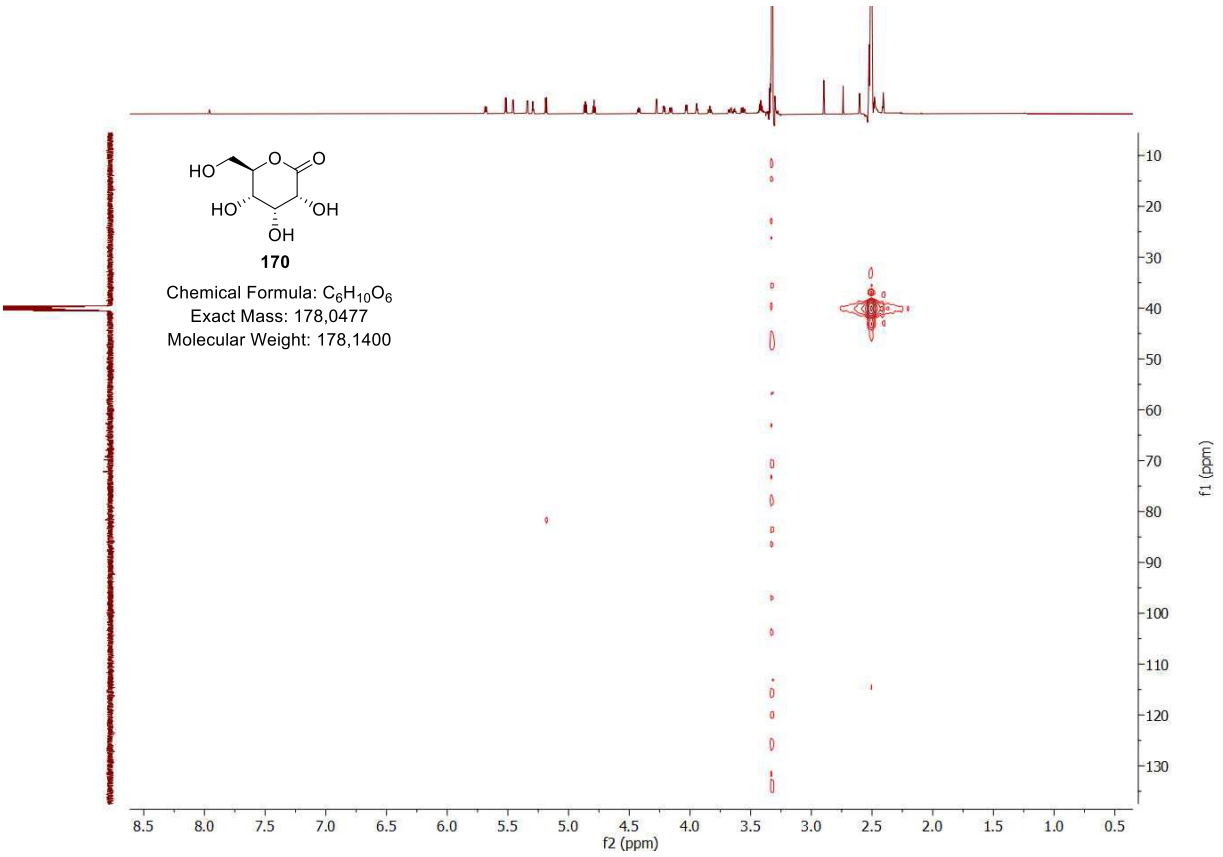

^{1}H, ^{13}C –HMBC spectrum of **170** (700 MHz, 175 MHz, DMSO-d6)

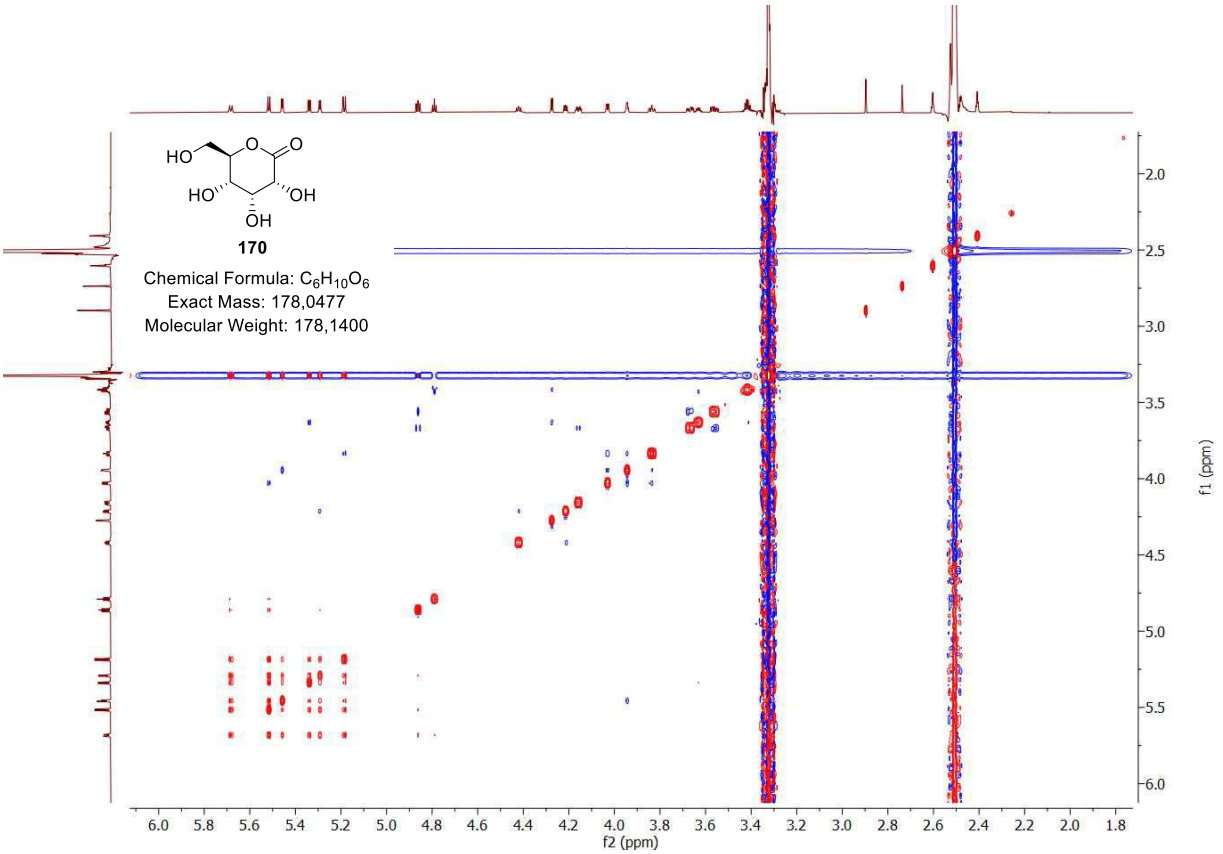

^{1}H, ^{1}H –NOESY spectrum of **170** (700 MHz, DMSO-d6)

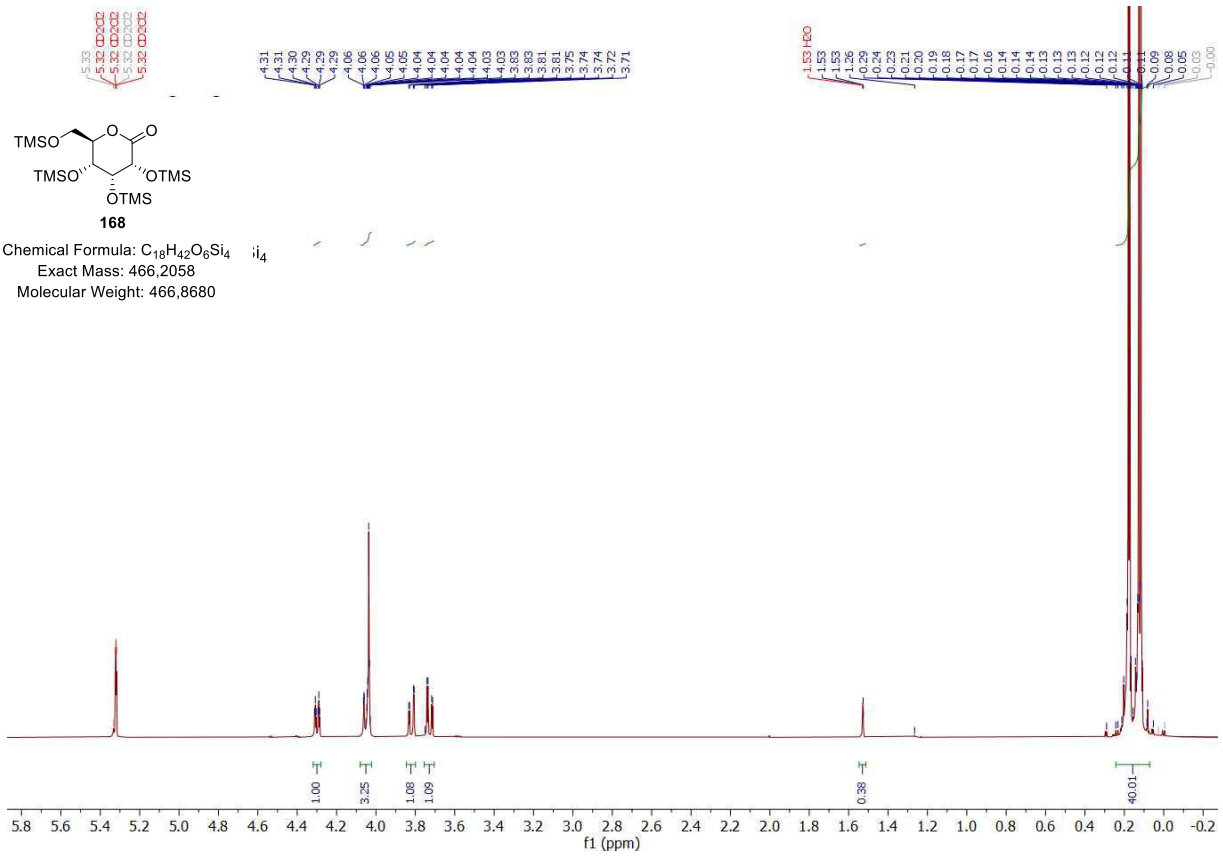

^{1}H – NMR spectrum of **168** (500 MHz, CD_2Cl_2)

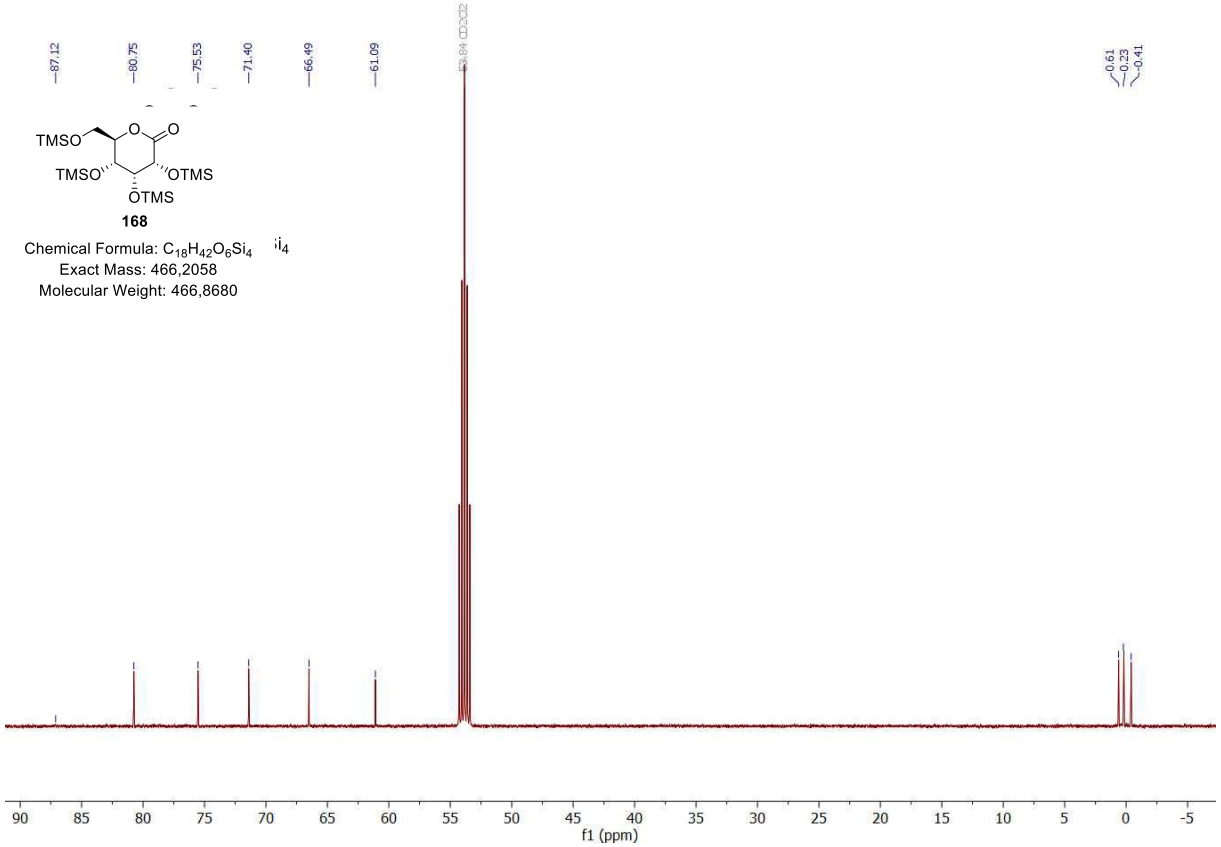

^{13}C – NMR spectrum of **168** (125 MHz, CD_2Cl_2)

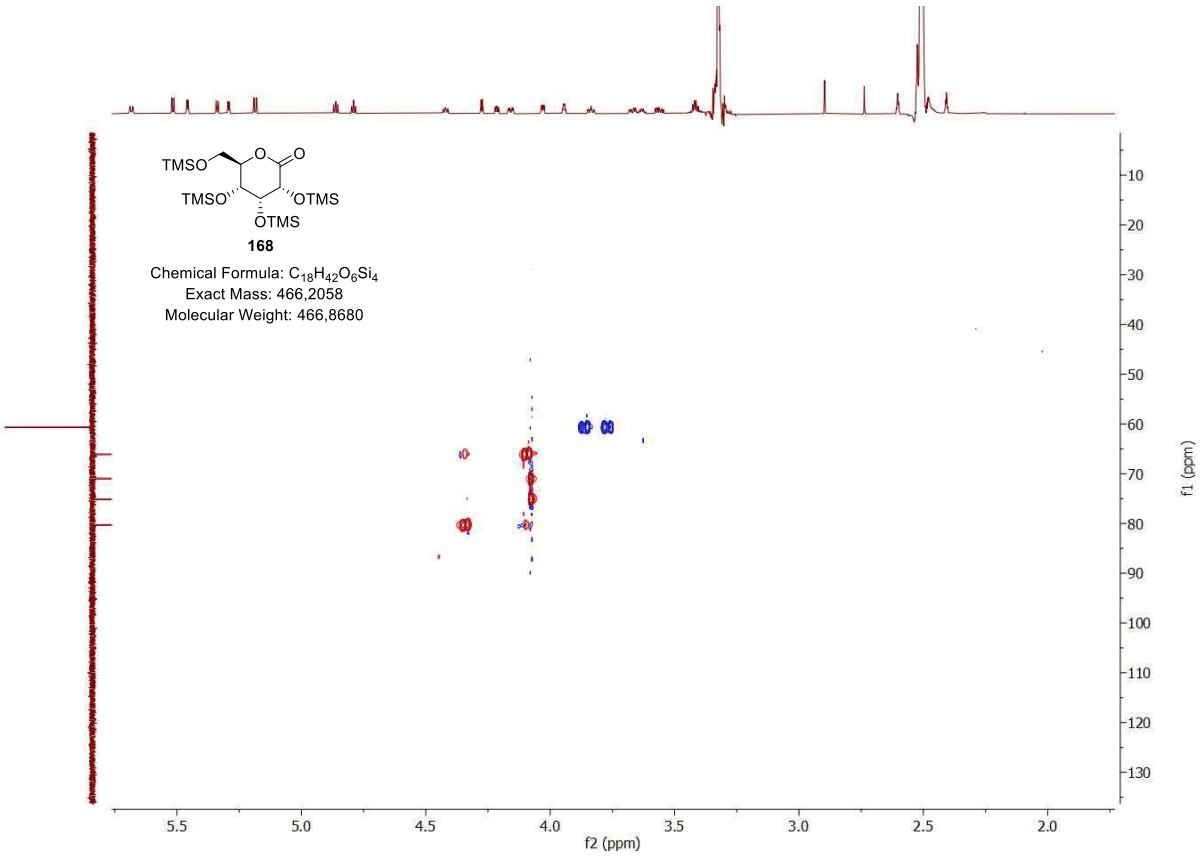

^{1}H, ^{13}C – HSQC spectrum of **168** (500 MHz, 125 MHz, CD_2Cl_2)

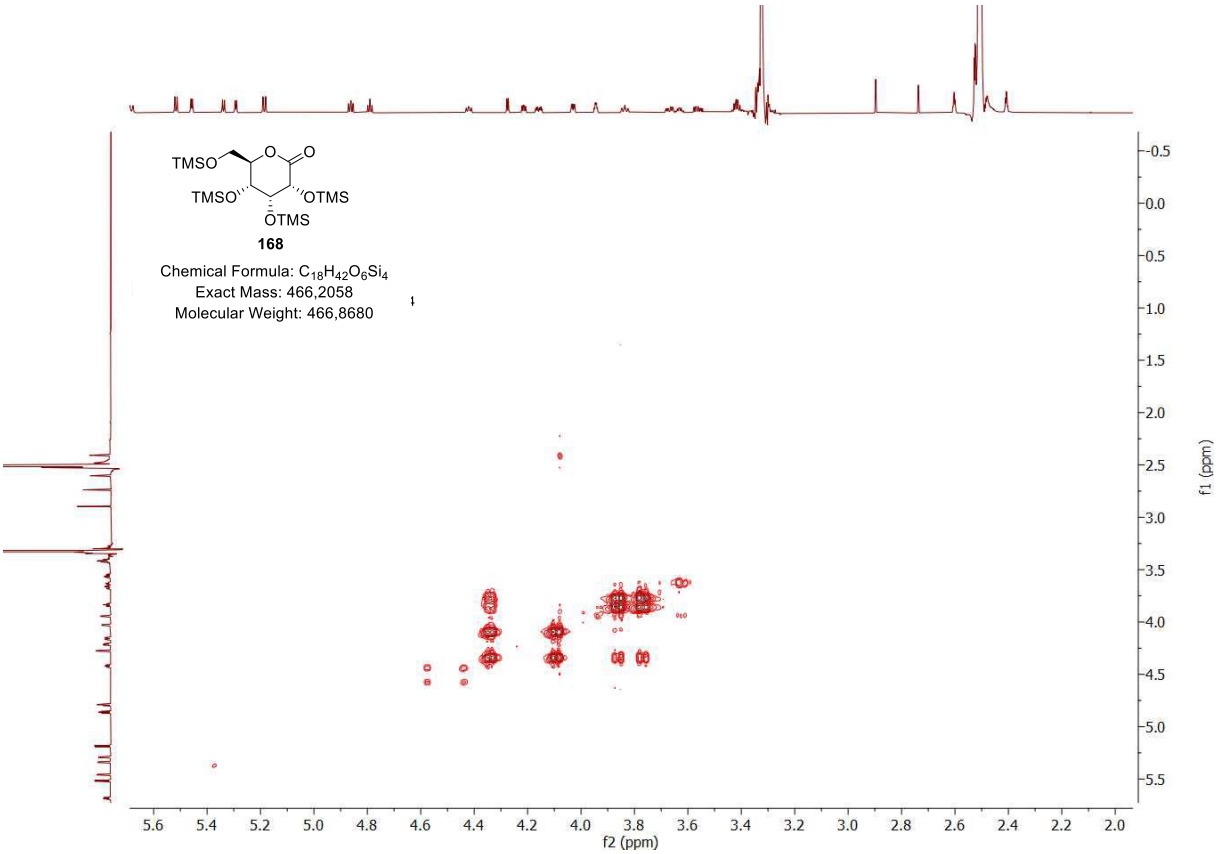

^{1}H, ^{1}H –COSY spectrum of **168** (500 MHz, CD_2Cl_2)

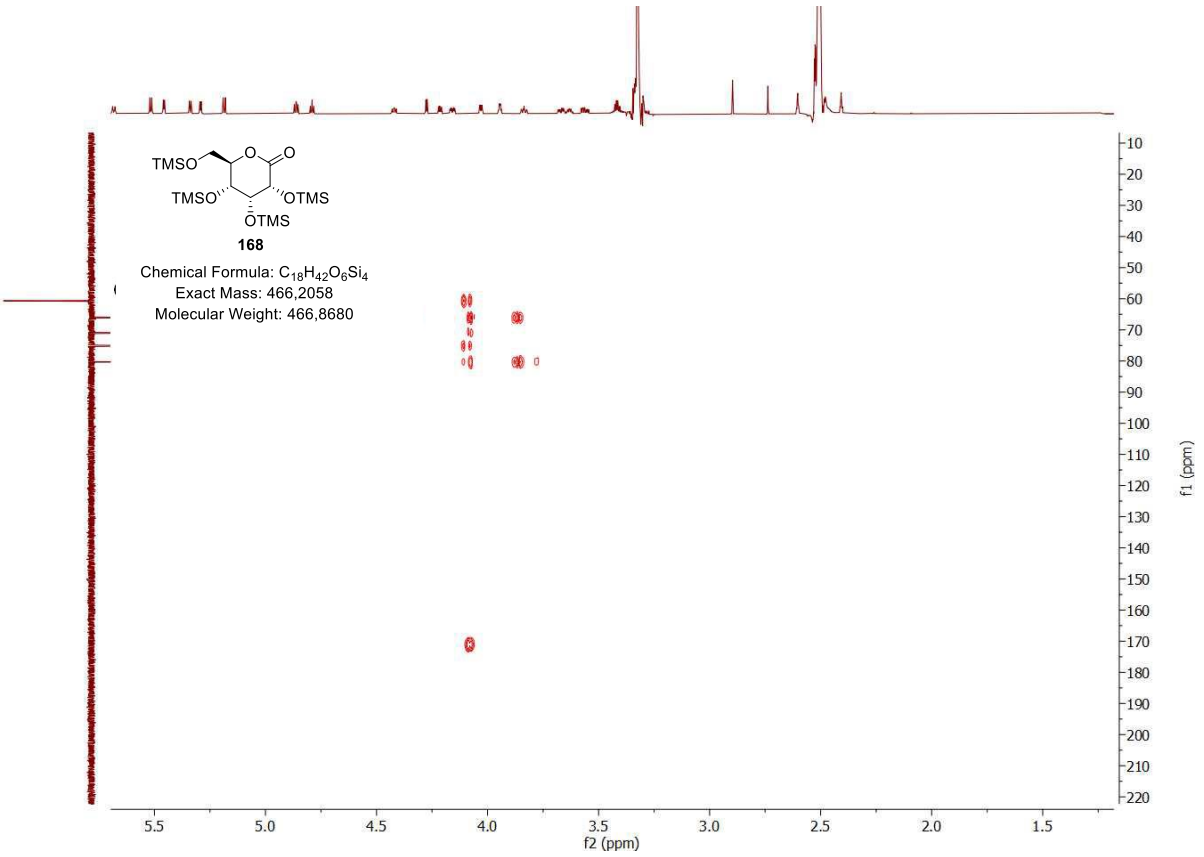

^{1}H, ^{13}C –HMBC spectrum of **168** (500 MHz, 125 MHz, CD_2Cl_2)

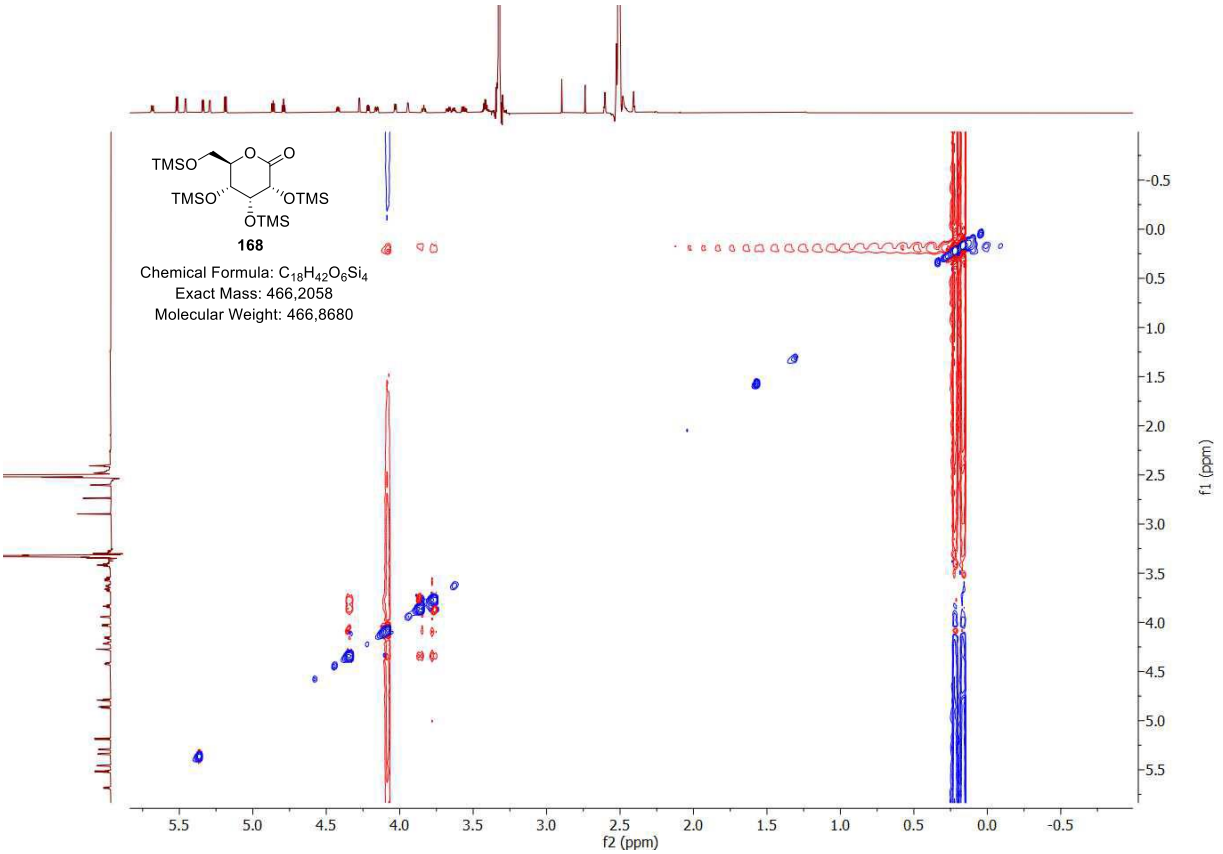

^{1}H, ^{1}H –NOESY spectrum of **168** (500 MHz, CD_2Cl_2)

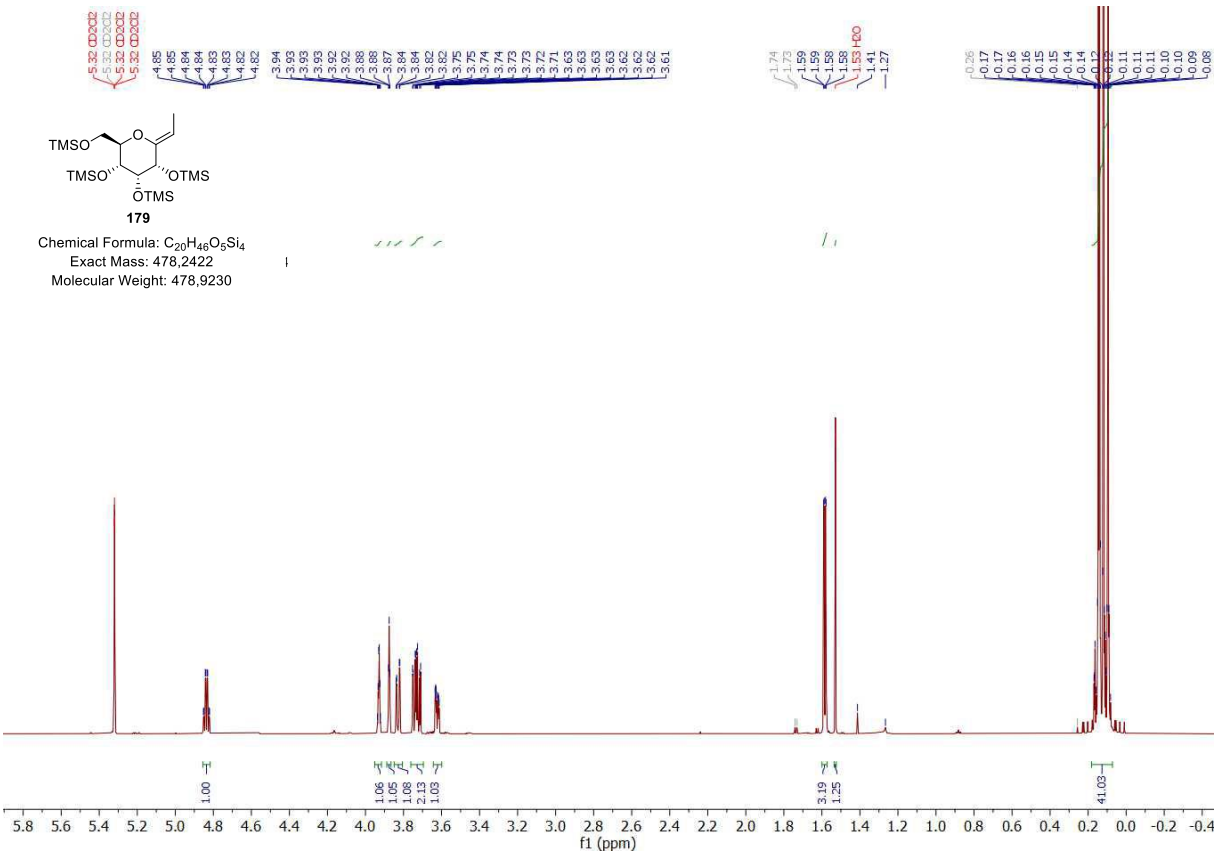

^{1}H – NMR spectrum of **179** (700 MHz, CD_2Cl_2)

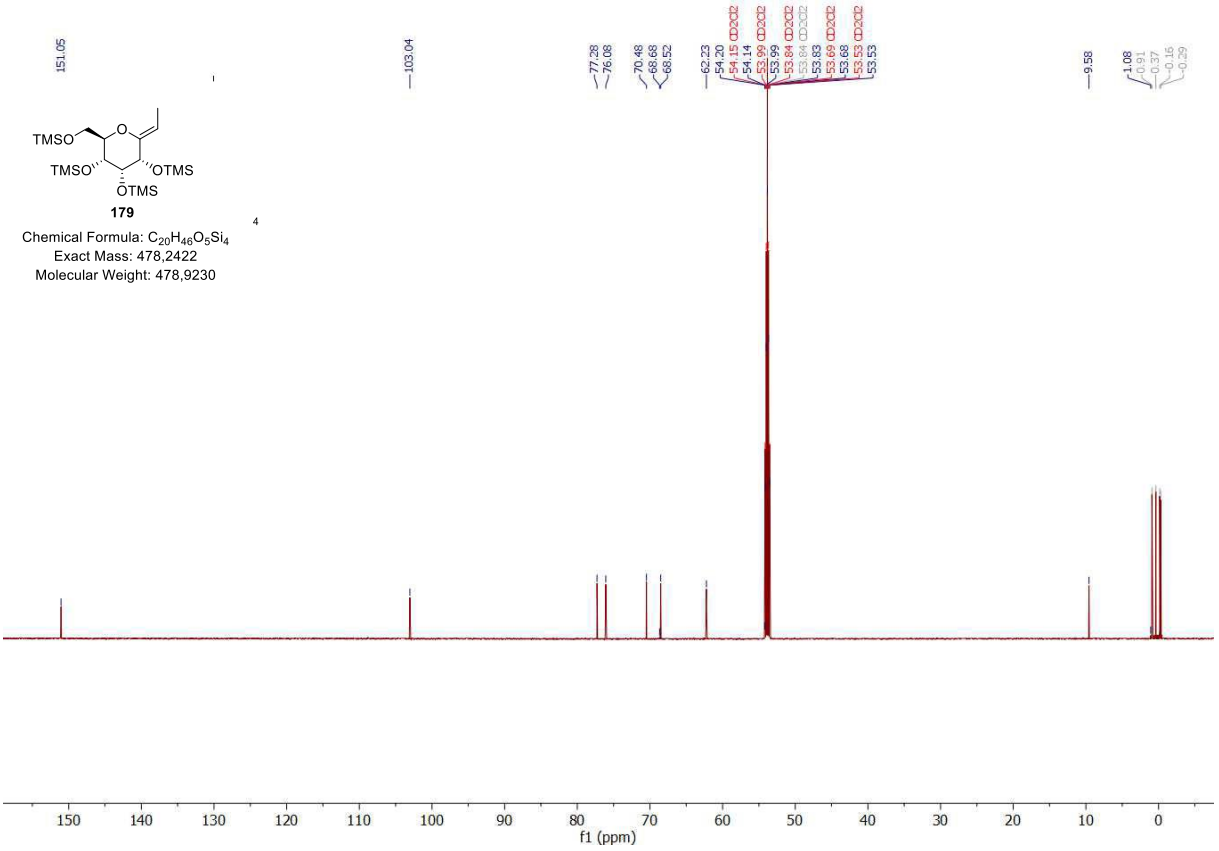

^{13}C – NMR spectrum of **179** (175 MHz, CD_2Cl_2)

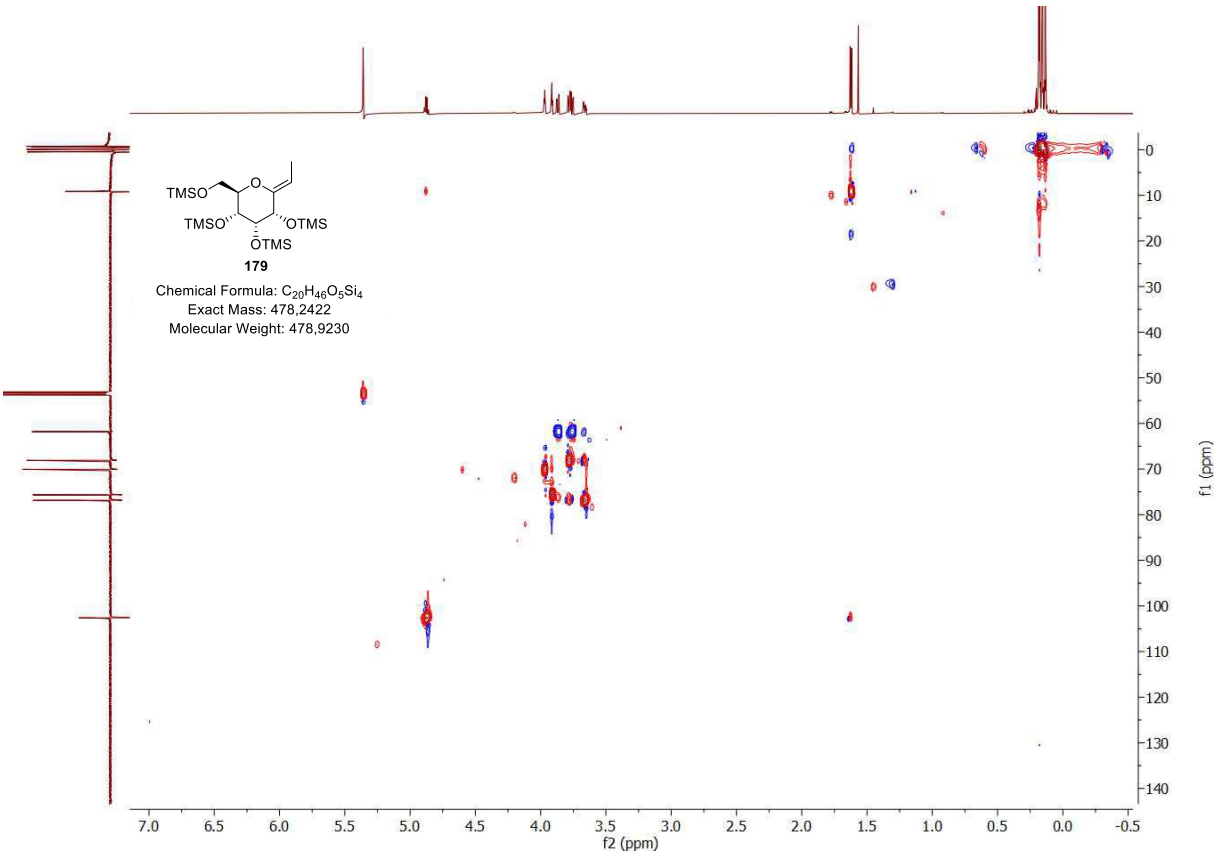

^{1}H, ^{13}C – HSQC spectrum of **179** (700 MHz, 175 MHz, CD_2Cl_2)

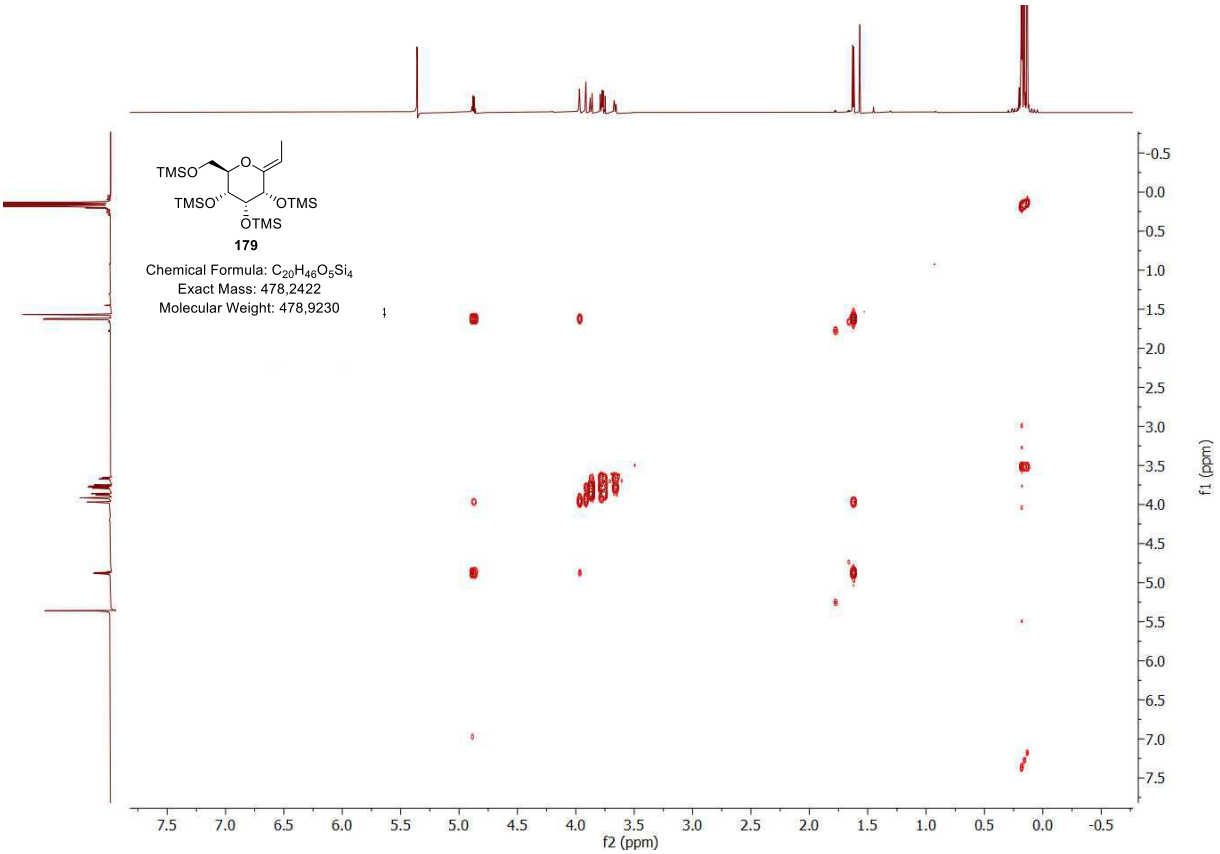

^{1}H, ^{1}H –COSY spectrum of **179** (700 MHz, CD_2Cl_2)

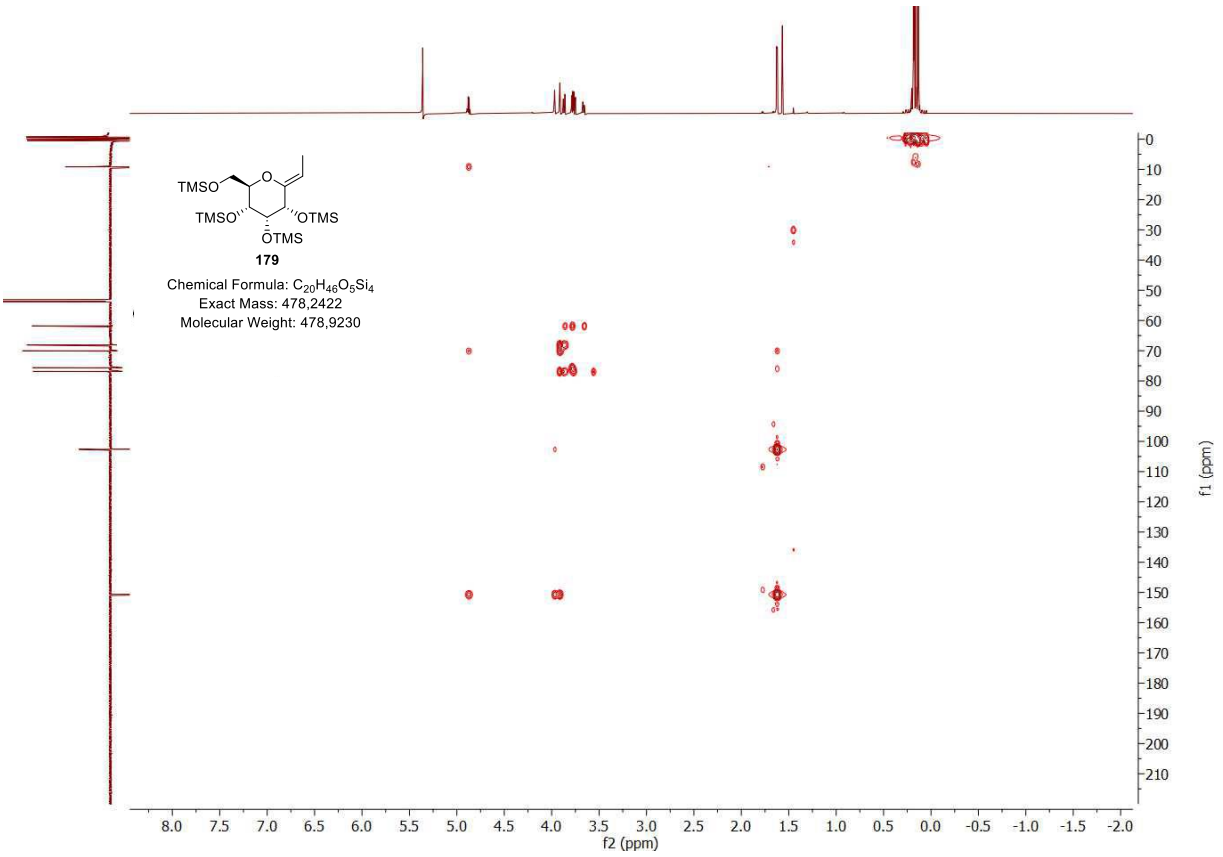

^{1}H, ^{13}C –HMBC spectrum of **179** (700 MHz, 175 MHz, CD_2Cl_2)

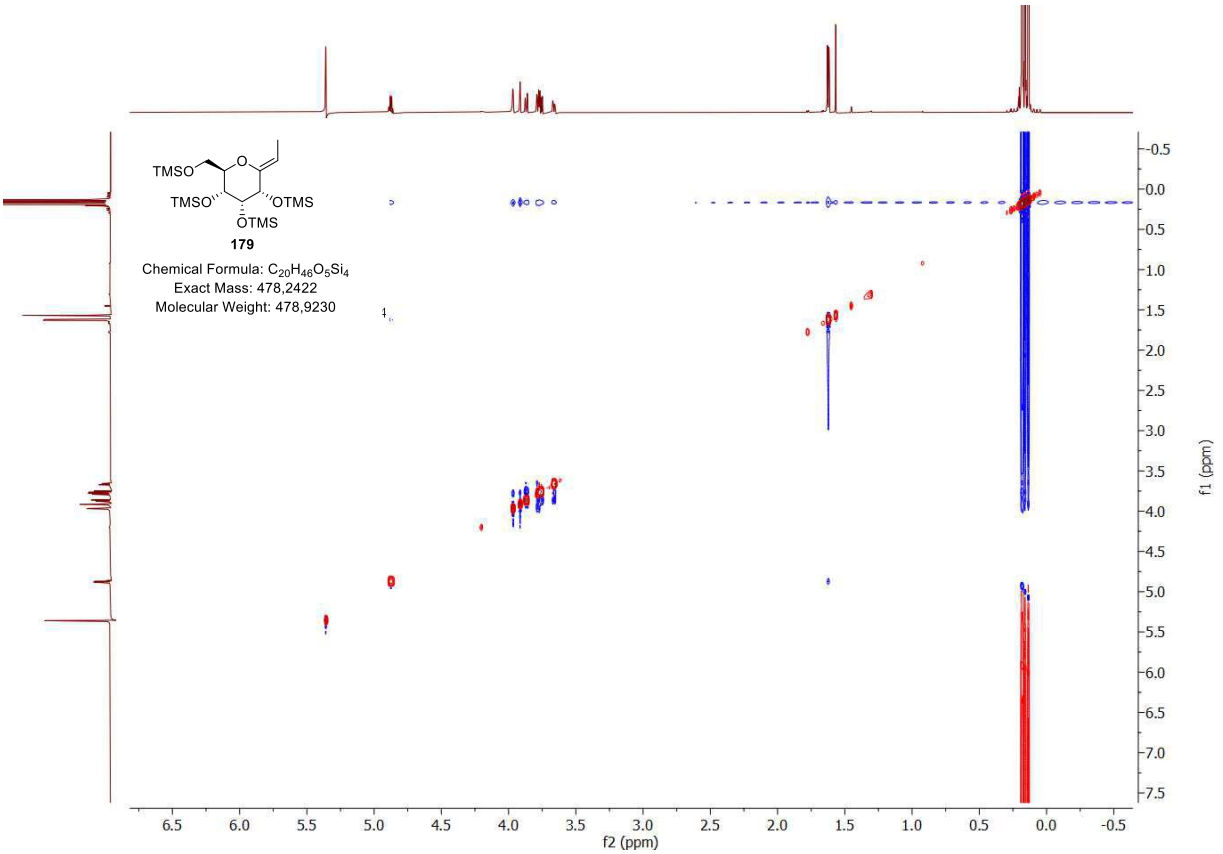

^{1}H, ^{1}H –NOESY spectrum of **179** (700 MHz, CD_2Cl_2)

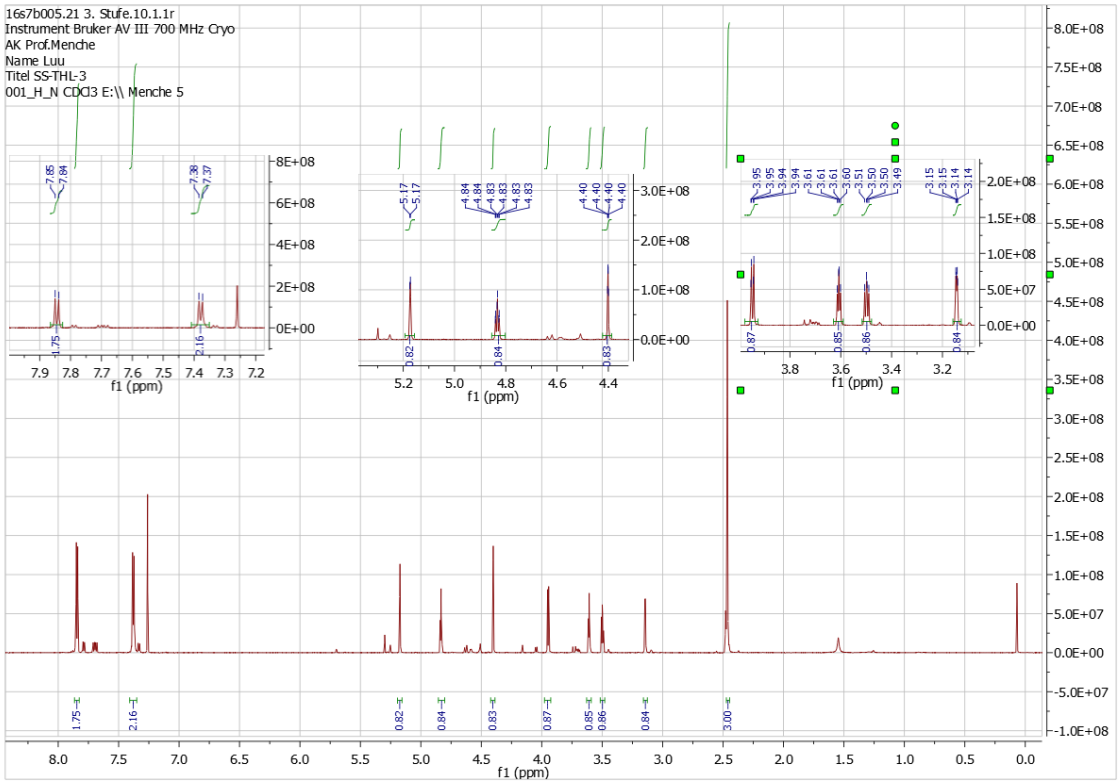

^{1}H – NMR spectrum of **142** (500 MHz, $CDCl_3$)

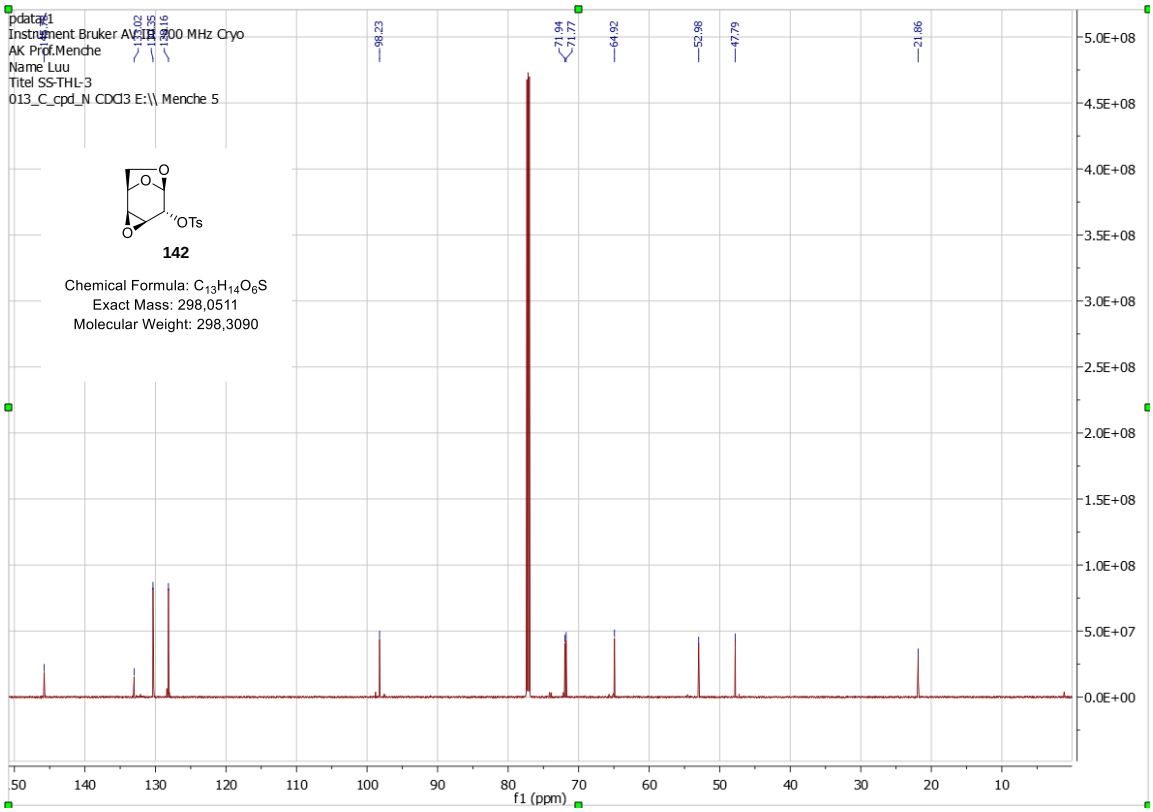

^{13}C – NMR spectrum of **142** (125 MHz, $CDCl_3$)

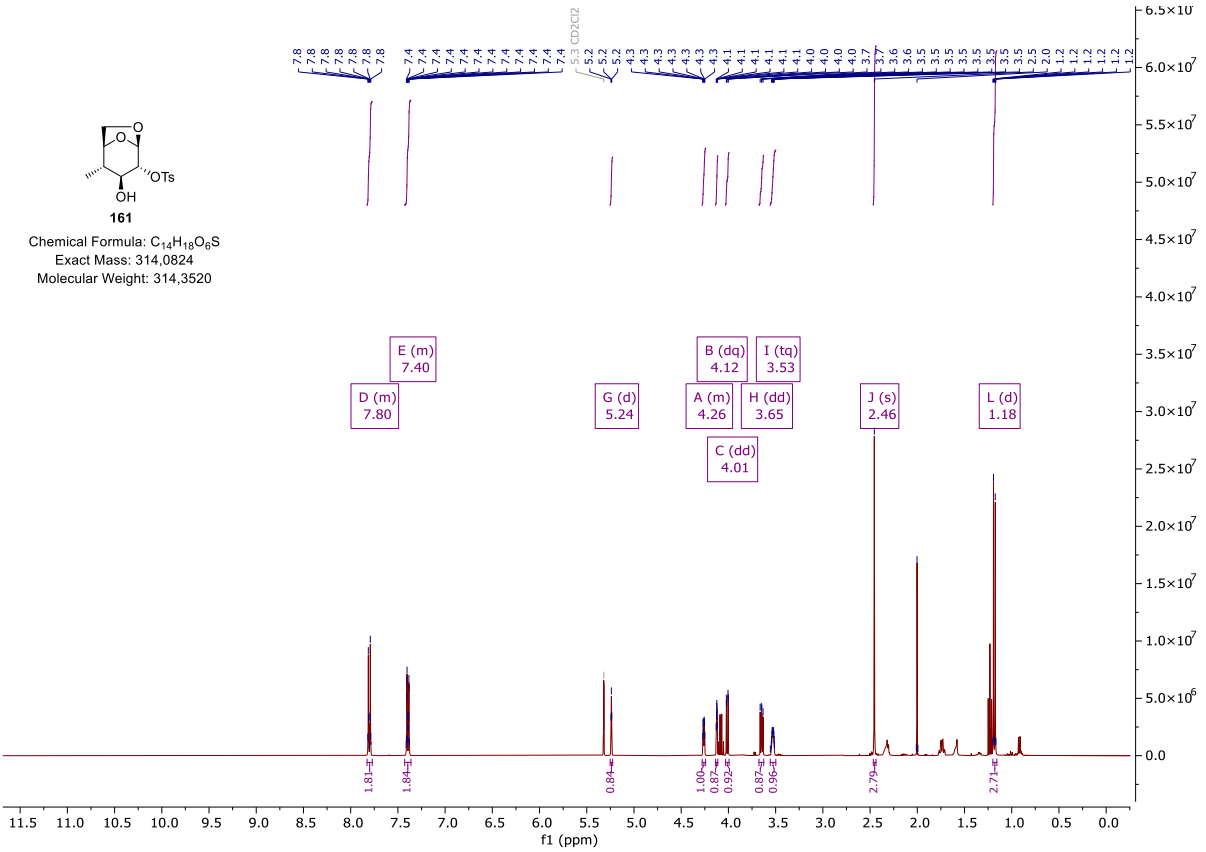

^{1}H – NMR spectrum of **161** (400 MHz, CD_2Cl_2)

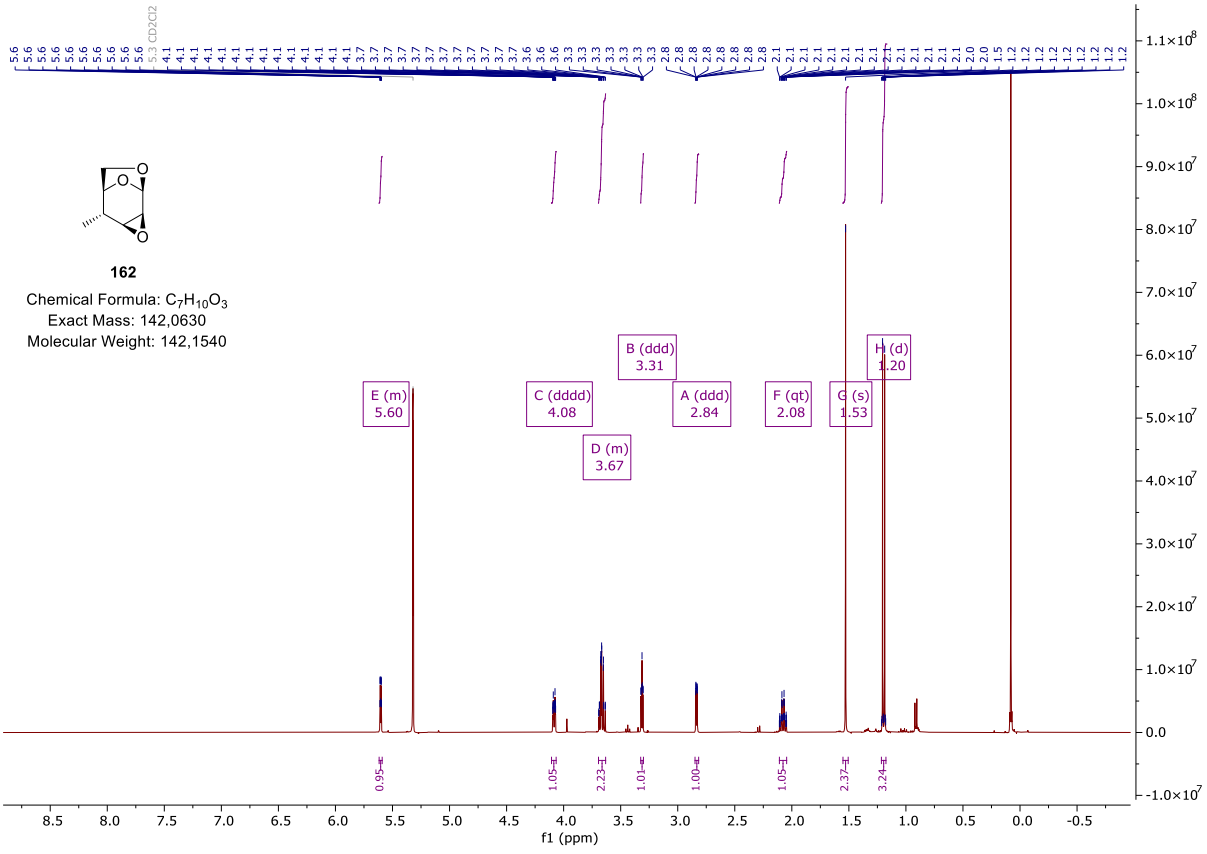

^{1}H – NMR spectrum of **162** (400 MHz, CD_2Cl_2)

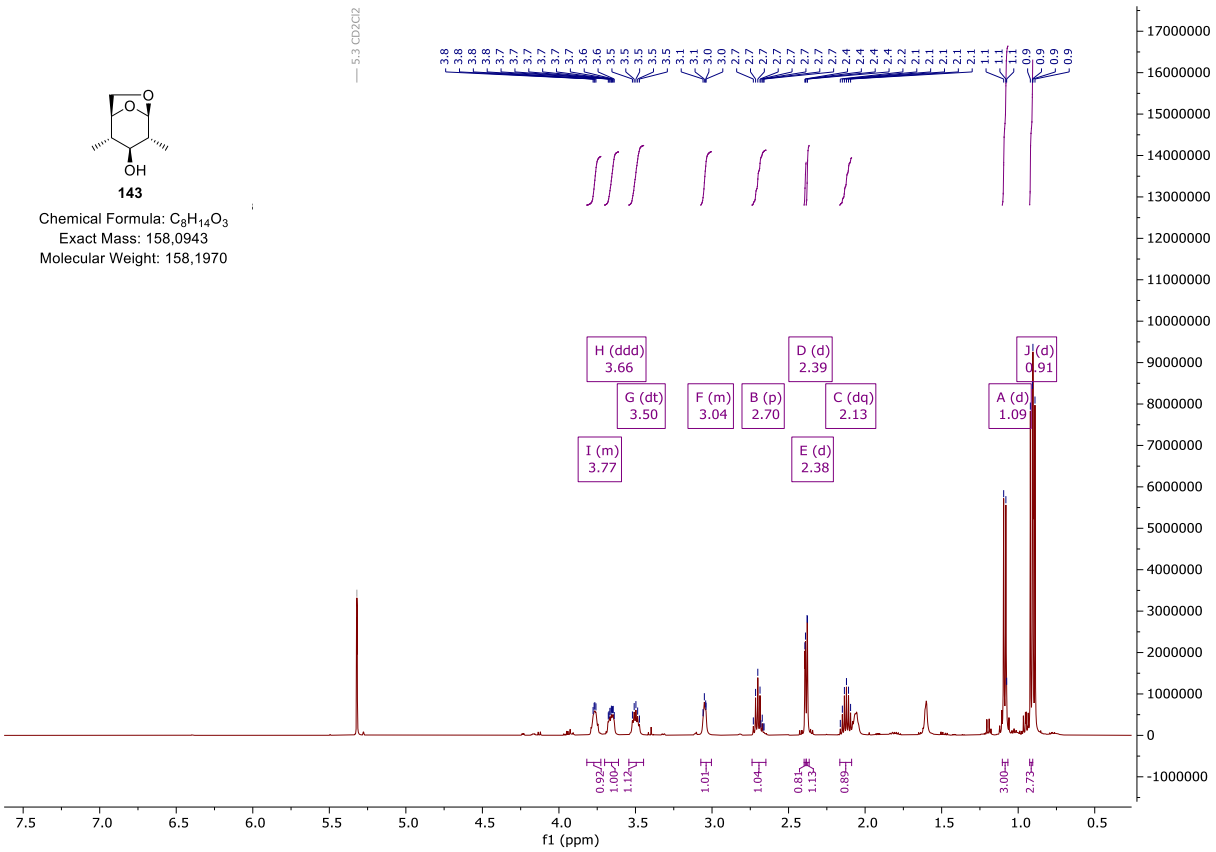

^{1}H – NMR spectrum of **143** (500 MHz, CD_2Cl_2)

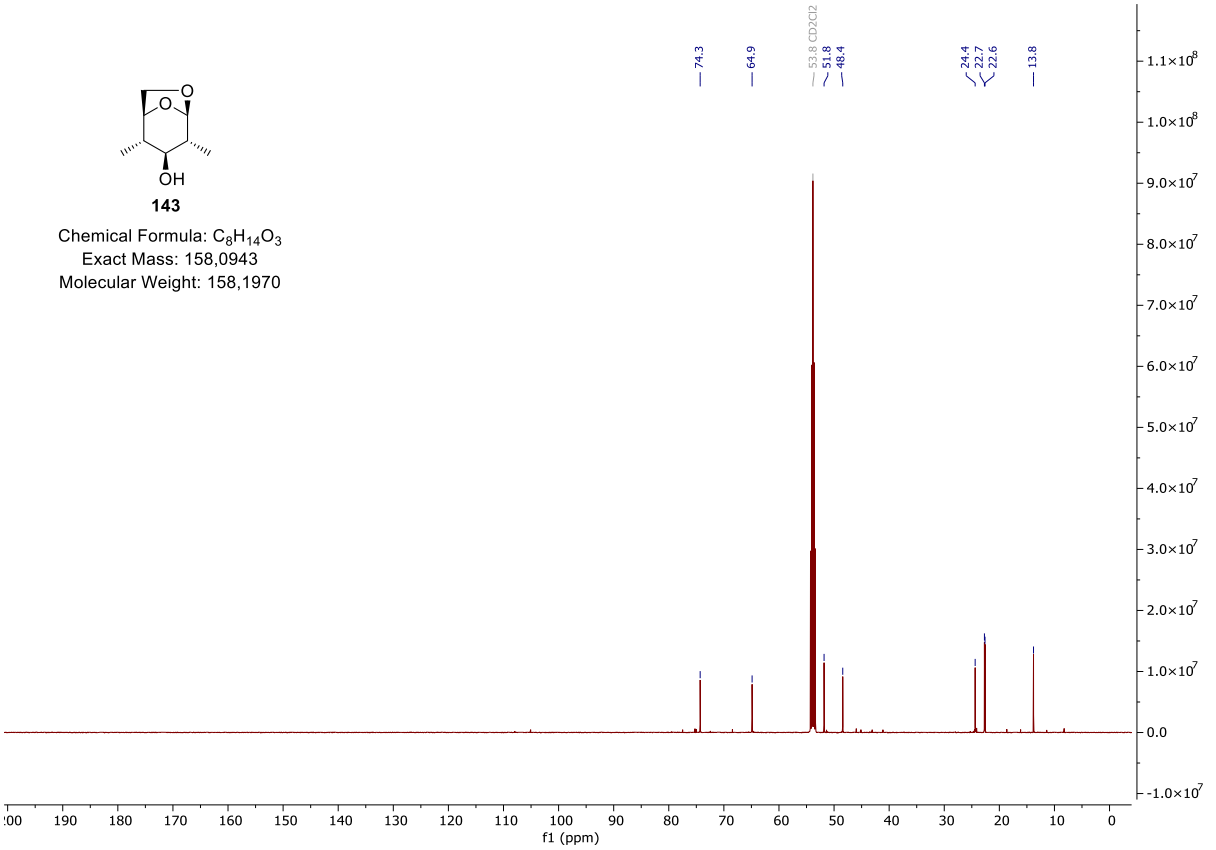

^{13}C – NMR spectrum of **143** (125 MHz, CD_2Cl_2)

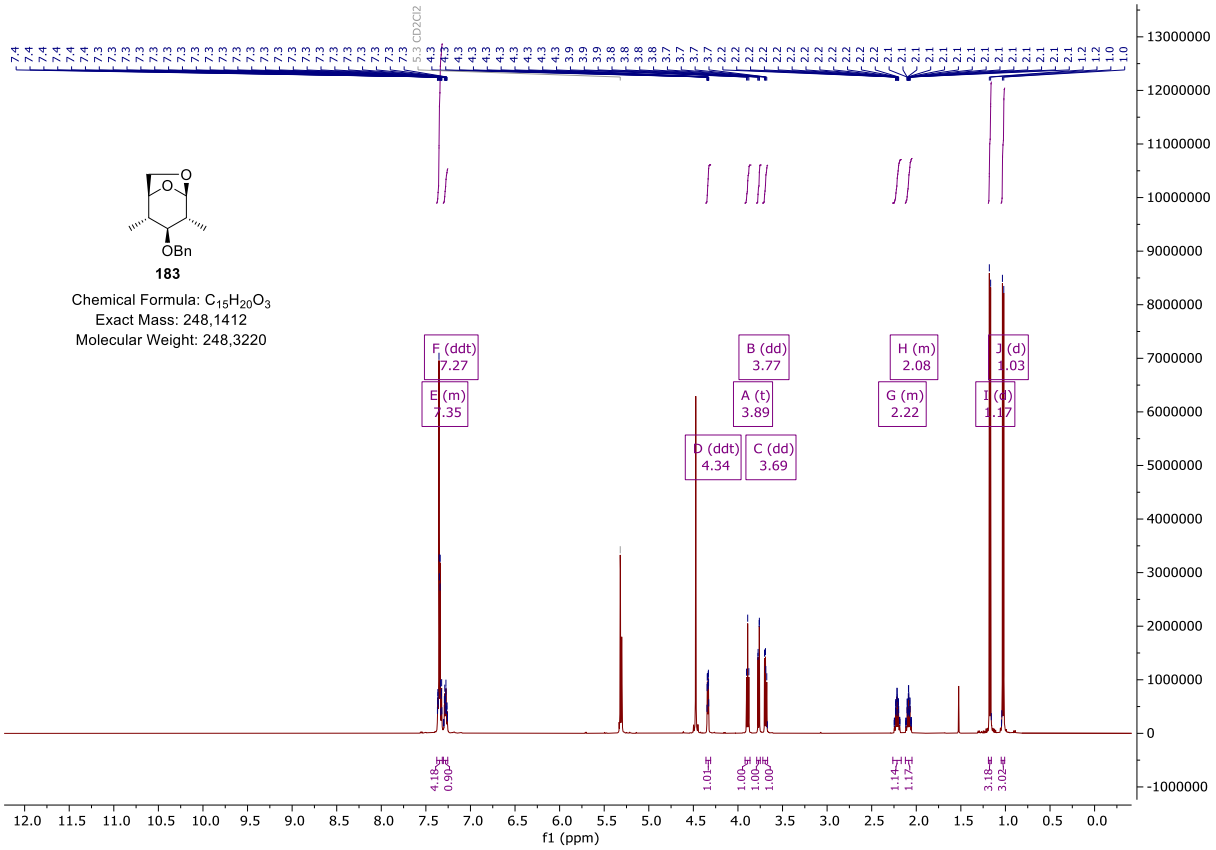

^{1}H – NMR spectrum of **183** (CD_2Cl_2)

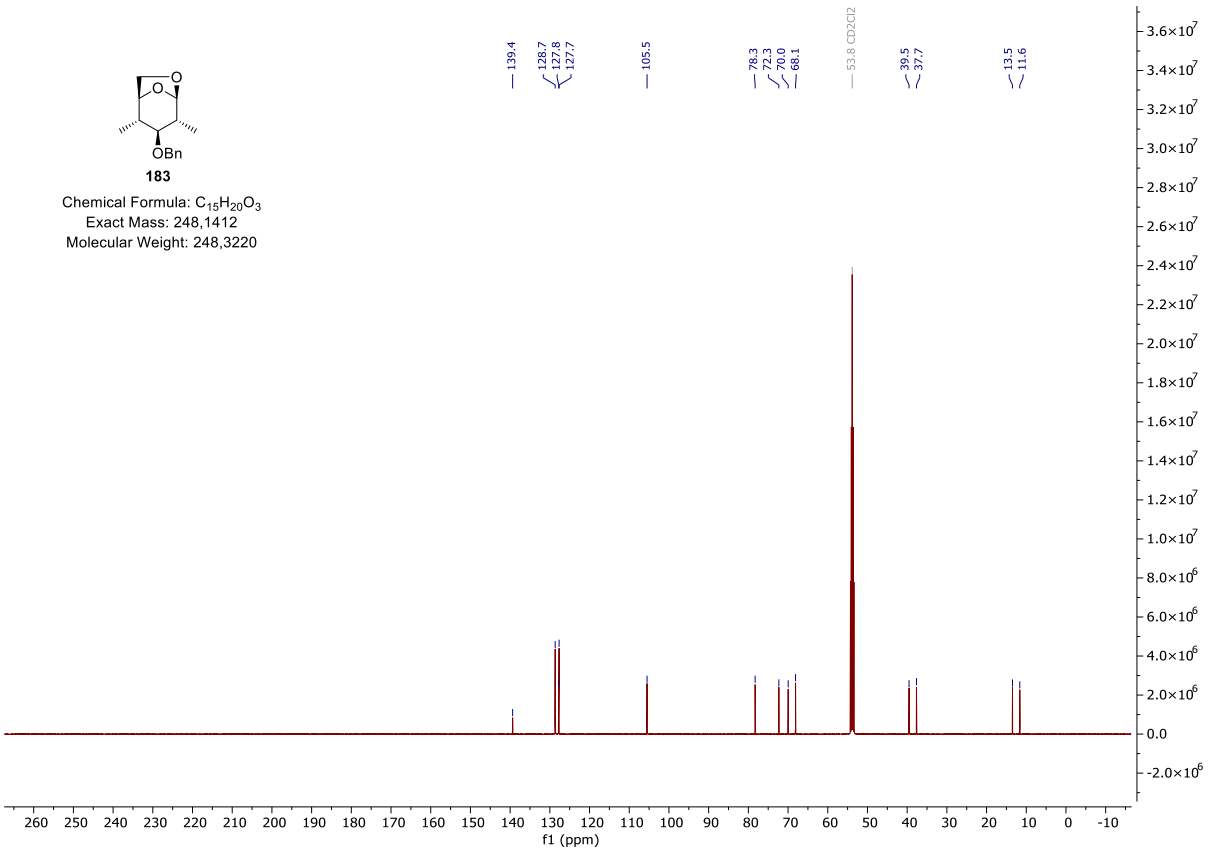

^{13}C – NMR spectrum of **183** (CD_2Cl_2)

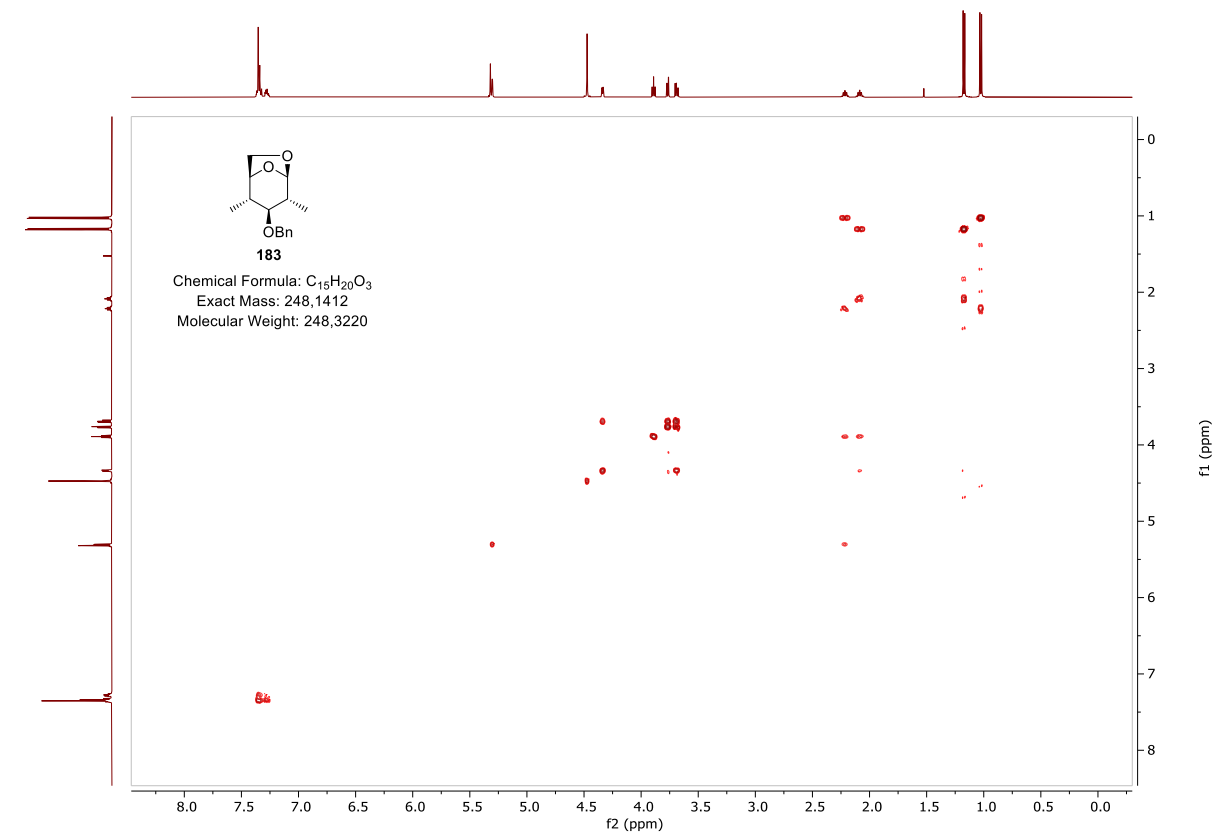

^{1}H, ^{1}H – COSY spectrum of **183** (500 MHz, $CDCl_3$)

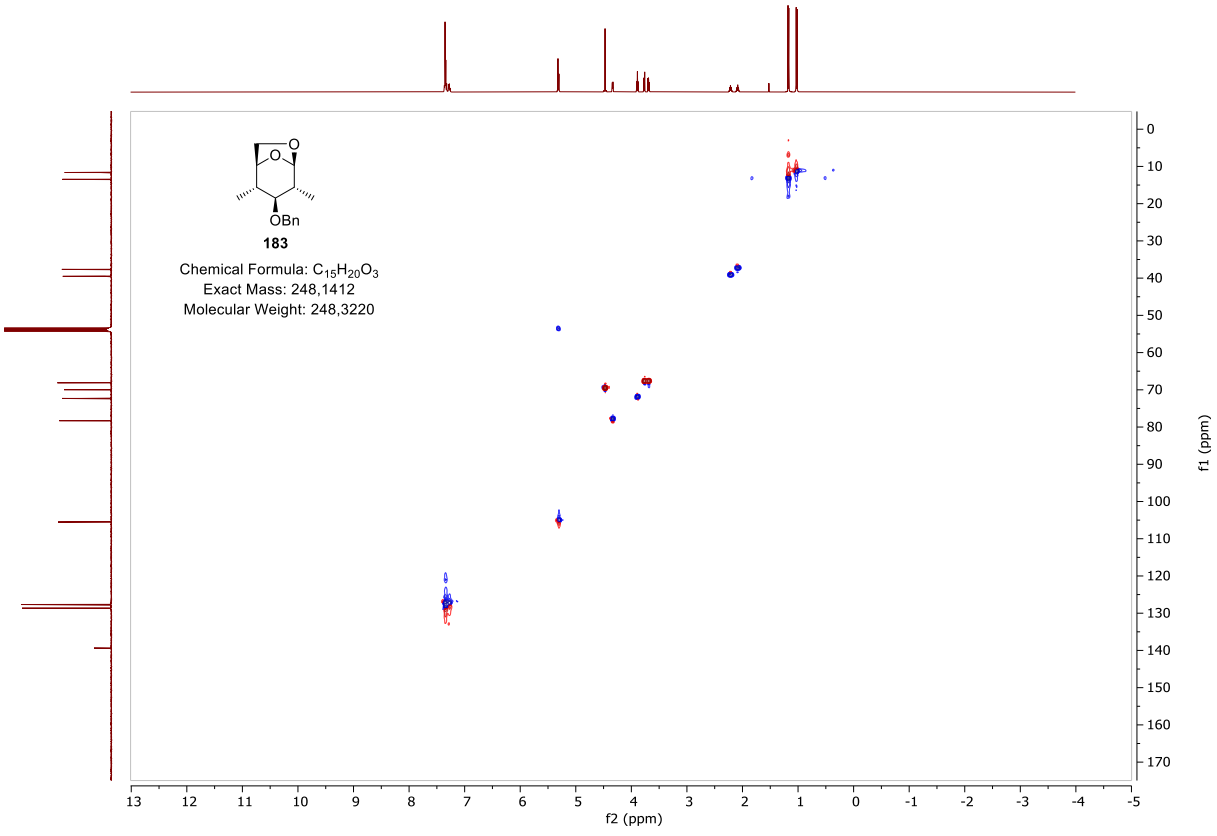

^{1}H, ^{13}C – HSQC spectrum of **183** (500 MHz, 125 MHz, $CDCl_3$)

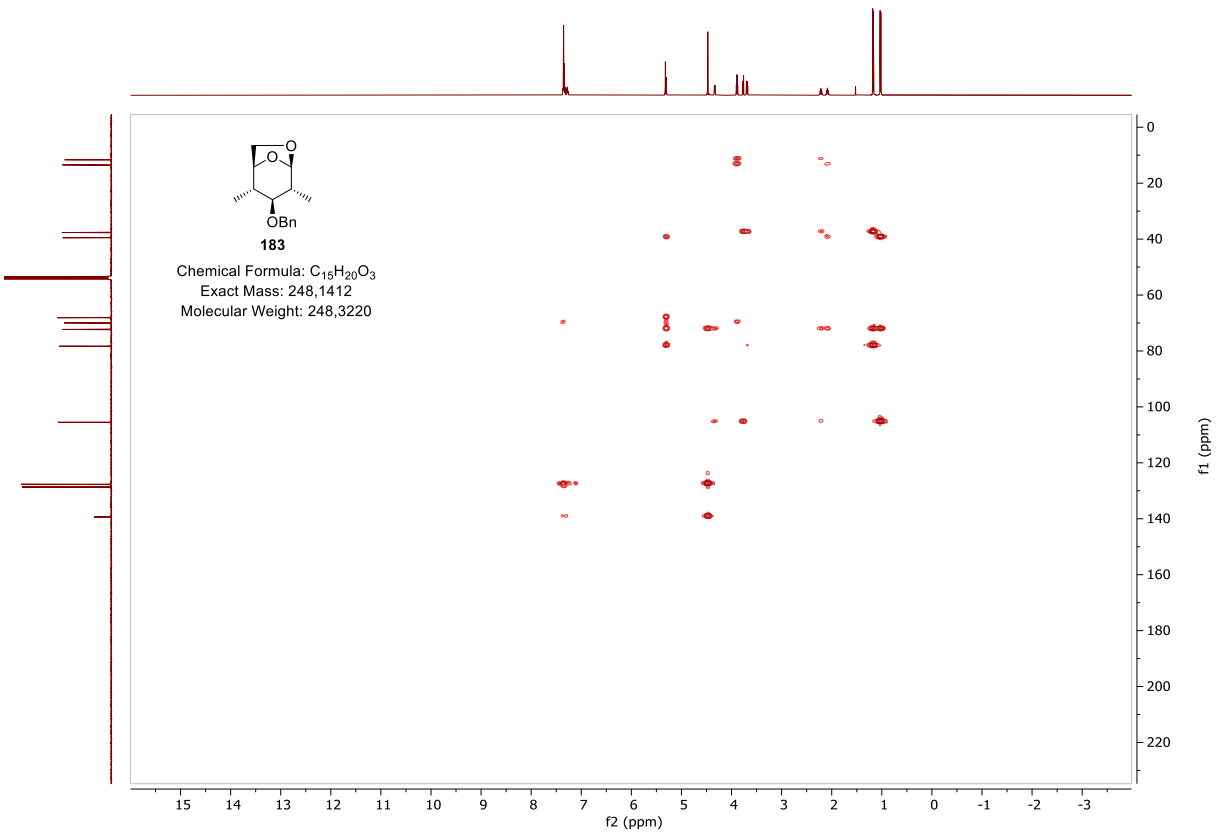

^{1}H, ^{13}C – HMBC spectrum of **183** (500 MHz, 125 MHz, $CDCl_3$)

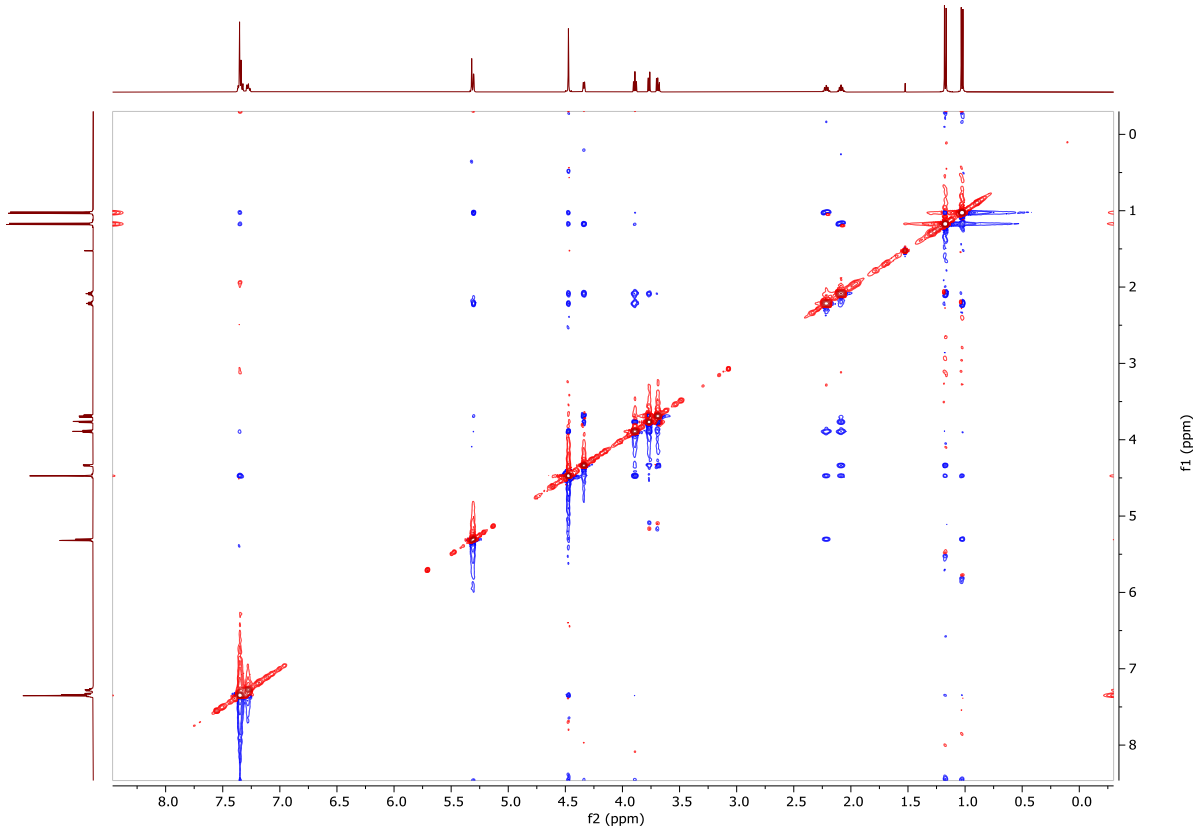

^{1}H, ^{1}H – NOESY spectrum of **183** (500 MHz, CD_2Cl_2)

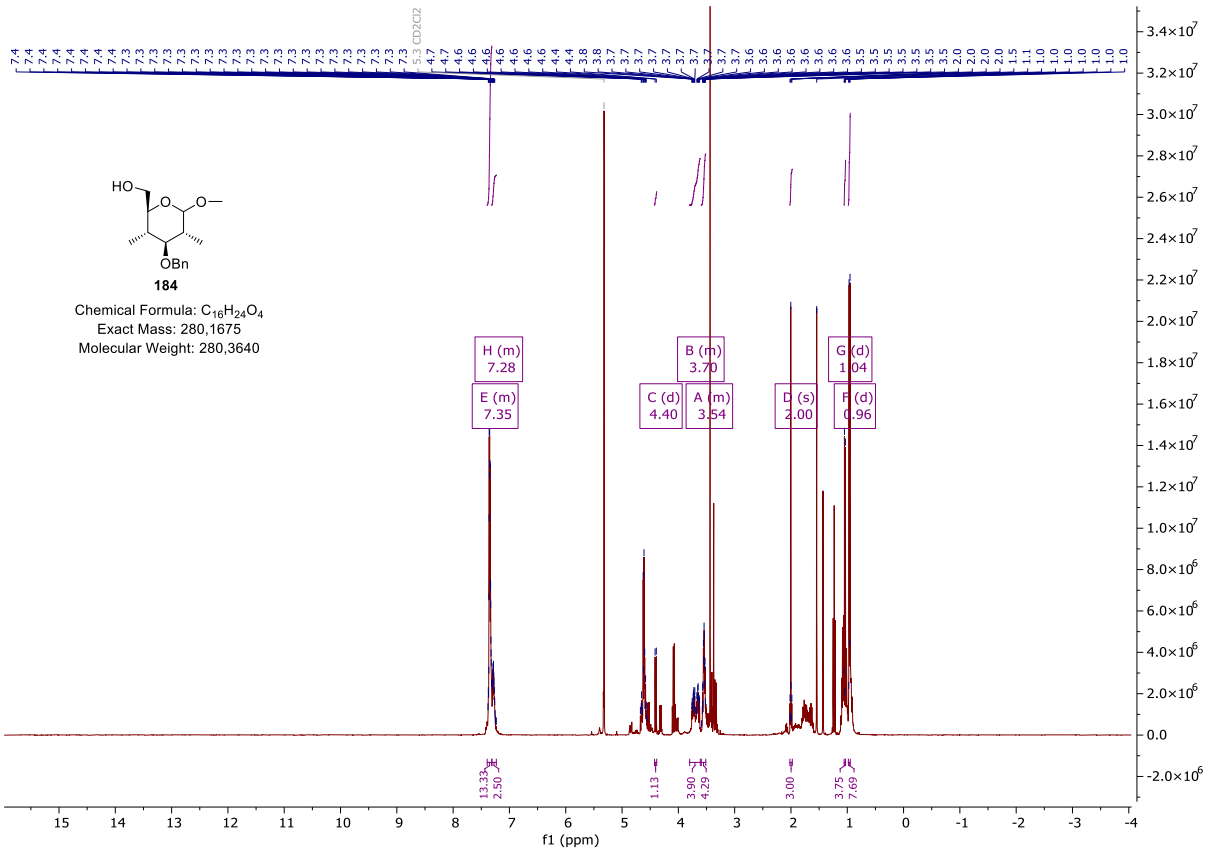

^{1}H – NMR spectrum of **184** (400 MHz, CD_2Cl_2)

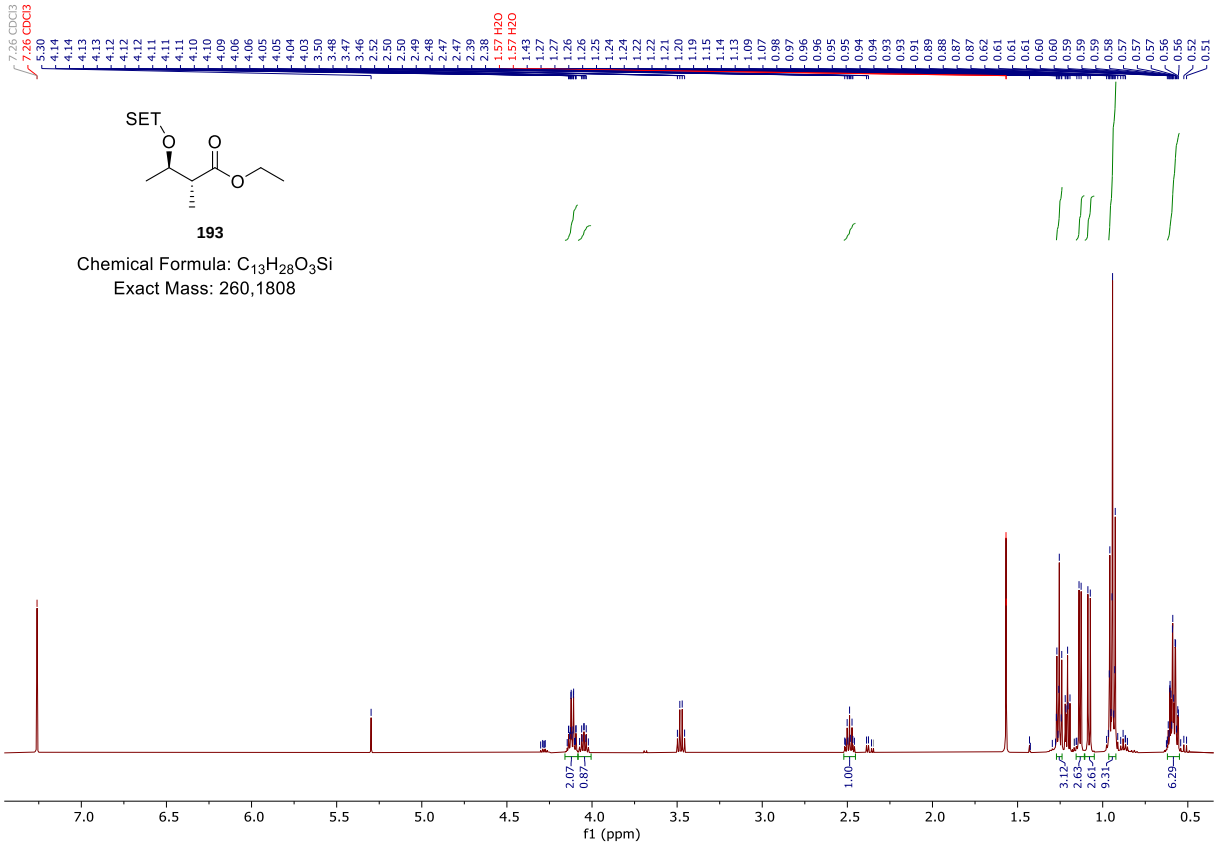

^{1}H – NMR spectrum of **193** (500 MHz, $CDCl_3$)

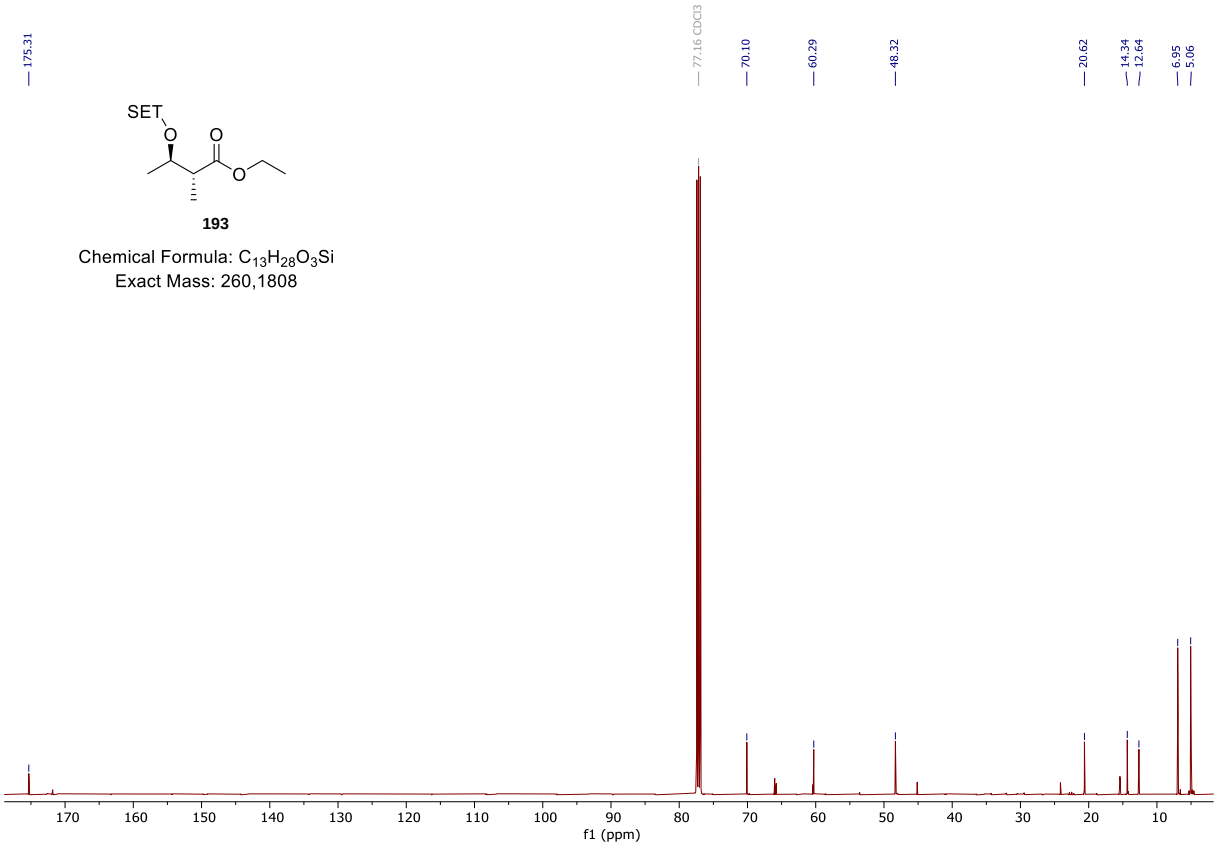

^{13}C – NMR spectrum of **193** ($CDCl_3$)

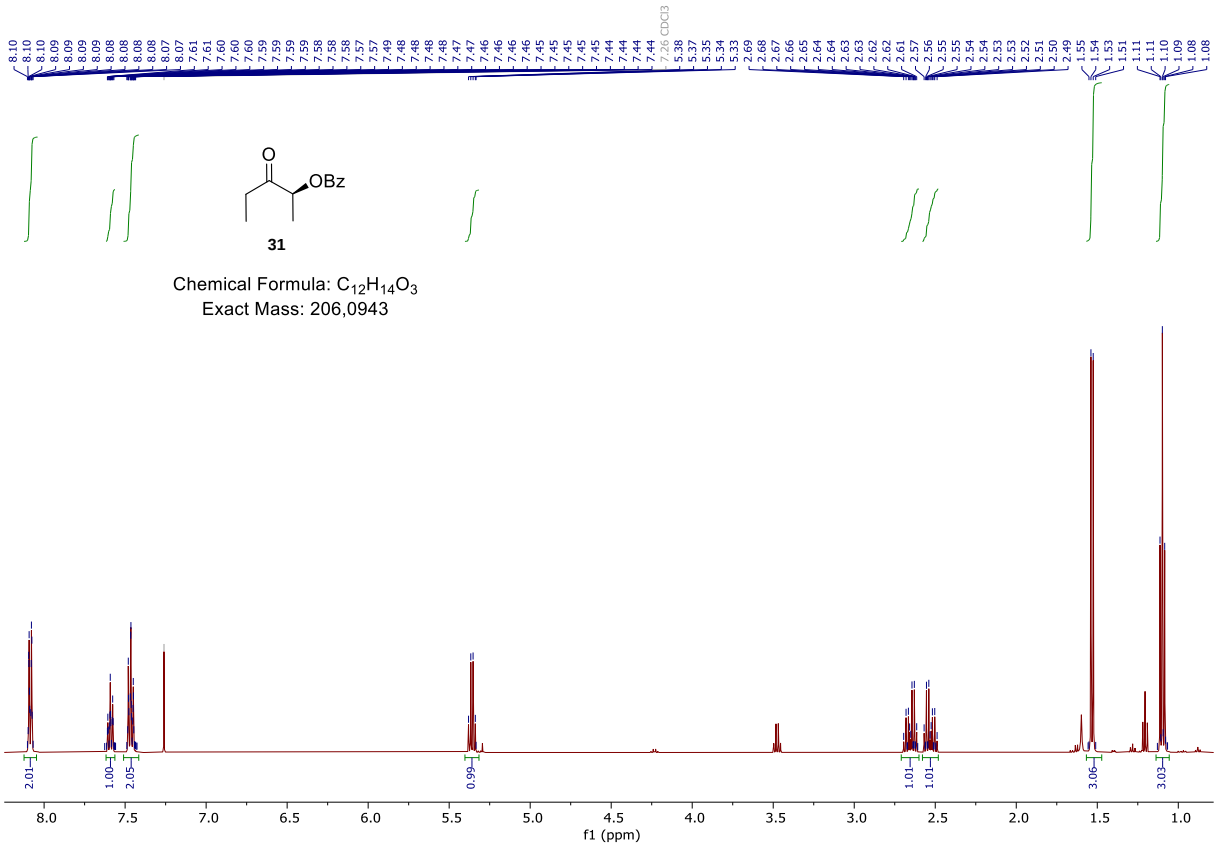

^{1}H – NMR spectrum of **31** ($CDCl_3$)

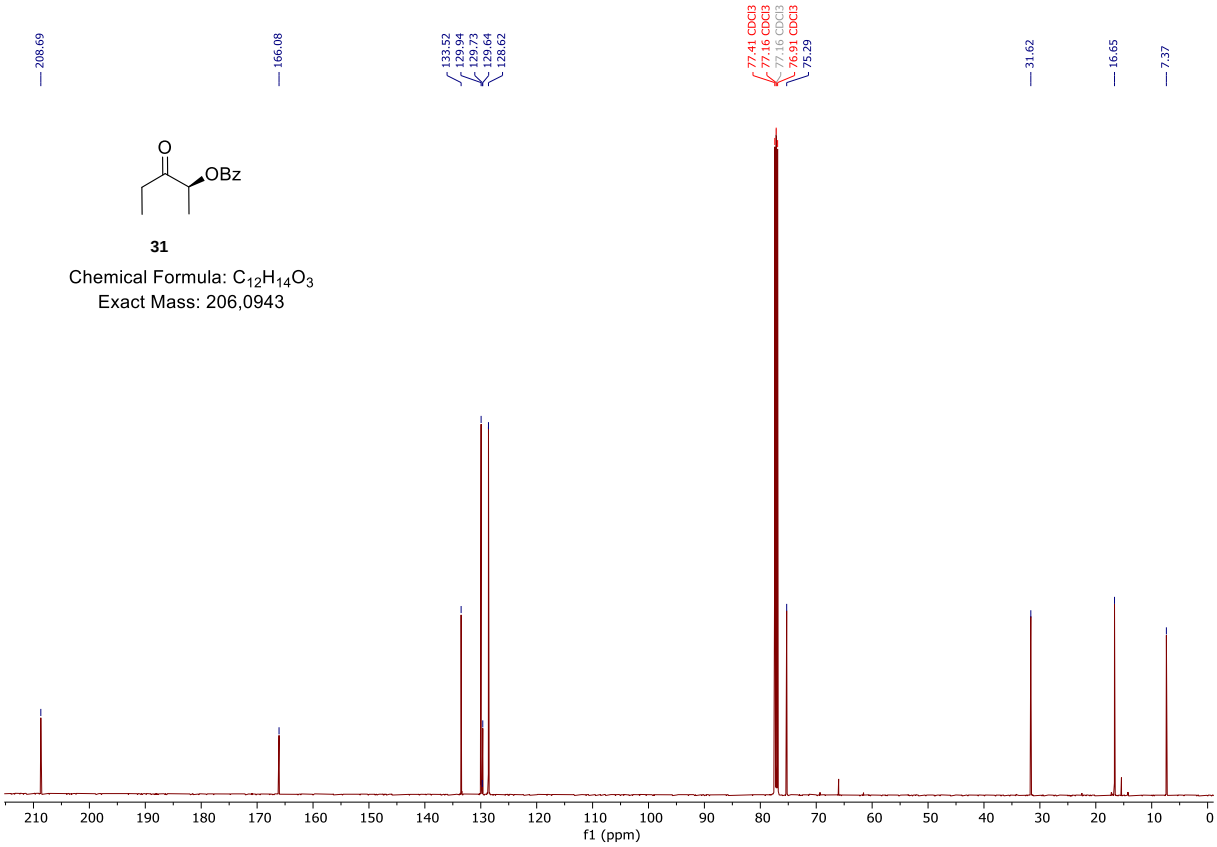

31

Chemical Formula: $C_{12}H_{14}O_3$
Exact Mass: 206,0943

^{13}C – NMR spectrum of **31** (125 MHz, $CDCl_3$)

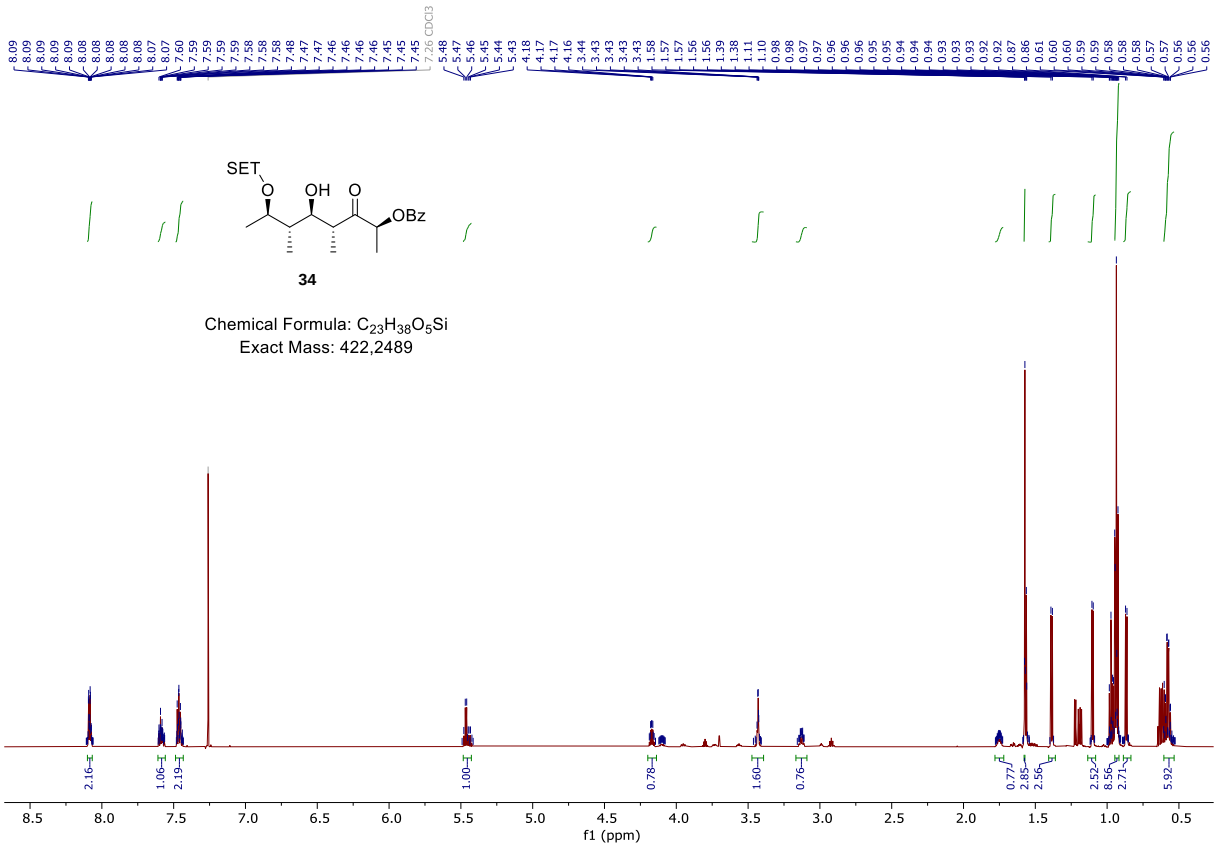

34

Chemical Formula: $C_{23}H_{38}O_5Si$
Exact Mass: 422,2489

^{1}H – NMR spectrum of **34** (500 MHz, $CDCl_3$)

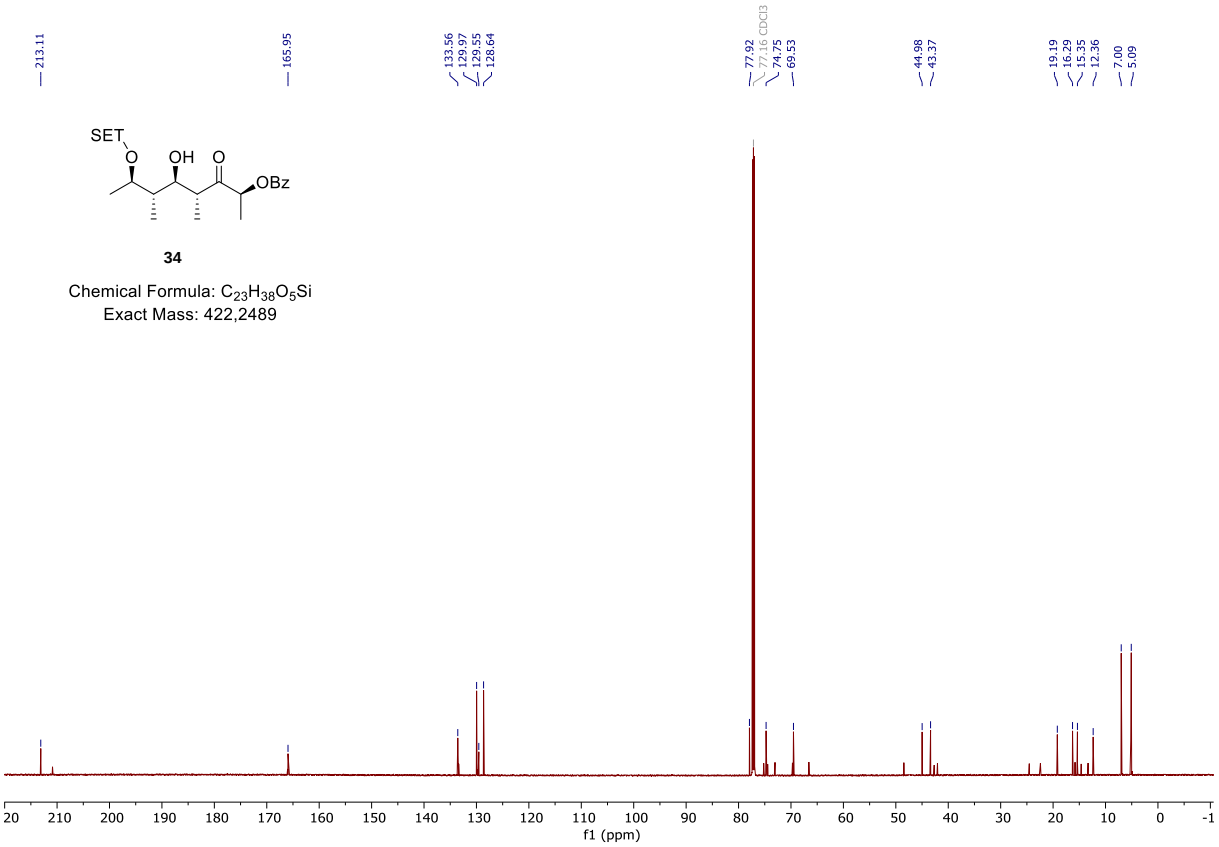

34

Chemical Formula: $C_{23}H_{38}O_5Si$
Exact Mass: 422,2489

^{13}C – NMR spectrum of **34** (125 MHz, $CDCl_3$)

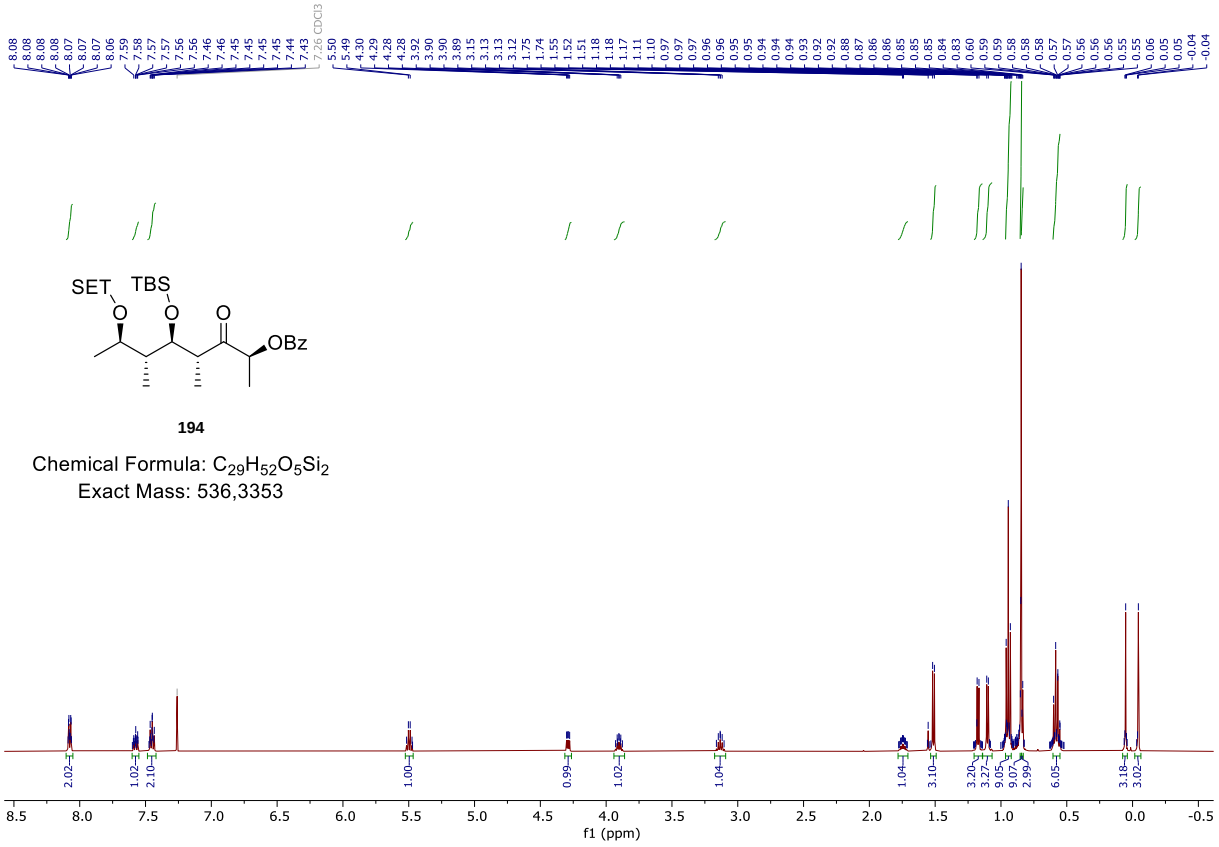

194

Chemical Formula: $C_{29}H_{52}O_5Si_2$
Exact Mass: 536,3353

^{1}H – NMR spectrum of **194** (500 MHz, $CDCl_3$)

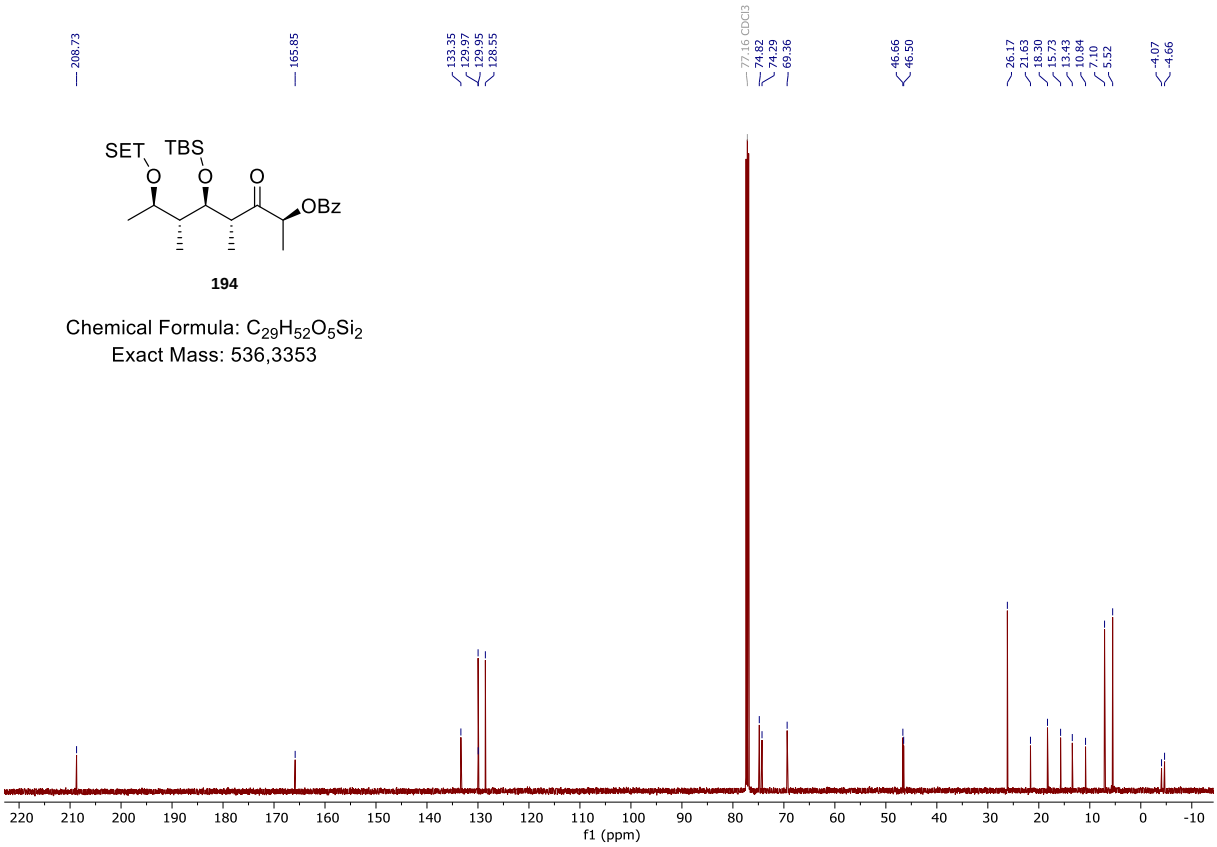

^{13}C – NMR spectrum of **194** (125 MHz, $CDCl_3$)

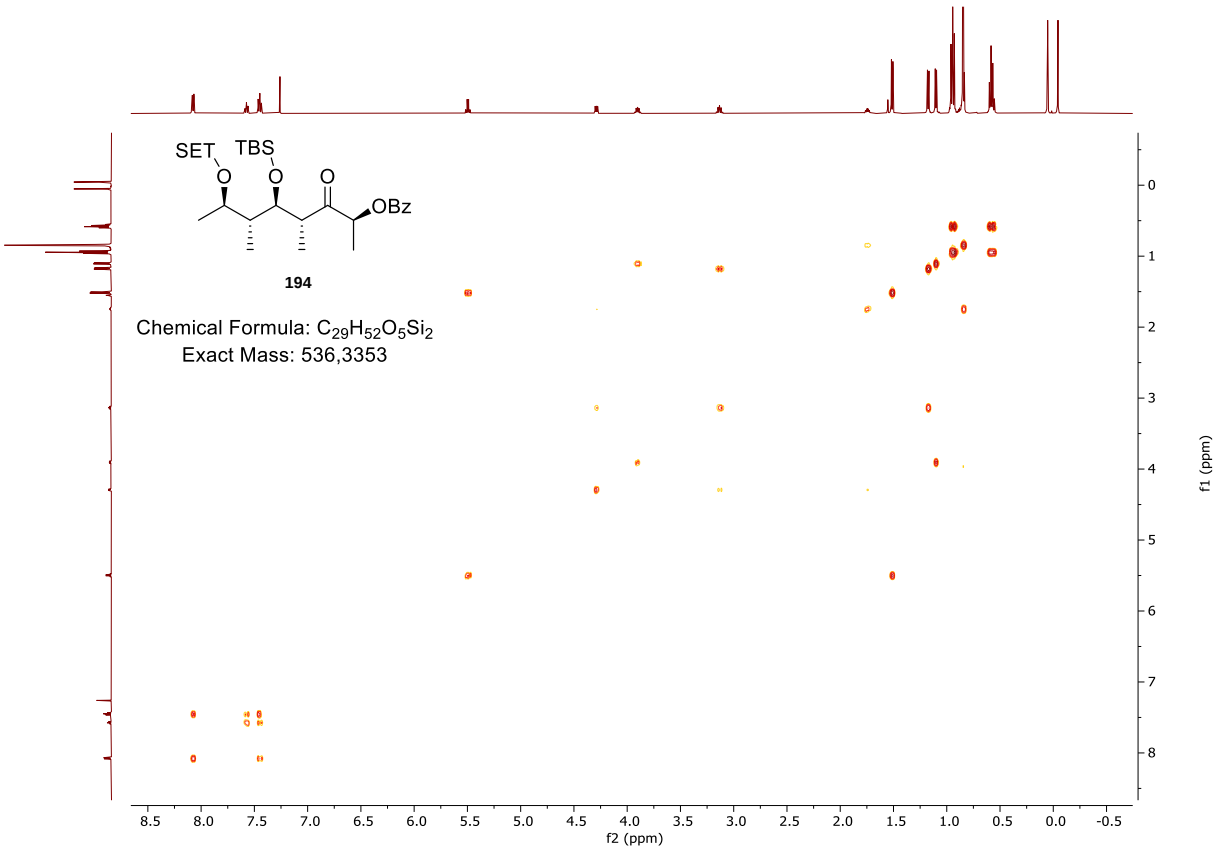

^{1}H, ^{1}H – COSY spectrum of **194** (500 MHz, $CDCl_3$)

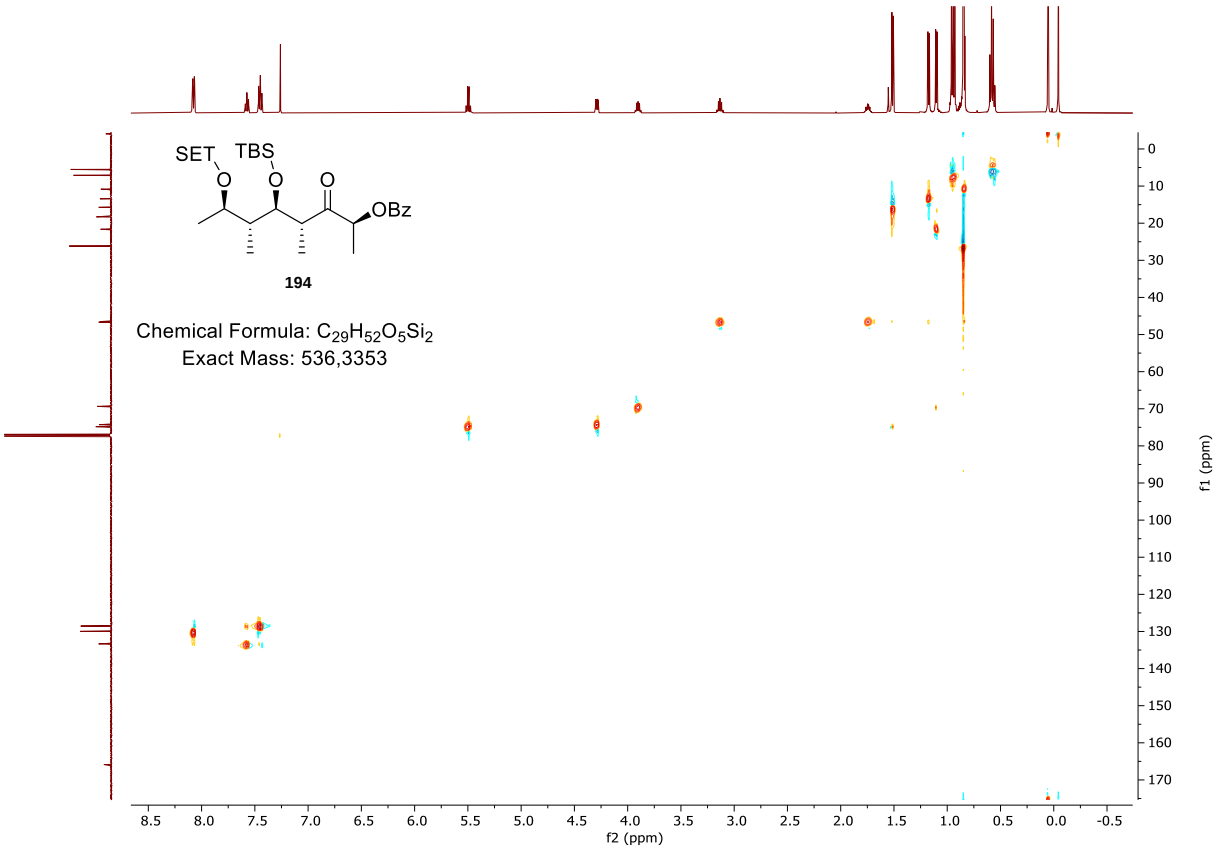

^{1}H, ^{13}C – HSQC spectrum of **194** (500 MHz, 125 MHz, $CDCl_3$)

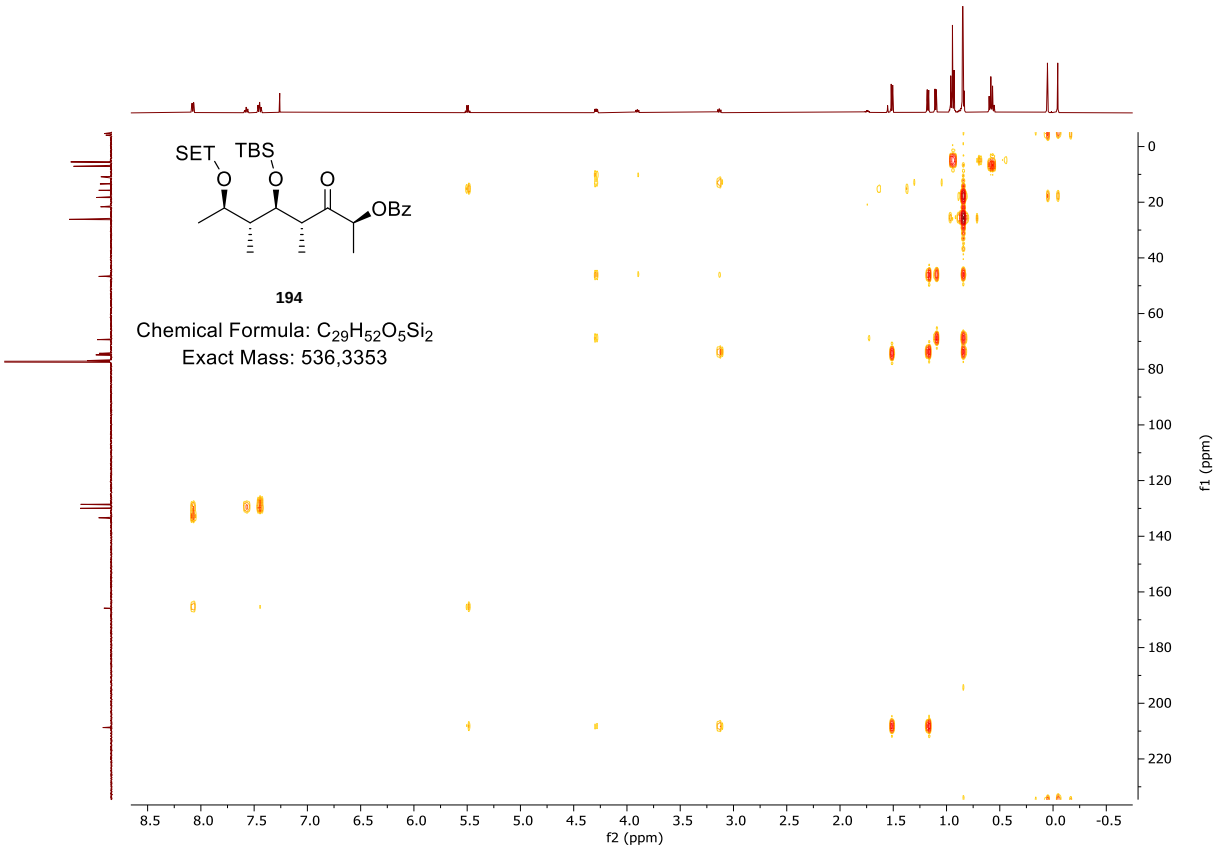

^{1}H, ^{13}C – HMBC spectrum of **194** (500 MHz, 125 MHz, $CDCl_3$)

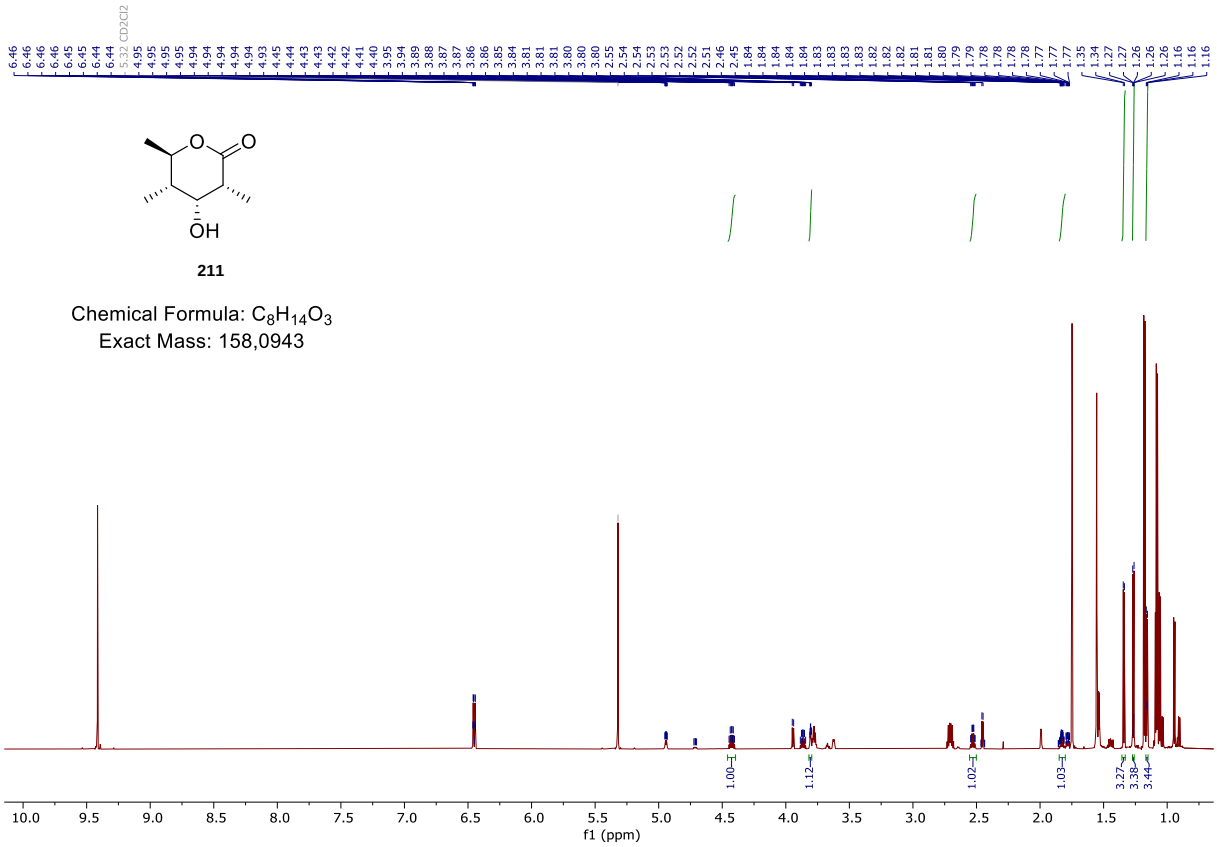

^{1}H – NMR spectrum of **211** (500 MHz, CD_2Cl_2)

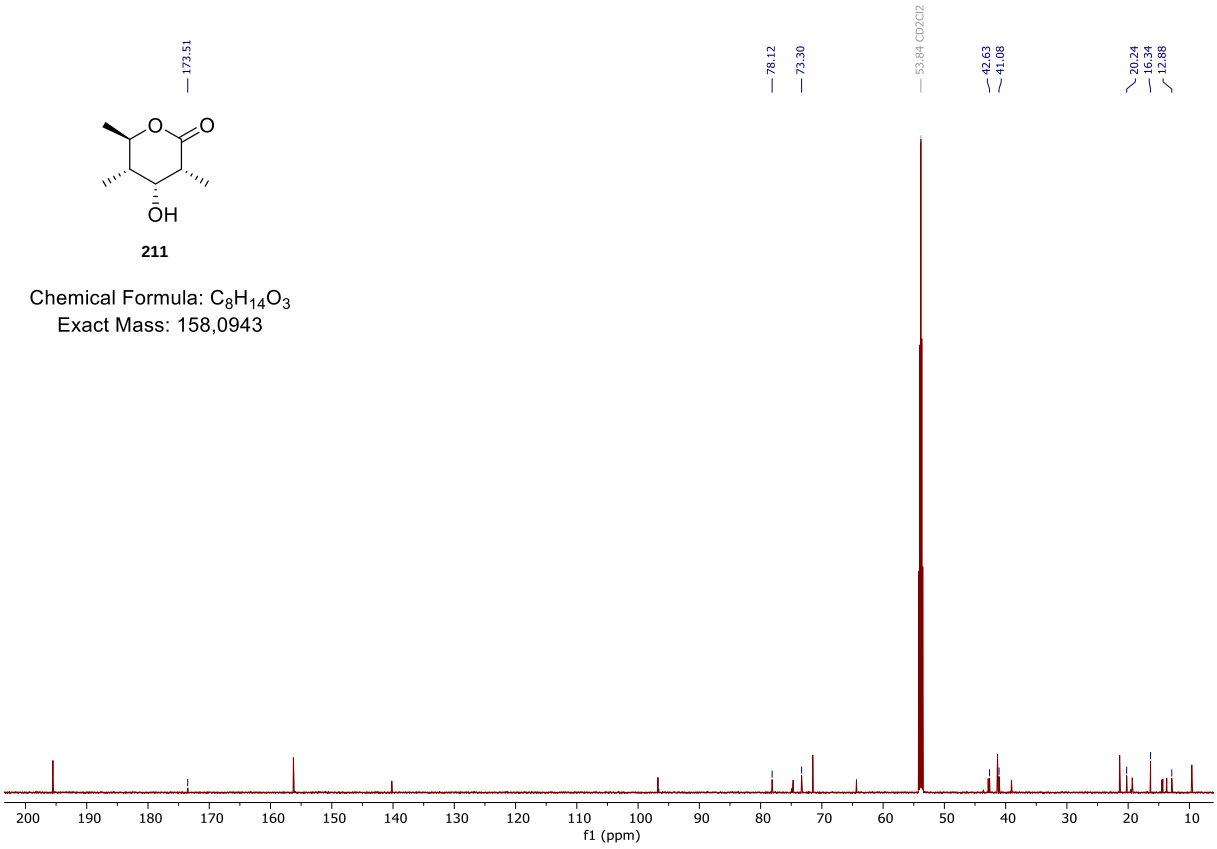

^{13}C – NMR spectrum of **211** (125 MHz, CD_2Cl_2)

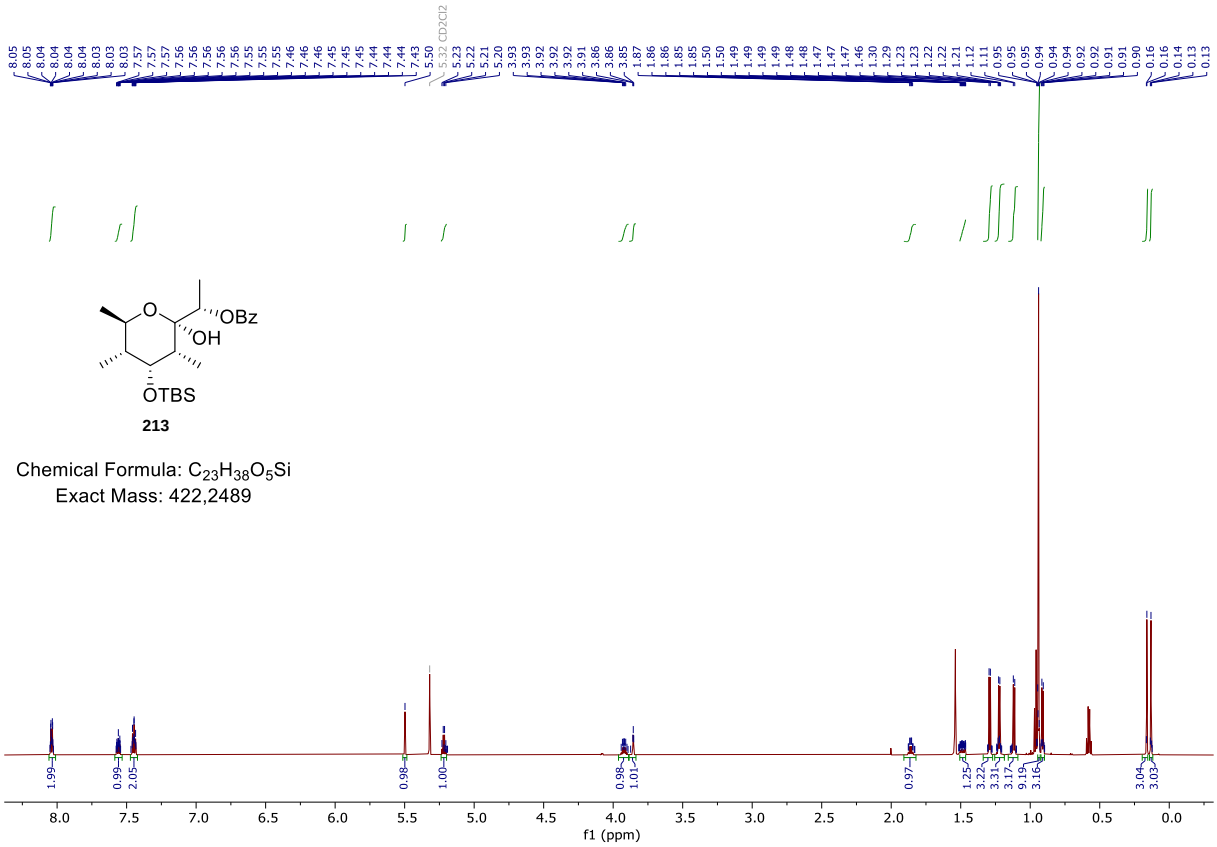

^{1}H – NMR spectrum of **213** (500 MHz, CD_2Cl_2)

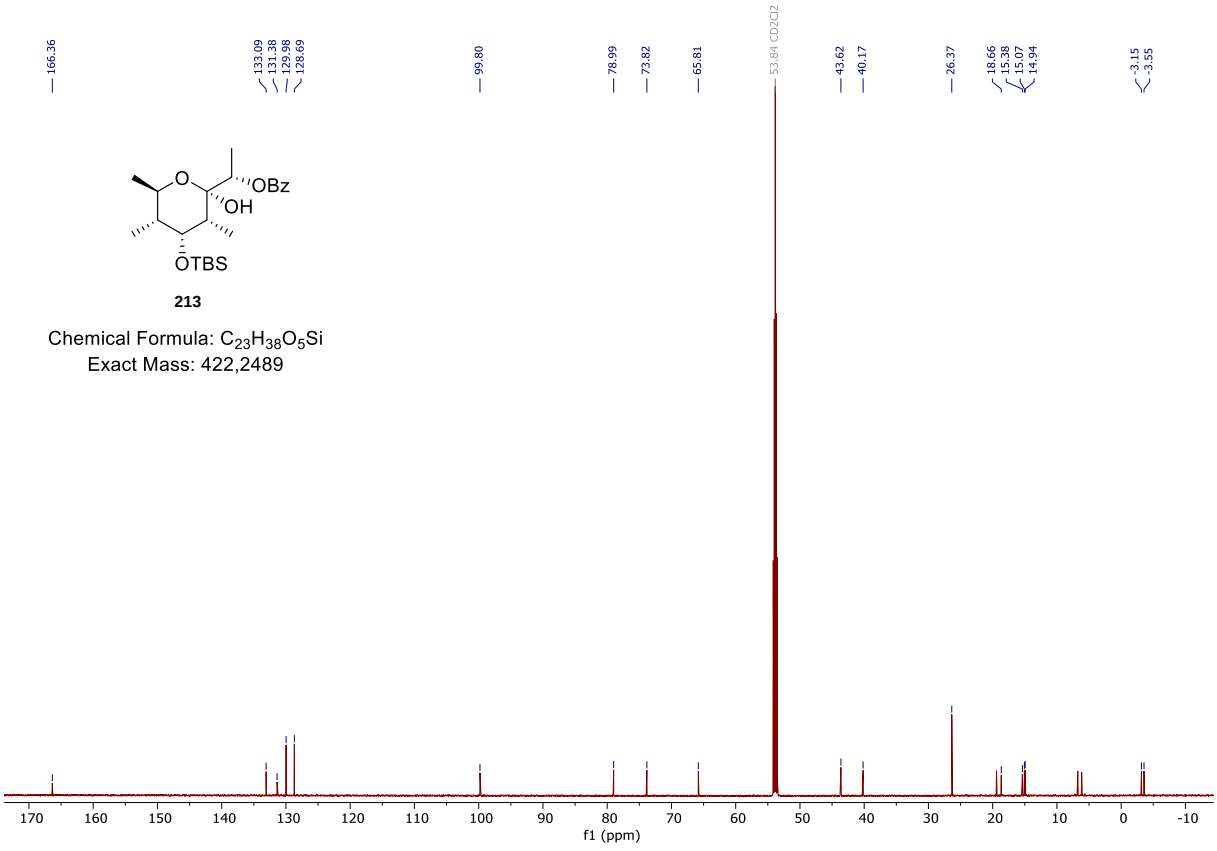

^{13}C – NMR spectrum of **213** (125 MHz, CD_2Cl_2)

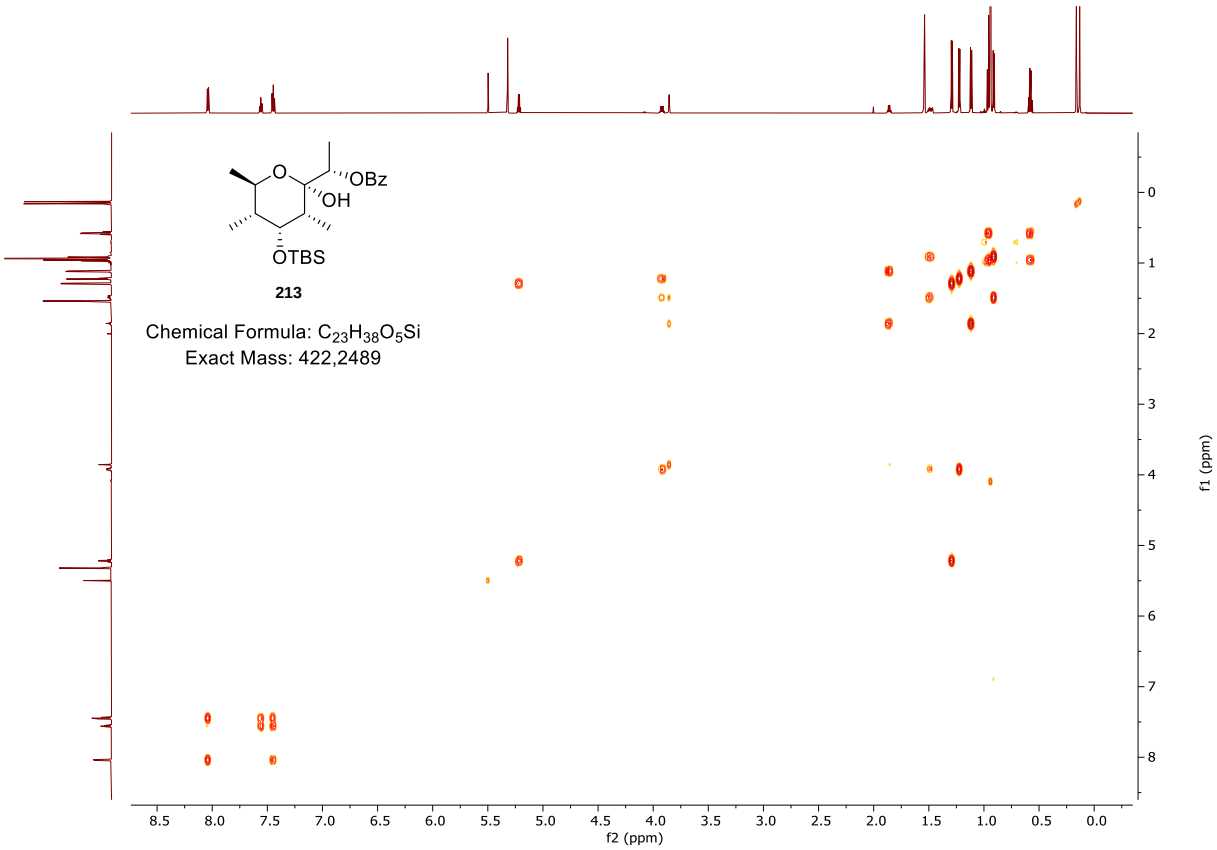

^{1}H, ^{1}H – COSY spectrum of **213** (500 MHz, CD_2Cl_2)

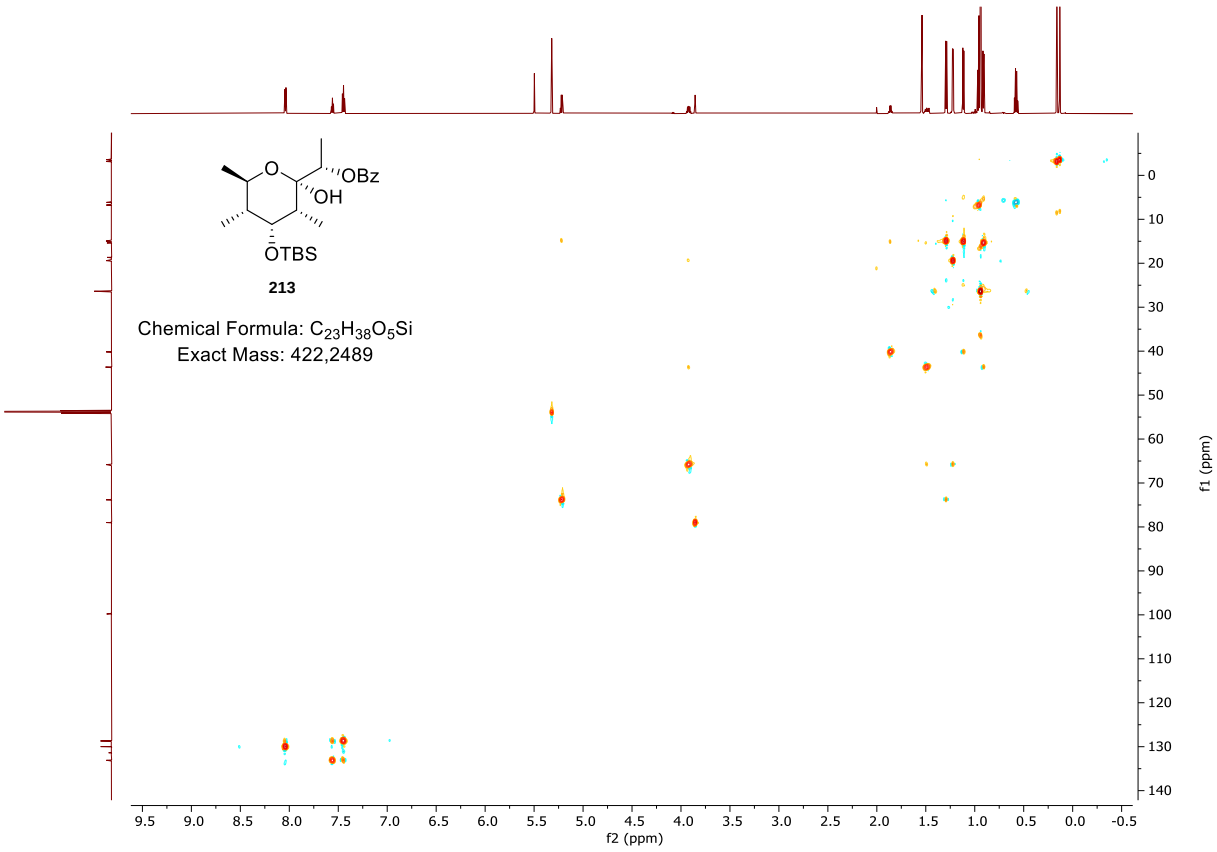

^{1}H, ^{13}C – HSQC spectrum of **213** (500 MHz, 125 MHz, CD_2Cl_2)

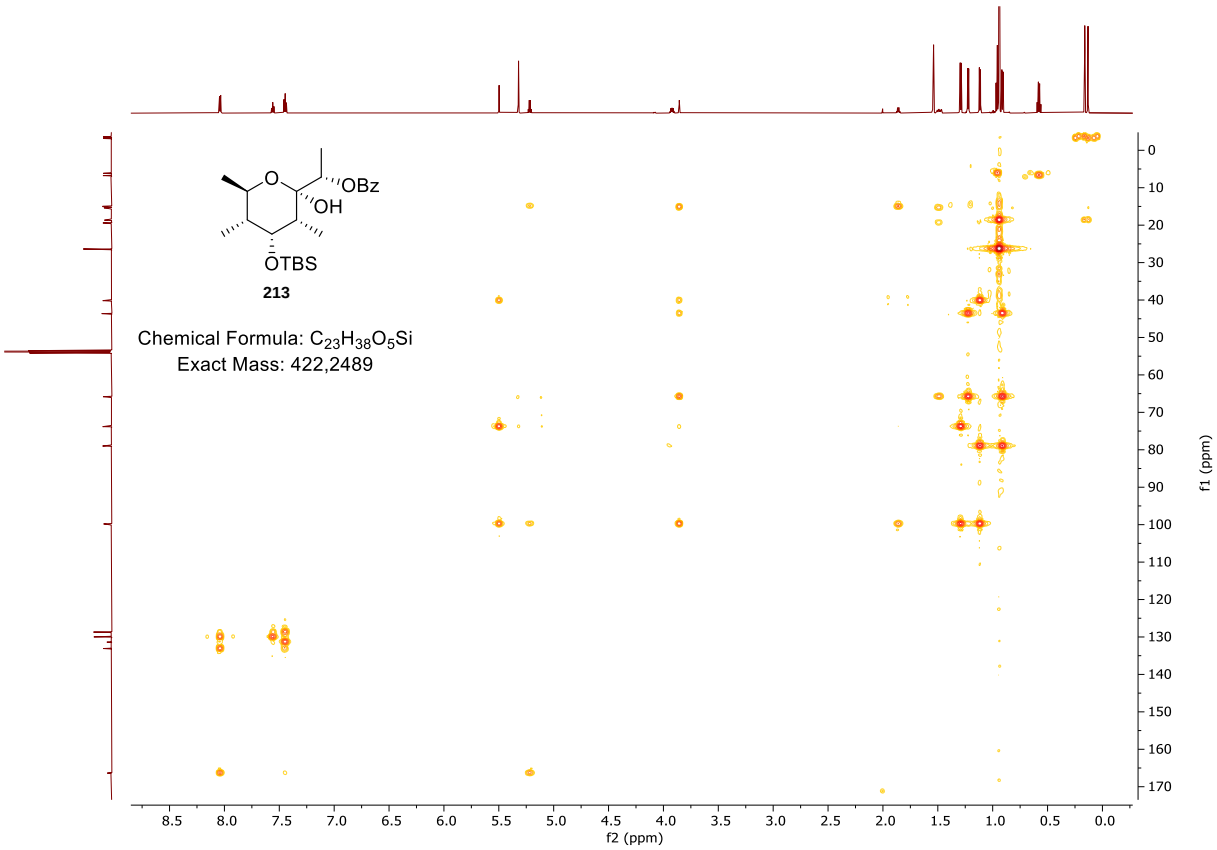

^{1}H, ^{13}C – HMBC spectrum of **213** (500 MHz, 125 MHz, CD_2Cl_2)

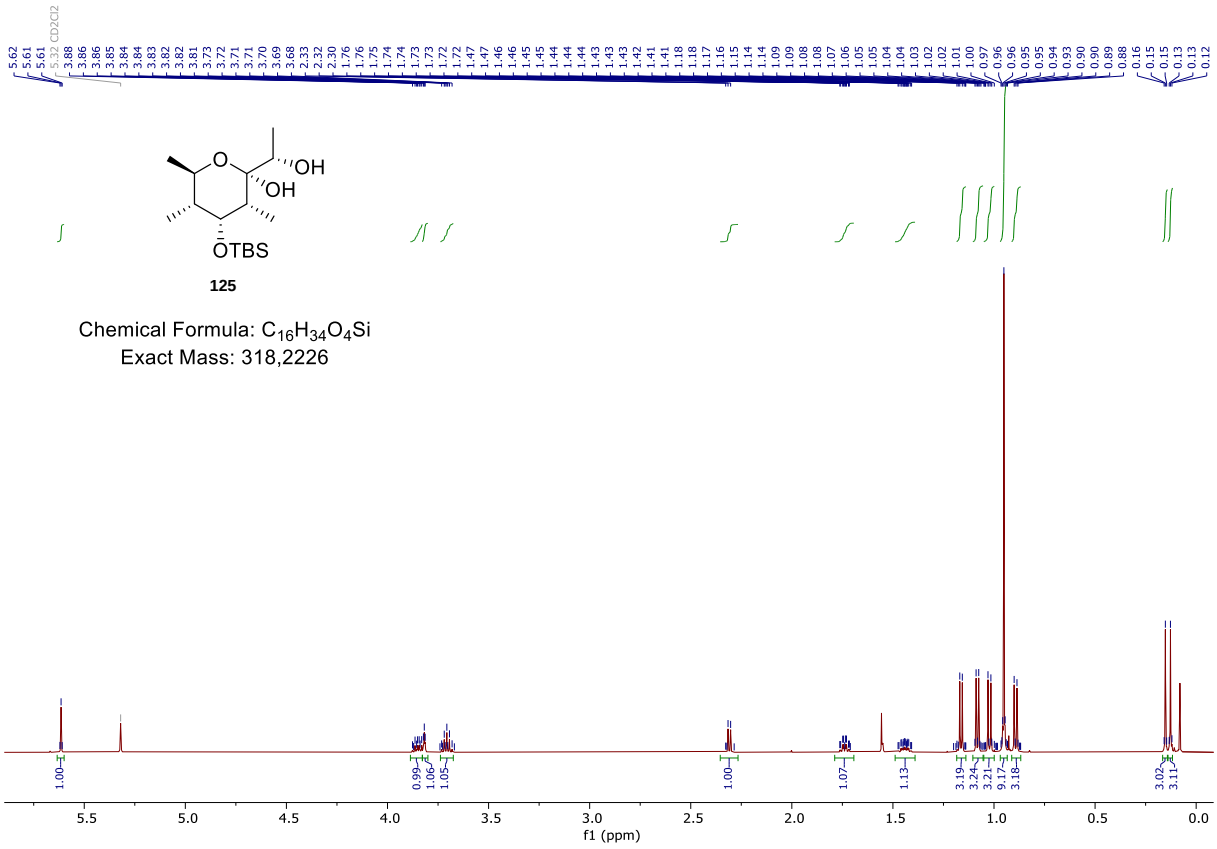

^{1}H – NMR spectrum of **125** (500 MHz, CD_2Cl_2)

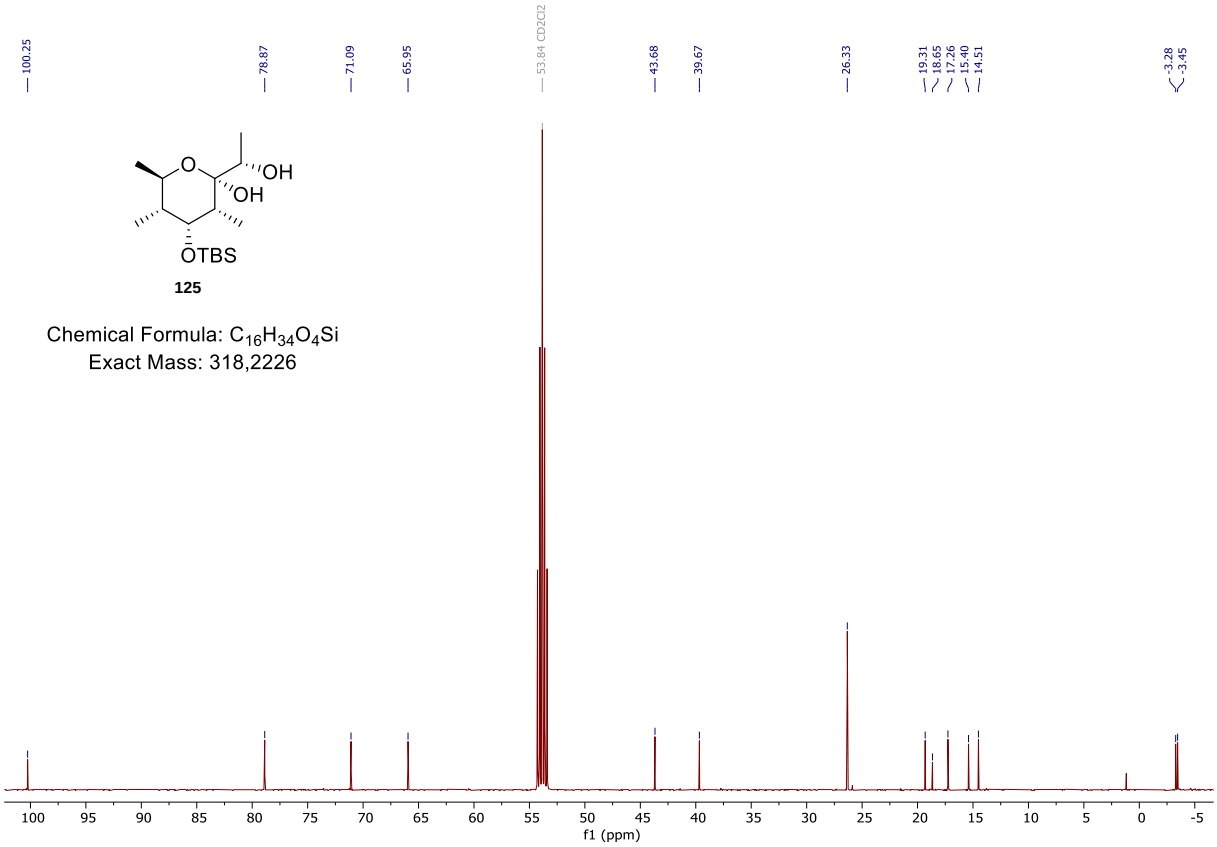

^{13}C – NMR spectrum of **125** (125 MHz, CD_2Cl_2)

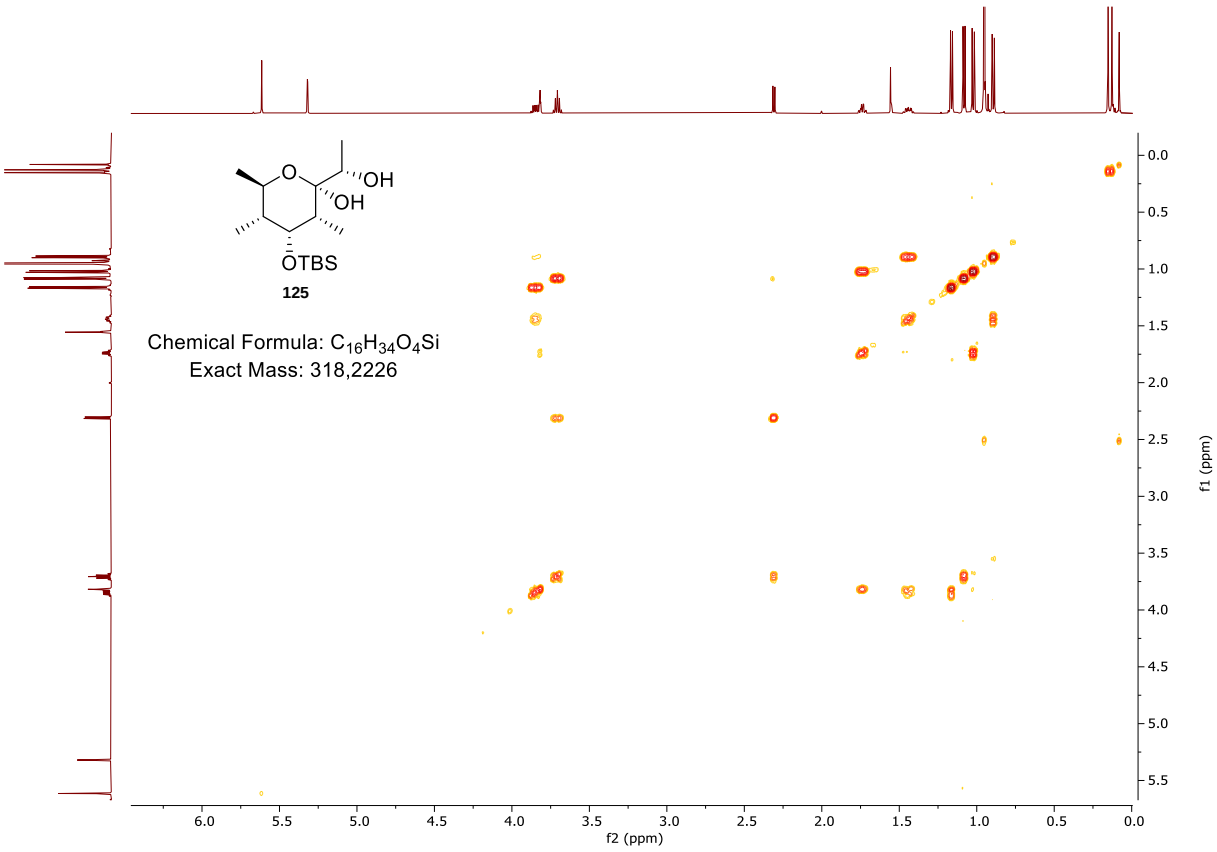

^{1}H, ^{1}H – COSY spectrum of **125** (500 MHz, CD_2Cl_2)

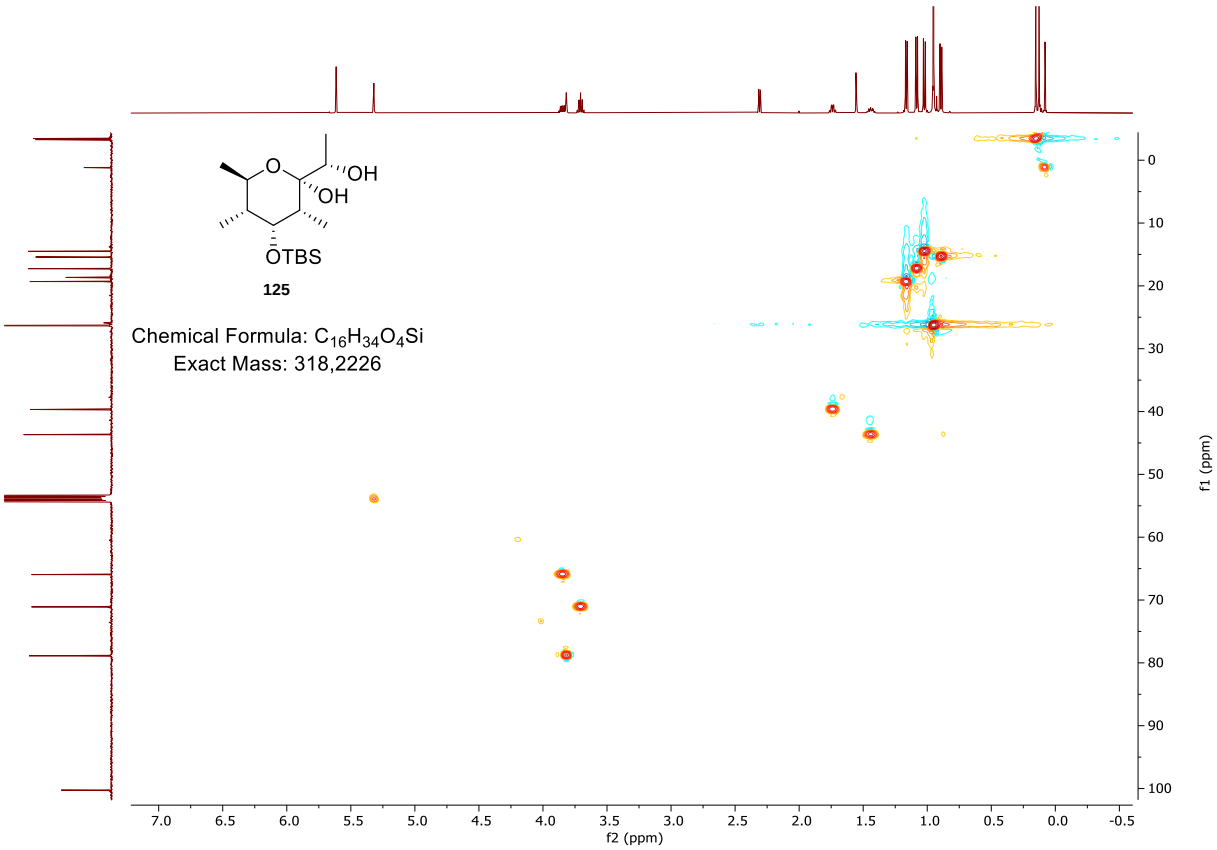

^{1}H, ^{13}C – HSQC spectrum of **125** (500 MHz, 125 MHz, CD_2Cl_2)

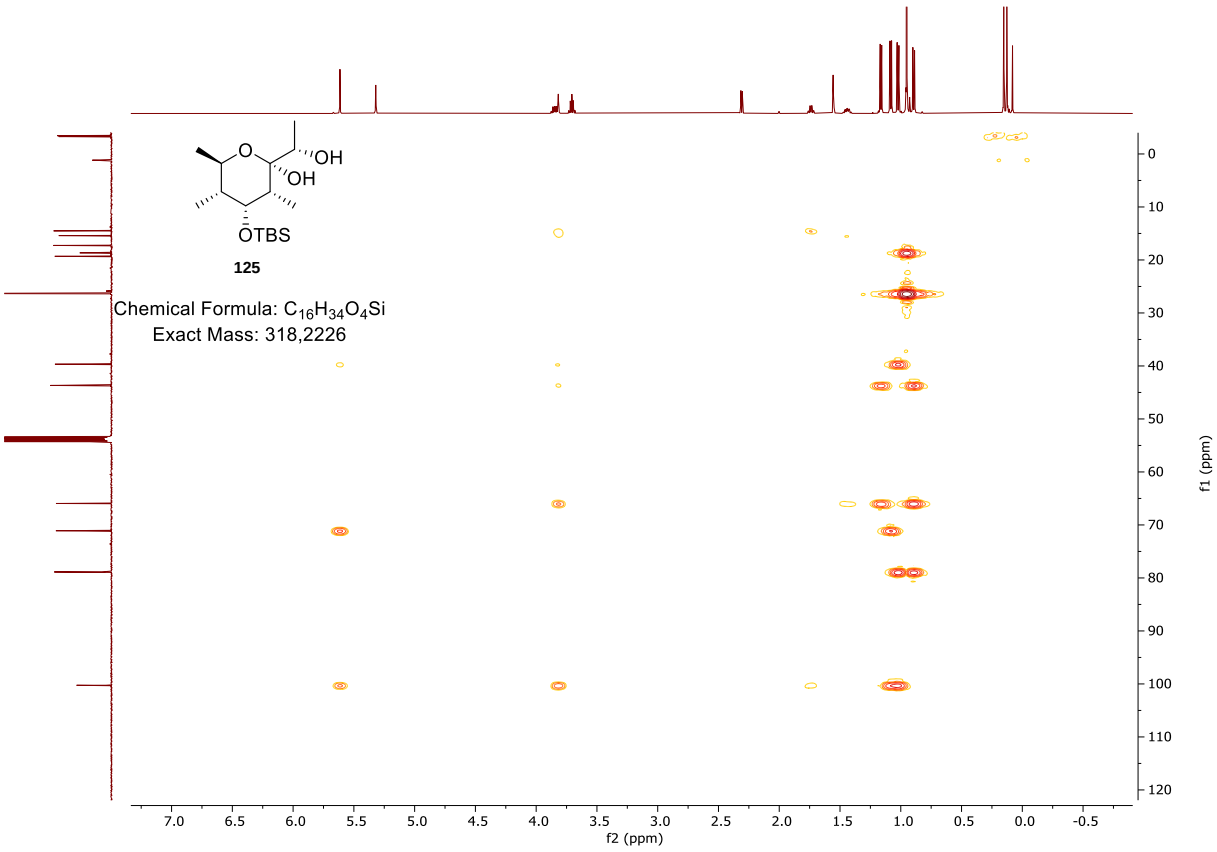

^{1}H, ^{13}C – HMBC spectrum of **125** (500 MHz, 125 MHz, CD_2Cl_2)

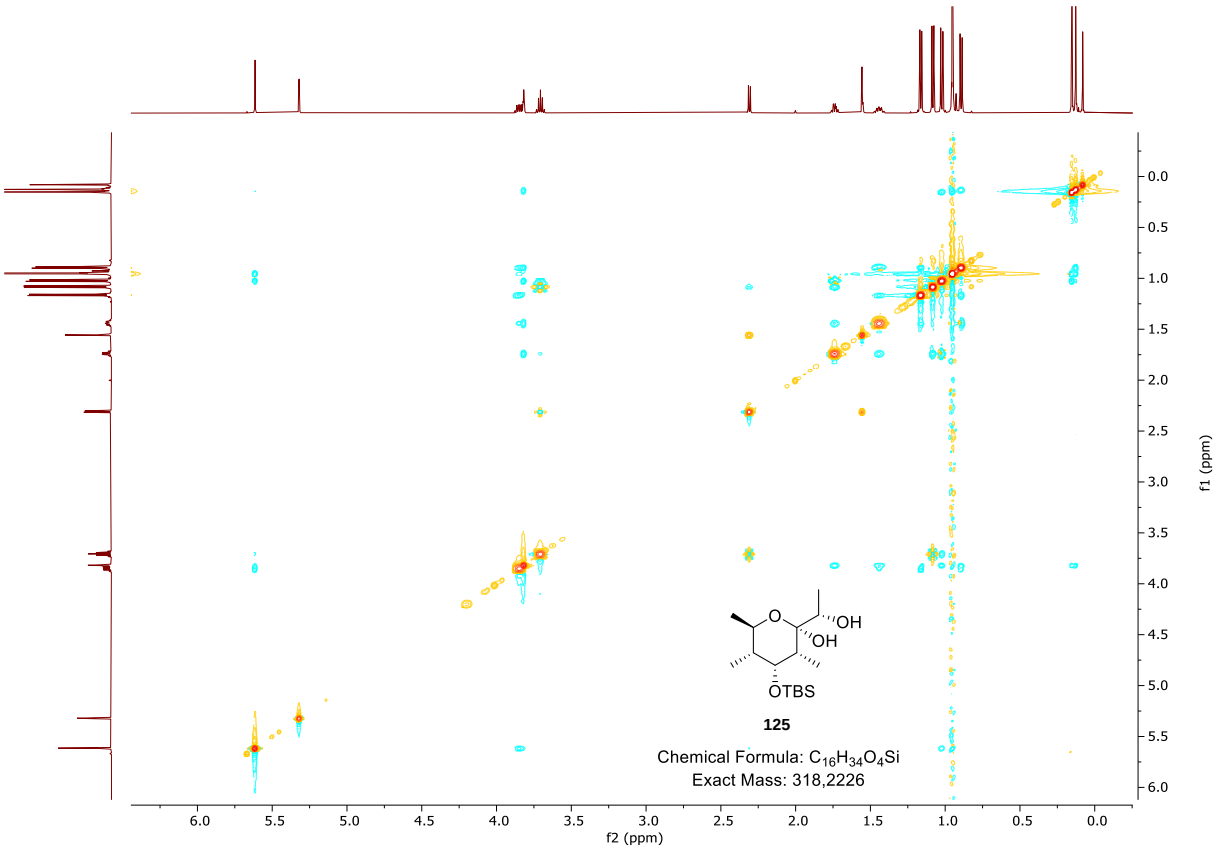

^{1}H, ^{1}H – NOESY spectrum of **125** (500 MHz, CD_2Cl_2)

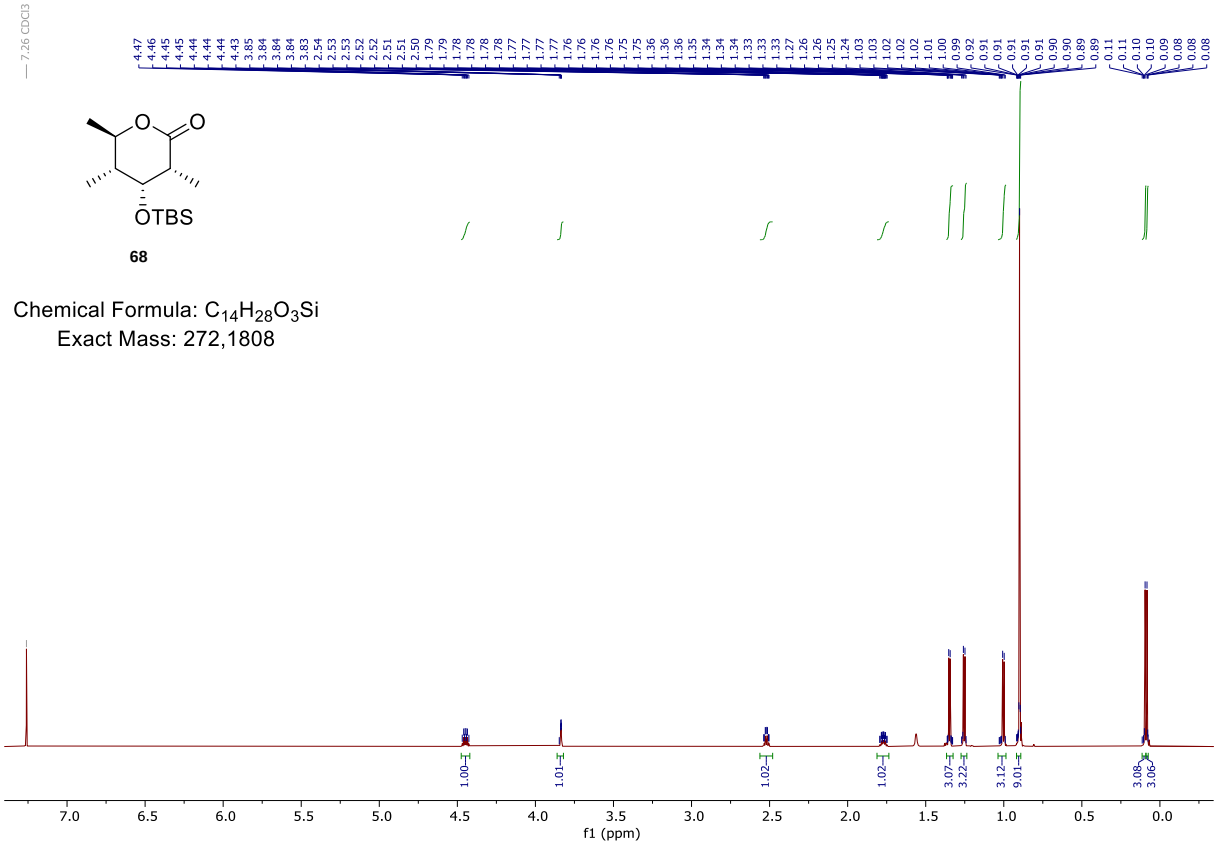

^{1}H – NMR spectrum of **68** (500 MHz, $CDCl_3$)

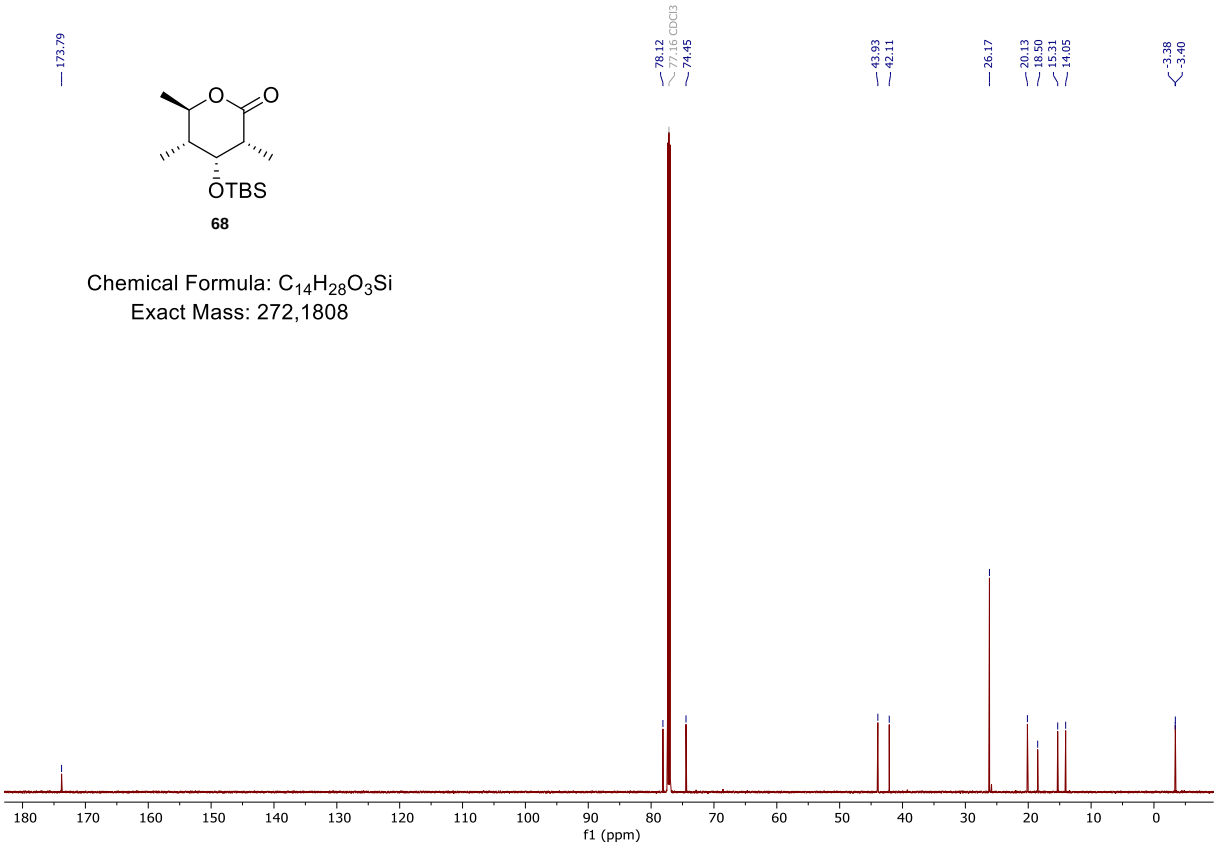

^{13}C – NMR spectrum of **68** (125 MHz, $CDCl_3$)

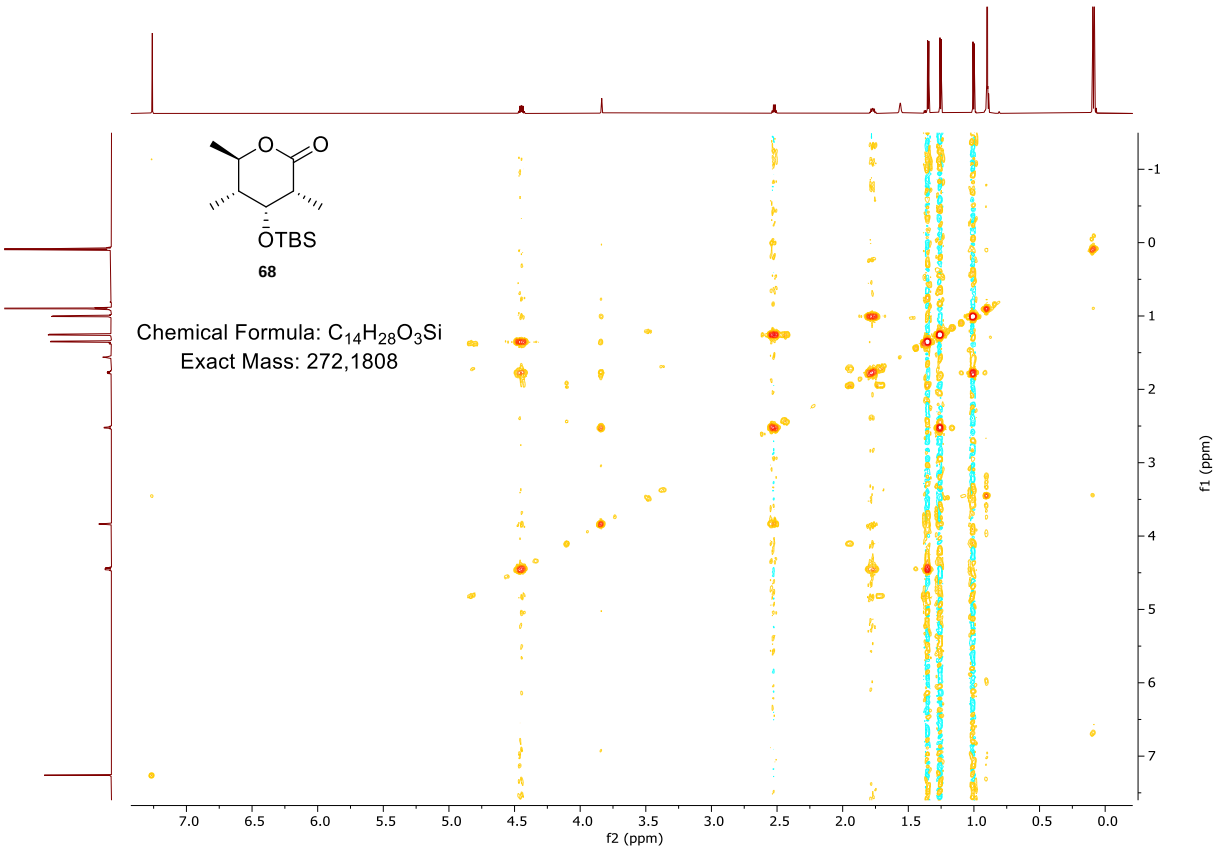

^{1}H, ^{1}H – COSY spectrum of **68** (500 MHz, $CDCl_3$)

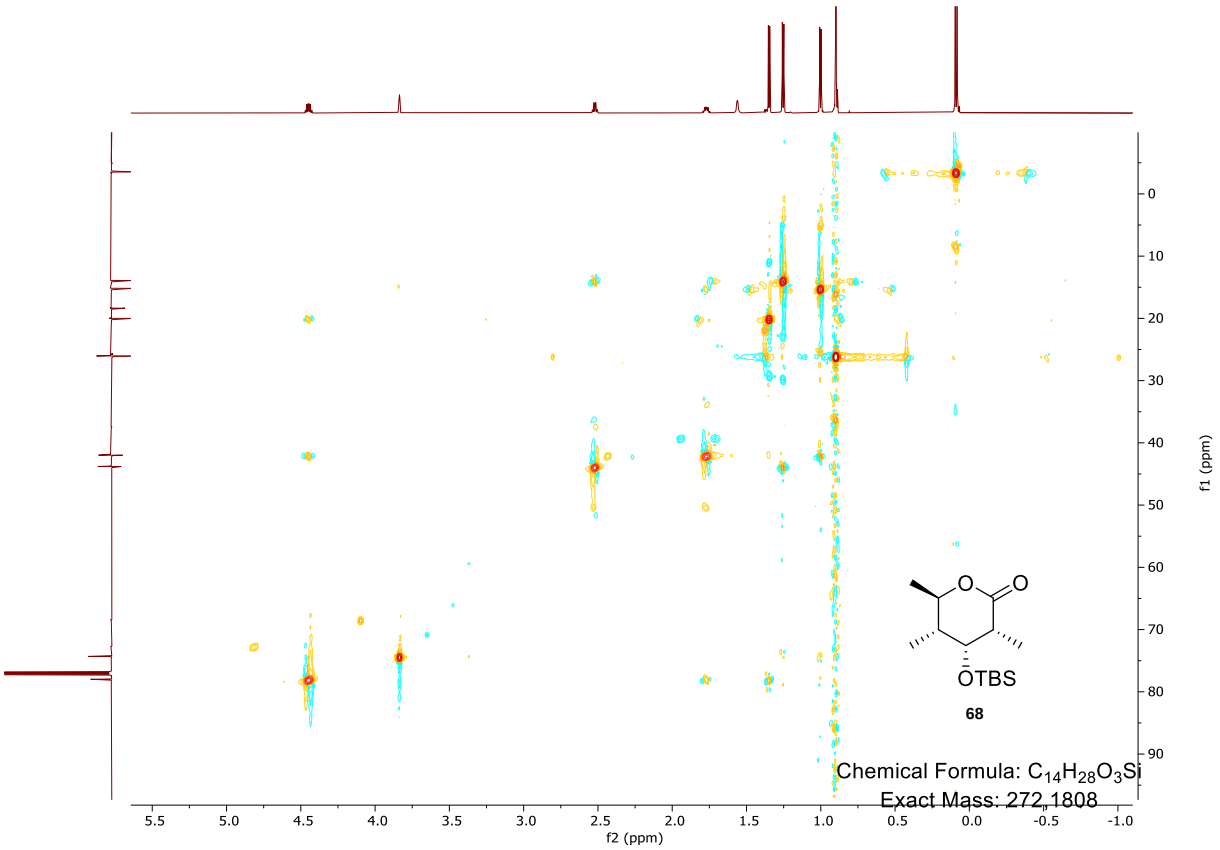

^{1}H, ^{13}C – HSQC spectrum of **68** (500 MHz, 125 MHz, $CDCl_3$)

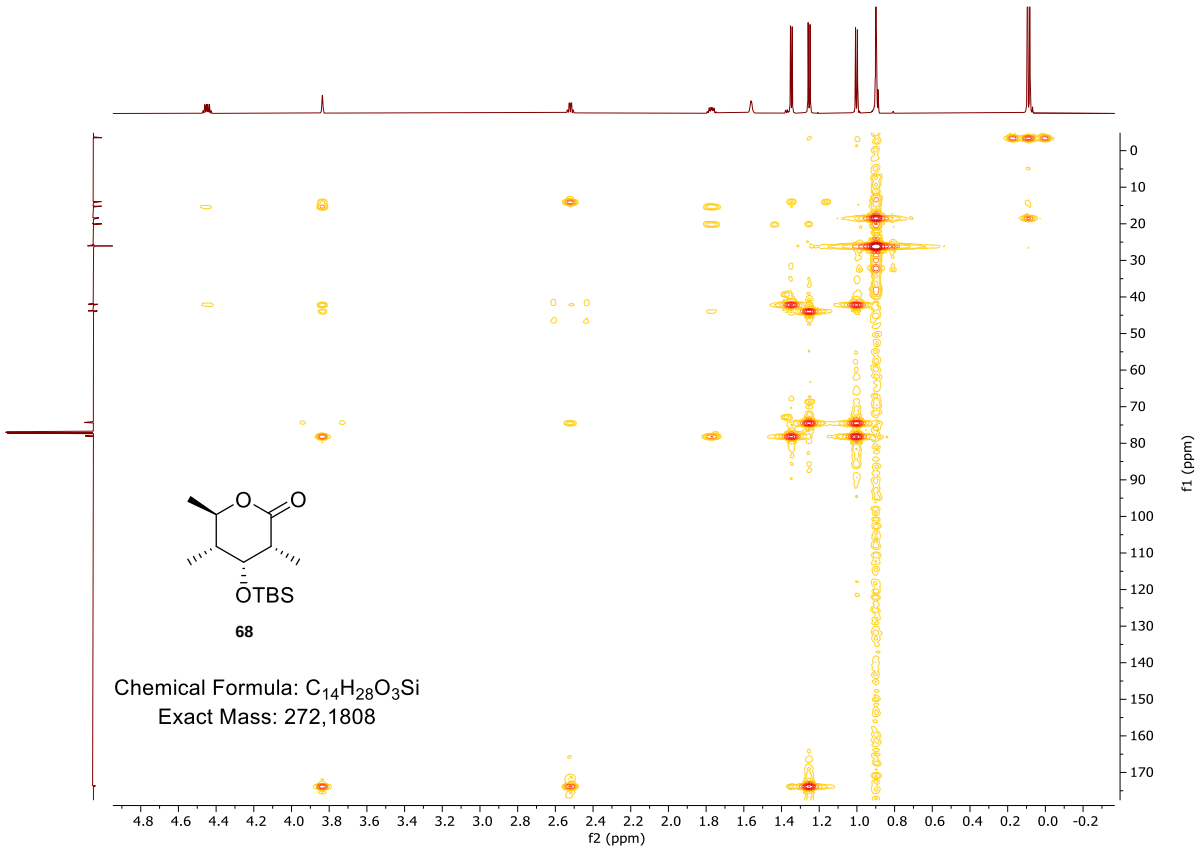

^{1}H, ^{13}C – HMBC spectrum of **68** (500 MHz, 125 MHz, $CDCl_3$)

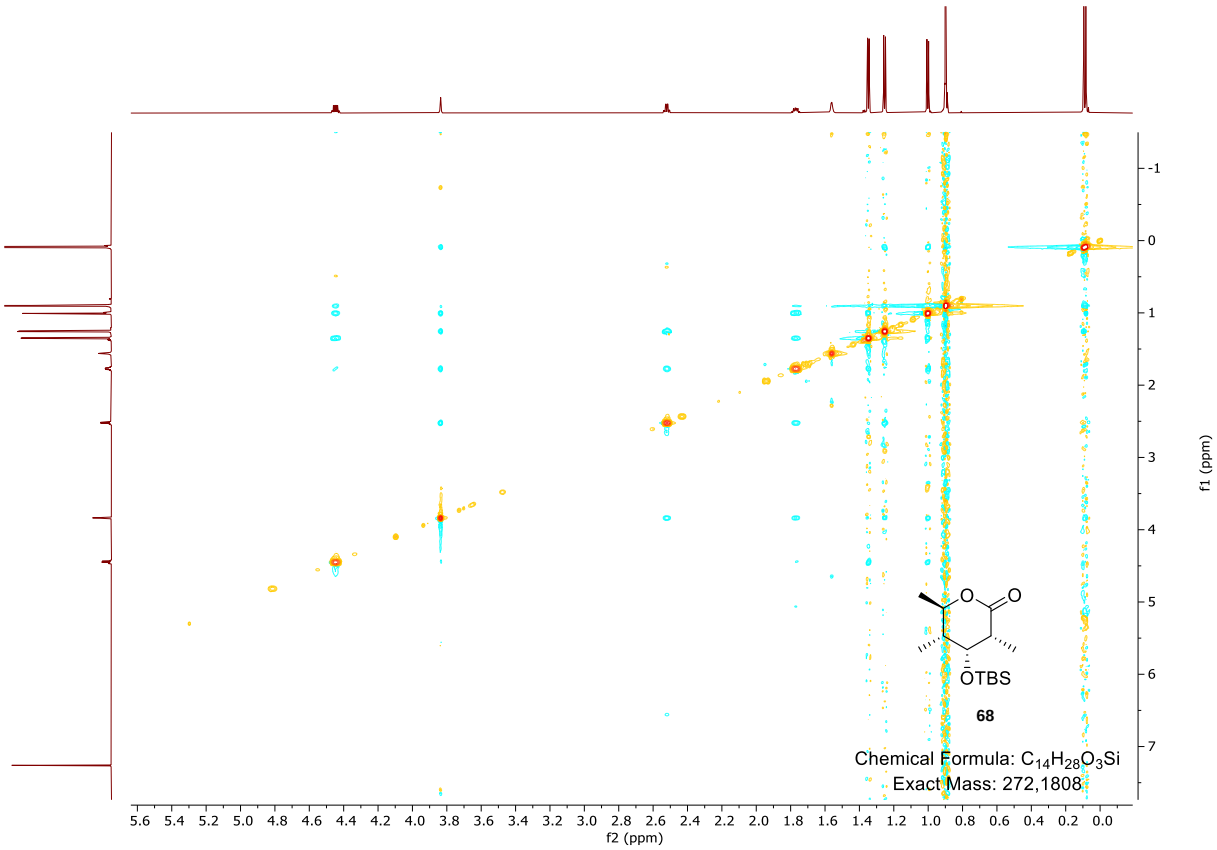

^{1}H, ^{1}H – NOESY spectrum of **68** (500 MHz, $CDCl_3$)

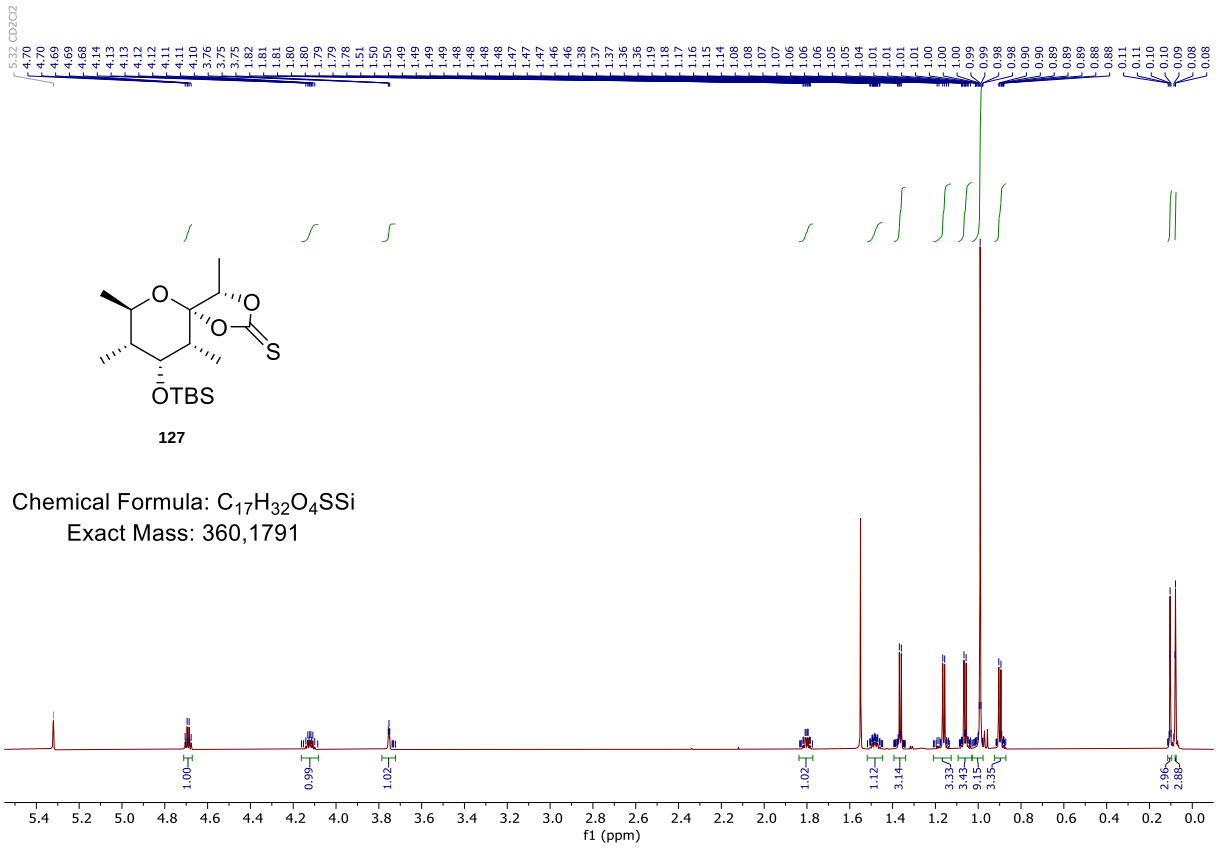

^{1}H – NMR spectrum of **127** (500 MHz, CD_2Cl_2)

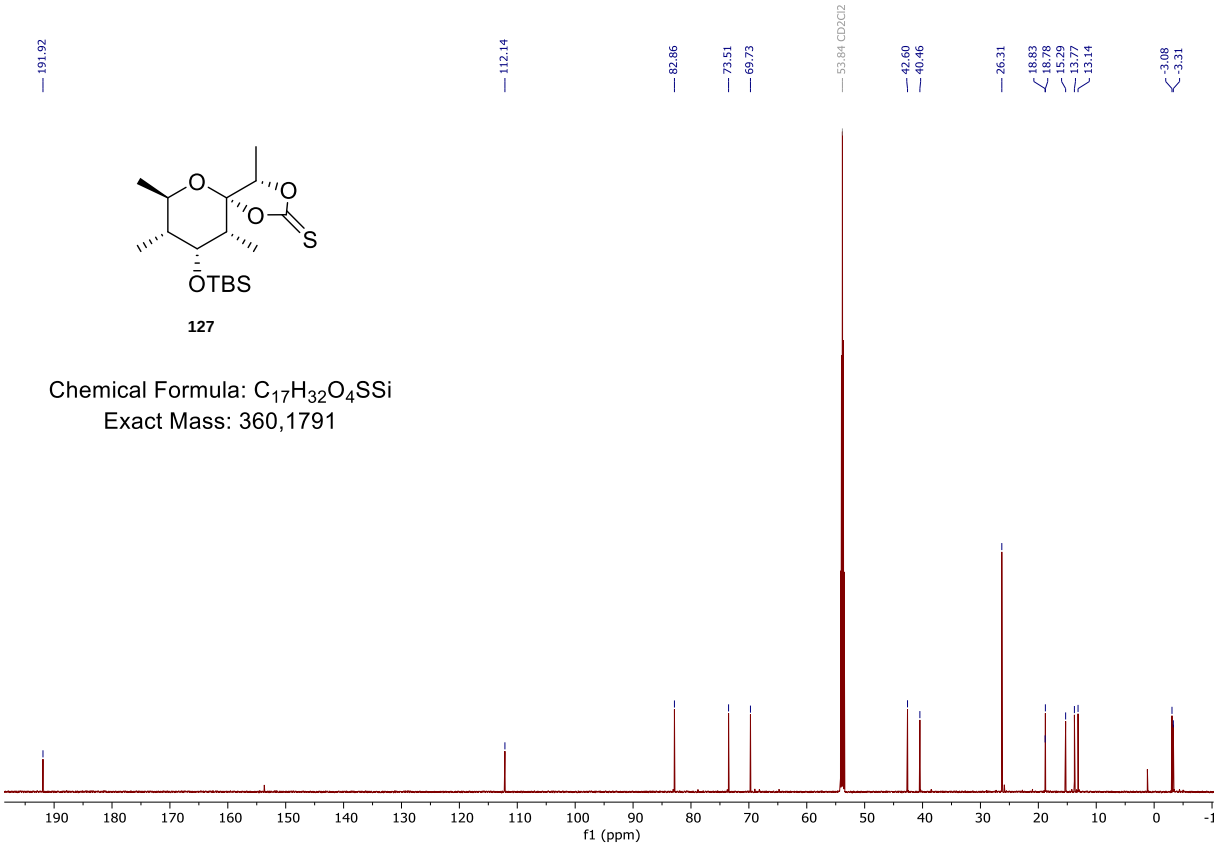

^{13}C – NMR spectrum of **127** (125 MHz, CD_2Cl_2)

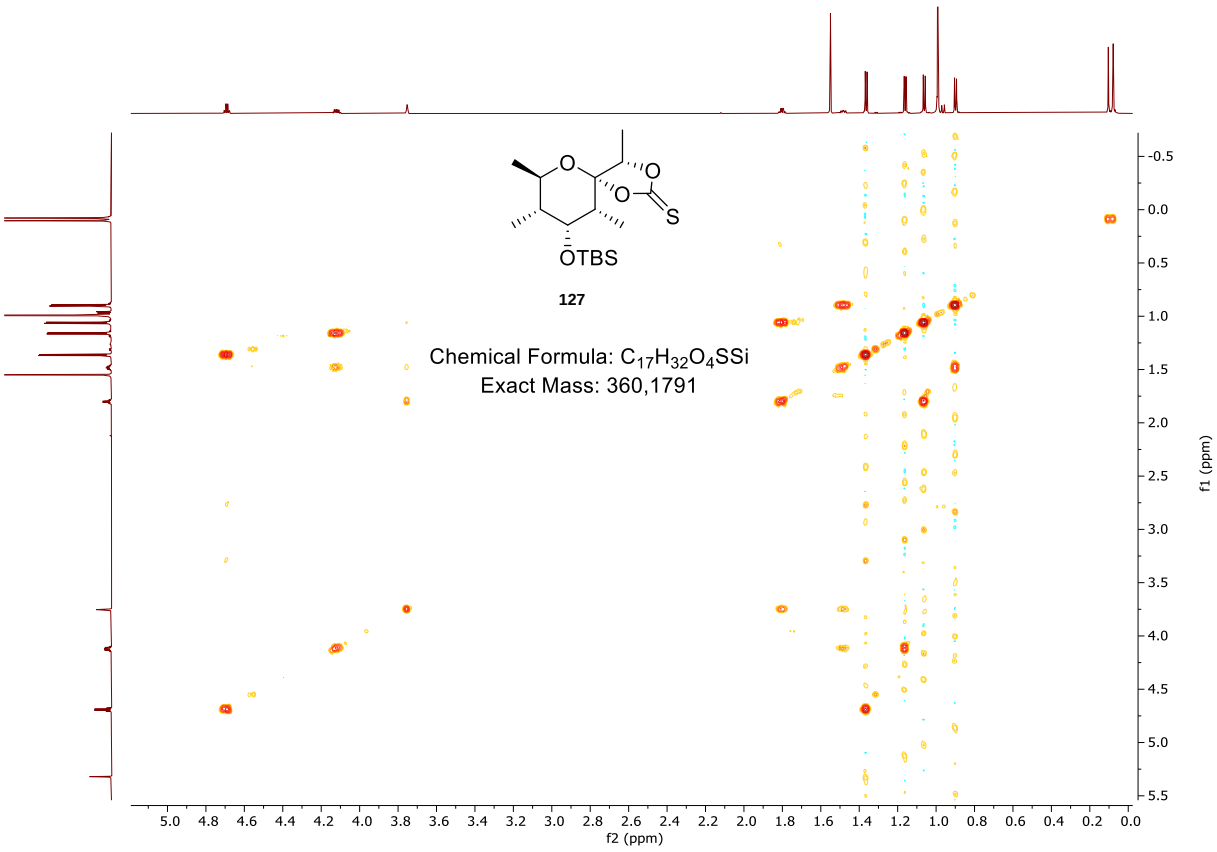

^{1}H, ^{1}H – COSY spectrum of **127** (500 MHz, CD_2Cl_2)

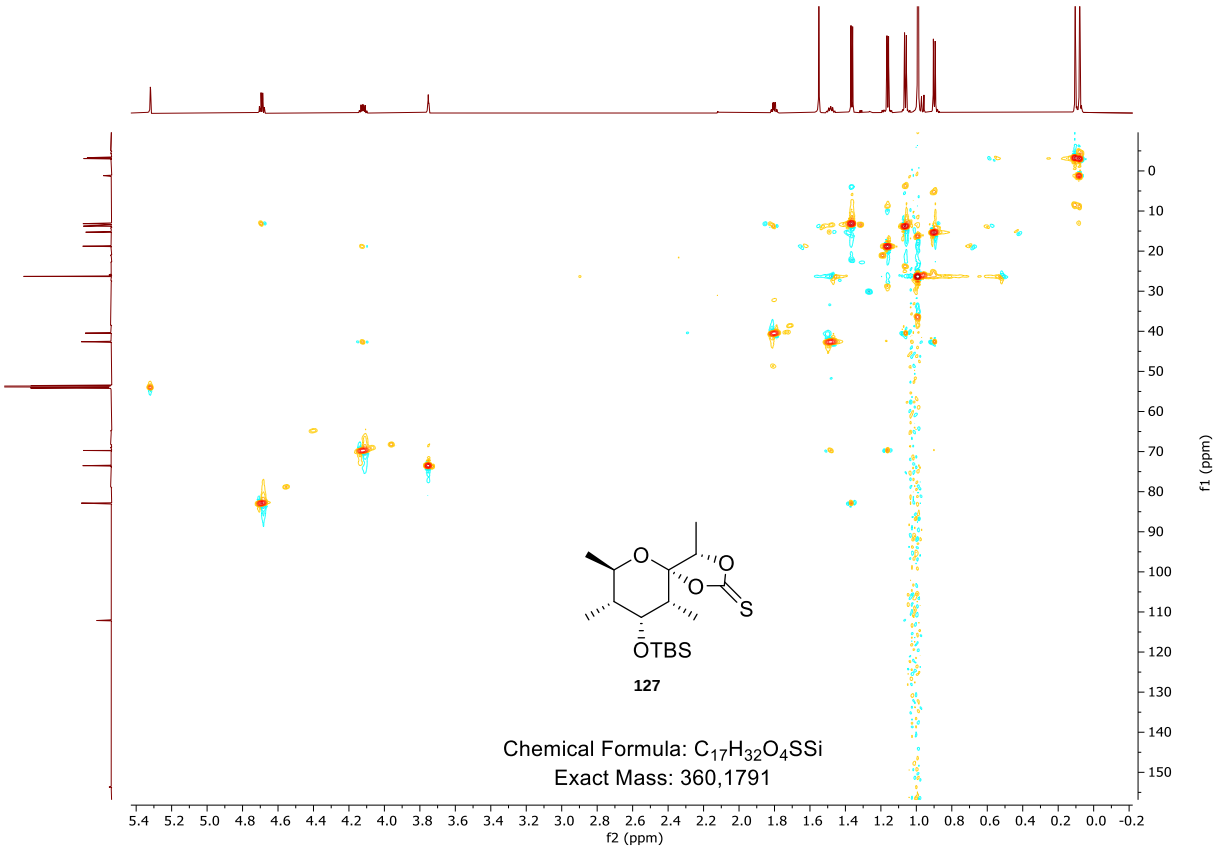

^{1}H, ^{13}C – HSQC spectrum of **127** (500 MHz, 125 MHz, CD_2Cl_2)

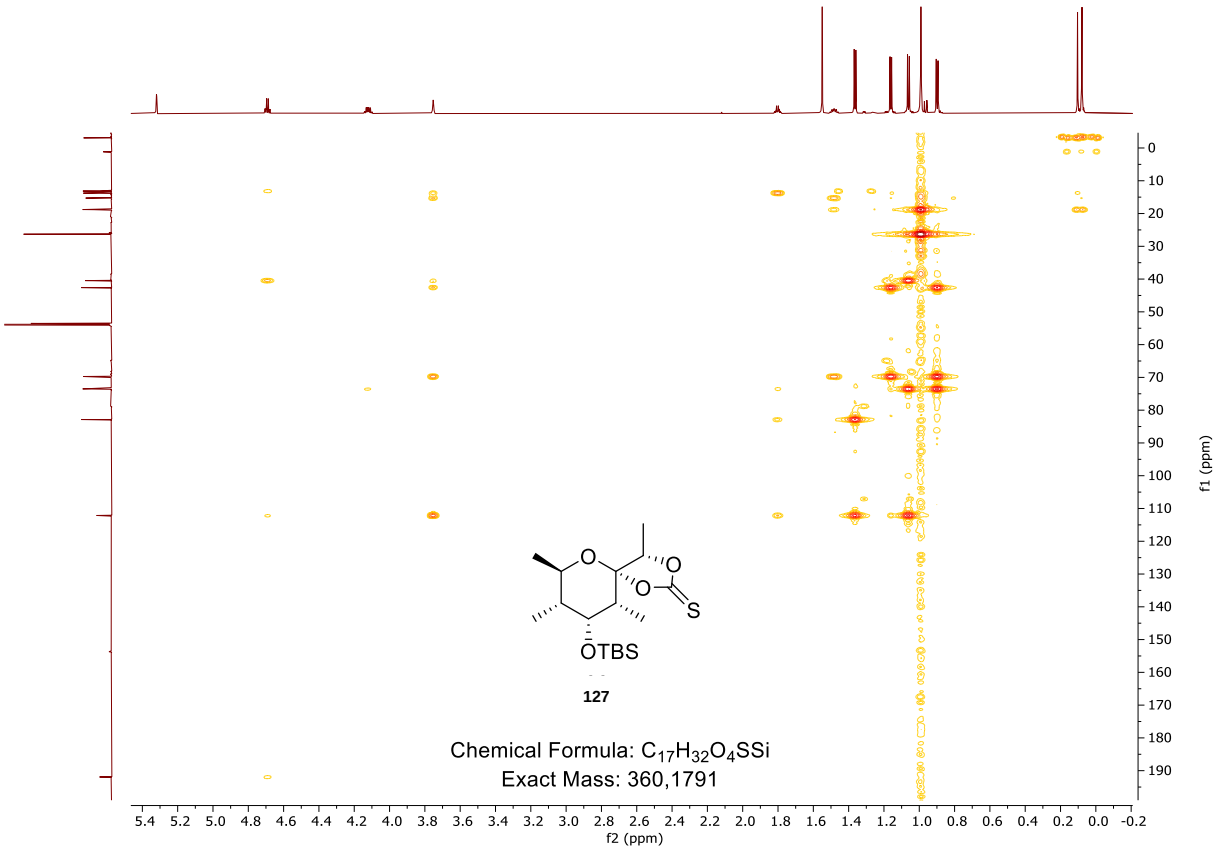

^{1}H, ^{13}C – HMBC spectrum of **127** (500 MHz, 125 MHz, CD_2Cl_2)

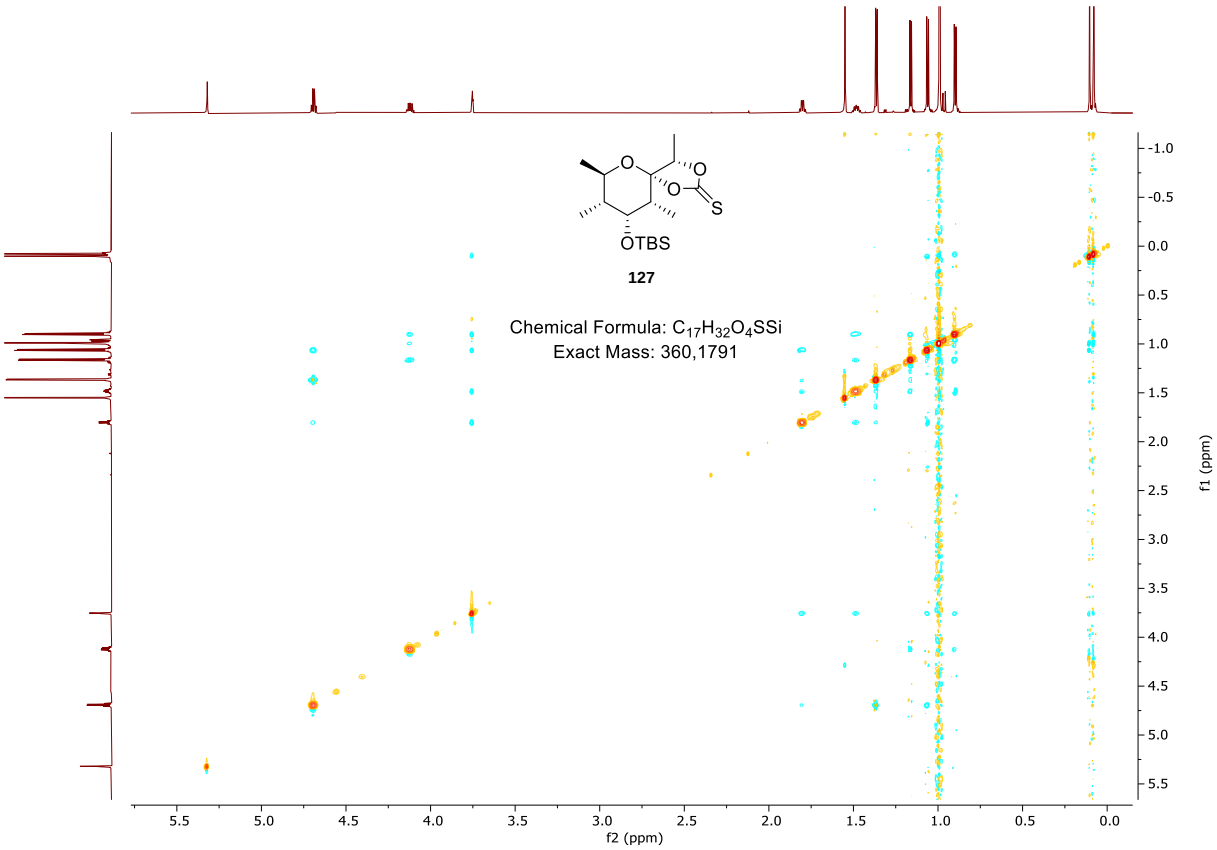

^{1}H, ^{1}H – NOESY spectrum of **127** (500 MHz, CD_2Cl_2)

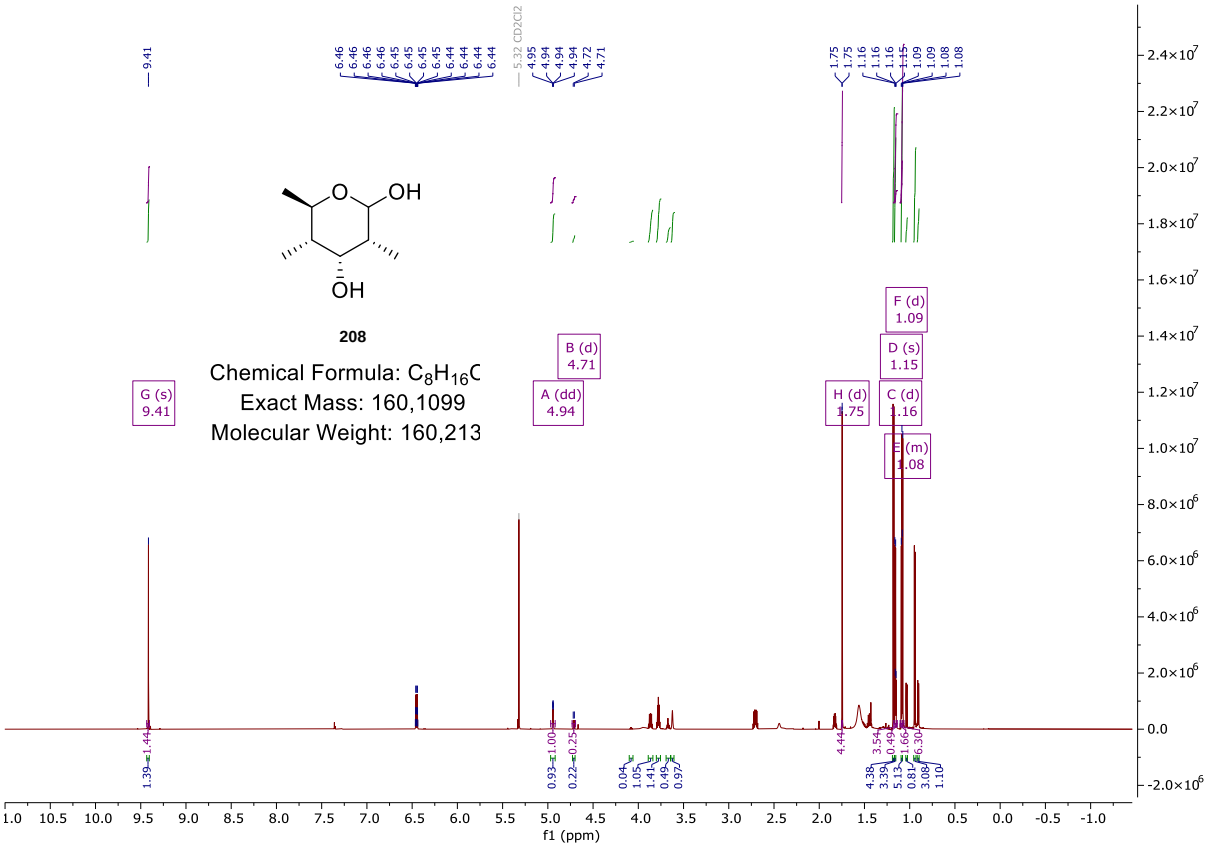

^{1}H – NMR spectrum of **208** (700 MHz, CD_2Cl_2)

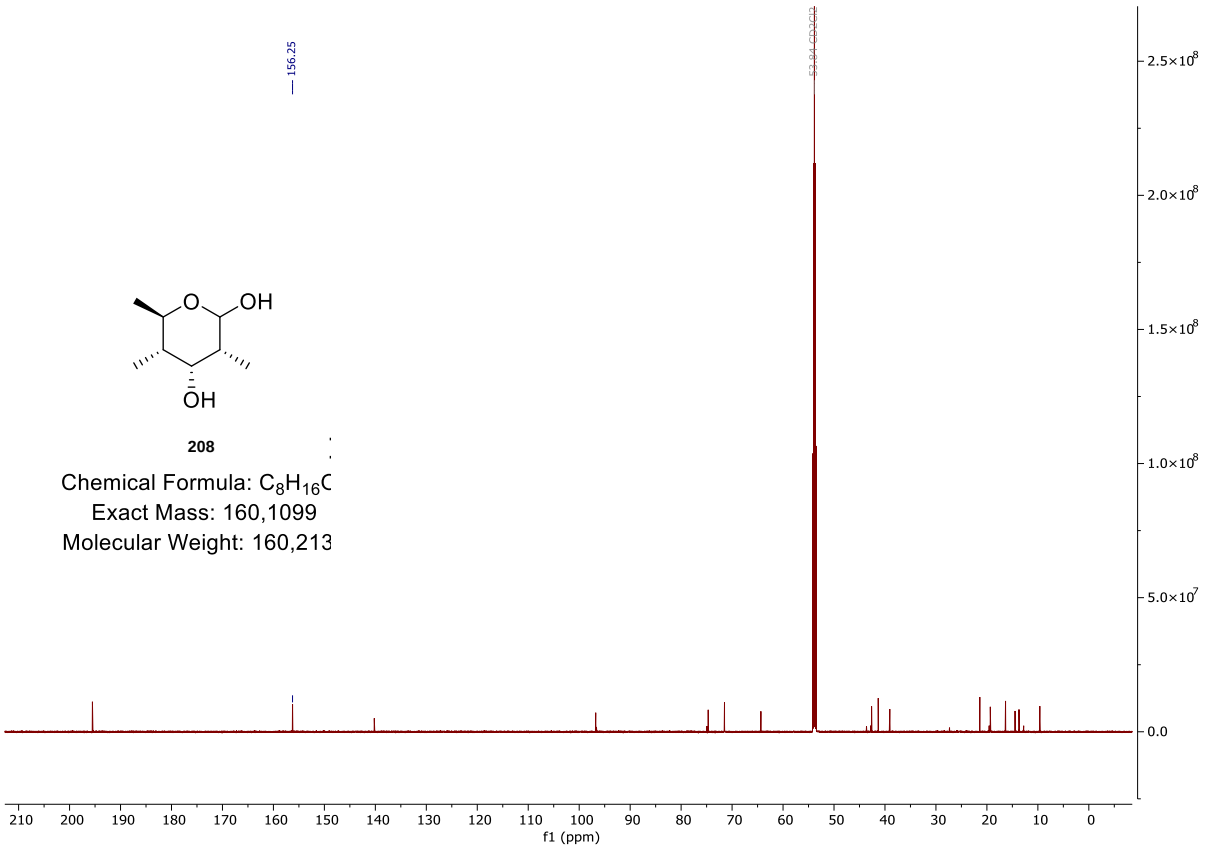

^{13}C – NMR spectrum of **208** (175 MHz, CD_2Cl_2)

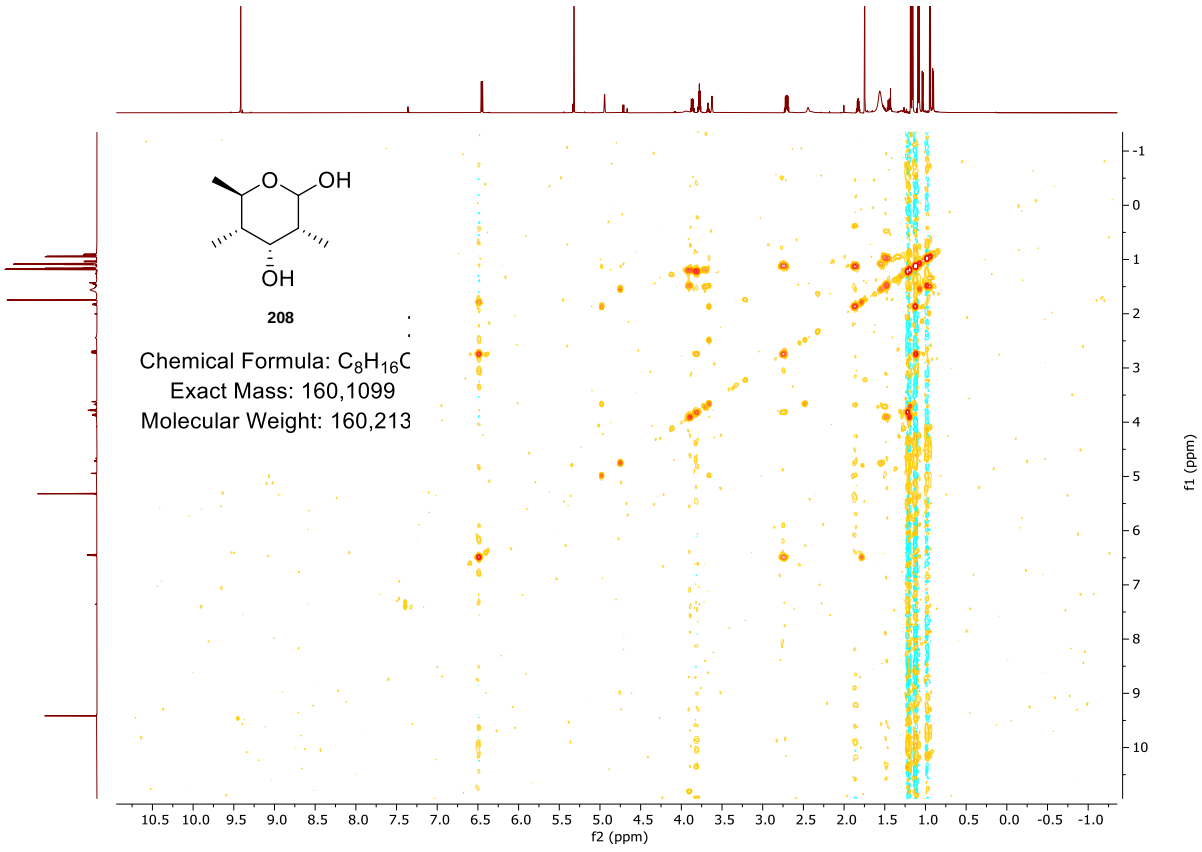

^{1}H, ^{1}H – COSY spectrum of **208** (700 MHz, CD_2Cl_2)

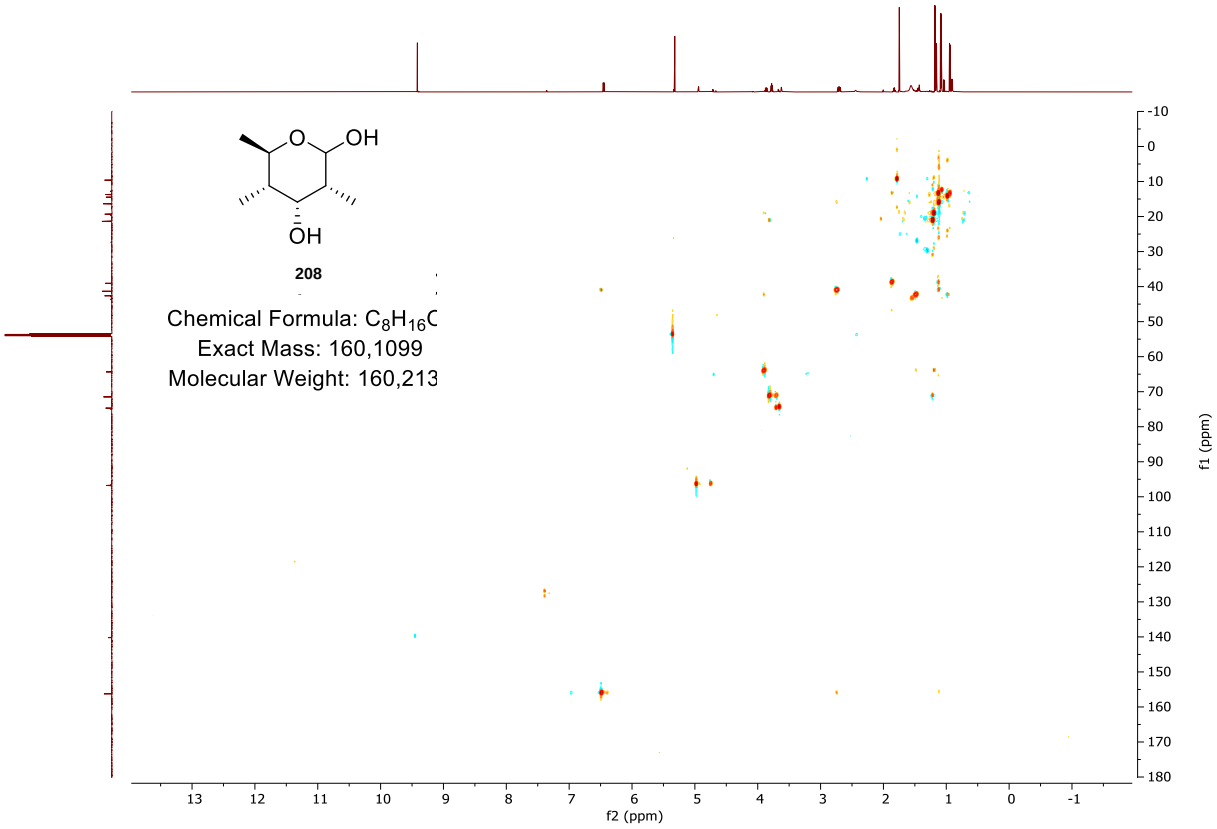

^{1}H, ^{13}C – HSQC spectrum of **208** (700 MHz, 175 MHz, CD_2Cl_2)

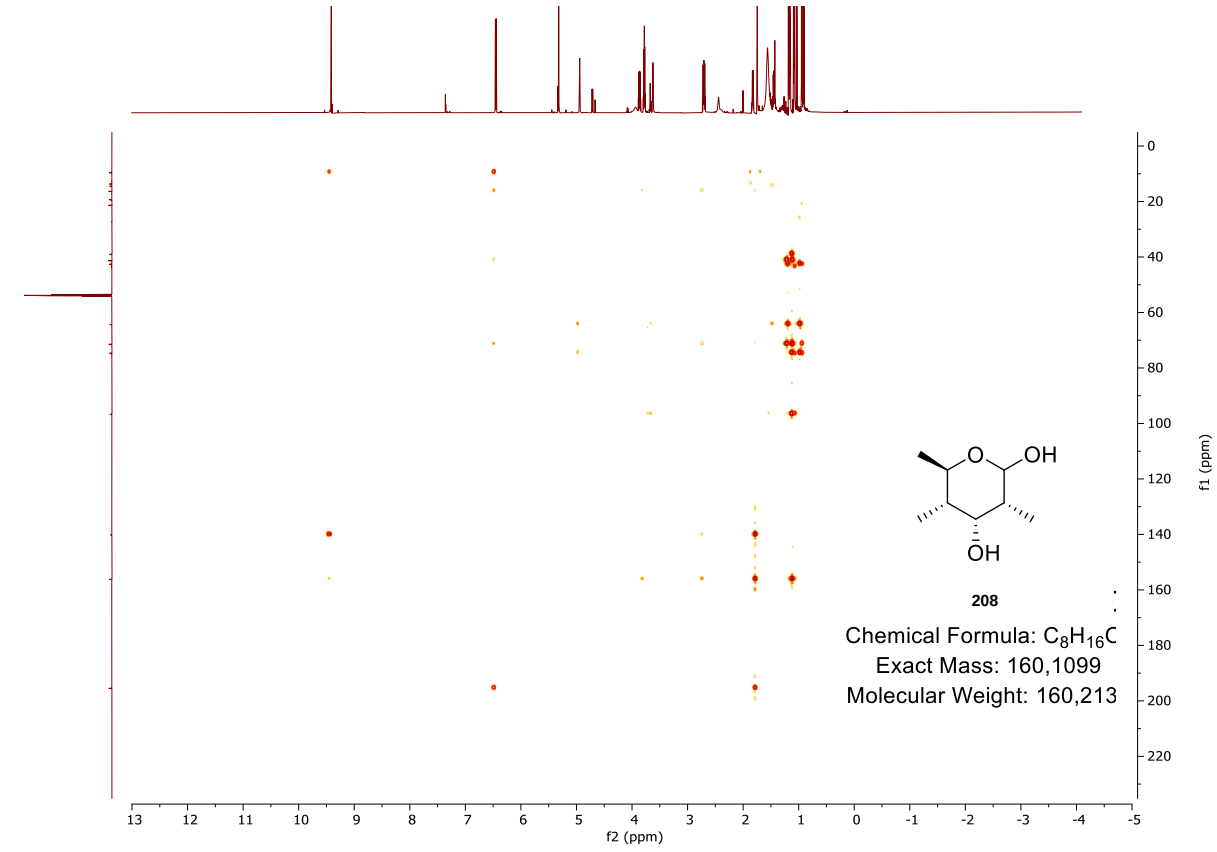

^{1}H, ^{13}C – HMBC spectrum of **208** (700 MHz, 175 MHz, CD_2Cl_2)

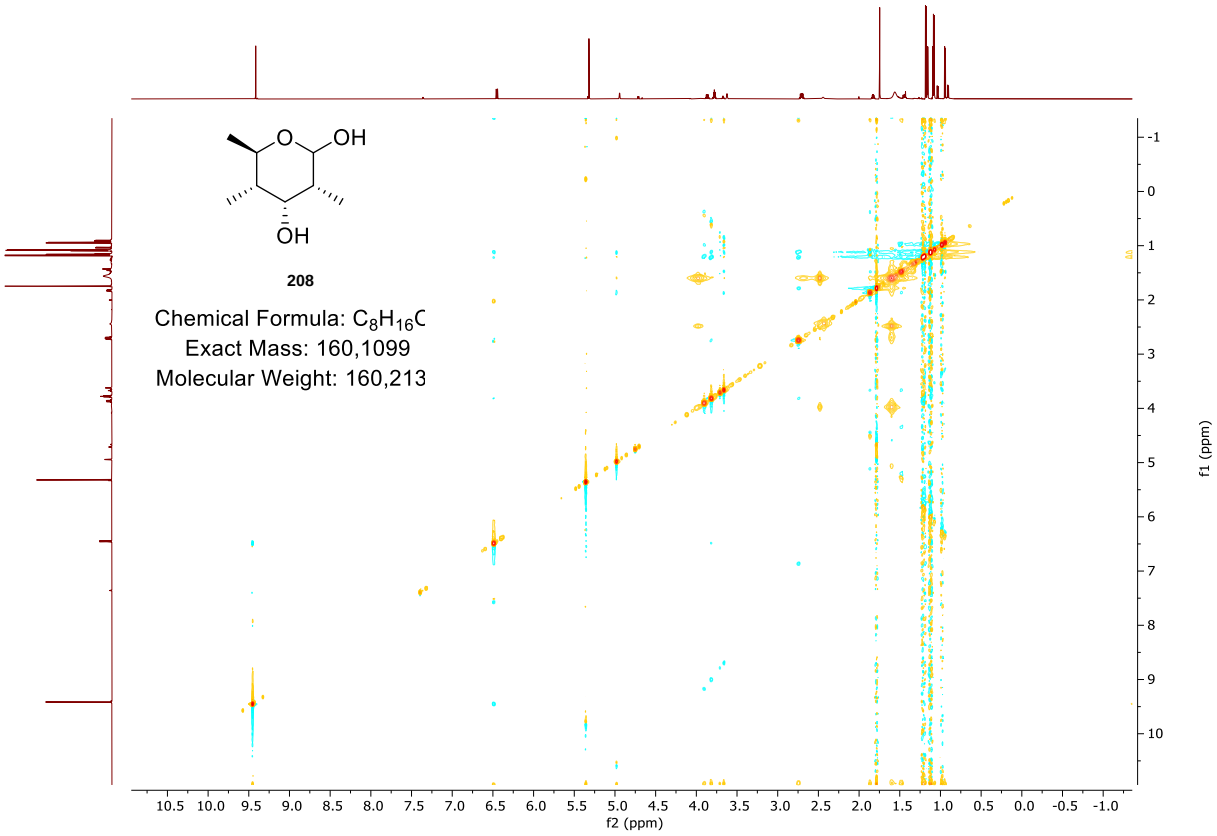

^{1}H, ^{1}H – NOESY spectrum of **208** (700 MHz, CD_2Cl_2)

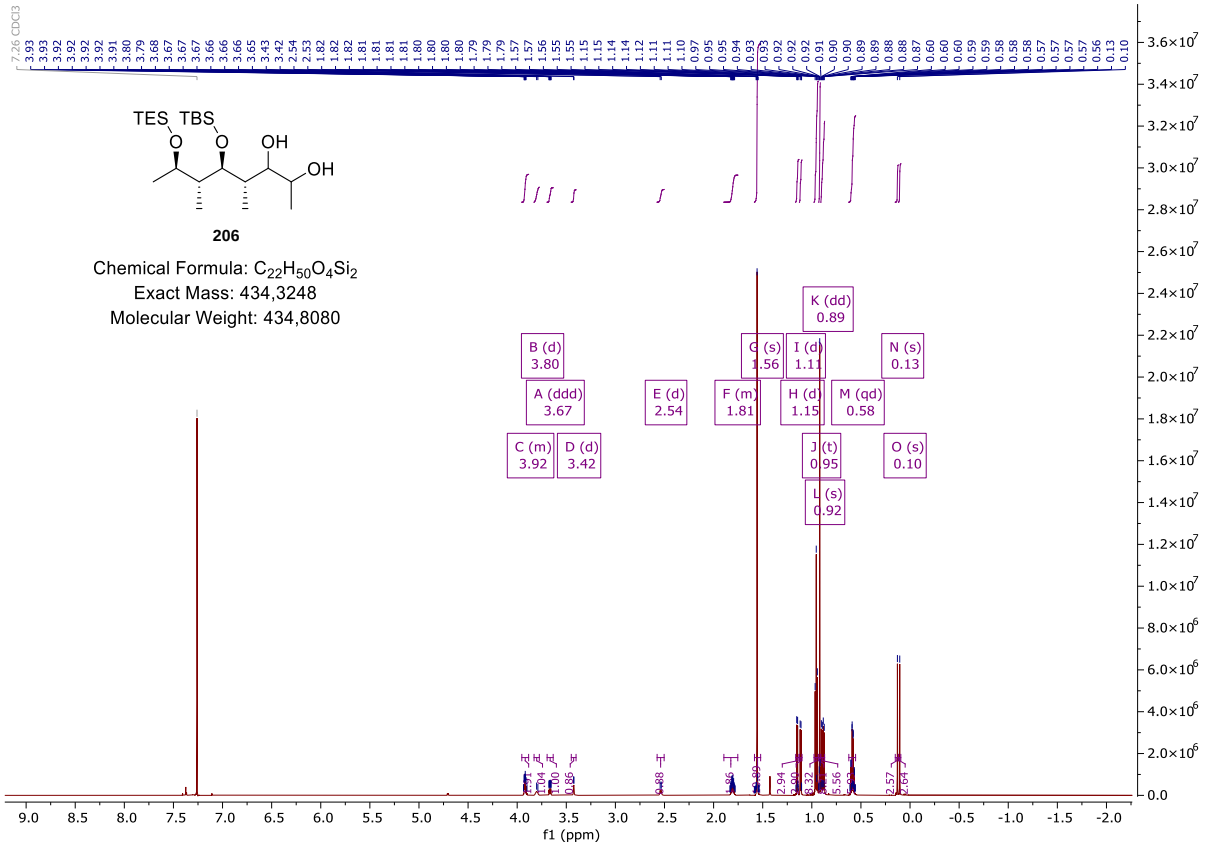

^{1}H – NMR spectrum of **206** (700 MHz, $CDCl_3$)

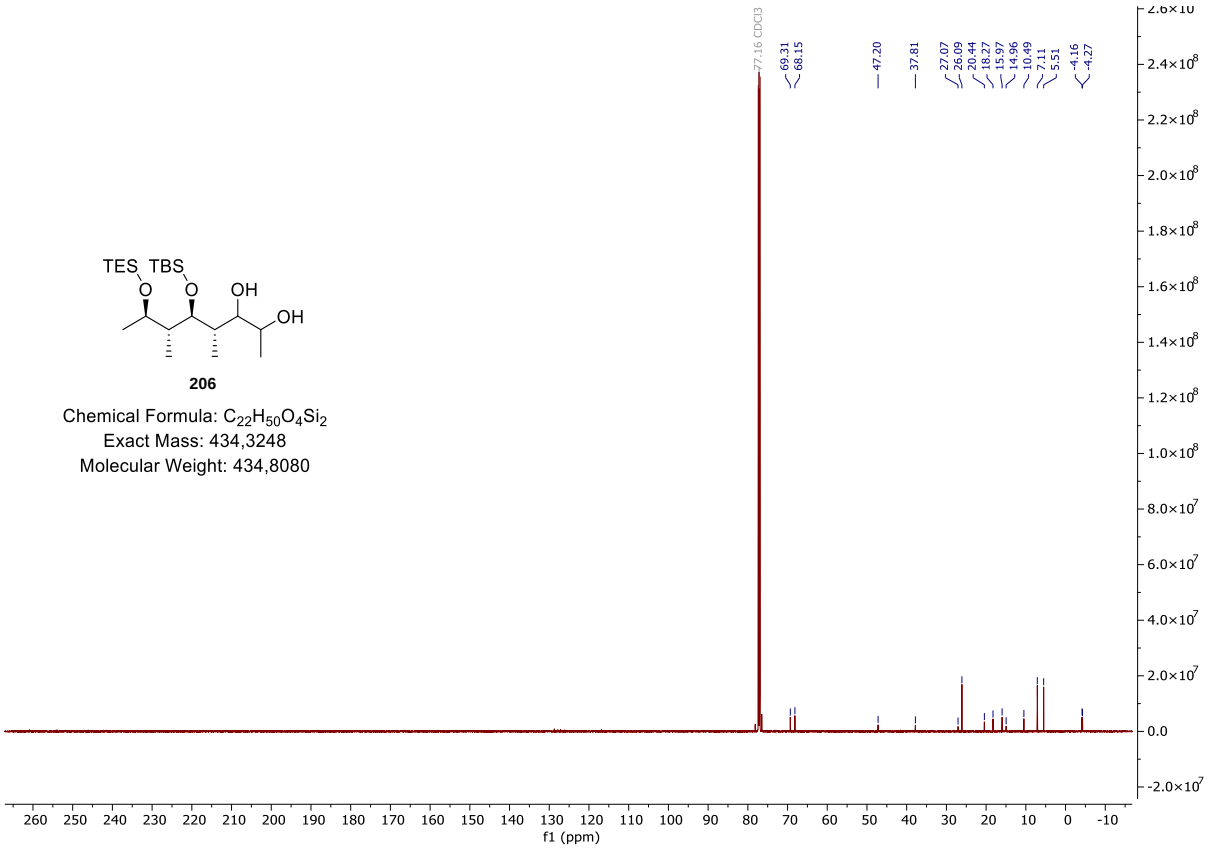

^{13}C – NMR spectrum of **206** ($CDCl_3$)

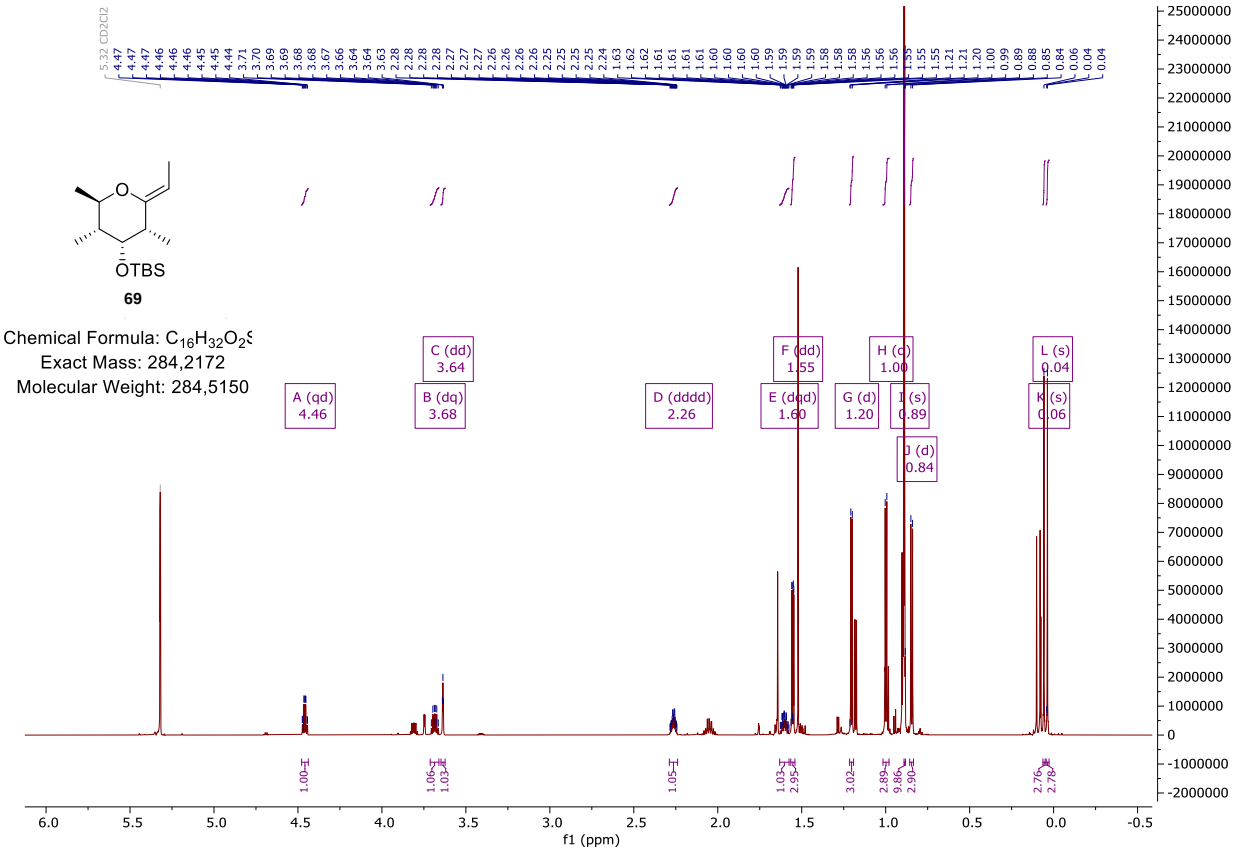

^{1}H – NMR spectrum of **69** (CD_2Cl_2)

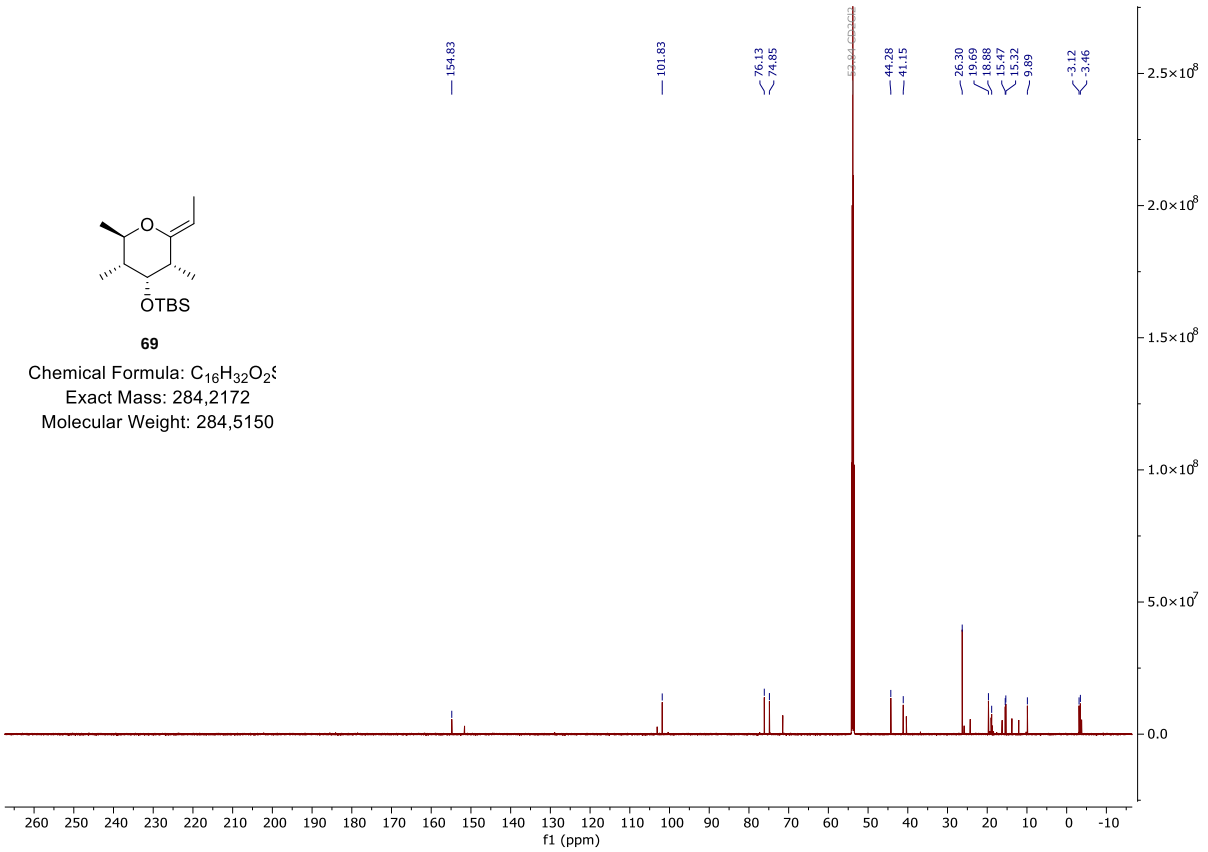

^{13}C – NMR spectrum of **69** (175 MHz, CD_2Cl_2)

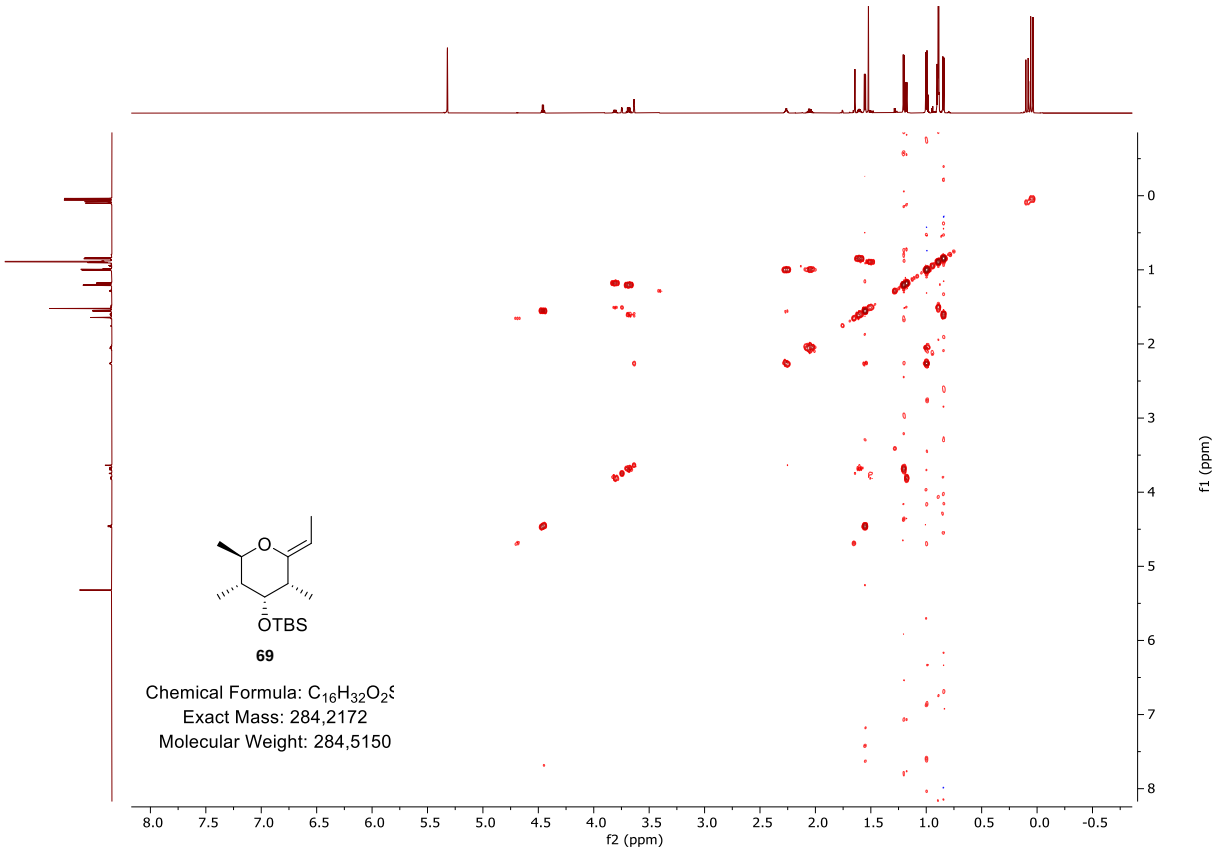

^{1}H, ^{1}H – COSY spectrum of **69** (700 MHz, CD_2Cl_2)

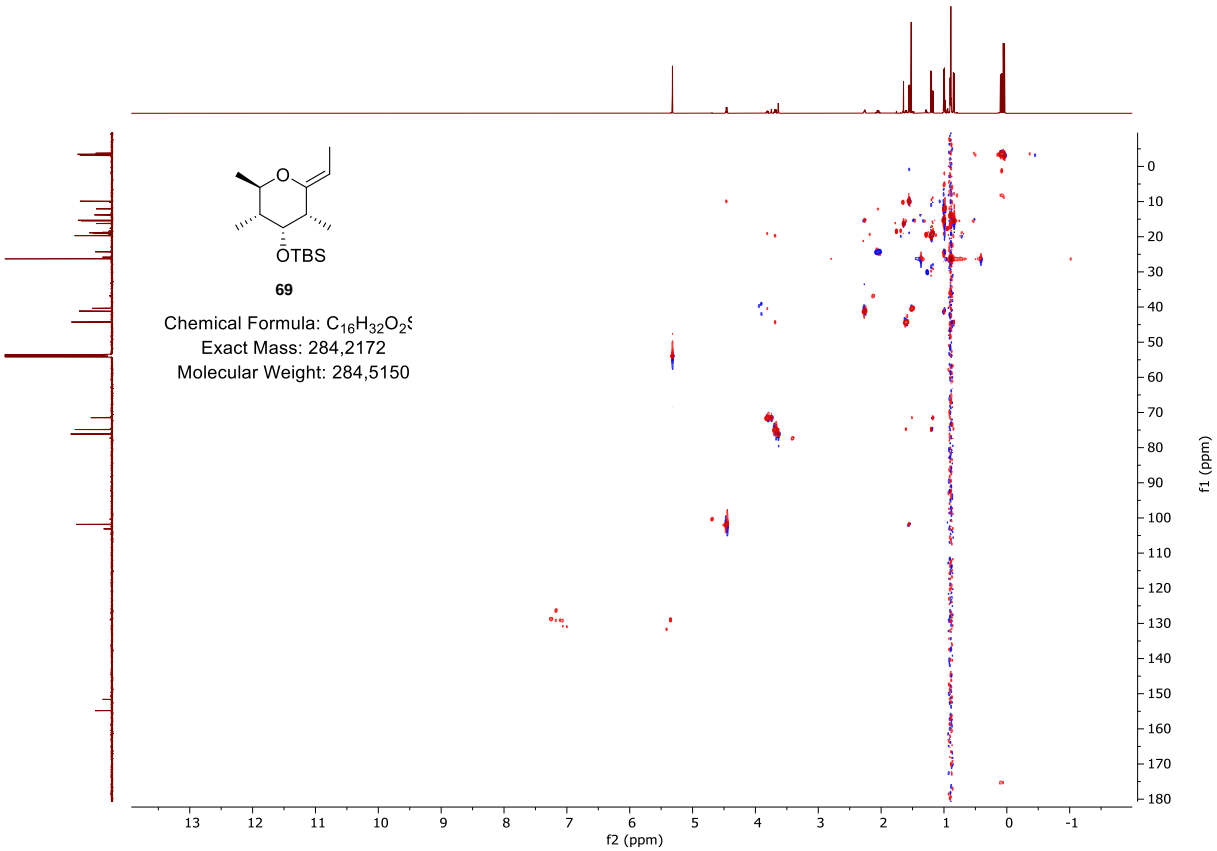

^{1}H, ^{13}C – HSQC spectrum of **69** (700 MHz, 175 MHz, CD_2Cl_2)

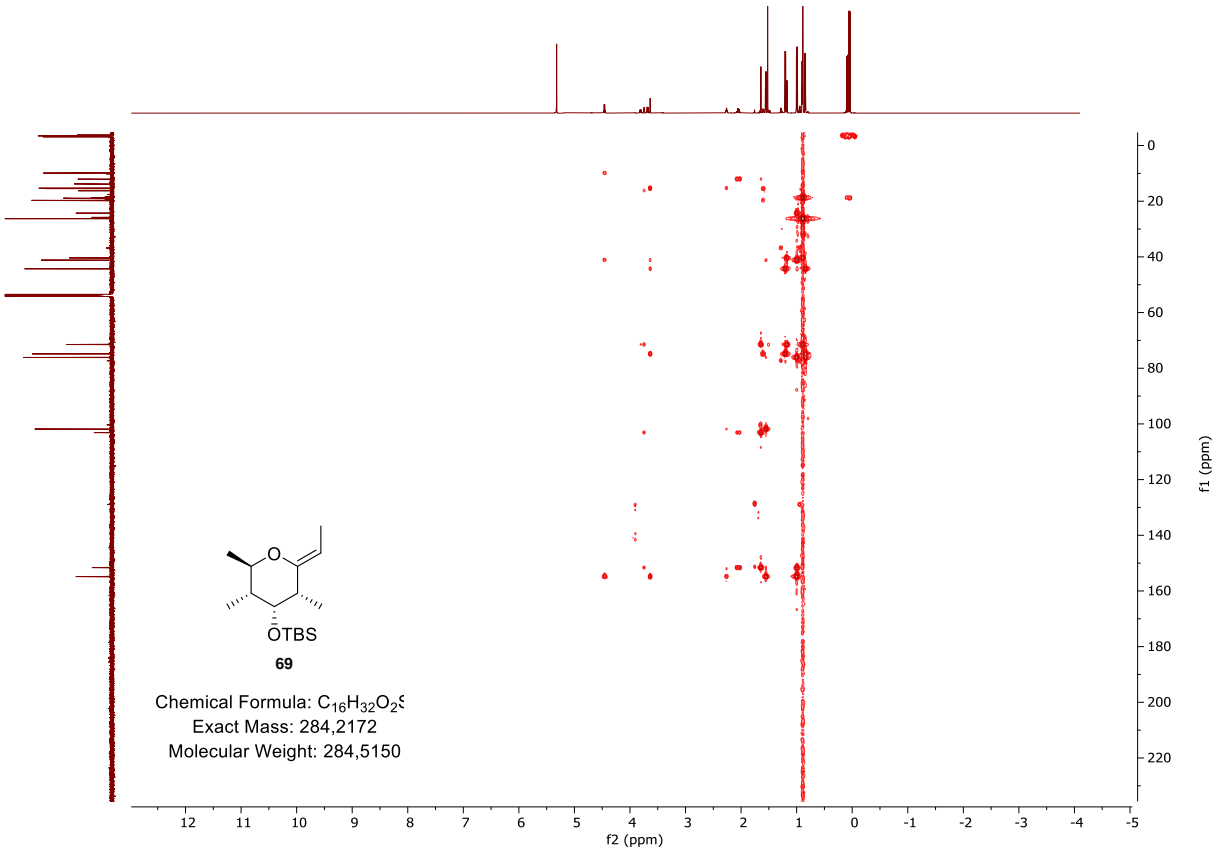

^{1}H, ^{13}C – HMBC spectrum of **69** (700 MHz, 175 MHz, CD_2Cl_2)

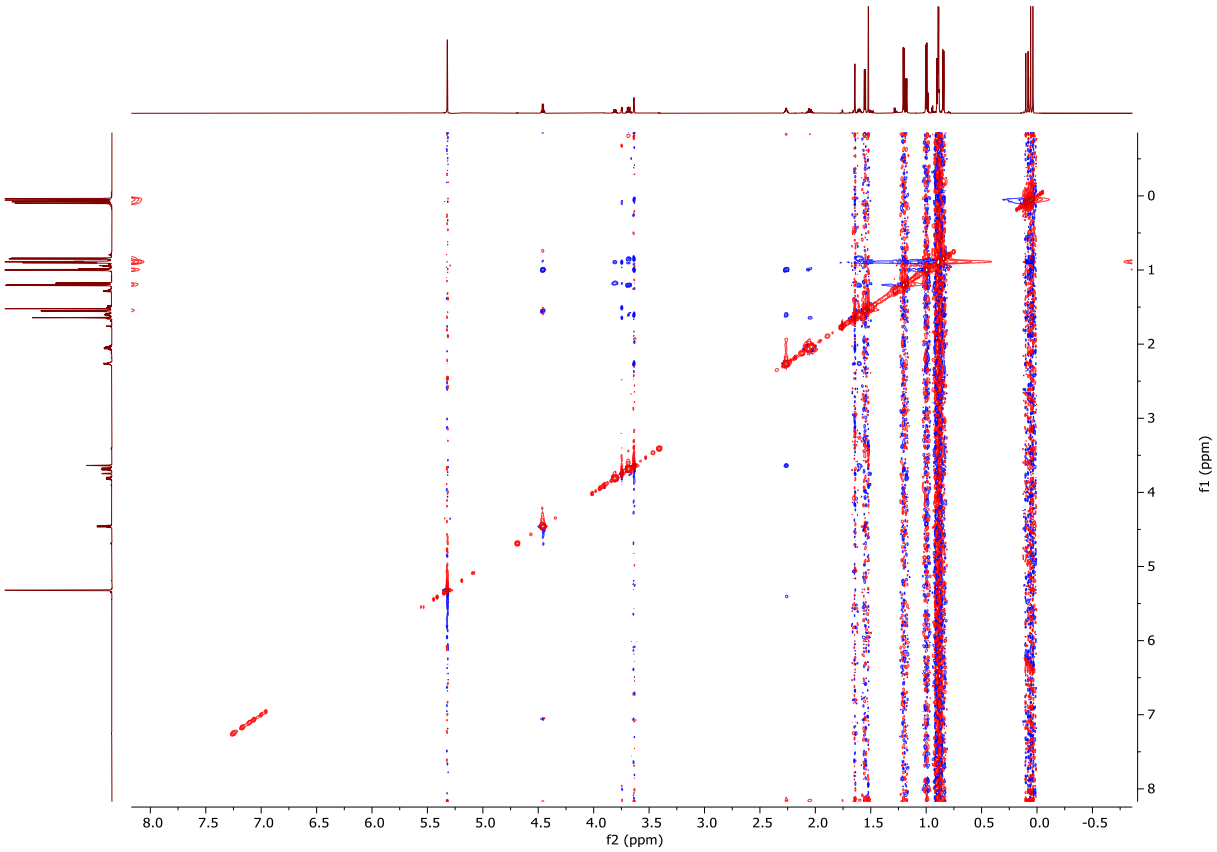

^{1}H, ^{1}H – NOESY spectrum of **69** (700 MHz, CD_2Cl_2)

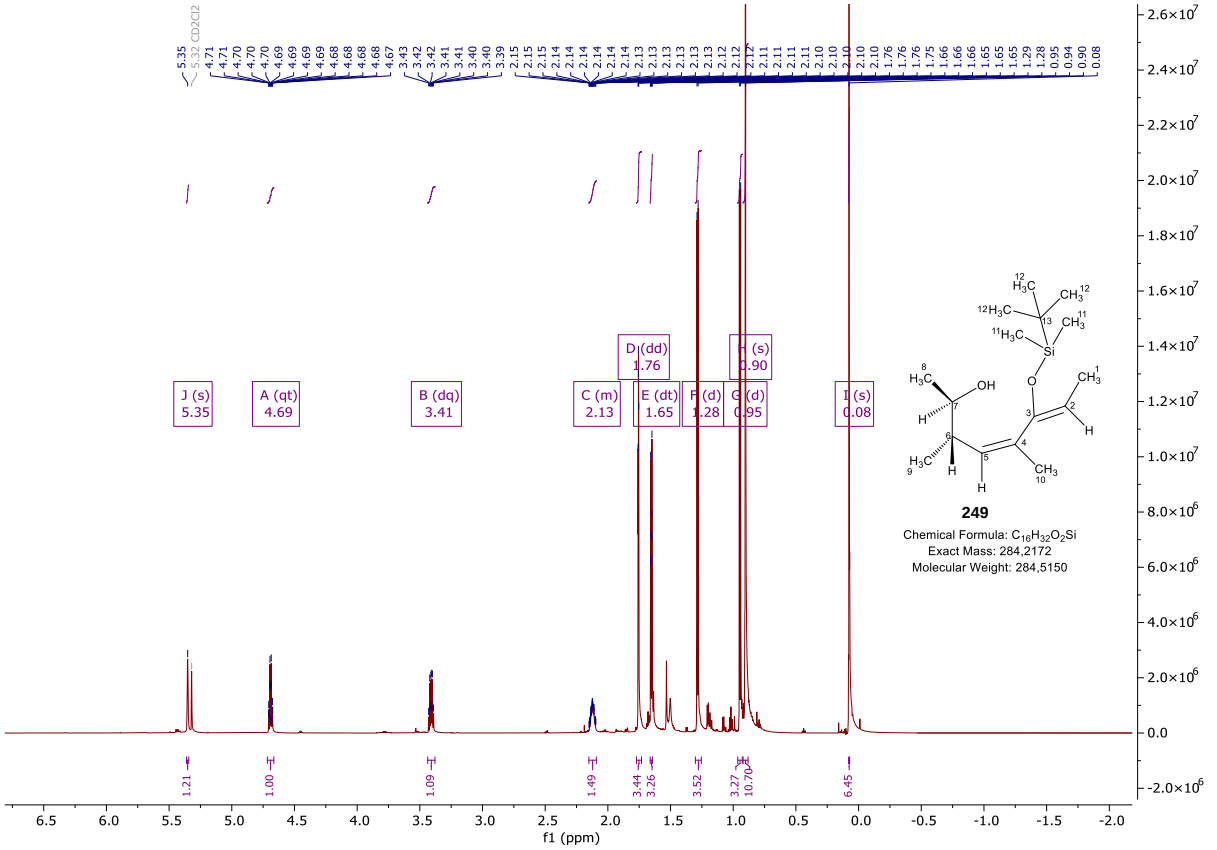

^{1}H – NMR spectrum of **249** (700 MHz, CD_2Cl_2)

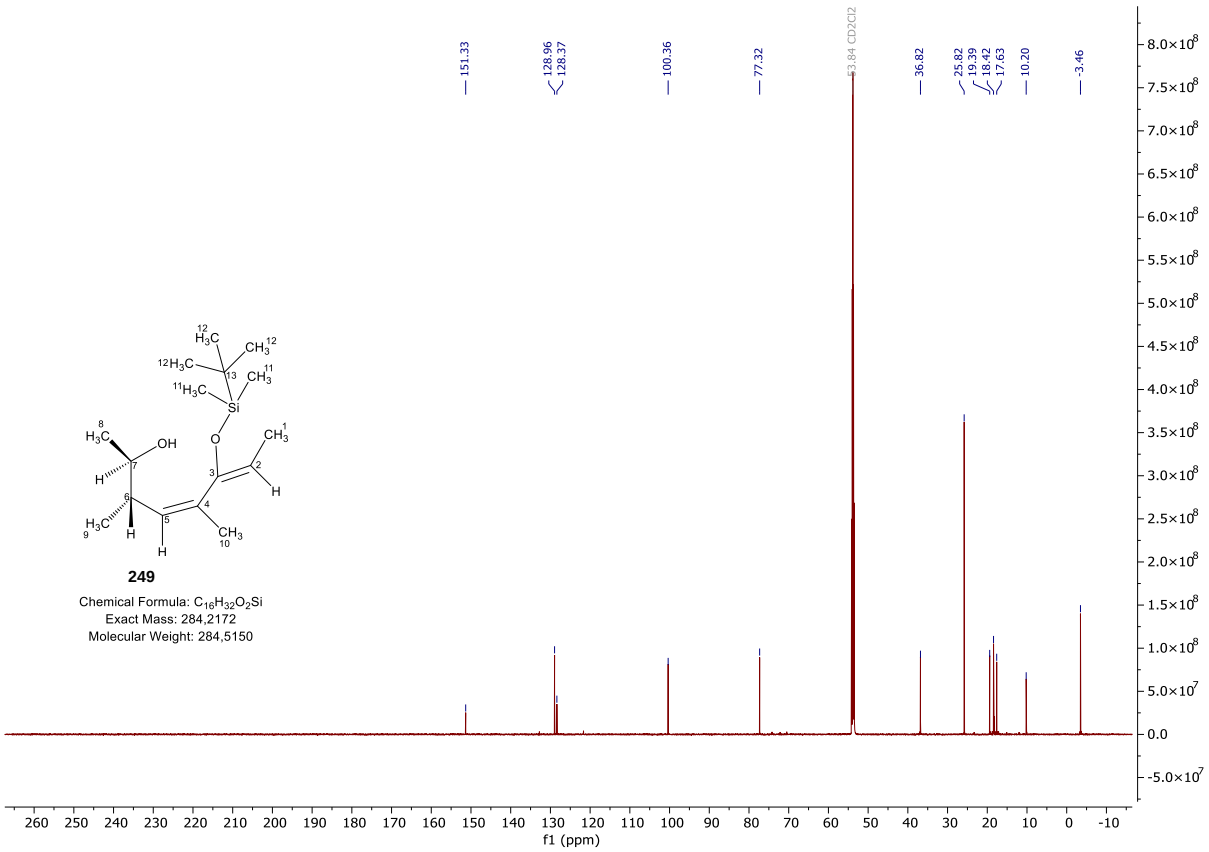

249

Chemical Formula: $C_{16}H_{32}O_2Si$
Exact Mass: 284,2172
Molecular Weight: 284,5150

^{13}C – NMR spectrum of **249** (175 MHz, CD_2Cl_2)

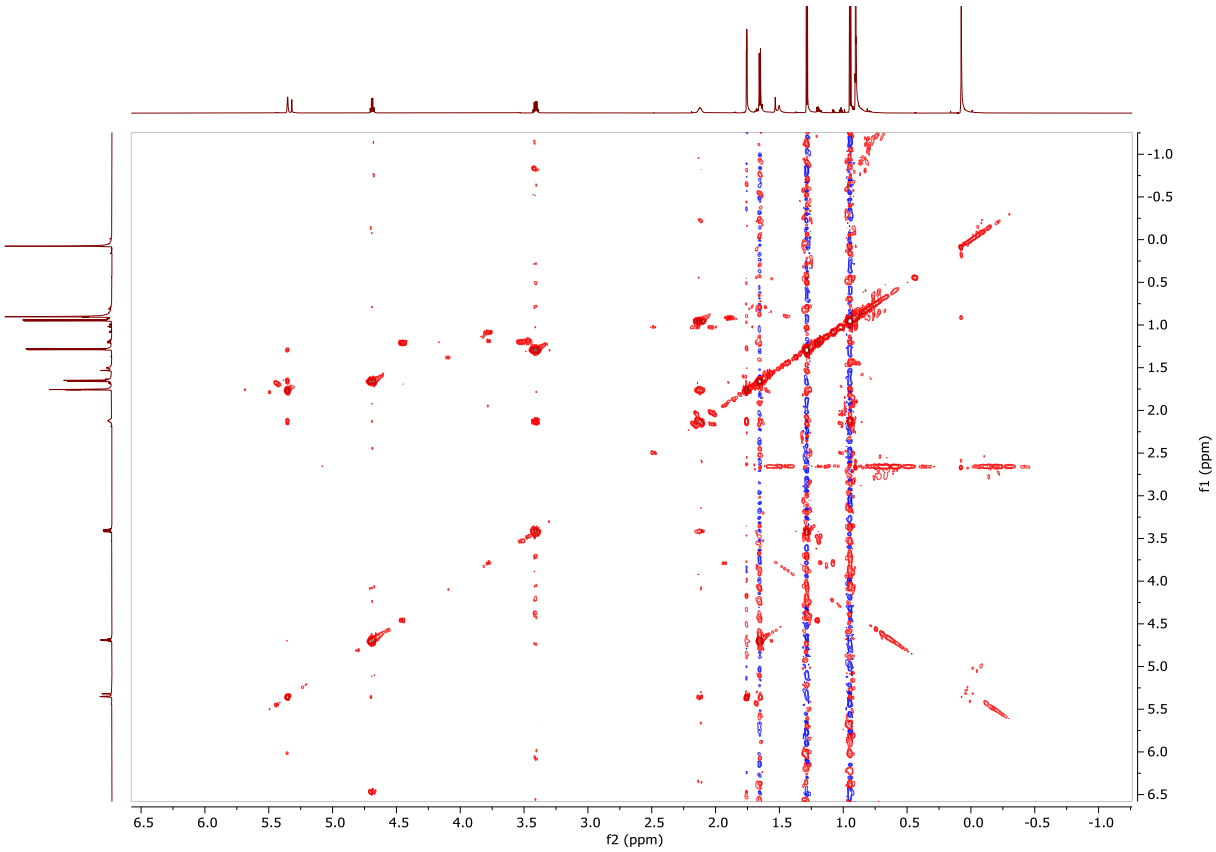

^{1}H, ^{1}H – COSY spectrum of **249** (700 MHz, CD_2Cl_2)

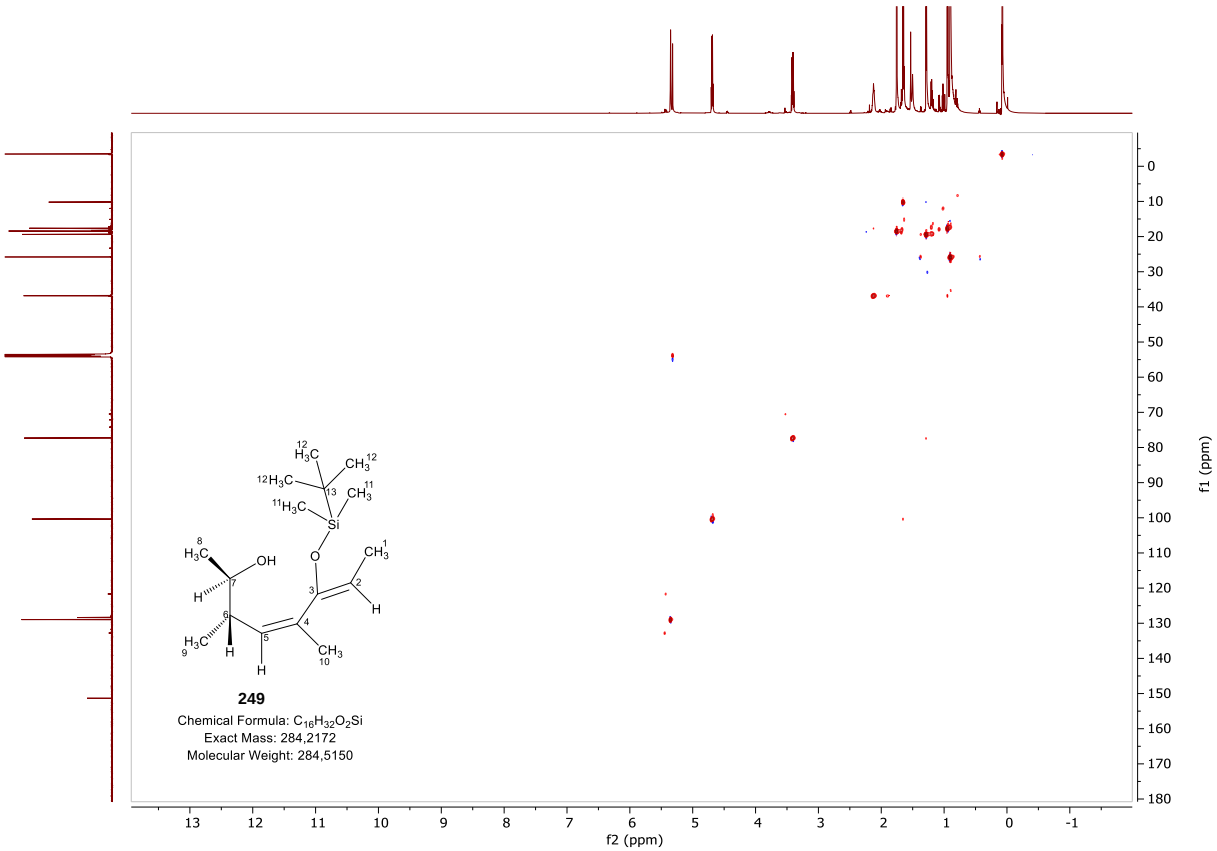

^{1}H, ^{13}C – HSQC spectrum of **249** (700 MHz, 175 MHz, CD_2Cl_2)

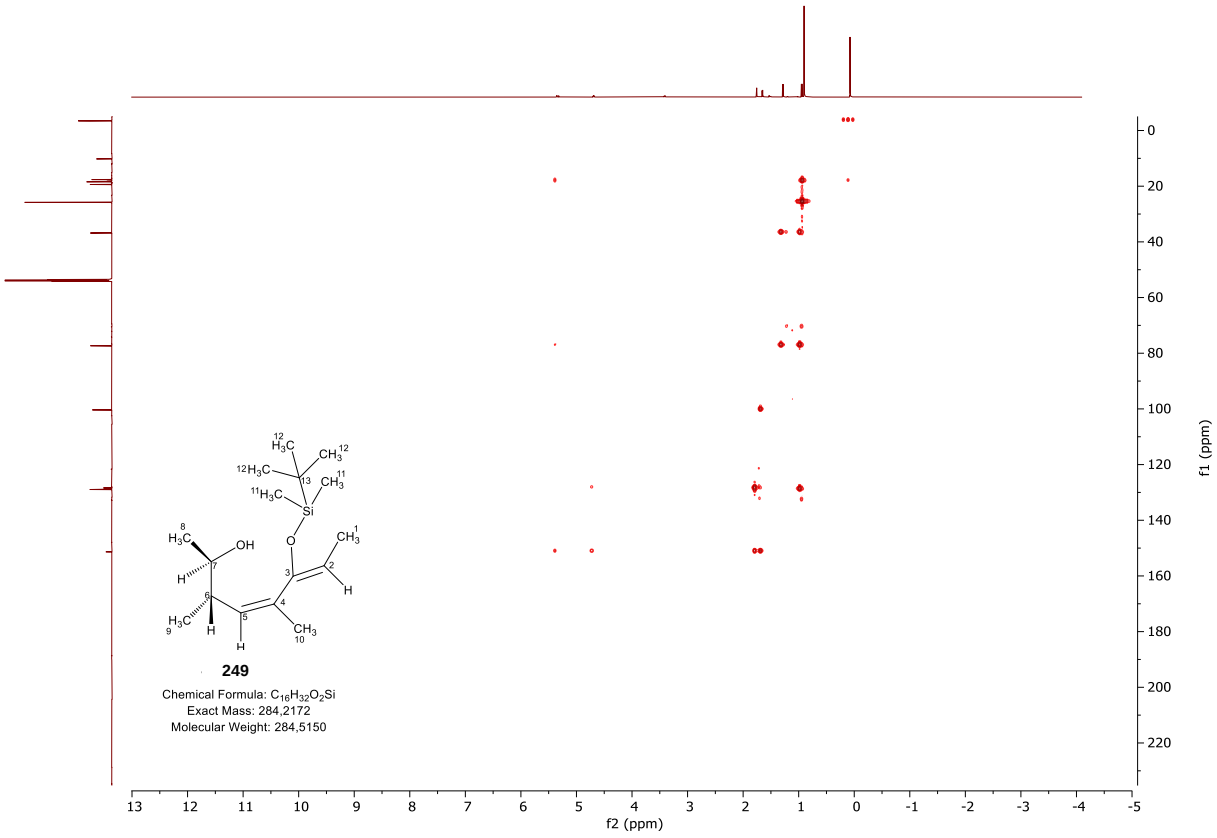

^{1}H, ^{13}C – HMBC spectrum of **249** (700 MHz, 175 MHz, CD_2Cl_2)

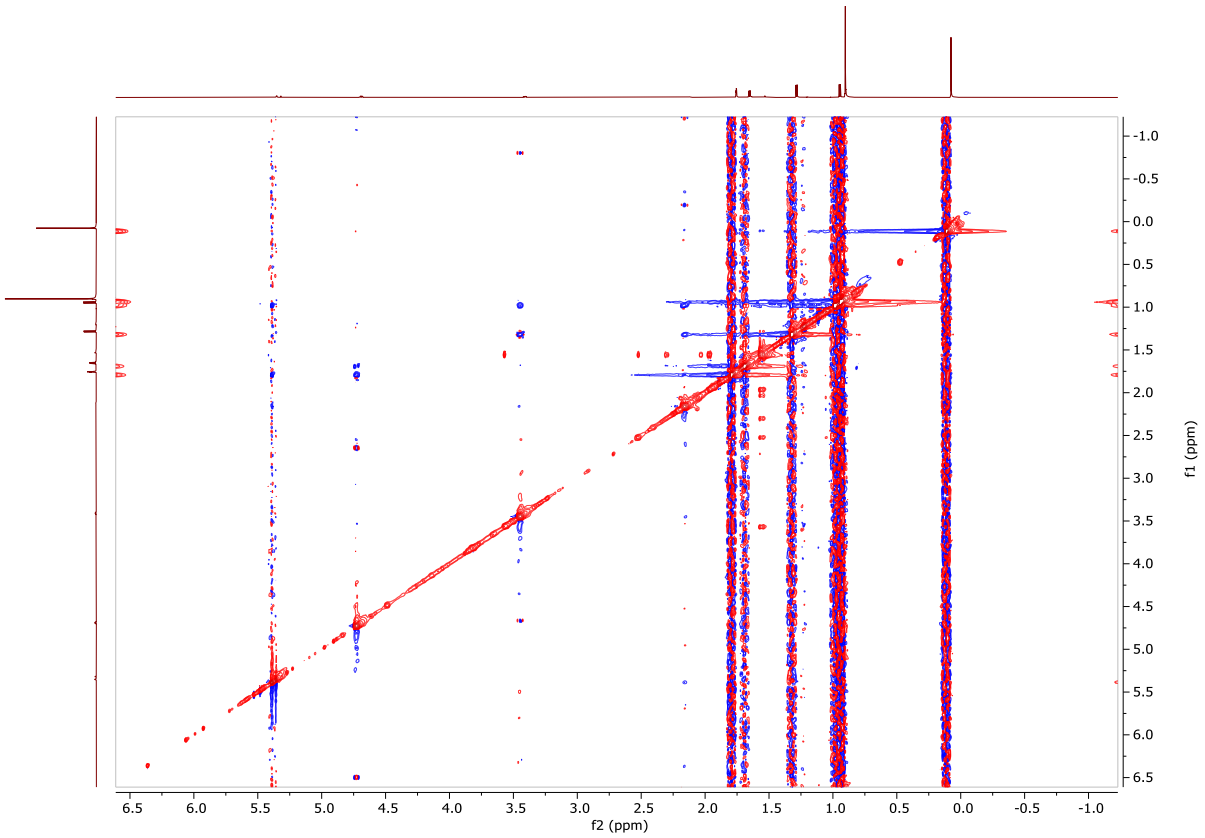

^{1}H, ^{1}H – NOESY spectrum of **249** (700 MHz, CD_2Cl_2)

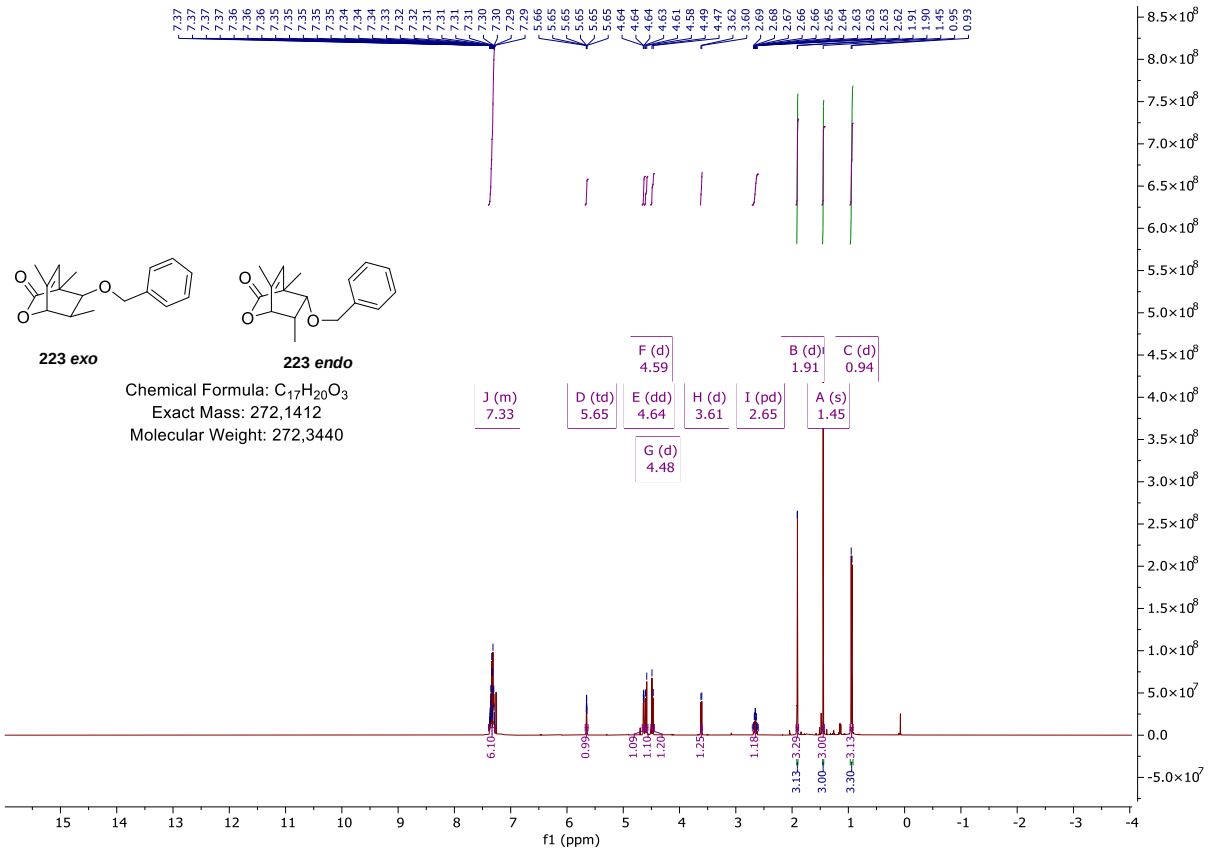

^{1}H – NMR spectrum of **223** (500 MHz, $CDCl_3$)

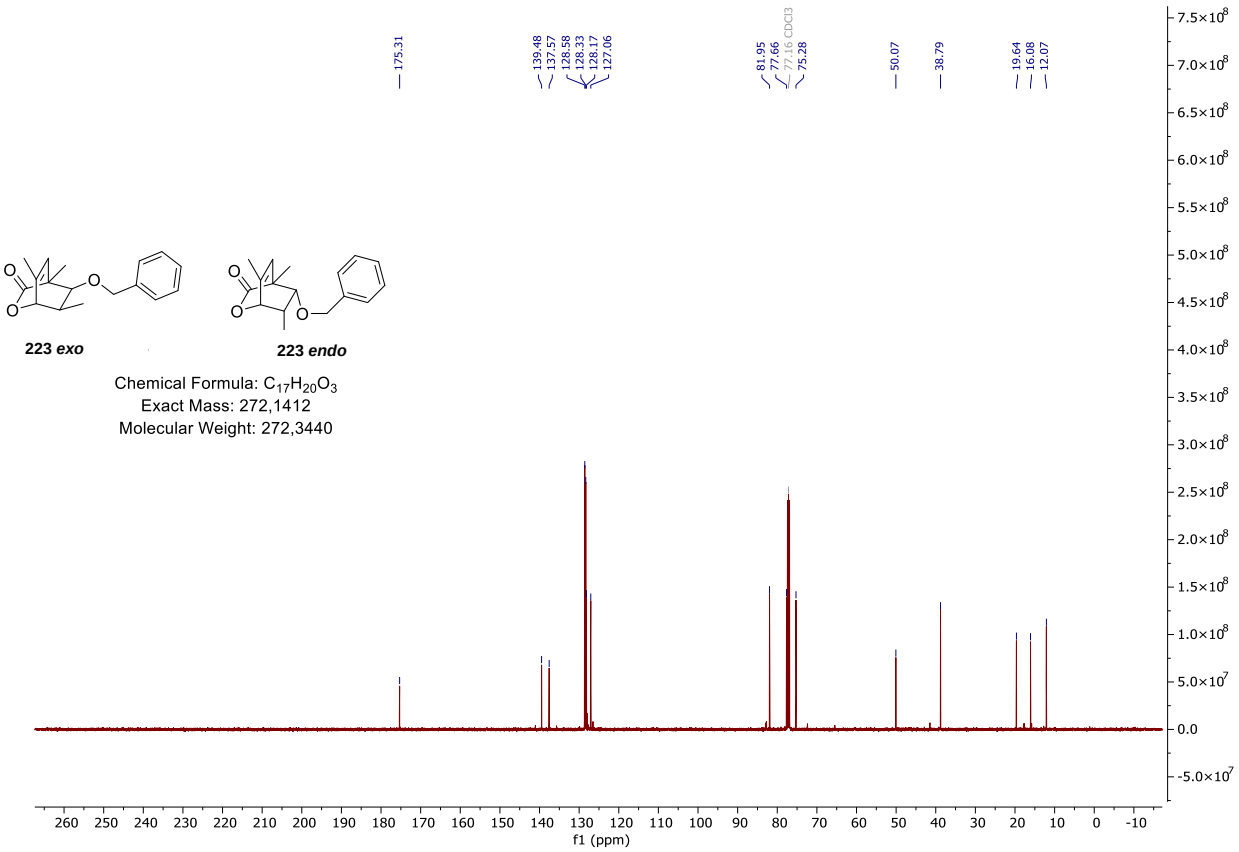

^{13}C – NMR spectrum of **223** (125 MHz, $CDCl_3$)

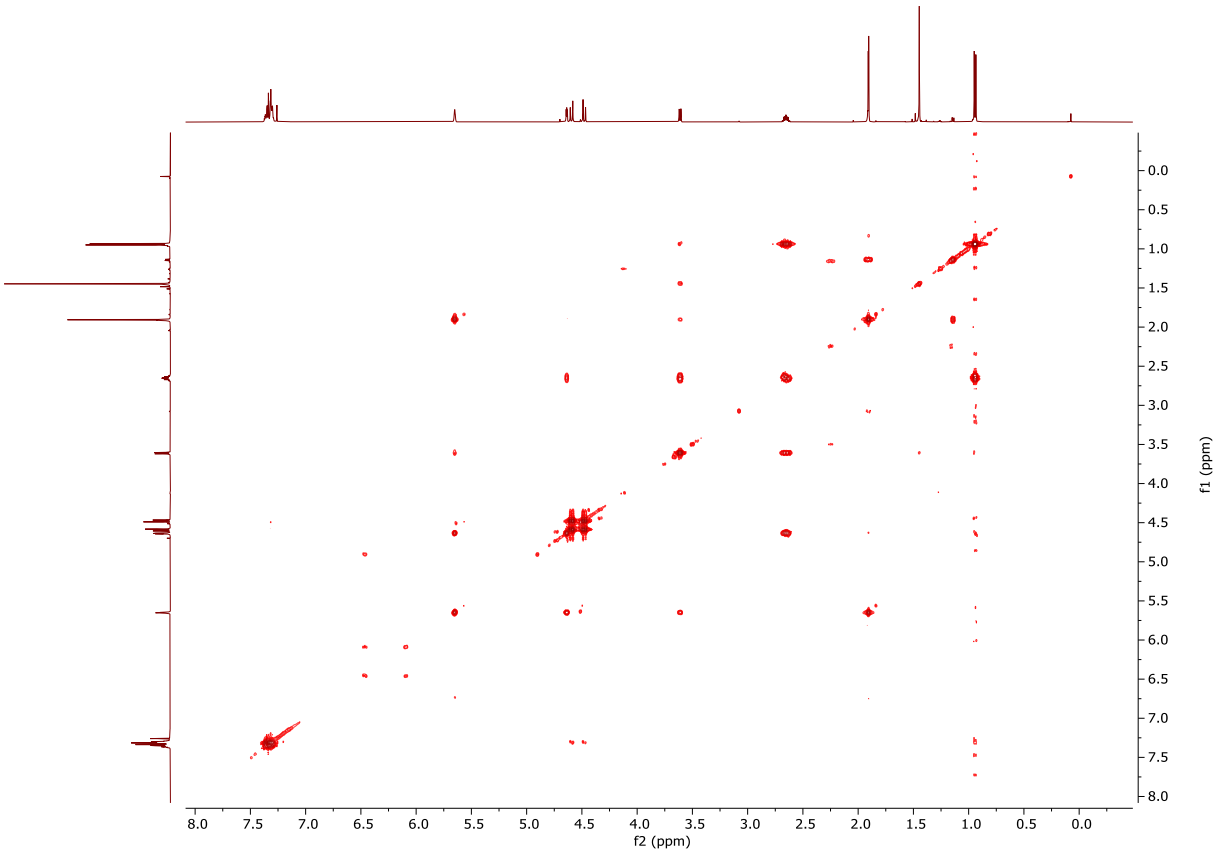

^{1}H, ^{1}H – COSY spectrum of **223** (500 MHz, $CDCl_3$)

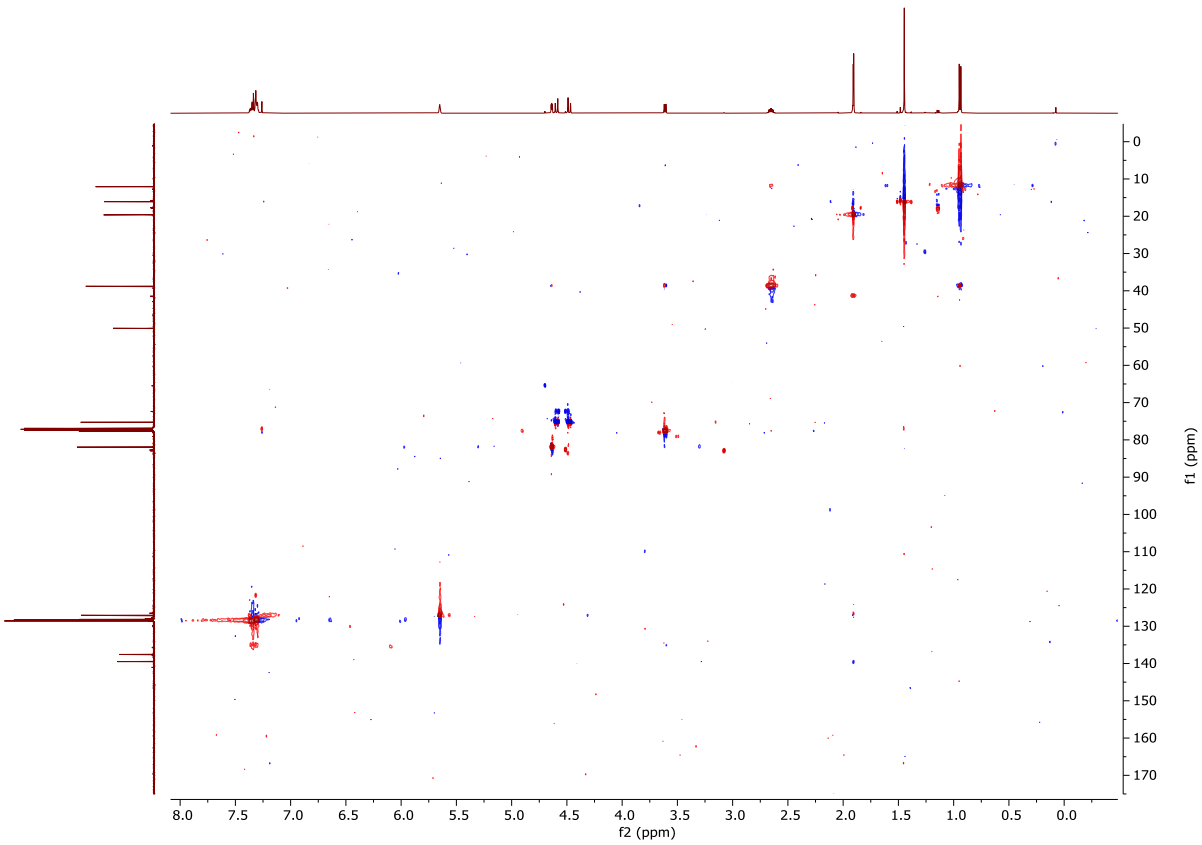

^{1}H, ^{13}C – HSQC spectrum of **223** (500 MHz, 125 MHz, $CDCl_3$)

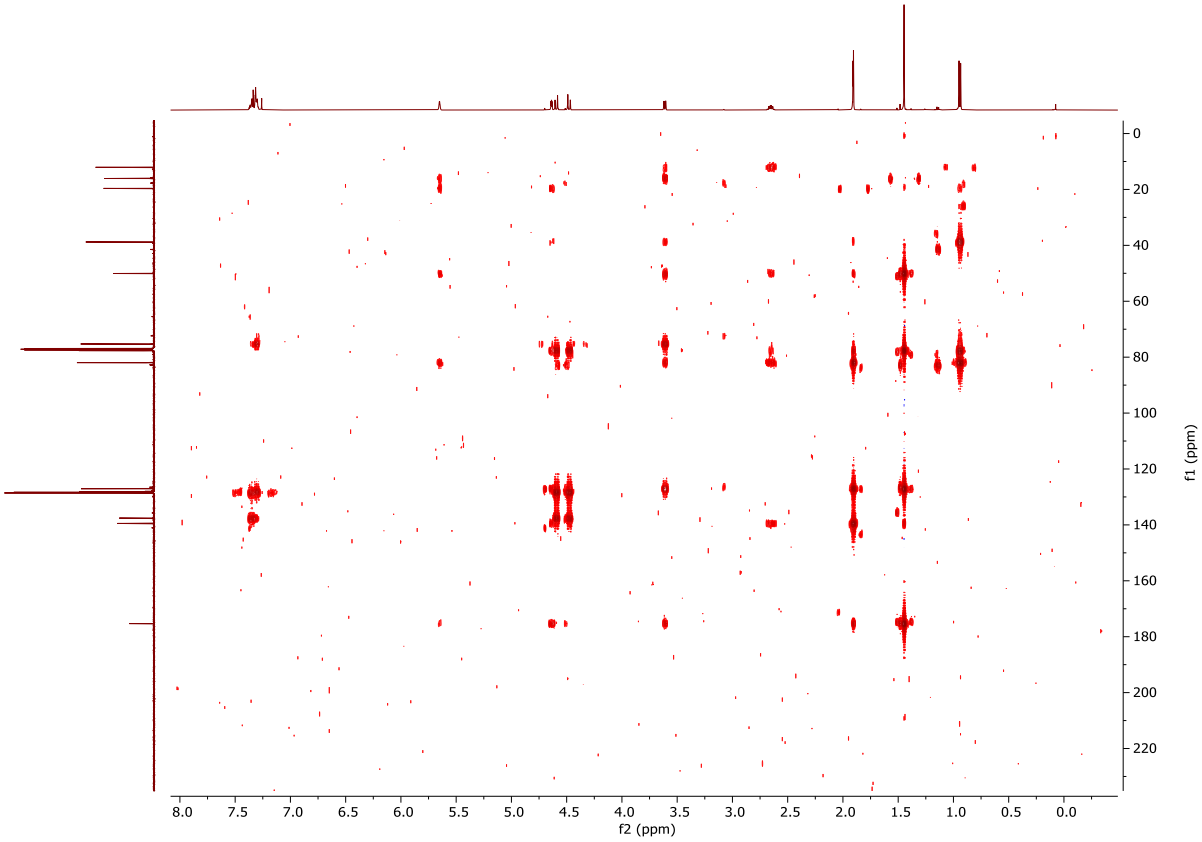

^{1}H, ^{13}C – HMBC spectrum of **223** (500 MHz, 125 MHz, $CDCl_3$)

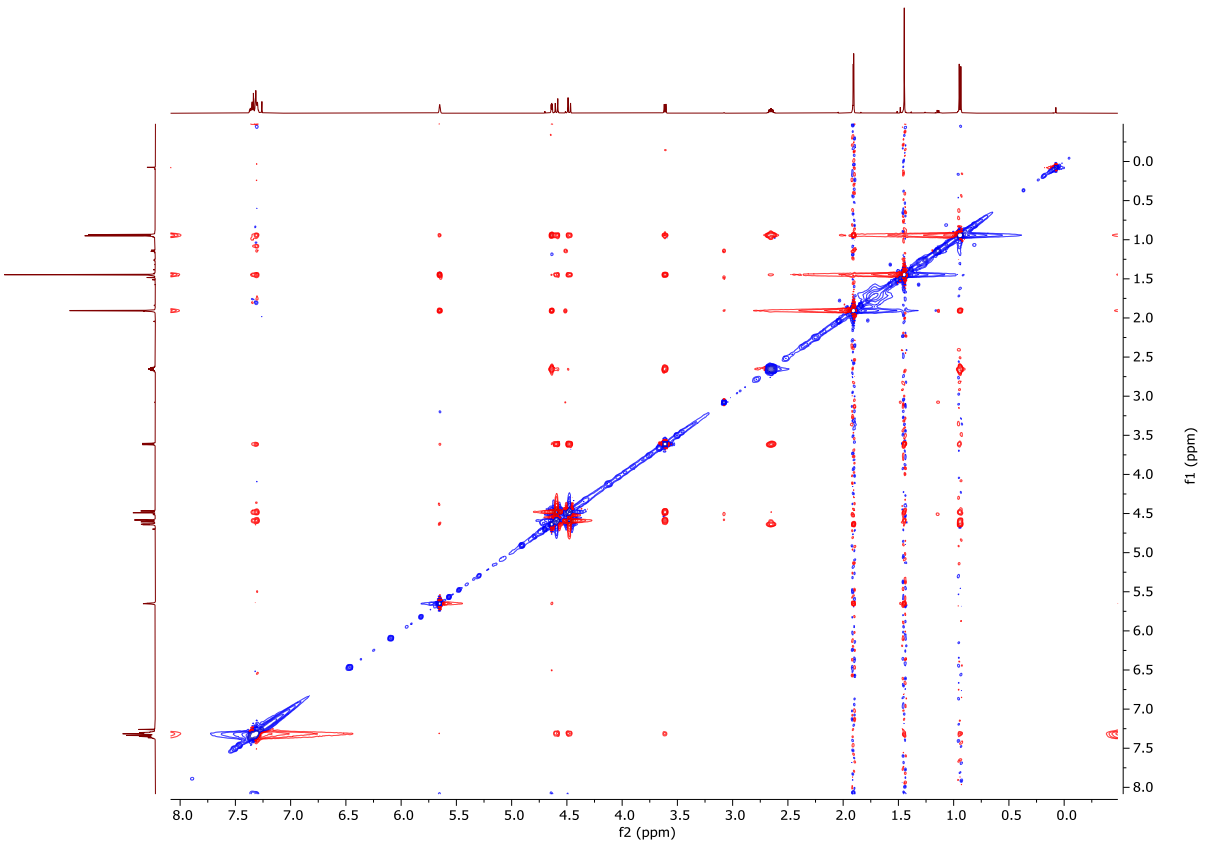

^{1}H, ^{1}H – NOESY spectrum of **223** (500 MHz, $CDCl_3$)

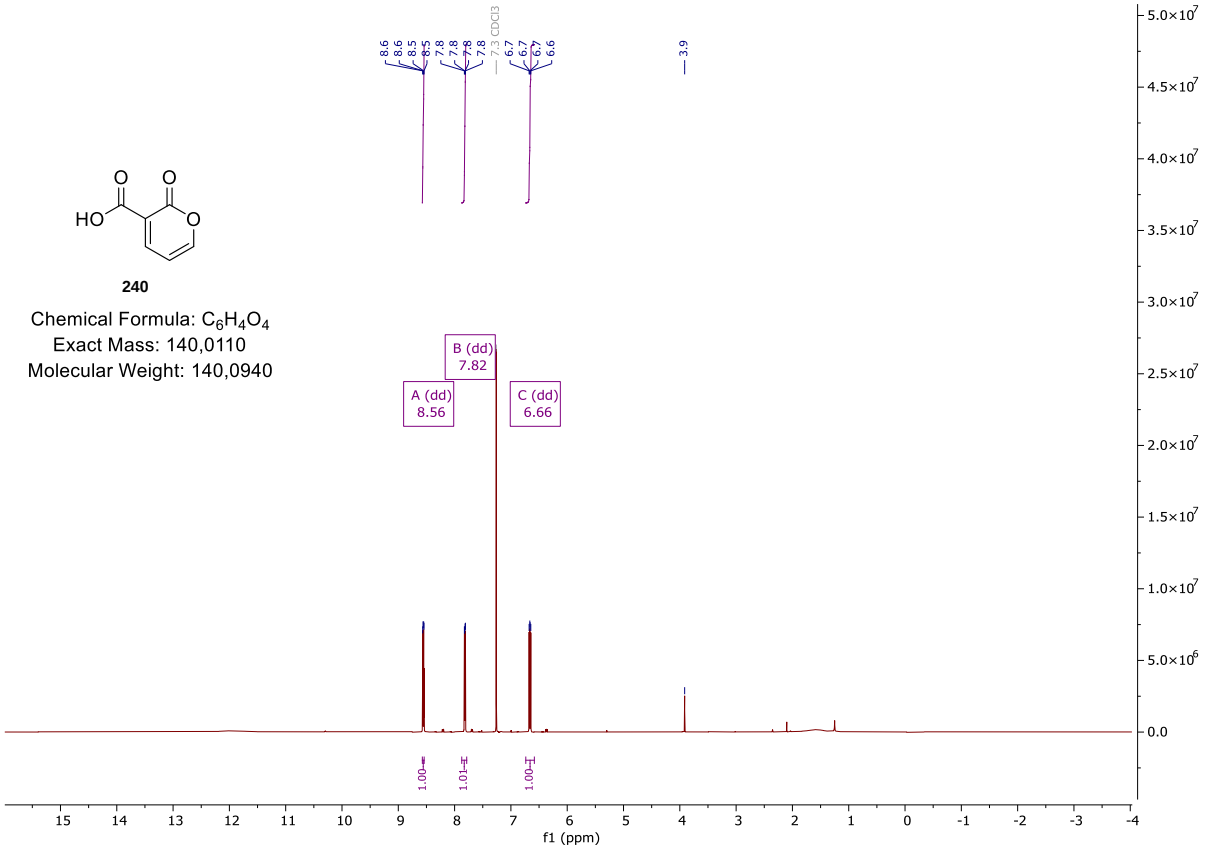

^{1}H – NMR spectrum of **240** (400 MHz, $CDCl_3$)

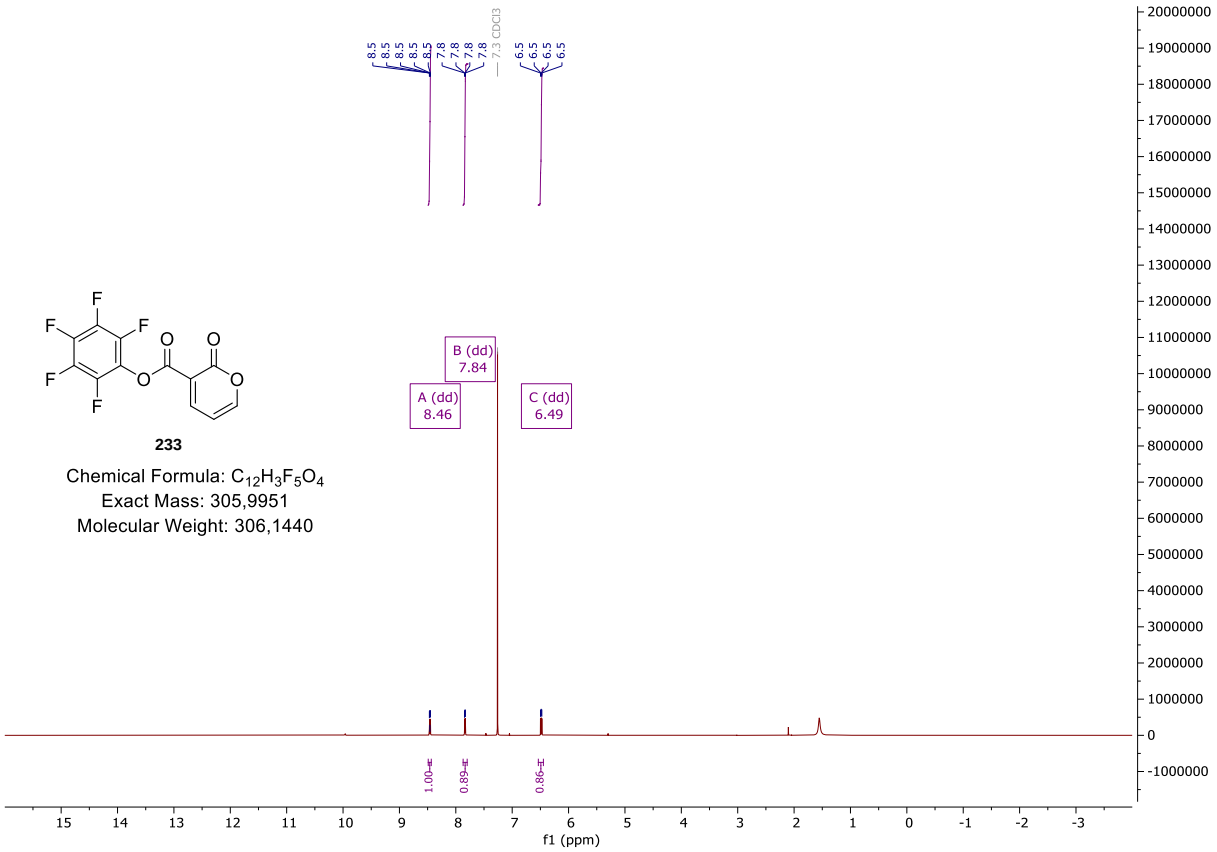

233

Chemical Formula: $C_{12}H_3F_5O_4$
Exact Mass: 305,9951
Molecular Weight: 306,1440

^{1}H – NMR spectrum of **233** (500 MHz, $CDCl_3$)

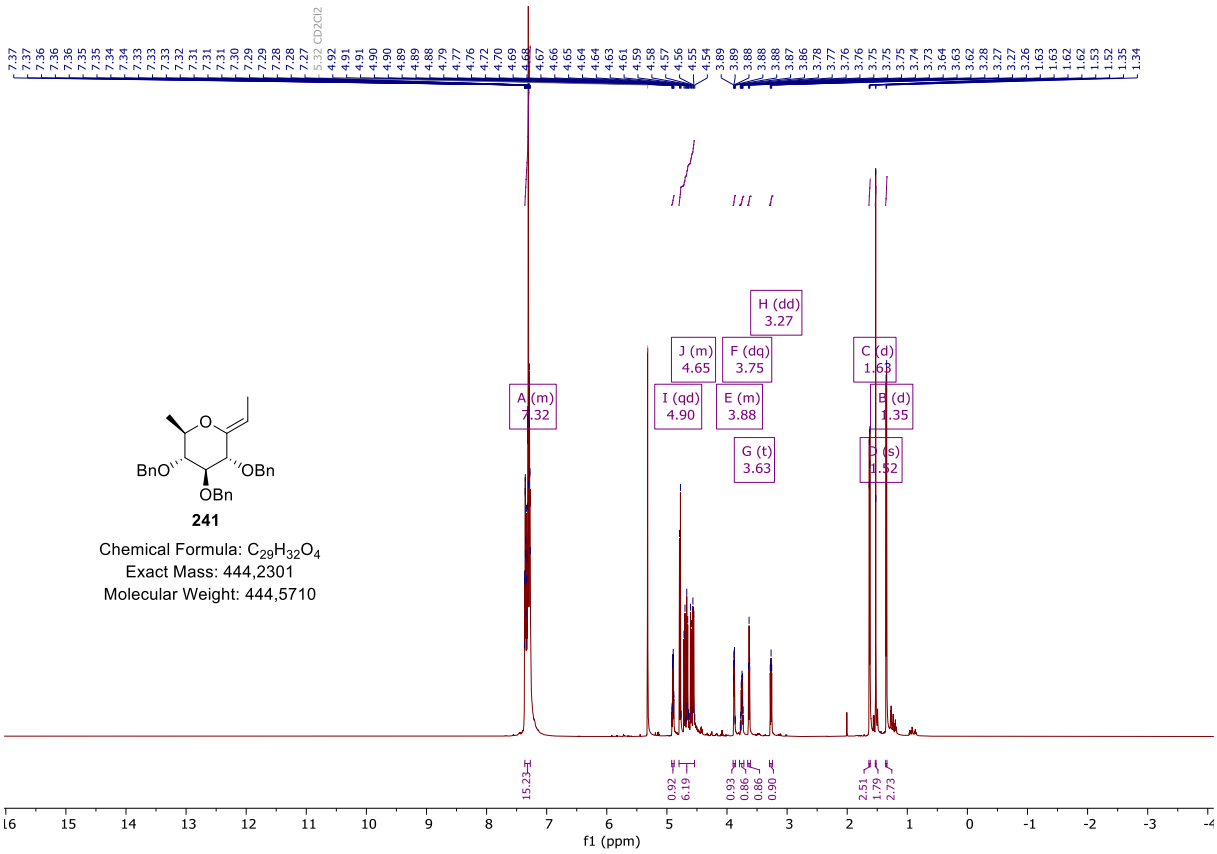

241

Chemical Formula: $C_{29}H_{32}O_4$
Exact Mass: 444,2301
Molecular Weight: 444,5710

^{1}H – NMR spectrum of **241** (700 MHz, CD_2Cl_2)

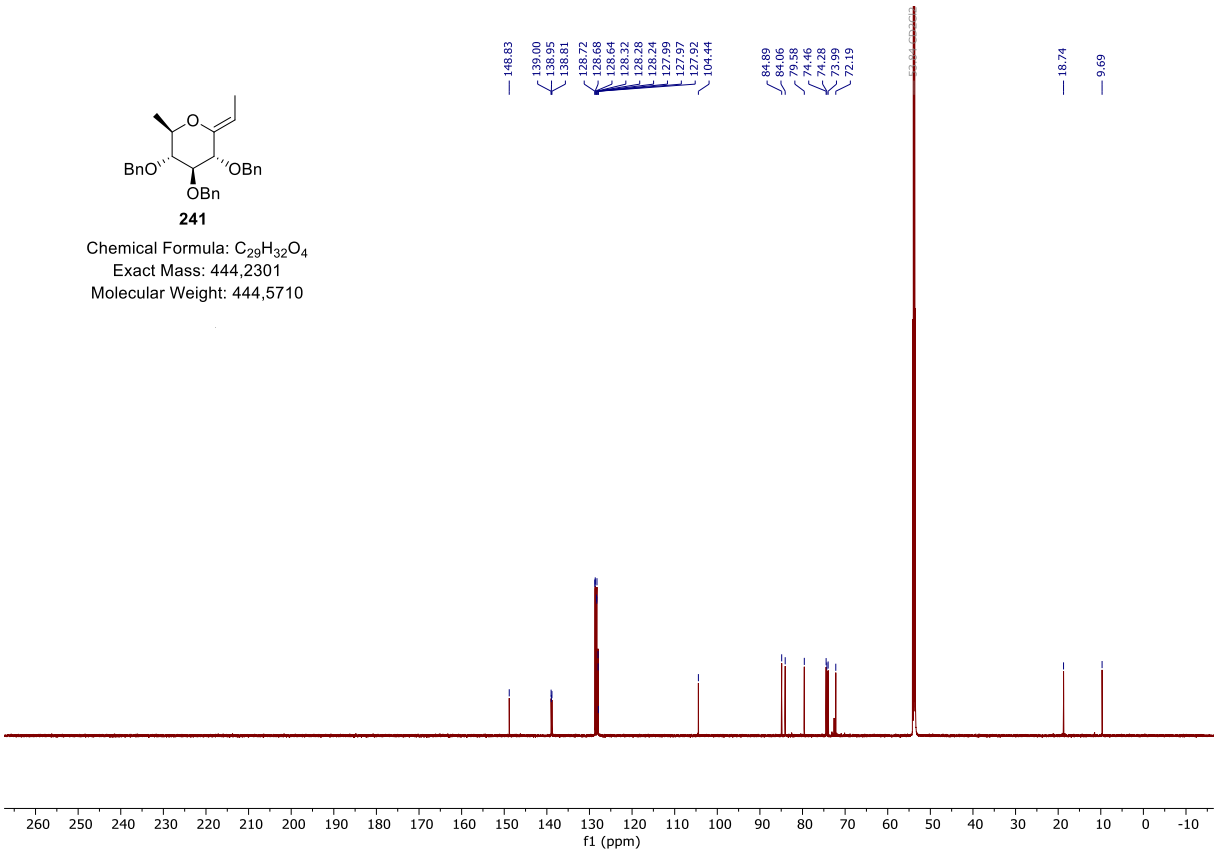

^{13}C – NMR spectrum of **241** (175 MHz, CD_2Cl_2)

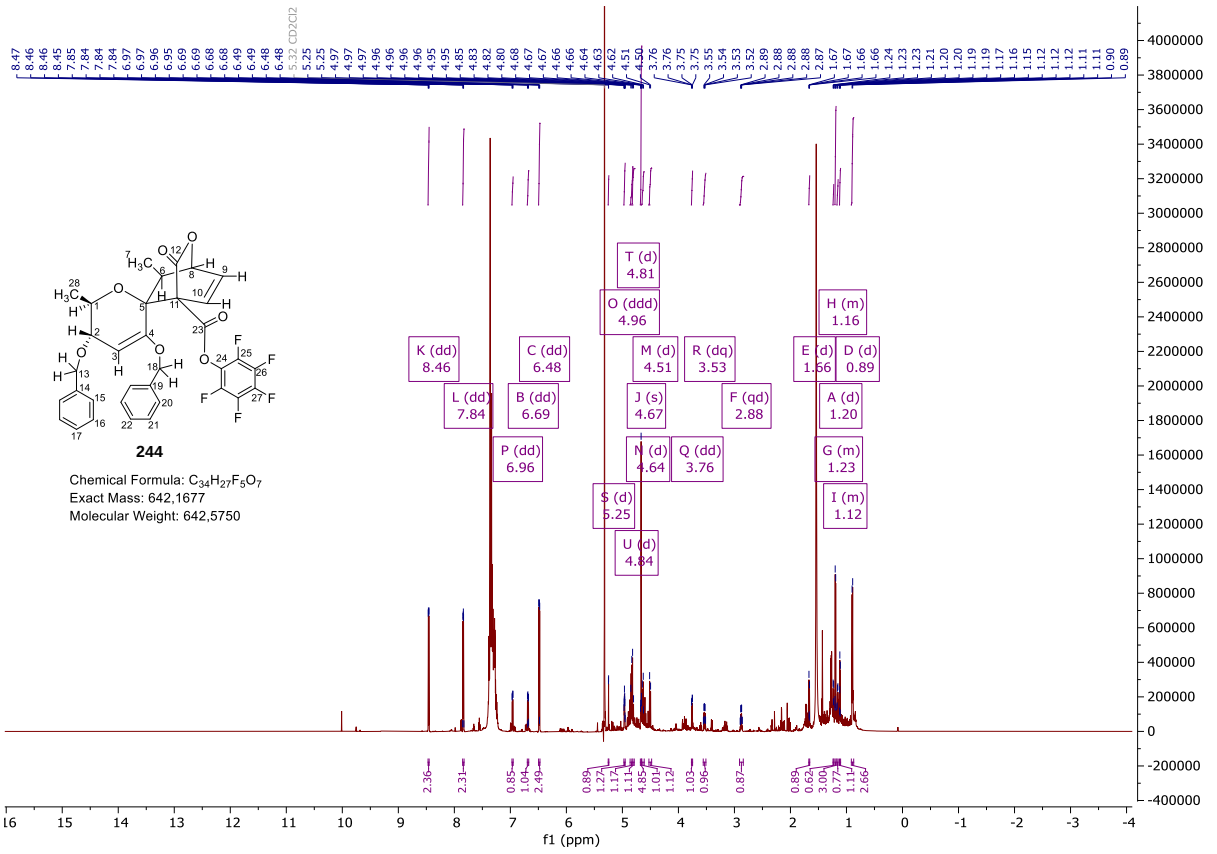

^{1}H – NMR spectrum of **244** (700 MHz, CD_2Cl_2)

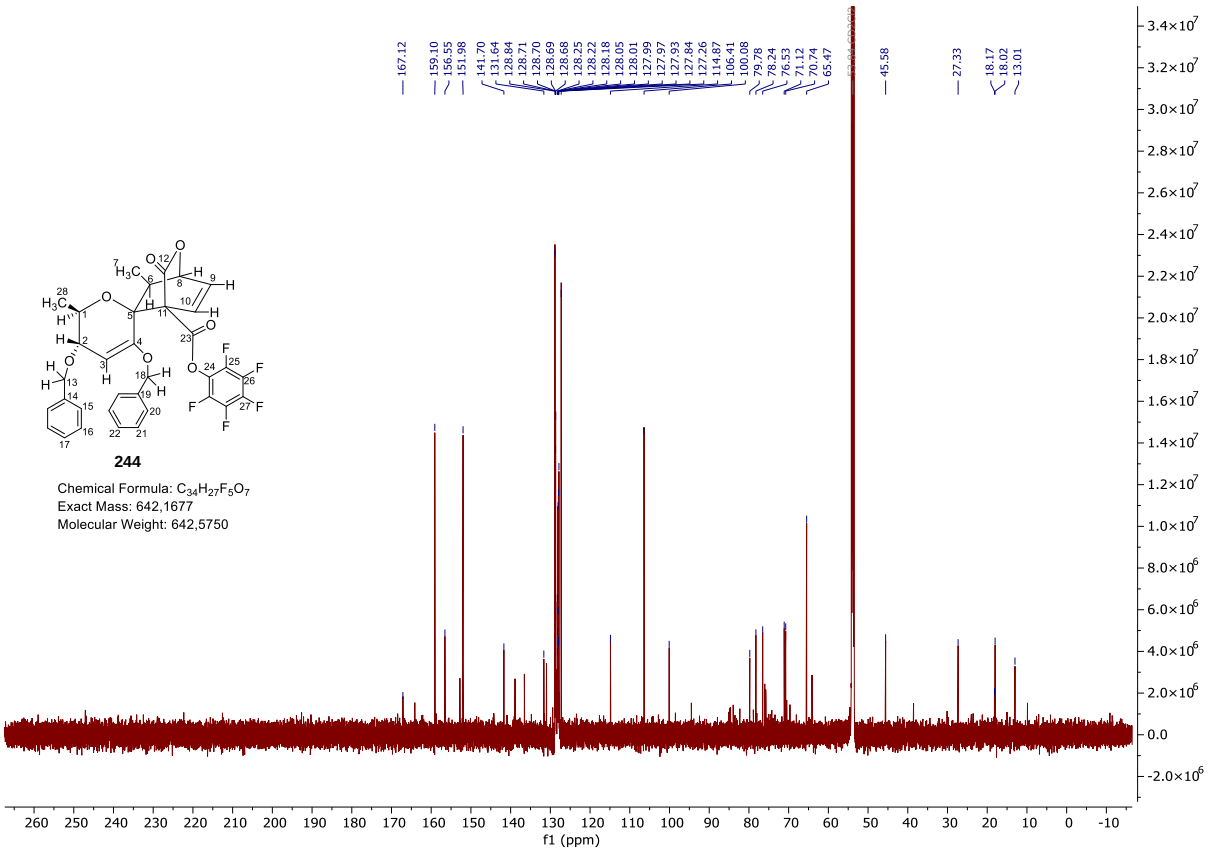

244

Chemical Formula: $C_{34}H_{27}F_5O_7$
Exact Mass: 642,1677
Molecular Weight: 642,5750

^{13}C – NMR spectrum of **244** (175 MHz, CD_2Cl_2)

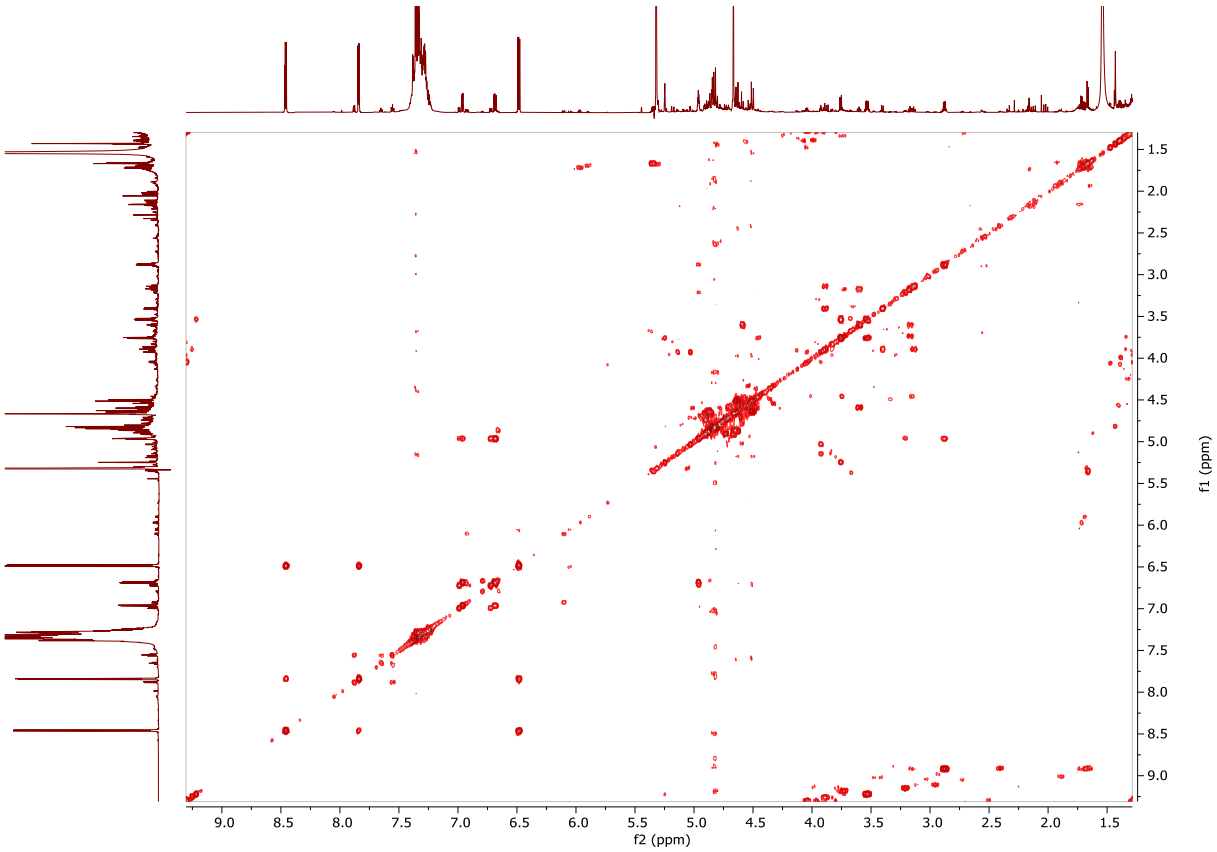

^{1}H, ^{1}H – COSY spectrum of **244** (700 MHz, CD_2Cl_2)

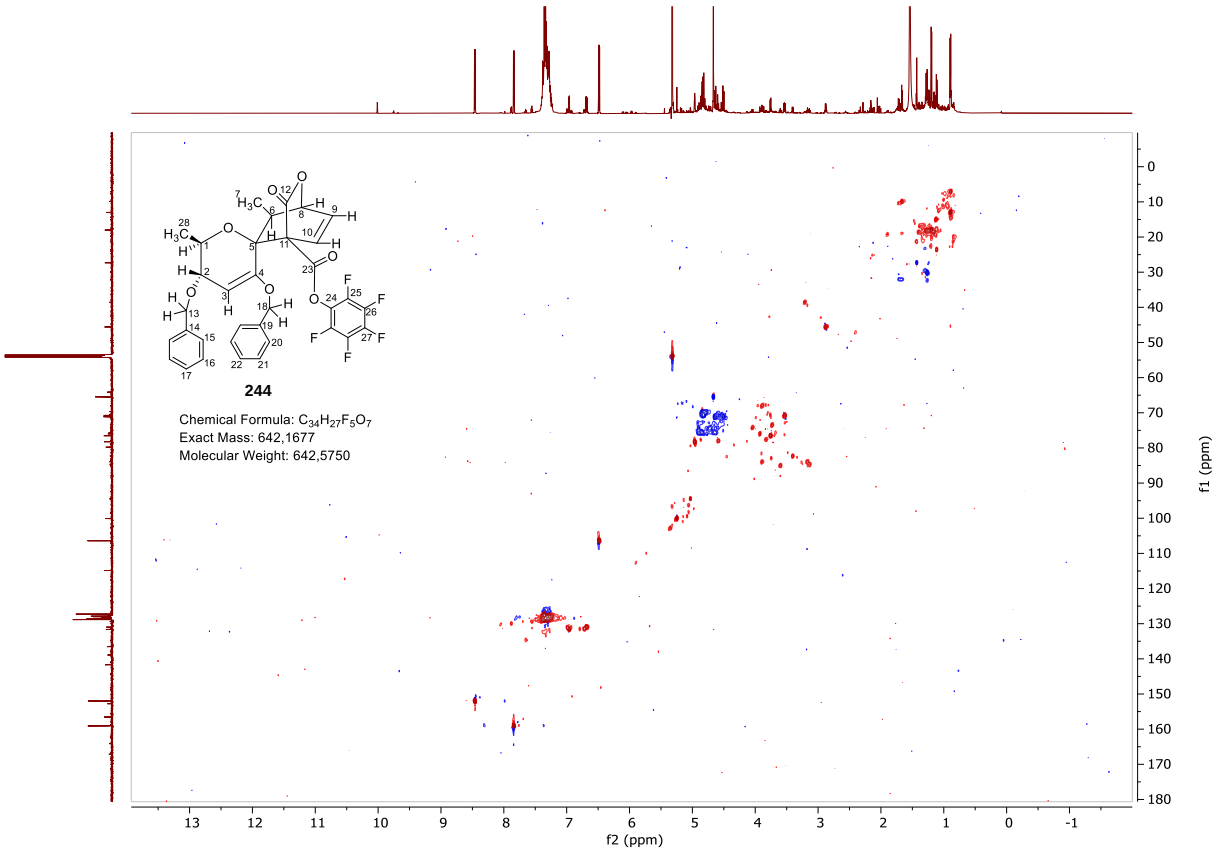

^{1}H, ^{13}C – HSQC spectrum of **244** (700 MHz, 175 MHz, CD_2Cl_2)

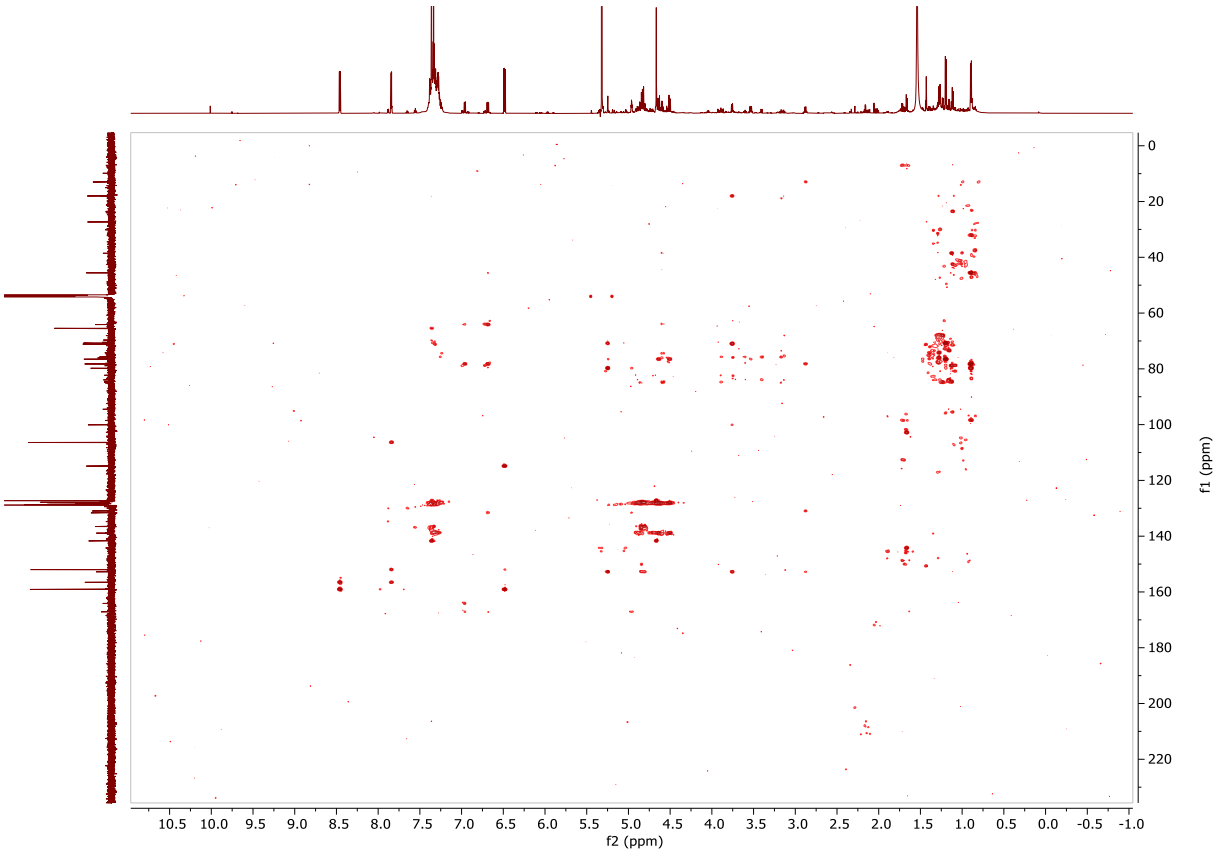

^{1}H, ^{13}C – HMBC spectrum of **244** (700 MHz, 175 MHz, CD_2Cl_2)

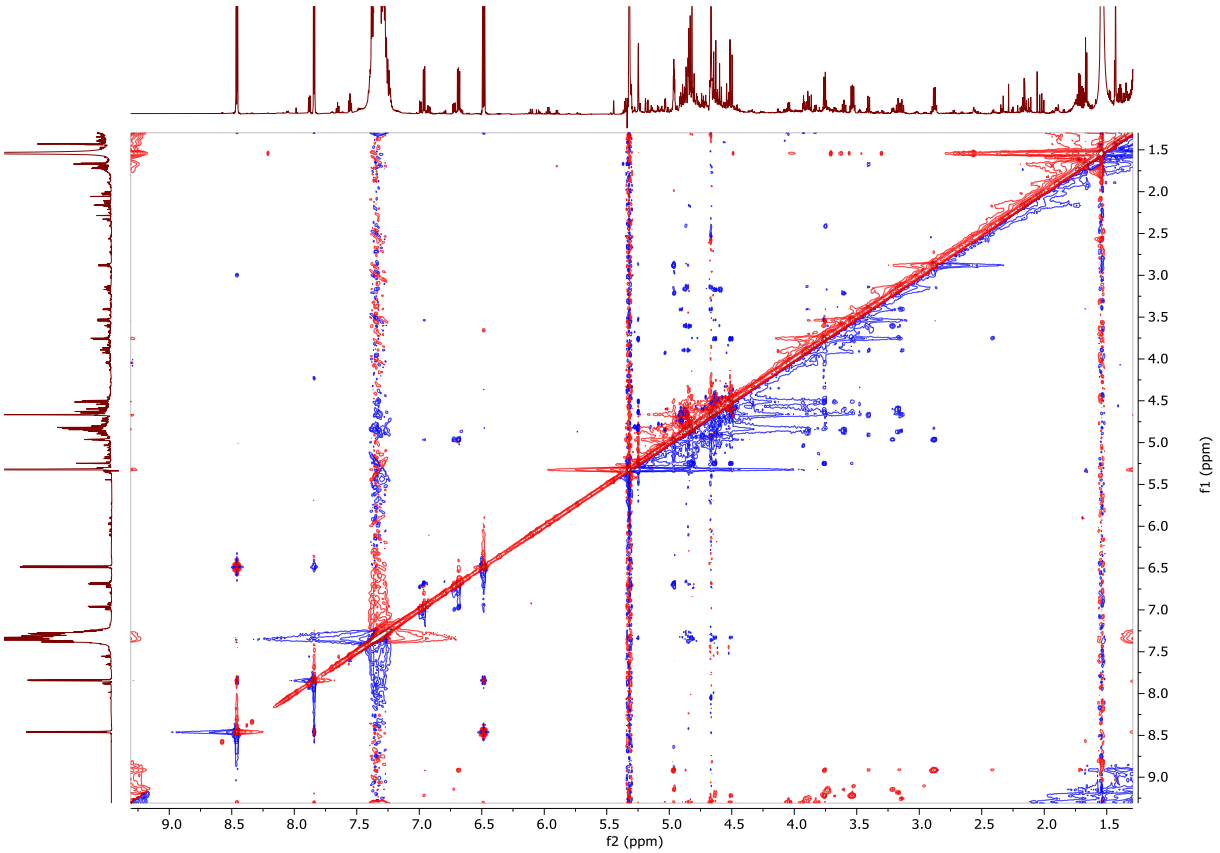

^{1}H, ^{1}H – NOESY spectrum of **244** (700 MHz, CD_2Cl_2)

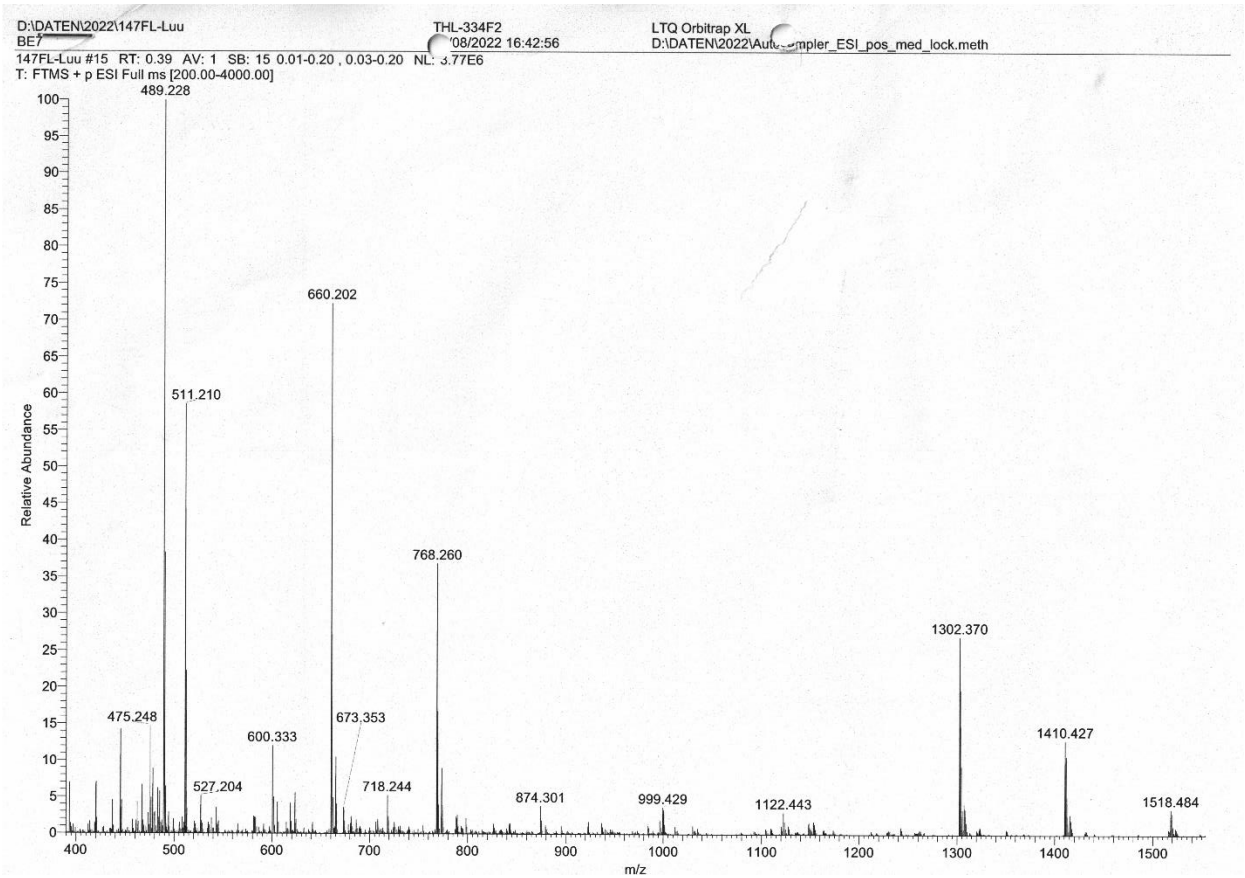

ESI Mass spectrum of **244**

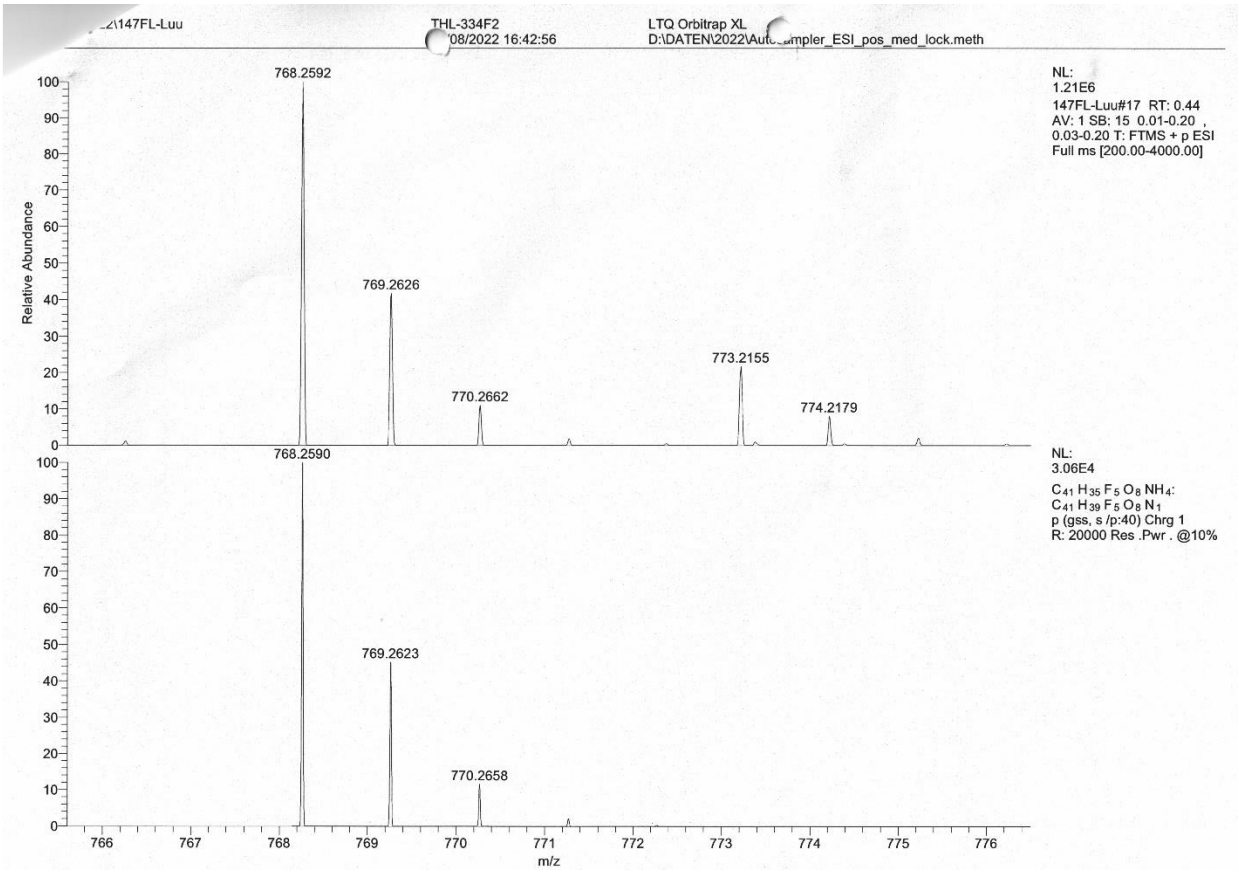

HRMS (ESI) for **242**.

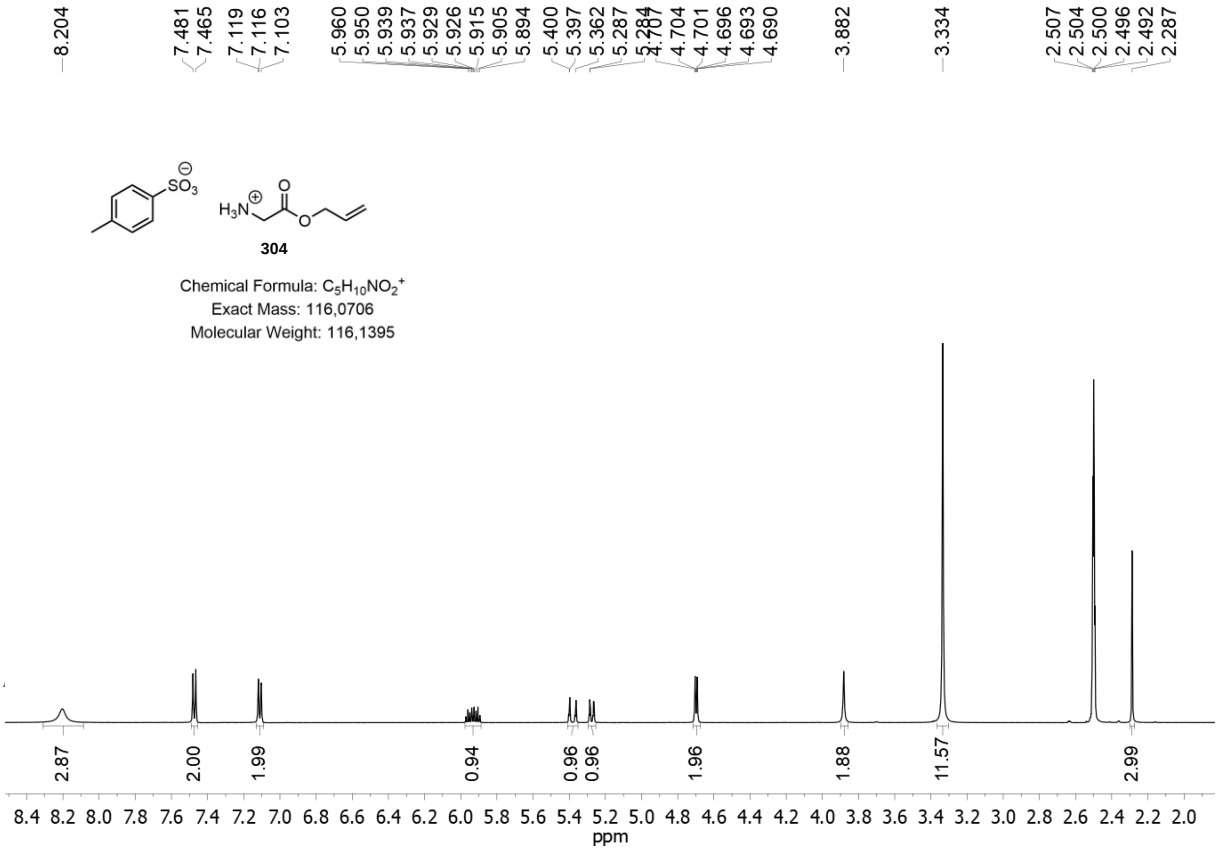

^{1}H – NMR spectrum of **304** (500 MHz, DMSO).

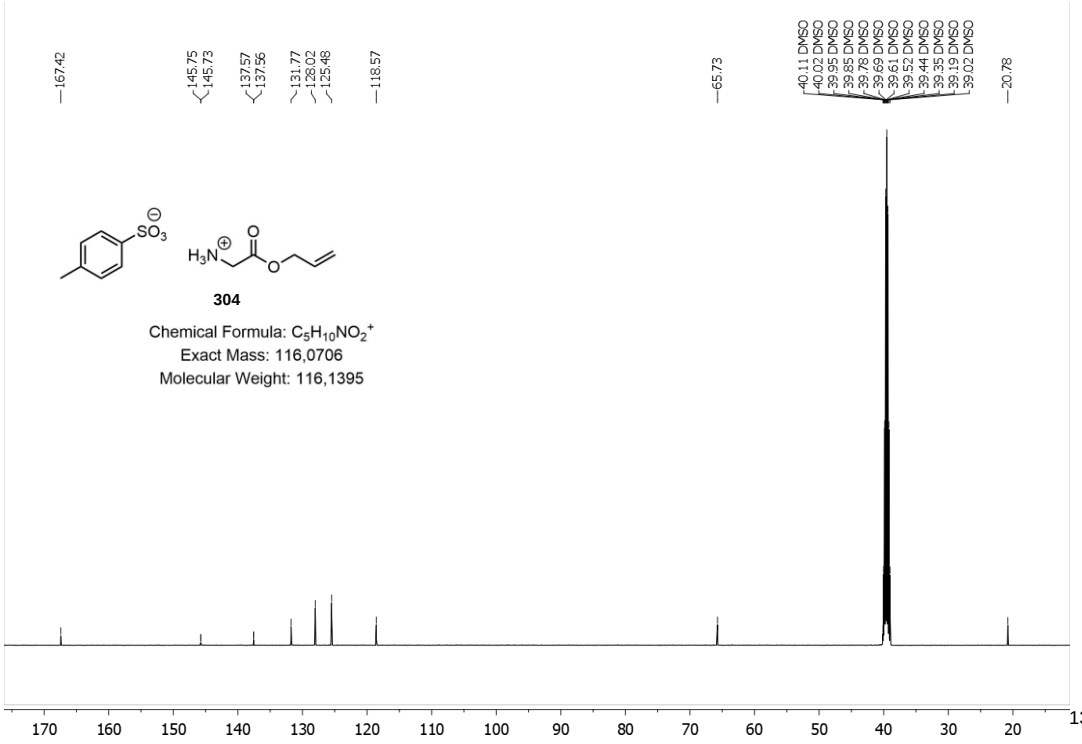

^{13}C – NMR

^{13}C – NMR spectrum of **304** (125 MHz, DMSO)

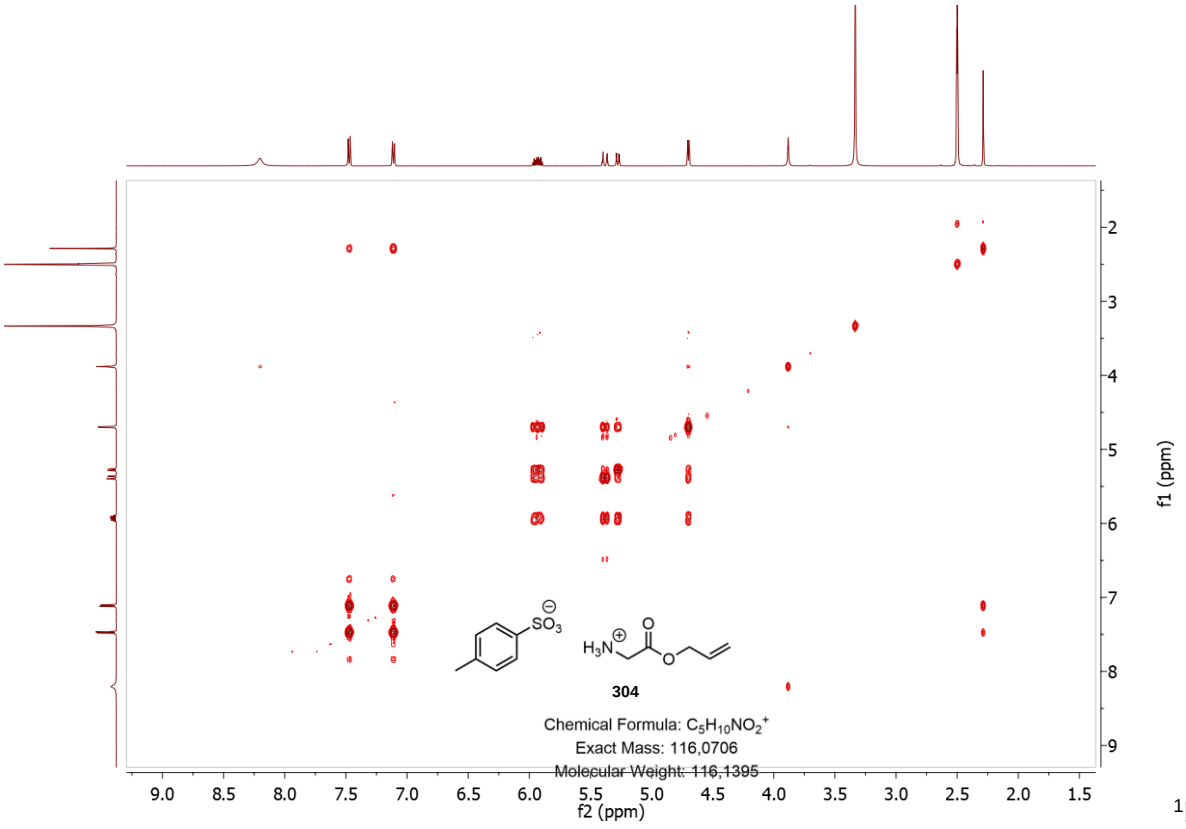

^{1}H,

^{1}H, ^{1}H – COSY spectrum of **304** (500 MHz, DMSO)

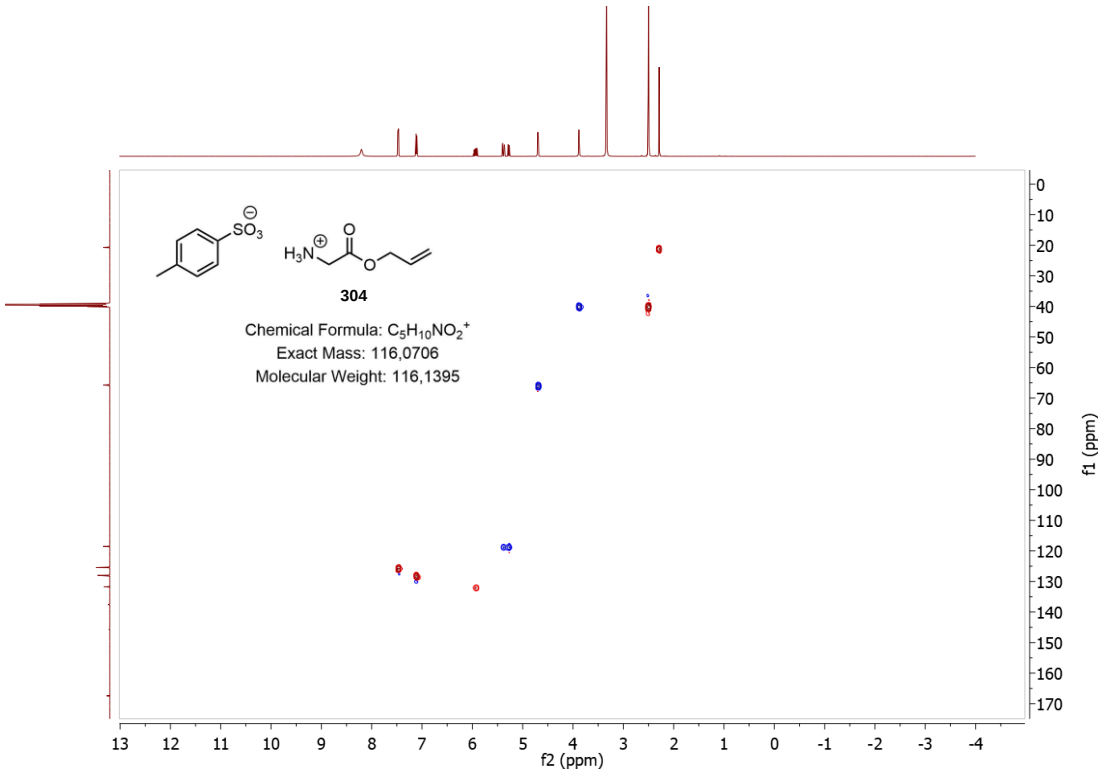

^{1}H, ^{13}C – HSQC spectrum of **304** (500 MHz, 125 MHz, DMSO)

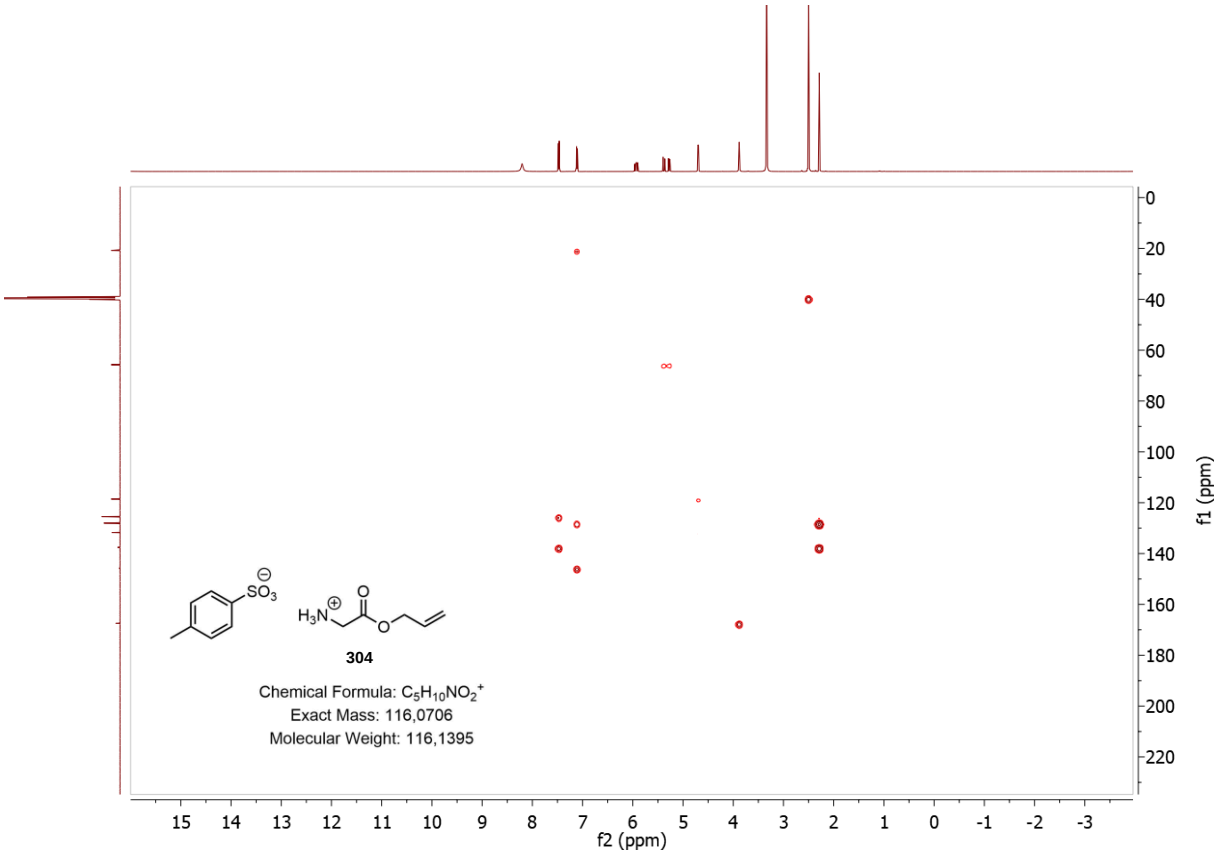

^{1}H, ^{13}C – HMBC spectrum of **304** (500 MHz, 125 MHz, DMSO)

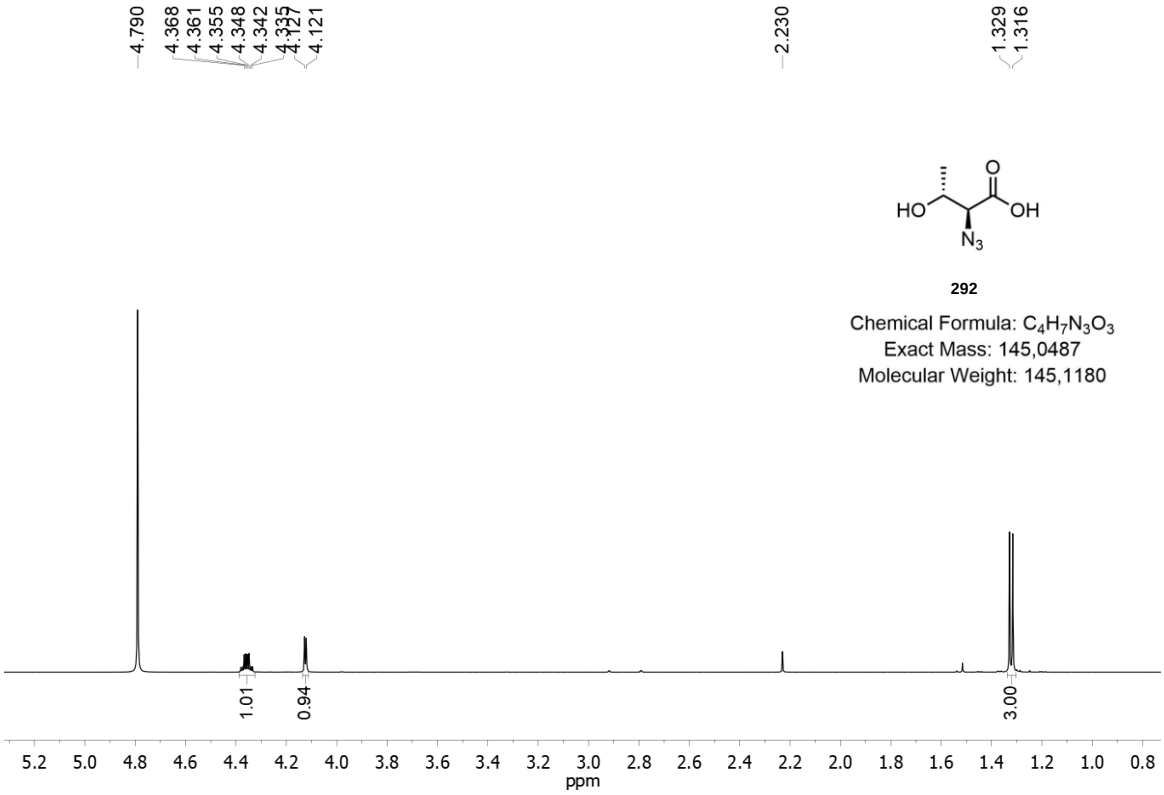

^{1}H – NMR spectrum of **292** (500 MHz, D_2O).

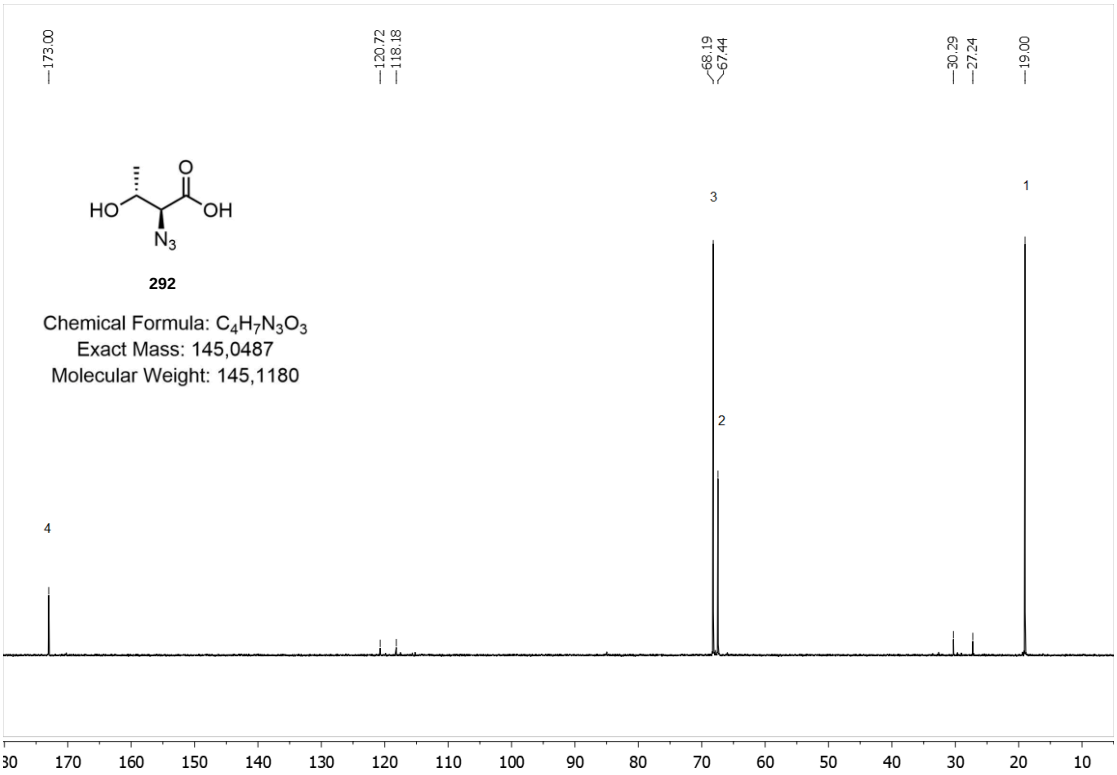

^{13}C – NMR spectrum of **292** (125 MHz, D_2O).

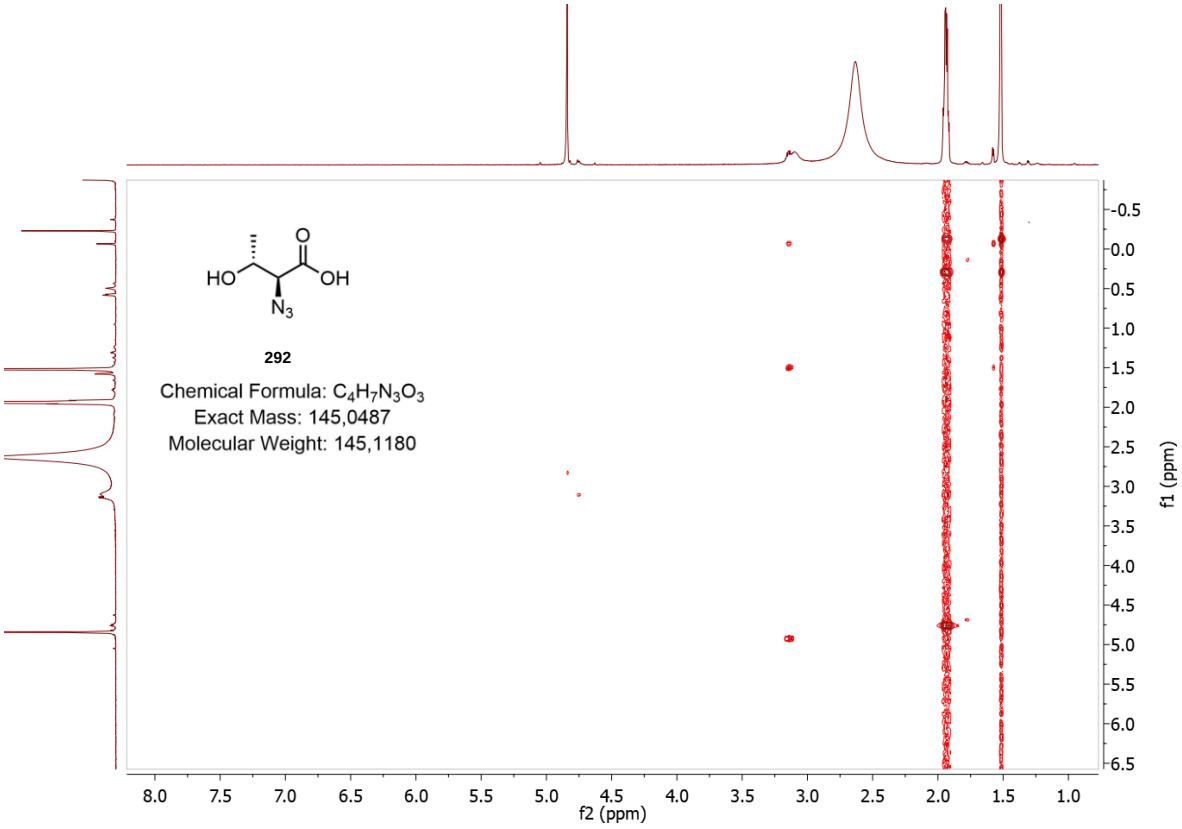

^{1}H, ^{1}H – COSY spectrum of **292** (500 MHz, D_2O).

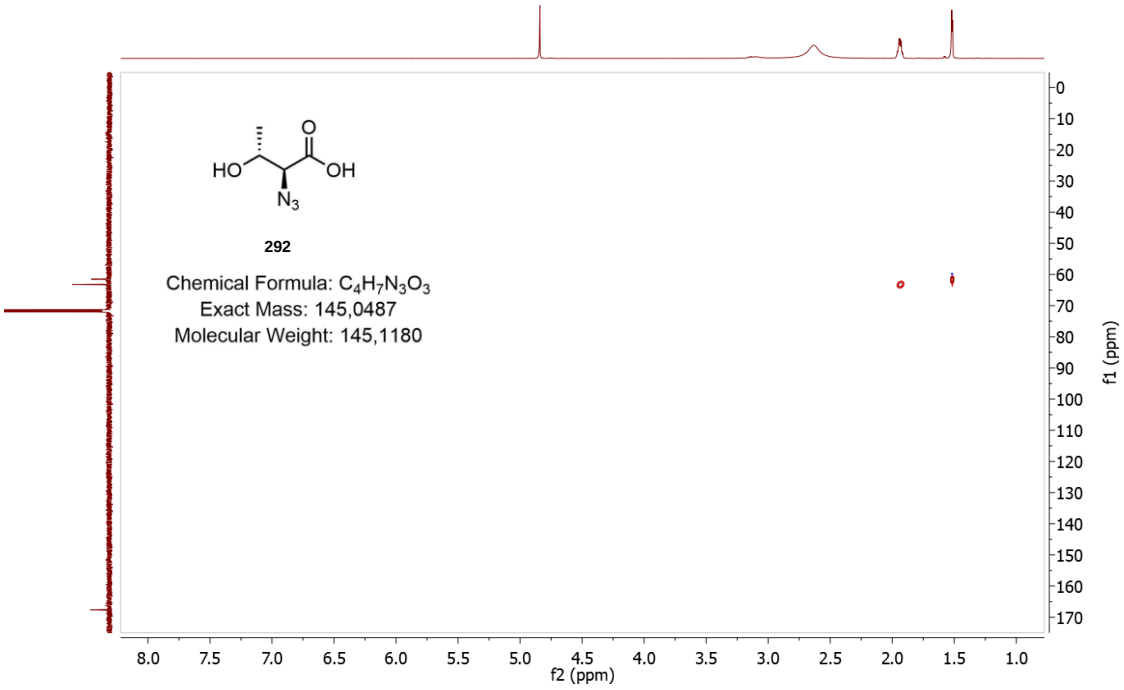

^{1}H, ^{13}C – HSQC spectrum of **292** (500 MHz, 125 MHz, D_2O)

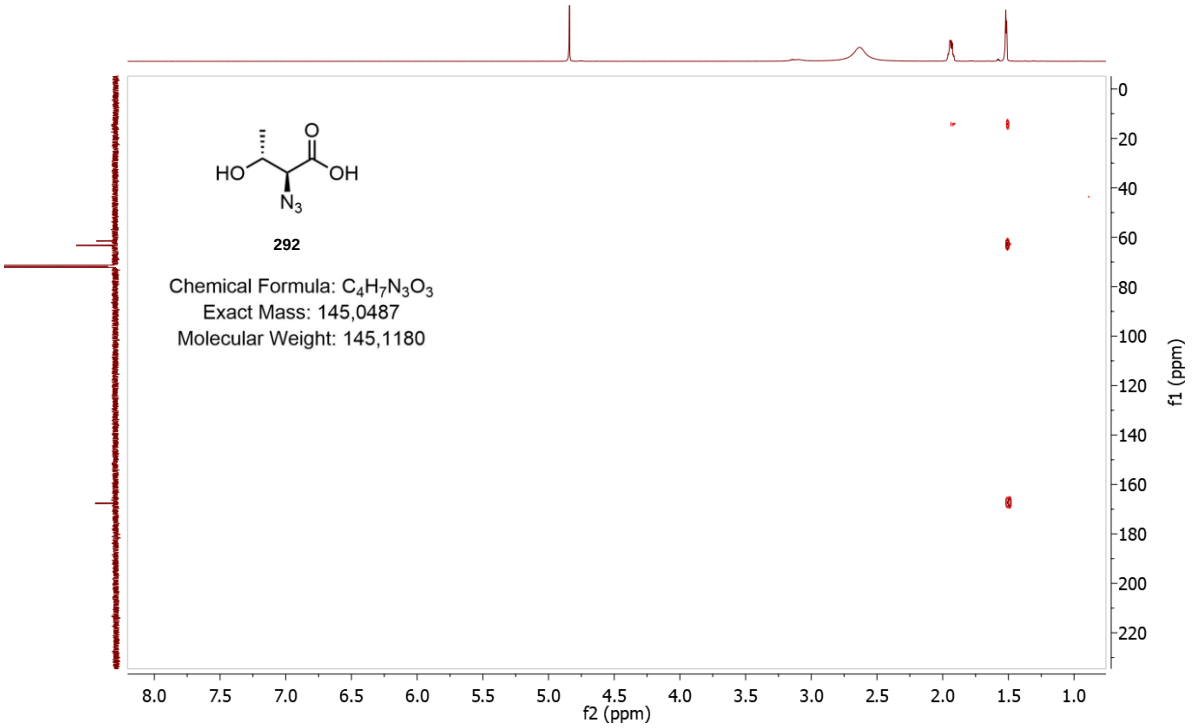

^{1}H, ^{13}C – HMBC spectrum of **292** (500 MHz, 125 MHz, D_2O)

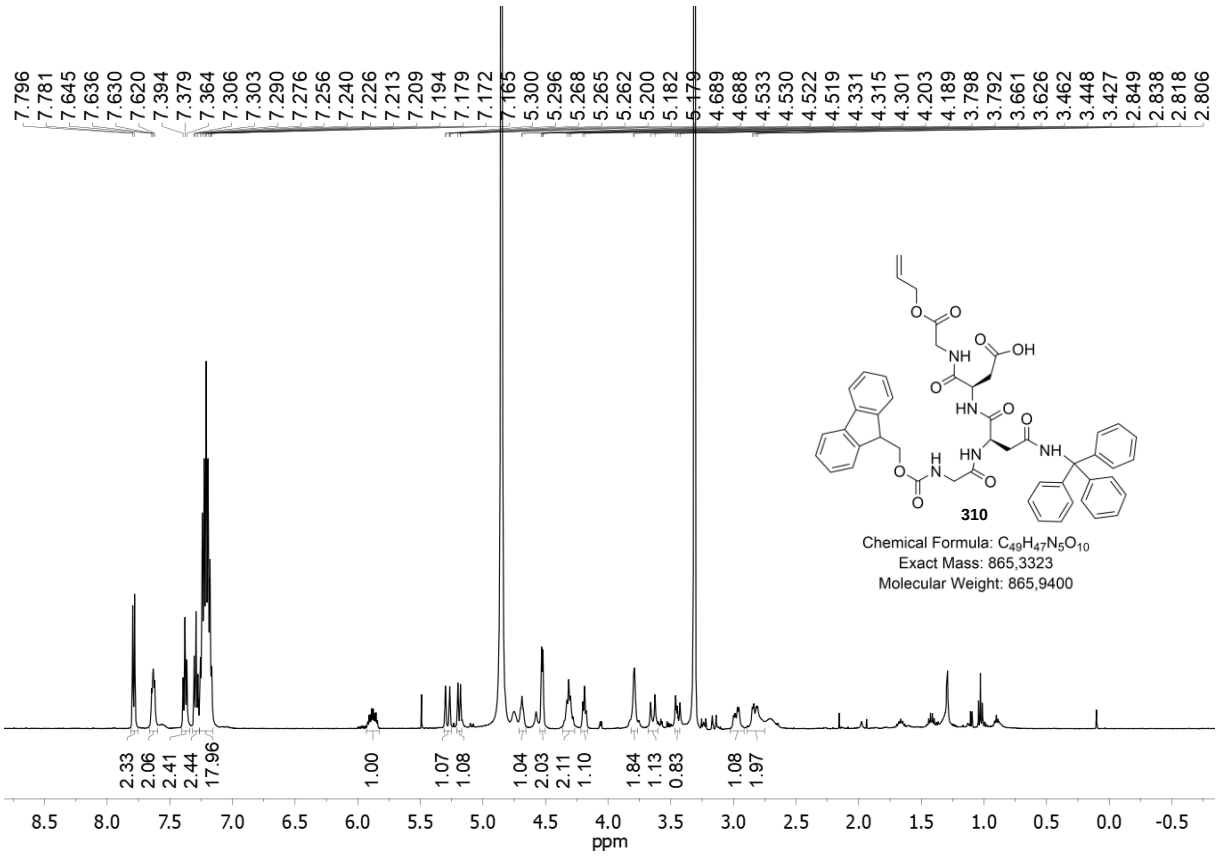

^{1}H – NMR spectrum of **310** (500 MHz, CD_3OD).

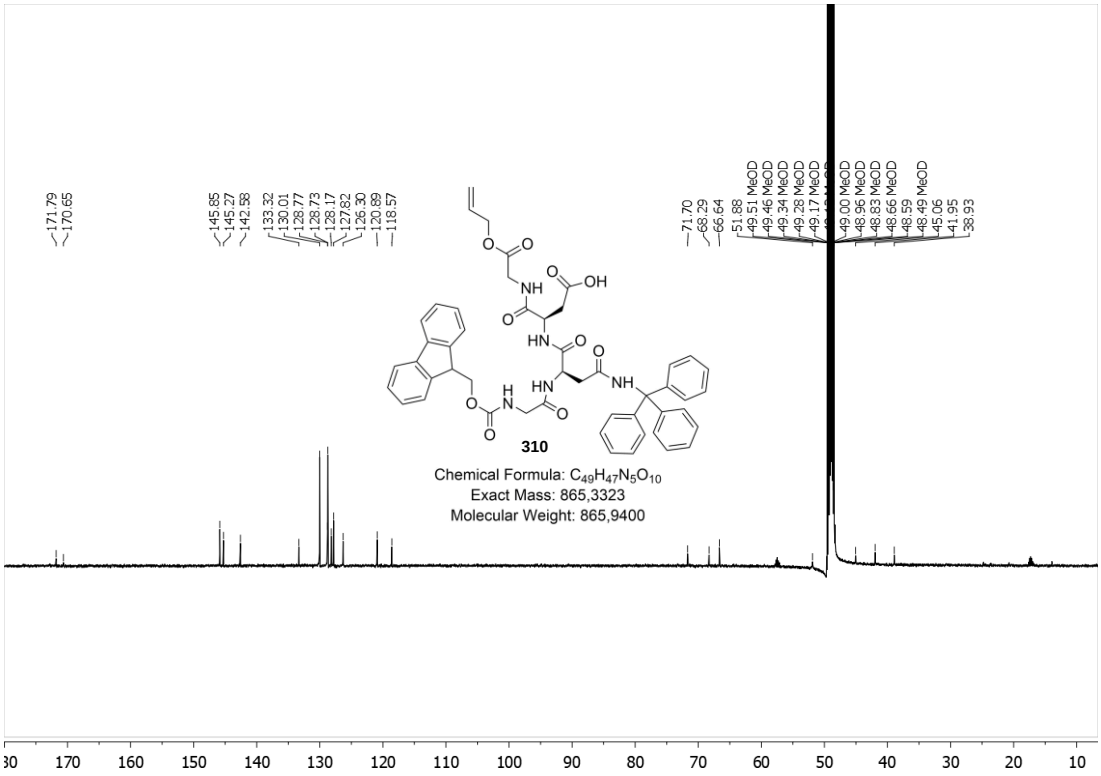

^{13}C – NMR spectrum of **310** (CD_3OD).

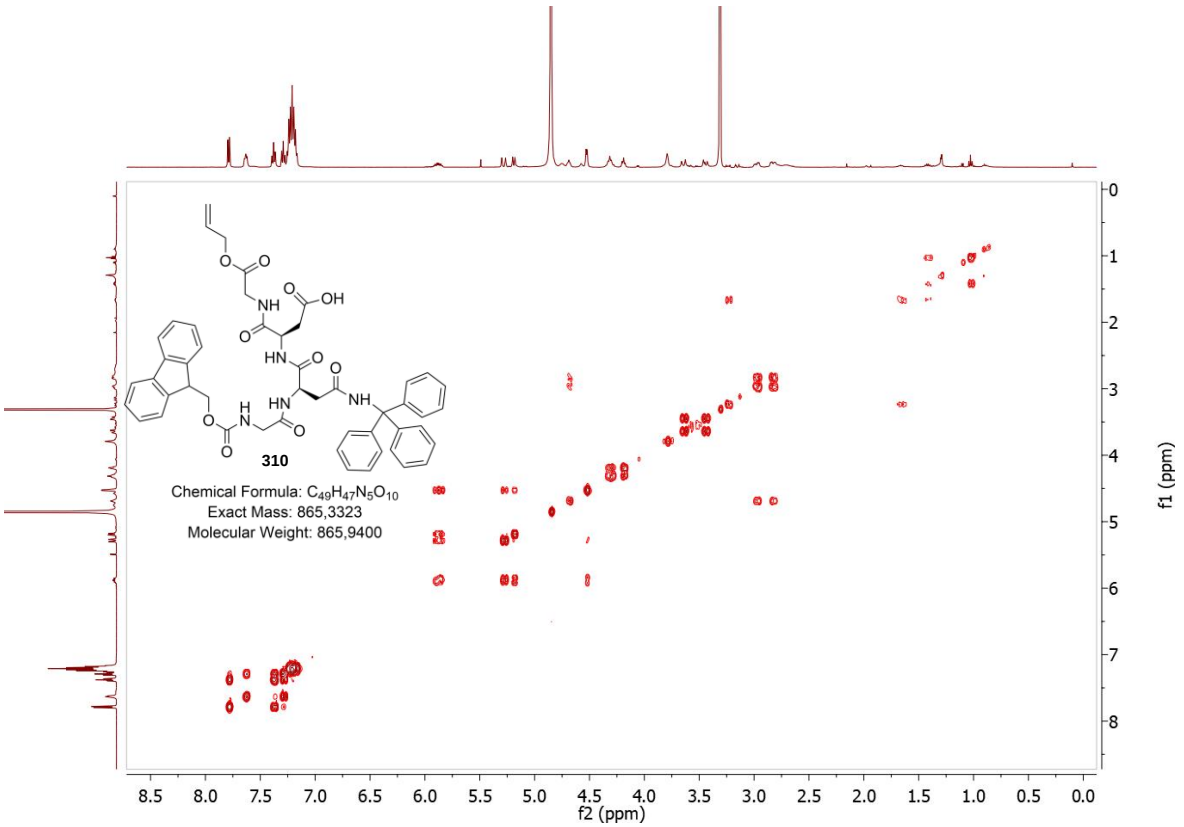

^{1}H, ^{1}H – COSY spectrum of **310** (CD_3OD).

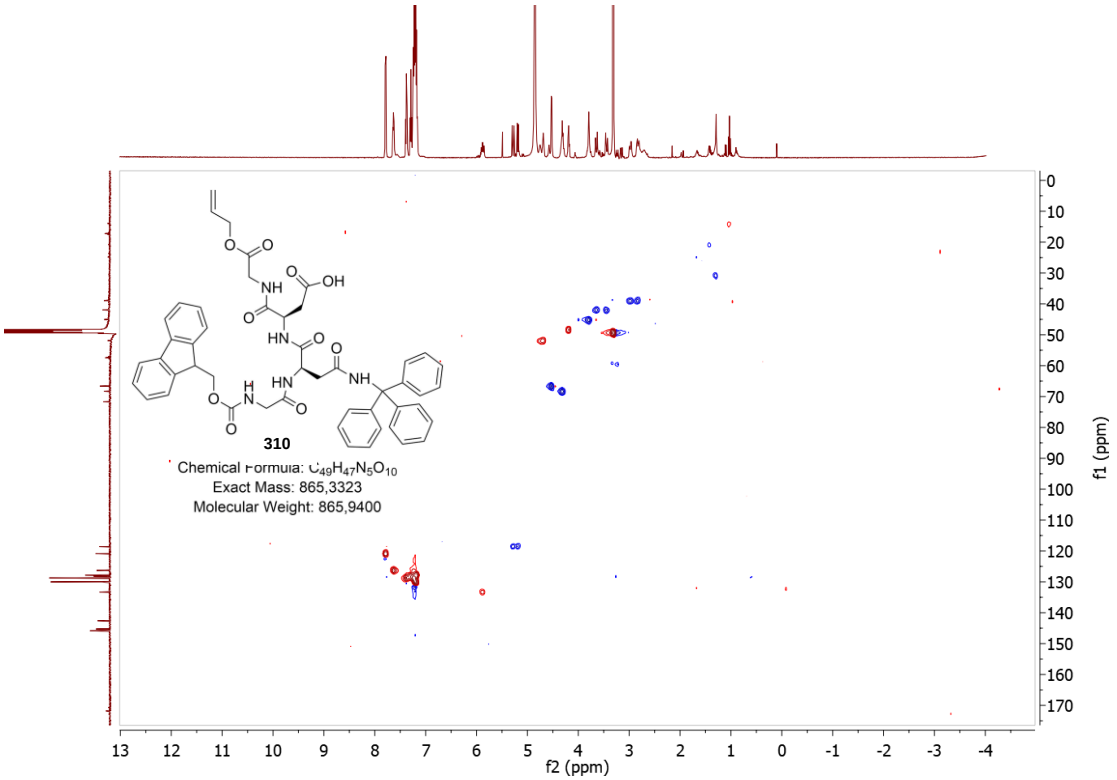

^{1}H, ^{13}C – HSQC spectrum of **310** (500 MHz, 125 MHz, CD_3OD)

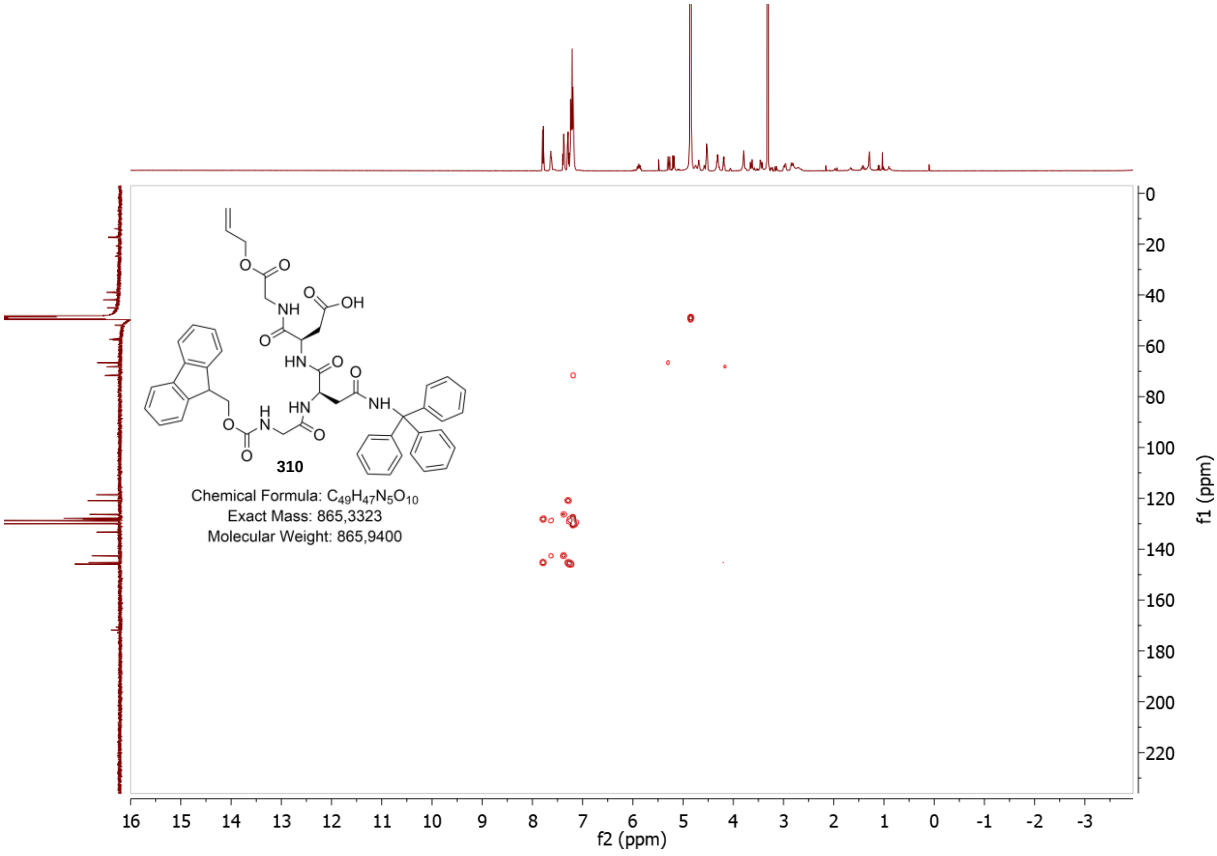

^{1}H, ^{13}C – HMBC spectrum of **310** (500 MHz, 125 MHz, CD_3OD)

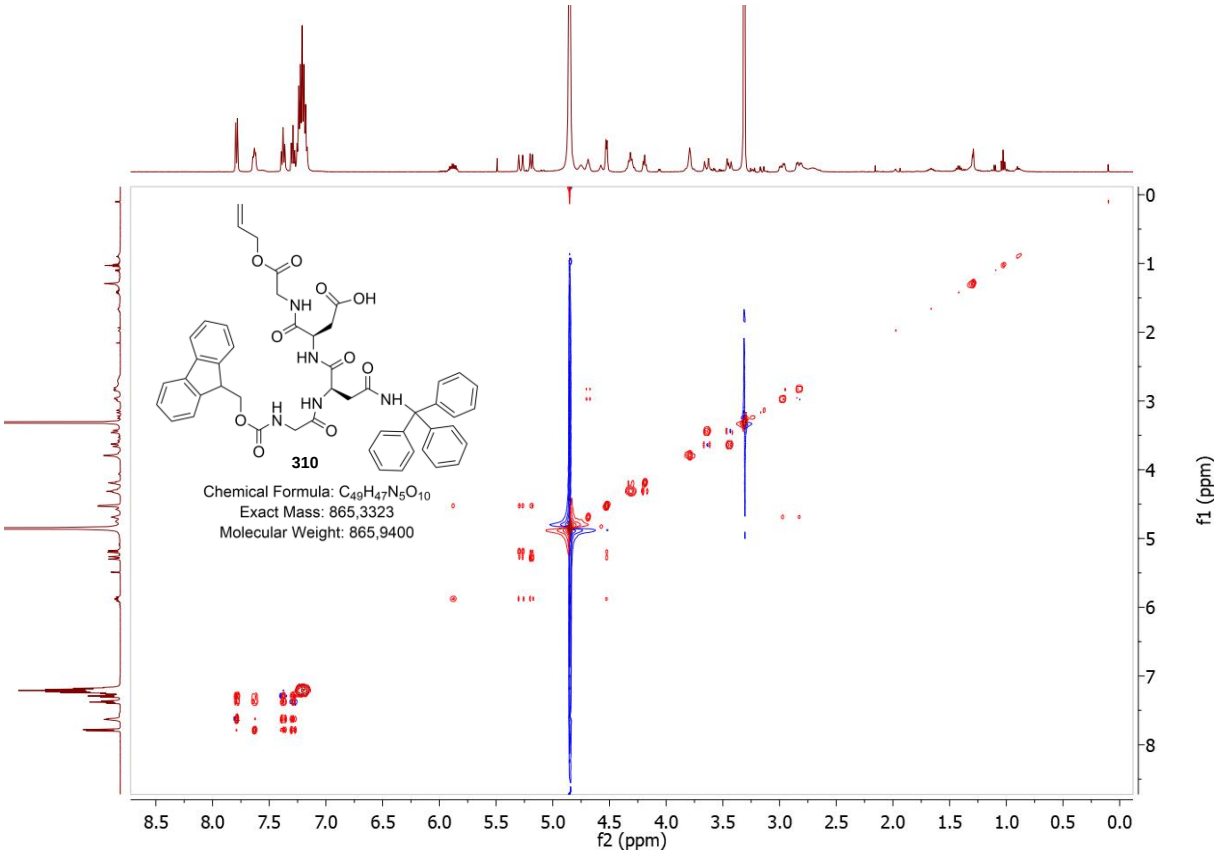

^{1}H, ^{1}H – TOCSY spectrum of **310** (500 MHz, CD_3OD)

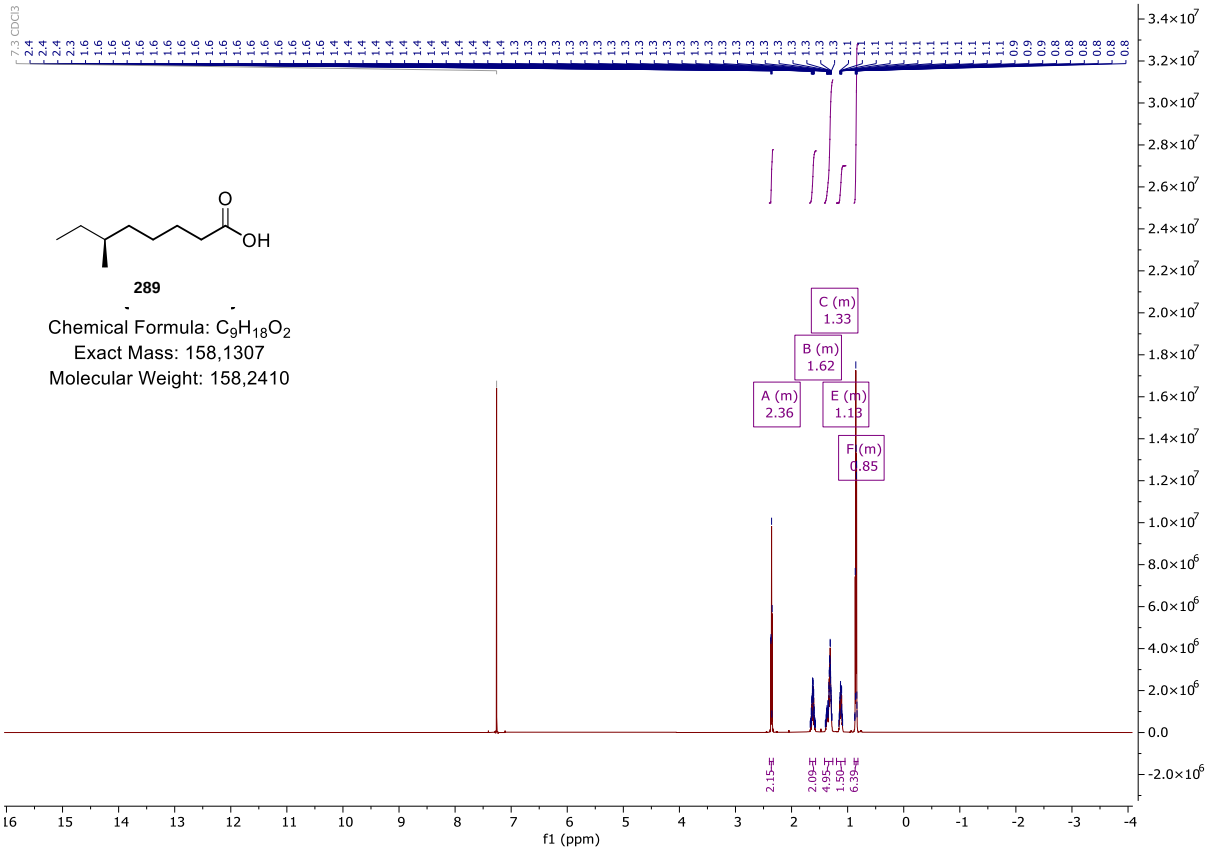

^{1}H – NMR spectrum of **289** (700 MHz, $CDCl_3$).

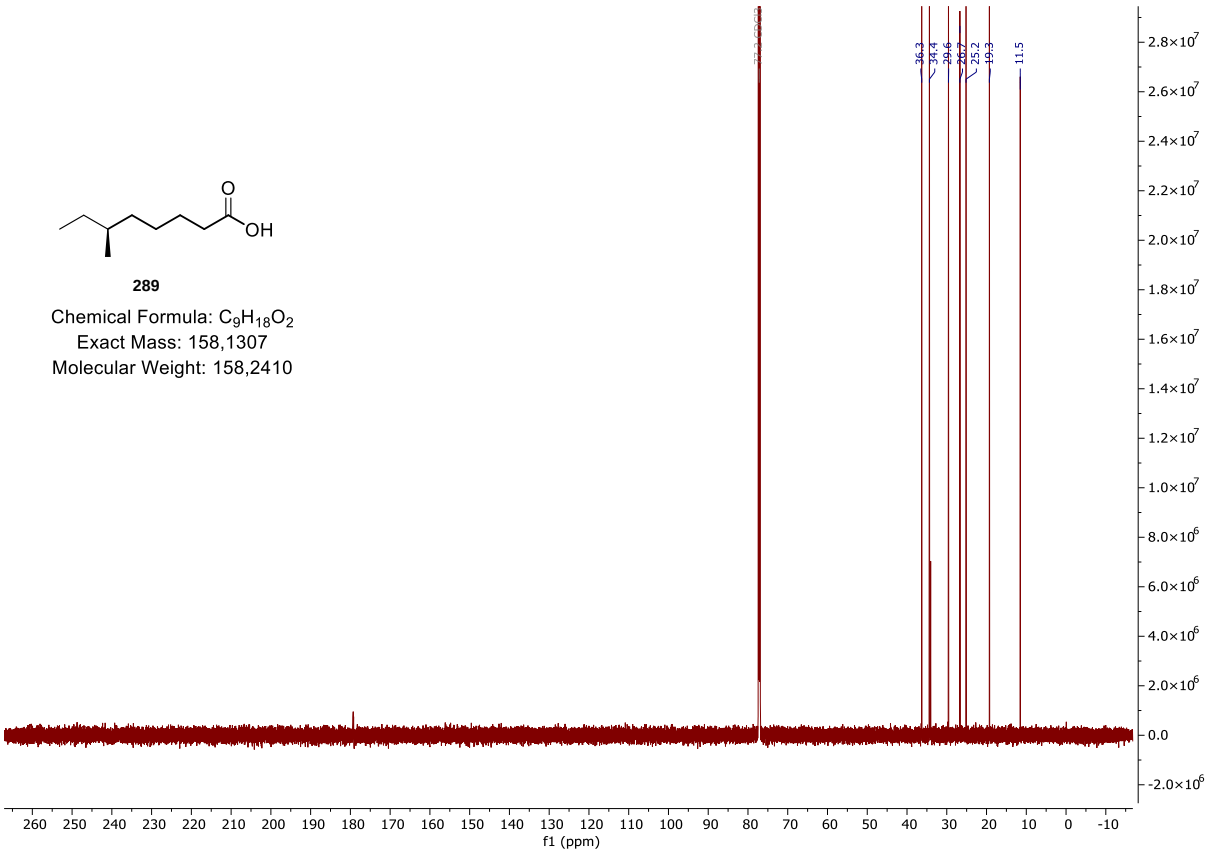

^{13}C – NMR spectrum of **289** (175 MHz, $CDCl_3$).

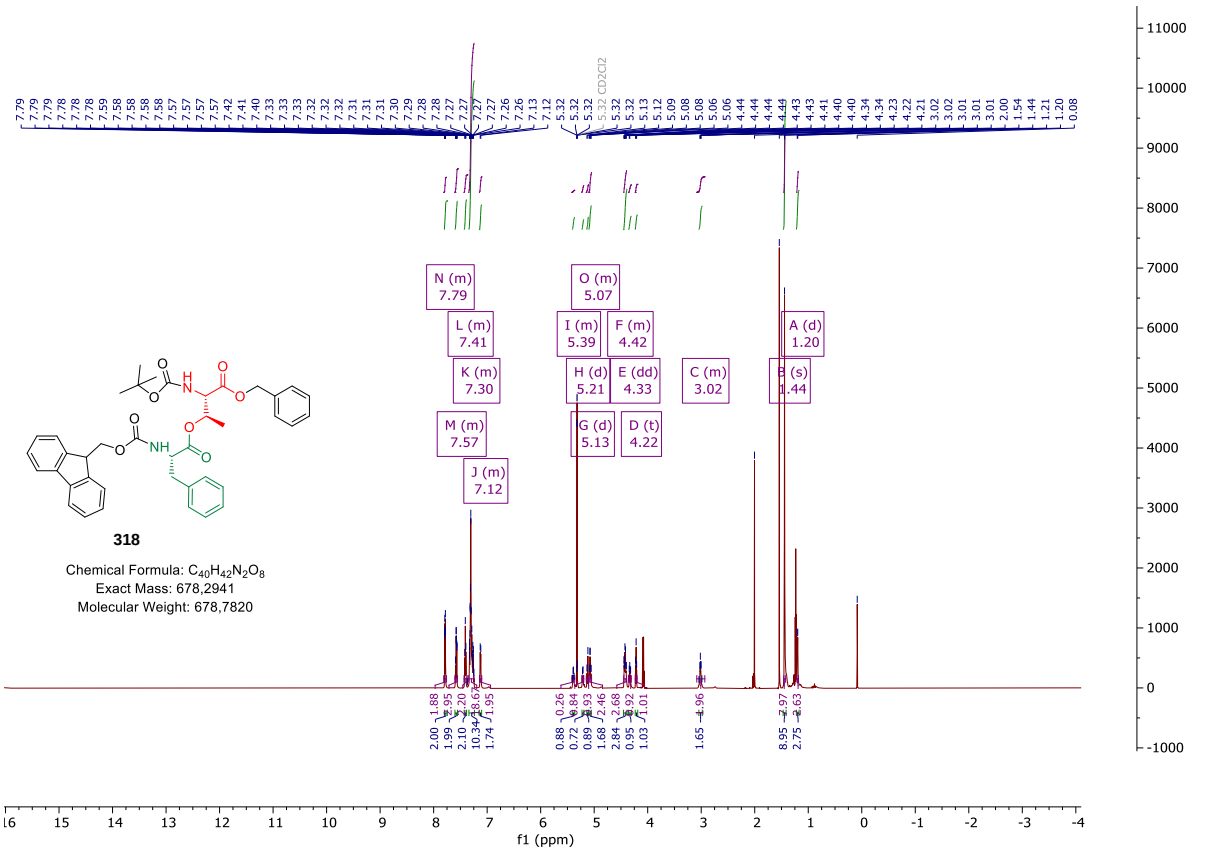

^{1}H – NMR spectrum of **318** (700 MHz, CD_2Cl_2)

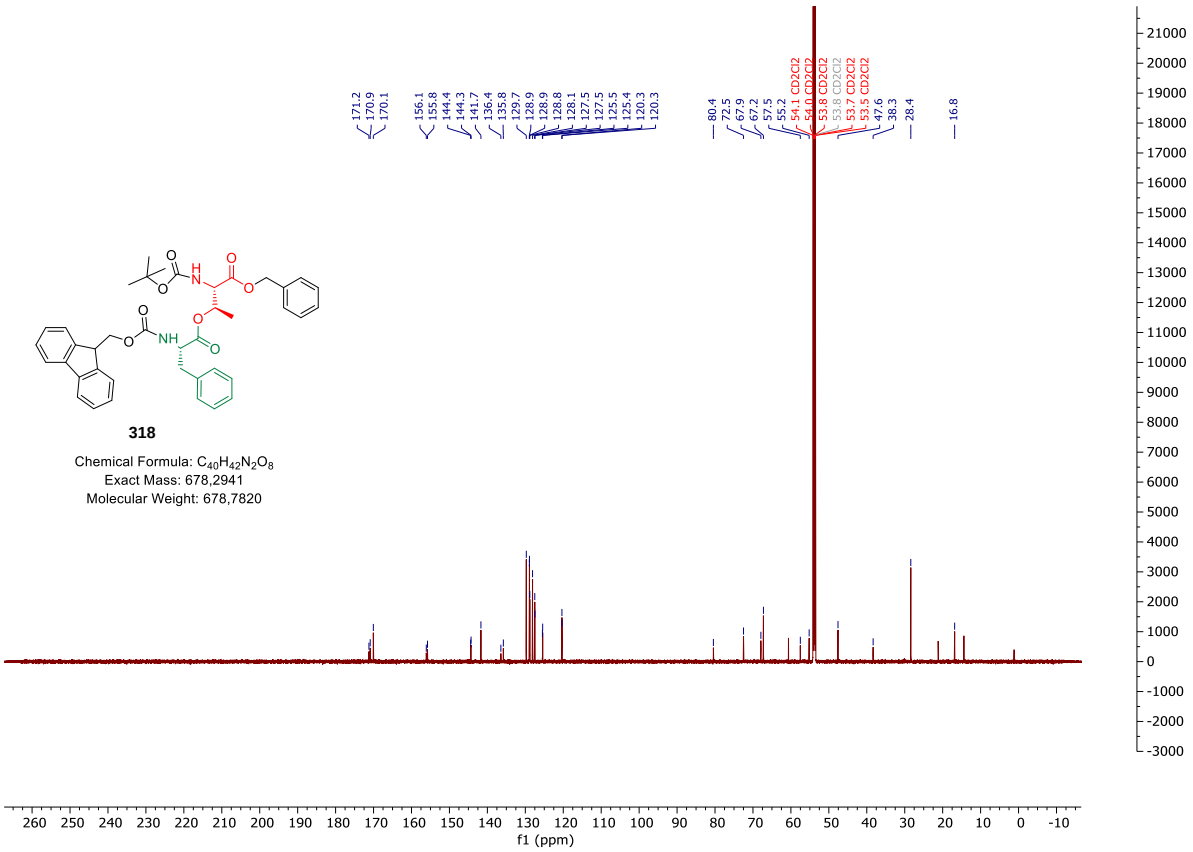

^{13}C – NMR spectrum of **318** (175 MHz, CD_2Cl_2)

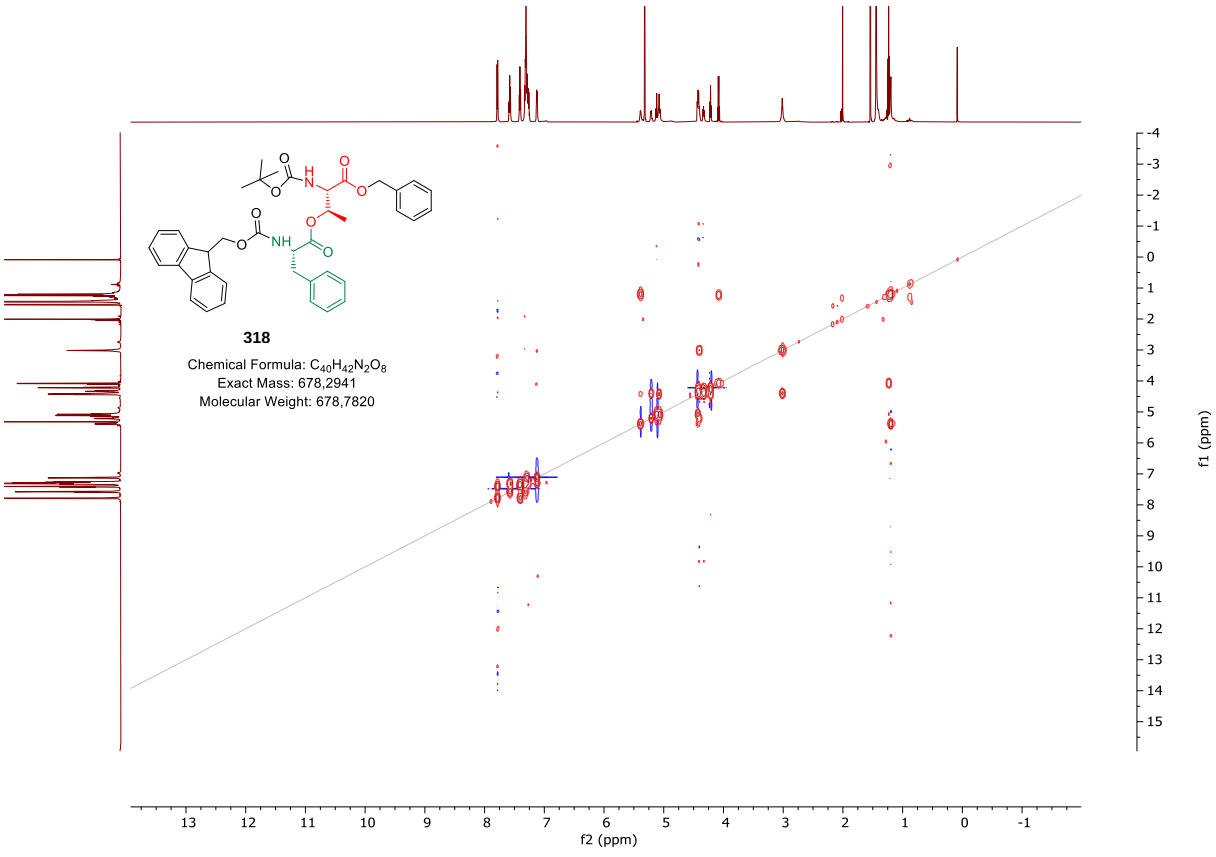

^{1}H, ^{1}H – COSY spectrum of **318** (700 MHz, CD_2Cl_2)

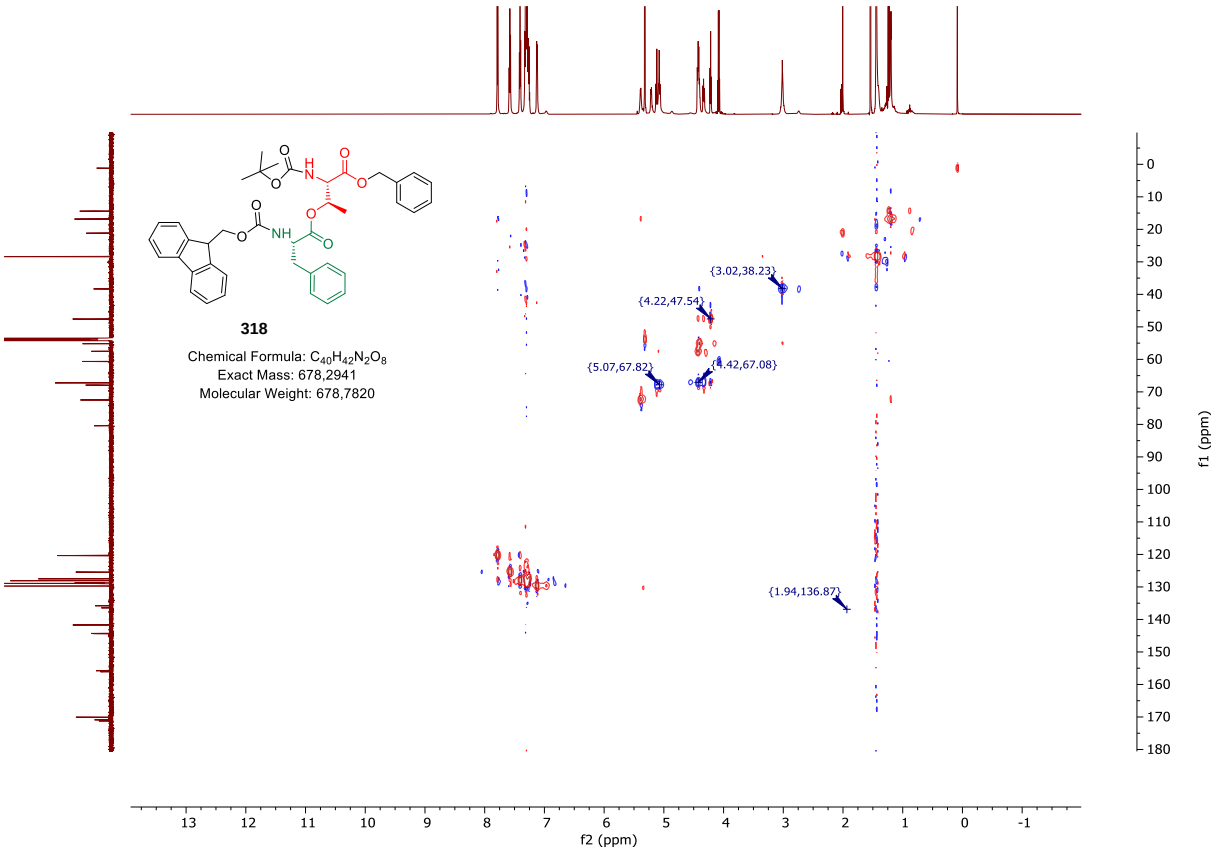

^{1}H, ^{13}C – HSQC spectrum of **318** (700 MHz, 175 MHz, CD_2Cl_2)

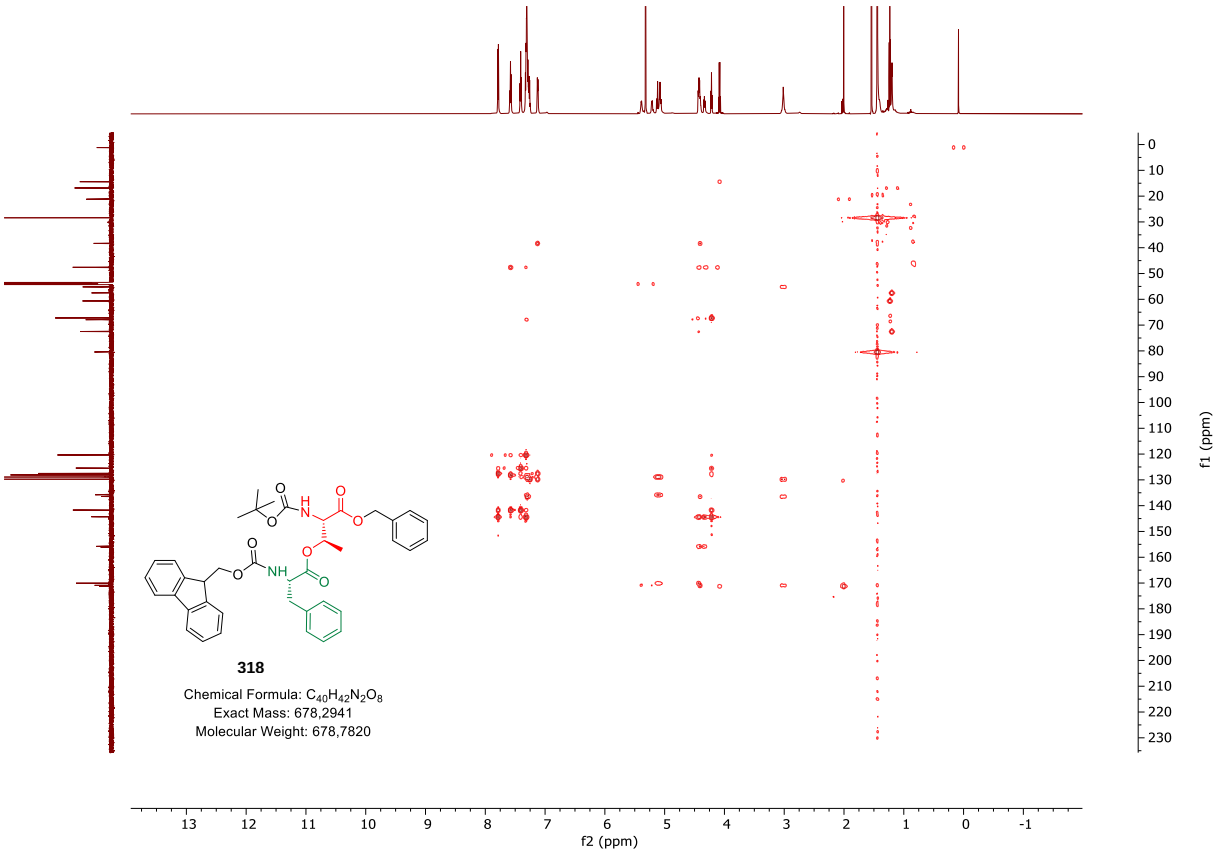

^{1}H, ^{13}C – HMBC spectrum of **318** (700 MHz, 175 MHz, CD_2Cl_2)

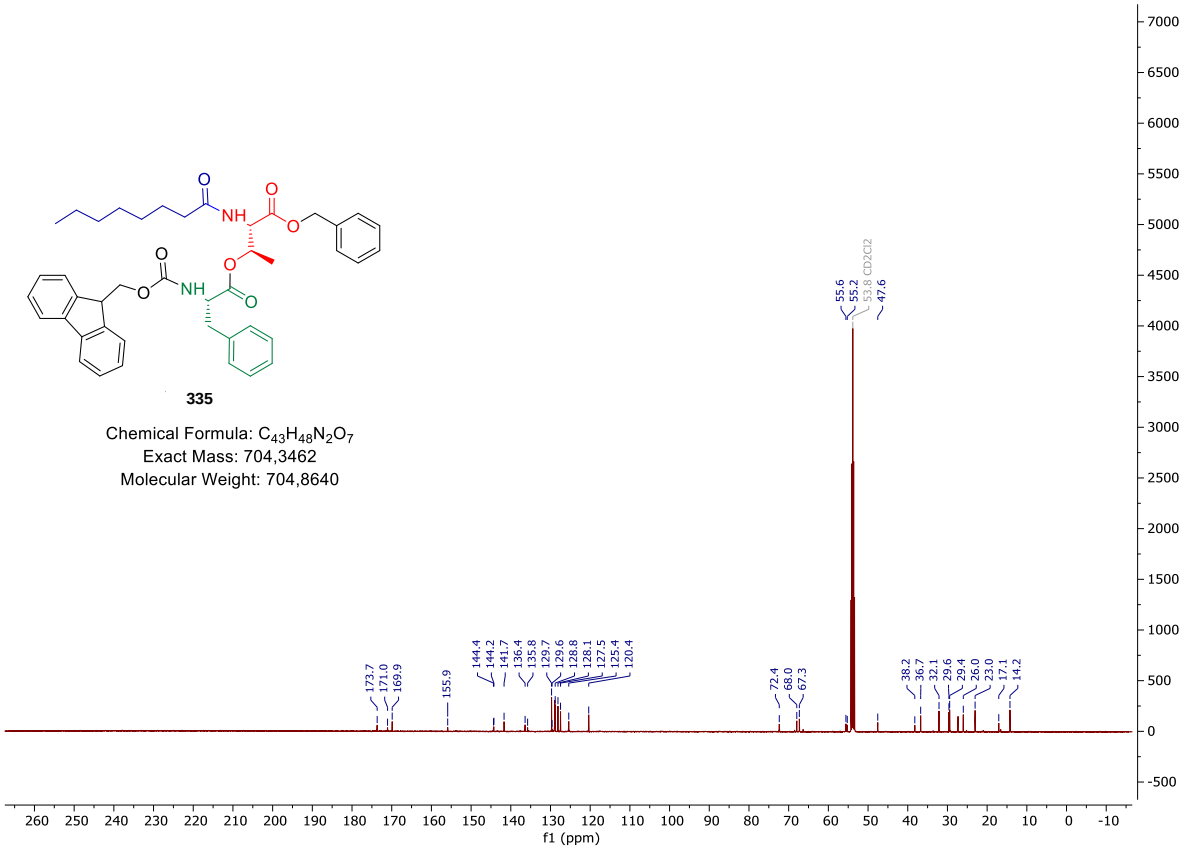

^{1}H – NMR spectrum of **335** (500 MHz, CD_2Cl_2)

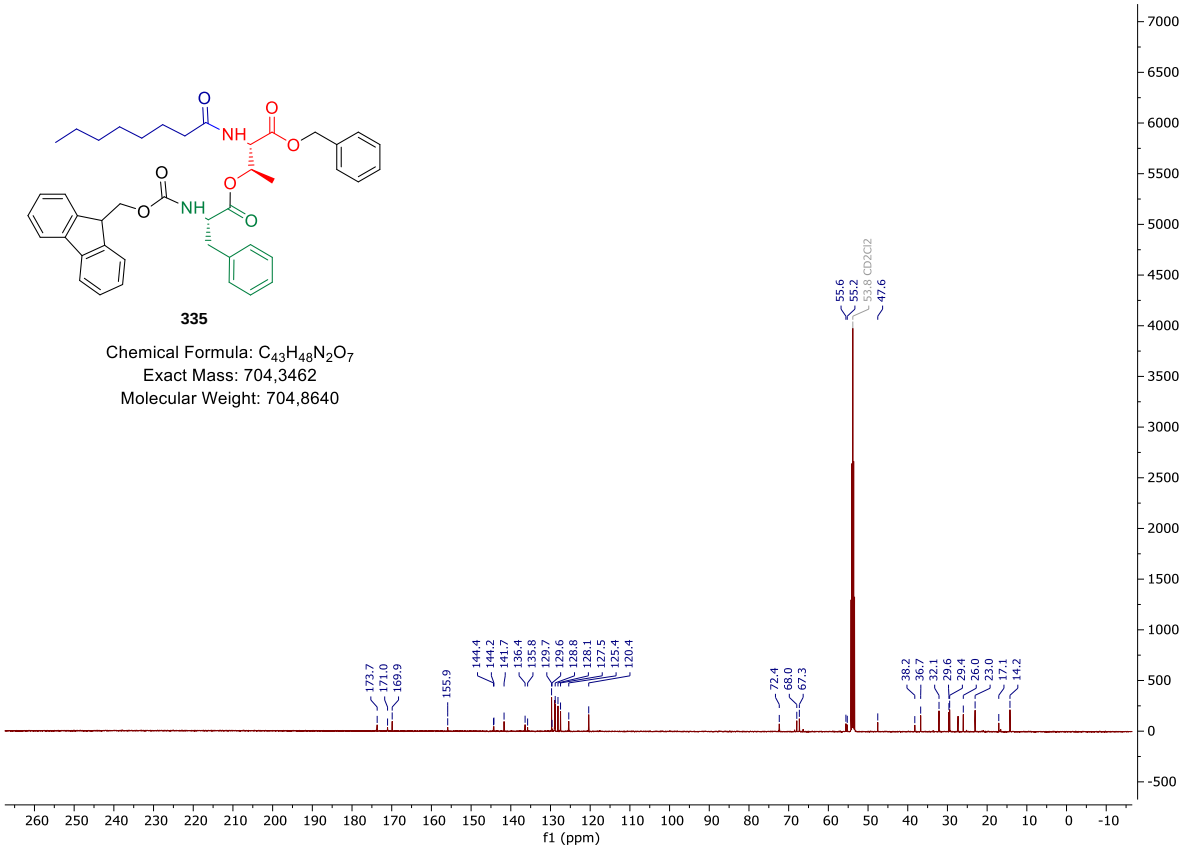

^{13}C – NMR spectrum of **335** (125 MHz, CD_2Cl_2)

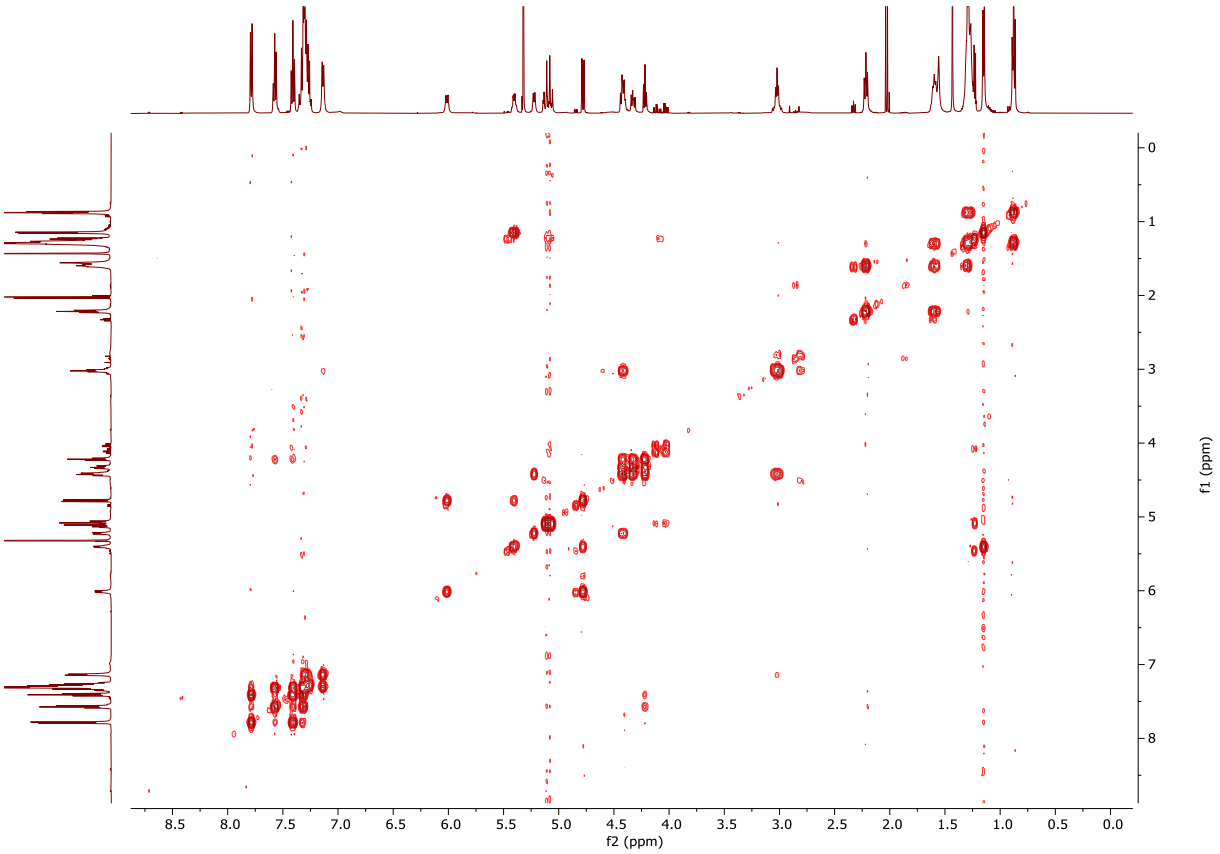

^{1}H, ^{1}H – COSY spectrum of **335** (500 MHz, CD_2Cl_2)

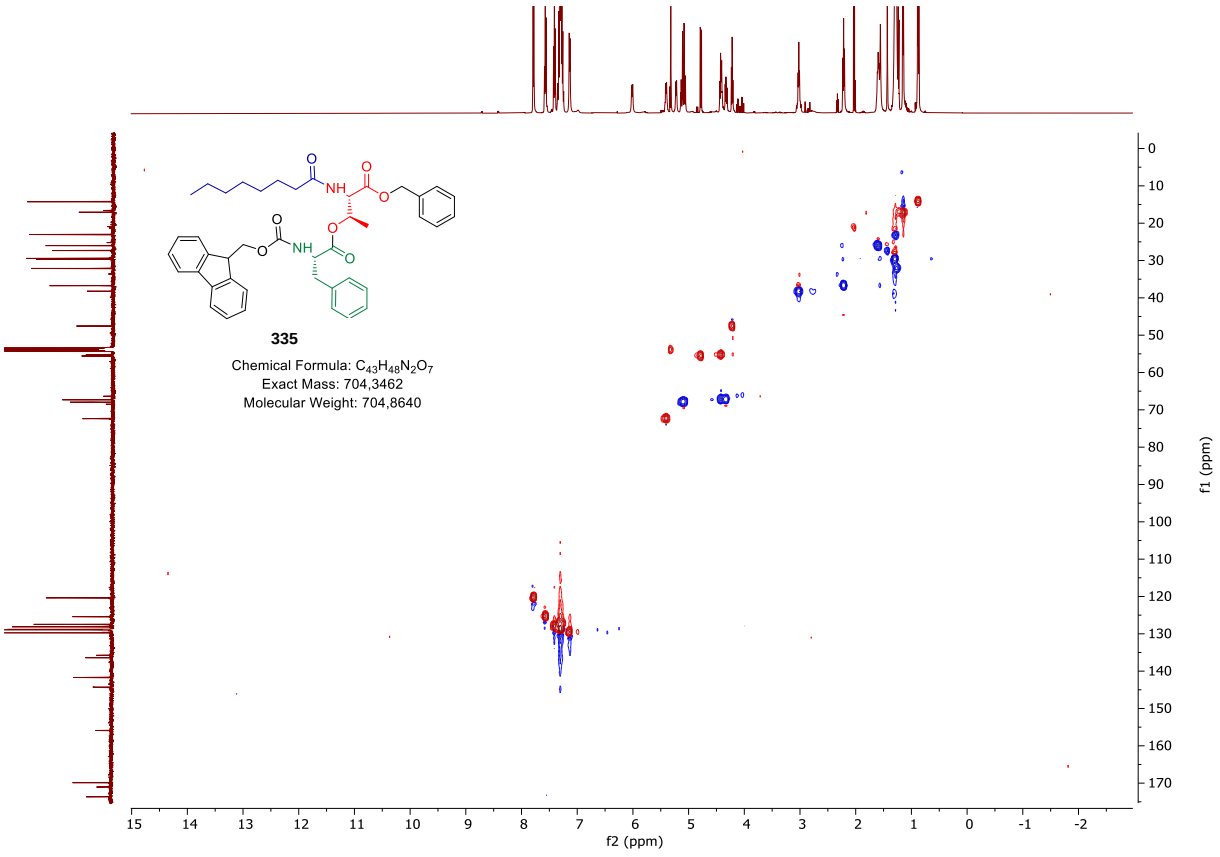

^{1}H, ^{13}C – HSQC spectrum of **335** (500 MHz, 125 MHz, CD_2Cl_2)

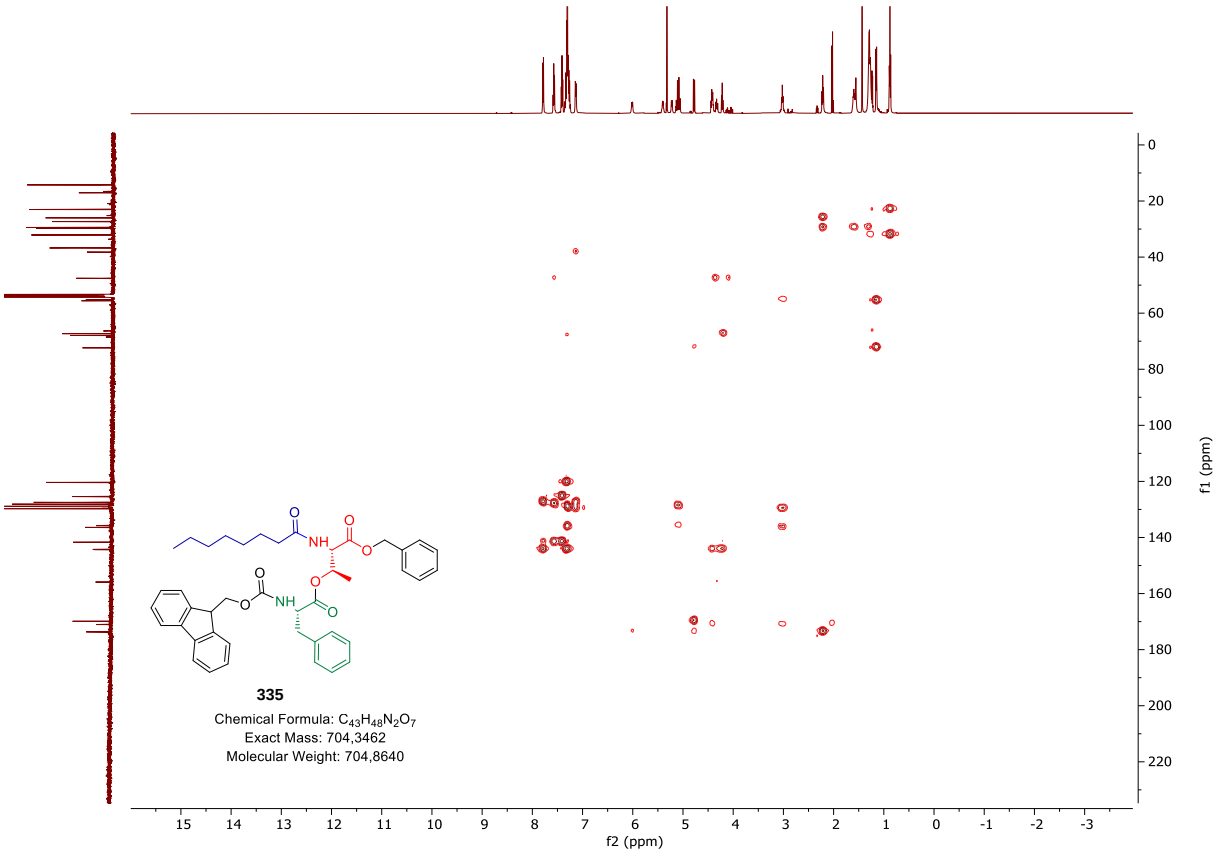

^{1}H, ^{13}C – HMBC spectrum of **335** (500 MHz, 125 MHz, CD_2Cl_2)

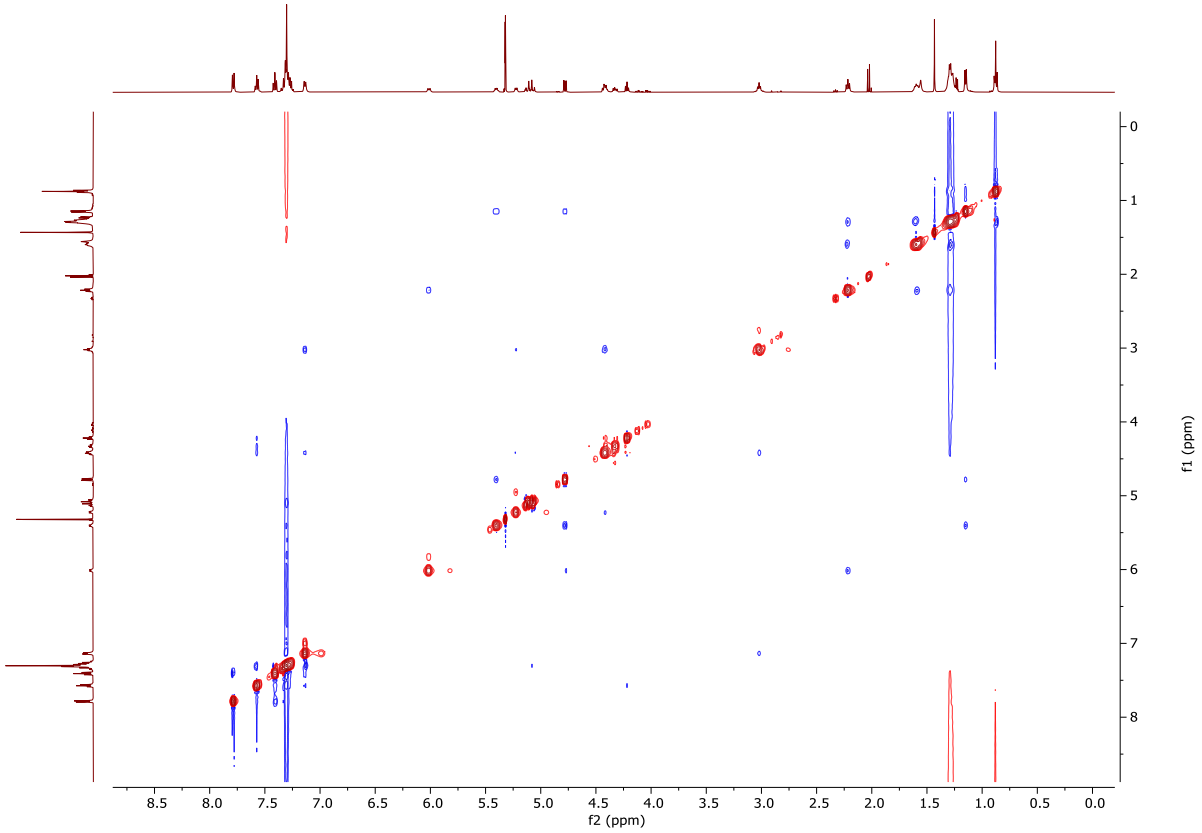

^{1}H, ^{1}H – NOESY spectrum of **335** (500 MHz, CD_2Cl_2)

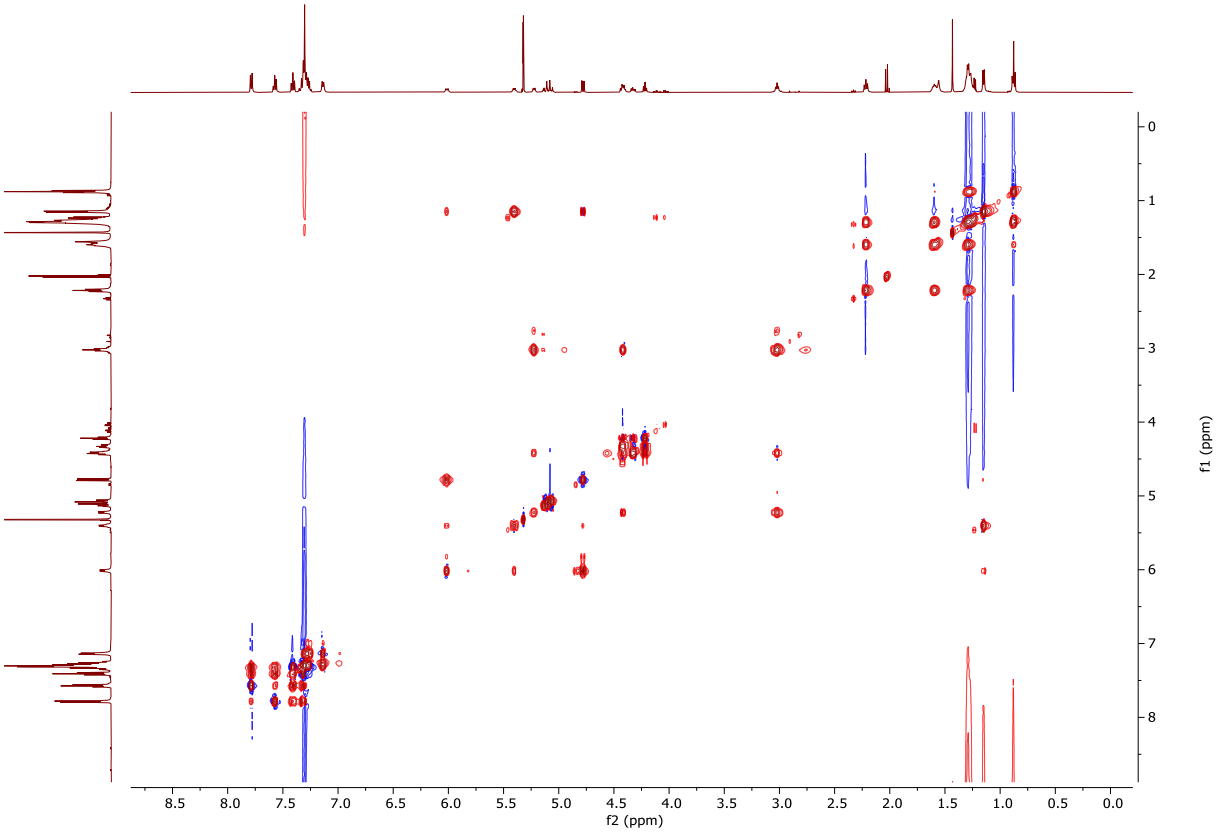

^{1}H, ^{1}H – TOCSY spectrum of **335** (500 MHz, CD_2Cl_2)

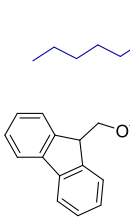

320

Chemical Formula: $C_{36}H_{42}N_2O_7$
Exact Mass: 614,2992
Molecular Weight: 614,7390

^{1}H – NMR spectrum of **320** (500 MHz, CD_2Cl_2)

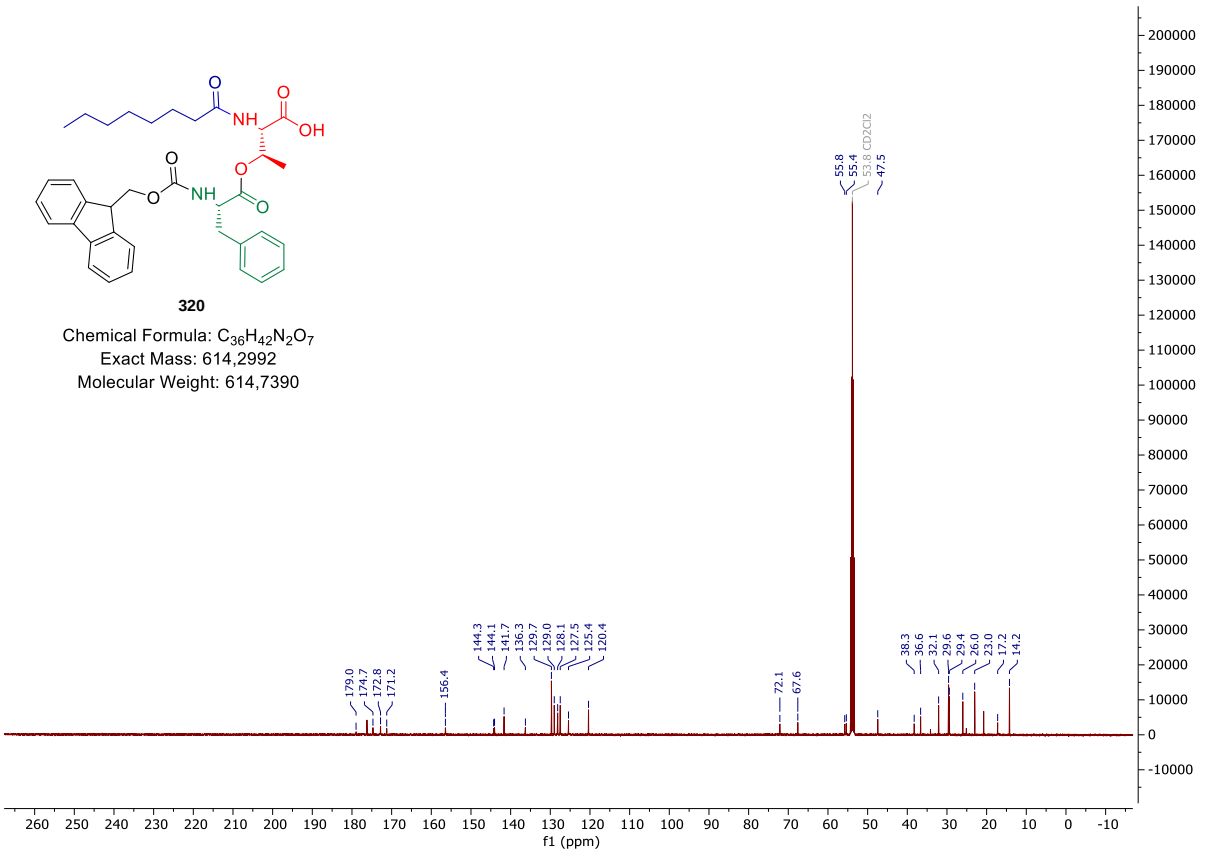

^{13}C – NMR spectrum of **320** (125 MHz, CD_2Cl_2)

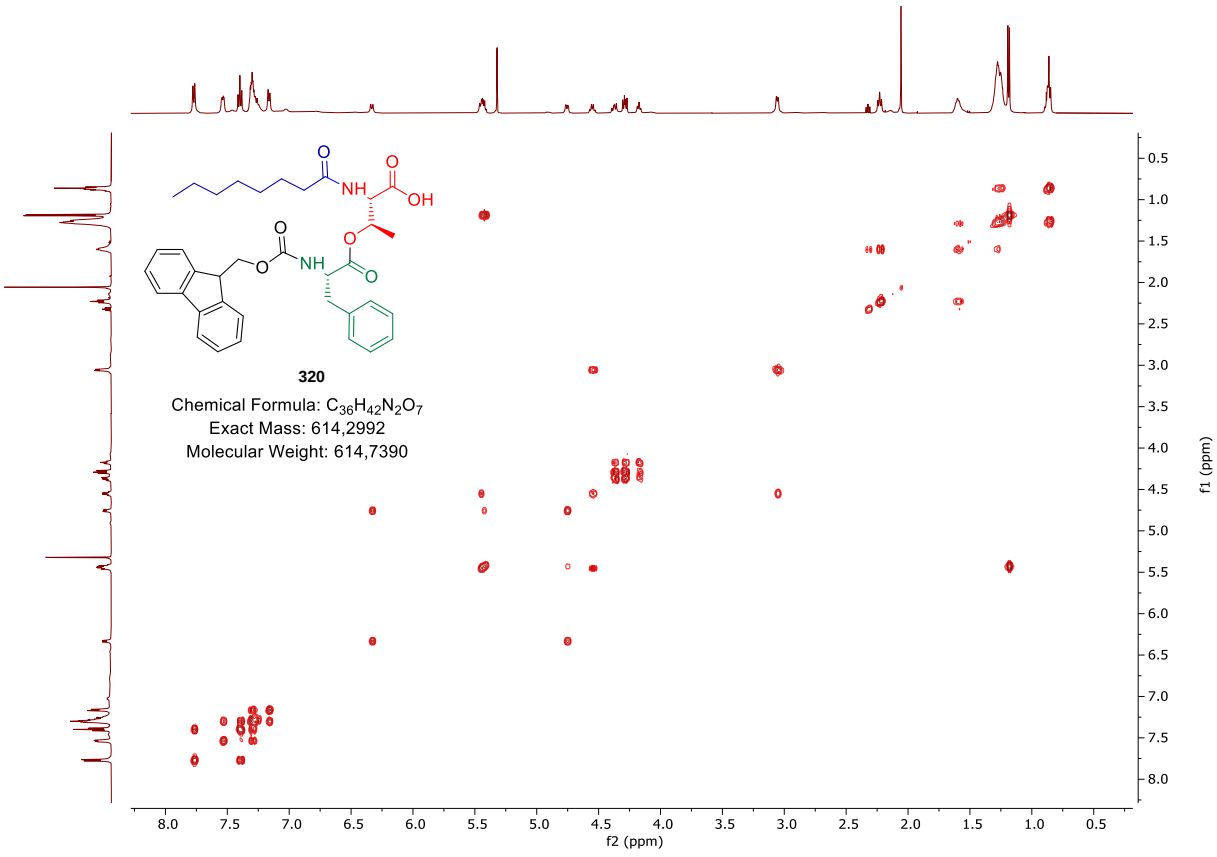

^{1}H, ^{1}H – COSY spectrum of **320** (500 MHz, CD_2Cl_2)

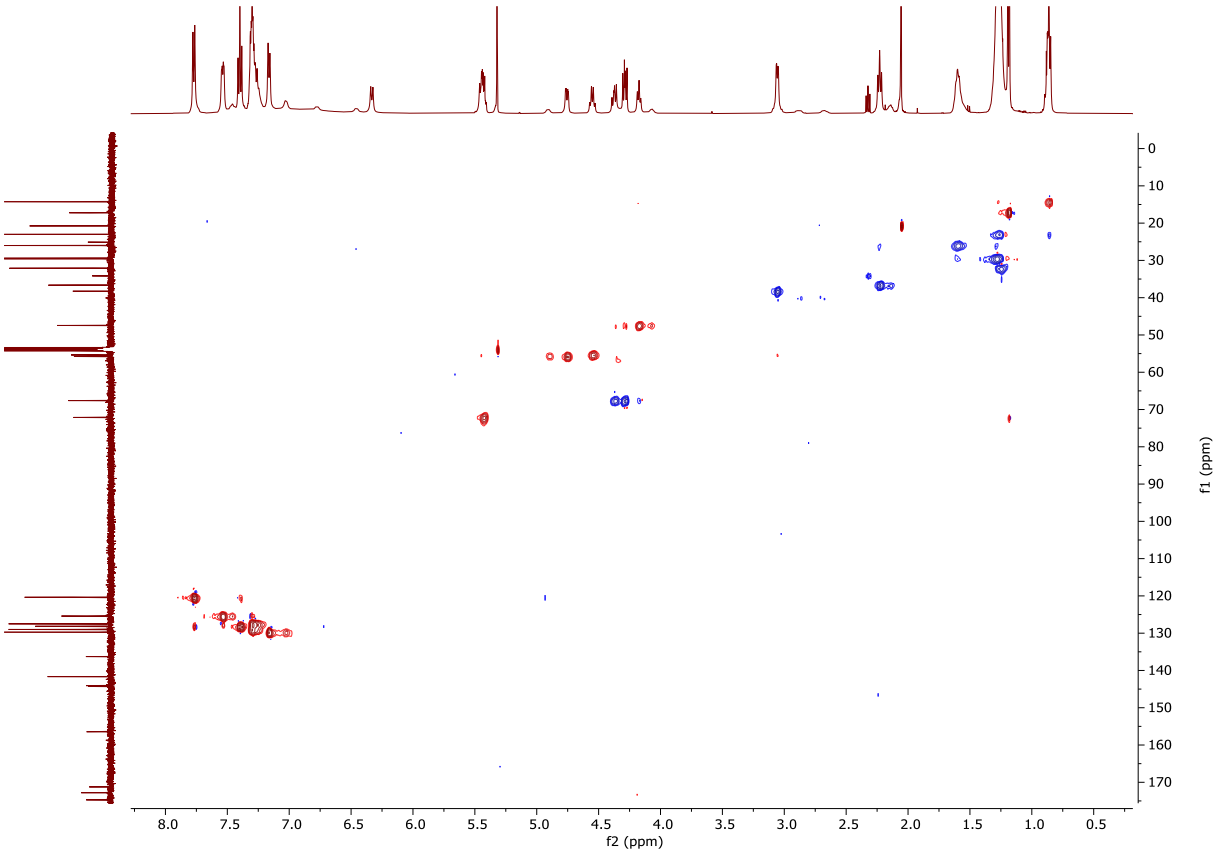

^{1}H, ^{13}C – HSQC spectrum of **320** (500 MHz, 125 MHz, CD_2Cl_2)

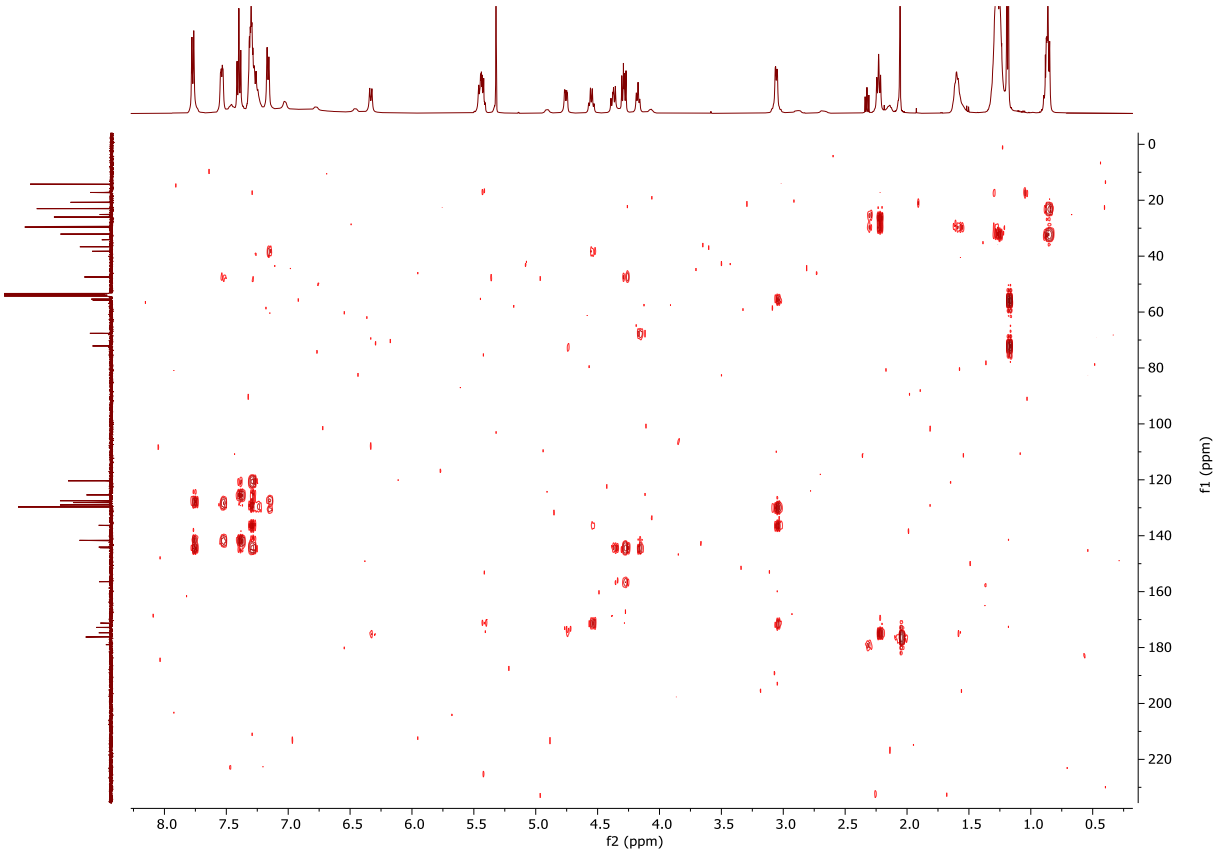

^{1}H, ^{13}C – HMBC spectrum of **320** (500 MHz, 125 MHz, CD_2Cl_2)

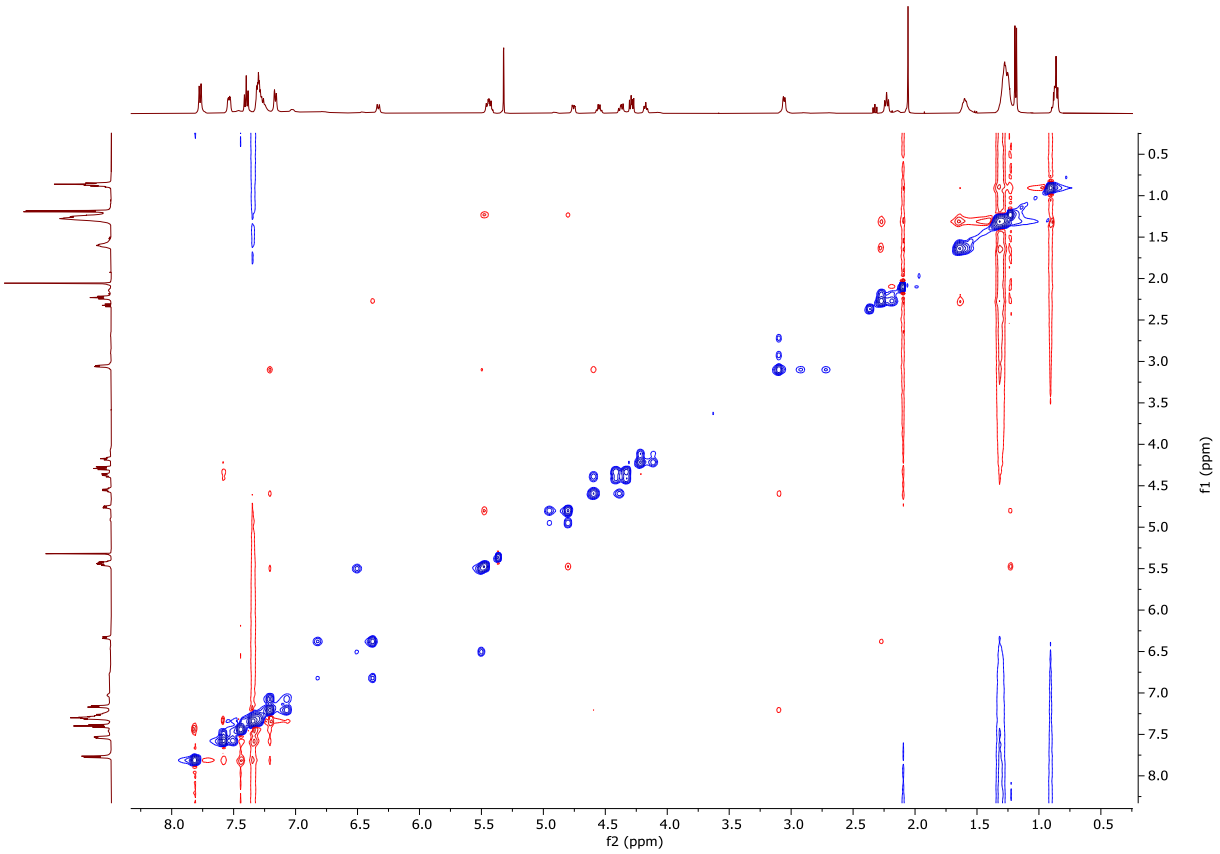

^{1}H, ^{1}H – NOESY spectrum of **320** (500 MHz, CD_2Cl_2)

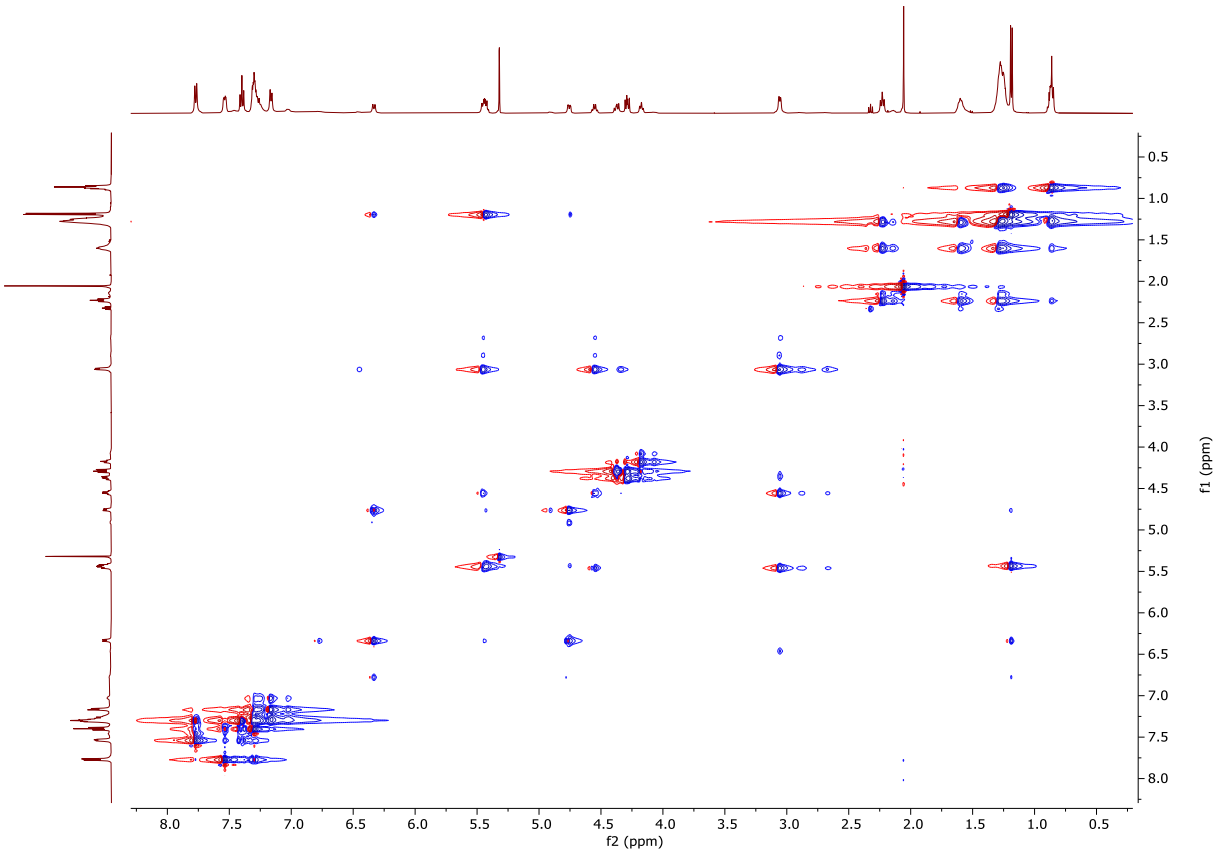

^{1}H, ^{1}H – TOCSY spectrum of **320** (500 MHz, CD_2Cl_2)

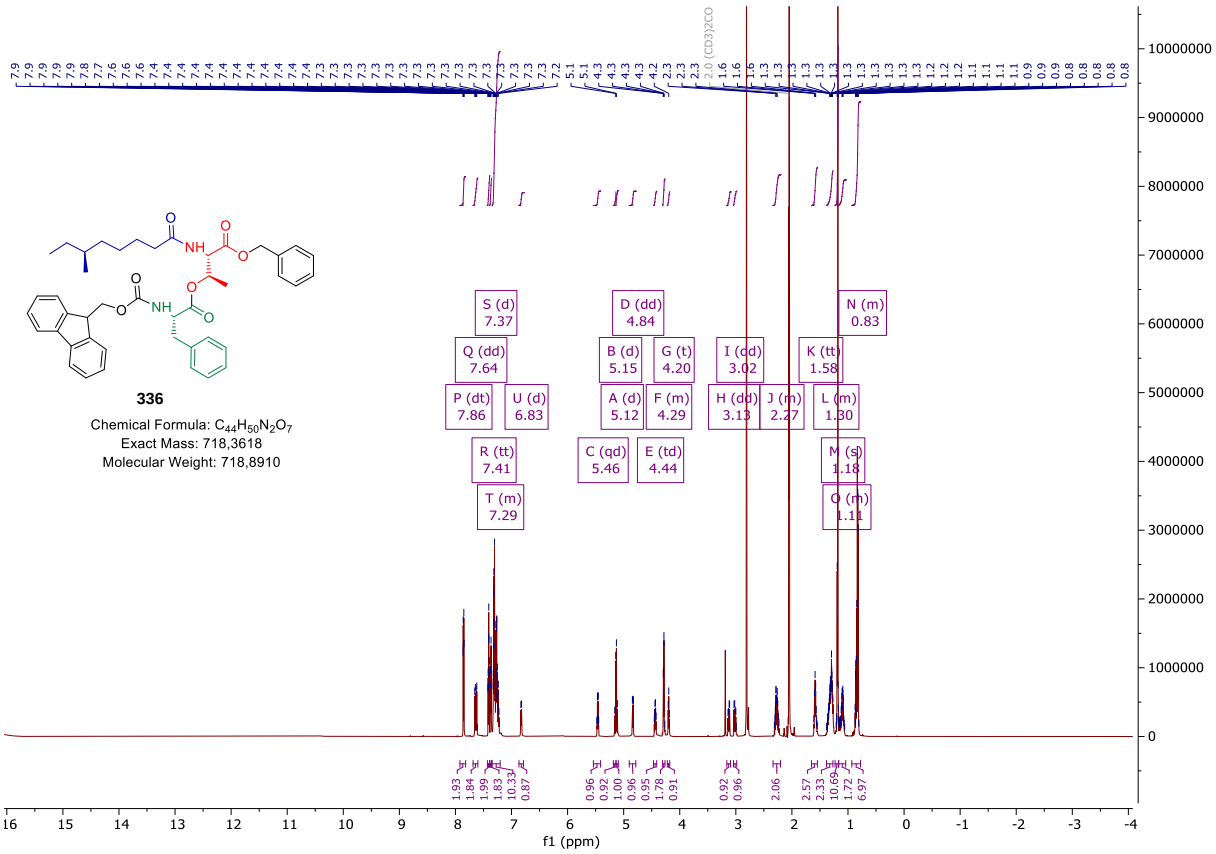

336

Chemical Formula: $C_{44}H_{50}N_2O_7$
Exact Mass: 718,3618
Molecular Weight: 718,8910

^{1}H – NMR spectrum of **336** (700 MHz, Aceton-d_6)

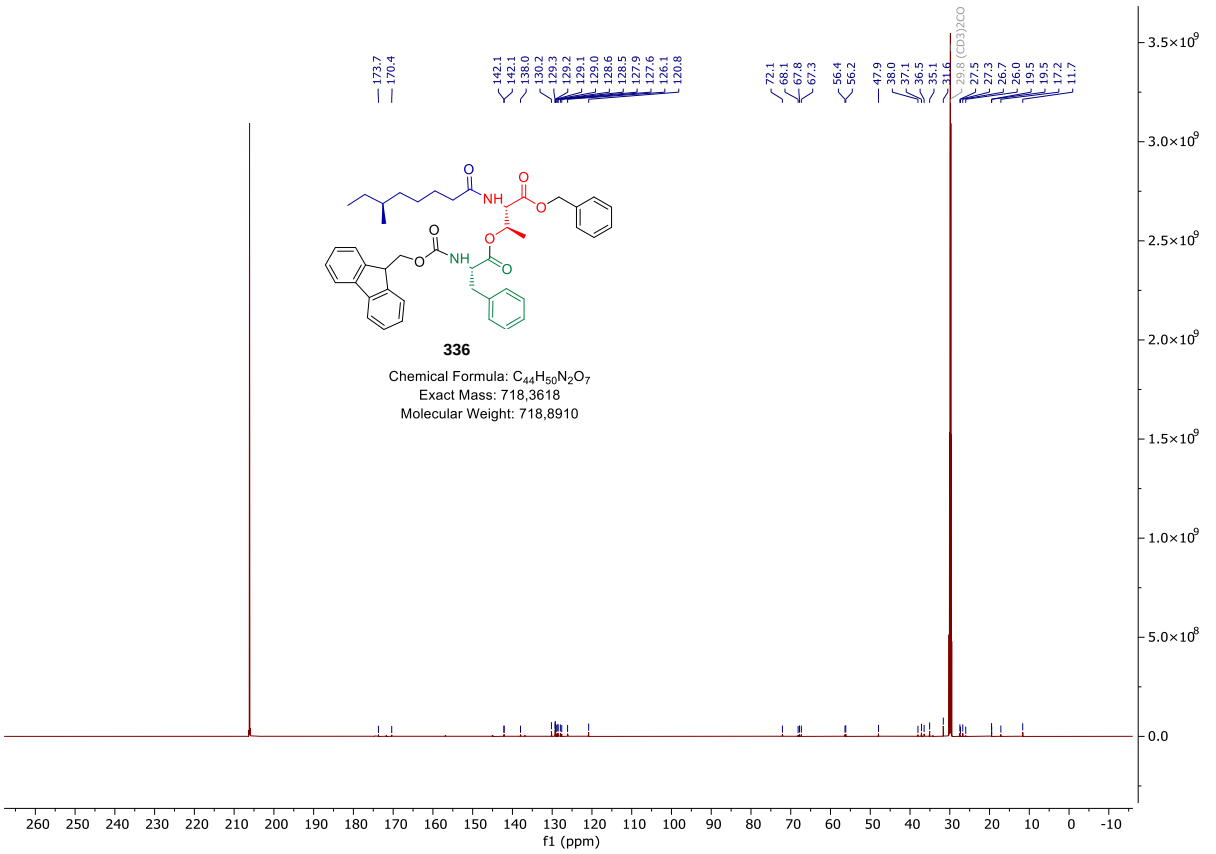

336

Chemical Formula: $C_{44}H_{50}N_2O_7$
Exact Mass: 718,3618
Molecular Weight: 718,8910

^{13}C – NMR spectrum of **336** (175 MHz, Aceton-d_6)

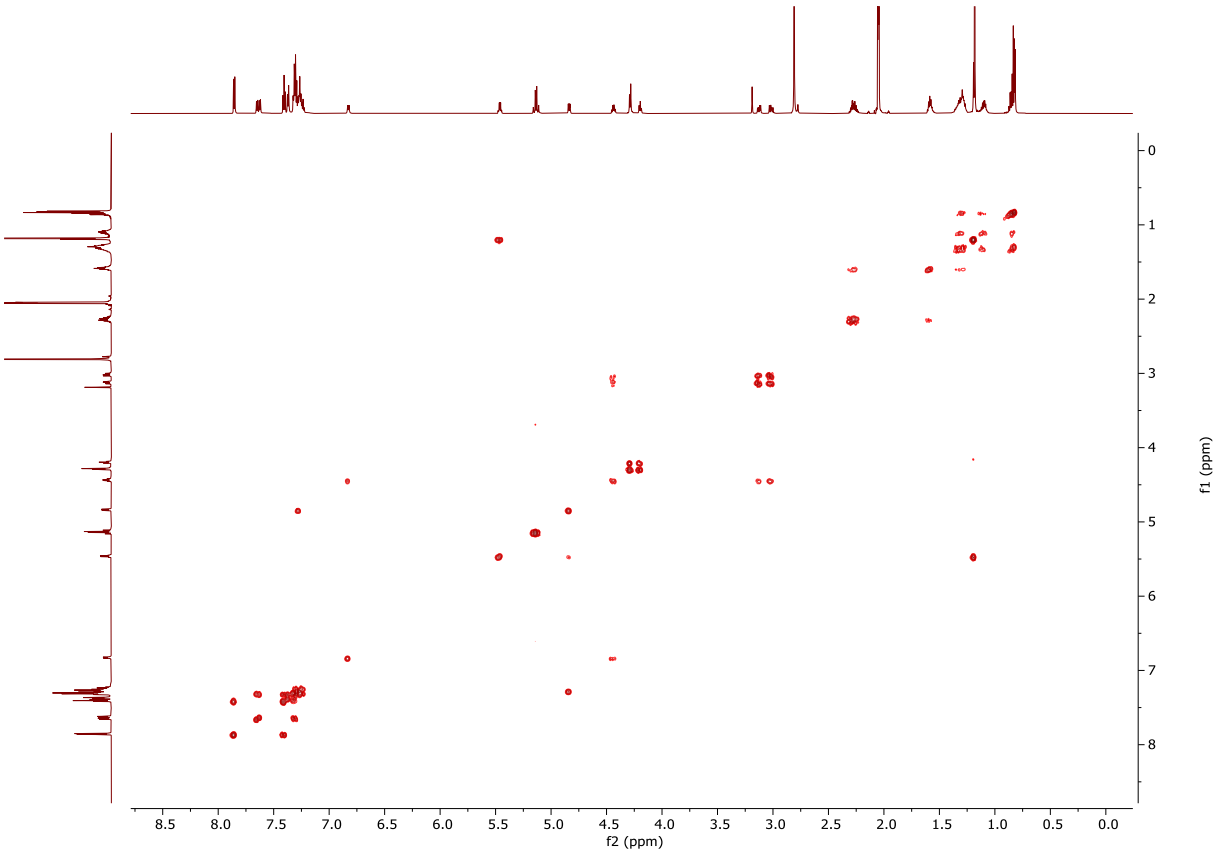

^{1}H, ^{1}H – COSY spectrum of **336** (700 MHz, Aceton-d_6)

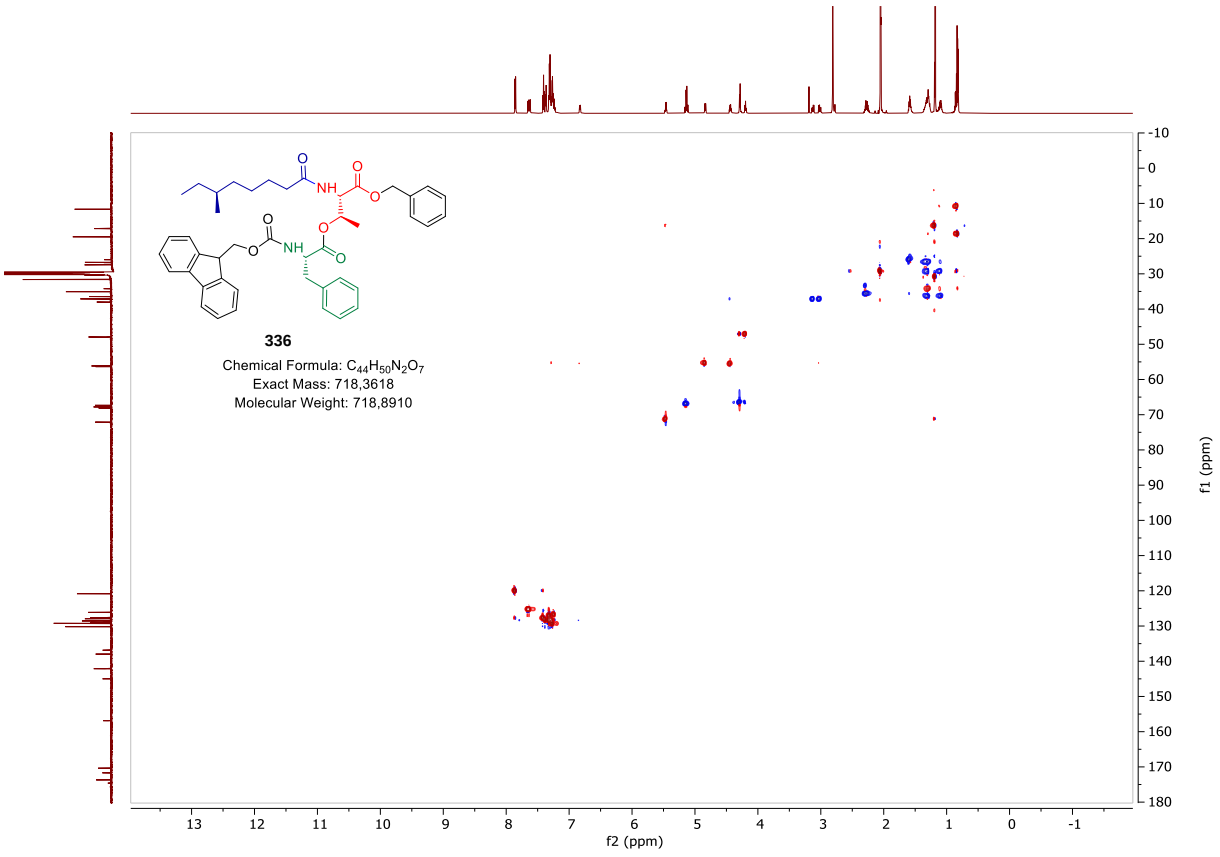

^{1}H, ^{13}C – HSQC spectrum of **336** (700 MHz, 175 MHz, Aceton-d_6))

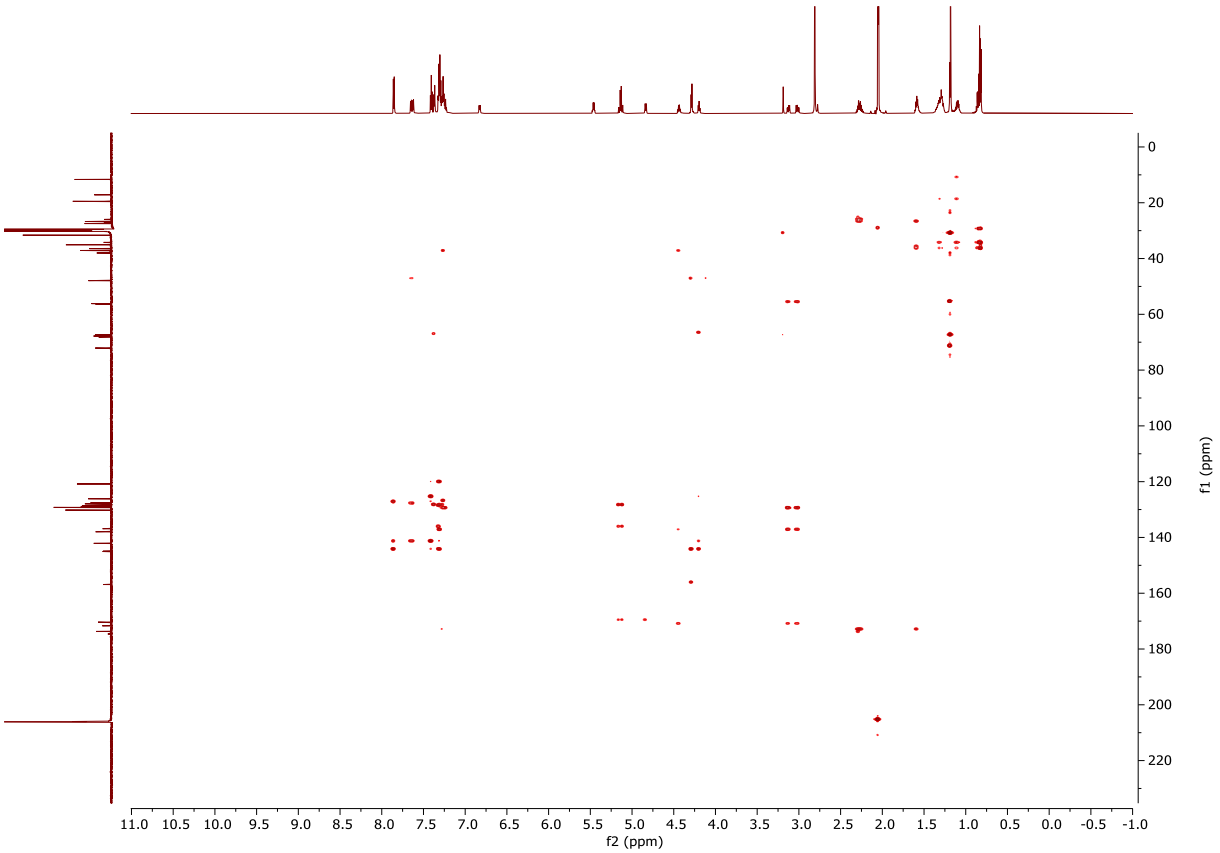

^{1}H, ^{13}C – HMBC spectrum of **336** (700 MHz, 175 MHz, Aceton-d_6)

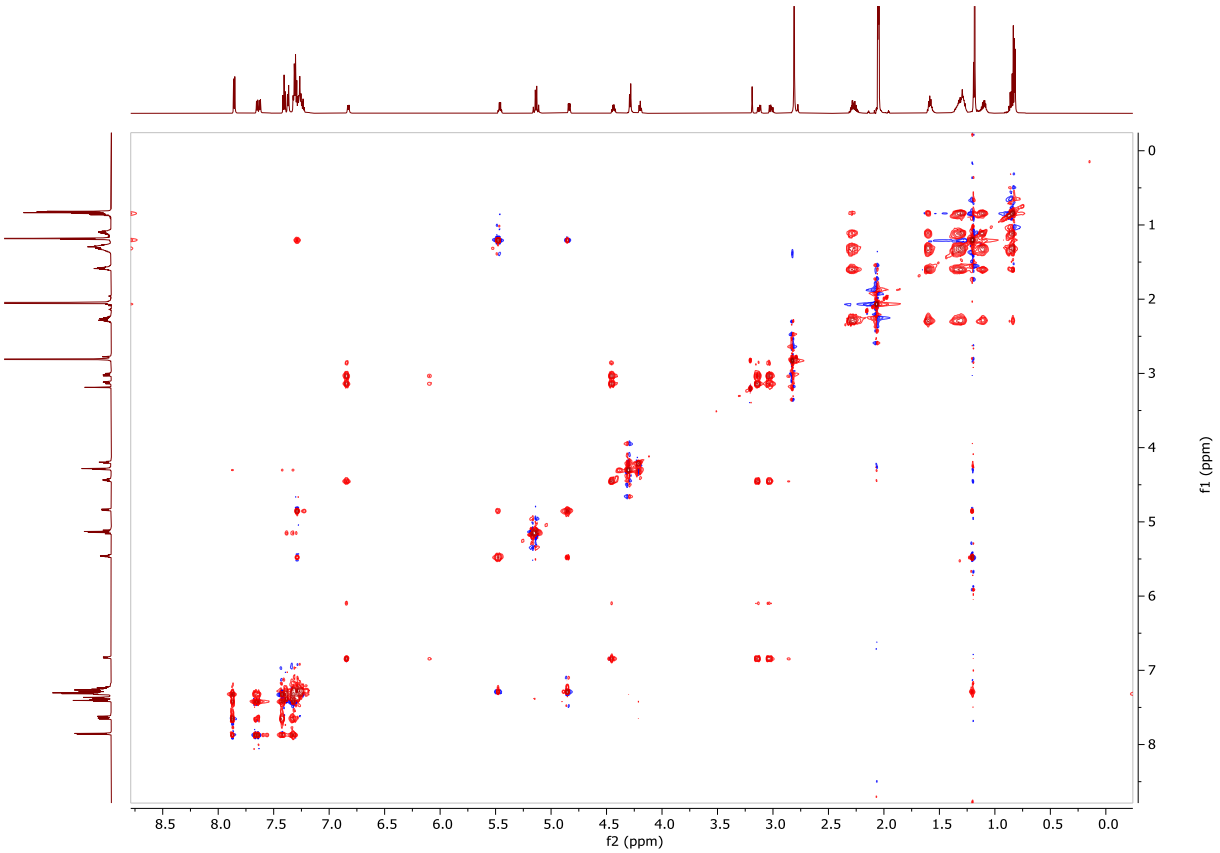

^{1}H, ^{1}H – TOCSY spectrum of **336** (700 MHz, Aceton-d_6)

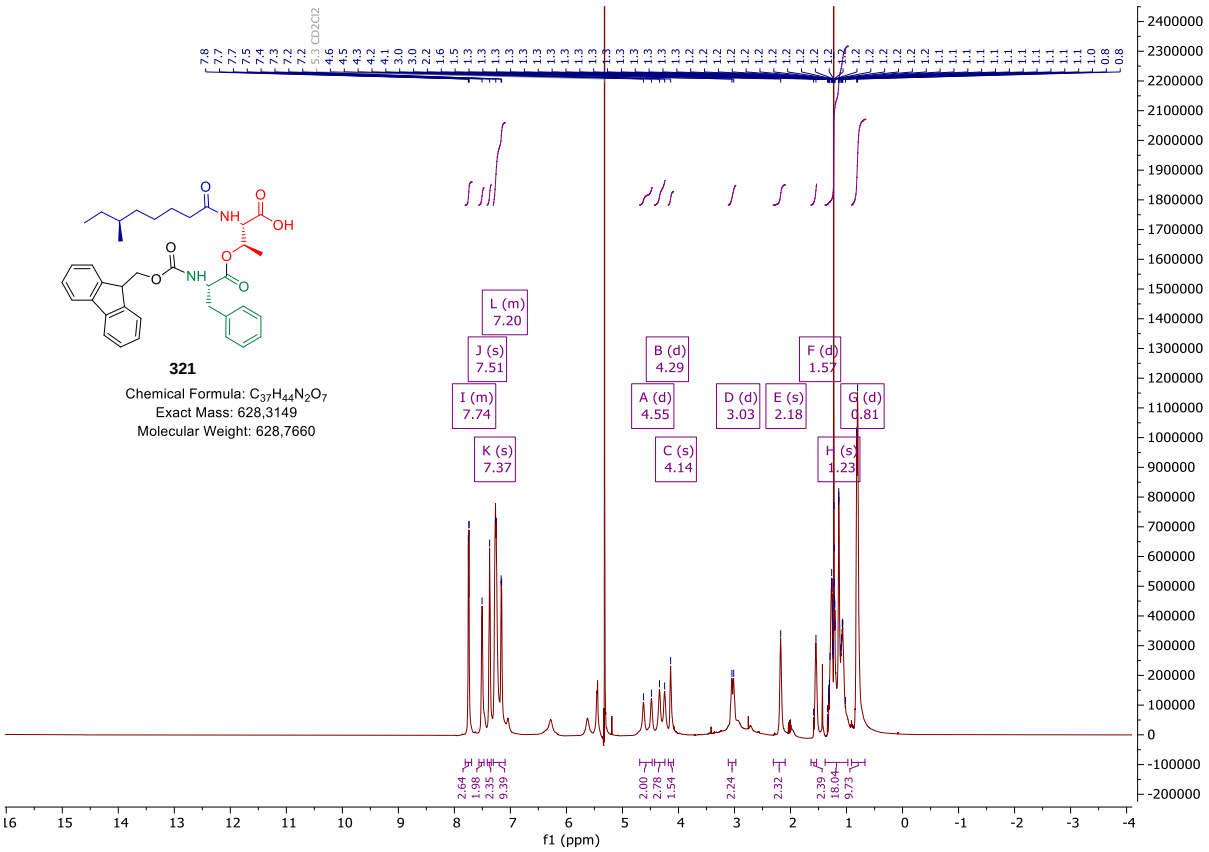

321

Chemical Formula: $C_{37}H_{44}N_2O_7$
Exact Mass: 628,3149
Molecular Weight: 628,7660

^{1}H – NMR spectrum of **321** (700 MHz, CD_2Cl_2).

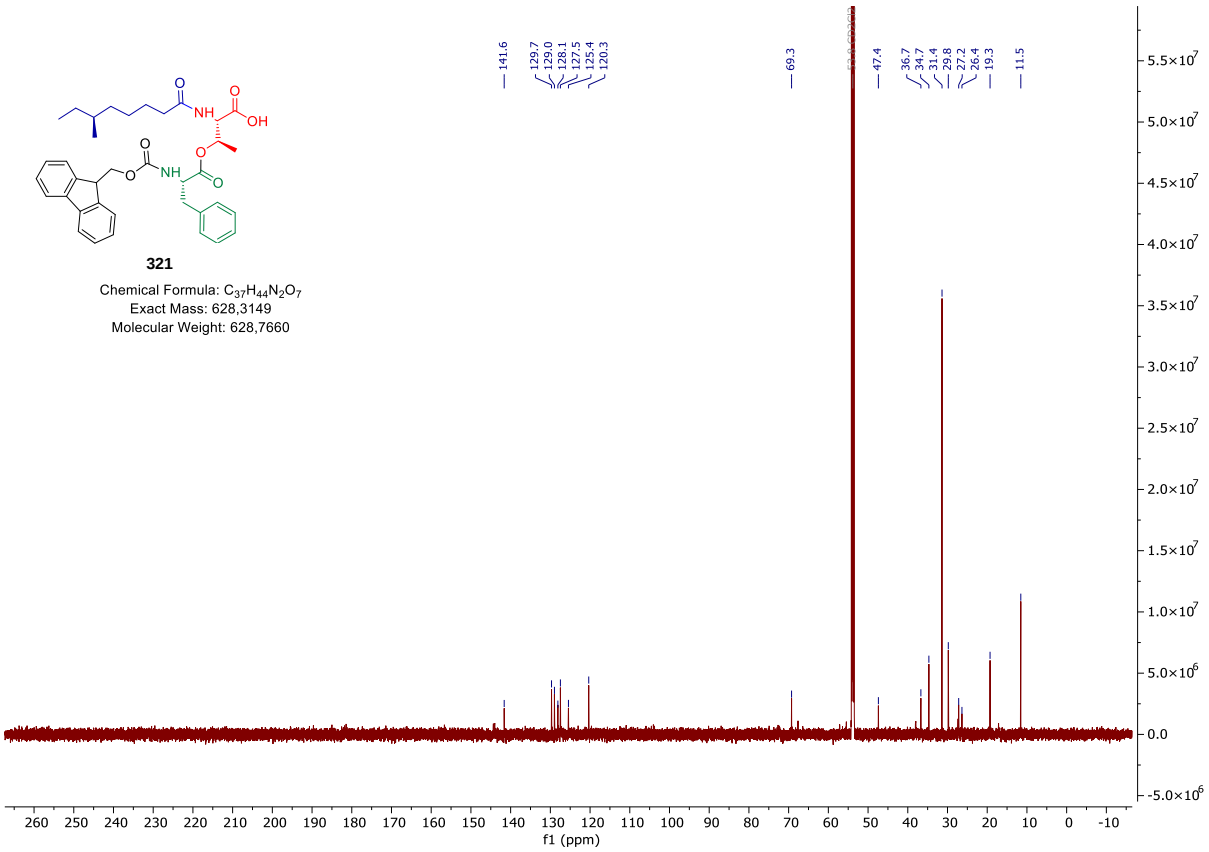

321

Chemical Formula: $C_{37}H_{44}N_2O_7$
Exact Mass: 628,3149
Molecular Weight: 628,7660

^{13}C – NMR spectrum of **321** (175 MHz, CD_2Cl_2).

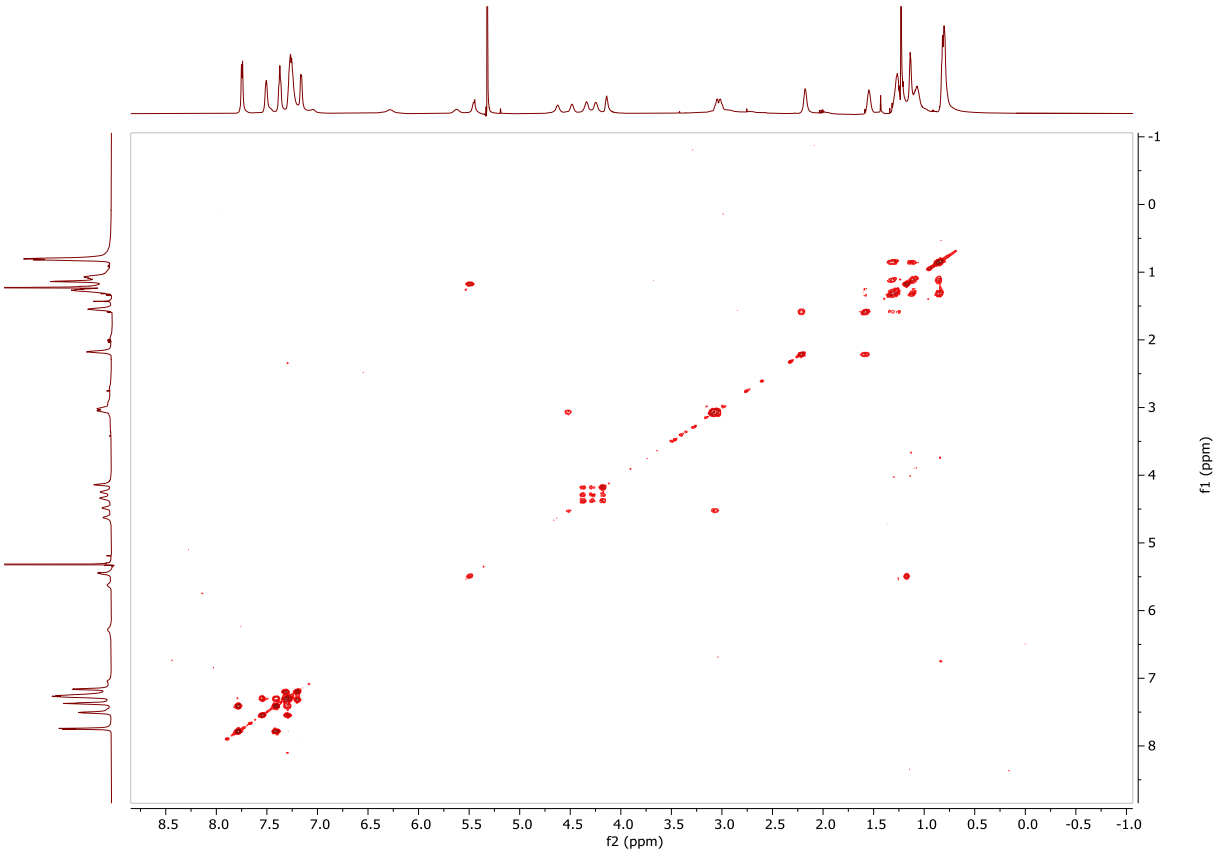

^{1}H, ^{1}H – COSY spectrum of **321** (700 MHz, CD_2Cl_2)

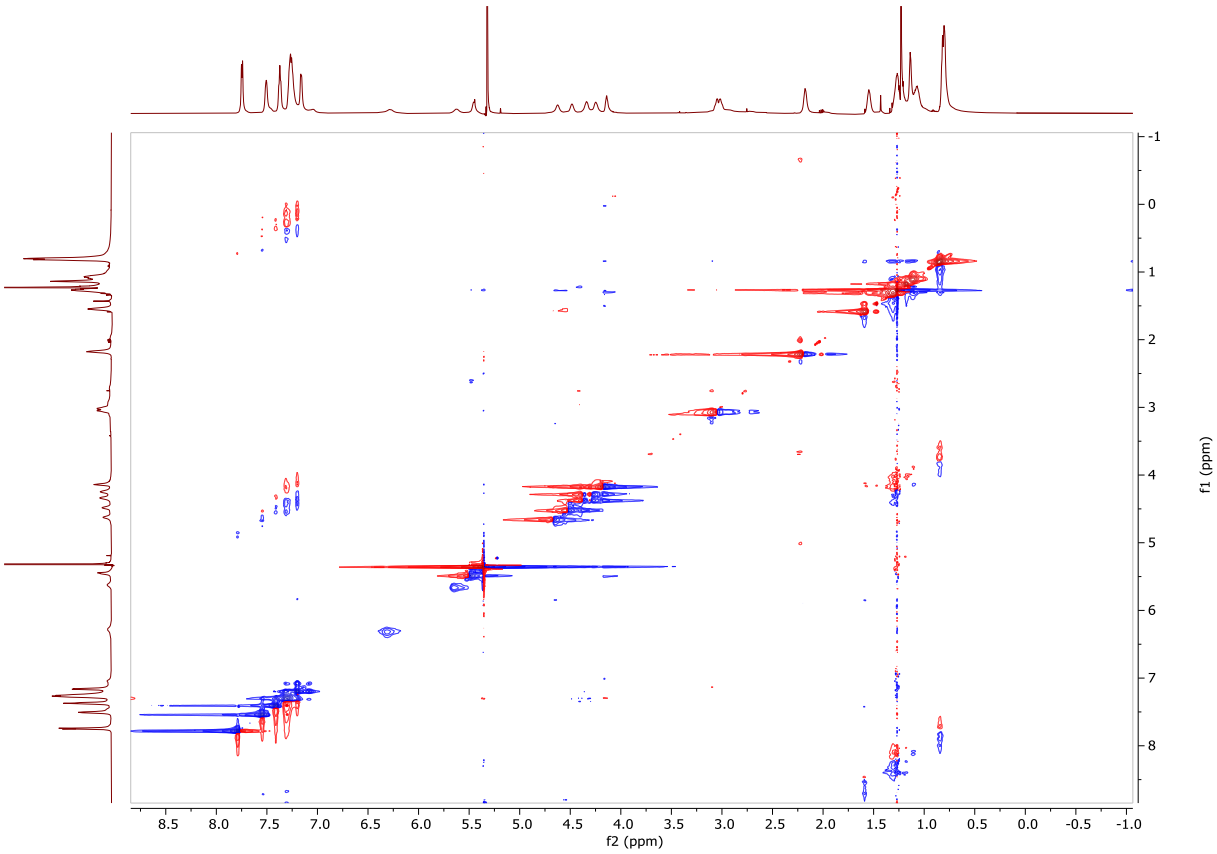

^{1}H, ^{1}H – NOESY spectrum of **321** (700 MHz, CD_2Cl_2)

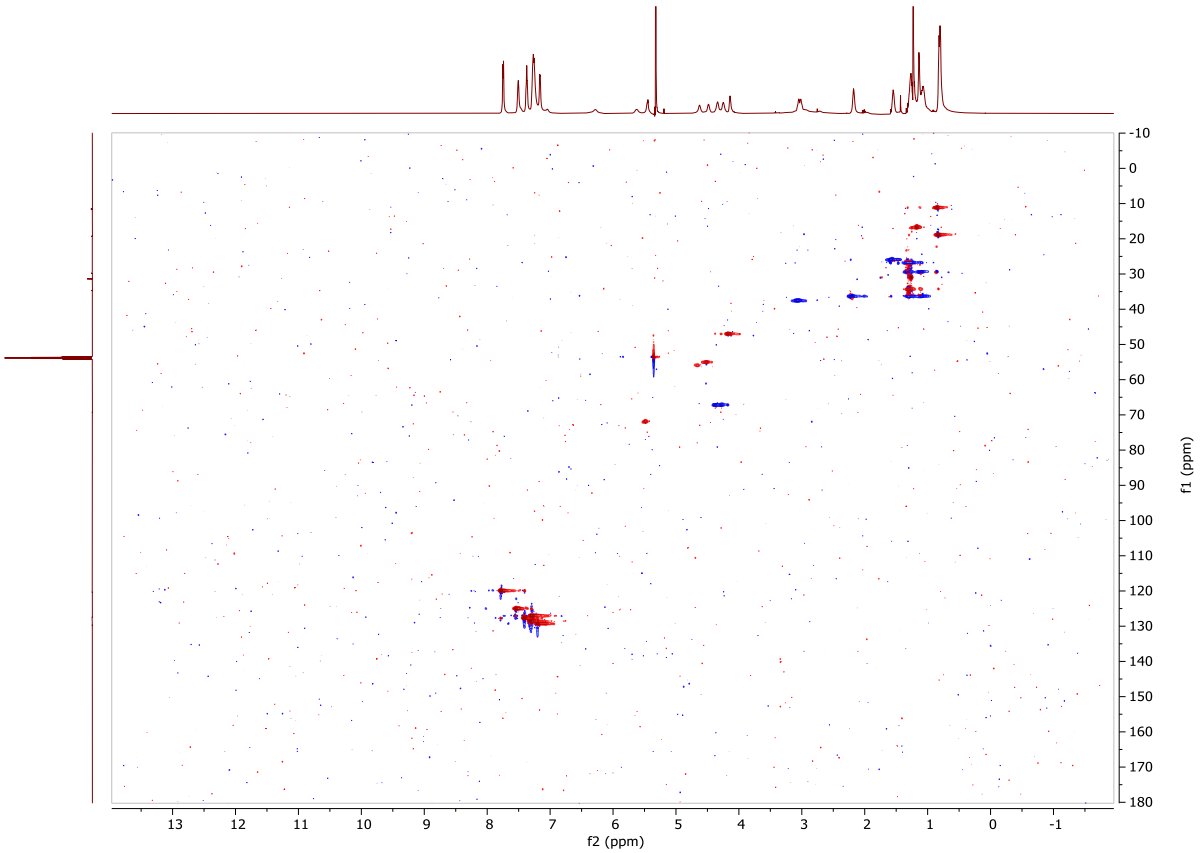

^{1}H, ^{13}C – HSQC spectrum of **321** (700 MHz, 175 MHz, CD_2Cl_2)

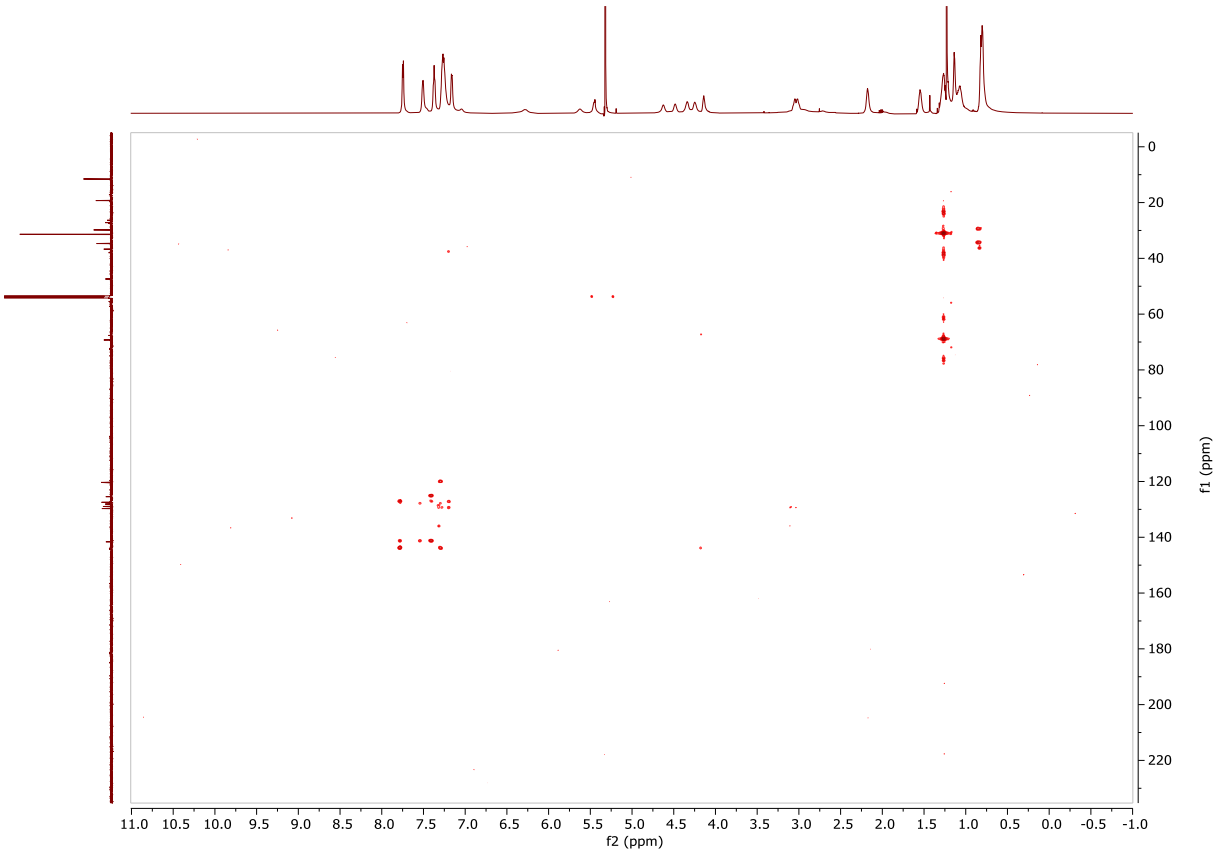

^{1}H, ^{13}C – HMBC spectrum of **321** (700 MHz, 175 MHz, CD_2Cl_2)

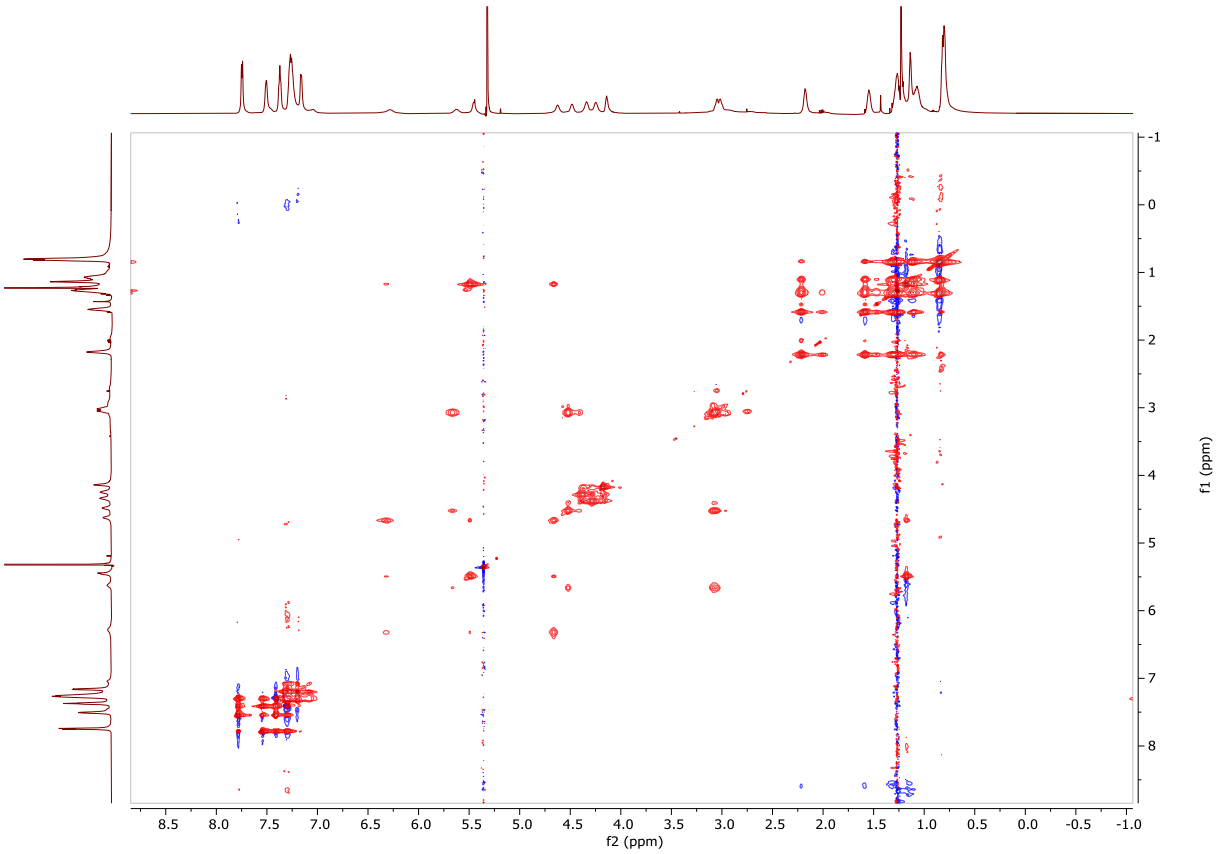

^{1}H, ^{1}H – TOCSY spectrum of **321** (700 MHz, CD_2Cl_2)

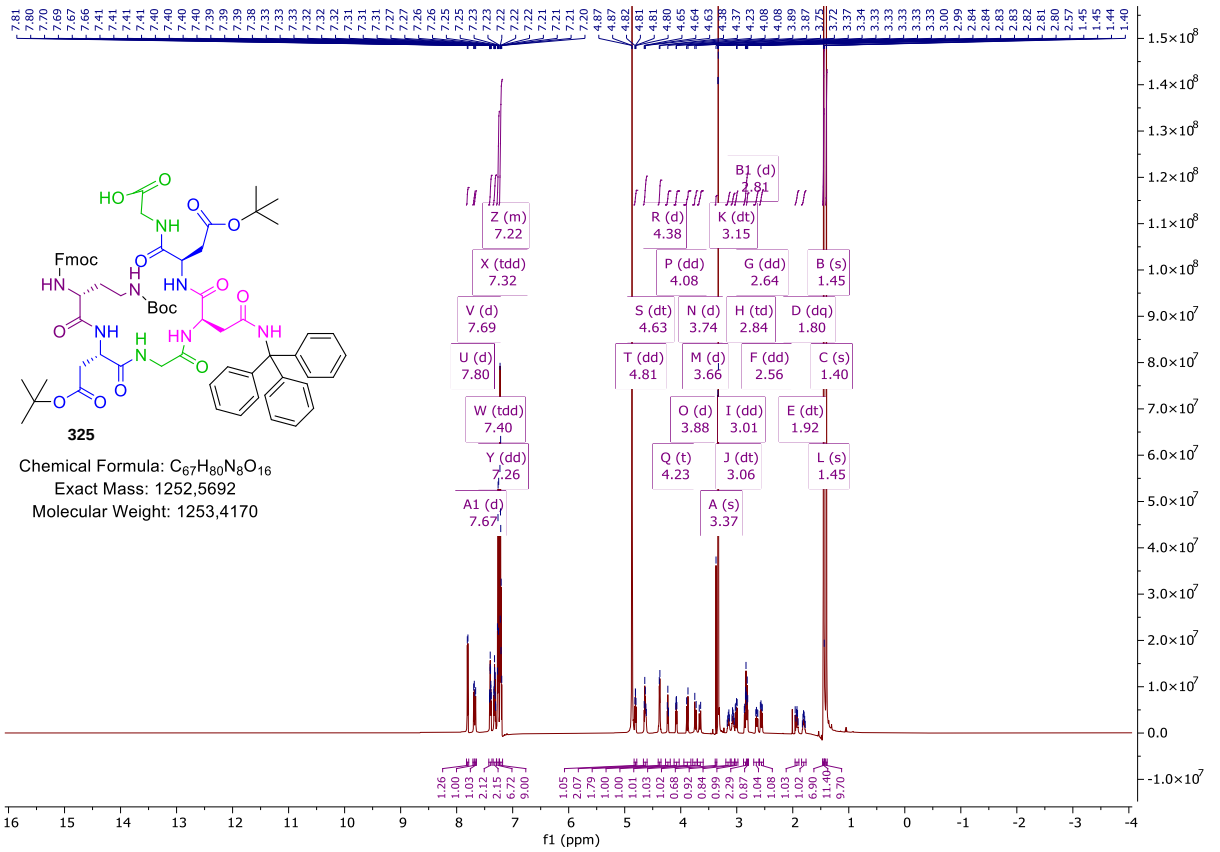

^{1}H – NMR spectrum of **325** (700 MHz, CD_3OD).

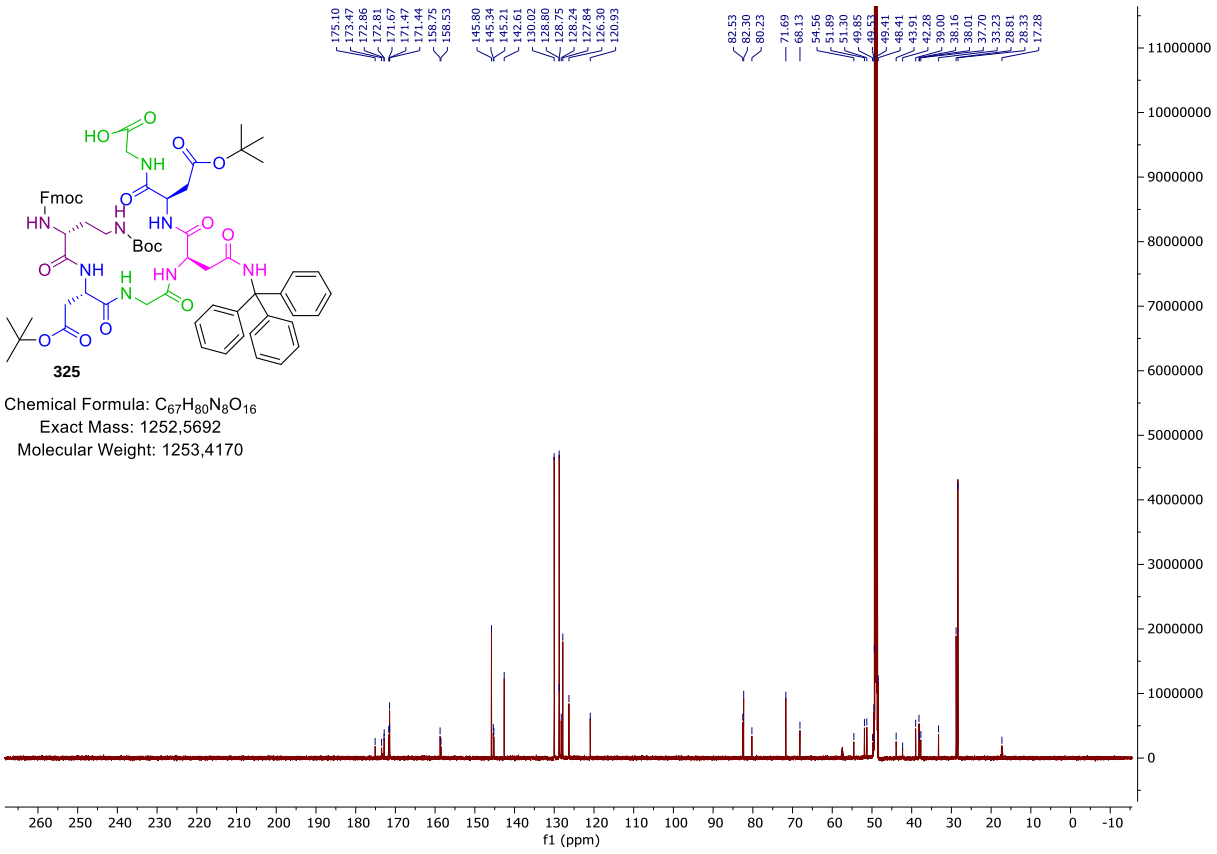

^{13}C – NMR spectrum of **325** (175 MHz, CD_3OD).

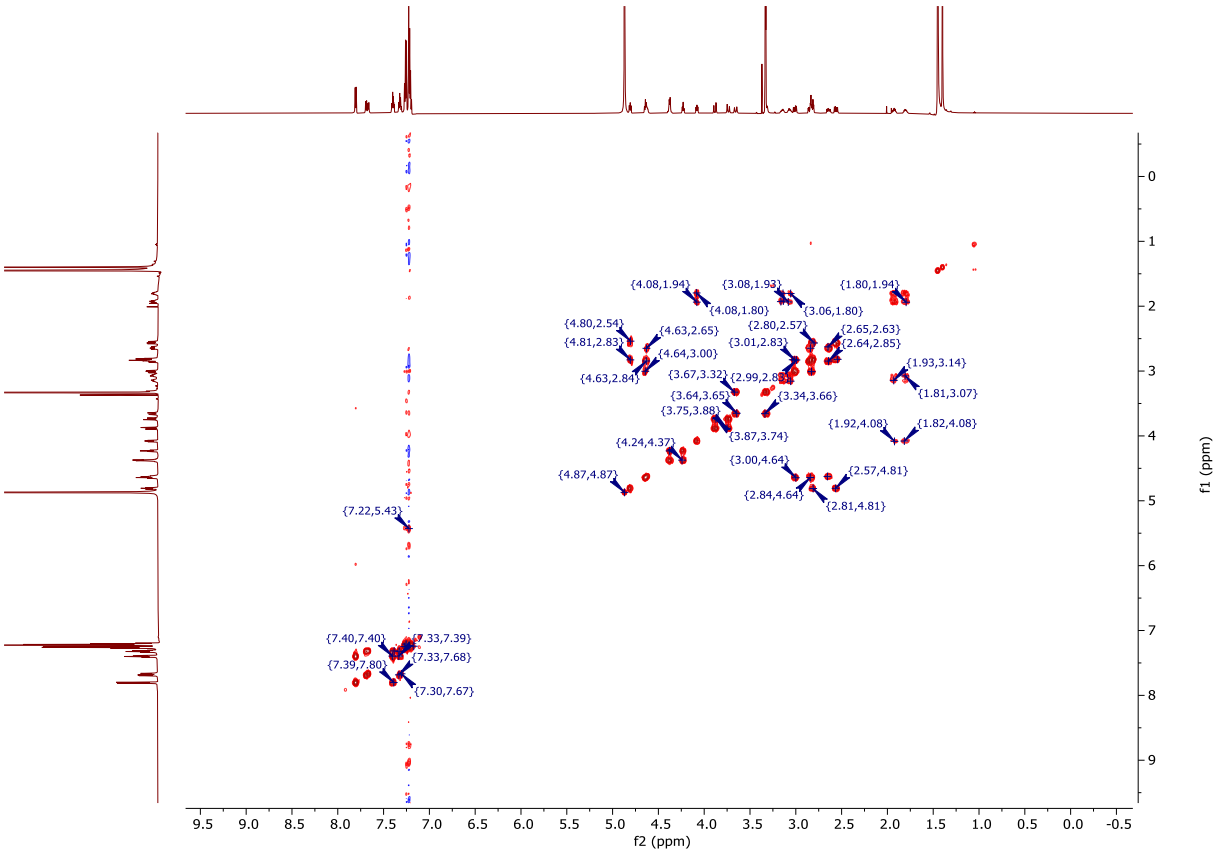

^{1}H, ^{1}H – COSY spectrum of **325** (700 MHz, CD_3OD).

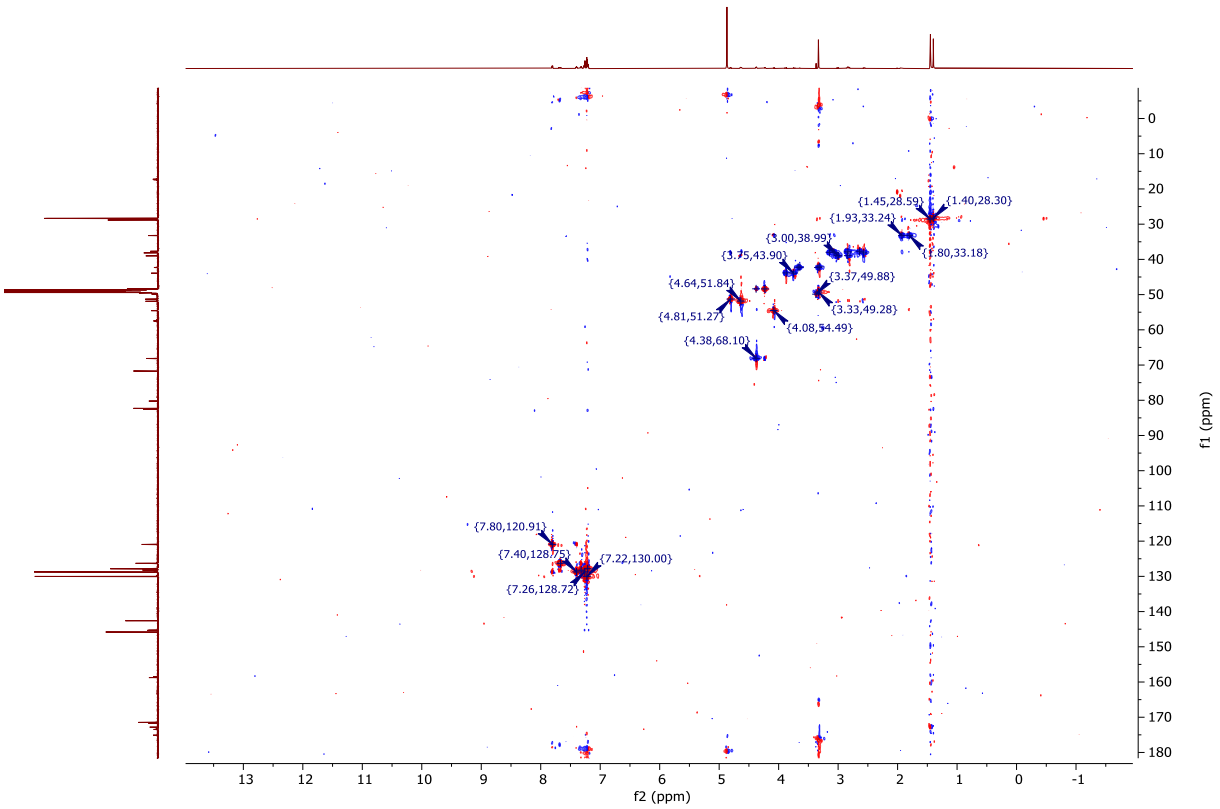

^{1}H, ^{13}C – HSQC spectrum of **325** (700 MHz, 175 MHz, CD_3OD).

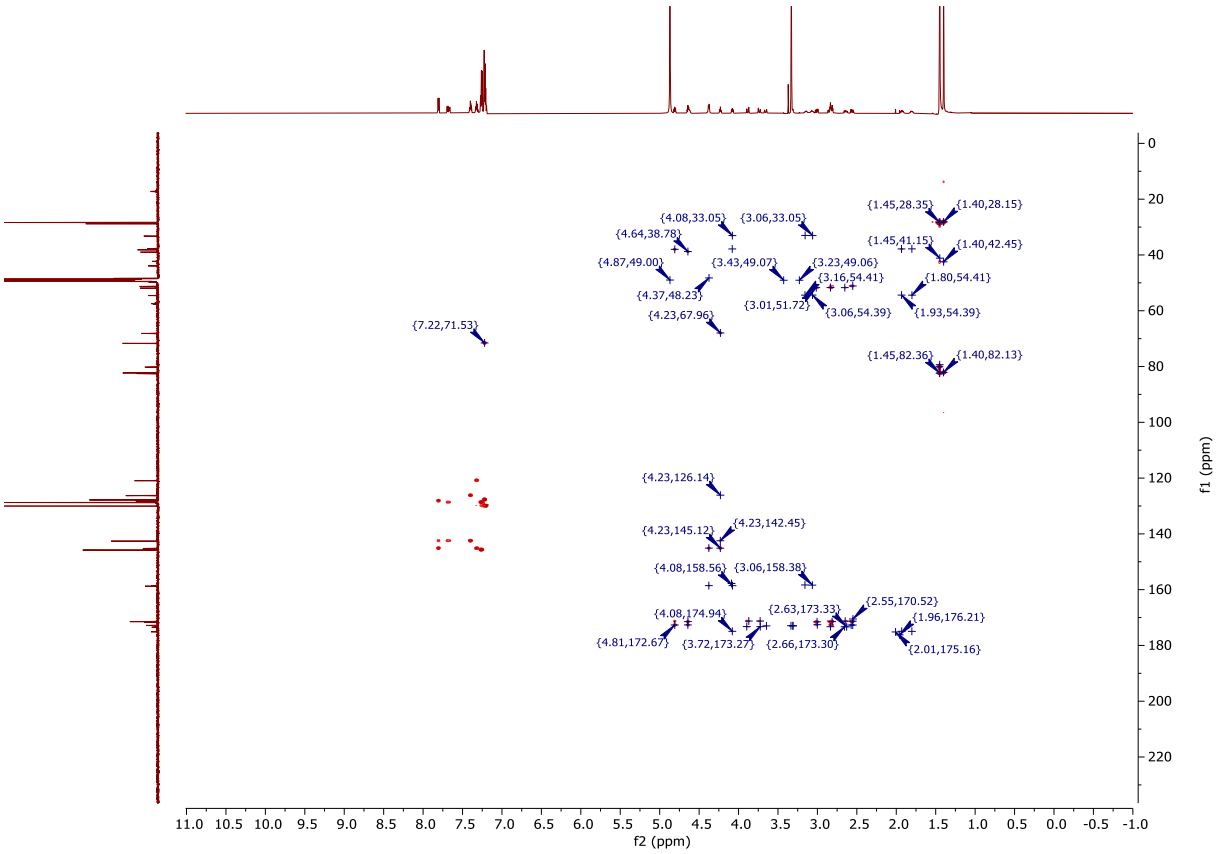

^{1}H, ^{13}C – HMBC spectrum of **325** (700 MHz, 175 MHz, CD_3OD)

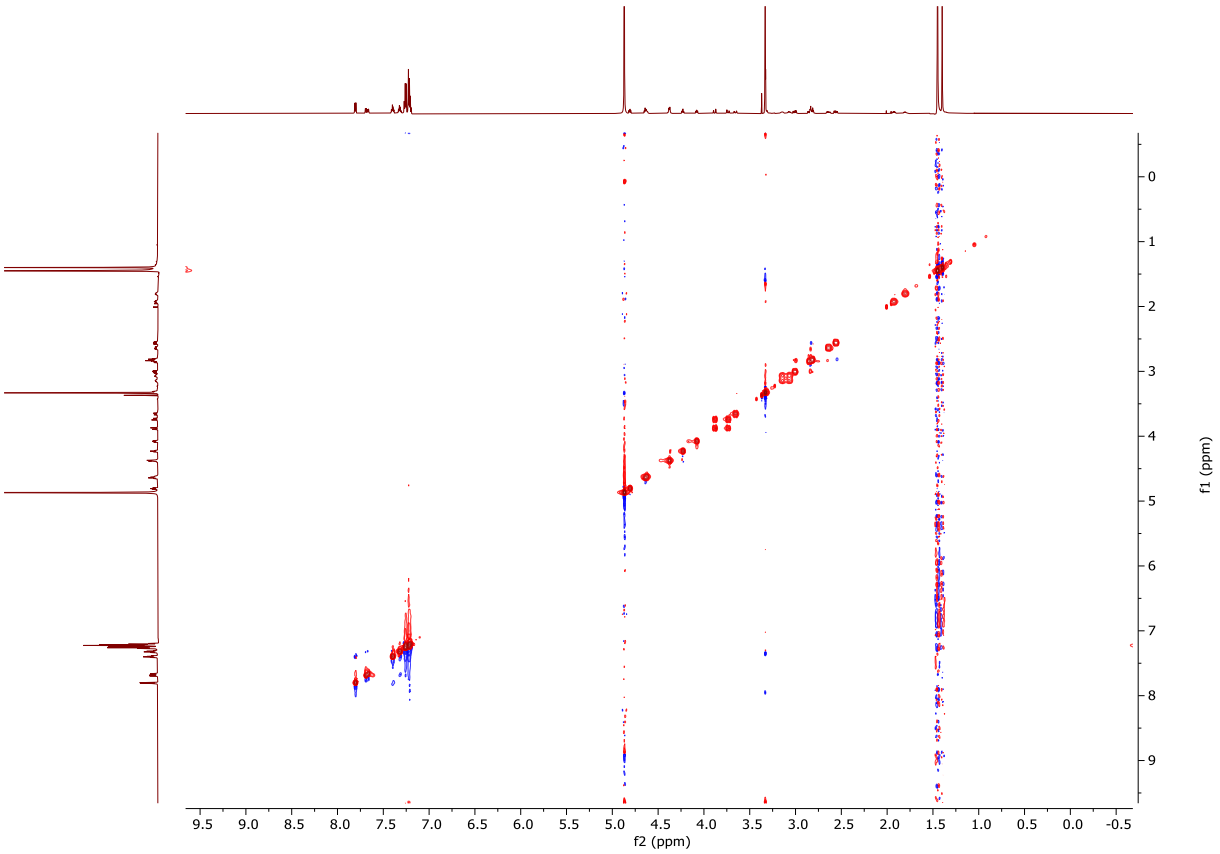

^{1}H, ^{1}H – NOESY spectrum of **325** (700 MHz, CD_3OD)

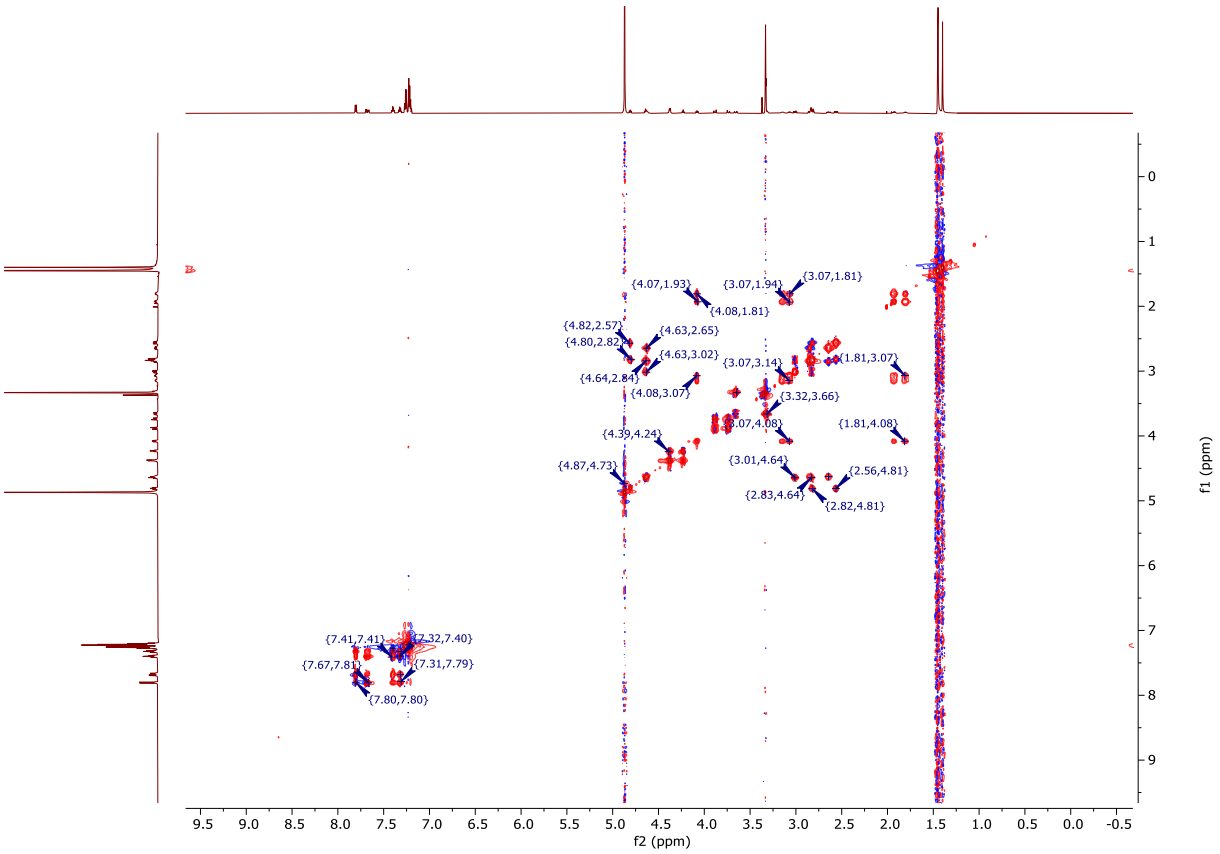

^{1}H, ^{1}H – TOCSY spectrum of **325** (700 MHz, CD_3OD)

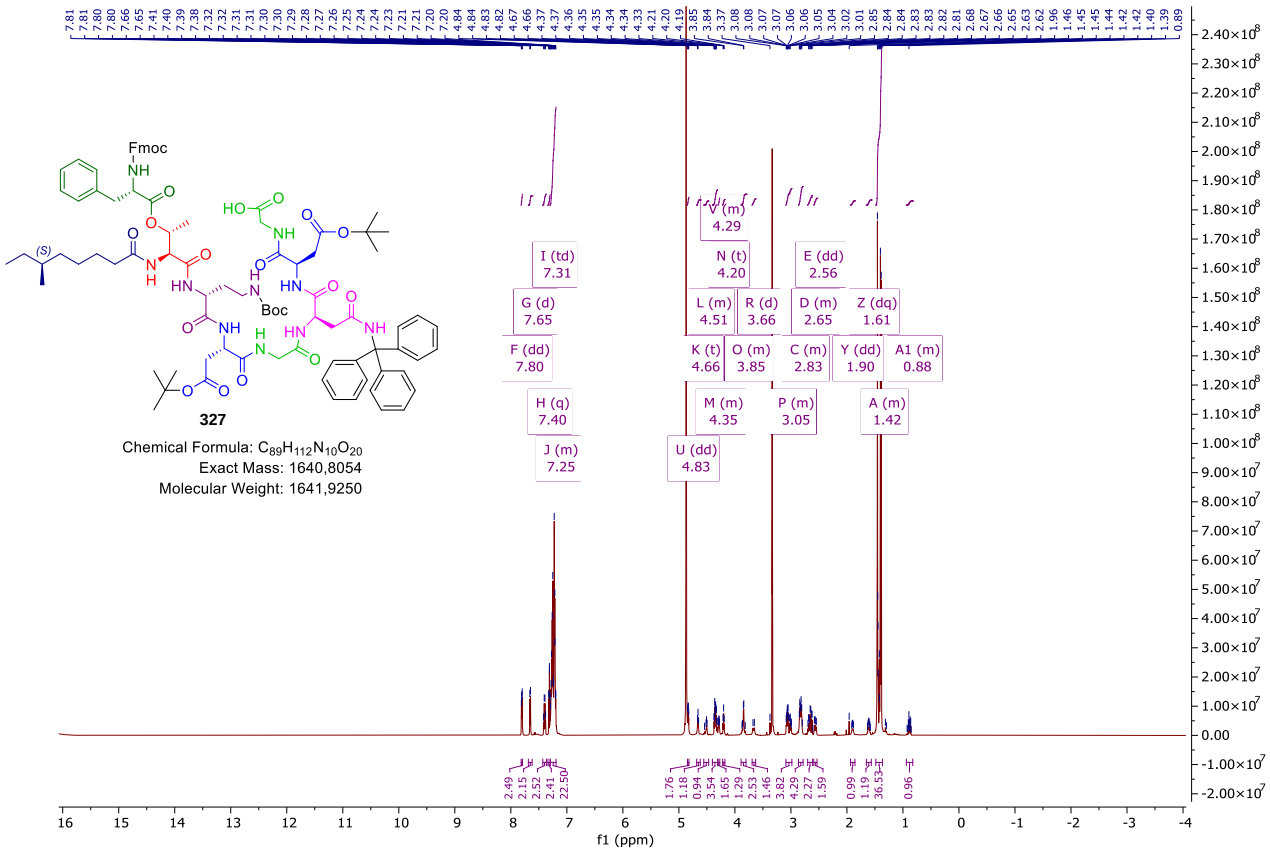

^{1}H – NMR spectrum of **327** (700 MHz, CD_3OD).

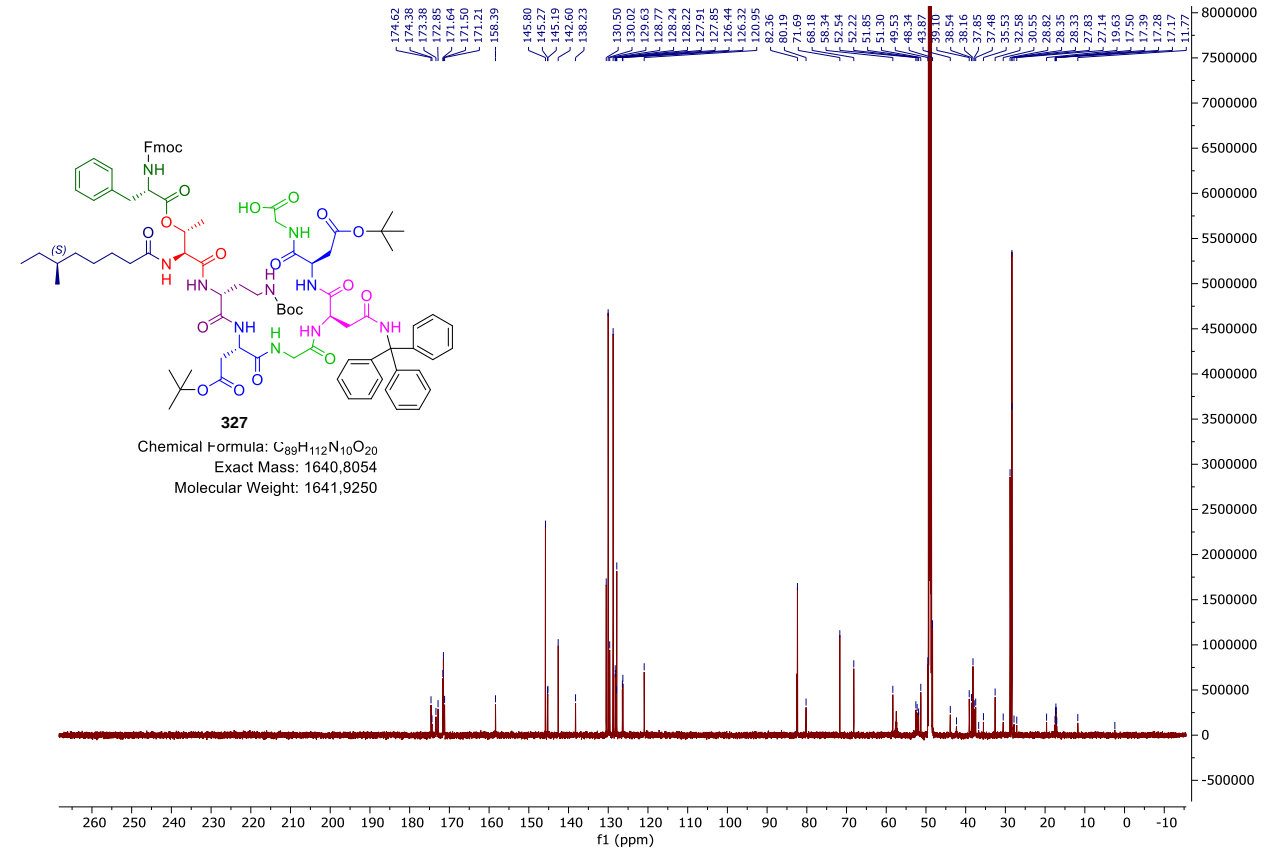

^{13}C – NMR spectrum of **327** (175 MHz, CD_3OD).

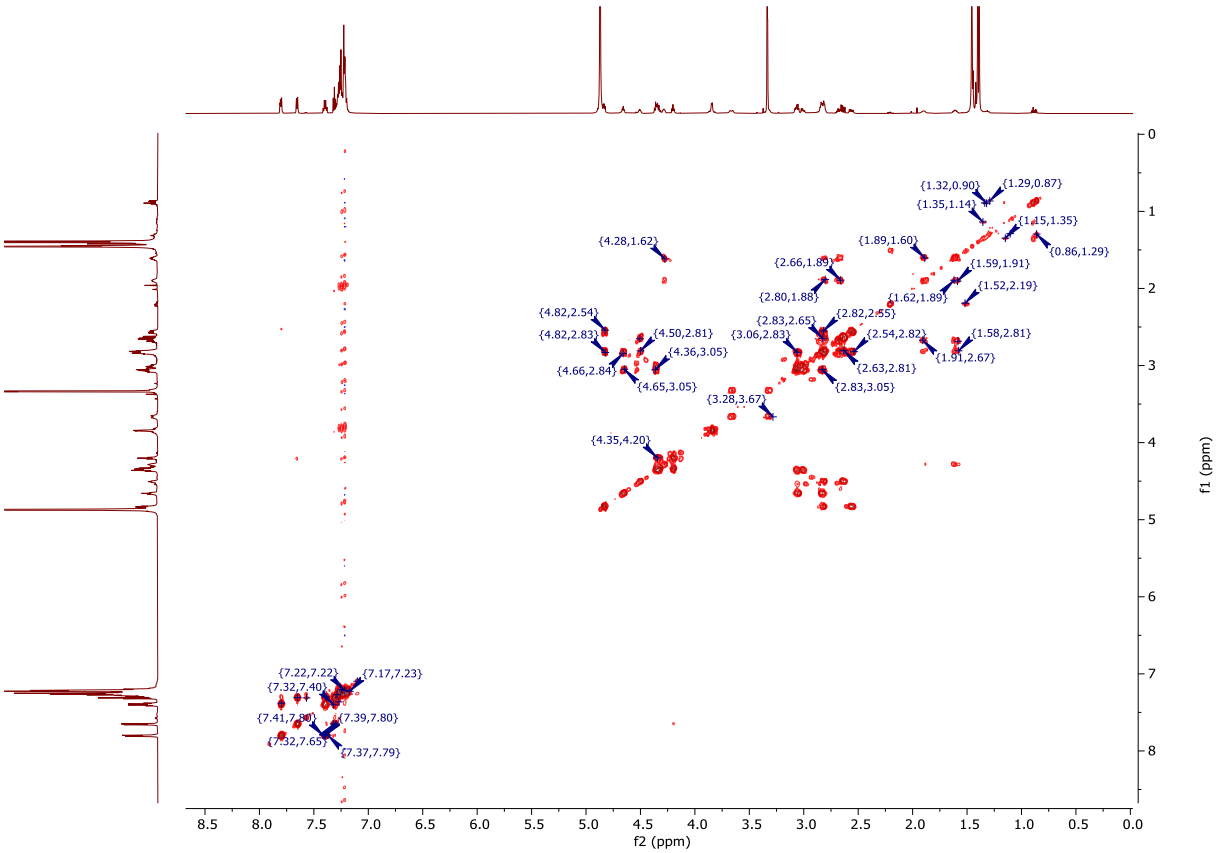

^{1}H, ^{1}H – COSY spectrum of **327** (700 MHz, CD_3OD).

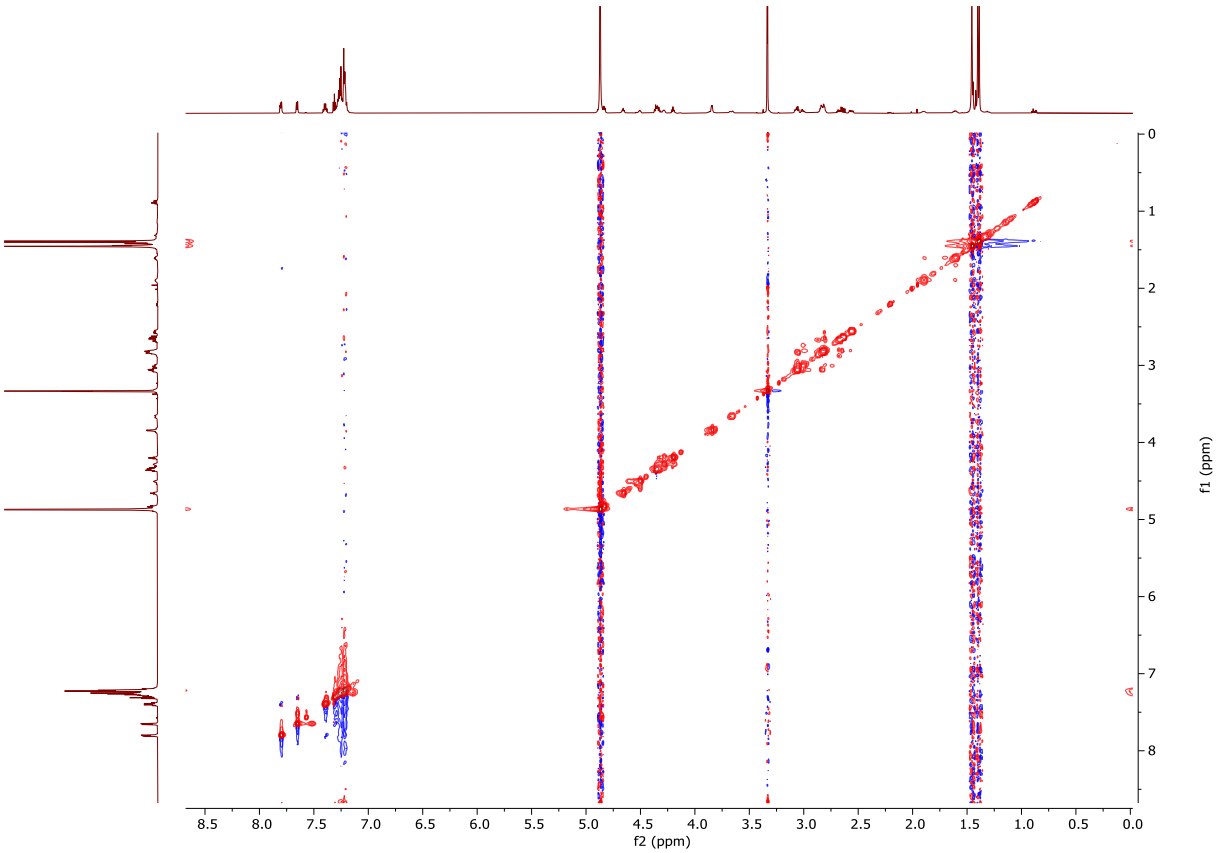

^{1}H, ^{1}H – NOESY spectrum of **327** (700 MHz, CD_3OD)

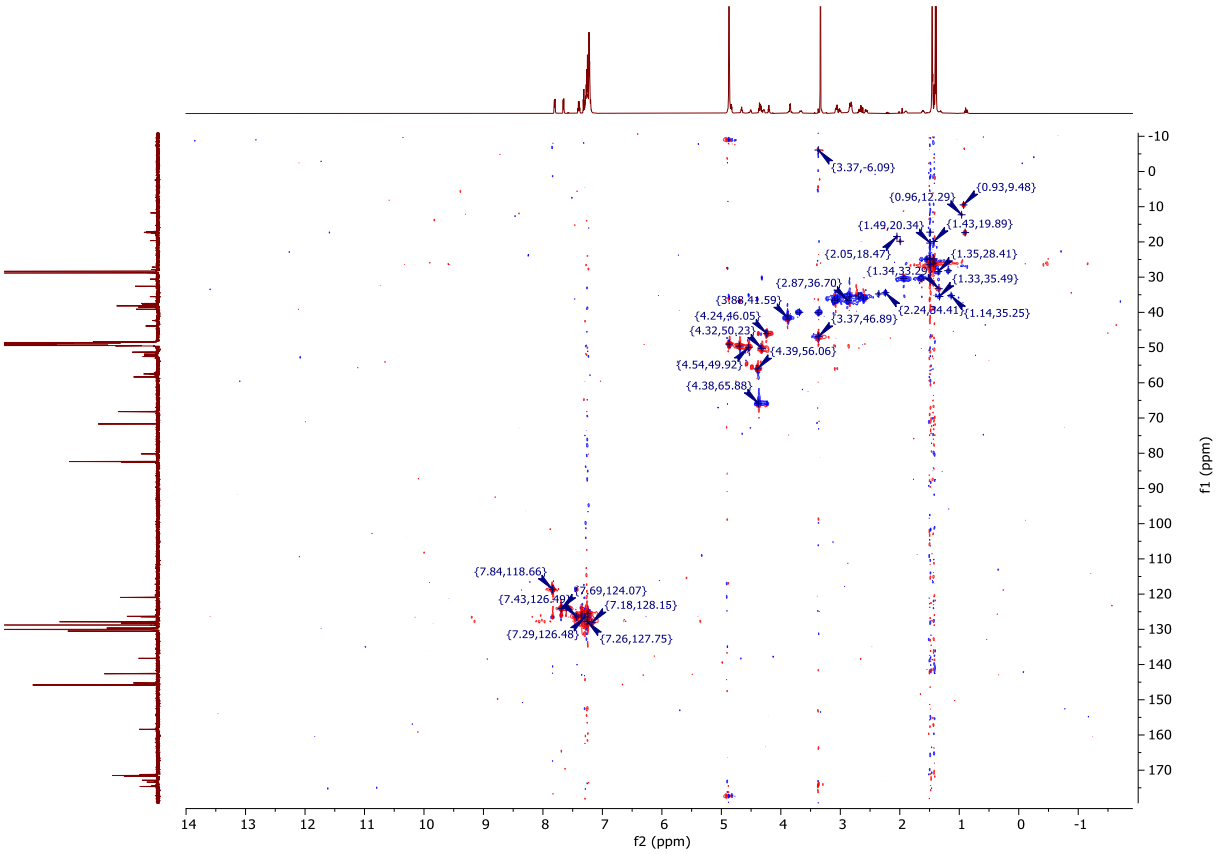

^{1}H, ^{13}C – HSQC spectrum of **327** (700 MHz, 175 MHz, CD_3OD).

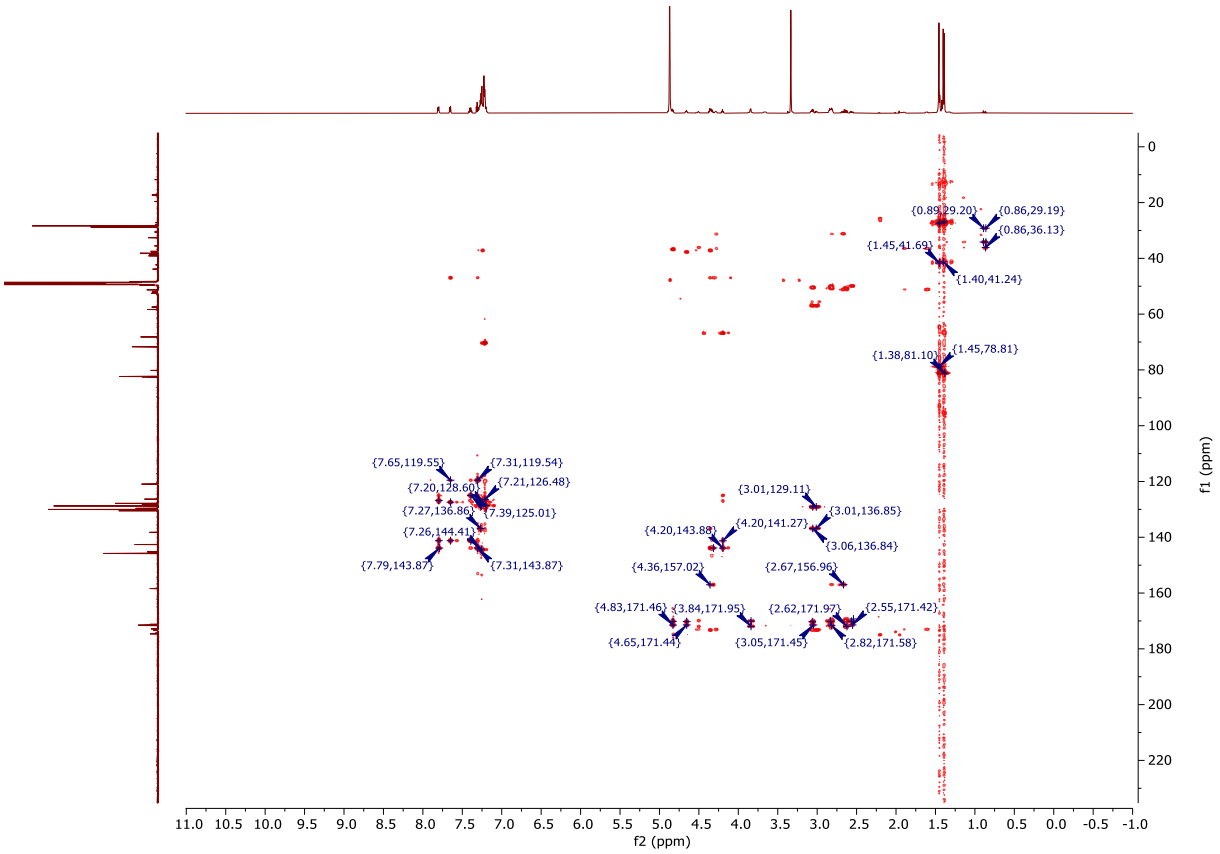

^{1}H, ^{13}C – HMBC spectrum of **327** (700 MHz, 175 MHz, CD_3OD)

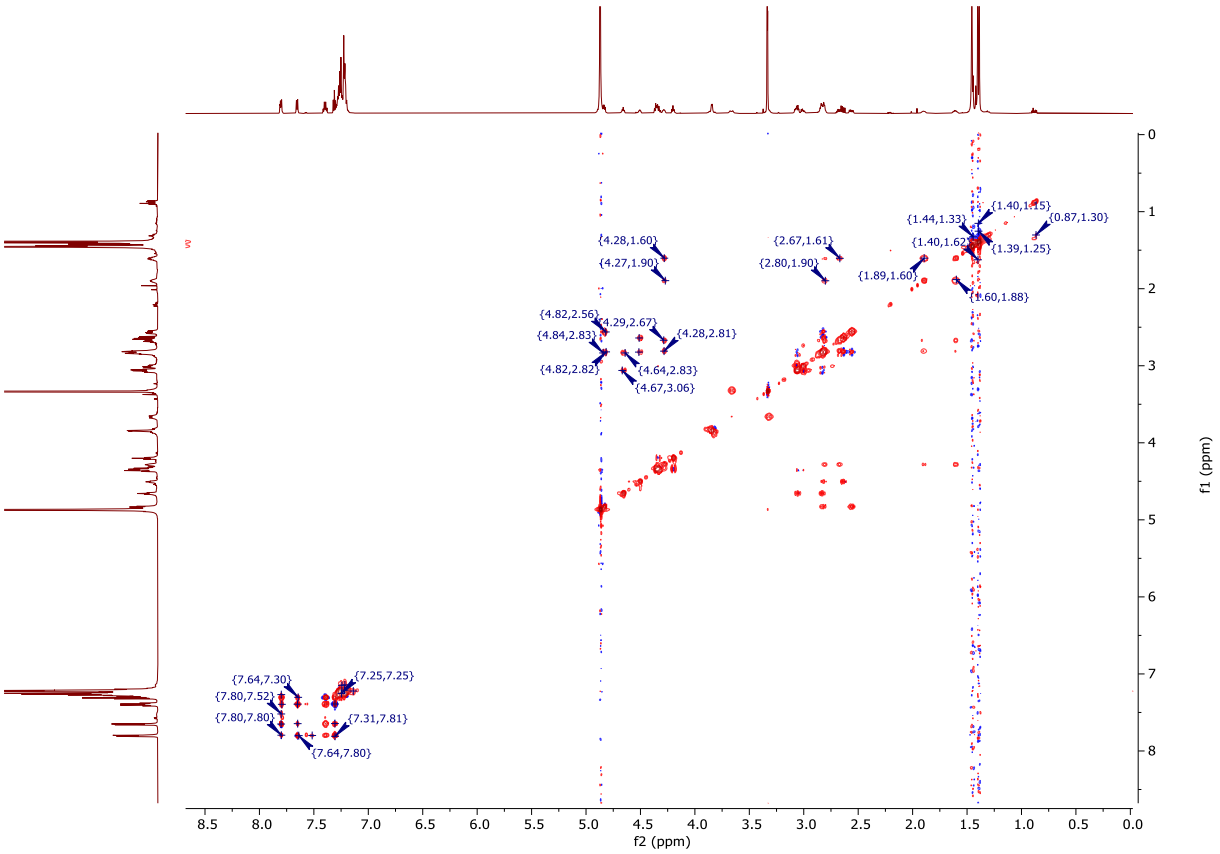

^{1}H, ^{1}H – TOCSY spectrum of **327** (700 MHz, CD_3OD)

*Table 13-1: NMR data of **329** in CD_3OD (700 MHz).*

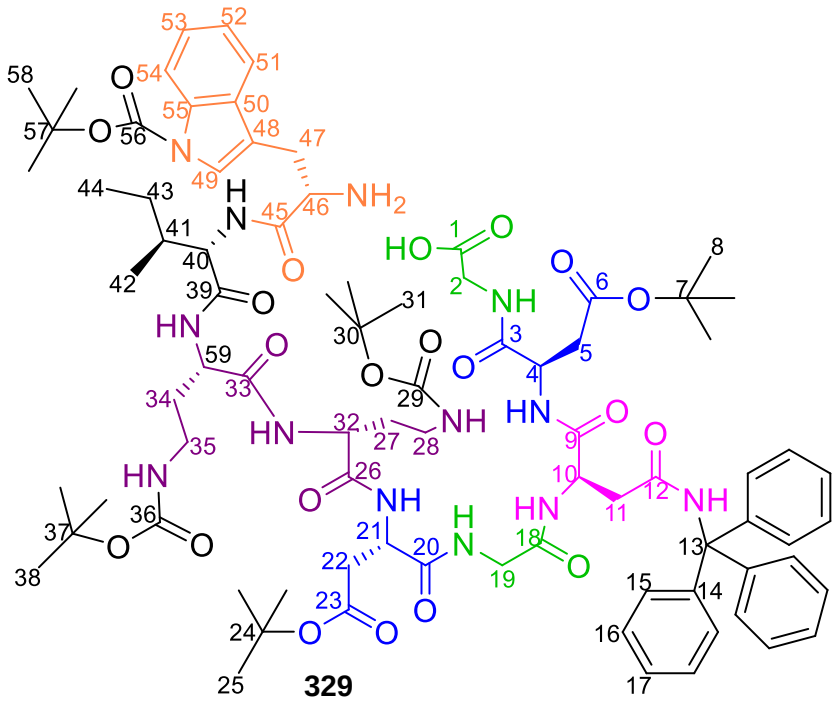

329

Nr.	δH [ppm] (m, J in Hz, Int.)	δC [ppm]
1	-	175.3
2a **2b**	3.69 (d, *J* = 17.3 Hz, 1H) 3.49 (d, *J* = 17.3 Hz, 1H)	44.3
3	-	172.6
4	4.87 (m, 1H)	51.3
5a/b	2.94 – 2.75 (m, 2H)	39.5
6	-	171.6
7	-	82.4
8	1.47 – 1.43 (m, 9H)	3 x 28.8
9	-	173.7
10	4.56 (pt, *J* = 7.7 Hz, 1H)	56.8
11a/b	3.00 – 2.95 (m, 2H)	39.2
12	-	173.6
13	-	71.8
14	-	3 x 145.8

15	7.31 – 7.10 (m, 6H)	6 x 130
16	7.31 – 7.10 (m, 6H)	6 x 128.8
17	7.31 – 7.10 (m, 3H)	3 x 127.8
18	-	173.2
19a **19b**	3.97 (d, *J* = 16.8 Hz, 1H) 3.90 (d, *J* = 16.6 Hz, 1H)	43.9
20	-	171.5
21	4.79 (pt, *J* = 6.9 Hz, 1H)	51.8
22a **22b**	2.60 – 2.54 (m, 1H) 2.75 – 2.62 (m, 1H)	38.6
23	-	171.5
24	-	82.5
25	1.47 – 1.43 (m, 9H)	3 x 28.9
26	-	174.3
27a **27b**	1.64 – 1.52 (m, 1H) 1.83 – 1.74 (m, 1H)	32.5
28a **28b**	2.94 – 2.75 (m, 1H) 2.75 – 2.62 (m, 1H)	37.8
29	-	158.3
30	-	80.2
31	1.47 – 1.43 (m, 9H)	3 x 28.5
32	4.11 (pt, *J* = 7.3 Hz, 1H)	53.1
33	-	173.2
34a **34b**	1.97 – 1.88 (m, 1H) 1.83 – 1.74 (m, 1H)	33.6
35a **35b**	3.15 (d, *J* = 8.8 Hz, 1H) 3.09 – 3.04 (m, 1H)	38.0
36	-	158.3
37	-	80.1

38	1.43 – 1.41 (m, 9H)	3 x 28.5
39	-	173.3
40	4.26 (d, *J* = 7.8 Hz, 1H)	59.8
41	1.83 – 1.74 (m, 1H)	38.2
42	0.91 – 0.84 (m, 3H)	16.0
43a **43b**	1.19 – 1.01 (m, 1H) 1.64 – 1.52 (m, 1H)	26.1
44	0.91 – 0.84 (m, 3H)	11.6
45	-	170.8
46	4.29 (d, *J* = 8.5 Hz, 1H)	54.2
47a **47b**	3.38 – 3.34 (m, 1H) 3.15 (d, *J* = 8.8 Hz, 1H)	28.5
48	-	114.9
49	7.62 (s, 1H)	126.6
50	-	131.2
51	7.71 (d, *J* = 7.9 Hz, 1H)	120.3
52	7.31 – 7.10 (m, 1H)	124.0
53	7.35 (dd, *J* = 7.4, 7.4 Hz, 1H)	125.9
54	8.13 (d, *J* = 8.3 Hz, 1H)	116.3
55	-	137.2
56	-	150.1
57	-	85.1
58	1.68 (s, 9H)	28.4
59	4.52 (d, *J* = 7.5 Hz, 2H)	52.1

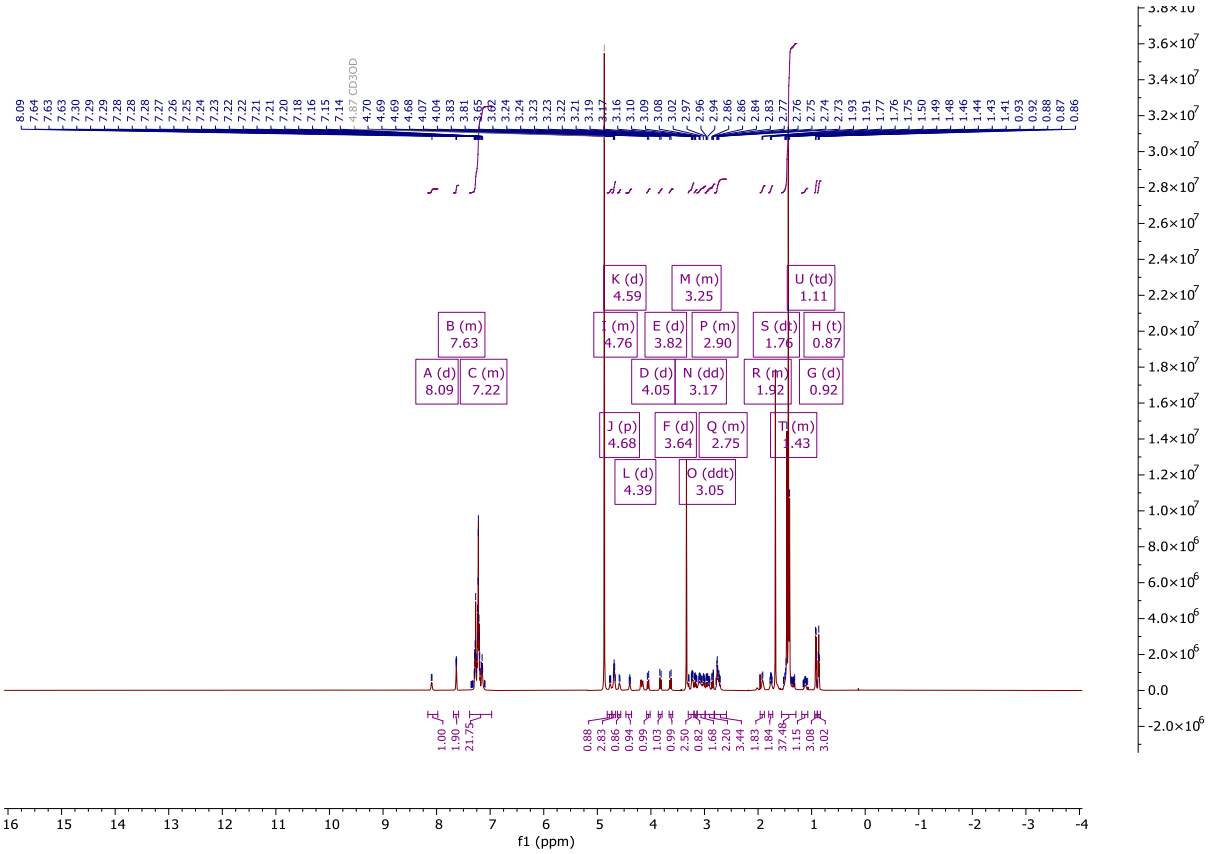

^{1}H – NMR spectrum of **329** (700 MHz, CD_3OD).

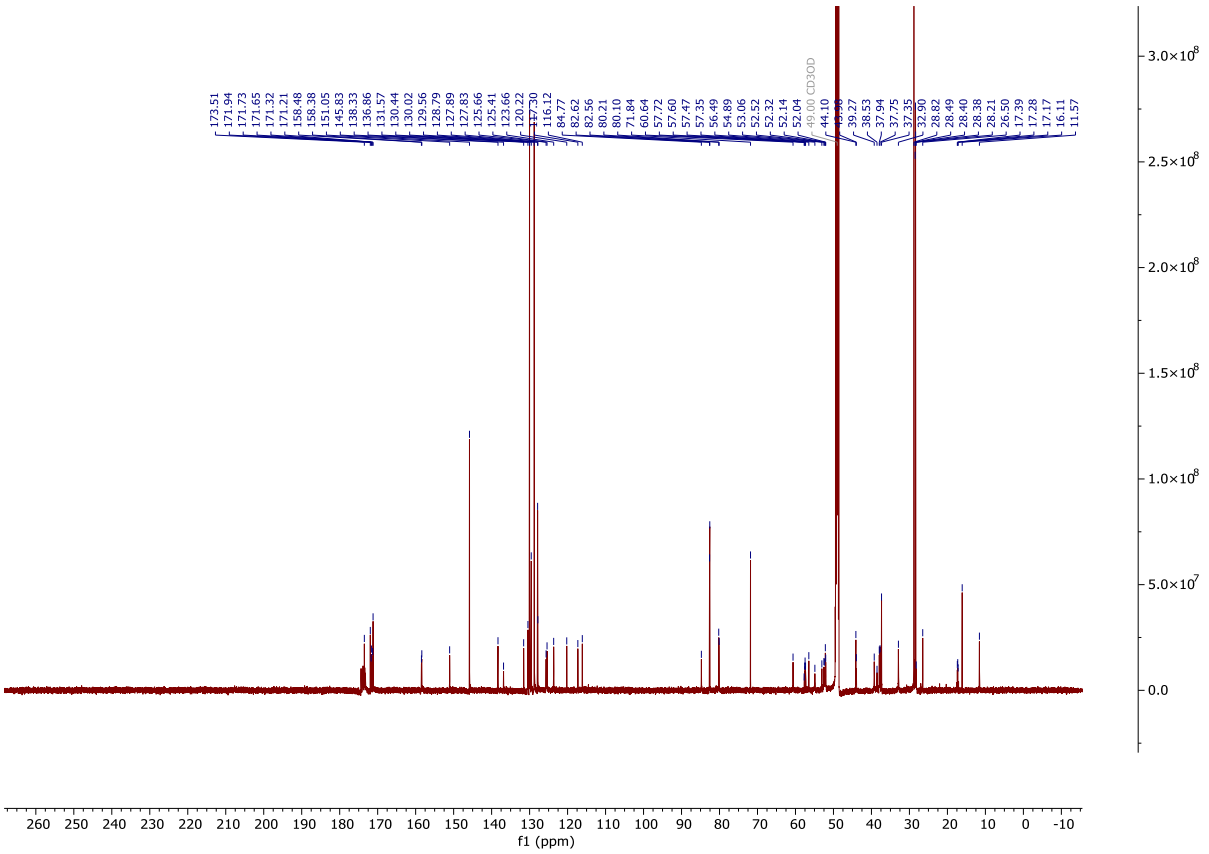

^{13}C – NMR spectrum of **329** (175 MHz, CD_3OD).

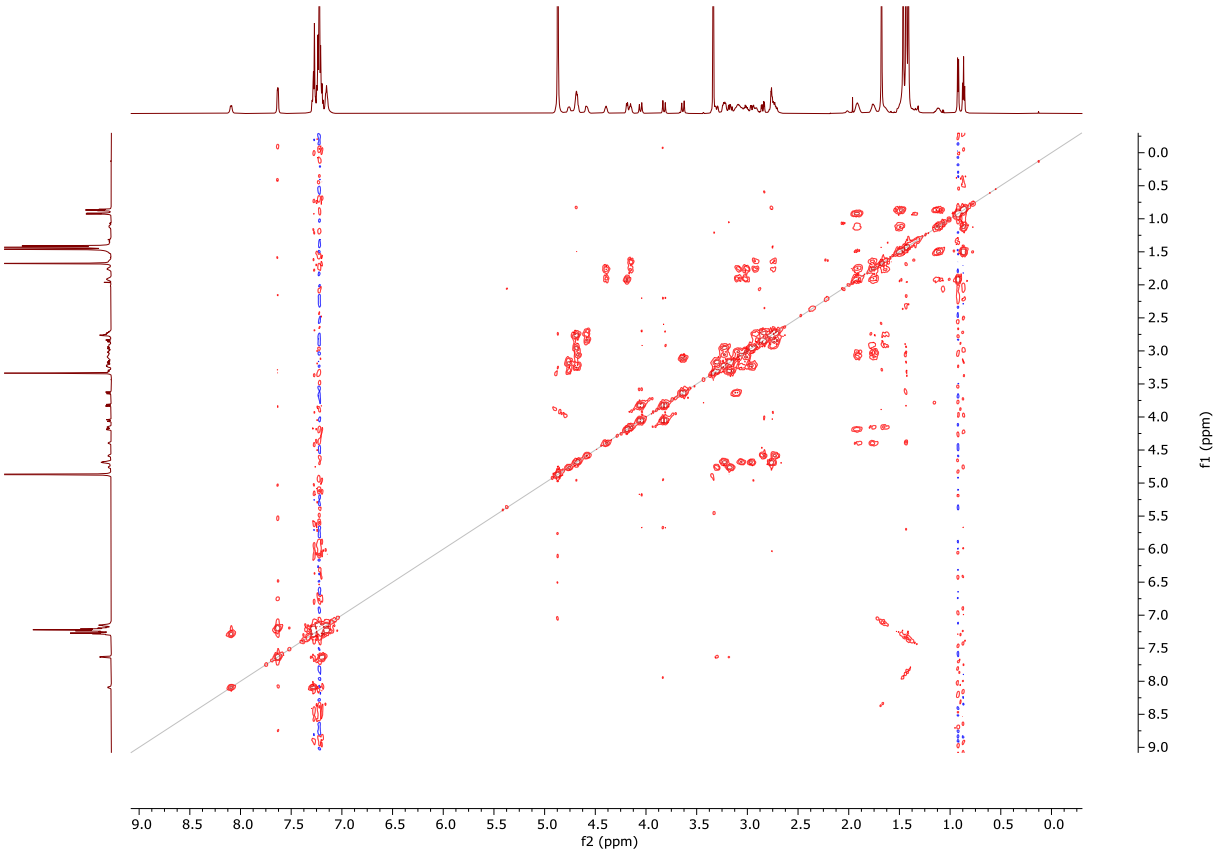

^{1}H, ^{1}H – COSY spectrum of **329** (700 MHz, CD_3OD).

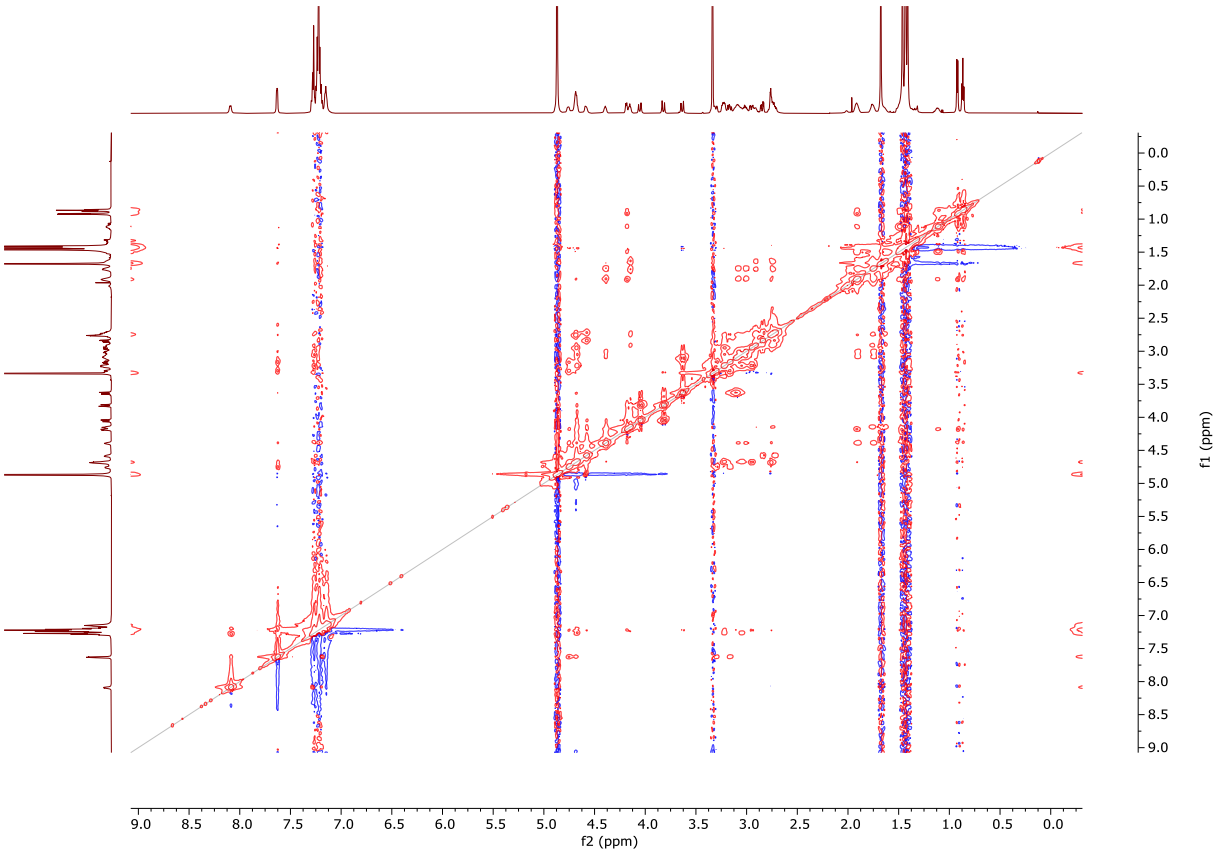

^{1}H, ^{1}H – NOESY spectrum of **329** (700 MHz, CD_3OD)

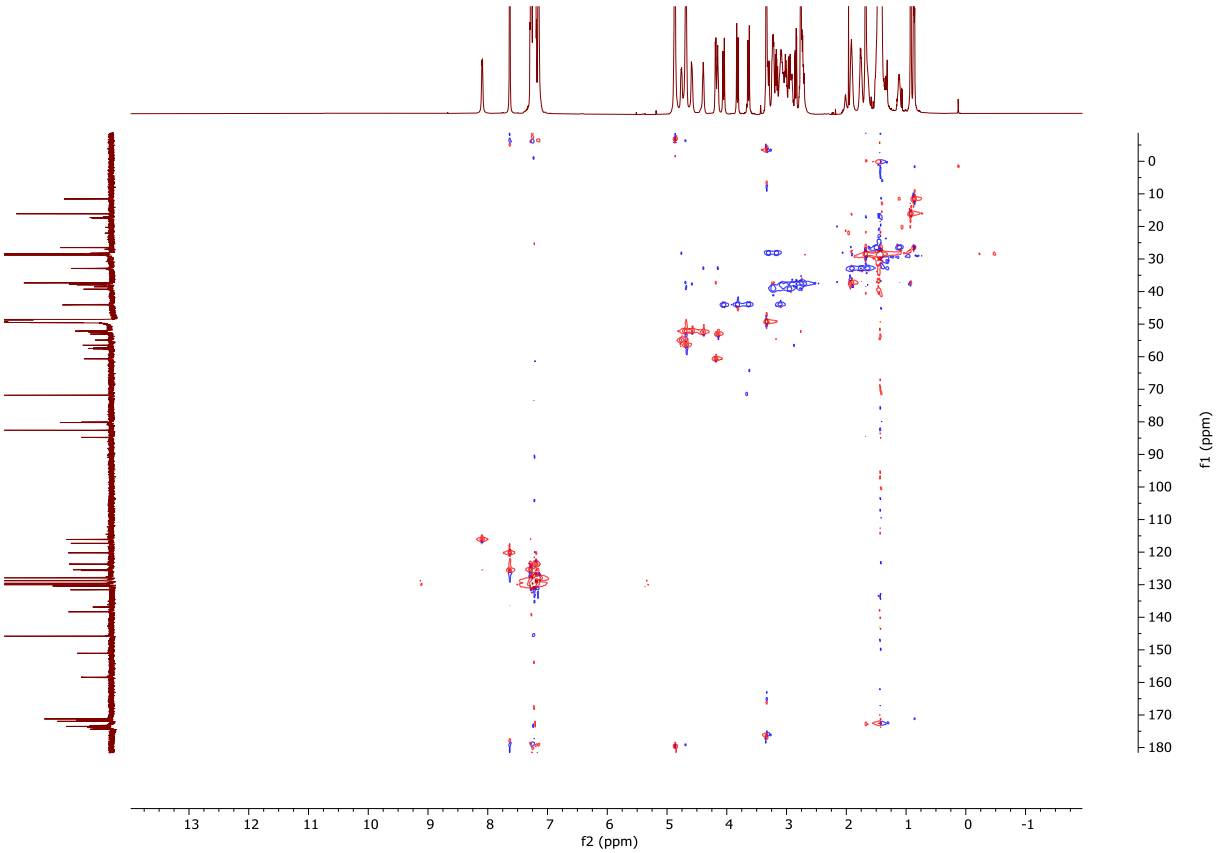

^{1}H, ^{13}C – HSQC spectrum of **329** (700 MHz, 175 MHz, CD_3OD).

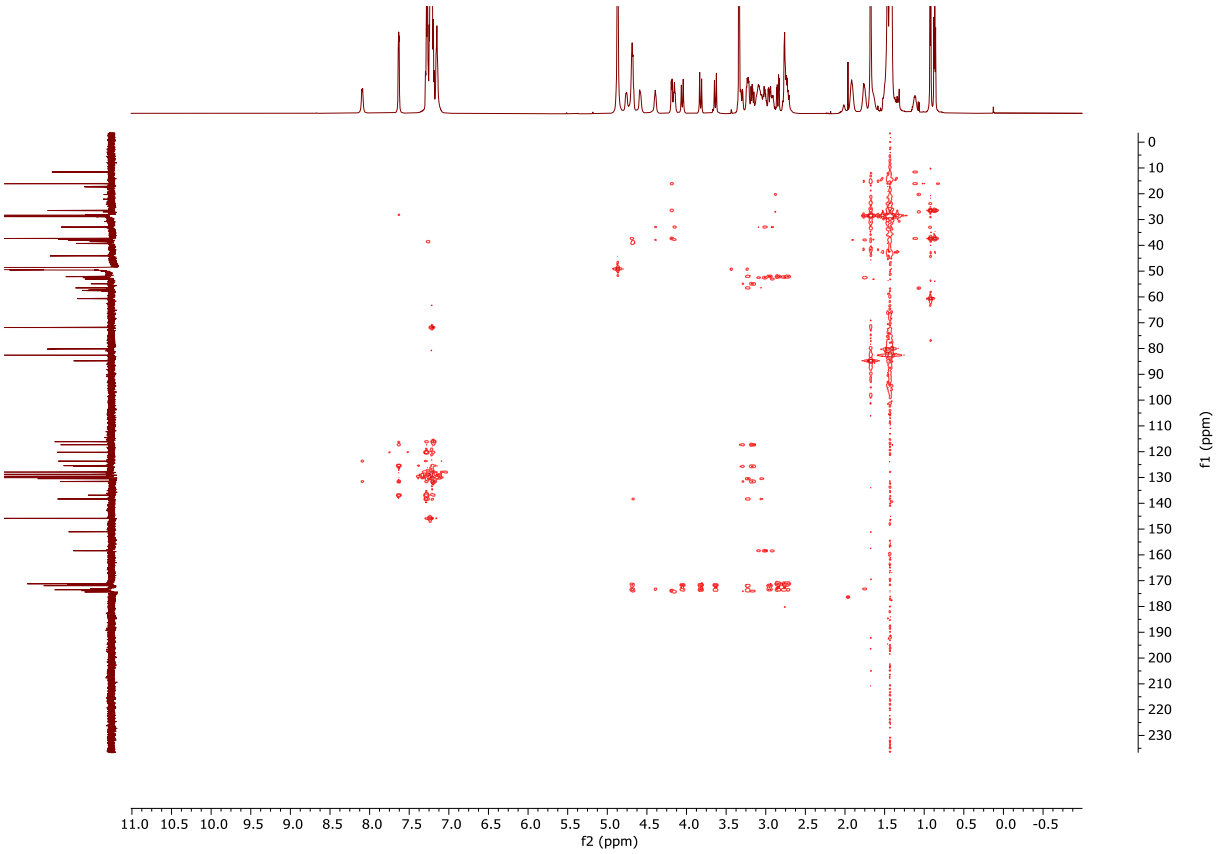

^{1}H, ^{13}C – HMBC spectrum of **329** (700 MHz, 175 MHz, CD_3OD)

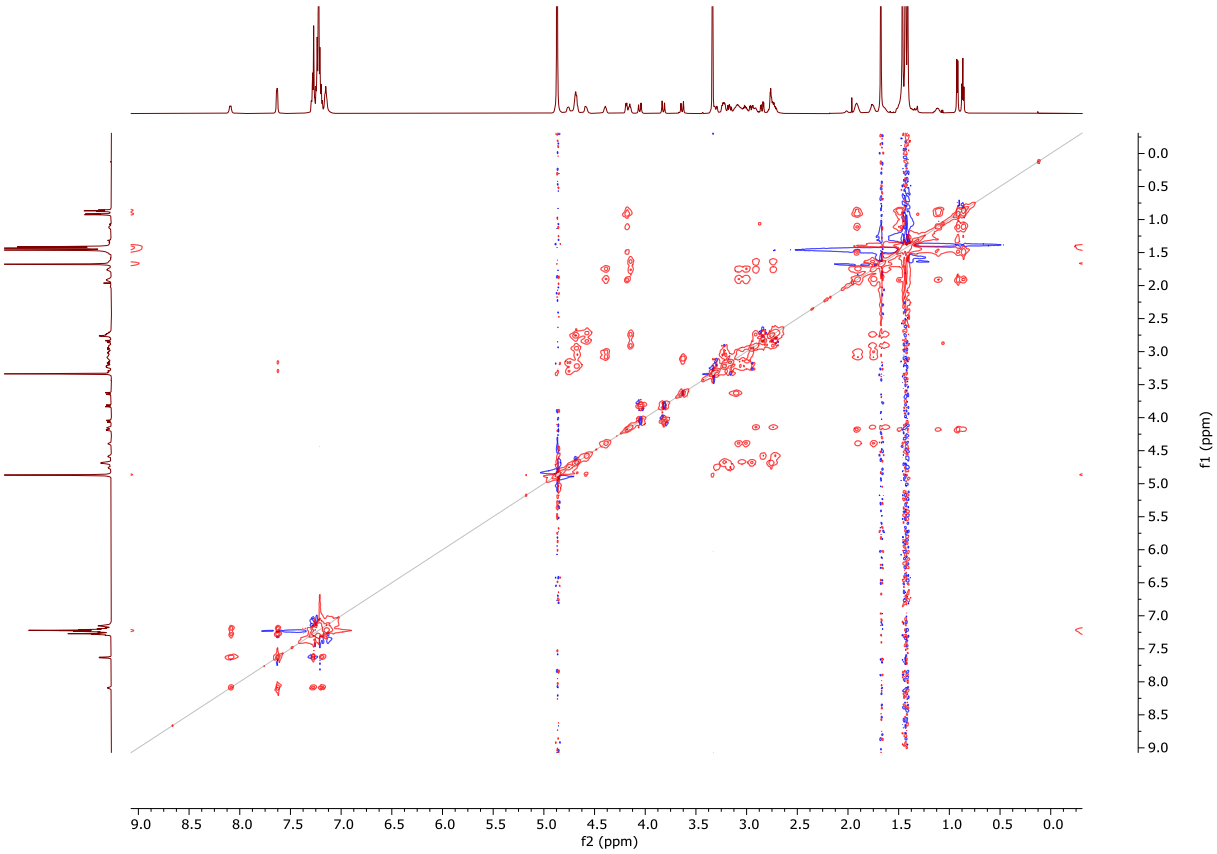

^{1}H, ^{1}H – TOCSY spectrum of **329** (700 MHz, CD_3OD)